INTERACTION OF PATHOGENIC ESCHERICHIA COLI WITH THE HOST: PATHOGENOMICS, VIRULENCE AND ANTIBIOTIC RESISTANCE

EDITED BY: Tânia Aparecida Tardelli Gomes, Ulrich Dobrindt, Mauricio J. Farfan and Roxane M. Piazza

PUBLISHED IN: Frontiers in Cellular and Infection Microbiology

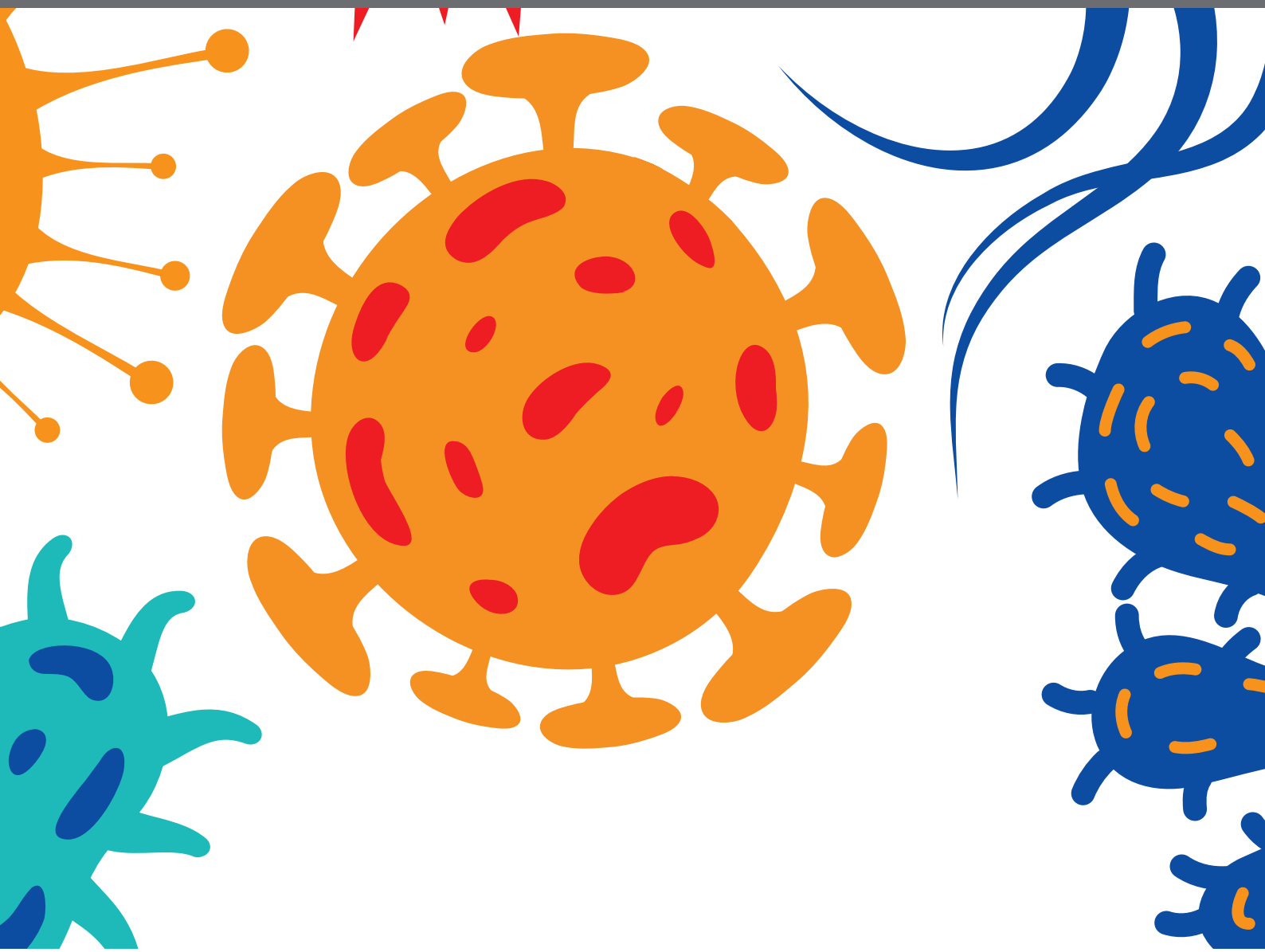

frontiers Research Topics

ISSN 1664-8714
ISBN 978-2-88966-797-0
DOI 10.3389/978-2-88966-797-0

About Frontiers

Frontiers is more than just an open-access publisher of scholarly articles: it is a pioneering approach to the world of academia, radically improving the way scholarly research is managed. The grand vision of Frontiers is a world where all people have an equal opportunity to seek, share and generate knowledge. Frontiers provides immediate and permanent online open access to all its publications, but this alone is not enough to realize our grand goals.

Frontiers Journal Series

The Frontiers Journal Series is a multi-tier and interdisciplinary set of open-access, online journals, promising a paradigm shift from the current review, selection and dissemination processes in academic publishing. All Frontiers journals are driven by researchers for researchers; therefore, they constitute a service to the scholarly community. At the same time, the Frontiers Journal Series operates on a revolutionary invention, the tiered publishing system, initially addressing specific communities of scholars, and gradually climbing up to broader public understanding, thus serving the interests of the lay society, too.

Dedication to Quality

Each Frontiers article is a landmark of the highest quality, thanks to genuinely collaborative interactions between authors and review editors, who include some of the world's best academicians. Research must be certified by peers before entering a stream of knowledge that may eventually reach the public - and shape society; therefore, Frontiers only applies the most rigorous and unbiased reviews.
Frontiers revolutionizes research publishing by freely delivering the most outstanding research, evaluated with no bias from both the academic and social point of view. By applying the most advanced information technologies, Frontiers is catapulting scholarly publishing into a new generation.

What are Frontiers Research Topics?

Frontiers Research Topics are very popular trademarks of the Frontiers Journals Series: they are collections of at least ten articles, all centered on a particular subject. With their unique mix of varied contributions from Original Research to Review Articles, Frontiers Research Topics unify the most influential researchers, the latest key findings and historical advances in a hot research area! Find out more on how to host your own Frontiers Research Topic or contribute to one as an author by contacting the Frontiers Editorial Office: frontiersin.org/about/contact

INTERACTION OF PATHOGENIC ESCHERICHIA COLI WITH THE HOST: PATHOGENOMICS, VIRULENCE AND ANTIBIOTIC RESISTANCE

Topic Editors:
Tânia Aparecida Tardelli Gomes, Federal University of São Paulo, Brazil
Ulrich Dobrindt, University of Münster, Germany
Mauricio J. Farfan, University of Chile, Chile
Roxane M. Piazza, Butantan Institute, Brazil

Citation: Gomes, T. A. T., Dobrindt, U., Farfan, M. J., Piazza, R. M., eds. (2021). Interaction of Pathogenic Escherichia coli with the Host: Pathogenomics, Virulence and Antibiotic Resistance. Lausanne: Frontiers Media SA.
doi: 10.3389/978-2-88966-797-0

Table of Contents

frontiers in Cellular and Infection Microbiology

EDITORIAL
published: 31 March 2021
doi: 10.3389/fcimb.2021.654283

Editorial: Interaction of Pathogenic *Escherichia coli* With the Host: Pathogenomics, Virulence and Antibiotic Resistance

Tânia A. T. Gomes[1]*, *Ulrich Dobrindt*[2], *Mauricio J. Farfan*[3,4] and *Roxane M. F. Piazza*[5]

[1] Departamento de Microbiologia, Imunologia e Parasitologia, Escola Paulista de Medicina, Universidade Federal de São Paulo, São Paulo, Brazil, [2] Institute of Hygiene, University of Muenster, Muenster, Germany, [3] Laboratorio Clínico, Hospital Dr. Luis Calvo Mackenna, Santiago, Chile, [4] Departamento de Pediatría y Cirugía Infantil, Hospital Dr. Luis Calvo Mackenna, Facultad de Medicina, Universidad de Chile, Santiago, Chile, [5] Laboratório de Bacteriologia, Instituto Butantan, São Paulo, Brazil

Keywords: ***Escherichia coli*, virulence factors, genome, antibiotic resistance, evolution**

Editorial on the Research Topic

Interaction of Pathogenic *Escherichia coli* With the Host: Pathogenomics, Virulence and Antibiotic Resistance

OPEN ACCESS

Edited and reviewed by:
Thomas Rudel,
Julius Maximilian University of Würzburg, Germany

***Correspondence:**
Tânia A. T. Gomes
tatg.amaral@unifesp.br

Specialty section:
This article was submitted to Bacteria and Host, a section of the journal Frontiers in Cellular and Infection Microbiology

Received: *15 January 2021*
Accepted: *17 March 2021*
Published: *31 March 2021*

Citation:
Gomes TAT, Dobrindt U, Farfan MJ and Piazza RMF (2021) Editorial: Interaction of Pathogenic Escherichia coli With the Host: Pathogenomics, Virulence and Antibiotic Resistance. Front. Cell. Infect. Microbiol. 11:654283. doi: 10.3389/fcimb.2021.654283

Escherichia coli live as commensals in the intestines of humans and warm-blooded animals (Leimbach et al., 2013). Although most *E. coli* strains rarely produce disease in healthy individuals, pathogenic strains can cause a wide range of diseases in the gastrointestinal tract or extraintestinal sites in healthy and immunocompromised individuals (Kaper et al., 2004). This variety of behaviors is due to the existence of virulence genes in mobile genetic elements and the large permissiveness of *E. coli* to acquire these elements by horizontal gene transfer (Dobrindt et al., 2004; Kaper et al., 2004; Croxen and Finlay, 2010; Leimbach et al., 2013; Johnson and Russo, 2018).

The acquisition of specific combinations of virulence genes defined the presently recognized diarrheagenic *E. coli* (DEC) pathotypes, which constitute the most critical contributors to diarrhea cases, especially in infants and young children in low- and middle-income countries (Gomes et al., 2016; Jesser and Levy, 2020). These pathotypes differ concerning their virulence mechanisms, preferential sites of intestinal colonization, symptoms, and clinical presentation. In turn, *E. coli* strains involved in extraintestinal infections are collectively known as extraintestinal pathogenic *E. coli* (ExPEC), as their virulence factor arsenal allows their spread to and multiplication in extraintestinal organs, leading to signs and symptoms mainly in the urinary tract, blood, and meninges (Russo and Johnson, 2000; Vila et al., 2016; Biran and Ron, 2018).

Although clinical outcomes may vary in severity, pathogenic *E. coli* remains a public health concern as they continue to gain novel traits, occasionally resulting in more virulent strains. This Research Topic highlights our growing understanding of the process of host-pathogen interactions as it relates to *E. coli*, addressing the genetic diversity, evolution, antimicrobial resistance, and novel molecular mechanisms and virulence strategies in their interaction with the host in various disease conditions. *E. coli* typing, diagnostic, and potential therapy procedures are also discussed.

NOVEL MECHANISMS OF PATHOGENICITY IN THE *E. COLI* PATHOTYPES

Shiga toxin-producing *E. coli* (STEC) and its subgroup, enterohemorrhagic *E. coli* (EHEC), is one of the most relevant DEC pathotypes. STEC/EHEC strains can cause diarrhea, hemorrhagic colitis in humans, and occasionally lead to hemolytic uremic syndrome (HUS) (Gianantonio et al., 1968; Boyce et al., 2002) and encephalopathy (Obata, 2010), which can be reversible or permanent (Melton-Celsa et al., 2012). STEC colonize the intestines and produce Shiga toxin 1 (Stx1) and/or 2 (Stx2) (Melton-Celsa, 2014), which are released into the intestinal lumen, translocated to the circulatory system, and then bound to their receptor, globotriaosylceramide (Gb3) (Zumbrun et al., 2010), in target cells. However, toxin uptake exhibits both a Gb3-dependent (Sandvig et al., 2002) and a Gb3-independent binding depending on the context (Malyukova et al., 2009; Lukyanenko et al., 2011; In et al., 2013). In this Research Topic, two relevant models, intestinal and microglial cells (MG), are presented to address the pathways of Stx2 uptake. Garimano et al. demonstrate that a hypervirulent O157:H7 STEC strain increases the Stx2 cytotoxic effect by stimulating several endocytic pathways and enhancing Stx2 translocation across HCT-8 monolayers in both the paracellular and transcellular pathways, employing dynamin-independent and Gb3-dependent mechanisms. Berdasco et al. hypothesize that Stx2, either the holotoxin or the Stx2B subunits, exerts a direct biological effect on MG. To determine whether culture conditions affect MG cell sensitivity and responsiveness, they analyze functional parameters; and demonstrated that MG cells exhibit both Gb3-independent and Gb3-canonical pathways for Stx2 uptake and have a pivotal role in the inflammatory processes observed in clinical HUS encephalopathy.

In addition to the production of Stx1, Stx2, and other virulence factors, recent studies revealed that EHEC can produce a type VI secretion system (T6SS) essential to disease development in a murine model (Wan et al., 2017), which has been associated with a higher prevalence of HUS. Vazquez-Lopez and Navarro-Garcia investigate *in silico* the EHEC T6SS core proteins and putative effector and immunity proteins. They compare the corresponding genes between two published genomes of the prototype EHEC O157:H7 strain EDL933 and with the genome of other O157:H7 strains. Unlike other typical T6SS *E. coli* effectors, the authors identify several Rhs family genes (recombination hotspot) (Bondage et al., 2016) in EHEC that could behave as T6SS effectors. These genes could serve as immunity proteins since they have several similar interaction motifs and structural homology with other known immunity proteins.

Of the six classical DEC pathotypes, enteroaggregative (EAEC) and diffusely adherent *E. coli* (DAEC) are the least characterized. To date, not a single DAEC genome and only a few different EAEC genomes have been sequenced. Meza-Segura et al. sequenced the whole genome of ten DAEC and ten typical EAEC strains (positive for the *aggR* gene, which encodes a transcriptional activator of EAEC virulence-associated genes) from diarrheic patients and one commensal *E. coli* strain isolated from a healthy child. They showed that DAEC and typical EAEC are phylogenetically related, but strains of the different pathotypes harbor genes encoding for different sets of virulence factors; DAEC carry more genes encoding for iron acquisition factors, while typical EAEC harbor genes encoding toxins and bacteriocins. Interestingly, the authors identified associations between the clinical characteristics of the diarrheal episode and specific virulence gene profiles in DAEC and typical EAEC.

Dias et al. present an extensive characterization of the typical and atypical EAEC. These authors characterized 220 EAEC isolates obtained from diarrheal patients during seven years (2010-2016) of epidemiological surveillance in Brazil. These isolates were classified into distinct phylogroups, with most isolates assigned to phylogroups A or B1. Interestingly, genes encoding aggregate-forming pili (AFP) were exclusively detected in atypical EAEC, representing a putative novel marker for increasing the efficiency of atypical EAEC diagnosis.

Virulence gene expression is a highly regulated process, mediated by environmental conditions and/or bacterial regulators, which can induce or silence its expression (Kitamoto et al., 2016). Under well-defined environmental conditions, virulence gene expression occurs at a specific site, allowing bacteria to initiate the infection process (Carlson-Banning and Sperandio, 2018). Gut microbiota, or its metabolites, play a fundamental role in regulating pathogenic mechanisms and colonization resistance (Vogt et al., 2015; Rolhion and Chassaing, 2016). In a pilot study, Gallardo et al. determine the composition of gut microbiota and metabolome in stool samples obtained from healthy children and children with diarrhea positive for DEC pathotype. Interestingly, a differential metabolome and microbiota composition was identified between these groups. Additionally, a strong correlation between a gut microbiota species and specific metabolites, such as histamine and L-ornithine, was found in the DEC group; such information might help identify mechanisms and signaling molecules involved in the crosstalk between microbiota and DEC pathotypes.

Besides the production of a variety of virulence factors, uropathogenic *E. coli* (UPEC) strains may produce the vacuolating autotransporter toxin (Vat), which is one of the so-called serine protease autotransporter proteins of the *Enterobacteriaceae* (SPATEs) toxin family (Henderson and Nataro, 2001; Dutta et al., 2002; Nichols et al., 2016). In an urothelium model of bladder cells, Díaz et al. showed that treatment with Vat resulted in time-dependent vacuole formation and loss of the intercellular contacts, leading to changes in the monolayer permeability with a limited amount of cell death. Cellular damage also included cytoskeletal alterations in the urothelium and lamina propria of the bladder and loss of integrity of the urothelium in an experimental *ex vivo* murine bladder model. The Vat-specific targets on the epithelial cell surface or the lamina propria, as well as the composition of the Vat-induced

vacuoles, remain to be determined to elucidate the contribution of this toxin to UPEC pathogenesis.

E. coli and other members of the *Enterobacteriaceae* may produce siderophore-microcins, which are peptides with antimicrobial activity that, by mimicking the iron–siderophore complexes, penetrate and kill phylogenetically related bacteria (Duquesne et al., 2007). Massip and Oswald provide an overview of the recent understanding of the siderophore-Mcc genetic determinants and biosynthesis, their mechanisms of action, and biological relevance in *E. coli*. They also show that the UPEC siderophore-microcin gene clusters and biosynthetic pathways differ from the "archetypal" types of fecal *E. coli* strains. Production of an active siderophore-microcin depends on the synergistic action of proteins encoded in other genomic islands and confers a strong selective advantage to control the colonic niche.

Rueter and Bielaszewska review the exciting topic of outer membrane vesicles (OMVs) production by Gram-negative bacteria, emphasizing intestinal pathogenic *E. coli*. OMVs are nanoscale proteoliposomes secreted from the cell envelope (Amano et al., 2010; Ellis and Kuehn, 2010; Kulp and Kuehn, 2010; O'Donoghue and Krachler, 2016). They represent a highly advanced mechanism for secretion and delivery of bacterial virulence factors into host cells, improving bacterial fitness, and supporting bacterial interactions with polymicrobial communities and the host (Manning and Kuehn, 2011; Duperthuy et al., 2013). OMV production contributes significantly to bacterial virulence since it makes it more able to reach and colonize distant host tissues, impair cell functions, and modulate the host's defenses. Therefore, efforts have been made to exploit the antigenic and adjuvant properties of OMVs as promising vaccine components. However, much knowledge is required to define the immunogenicity and protective efficacy of OMVs and to identify their components involved in the immune responses and mechanisms underlying OMV-elicited protective immunity.

DIAGNOSIS, TYPING, AND GENOMIC EVOLUTION IN THE *E. COLI* PATHOTYPES

Molecular diagnostics is becoming increasingly important to allow detection and diagnosis of pathogens also culture-independently. They are interesting for medical applications and fundamental questions, e.g., regarding the prevalence and ecology of pathogens and food safety (Ramanan et al., 2017; Sekse et al., 2017). For example, the current focus of routine STEC detection is still on the predominant "big seven" serotypes associated with clinical symptoms. Nevertheless, comprehensive diagnostic tests for all clinically relevant STEC serogroups are required. Ludwig et al. took advantage of available genomic sequence information of STEC O antigen-specific genes and developed and validated multiplex PCR (mPCR) assays for the discrimination and detection of 137 "non-big seven" STEC serogroups, which can be associated with cattle. These mPCR assays can, for instance, help to systematically screen the prevalence of STEC in the environment or animals.

Merino et al. applied real-time quantitative PCR (qPCR) to analyze in a culture-independent way the prevalence of bacterial enteropathogens in stool samples of children below seven years with and without diarrhea in São Paulo, Brazil. They detected the tested enteropathogens' virulence markers significantly more frequently in stool samples from diarrhea cases than asymptomatic controls. Also, the relevant marker copy number was significantly higher in diarrheal patients than in stool from asymptomatic children. This analysis demonstrates that asymptomatic children of an urban area, such as São Paulo, may be a reservoir of enteropathogens.

Michelacci et al. analyzed whole-genome sequences of highly virulent enteroinvasive *E. coli* (EIEC) O96:H19 isolates. Sequence comparison of the EIEC virulence plasmid indicated that IS element-mediated recombination might be responsible for the absence of the conjugation determinant in most EIEC and Shigella virulence plasmids. The authors hypothesize that the acquisition of virulence plasmids *via* conjugation led to the evolution of EIEC from non-pathogenic *E. coli* and may promote the establishment of new virulent EIEC clones.

Flament-Simon et al. studied the epidemiological differences of 188 extended spectrum beta-lactamase (ESBL)-producing extraintestinal pathogenic *E. coli* isolates from two hospitals in Spain and France. Although these isolates were markedly diverse, most of them belonged to only three clonal complexes. The new globally emerging clone ST1193 was identified in two isolates from France and Spain in 2015.

E. coli is characterized by high genomic plasticity and frequent exchange of genetic material. Thus, unambiguous typing of clinical isolates may be complicated due to the existence of hybrid strains combining different pathotypes' traits. Comparative genomics is, therefore, instrumental in understanding pheno- and genotypic variability among clinical isolates. Valiatti et al. characterized geno- and phenotypically uropathogenic *E. coli* isolate 252 (UPEC 252) and demonstrated that this strain represents an atypical enteropathogenic *E. coli* (EPEC) strain. The ability to grow in human blood serum and adhere to human epithelial cell lines of the urinary and intestinal tract enables UPEC 252 to cause intestinal and extraintestinal infections.

HYBRID- AND HETERO-PATHOGENIC *E. COLI* STRAINS

It has been reported that certain pathogenic *E. coli* strains combine different pathotypes' main virulence traits, encompassing potentially more virulent hybrid strains (Dobrindt et al., 2003; Bielaszewska et al., 2007; Khan et al., 2018). The terms hybrid- and hetero-pathogenic *E. coli* were created to depict new combinations of virulence factors among classic *E. coli* pathotypes. Two mini-reviews on this topic can be appreciated in this Research Topic. Santos et al. review the studies that introduced the hybrid- and hetero-pathogenic *E. coli* classifications, emphasizing the *E. coli* genomic plasticity that

emerged in mixed pathotypes exhibiting unique pathogenic mechanisms. The potential of such hybrid strains to emerge in new and severe outbreaks and their potential implication in more severe diseases are also discussed. Braz et al. add an important topic to this discussion, i.e., the increasing acquisition of antimicrobial resistance by *E. coli* strains. The consequences related to this genetically versatile species are the growing need to develop unconventional therapies and more precise diagnostic methods to combat the infections caused by these hybrid strains.

NOVEL PROCEDURES FOR DEC INFECTIONS THERAPY

Gut microbiota has been associated with resistance to pathogen colonization in the intestine. Several molecules have been proven to modify the composition of the gut microbiota (Pamer, 2016; Jacobson et al., 2018). Liu et al. investigated the changes in gut microbiota induced by *Pulsatilla decoction* (PD), a traditional Chinese medicinal herb used to treat fever and dysentery, which also has a good curative effect on bacterial diarrhea and inflammatory bowel disease. The authors studied changes in gut microbiota after PD therapy of *E. coli* infection in rats and found that PD helped restore *Bacteroidetes* spp. composition in the gut. These findings might be essential to determine the mechanism of the Chinese herbal formula for preventing and treating bacterial infections.

The use of antibiotics to treat STEC infections has long been controversial due to reports that such treatments may increase Shiga toxin secretion (Wong et al., 2000); currently, the recommended therapy is mainly supportive. Mühlen and Dersch reviewed the current understanding and progress in developing treatment options against STEC infections. In recent years, several strategies have progressed to the clinical trial stages. Receptor analogs such as Synsorb Pk, or the use of Eculizumab looked promising in phase II trials but showed little evidence of success when evaluated systematically or in phase III trials (Trachtman et al., 2003; Monet-Didailler et al., 2019). On the other hand, a prophylactic vaccine may only be of interest for countries where these infections are endemic. In general, phase II clinical trials can be carried out, but patients with STEC infections for phase III trials are limited.

CONCLUSIONS

The recent progression of genome sequencing techniques allowed identifying novel virulence factors that enable *E. coli* strains to harm the human host. The *E. coli* genetic plasticity favors the emergence and spread of virulence traits and antimicrobial resistance, resulting in novel virulent variants. These isolates include the so-called hybrid- and hetero-pathogenic strains, which exceed the borders currently established in defining the different *E. coli* pathotypes and represent an emerging threat that challenges the development of novel diagnosis and typing methods. Knowing the different virulence strategies employed by *E. coli* in its interaction with the host in various disease conditions reveals potential new targets for disease prevention and treatment.

AUTHOR CONTRIBUTIONS

All authors listed have made a substantial, direct, and intellectual contribution to the work, and approved it for publication. All authors contributed to the article and approved the submitted version.

ACKNOWLEDGMENTS

The editors thank all the contributors to this issue.

REFERENCES

Amano, A., Takeuchi, H., and Furuta, N. (2010). Outer membrane vesicles function as offensive weapons in host-parasite interactions. *Microbes Infect.* 12, 791–798. doi: 10.1016/j.micinf.2010.05.008

Bielaszewska, M., Dobrindt, U., Gärtner, J., Gallitz, I., Hacker, J., Karch, J., et al. (2007). Aspects of genome plasticity in pathogenic *Escherichia coli*. *Int. J. Med. Microbiol.* 297 (7-8), 625–639. doi: 10.1016/j.ijmm.2007.03.001

Biran, D., and Ron, E. Z. (2018). Extraintestinal Pathogenic *Escherichia coli*. *Curr. Top. Microbiol. Immunol.* 416, 149–161. doi: 10.1007/82_2018_108

Bondage, D. D., Lin, J.-S., Ma, L.-S., Kuo, C.-H., and Lai, E.-M. (2016). VgrG C-terminus confers the type VI effector transport specificity and is required for binding with PAAR and adaptor-effector complex. *Proc. Natl. Acad. Sci. U. S. A.* 113, E3931–E3940. doi: 10.1073/pnas.1600428113

Boyce, T. G., Swerdlow, D. L., and Griffin, P. M. (2002). *Escherichia coli* O157:H7 and the hemolytic–uremic syndrome. *N. Engl. J. Med.* 333, 364–368. doi: 10.1056/NEJM199508103330608

Carlson-Banning, K. M., and Sperandio, V. (2018). Enterohemorrhagic *Escherichia coli* outwits hosts through sensing small molecules. *Curr. Opin. Microbiol.* 41, 83–88. doi: 10.1016/j.mib.2017.12.002

Croxen, M. A., and Finlay, B. B. (2010). Molecular mechanisms of *Escherichia coli* pathogenicity. *Nat. Rev. Microbiol.* 8, 26–38. doi: 10.1038/nrmicro2265

Dobrindt, U., Agerer, F., Michaelis, K., Janka, A., Buchrieser, C., Samuelson, M., et al. (2003). Analysis of genome plasticity in pathogenic and commensal *Escherichia coli* isolates by use of DNA arrays. *J. Bacteriol.* 185 (6), 1831–1840. doi: 10.1128/jb.185.6.1831-1840.2003

Dobrindt, U., Hochhut, B., Hentschel, U., and Hacker, J. (2004). Genomic islands in pathogenic and environmental microorganisms. *Nat. Rev. Microbiol.* 2 (5), 414–424. doi: 10.1038/nrmicro884

Duperthuy, M., Sjöström, A. E., Sabharwal, D., Damghani, F., Uhlin, B. E., and Wai, S. N. (2013). Role of the *Vibrio cholerae* matrix protein Bap1 in cross-resistance to antimicrobial peptides. *PLoS Pathog.* 9, e1003620. doi: 10.1371/journal.ppat.1003620

Duquesne, S., Destoumieux-Garzón, D., Peduzzi, J., and Rebuffat, S. (2007). Microcins, gene-encoded antibacterial peptides from enterobacteria. *Nat. Prod. Rep.* 24, 708–734. doi: 10.1039/b516237h

Dutta, P. R., Cappello, R., Navarro-García, F., and Nataro, J. P. (2002). Functional comparison of serine protease autotransporters of Enterobacteriaceae. *Infect. Immun.* 70, 7105–7113. doi: 10.1128/iai.70.12.7105-7113.2002

Ellis, T. N., and Kuehn, M. J. (2010). Virulence and immunomodulatory roles of bacterial outer membrane vesicles. *Microbiol. Mol. Biol. Rev.* 74, 81–94. doi: 10.1128/MMBR.00031-09

Gianantonio, C. A., Vitacco, M., Mendilaharzu, F., and Gallo, G. (1968). The hemolytic-uremic syndrome. Renal status of 76 patients at long-term follow-up. *J. Pediatr.* 72, 757–765. doi: 10.1016/S0022-3476(68)80427-5

Gomes, T. A. T., Elias, W. P., Scaletsky, I. C., Guth, B. E., Rodrigues, J. F., Piazza, R. M., et al. (2016). Diarrheagenic *Escherichia coli*. *Braz. J. Microbiol.* 47 (Suppl 1), 3–30. doi: 10.1016/j.bjm.2016.10.015

Henderson, I., and Nataro, J. (2001). Virulence functions of autotransporter proteins. *Infect. Immun.* 69, 1231–1243. doi: 10.1128/IAI.69.3.1231-1243.2001

In, J., Lukyanenko, V., Foulke-Abel, J., Hubbard, A. L., Delannoy, M., Hansen, A. M., et al. (2013). Serine Protease EspP from enterohemorrhagic *Escherichia coli* is sufficient to induce Shiga toxin macropinocytosis in intestinal epithelium. *PLoS One* 8, e69196. doi: 10.1371/journal.pone.0069196

Jacobson, A., Lam, L., Rajendram, M., Tamburini, F., Honeycutt, J., Pham, T., et al. (2018). A Gut Commensal-Produced Metabolite Mediates Colonization Resistance to *Salmonella* Infection. *Cell Host Microbe* 24 (2), 296–307.e7. doi: 10.1016/j.chom.2018.07.002

Jesser, K. J., and Levy, K. (2020). Updates on defining and detecting diarrheagenic *Escherichia coli* pathotypes. *Curr. Opin. Infect. Dis.* 33 (5), 372–380. doi: 10.1097/QCO.0000000000000665

Johnson, J. R., and Russo, T. A. (2018). Molecular epidemiology of extraintestinal pathogenic *Escherichia coli*. *EcoSal Plus* 8, Q13. doi: 10.1128/ecosalplus.ESP-0004-2017

Kaper, J. B., Nataro, J. P., and Mobley, H. L. T. (2004). Pathogenic *Escherichia coli*. *Nat. Rev. Microbiol.* 2, 123–140. doi: 10.1038/nrmicro818

Khan, A., Miller, W. R., and Arias, C. A. (2018). Mechanisms of antimicrobial resistance among hospital-associated pathogens. *Expert Rev. Anti Infect. Ther.* 16 (4), 269–287. doi: 10.1080/14787210.2018.1456919

Kitamoto, S., Nagao-Kitamoto, H., Kuffa, P., and Kamada, N. (2016). Regulation of virulence: the rise and fall of gastrointestinal pathogens. *J. Gastroenterol.* 51, 195–205. doi: 10.1007/s00535-015-1141-5

Kulp, A., and Kuehn, M. J. (2010). Biological functions and biogenesis of secreted bacterial outer membrane vesicles. *Annu. Rev. Microbiol.* 64, 163–184. doi: 10.1146/annurev.micro.091208.073413

Leimbach, A., Hacker, J., and Dobrindt, U. (2013). *E. coli* as an all-rounder: The thin line between commensalism and pathogenicity. *Curr. Top. Microbiol. Immunol.* 358, 3–32. doi: 10.1007/82_2012_303

Lukyanenko, V., Malyukova, I., Hubbard, A., Delannoy, M., Boedeker, E., Zhu, C., et al. (2011). Enterohemorrhagic *Escherichia coli* infection stimulates Shiga toxin 1 macropinocytosis and transcytosis across intestinal epithelial cells. *Am. J. Physiol. Physiol.* 301, C1140–C1149. doi: 10.1152/ajpcell.00036.2011

Malyukova, I., Murray, K. F., Zhu, C., Boedeker, E., Kane, A., Patterson, K., et al. (2009). Macropinocytosis in Shiga toxin 1 uptake by human intestinal epithelial cells and transcellular transcytosis. *Am. J. Physiol. - Gastrointest. Liver Physiol.* 296, 78–92. doi: 10.1152/ajpgi.90347.2008

Manning, A. J., and Kuehn, M. J. (2011). Contribution of bacterial outer membrane vesicles to innate bacterial defense. *BMC Microbiol.* 11:258. doi: 10.1186/1471-2180-11-258

Melton-Celsa, A., Mohawk, K., Teel, L., and O'Brien, A. (2012). Pathogenesis of Shiga-toxin producing *Escherichia coli*. *Curr. Top. Microbiol. Immunol.* 357, 367–103. doi: 10.1007/82_2011_176

Melton-Celsa, A. R. (2014). Shiga toxin (Stx) classification, structure, and function. *Microbiol. Spectr.* 2, 1–21. doi: 10.1128/microbiolspec.EHEC-0024-2013

Monet-Didailler, C., Chevallier, A., Godron-Dubrasquet, A., Allard, L., Delmas, Y., Contin-Bordes, C., et al. (2019). Outcome of children with shiga toxin associated haemolytic uraemic syndrome treated with eculizumab: a matched cohort study. *Nephrol. Dial. Transplant.* 14:gfz158. doi: 10.1093/ndt/gfz158

Nichols, K., Totsika, M., Moriel, D., Lo, A., Yang, J., Wurpel, D., et al. (2016). Molecular characterization of the vacuolating autotransporter toxin in uropathogenic *Escherichia coli*. *J. Bacteriol.* 198, 1487–1498. doi: 10.1128/JB.00791-15

Obata, F. (2010). Influence of *Escherichia coli* Shiga toxin on the mammalian central nervous system. *Adv. Appl. Microbiol.* 71, 1–19. doi: 10.1016/S0065-2164(10)71001-7

O'Donoghue, E. J., and Krachler, A. M. (2016). Mechanisms of outer membrane vesicle entry into host cells. *Cell. Microbiol.* 18, 1508–1517. doi: 10.1111/cmi.12655

Pamer, E. G. (2016). Resurrecting the intestinal microbiota to combat antibiotic-resistant pathogens. *Science* 352 (6285), 535–538. doi: 10.1126/science.aad9382

Ramanan, P., Bryson, A. L., Binnicker, M. J., Pritt, B. S., and Patel, R. (2017). Syndromic Panel-Based Testing in Clinical Microbiology. *Clin. Microbiol. Rev.* 31 (1), e00024–e00017. doi: 10.1128/CMR.00024-17

Rolhion, N., and Chassaing, B. (2016). When pathogenic bacteria meet the intestinal microbiota. *Philos. Trans. R. Soc Lond. B. Biol. Sci.* 371, 20150504. doi: 10.1098/rstb.2015.0504

Russo, T. A., and Johnson, J. R. (2000). Proposal for a new inclusive designation for extraintestinal pathogenic isolates of *Escherichia coli*: ExPEC. *J. Infect. Dis.* 181, 1753–1754. doi: 10.1086/315418

Sandvig, K., Grimmer, S., Lauvrak, S., Torgersen, M., Skretting, G., Van Deurs, B., et al. (2002). Pathways followed by ricin and Shiga toxin into cells. *Histochem. Cell Biol.* 117, 131–141. doi: 10.1007/s00418-001-0346-2

Sekse, C., Holst-Jensen, A., Dobrindt, U., Johannessen, G. S., Li, W., Spilsberg, B., et al. (2017). High Throughput Sequencing for Detection of Foodborne Pathogens. *Front. Microbiol.* 8:2029. doi: 10.3389/fmicb.2017.02029

Trachtman, H., Cnaan, A., Christen, E., Gibbs, K., Zhao, S., Acheson, D. W., et al. (2003). Effect of an oral Shiga toxin-binding agent on diarrhea-associated hemolytic uremic syndrome in children: a randomized controlled trial. *JAMA* 290, 1337–1344. doi: 10.1001/jama.290.10.1337

Vila, J., Sáez-López, E., Johnson, J. R., Römling, U., Dobrindt, U., Cantón, R., et al. (2016). *Escherichia coli*: an old friend with new tidings. *FEMS Microbiol. Rev.* 40 (4), 437–463. doi: 10.1093/femsre/fuw005

Vogt, S. L., Pena-Diaz, J., and Finlay, B. B. (2015). Chemical communication in the gut: effects of microbiota-generated metabolites on gastrointestinal bacterial pathogens. *Anaerobe* 34, 106–115. doi: 10.1016/j.anaerobe.2015.05.002

Wan, B., Zhang, Q., Ni, J., Li, S., Wen, D., Li, J., et al. (2017). Type VI secretion system contributes to Enterohemorrhagic *Escherichia coli* virulence by secreting catalase against host reactive oxygen species (ROS). *PLoS Pathog.* 13, e1006246. doi: 10.1371/journal.ppat.1006246

Wong, C. S., Jelacic, S., Habeeb, R. L., Watkins, S. L., and Tarr, P. I. (2000). The risk of the hemolytic-uremic syndrome after antibiotic treatment of *Escherichia coli* O157: H7 infections. *N. Engl. J. Med.* 342, 1930–1936. doi: 10.1056/NEJM200006293422601

Zumbrun, S. D., Hanson, L., Sinclair, J. F., Freedy, J., Melton-Celsa, A. R., Rodriguez-Canales, J., et al. (2010). Human intestinal tissue and cultured colonic cells contain globotriaosylceramide synthase mRNA and the alternate Shiga toxin receptor globotetraosylceramide. *Infect. Immun.* 78, 4488–4499. doi: 10.1128/IAI.00620-10

Conflict of Interest: The authors declare that the research was conducted in the absence of any commercial or financial relationships that could be construed as a potential conflict of interest.

frontiers in Cellular and Infection Microbiology

ORIGINAL RESEARCH
published: 21 November 2019
doi: 10.3389/fcimb.2019.00396

Endocytosis, Cytotoxicity, and Translocation of Shiga Toxin-2 Are Stimulated by Infection of Human Intestinal (HCT-8) Monolayers With an Hypervirulent *E. coli* O157:H7 Lacking *stx2* Gene

*Nicolás Garimano, María Marta Amaral and Cristina Ibarra**

Laboratorio de Fisiopatogenia, Departamento de Fisiología, Facultad de Medicina, Instituto de Fisiología y Biofísica Bernardo Houssay (IFIBIO Houssay-CONICET), Universidad de Buenos Aires, Buenos Aires, Argentina

OPEN ACCESS

Edited by:
Roxane M. Piazza, Butantan Institute, Brazil

Reviewed by:
Dakshina Jandhyala, University of Houston, United States
Azucena Mora Gutiérrez, University of Santiago de Compostela, Spain

***Correspondence:**
Cristina Ibarra
ibarra@fmed.uba.ar

Specialty section:
This article was submitted to Molecular Bacterial Pathogenesis, a section of the journal Frontiers in Cellular and Infection Microbiology

Received: *27 August 2019*
Accepted: *05 November 2019*
Published: *21 November 2019*

Citation:
Garimano N, Amaral MM and Ibarra C (2019) Endocytosis, Cytotoxicity, and Translocation of Shiga Toxin-2 Are Stimulated by Infection of Human Intestinal (HCT-8) Monolayers With an Hypervirulent E. coli O157:H7 Lacking stx2 Gene. Front. Cell. Infect. Microbiol. 9:396. doi: 10.3389/fcimb.2019.00396

Shiga toxin-producing *Escherichia coli* (STEC) strains are responsible for multiple clinical syndromes, including hemolytic uremic syndrome (HUS). *E. coli* O157:H7 is the most prevalent serotype associated with HUS and produces a variety of virulence factors being Stx2 the responsible of the most HUS severe cases. After intestinal colonization by STEC, Stx2 is released into the intestinal lumen, translocated to the circulatory system and then binds to its receptor, globotriaosylceramide (Gb3), in target cells. Thus, Stx2 passage through the colonic epithelial barrier is a key step in order to produce disease, being its mechanisms still poorly understood. We have previously reported that STEC interaction with the human colonic mucosa enhanced Stx2 production. In the present work, we have demonstrated that infection with O157:H7Δstx2, a mutant unable to produce Stx2, enhanced either Stx2 cytotoxicity on an intestinal cell line (HCT-8), or translocation across HCT-8 monolayers. Moreover, we found that translocation was enhanced by both paracellular and transcellular pathways. Using specific endocytosis inhibitors, we have further demonstrated that the main mechanisms implicated on Stx2 endocytosis and translocation, either when O157:H7Δstx2 was present or not, were Gb3-dependent, but dynamin-independent. On the other hand, dynamin dependent endocytosis and macropinocytosis became more relevant only when O157:H7Δstx2 infection was present. Overall, this study highlights the effects of STEC infection on the intestinal epithelial cell host and the mechanisms underlying Stx2 endocytosis, cytotoxic activity and translocation, in the aim of finding new tools toward a therapeutic approach.

Keywords: shiga toxin, HCT-8, STEC, O157, endocytosis, cytotoxicity, transcytosis, translocation

INTRODUCTION

Shiga toxin-producing *Escherichia coli* (STEC) strains are responsible for multiple clinical syndromes including bloody diarrhea, hemorrhagic colitis, and hemolytic uremic syndrome (HUS) (Karmali et al., 1985). HUS is a systemic disease that can be fatal and is developed several days after STEC infection in up to 15% of children infected (Tarr et al., 2005).

HUS is characterized by thrombotic microangiopathy, hemolytic anemia, thrombocytopenia, and acute renal failure (Gianantonio et al., 1968; Boyce et al., 2002). STEC are usually carried by cattle and bacterial ingestion frequently occurs via contaminated undercooked meat, unpasteurized dairy products, contaminated fruits, vegetables and water, and through animal to person or person to person contact (Ferens and Hovde, 2011). *E. coli* O157:H7 is the most prevalent serotype associated with HUS although multiple serotypes of STEC, including O157:NM strains and non-O157 serotypes such as O26:H11, O103:H2, O111:NM, O121:H19, and O145:NM have been associated with hemorrhagic colitis cases (Karmali et al., 2003). Some STEC strains commonly associated with serious disease possess a chromosomal pathogenicity island known as the locus of enterocyte effacement (LEE) (Nataro and Kaper, 1998), though LEE-negative strains which encode additional virulence, and colonization factors have also been associated with severe disease (Newton et al., 2009; Beutin and Martin, 2012; McWilliams and Torres, 2014). The genes encoded in the LEE are responsible for intimate adhesion of STEC to colonic epithelial cells (McWilliams and Torres, 2014), which is followed by injection of bacterial effector proteins into the host cell through a type III secretion system (T3SS) (Jerse et al., 1990). These effector proteins produce attaching and effacing (A/E) lesions on intestinal cells and interfere with host cells in many ways, inducing a profound rearrangement of cell cytoskeleton, and a loss of tight junction and membrane integrity (Knutton et al., 1989; Holmes et al., 2010; Ugalde-Silva et al., 2016). Additionally, STEC can produce either Stx1 and/or Stx2 prototypes, for which both have multiple subtypes (Melton-Celsa, 2014). Stx2 is widely recognized as the most important virulence factor of *E. coli* O157:H7 responsible for HUS (Palermo et al., 2009). This toxin is an AB5 toxin composed of an A subunit (Stx2A) and five B subunits (Stx2B). Stx2A possesses a N-glycosidase activity against 28S rRNA of 60S ribosomes in the cytosol. This activity results in an inhibition of protein synthesis in eukaryotic cells and activation of a proinflammatory signaling cascade known as the ribotoxic stress response, which is also involved in apoptosis induction (Smith et al., 2003).

On the other hand, Stx2B is arranged as pentamers of identical composition and has high affinity to the cell surface, glucosylceramide derived glycolipids, globotriaosylceramide (Gb3) and globotetraosylceramide (Gb4), though it has been found that only Gb3 may act as a functional receptor (Zumbrun et al., 2010). These glycolipids are generally located in cholesterol-rich cell membrane microdomains denominated lipid rafts (Hanashima et al., 2008; Legros et al., 2018) and are associated with toxin entry into target cells. Stx2 internalization has been shown to occur in two ways, one requiring specific binding of Stx2 to Gb3 receptor (Sandvig et al., 2002) and an unspecific macropinocytic pathway (Malyukova et al., 2009; Lukyanenko et al., 2011; In et al., 2013). Gb3 availability and microdomain location (Betz et al., 2011) and actin organization (Gaus et al., 2010) have been found to play a central role on Stx internalization. These factors are relevant on the mechanisms preceding endocytosis, as they impact clustering of Stx-Gb3 complexes on the cell membrane (Pezeshkian et al., 2017) and its capacity to ultimately form tubular invaginations prior to toxin internalization (Römer et al., 2007). The last step required for toxin internalization is vesicular scission, which has been found to occur via clathrin and dynamin (Lauvrak, 2004), dynamin only (Römer et al., 2007), and/or actin and cholesterol (Gaus et al., 2010) dependent mechanisms.

Several mechanisms for toxin translocation across intestinal epithelium have been proposed. Non-Gb3 associated translocation has been found to occur via the paracellular pathway, stimulated by neutrophil transmigration and actin rearrangements during STEC infection (Hurley et al., 2001), but also via the transcellular pathway, implicating an unspecific macropinocytic mechanism that does not involve the Gb3 receptor (Lukyanenko et al., 2011). There is also evidence that Stx2 transcellular transcytosis may be due to Gb3-linked Stx2 endocytosis, as it was described that a percentage of apical recycling endosomes containing Stx2 are released on the basolateral side (Müller et al., 2017), although Gb3 presence on colonic epithelium is still under debate (Schüller et al., 2004; Zumbrun et al., 2010). Previous studies have described that these routes can be selectively and efficiently inhibited (Macia et al., 2006; Huang et al., 2010; Koivusalo et al., 2010; Dutta and Donaldson, 2012; Shayman, 2013; Kaissarian et al., 2018), even though their particular relevance to Stx2 endocytosis and translocation is still unclear.

In vitro studies using human intestinal epithelial cell lines have demonstrated that epithelial cell infection with STEC may lead to enhanced Stx2 translocation depending on the strain virulence profile (Tran et al., 2018). In turn, intestinal epithelial cell-derived molecules could also modify STEC virulence by increasing adhesion and upregulating virulent genetic profiles (Bansal et al., 2013). In our previous work, we investigated the effect of *E. coli* O157:H7 expressing Stx2 on human colonic mucosa and showed that bacterial interaction with colonic epithelium enhanced Stx2 production that, in turn, caused a marked inhibition of water absorption concomitant with histological damages on the surface epithelium (Albanese et al., 2015). In this study, we analyze the effects of *E. coli* O157:H7Δstx2 infection on Stx2 cytotoxic effects, endocytosis and translocation across polarized HCT-8 cells, which express Gb3 and Gb4 receptors (Kouzel et al., 2017). To this aim, we used specific endocytosis inhibitors, in order to demonstrate which pathways are stimulated upon infection, providing an *in vitro* basis to further develop therapeutic targets.

MATERIALS AND METHODS

Materials

Purified Stx2a was provided from Phoenix Laboratory (Tufts Medical Center, Boston, MA, USA). Eliglustat (Cerdelga, Sanofis-Genzyme) used as an inhibitor of glucosylceramide synthase (Shayman, 2013) was purchased from MedKoo Biosci, Morrisville, USA. Dynasore, a specific dynamin-mediated endocytic inhibitor (Macia et al., 2006), Methyl-β-cyclodextrin (MβCD), a membrane cholesterol extractor (Zidovetzki and Levitan, 2007), and Amiloride hydrochloride, a macropinocytosis inhibitor (Koivusalo et al., 2010) were purchased from Sigma Aldrich, St. Louis, MO, USA. A fluorescein isothiocyanate

(FITC)-labeled Dextran (average molecular weight of 70 kDa, Sigma Aldrich, catalog # 46945) was used as a marker of paracellular permeability (Chattopadhyay et al., 2017). A mouse monoclonal antibody against the A-subunit of Stx2 (Mab 2E11) was provided by Roxane Piazza (Butantan Institute, São Paulo, SP, Brazil) (Rocha et al., 2012) and an Alexa 647-conjugated anti-mouse secondary antibody (AbCam, catalog #ab150115) were used for flow cytometry.

Bacterial Strains and Growth Conditions

E. coli O157:H7 strain 125/99 wild type (O157:H7) isolated from a patient with HUS has been previously described (Rivas et al., 2006). A mutant lacking *stx2* gene from the parenteral *E. coli* O157:H7 strain 125/99wt (O157:H7Δstx2) was previously obtained (Albanese et al., 2015). O157:H7Δstx2 was grown in Luria Broth medium for 18 h at 37°C with shaking at 150 rpm and then diluted 1/10 in DMEM/F12 medium (Sigma Aldrich, USA) with the addition of HEPES 10 mM and grown to exponential phase ($OD_{600} = 0.3–0.4$) at 37°C with shaking at 150 rpm. O157:H7Δstx2 density corresponded to $\sim 4 \times 10^9$ colony-forming units per ml (CFU/ml). O157:H7Δstx2 supernatant (SN O157:H7) was collected after centrifugation at 10,000 g for 5 min, followed by filtration through a 0.22-μm filter (Millipore, Billerica, MA, USA).

Cell Cultures

The human intestinal cell line HCT-8 (ATCC CCL-244, Manassas, VA, USA) was maintained in RPMI-1640 medium (ATCC) and the monkey kidney cell line Vero (ATCC CCL-81) was grown in DMEM/F12 (Sigma Aldrich, St. Louis, MO USA). Both media were supplemented with 10% fetal bovine serum (FBS, Internegocios S.A., Buenos Aires, Argentina), 100 U/ml penicillin and 100 μg/ml streptomycin. Additionally, 1 mM L-glutamine, 10 mM sodium pyruvate, 10 mM HEPES, 10 mM glucose were also supplemented in HCT-8 cultures. Cells were grown at 37°C in a humidified 5% CO_2 incubator. Cells were subcultured after 80% confluence was reached (7–10 days) in antibiotic-free medium. During experiments, HCT-8 cells were maintained in growth-arrested conditions (medium without FBS).

Cytotoxicity and Neutralization Assay on HCT-8 Cells

Purified Stx2 and O157:H7Δstx2 induced cytotoxicity were assayed on HCT-8 cells cultured on fixed support. Briefly, HCT-8 cells monolayers grown on 96-well plates were treated for 4 h under growth-arrested conditions (Culture media without FBS) and antibiotic free conditions with 100 ng/ml Stx2 and/or 4×10^8 CFU/ml O157:H7Δstx2. In selected experiments, cells were preincubated with Eliglustat (200 nM, 48 h Kaissarian et al., 2018), Dynasore (80 μM, 30 min), MβCD (4 mM, 30 min), or Amiloride (1 mM, 30 min) and washed twice with PBS before treatment. At the end of the incubation time, plates were washed twice with PBS (145 mM NaCl, 10 mM NaH_2PO_4, pH 7.2) and subsequently incubated in growth-arrested media for 72 h. Then, cell viability was assayed by neutral red uptake (Repetto et al., 2008).

Cytotoxic activity neutralization was calculated using the following equation.

$$Cytotoxic\ Activity\ Neutralization = 100 * \frac{I - T}{100 - T} \quad (1)$$

In this Equation, I and T are % cell viability of HCT-8 cells pre-treated or not with endocytosis inhibitors respectively.

Neutral Red Uptake Assay

Neutral red uptake assay was performed as previously described, with minor modifications (Repetto et al., 2008). After treatment, cells were washed twice with PBS (145 mM NaCl, 10 mM NaH_2PO_4, pH 7.2) and incubated for 2 h with freshly diluted neutral red in PBS to a final concentration of 50 μg/ml. Cells were then washed with 1% $CaCl_2$ and 4% formaldehyde twice and were then solubilized in 1% acetic acid and 50% ethanol. Absorbance at 546 nm was read in an automated plate spectrophotometer. Results were expressed as percent viability, with 100% represented by cells incubated under identical conditions but without treatment. The 50% cytotoxic dose (CD_{50}) corresponded to the dilution required to kill 50% of the cells.

Cell Monolayer Culture

HCT-8 were seeded on Milicell culture inserts (PIHP01250, Millipore, Billerica, MA, USA) of 12 mm diameter and 0.4 um pore size (filter area: 1.13 cm) placed on a 24-well plate and grown for about 7–10 days as previously described until a continuous monolayer was achieved. The development of monolayers was monitored with the electrical resistance (TEER) measured with a Millicell-ERS electric resistance system (Millipore, Billerica, MA, USA) until TEER values were stable for 2 consecutive days and higher than 1,200 $\Omega.cm^2$, which is consistent with cell polarization (Hurley et al., 1999).

Translocation Assays

Briefly, after HCT-8 cell monolayer formation, complete medium was removed from upper (apical) and lower (basolateral) chambers and replaced with growth-arrested and antibiotic free medium. Apical side of the HCT-8 cells were exposed to Stx2 (100 ng/ml) in the absence or presence of O157:H7Δstx2 (4×10^8 CFU/ml), its filtered supernatant SN-O157:H7Δstx2 (1:10 diluted) or EDTA (10 mM) as a tight junction disruptor for 4 h at 37°C in 5% CO_2 atmosphere. Following the incubation period, the media from the lower chamber was filter-sterilized to determine Stx2 concentration by Vero cell cytotoxic assays. In selected experiments, cells were preincubated with Eliglustat (200 nM, 48 h), Dynasore (80 μM, 30 min), MβCD (4 mM, 30 min), or Amiloride (1 mM, 30 min) and washed twice with PBS before treatments were applied.

Stx2 Quantification by Vero Cell Cytotoxicity Assay

Vero cells grown in 96-well culture plate until confluence were treated in serum-free medium for 24 h with different concentrations of purified Stx2 or different dilutions of experimental samples. At the end of the incubation, cell viability

was analyzed by neutral red uptake. Stx2 concentrations were calculated from Stx2 standard curves. When the cytotoxic effect elicited by filter-sterilized SN from O157:H7 grown to exponential phase was compared to a purified Stx2 curve used as standard, the average cytotoxicity of the filtered SN was equivalent to 100 ± 6 ng/ml Stx2 (data not shown).

Paracellular Permeability

Paracellular permeability in HCT-8 monolayers was determined by measuring FITC-Dextran passage from the apical- to basolateral side of monolayers, taking into account that Dextran (MW 70 kDa) cannot penetrate the cellular membrane under physiological conditions being its molecular weight similar to Stx2 (Hashida et al., 1986; Balda et al., 1996; Matter and Balda, 2003). FITC-Dextran was measured according to methods described previously with some modifications (Balda et al., 1996). FITC-Dextran (1 mg/ml) was added on the upper (apical) chamber at the beginning of each experiment. Following the incubation period, 100 µl of media from the upper (apical) and lower (basolateral) chamber collected separately were placed in a 96-well plate and the concentration of FITC-Dextran was measured on a fluorescence multiplate reader (FLUOstar Omega, excitation, 486 nm; emission, 520 nm). Relative fluorescence was then calculated as a ratio between lower (basolateral) chamber fluorescence and total fluorescence. Sample readings were performed in triplicate.

Adhesion of O157:H7Δstx2 to HCT-8 Cells

HCT-8 cells were grown on 24-wells plates until a confluent monolayer was achieved. Monolayers were pretreated with Eliglustat (200 nM, 48 h), Dynasore (80 µM, 30 min), MβCD (4 mM, 30 min), or Amiloride (1 mM, 30 min), washed twice with PBS and then treated for 4 h with 4×10^8 CFU/ml O157:H7Δstx2 in the presence of 100 ng/ml Stx2. To count CFU number, cells were washed 5 times with PBS to remove non-attached bacteria and lysed using 0.2% Triton-PBS solution for 30 min. Serial dilutions of these suspensions were spread on LB-agar coated Petri dishes and incubated at 37°C for 24 h for optical counting.

Stx2 Flow Cytometry Detection

The presence of intracellular and extracellular Stx2 in HCT-8 cells pre-incubated with endocytic inhibitors was evaluated in HCT-8 cells by flow cytometry. For that purpose, cells were fixed after treatment in 0.5% paraformaldehyde, and for intracellular staining, permeabilized with saponin 0.1% in phosphate-buffered saline (PBS). Then, cells were incubated in PBS 0.5% FBS with Mab 2E11 for 2 h, followed by a 1 h incubation with an Alexa 647-conjugated anti-mouse secondary antibody for 1 h. Cells were subsequently washed and resuspended in PBS. The staining was analyzed by flow cytometry on PARTEC PAS III using Cyflogic software 1.2.1. Results are expressed as percentage of Stx2 positive events and median intensity of fluorescence (MIF) in cells treated compared to cells not pre-treated with inhibitors.

Statistical Analysis

Cytotoxicity curves were fitted using linear or logarithmic regression. Statistical significance for all assays was assessed using one-way ANOVA with Tukey's or Bonferroni's multiple comparison test or Student's *t*-test. Analysis was performed using Graphpad Prism v6.01 software. Statistical significance was set at $^*p < 0.05$.

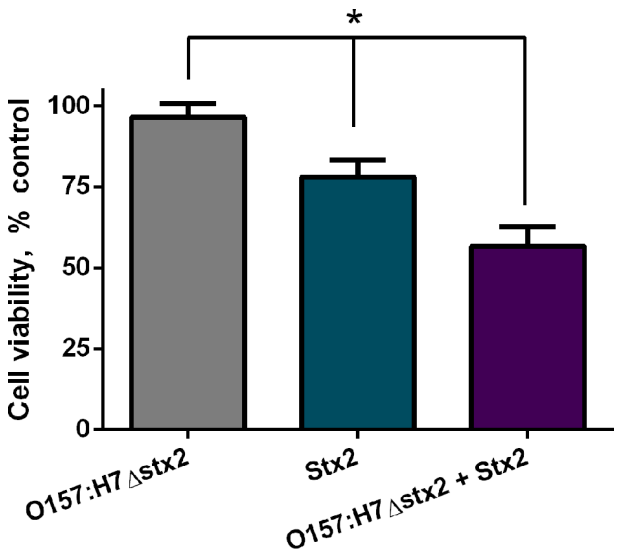

FIGURE 1 | Stx2 and O157:H7Δstx2 cytotoxicity on HCT-8 cells. HCT-8 cells were incubated with either 100 ng/ml Stx2 alone or in the presence of 4 x 10^8 CFU/ml O157:H7Δstx2 (O157:H7Δstx2 + Stx2) for 4 h and compared with 4 × 10^8 O157:H7Δstx2 alone. HCT-8 viability was measured by neutral red uptake after 72 h. Data is shown as means ± SEM from six independent experiments performed in triplicate. Stx2 vs. O157:H7Δstx2 or Stx2 vs. O157:H7Δstx2 + Stx2. $^*p < 0.05$.

RESULTS

Effects of O157:H7Δstx2 Infection on Stx2 Cytotoxicity

To examine if Stx2 cytotoxicity could be modulated by O157:H7Δstx2 infection, cell viability was measured on HCT-8 cells incubated with either 100 ng/ml Stx2 alone or in presence of 4 × 10^8 CFU/ml O157:H7Δstx2 (O157:H7Δstx2+Stx2) and compared with HCT-8 cells incubated with O157:H7Δstx2 alone. As shown in **Figure 1**, the cytotoxic effect caused by O157:H7Δstx2 + Stx2 was significantly greater compared to Stx2 alone, while O157:H7Δstx2 did not show any cytotoxic effect. These results suggest that an increase in Stx2 cytotoxicity is elicited by O157:H7Δstx2 infection.

Effect of Endocytic-Pathway Inhibitors on Stx2 Uptake and Cytotoxic Effects

The finding that O157:H7Δstx2 infection significantly increased Stx2 cytotoxicity in HCT-8 cells led the studies to determine which pathways are involved in Stx2 uptake and cytotoxicity and, in turn, which ones were stimulated by O157:H7Δstx2 infection. HCT-8 cells were pre-treated with Eliglustat (200 nM, 48 h), an inhibitor of glucosylceramide (GL1) synthase (Shayman, 2013), MβCD (4 mM, 30 min), a membrane cholesterol extractor

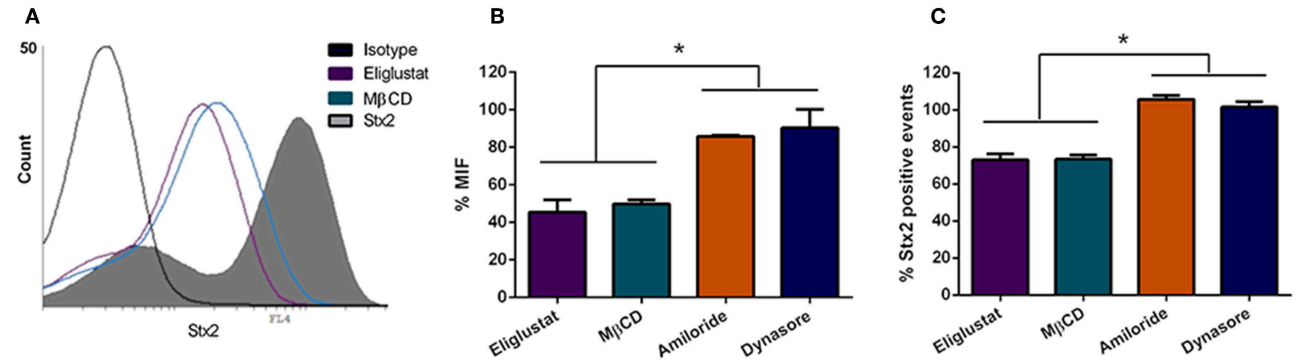

FIGURE 2 | Stx2 uptake by HCT-8 cells. **(A)** Cells pre-treated or not with endocytosis inhibitors were exposed to 100 ng/ml Stx2 and then analyzed by flow cytometry. Histograms represent the log fluorescence of Stx2 for each treatment. A Representative experiment is shown. Amiloride and Dynasore curves are not shown due to superimposition with Stx2 curve. **(B)** Bar graph representing the Median Intensity of Fluorescence (% MIF) for each inhibitor treatment relative to cells only treated with Stx2. **(C)** Stx2 positive events (%) for each inhibitor treatment relative to cells only treated with Stx2. Bars represent the mean ± SEM of three independent experiments. *$p < 0.05$.

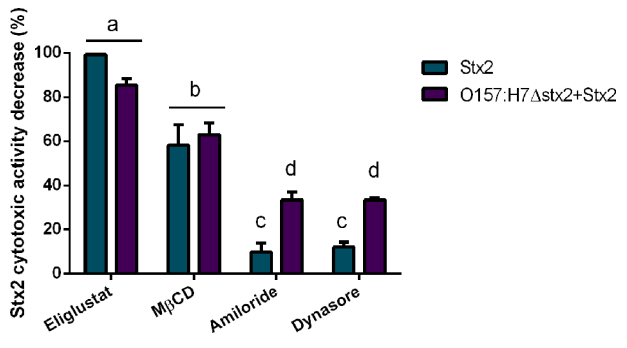

FIGURE 3 | Effect of endocytosis inhibitors on Stx2 cytotoxicity in HCT-8 cells. Cells were pre-incubated with Eliglustat (200 nM, 48 h), MβCD (4 mM, 30 min), Dynasore (80 μM, 30 min), or Amiloride (1 mM, 30 min) and washed twice with PBS before treatment for 4 h of 100 ng/ml Stx2 with or without O157:H7Δstx2. Data is shown as means ± SEM from six independent experiments performed in triplicate. Significant differences were found between the groups, labeled a, b, c, and d.

(Zidovetzki and Levitan, 2007), Dynasore (80 μM, 30 min), a specific dynamin-mediated endocytic inhibitor (Macia et al., 2006) or Amiloride (1 mM, 30 min), a specific dynamin-mediated endocytic inhibitor (Macia et al., 2006). Cells were then incubated with 100 ng/ml Stx2 during 4 h. Finally, toxin uptake was measured by flow cytometry. As it can be seen on **Figure 2**, both % MIF and % Stx2 positive events were significantly lower when cells were pre-incubated with Eliglustat or MβCD, compared to Dynasore or Amiloride, indicating that Stx2 uptake may be sensitive to glucosylceramide synthase inhibition (presumably due to Gb3 synthesis inhibition) and/or cholesterol dependent but not significantly dynamin or macropinocytosis dependent.

In agreement with the reduced level of Stx2 uptake observed following inhibitor treatments, Stx2 cytotoxicity was also decreased by the inhibitors Eliglustat and MβCD (**Figure 3**), with Eliglustat having a more pronounced effect.

Notably, the neutralizing effect on cytotoxicity by Eliglustat was maximal when O157:H7Δstx2 were not present and appeared lower when O157:H7Δstx2 were present, though no statistically significant differences were found. On the other hand, Amiloride and Dynasore showed a significantly lower protective capability than Eliglustat and MβCD, but both showed a significantly higher neutralizing capability when cells were treated with O157:H7Δstx2+Stx2 compared to Stx2 alone (**Figure 3**). None of these inhibitors showed cytotoxic activity *per se* when they were tested alone (data not shown). This data is consistent with a necessary interaction between Stx2 and the Gb3 receptor, presented in the apical surface of HCT-8 cells, to cause cytotoxicity, although these effects appear to be less dependent on the lipid environment compared to the net Stx2 uptake measured by flow cytometry. However, dynamin-dependent and Gb3-independent macropinocytic endocytosis pathways became relevant only when O157:H7Δstx2 were present, suggesting that these mechanisms are sensitive to O157:H7Δstx2 infection.

None of the inhibitors used for pre-incubation showed a significant effect on O157:H7Δstx2 adhesion to HCT-8 cells (**Figure S1**).

Effect of O157:H7 Infection on Stx2 Translocation

To determine whether Stx2 translocation across the intestinal barrier was affected by the presence of O157:H7Δstx2, HCT-8 monolayers were incubated with 100 ng/ml of Stx2 alone or in the presence of: 4 x 10^8 CFU/ml O157:H7Δstx2, 10 mM EDTA, or O157:H7Δstx2 supernatant from O157:H7Δstx2 (SN O157:H7Δstx2), added on the upper (apical) chamber. After 4 h of incubation, Stx2 passage was quantified on the lower (basolateral) chamber by Vero cell cytotoxicity assay (**Figure 4A**).

Since Stx has been shown to be able to cross polarized epithelial cells through both transcellular and paracellular pathways (Hurley et al., 2001; Malyukova et al., 2009; Lukyanenko et al., 2011; Tran et al., 2018), FITC-Dextran passage from apical to basolateral side was simultaneously

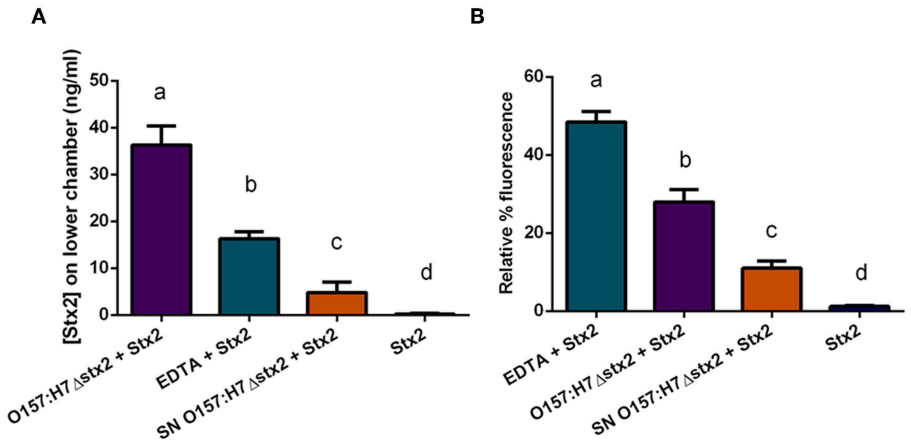

FIGURE 4 | Stx2 translocation across HCT-8 monolayers. **(A)** Stx2 concentration in the lower (basolateral) chamber was determined by Vero cell cytotoxicity assays. **(B)** Relative FITC-Dextran passage (%) to the lower (basolateral) chamber was measured. Significant differences were found between the groups, labeled a, b, c, and d.

measured (**Figure 4B**). Maximum Stx2 translocation across the HCT-8 monolayers was found in the presence of O157:H7Δstx2 compared to the other experimental conditions (**Figure 4A**). Instead, maximum FITC-Dextran passage was found in the presence of EDTA, a potent tight junction disruptor agent, followed by O157:H7Δstx2 treatment (**Figure 4B**). Taken together, these results have demonstrated that O157:H7Δstx2 stimulates not only paracellular, but also transcellular Stx2 translocation.

On the other hand, monolayers exposed to SN O157:H7Δstx2 also resulted in a significant increase of Stx2 and FITC-Dextran passage (**Figures 4A,B**, respectively) indicating that O157:H7Δstx2 SN affected at least the paracellular permeability but to a lesser extent than that observed with O157:H7Δstx2 (**Figure 4B**b vs. c), compared to treatment with Stx2 alone (**Figure 4B**d).

To confirm the effects of O157:H7Δstx2 and its filtered SN on epithelial barrier function leading to Stx2 paracellular translocation, we analyzed the integrity of the tight junctional barrier by TEER measurements before and after each treatment (**Figure 5**). The integrity of tight junctions clearly declined in monolayers treated with O157:H7Δstx2 and SN O157:H7Δstx2 in the presence of Stx2, proportionally to the increase of FITC-Dextran passage. As it was expected, minimum TEER value was observed after incubation with 10 mM EDTA. However, the Stx2 passage was higher in the presence of O157:H7Δstx2 than with EDTA, supporting the hypothesis that O157:H7Δstx2 stimulates Stx2 translocation across transcellular and paracellular pathways.

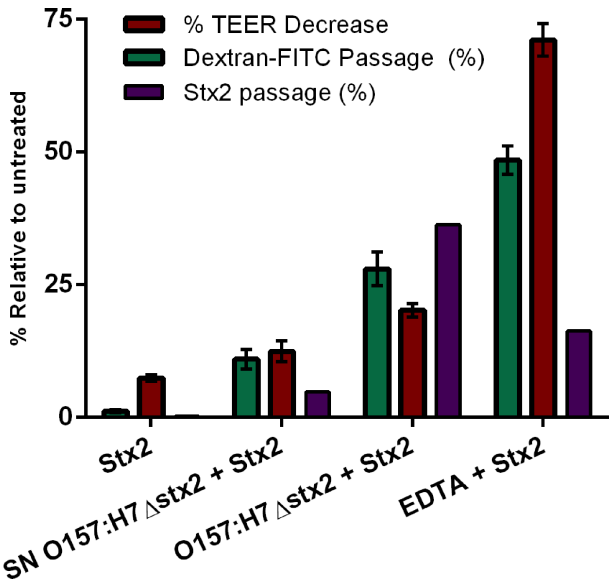

FIGURE 5 | Stx2 translocation was not entirely correlated to tight junction barrier disruption. The correlation between Stx2 translocation and the disruptive effects on tight junctional barrier measured as TEER and FITC-Dextran passage was analyzed in HCT-8 cell monolayers after 4 h incubation with O157:H7Δstx2, SN O157:H7Δstx2 and EDTA. Stx2 concentration was determined in the lower (basolateral) chamber by Vero cell cytotoxicity assays and it was relativized to initial Stx2 concentration (100 ng/ml). Relative FITC-Dextran passage was calculated as a ratio between lower (basolateral) chamber fluorescence and total fluorescence relative to cell free control. TEER was measured at the end of treatments and expressed as a percentage of the corresponding TEER immediately before the start of treatments.

Effects of Endocytosis Inhibitors on Stx2 Passage Across the Transcellular Pathway

To assess which endocytic mechanisms previously described are involved in Stx2 transcytosis in presence of O157:H7Δstx2, HCT-8 cells monolayers were pre-incubated with Eliglustat, Dynasore, MβCD, or Amiloride as previously described, followed by incubation with O157:H7Δstx2+Stx2. Stx2 translocation, measured as indicated above, was significantly inhibited by all treatments, with a maximum inhibition observed after MβCD treatment, followed by Eliglustat, and

lastly, Dynasore and Amiloride (**Figure 6A**). In addition, none of these inhibitors significantly disrupted the epithelial barrier function measured as FITC-Dextran translocation (**Figure 6B**). These results suggest that cholesterol disruption was more efficient than glucosylceramide synthesis inhibition at decreasing endocytosis-dependent translocation, suggesting a wider implication of cholesterol in the transcytosis process. In addition, Stx2 translocation via dynamin and macropinocytic pathways was also significantly decreased, showing that both mechanisms also may play a role on Stx2 transcytosis during O157:H7Δstx2 infection.

DISCUSSION

We have previously reported that Stx2-mediated physiological and morphological alterations to human colonic mucosa was enhanced by exposure to O157:H7 bacteria (Albanese et al., 2015). In the present study, we demonstrate that infection of human colonic epithelial (HCT-8) monolayers by O157:H7Δstx2 also impacts Stx2 endocytosis, cytotoxic action, and translocation across intestinal epithelial monolayers.

In this report, HCT-8 cells infected with O157:H7Δstx2 supplemented with Stx2 exhibited a significantly higher cytotoxic activity compared to the same concentration of Stx2 alone, indicating that O157:H7Δstx2 infection led to host cell modifications that enhanced Stx2 cytotoxicity (**Figure 1**). Regarding Stx2 effects on uninfected cells, we have seen that inhibition of glucosylceramide synthesis by Eliglustat led to a maximum decrease in Stx2 entry into cells and cytotoxic effects on HCT-8 cells (**Figures 2**, **3**). This inhibitor has been used at optimal concentration and incubation time according to previous works with endothelial cells (Kaissarian et al., 2018) and to previous experience with another glucosylceramide synthase inhibitor (Miglustat, Acetilon Pharm) (Girard et al., 2015) that also reduces Gb3 synthesis. It is worth noting that Eliglustat inhibits the synthesis of multiple glucosylceramides besides Gb3, some of which have been implied in membrane traffic and endocytic pathway modulation (Sillence et al., 2002). In this direction, it is possible that the absence of these glucosylceramides may account for some of the effects observed, but we speculate that their relative relevance on Stx2 uptake and cytotoxic activity should be minor compared to Gb3 absence. Our results indicate that, although Eliglustat prevented Stx2 cytotoxic effects (**Figure 3**), it did not completely inhibit net Stx2 internalization (**Figure 2**). We propose that this observed Stx2 uptake may be due to Gb3-independent endocytic mechanisms (Chan and Ng, 2016), although it may not have been enough to exert Stx2 cytotoxic effects. Similarly, removal of cholesterol by using MβCD reduced Stx2 uptake and cytotoxicity, although it appeared to do so to a lesser extent than that observed with Eliglustat. Cholesterol is known to be a major component of the microenvironment in which Gb3 is embedded, and it has previously been implicated on Gb3 avidity for Stx2 (Gallegos et al., 2012) and Stx2-induced tubule scission (Gaus et al., 2010). It was also suggested that cholesterol may play a role on macropinocytosis and membrane ruffling (Grimmer et al., 2002). Although significant differences were not found, Eliglustat appeared to be less effective on decreasing Stx2 cytotoxicity when O157:H7Δstx2 was present, compared to the bacterial-free condition (**Figure 3**). Even though the methods used may have not been sensitive enough to provide significant differences in this scenario, we speculate that this result is relevant as it may account for the significant stimulation observed of alternative mechanisms, such as macropinocytosis and dynamin-dependent pathways, upon O157:H7Δstx2 infection. On the other hand, dynamin's role on Stx2 induced tubule scission after Gb3 binding is highly controversial, as a putative spontaneous, actin-dependent mechanism has also been described (Gaus et al., 2010). In this study, we found that dynamin-dependent Stx2 endocytosis had no relevance on Stx2 uptake (**Figure 2**) or cytotoxic effects when O157:H7Δstx2 was absent but did significantly contribute to Stx2 cytotoxicity upon O157:H7Δstx2 infection (**Figure 3**). We speculate that these differences may be explained as it was observed that O157:H7Δstx2 infection could exert a positive action on dynamin recruitment around vesicles, which is required for actin pedestal formation (Unsworth et al., 2007). Alternatively, we hypothesize that actin rearrangement induced by O157:H7Δstx2 may have affected actin-dependent vesicle scission mechanisms (Gaus et al., 2010), which may in turn increase dynamin dependent scission, although the exact underlying causes remain a subject for future studies. Macropinocytosis involvement in Stx2 internalization during STEC infection and the molecular mechanisms implicated has been previously described (Malyukova et al., 2009; Lukyanenko et al., 2011; In et al., 2013). In this study, we found that macropinocytosis significantly contributed to Stx2 internalization only when O157:H7Δstx2 were present, indicating that bacterial infection exerts a positive effect on cell's macropinocytosis regulation (**Figure 3**).

As O157:H7 is generally believed to be non-invasive, Stx2 must translocate across the epithelial barrier of the intestine in order to reach target organs and cause HUS (Boyce et al., 2002). In this study, we demonstrate that Stx2 passage across polarized HCT-8 monolayers is enhanced by O157:H7Δstx2 infection. This increase is not exclusively due to soluble metabolites, as SN O157:H7Δstx2 exerted a much lesser, although statistically significant, effect on transcytosis (**Figure 4A**). Previous studies have shown that Stx2 may translocate the intestinal barrier by a paracellular in addition to a transcellular/endocytic pathway (Hurley et al., 2001; Müller et al., 2017). We used EDTA, a chelating agent extensively described as a tight junction disruptor (Ward et al., 2000), to estimate the maximum passage allowed by the paracellular route. We confirmed by TEER and FITC-Dextran measurements that paracellular passage and permeability were maximum when EDTA was added, followed by O157:H7Δstx2 treatment (**Figures 4B**, **5**). However, Stx2 translocation in presence of O157:H7Δstx2 was significantly higher than with EDTA treatment (**Figure 5**), suggesting that both paracellular and transcellular translocation routes can be

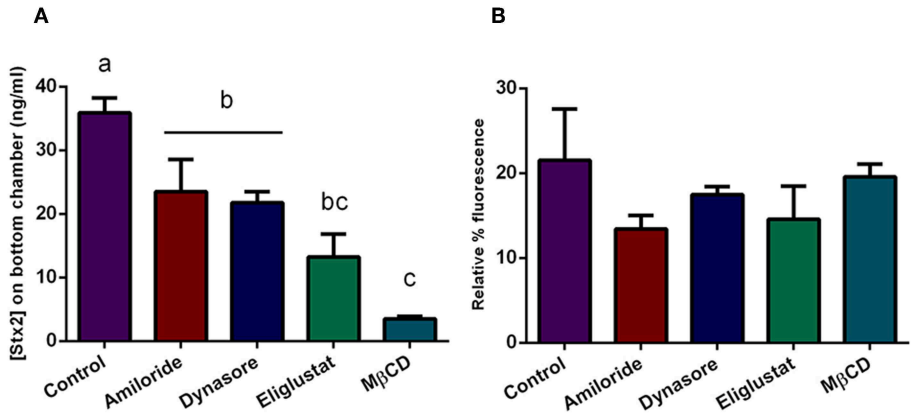

FIGURE 6 | Stx2 translocation in presence of endocytosis inhibitors. Cells were pre-incubated with Eliglustat (200 nM, 48 h), MBCD (4 mM, 30 min), Dynasore (80 μM, 30 min), or Amiloride (1 mM, 30 min), and washed twice with PBS followed by treatment with O157:H7Δstx2 + 100 ng/ml Stx2 for 4 h. Control cells were not pre-treated with inhibitors. **(A)** Estimated Stx2 concentration in the lower (basolateral) chamber. **(B)** Relative FITC-Dextran passage (%) to the lower (basolateral) chamber. Significant differences were found between groups with different letters, labeled a, b, and c.

upregulated by O157:H7Δstx2. Again, SN O157:H7Δstx2 was able to exert a significant effect over tight junction integrity compared to Stx2 alone, but much less than that exerted by O157:H7Δstx2 infection. Previous reports showed that Stx2 translocation across a polarized colonic epithelial T84 cell line is enhanced by O157:H7 infection and may only occur via a transcellular pathway because TEER remains constant during infection with several STEC O157:H7 strains (Tran et al., 2014, 2018). In the same fashion, we found that the transcellular pathway is stimulated by O157:H7Δstx2 infection, but we also observed that the paracellular pathway, measured as TEER and FITC-Dextran permeability, was significantly affected after infection with O157:H7Δstx2 (**Figure 5**). The apparent discrepancy could be due to differences in STEC strains, as the one used in this study belongs to the hypervirulent clade 8, which was found to overexpress several virulence proteins (Amigo et al., 2015, 2016). Differences in intestinal cell lines used may also explain these discrepancies, as they show differences in key characteristics such as monolayers TEER values (Hurley et al., 2016), which we speculate may account for differences in sensitivity of tight junction to O157:H7 infection.

Overall, our data suggests that O157:H7Δstx2 infection greatly stimulated Stx2 passage through both paracellular and transcellular pathways, and that this stimulation is mainly due to O157:H7Δstx2 co-incubation with epithelial cells, and to a lesser extent, to soluble metabolites released by O157:H7Δstx2 to the culture supernatant.

We also tested if the same endocytic pathways involved in cytotoxicity could account for the increased transcytosis. Surprisingly, we found that cholesterol depletion by MβCD appears to be more effective decreasing Stx2 transcytosis than glucosylceramide synthesis inhibition by Eliglustat (**Figure 6**), though the opposite was observed when cytotoxic effects were analyzed (**Figure 3**). Being the exact mechanisms that determine vesicle trafficking and its destiny still unknown, we can hypothesize that membrane cholesterol may be more strongly implied on the basolateral trafficking leading to translocation, rather than on the retrograde transport leading to cytotoxicity. On the other hand, Amiloride and Dynasore led to a moderate transcytosis decrease (**Figure 6**) in the same fashion as that observed in cytotoxic neutralization (**Figure 3**), suggesting that O157:H7Δstx2 could also stimulate macropinocytosis and dynamin-dependent translocation. As these endocytosis inhibitors showed similar effects on both cytotoxicity and transcytosis, we can hypothesize that, to a degree, the mechanisms leading to both outcomes may have the same endocytic origin (Malyukova et al., 2009; Müller et al., 2017).

To summarize, our results showed that *E. coli* O157:H7Δstx2 infection increases Stx2 cytotoxic effect by stimulation of several endocytic pathways. Furthermore, we demonstrated that O157:H7Δstx2 infection enhances Stx2 translocation across HCT-8 monolayers in both paracellular and transcellular pathways. We showed that dynamin-independent and Gb3-dependent mechanisms are mostly implicated in Stx2 endocytosis and translocation, though dynamin dependent endocytosis and macropinocytosis became more relevant when O157:H7Δstx2 infection was present.

This study provides insight on how O157:H7 infection may promote Stx2 associated disease by affecting Stx2 intestinal toxicity, uptake, and/or translocation into the systemic circulation resulting in intoxication of distal target organs. These studies may open the door to the development of novel therapeutic approaches for treating EHEC associated disease.

DATA AVAILABILITY STATEMENT

The datasets generated for this study are available on request to the corresponding author.

AUTHOR CONTRIBUTIONS

All authors listed have made a substantial, direct and intellectual contribution to the work, and approved it for publication.

FUNDING

This study was supported by the National Agency for Promotion of Science and Technology (ANPCYT-PICT2016-0292), the University of Buenos Aires (UBACYT-2018-20020170100600BA), and the National Scientific and Technical Research Council (CONICET PUE-2017-0041). NG has a fellowship of the National Council of Research (CONICET). CI and MA are members of CONICET.

ACKNOWLEDGMENTS

We are grateful to Roxane M. F. Piazza (Laboratorio de Bacteriología, Instituto Butantan, São Paulo, SP, Brasil) for kindly providing Mab 2E11 directed against the A-subunit of Stx2.

SUPPLEMENTARY MATERIAL

The Supplementary Material for this article can be found online at: https://www.frontiersin.org/articles/10.3389/fcimb.2019.00396/full#supplementary-material

REFERENCES

Albanese, A., Gerhardt, E., Garcia, H., Amigo, N., Cataldi, A., Zotta, E., et al. (2015). Inhibition of water absorption and selective damage to human colonic mucosa induced by Shiga toxin-2 are enhanced by *Escherichia coli* O157:H7 infection. *Int. J. Med. Microbiol.* 305, 348–354. doi: 10.1016/j.ijmm.2015.02.002

Amigo, N., Mercado, E., Bentancor, A., Singh, P., Vilte, D., Gerhardt, E., et al. (2015). Clade 8 and clade 6 strains of *Escherichia coli* O157:H7 from cattle in Argentina have hypervirulent-like phenotypes. *PLoS ONE* 10:e0127710. doi: 10.1371/journal.pone.0127710

Amigo, N., Zhang, Q., Amadio, A., Zhang, Q., Silva, W. M., Cui, B., et al. (2016). Overexpressed proteins in hypervirulent clade 8 and clade 6 strains of *Escherichia coli* O157:H7 compared to *E. coli* O157:H7 EDL933 clade 3 strain. *PLoS ONE* 11:e0166883. doi: 10.1371/journal.pone.0166883

Balda, M. S., Whitney, J. A., Flores, C., González, S., Cereijido, M., and Matter, K. (1996). Functional dissociation of paracellular permeability and transepithelial electrical resistance and disruption of the apical-basolateral intramembrane diffusion barrier by expression of a mutant tight junction membrane protein. *J. Cell Biol.* 134, 1031–1049. doi: 10.1083/jcb.134.4.1031

Bansal, T., Dae Nyun, K., Slininger, T., Wood, T. K., and Jayaraman, A. (2013). Human intestinal epithelial cell-derived molecules increase enterohemoorhagic Esherichia coli virulence. *FEMS Immunol. Med. Microbiol.* 66, 399–410. doi: 10.1111/1574-695X.12004

Betz, J., Bielaszewska, M., Thies, A., Humpf, H.-U., Dreisewerd, K., Karch, H., et al. (2011). Shiga toxin glycosphingolipid receptors in microvascular and macrovascular endothelial cells: differential association with membrane lipid raft microdomains. *J. Lipid Res.* 52, 618–634. doi: 10.1194/jlr.M010819

Beutin, L., and Martin, A. (2012). Outbreak of shiga toxin-producing *Escherichia coli* (STEC) O104:H4 infection in Germany causes a paradigm shift with regard to human pathogenicity of STEC strains. *J. Food Prot.* 75, 408–418. doi: 10.4315/0362-028X.JFP-11-452

Boyce, T. G., Swerdlow, D. L., and Griffin, P. M. (2002). *Escherichia coli* O157:H7 and the hemolytic–uremic syndrome. *N. Engl. J. Med.* 333, 364–368. doi: 10.1056/NEJM199508103330608

Chan, Y. S., and Ng, T. B. (2016). Shiga toxins: from structure and mechanism to applications. *Appl. Microbiol. Biotechnol.* 100, 1597–1610. doi: 10.1007/s00253-015-7236-3

Chattopadhyay, R., Raghavan, S., and Rao, G. N. (2017). Resolvin D1 via prevention of ROS-mediated SHP2 inactivation protects endothelial adherens junction integrity and barrier function. *Redox Biol.* 12, 438–455. doi: 10.1016/j.redox.2017.02.023

Dutta, D., and Donaldson, J. G. (2012). Search for inhibitors of endocytosis Intended specificity and unintended consequences. *Cell. Logist.* 2, 203–208. doi: 10.4161/cl.23967

Ferens, W. A., and Hovde, C. J. (2011). *Escherichia coli* O157:H7: animal reservoir and sources of human infection. *Foodborne Pathog. Dis.* 8, 465–487. doi: 10.1089/fpd.2010.0673

Gallegos, K. M., Conrady, D. G., Karve, S. S., Gunasekera, T. S., Herr, A. B., and Weiss, A. A. (2012). Shiga toxin binding to glycolipids and glycans. *PLoS ONE* 7:e30368. doi: 10.1371/journal.pone.0030368

Gaus, K., Johannes, L., Lamaze, C., and Bassereau, P. (2010). Actin dynamics drive membrane reorganization and scission in clathrin-independent endocytosis. *Cell* 140, 540–553. doi: 10.1016/j.cell.2010.01.010

Gianantonio, C. A., Vitacco, M., Mendilaharzu, F., and Gallo, G. (1968). The hemolytic-uremic syndrome. Renal status of 76 patients at long-term follow-up. *J. Pediatr.* 72, 757–65. doi: 10.1016/S0022-3476(68)80427-5

Girard, M. C., Sacerdoti, F., Rivera, F. P., Repetto, H. A., Ibarra, C., and Amaral, M. M. (2015). Prevention of renal damage caused by Shiga toxin type 2: action of miglustat on human endothelial and epithelial cells. *Toxicon 2015*, 105, 27–33. doi: 10.1016/j.toxicon.2015.08.021

Grimmer, S., van Deurs, B., and Sandvig, K. (2002). Membrane ruffling and macropinocytosis in A431 cells require cholesterol. *J. Cell Sci* 115, 2953–2962.

Hanashima, T., Miyake, M., Yahiro, K., Iwamaru, Y., Ando, A., Morinaga, N., et al. (2008). Effect of Gb3 in lipid rafts in resistance to Shiga-like toxin of mutant Vero cells. *Microb. Pathog.* 45, 124–133. doi: 10.1016/j.micpath.2008.04.004

Hashida, R., Anamizu, C., Yagyu-Mizuno, Y., Ohkuma, S., and Takano, T. (1986). Transcellular transport of fluorescein dextran through an arterial endothelial cell monolayer. *Cell Struct. Funct.* 11, 343–349. doi: 10.1247/csf.11.343

Holmes, A., Mühlen, S., Roe, A. J., and Dean, P. (2010). The EspF effector, a bacterial pathogen's swiss army knife. *Infect. Immun.* 78, 4445–4453. doi: 10.1128/IAI.00635-10

Huang, J., Motto, D. G., Bundle, D. R., and Sadler, J. E. (2010). Shiga toxin B subunits induce VWF secretion by human endothelial cells and thrombotic microangiopathy in ADAMTS13-deficient mice. *Blood* 116, 3653–3659. doi: 10.1182/blood-2010-02-271957

Hurley, B. P., Jacewicz, M., Thorpe, C. M., Lincicome, L. L., King, A. J., Keusch, G. T., et al. (1999). Shiga toxin 1 and 2 translocate differently across polarized intestinal epithelial cells. *Infect. Immun* 67, 6670–6677.

Hurley, B. P., Pirzai, W., Eaton, A. D., Harper, M., Roper, J., Zimmermann, C., et al. (2016). An experimental platform using human intestinal epithelial cell lines to differentiate between hazardous and non-hazardous proteins. *Food Chem. Toxicol.* 92, 75–87. doi: 10.1016/j.fct.2016.04.003

Hurley, B. P., Thorpe, C. M., and Acheson, D. W. K. (2001). Shiga toxin translocation across intestinal epithelial cells is enhanced by neutrophil transmigration. *Infect. Immun.* 69, 6148–6155. doi: 10.1128/IAI.69.10.6148-6155.2001

In, J., Lukyanenko, V., Foulke-Abel, J., Hubbard, A. L., Delannoy, M., Hansen, A. M., et al. (2013). Serine Protease EspP from enterohemorrhagic *Escherichia coli*

is sufficient to induce shiga toxin macropinocytosis in intestinal epithelium. *PLoS ONE* 8:e69196. doi: 10.1371/journal.pone.0069196

Jerse, A. E., Yu, J., Tall, B. D., and Kaper, J. B. (1990). A genetic locus of enteropathogenic *Escherichia coli* necessary for the production of attaching and effacing lesions on tissue culture cells. *Proc. Natl. Acad. Sci. U.S.A.* 87, 7839–7843. doi: 10.1073/pnas.87.20.7839

Kaissarian, N., Kang, J., Shu, L., Ferraz, M. J., Aerts, J. M., and Shayman, J. A. (2018). Dissociation of globotriaosylceramide and impaired endothelial function in α-galactosidase-A deficient EA.hy926 cells. *Mol. Genet. Metab.* 125, 338–344. doi: 10.1016/j.ymgme.2018.10.007

Karmali, M. A., Mascarenhas, M., Shen, S., Ziebell, K., Johnson, S., Reid-Smith, R., et al. (2003). Association of genomic o island 122 of *Escherichia coli* EDL 933 with verocytotoxin-producing *Escherichia coli* seropathotypes that are linked to epidemic and/or serious disease. *J. Clin. Microbiol.* 41, 4930–4940. doi: 10.1128/JCM.41.11.4930-4940.2003

Karmali, M. A., Petric, M., Lim, C., Cheung, R., and Arbus, G. S. (1985). Sensitive method for detecting low numbers of Verotoxin-producing *Escherichia coli* in mixed cultures by use of colony sweeps and polymyxin extraction of Verotoxin. *J. Clin. Microbiol* 22, 614–619.

Knutton, S., Baldwin, T., Williams, P. H., and McNeish, A. S. (1989). Actin accumulation at sites of bacterial adhesion to tissue culture cells: Basis of a new diagnostic test for enteropathogenic and enterohemorrhagic *Escherichia coli*. *Infect. Immun* 57, 1290–1298.

Koivusalo, M., Welch, C., Hayashi, H., Scott, C. C., Kim, M., Alexander, T., et al. (2010). Amiloride inhibits macropinocytosis by lowering submembranous pH and preventing Rac1 and Cdc42 signaling. *J. Cell Biol.* 188, 547–563. doi: 10.1083/jcb.200908086

Kouzel, I. U., Pohlentz, G., Schmitz, J. S., Steil, D., Humpf, H. U., Karch, H., et al. (2017). Shiga toxin glycosphingolipid receptors in human Caco-2 and HCT-8 colon epithelial cell lines. *Toxins* 9, 1–27. doi: 10.3390/toxins9110338

Lauvrak, S. U. (2004). Efficient endosome-to-Golgi transport of Shiga toxin is dependent on dynamin and clathrin. *J. Cell Sci.* 117, 2321–2331. doi: 10.1242/jcs.01081

Legros, N., Pohlentz, G., Steil, D., and Müthing, J. (2018). Shiga toxin-glycosphingolipid interaction: status quo of research with focus on primary human brain and kidney endothelial cells. *Int. J. Med. Microbiol.* 308, 1073–1084. doi: 10.1016/j.ijmm.2018.09.003

Lukyanenko, V., Malyukova, I., Hubbard, A., Delannoy, M., Boedeker, E., Zhu, C., et al. (2011). Enterohemorrhagic *Escherichia coli* infection stimulates Shiga toxin 1 macropinocytosis and transcytosis across intestinal epithelial cells. *Am. J. Physiol. Physiol* 301, C1140–C1149. doi: 10.1152/ajpcell.00036.2011

Macia, E., Ehrlich, M., Massol, R., Boucrot, E., Brunner, C., and Kirchhausen, T. (2006). Dynasore, a cell-permeable inhibitor of dynamin. *Dev. Cell* 2006, 10, 839–850. doi: 10.1016/j.devcel.2006.04.002

Malyukova, I., Murray, K. F., Zhu, C., Boedeker, E., Kane, A., Patterson, K., et al. (2009). Macropinocytosis in Shiga toxin 1 uptake by human intestinal epithelial cells and transcellular transcytosis. *Am. J. Physiol. - Gastrointest. Liver Physiol* 296, 78–92. doi: 10.1152/ajpgi.90347.2008

Matter, K., and Balda, M. S. (2003). Functional analysis of tight junctions. *Methods* 30, 228–234. doi: 10.1016/S1046-2023(03)00029-X

McWilliams, B. D., and Torres, A. G. (2014). Enterohemorrhagic *Escherichia coli* adhesins. *Microbiol. Spectr.* 2. doi: 10.1128/microbiolspec.EHEC-0003-2013

Melton-Celsa, A. R. (2014). Shiga toxin (Stx) classification, structure, and function. *Microbiol. Spectr.* 2, 1–21. doi: 10.1128/microbiolspec.EHEC-0024-2013

Müller, S. K., Wilhelm, I., Schubert, T., Zittlau, K., Madl, J., Eierhoff, T., et al. (2017). Expert opinion on drug delivery Gb3-binding lectins as potential carriers for transcellular drug delivery. *Expert Opin. Drug Deliv.* 14, 1–13. doi: 10.1080/17425247.2017.1266327

Nataro, J. P., and Kaper, J. B. (1998). Diarrheagenic *Escherichia coli*. *Clin. Microbiol. Rev.* 11, 142–201. doi: 10.1128/CMR.11.1.142

Newton, H. J., Sloan, J., Bulach, D. M., Seemann, T., Allison, C. C., Tauschek, M., et al. (2009). Shiga toxin-producing *Escherichia coli* strains negative for locus of enterocyte effacement. *Emerg. Infect. Dis.* 15, 372–380. doi: 10.3201/eid1503.080631

Palermo, M. S., Exeni, R. A., and Fernández, G. C. (2009). Hemolytic uremic syndrome: Pathogenesis and update of interventions. *Expert Rev. Anti Infect. Ther.* 7, 697–707. doi: 10.1586/eri.09.49

Pezeshkian, W., Gao, H., Arumugam, S., Becken, U., Bassereau, P., Florent, J. C., et al. (2017). Mechanism of Shiga toxin clustering on membranes. *ACS Nano* 11, 314–324. doi: 10.1021/acsnano.6b05706

Repetto, G., del Peso, A., and Zurita, J. L. (2008). Neutral red uptake assay for the estimation of cell viability/cytotoxicity. *Nat. Protoc.* 3, 1125–1131. doi: 10.1038/nprot.2008.75

Rivas, M., Miliwebsky, E., Chinen, I., Roldán, C. D., Balbi, L., García, B., et al. (2006). Characterization and epidemiologic subtyping of Shiga toxin-producing *Escherichia coli* strains isolated from hemolytic uremic syndrome and diarrhea cases in Argentina. *Foodborne Pathog. Dis.* 3, 88–96. doi: 10.1089/fpd.2006.3.88

Rocha, L. B., Luz, D. E., Moraes, C. T. P., Caravelli, A., Fernandes, I., Guth, B. E. C., et al. (2012). Interaction between shiga toxin and monoclonal antibodies: binding characteristics and *in vitro* neutralizing abilities. *Toxins* 4, 729–747. doi: 10.3390/toxins4090729

Römer, W., Berland, L., Chambon, V., Gaus, K., Windschiegl, B., Tenza, D., et al. (2007). Shiga toxin induces tubular membrane invaginations for its uptake into cells. *Nature* 450, 670–675. doi: 10.1038/nature05996

Sandvig, K., Grimmer, S., Lauvrak, S., Torgersen, M., Skretting, G., Van Deurs, B., et al. (2002). Pathways followed by ricin and Shiga toxin into cells. *Histochem. Cell Biol.* 117, 131–141. doi: 10.1007/s00418-001-0346-2

Schüller, S., Frankel, G., and Phillips, A. D. (2004). Interaction of Shiga toxin from *Escherichia coli* with human intestinal epithelial cell lines and explants: Stx2 induces epithelial damage in organ culture. *Cell. Microbiol.* 6, 289–301. doi: 10.1046/j.1462-5822.2004.00370.x

Shayman, J. A. (2013). Eliglustat tartrate, a prototypic glucosylceramide synthase inhibitor. *Expert Rev. Endocrinol. Metab.* 8, 491–504. doi: 10.1586/17446651.2013.846213

Sillence, D. J., Puri, V., Marks, D. L., Butters, T. D., Dwek, R. A., Pagano, R. E., et al. (2002). Glucosylceramide modulates membrane traffic along the endocytic pathway. *J. Lipid Res.* 43, 1837–1845. doi: 10.1194/jlr.M200232-JLR200

Smith, W. E., Kane, A. V., Campbell, S.T., Acheson, D.W.K., Cochran, B.H., and Thorpe, C.M. (2003). Shiga toxin 1 triggers a ribotoxic stress response leading to p38 and JNK activation and induction of apoptosis in intestinal epithelial cells. *Infect. Immun.* 71, 1497–504. doi: 10.1128/IAI.71.3.1497-1504.2003

Tarr, P. I., Gordon, C. A., and Chandler, W. L. (2005). Shiga-toxin-producing *Escherichia coli* and haemolytic uraemic syndrome. *Lancet* 365, 1073–1086. doi: 10.1016/S0140-6736(05)74232-X

Tran, S. L., Billoud, L., Lewis, S. B., Phillips, A. D., and Schüller, S. (2014). Shiga toxin production and translocation during microaerobic human colonic infection with Shiga toxin-producing *E.coli* O157: H7 and O104: H4. *Cell. Microbiol.* 16, 1255–1266. doi: 10.1111/cmi.12281

Tran, S. L., Jenkins, C., Livrelli, V., and Schüller, S. (2018). Shiga toxin 2 translocation across intestinal epithelium is linked to virulence of shiga toxin-producing *Escherichia coli* in humans. *Microbiol* 164, 509–516. doi: 10.1099/mic.0.000645

Ugalde-Silva, P., Gonzalez-Lugo, O., and Navarro-Garcia, F. (2016). Tight junction disruption induced by type 3 secretion system effectors injected by enteropathogenic and enterohemorrhagic *Escherichia coli*. *Front. Cell. Infect. Microbiol.* 6:87. doi: 10.3389/fcimb.2016.00087

Unsworth, K. E., Mazurkiewicz, P., Senf, F., Zettl, M., McNiven, M., Way, M., et al. (2007). Dynamin is required for F-actin assembly and pedestal formation by enteropathogenic *Escherichia coli* (EPEC). *Cell. Microbiol.* 9, 438–449. doi: 10.1111/j.1462-5822.2006.00801.x

Ward, P. D., Tippin, T. K., and Thakker, D. R. (2000). Enhancing paracellular permeability by modulating epithelial tight junctions. *Pharm. Sci. Technol. Today* 2000, 3, 346–358. doi: 10.1016/S1461-5347(00)00302-3

Zidovetzki, R., and Levitan, I. (2007). Use of cyclodextrins to manipulate plasma membrane cholesterol content: Evidence, misconceptions and control strategies. *Biochim. Biophys. Acta - Biomembr* 1768, 1311–1324. doi: 10.1016/j.bbamem.2007.03.026

Zumbrun, S. D., Hanson, L., Sinclair, J. F., Freedy, J., Melton-Celsa, A. R., Rodriguez-Canales, J., et al. (2010). Human intestinal tissue and cultured colonic cells contain globotriaosylceramide synthase mRNA and the alternate shiga toxin receptor globotetraosylceramide. *Infect. Immun.* 78, 4488–4499. doi: 10.1128/IAI.00620-10

Conflict of Interest: The authors declare that the research was conducted in the absence of any commercial or financial relationships that could be construed as a potential conflict of interest.

frontiers in Cellular and Infection Microbiology

ORIGINAL RESEARCH
published: 08 January 2020
doi: 10.3389/fcimb.2019.00442

Environmental Cues Modulate Microglial Cell Behavior Upon Shiga Toxin 2 From Enterohemorrhagic *Escherichia coli* Exposure

Clara Berdasco[1], *Maite Duhalde Vega*[2], *María Victoria Rosato-Siri*[2*†] and *Jorge Goldstein*[1*]

[1] Laboratorio de Neurofisiopatología, Consejo Nacional de Investigaciones Científicas y Técnicas, Facultad de Medicina, Instituto de Fisiología y Biofísica "Houssay", Universidad de Buenos Aires, Buenos Aires, Argentina, [2] Instituto de Química y Fisicoquímica Biológicas, Universidad de Buenos Aires, CONICET, Buenos Aires, Argentina

OPEN ACCESS

Edited by:
Roxane M. Piazza,
Butantan Institute, Brazil

Reviewed by:
Deepak Saxena,
New York University, United States
Weipeng Zhang,
Ocean University of China, China
Vernon L. Tesh,
Texas A&M University, College of Medicine, United States

***Correspondence:**
María Victoria Rosato-Siri
victoriarosatosiri@gmail.com
Jorge Goldstein
jogol@fmed.uba.ar

†ORCID:
María Victoria Rosato-Siri
orcid.org/0000-0002-5073-3937

Specialty section:
This article was submitted to Bacteria and Host, a section of the journal Frontiers in Cellular and Infection Microbiology

Received: 15 August 2019
Accepted: 09 December 2019
Published: 08 January 2020

Citation:
Berdasco C, Duhalde Vega M, Rosato-Siri MV and Goldstein J (2020) Environmental Cues Modulate Microglial Cell Behavior Upon Shiga Toxin 2 From Enterohemorrhagic Escherichia coli Exposure. Front. Cell. Infect. Microbiol. 9:442. doi: 10.3389/fcimb.2019.00442

Shiga toxin (Stx) produced by enterohemorrhagic *E. coli* produces hemolytic uremic syndrome and encephalopathies in patients, which can lead to either reversible or permanent neurological abnormalities, or even fatal cases depending on the degree of intoxication. It has been observed that the inflammatory component plays a decisive role in the severity of the disease. Therefore, the objective of this work was to evaluate the behavior of microglial cell primary cultures upon Stx2 exposure and heat shock or lipopolysaccharide challenges, as cues which modulate cellular environments, mimicking fever and inflammation states, respectively. In these contexts, activated microglial cells incorporated Stx2, increased their metabolism, phagocytic capacity, and pro-inflammatory profile. Stx2 uptake was associated to receptor globotriaosylceramide (Gb3)-pathway. Gb3 had three clearly distinguishable distribution patterns which varied according to different contexts. In addition, toxin uptake exhibited both a Gb3-dependent and a Gb3-independent binding depending on those contexts. Altogether, these results suggest a fundamental role for microglial cells in pro-inflammatory processes in encephalopathies due to Stx2 intoxication and highlight the impact of environmental cues.

Keywords: Shiga Toxin 2, microglial cell primary cultures, LPS challenge, heat shock exposure, receptor Gb3-pathway

INTRODUCTION

Shiga toxin-producing *Escherichia coli* (STEC) causes hemorrhagic colitis, and hemolytic uremic syndrome (HUS) once the toxin enters circulation from the gut (Karmali, 2004). HUS is an orally acquired infective illness produced by the ingestion of contaminated food, water and/or cross infection, and includes thrombocytopenia, microangiopathic hemolytic anemia, and acute renal failure (Gianantonio et al., 1973). In addition, Shiga toxin 2 (Stx2) targets other organs like the brain, inducing encephalopathies (Obata, 2010). Neurological damage produced by Stx2 (Ashkenazi et al., 1994; Siegler, 1994) has gained notoriety in Argentina and throughout the world. A multicenter, observational, retrospective, and cross-sectional study recently conducted by the National Epidemiological Surveillance System of Argentina concluded that central nervous system

(CNS) involvement by STEC was the main predictor of death in patients with HUS (Alconcher et al., 2018).

STEC may produce two variants of Shiga toxin, Shiga toxin type 1 (Stx1) and/or Shiga toxin type 2 (Stx2); both have the same mode of action but they are antigenically different (Melton-Celsa, 2014). Stx2, the endemic variant that predominates in Argentina, is a protein formed by a catalytic subunit A (StxA) and five subunits B (StxB) related with toxin binding. StxA possesses N-glycosidase activity and inhibits protein biosynthesis. To perform this task it must be transported to the cytosol by StxB (Johannes and Decaudin, 2005; Sandvig and van Deurs, 2005) through its receptor, located in the cell membrane. Globotriaosylceramide (Gb3) is a glycosphingolipid expressed on the cell membrane of some mammalian cells and it was described to be involved in cellular signaling. In addition, Gb3 has been identified as a primary receptor for various toxins including Stx1 and Stx2 (Bekri et al., 2006). Gb3 may serve as a precursor for the synthesis of more complex globo-series glycosphingolipids, such as globotetraosylceramide (Gb4) (Kavaliauskiene et al., 2017).

It has been observed that Stx2 intracerebroventricular-administration in rat brains exerts its neurotoxic effect through its Gb3 receptor in post-synaptic neurons (Tironi-Farinati et al., 2010). Indeed, neuronal degeneration and astrocytic reaction were found in several regions of the brain (Boccoli et al., 2008).

An inflammatory component of HUS in the brain was postulated through the observation that damage to the neurovascular component could be attenuated by the administration of dexamethasone, an anti-inflammatory drug (Pinto et al., 2013). These results were in agreement with previous studies by other groups in endothelial cells cultures which showed the contribution of pro-inflammatory lipopolysaccharide (LPS) to cytotoxicity upon Shiga toxins exposure (Louise and Obrig, 1992).

Microglial (MG) cells can be postulated as a central target in the harmful action caused by Stx2, as they belong to the monocyte-macrophage immune cell lineage (Xing et al., 2011). Along the same lines, our group has recently demonstrated in a translational murine model of HUS-derived encephalopathy that systemic sub lethal Stx2 induces MG cell reactivity in the striatum and the hippocampus (Pinto et al., 2018; Berdasco et al., 2019). We hypothesized that MG cells might play a pivotal role in the inflammatory effects of Stx2 observed in the brain and, thus, define the severity of encephalopathies in patients. This state of affairs prompted us to hypothesize that Stx2, either the holotoxin or the Stx2B subunits, exerted a direct biological effect on MG cell primary cultures. Therefore, functional parameters, such as MG cell activation, cytology, metabolism, cytokine expression levels, and phagocytic status were assayed using heat shock exposure and LPS challenge to determine whether culture conditions affect MG cell sensitivity and responsiveness. The present work demonstrates that MG cells exhibit both a Gb3-independent and Gb3-cannonical pathway for Stx2 uptake. Altogether, the present results suggest a fundamental role of MG cells in the pro-inflammatory processes underlying encephalopathies due to STEC exposure.

MATERIALS AND METHODS

Ethics Statement

All experimental procedures were performed in accordance with the guidelines of the Institutional Review Board at Buenos Aires University Council of Animal Care and were in accordance with the National Institutes of Health Guide for the Care and Use of Laboratory Animals. Animal protocols were approved by the School of Medicine Committee on Ethics and Animal Research (CICUAL Number: 046/2017).

Animals

Wistar rats were housed under controlled temperature (22 ± 2°C) in an artificially lit animal room under a 12 h-light/dark cycle and fed water and food *ad libitum*.

MG Cell Primary Cultures

Total brains of post-natal day (P) 0–1 Wistar rat pups from both sex (8–10 animals/litter) were dissected and plated on T75 polylysinated flasks and cultured in Dulbecco's Modified Eagle's medium (DMEM) supplemented with F12 (DMEM/F12) and 10% fetal calf serum (FCS) for 11–13 days. Following the original protocol (de Vellis and Cole, 2012; Rosato-Siri et al., 2018), MG cells were obtained by differential centrifugation and plated on uncoated surfaces, suitable for the subsequent assay (**Figure 1**). MG cells culture purity (CD11b positive cells) was checked regarding neuron, oligodendrocytes and astrocytes contamination by NeuN, O4, and GFAP ICC, respectively, rendering 98% pure MG cells cultures (data not shown).

MG Cell Treatments

MG cells were cultured maintaining DMEM/F12 + 10% FCS and, 48 h after plating, media were changed to DMEM/F12 + 10% FCS (Control) or DMEM/F12 + 10% FCS and the corresponding treatment. Two culture contexts were evaluated: lipopolysaccharide challenge (LPS) (Landoni et al., 2010) and heat shock exposure (HS) (Sugimoto et al., 2014) (**Figure 1** and **Table 1**).

BrdU Incorporation

BrdU (10 μM) was added concomitantly with treatments (**Figure 1**, red arrows).

Immunofluorescence Assay

Immunocytochemistry (ICC) was performed as previously described (Rosato-Siri et al., 2018). Briefly, covers were washed with phosphate buffered saline (PBS), permeabilized (PBS + 0.1% Triton X-100 + 5% FCS) for 3 h and sequentially exposed to primary antibodies (PBS + 0.1% Triton X-100 + 1% FCS) and secondary antibodies (PBS + 0.1% Triton X-100 + 1% FCS) (**Table 2**). BrdU was incorporated before the ICC protocol by incubated cells in a 2 N HCl solution for 30 min at room temperature and subsequent washes with 100 mM buffer borate, pH 8.5. No immunolabeling was detected when primary antibodies were omitted.

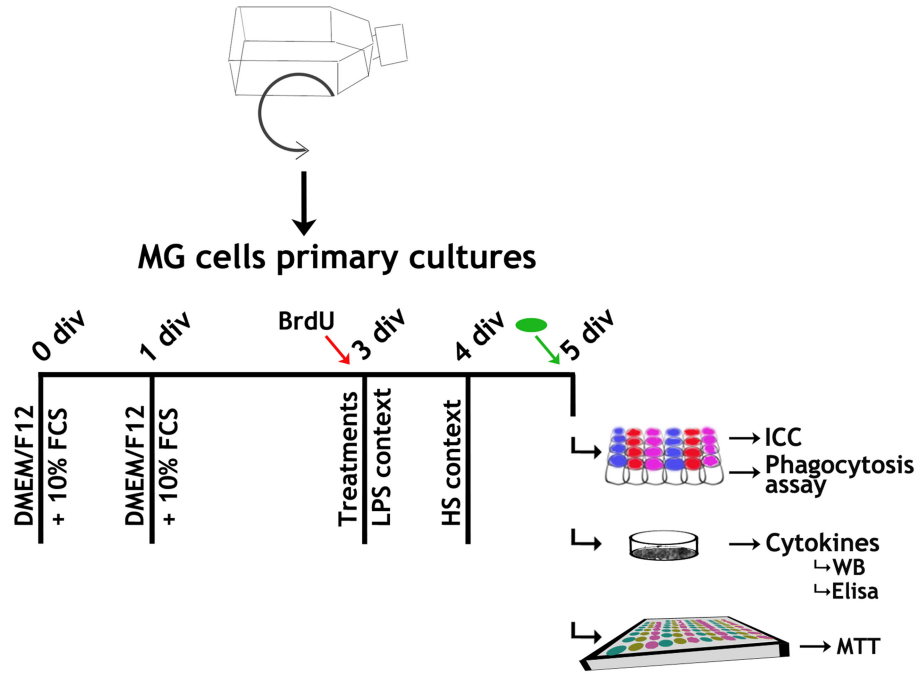

FIGURE 1 | Experimental design. Brains from P0-1 pups born to Wistar rats were dissected and plated on T75 polylysinated flasks. Microglial (MG) cells were harvested by 2 h shaking at 37°C. MG cells were plated either on uncoated coverslips placed in a 24-well plate (7×10^3 cells/well) for ICC and phagocytosis assays, 96-well plate (2×10^4 cells/well) for MTT assays, or 25 mm ø/ Petri dishes (7×10^5 cells/dish) for cytokine quantification, and cultured in Dulbecco's Modified Eagle's medium supplemented with F12 (DMEM/F12) and 10% FCS for 24 h, when medium was changed to remove non-attached cells. At 3 *div*, medium was replaced by the corresponding Stx2 incubation and LPS context applied concurrently with BrdU incorporation (red arrow) where appropriate. At 4 *div*, HS context was applied. At 5 *div*, where applicable, FITC-yeast conjugated incubation (green oval) was performed before fixation. Cultures suitable for ICC and phagocytosis assays were fixed by cold 100% methanol incubation (30 min, −20°C) and washed twice with PBS. On the other hand, for MTT assays and cytokine quantifications, cultures were washed with PBS without fixing.

TABLE 1 | Experimental groups.

Culture contexts	**Control**	**LPS**	**HS**	**LPS + HS**
Stx2 concentration range	**Stx2 (ng/ml)**			
	1	**10**	**100**	**1,000**
Treatments	Stx2 100 ng/ml W/O	Stx2 100 ng/ml +LPS	Stx2 100 ng/ml +HS	Stx2 100 ng/ml +LPS + HS
	Stx2B 100 ng/ml (W/O)	Stx2B 100 ng/ml +LPS	Stx2B 100 ng/ml +HS	Stx2B 100 ng/ml +LPS +HS

MG cell behavior was initially evaluated in four culture contexts: Control, LPS, HS, and LPS + HS. In order to evaluate toxin uptake, Stx2 concentration range (1, 10, 100, and 1,000 ng/ml) was assayed. Given that Stx2 100 ng/ml was the concentration condition for which toxin detection was most clearly positive regardless of culture context, effects on toxin uptake were compared at this concentration from here onwards. LPS: 500 ng/ml of lipopolysaccharide was added together with Stx2/Stx2B to culture media. HS: MG cultures were exposed to 42°C for 30 min. W/O: without context. Stx2B was a generous gift from Dr. Mariano Enrique Fernandez-Miyakawa (Instituto de Patobiología, CNIA-INTA).

Microscopy and Image Analysis

Digital images were acquired either with an epifluorescence Olympus BX50 microscope equipped with a CoolSnap digital camera or with a confocal Olympus FV1000 microscope.

Quantification Strategies: FIJI Software Was Used Throughout

Incorporated Stx2 or Iba1 expression: images were subjected to Image<Color<Split Channels, and "Wand tool" was used to select the corresponding marker. "Threshold tool" and Shanbhag or Triangle algorithm, were used to determine fluorescent values expressed as integrated optical density (IOD) average. For Iba1 plot, the control value was subtracted from the treatment ones.

Cytokines in WB membranes: images were converted to 8-bit Image<Type<8-bit. "Rectangle tool" was used to select each band surface. "Wand tool" was used to measure histogram areas under the curve. Values were referred to those of β-actin.

Irregular nuclei: a criterion was used to determine normal and irregular nuclei. Round nuclei were regarded as normal, while all nuclei phenotypes different from this were considered

TABLE 2 | ICC working antibody dilutions.

ICC markers	Catalog number	Dilution	Secondary antibodies (1:500)
Anti-Stx2	**	1:500	Anti-Rb Alexa 488
Anti-CD11b	CBL1512 (Millipore)	1:500	Anti-Mo Alexa 647
Anti-Iba1	Ab5076 (Abcam)	1:250	Anti-Gt Cy3
Anti-Gb3	357102 (BioLegend)	1:200	Anti-Mo Alexa 488
Anti-BrdU	11170376001 (Sigma)	1:500	Anti-Mo Alexa 488

***Anti-Stx2 was a generous gift from Dr. Mariano Enrique Fernandez-Miyakawa. Hoechst dye was added together with the secondary antibody solution. Secondary antibodies were purchased from Jackson ImmunoResearch.*

TABLE 3 | WB working antibody dilutions.

WB markers	Catalog number	Dilution
Anti-IL1β, clone B122	sc-12742 (Santa Cruz, Biotech.)	1:1,000
Biotin anti-IFNγ	505803 (BioLegend)	1:1,000
Biotin anti-IL10	554465 (BD Biosciences)	1:500
Biotin anti-TGFβ	555053 (BD Biosciences)	1:500
Anti-β-actin	622101 (BioLegend)	1:500

The corresponding horseradish peroxidase (HRP)-conjugated secondary antibodies were purchased from Jackson ImmunoResearch. Streptavidin-horseradish peroxidase (SAv-HRP) was purchased from BioLegend and used for biotin-tag detection. Loading control: β-actin.

irregular. "Multi-point tool" was used in RGB images to quantify different Hoechst nuclei phenotypes. Values were expressed as percentages.

$BrdU^+$ cells or FITC-yeast: RGB images were combined with Image < Color < Merge channels, Hoechst labeling was assigned to the blue channel and $BrdU^+$ cells or FITC-yeast were assigned to the green channel. Contrast was established to create clear images. "Multi-point tool" was used to quantify events/field. Values were expressed as percentages.

MTT Reduction Assay

3-(4,5-dimethyl-thiazol-2-yl)-2,5-diphenyl-tetrazolium bromide (MTT) reduction assay was carried out according to the protocol described by Mosmann (1983). Measurements were expressed as absorbance at 570 nm of each sample relative to the Control group.

Phagocytosis Assay

MG cells were incubated 15, 30, and 60 min with FITC-yeast conjugated (2.5×10^5 yeast/ml). After incubation, cultures were generously washed with PBS to remove non-phagocytized yeast before fixing (**Figure 1**, green arrows). Data were expressed either as the number of phagocytized yeast/cell or as a phagocytic index,

$$phagocytic\ index = \frac{number\ of\ phagocytic\ cell\ treatment/field}{number\ of\ phagocytic\ cell\ Control/field}$$

Cytokine Expression Levels

Preparation of Lysates From Cell Cultures

The cell suspension was transferred into a microcentrifuge tube, added ice-cold lysis buffer (1 ml per 10^6 cells, 150 mM sodium chloride, 1.0% NP−40, 0.5% sodium deoxycholate, 0.1% SDS, 50 mM Tris, pH 8.0 and protease inhibitor cocktail) and incubated 15 min at 4°C. The suspension was then centrifuged at 4°C (20 min at 12,000 rpm). The supernatants were placed in a fresh tube and Bradford's method was used to determine protein concentration.

Protein Precipitation

The supernatant was mixed with 100% (w/v) trichloroacetic acid (relation 4:1), incubated for 10 min at 4°C and centrifuged for 5 min at 14,000 rpm. The supernatant was then removed and washed three times in cold acetone with 5 min centrifugation at 14,000 rpm each time. Finally, the pellet was dried at 95°C for 5 min and re-suspended on sample buffer 2× for SDS-PAGE.

Western Blot Analysis

Cell extracts (50μg protein) were separated by 12% SDS-PAGE and transferred onto nitrocellulose sheets (GE Life Sciences). After transfer, non-specific binding sites were blocked with 3% BSA in 30 mM Tris, 0.14 M NaCl, 0.1% (v/v), Tween 20, pH 8.0 for 1 h at room temperature with shaking. Specific antibodies were incubated at 4°C overnight (**Table 3**).

ELISA

The supernatant cytokine levels were measured by ELISA BD OptEIA kit (BD Biosciences, 559603 and 555138) according to the manufacturer's instructions.

Statistical Analysis

Data ($n = 9$, independent cultures) were subjected to non-parametric tests suitable for normally distributed populations. Statistical analysis was performed using one-way ANOVA followed by different post-tests (GraphPad Prism, GraphPad Software Inc.). The corresponding replicates for consistency, *p*-values and post-tests are provided in each figure legend.

RESULTS

MG Uptake of Stx2 Depends on Toxin Concentration and Culture Contexts

MG cell behavior was initially evaluated in four culture contexts: Control, LPS, HS, and LPS + HS. CD11b detection, a marker for all types of sensing and responsive MG cell phenotypes, showed that neither viability nor survival were affected in 98% pure MG cell cultures in any context assayed (**Figure 2A**). MG cells were incubated in a Stx2 concentration range (1, 10, 100, and 1,000 ng/ml) in order to evaluate toxin uptake. Stx2 immunodetection was clearly positive in $CD11b^+$ cells incubated with 100 and 1,000 ng/ml (**Figure 2B**) but weakly positive and negative when MG cells were incubated with 10 ng/ml and 1 ng/ml (data not shown), respectively. In addition, the Stx2 concentration range was evaluated in two culture contexts. Interestingly, Stx2 uptake at 10 ng/ml turned out to be positive in LPS and HS as compared to Stx2 incubation without (W/O) context, while Stx2 uptake at 1 ng/ml was only positive in HS. Stx2 uptake at 100 ng/ml and 1,000 ng/ml increased in both contexts tested as compared to incubations W/O context (**Figure 2C**). Given that Stx2 100 ng/ml was the concentration

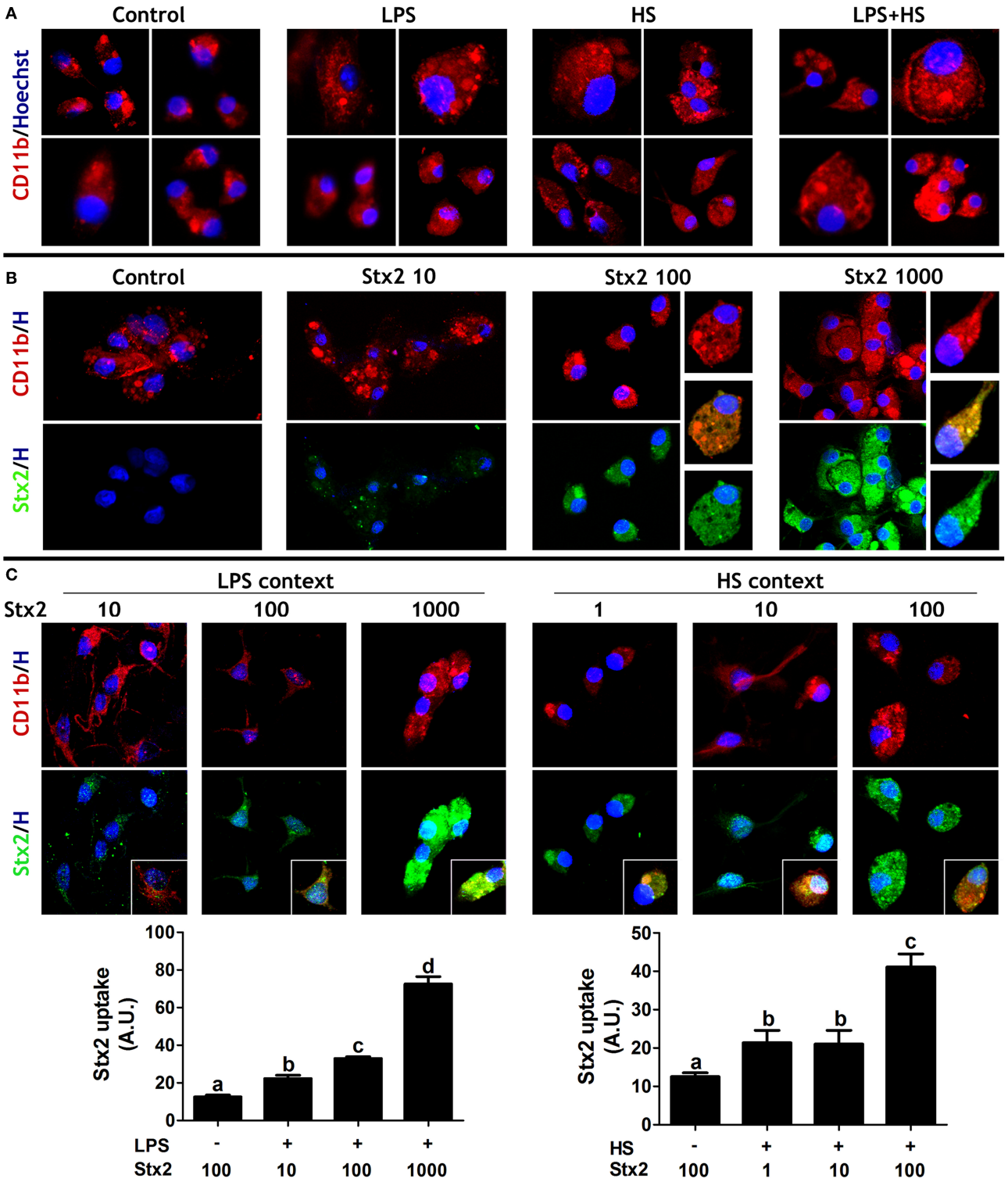

FIGURE 2 | MG cell culture contexts and Stx2 uptake. **(A)** MG cells behavior was evaluated in different contexts: Control, LPS, HS, or LPS + HS. **(B)** Stx2 uptake was evaluated upon different toxin concentrations (1, 10, 100, or 1,000 ng/ml). **(C)** Stx2 uptake was also evaluated and quantified in LPS and HS contexts. Significant differences are indicated by different letters (a–d, $p < 0.05$). Bonferroni's *post-hoc* test $n = 5$, replicates = 3. CD11b (red) and Stx2 (green) ICC showed MG cells specific uptake of Stx2. Insets: Higher magnifications of double positive cells (merge images).

condition for which toxin detection was most clearly positive regardless of culture context, effects on toxin uptake were compared at this concentration from here onwards.

MG Cell Activation Increases With Stx2 and Challenged Culture Contexts

Ionized calcium-binding adaptor protein1 (Iba1) is an actin-binding protein constitutively and specifically expressed in all MG cells while activated MG cells are associated with increased Iba1 expression (Imai et al., 1996; Sasaki et al., 2001). MG cell activation status was determined by Iba1 immunofluorescence in the contexts previously described. Iba1 expression levels were increased in both LPS and HS, taken together or separately in comparison with Control (**Figures 3A,C**). MG cell activation was also evaluated upon Stx2 at 100 ng/ml incubation. Toxin *per se* produced an increase in Iba1 expression levels in comparison with Control. This increase was significantly more evident when cultures were exposed to Stx2 and LPS or HS and showed a synergistic effect when LPS + HS were applied (**Figure 3B**, upper panel and **Figure 3C**). In addition, Stx2 uptake quantification at 100 ng/ml verified the qualitative increase observed in culture contexts (**Figure 2B**). Interestingly, toxin uptake was markedly increased in LPS + HS (**Figure 3B**, lower panel and **Figure 3C**).

MG Cell Metabolic Activity Increases With Stx2 and LPS-Challenged Culture Contexts

To further describe MG cell behavior, cytological, and metabolic features were evaluated concurrently with culture conditions. Nuclear morphology was typified considering shape, size, cellular location, and staining intensity. Normal nuclei were round with a defined edge, often centrally located and with homogenous Hoechst fluorescence staining. In contrast, irregular nuclei were larger and not round, exhibiting peripheral location and diffuse Hoechst staining (**Figure 4A**, yellow arrows). Only Stx2 + LPS and Stx2 + LPS + HS showed an increase in the mean number of irregular nuclei (**Figure 4A**), in addition to a Höechst-positive

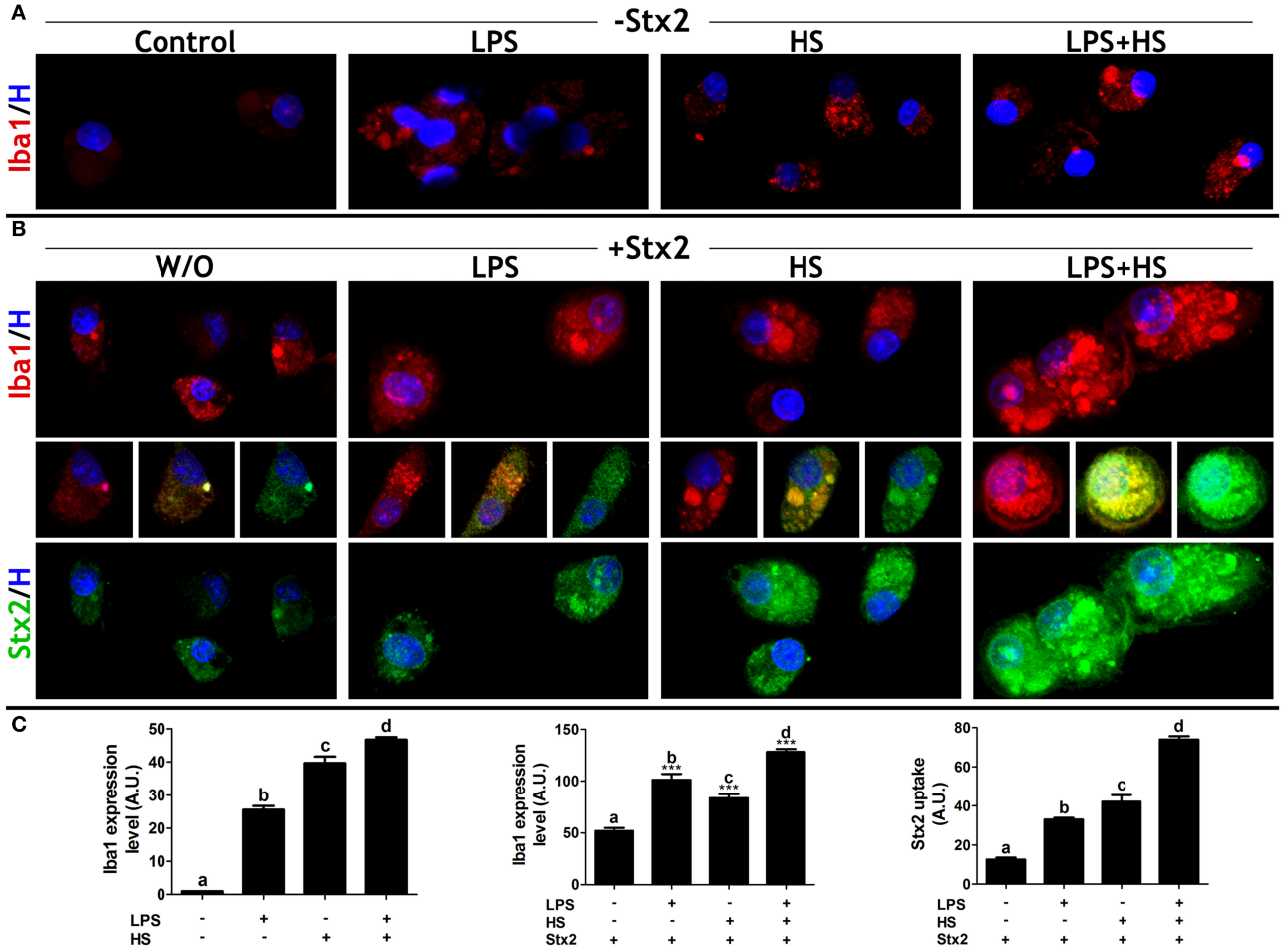

FIGURE 3 | MG responsiveness and Stx2 uptake. **(A)** Iba1 ICC in MG cells cultured in different contexts. **(B)** Iba1 expression level (upper panel) and Stx2 uptake (lower panel) by ICC in MG cells exposed to Stx2 100 ng/ml. Middle images: merged Iba1, Stx2, and Hoechst labels. **(C)** Iba1 expression level and Stx2 uptake quantifications. Significant differences are indicated in comparison with Control (a–d, $p < 0.05$) or in comparison with Stx2 W/O context (***$p < 0{,}001$). Bonferroni's *post-hoc* test; $n = 5$; replicates = 3.

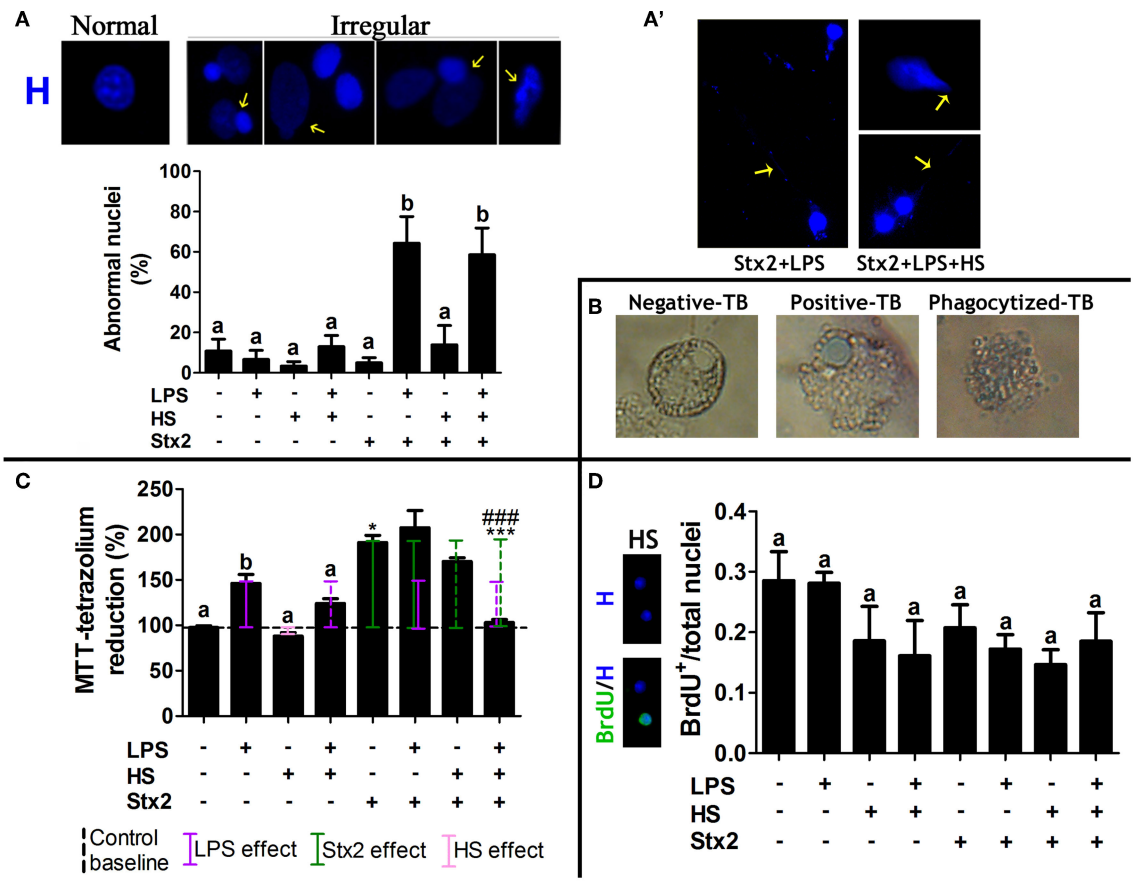

FIGURE 4 | MG cell cytological and metabolic features. **(A)** Quantification of irregular nuclei phenotype (yellow arrows). Significant differences are indicated by different letters in comparison with Control ($p < 0.05$). Bonferroni's *post-hoc* test. $n = 5$; replicates = 5. **(A')** Extra-cellular trap-like structure (ET-LS) was only observed in Stx2 + LPS and Stx2 + LPS + HS. **(B)** TB staining (1:1 dilution of the cell suspension and a 0.4% Trypan Blue solution). **(C)** MTT assay. Significant differences are indicated as follows: a and b, between context effects and Control ($p < 0.05$); * between Stx2 W/O context and Control ($p < 0.05$); *** between Stx2 + LPS + HS and all the other Stx2 incubations ($p < 0.001$), and ### between Stx2 + LPS + HS and Stx2 + LPS ($p < 0.001$). Newman-Keuls's *post-hoc* test; $n = 5$; replicates = 12. **(D)** BrdU-positive nuclei quantification showed no significant differences across contexts; Bonferroni's *post-hoc* test; $n = 4$; replicates = 3.

configuration resembling extra cellular trap-like structures (ET-LS) (**Figure 4A'**).

The Trypan blue (TB) viability assay was performed to evaluate cell death. Three different situations regarding TB staining were observed, i.e., negative and positive nuclear staining, and a third staining corresponding to phagocytized TB (**Figure 4B**); the latter, would be recorded as a positive stain if TB intracellular localization had not been considered. Phase contrast images showed no significant differences of TB-positive nuclear staining across groups (data not shown). Unlike HS, LPS alone increased the MTT score (**Figure 4C**, solid violet line) as compared to Control (**Figure 4C**, dashed black line). Stx2 also significantly increased the MTT score over Control (**Figure 4C**, solid green line). Interestingly, opposite effects were observed when Stx2 exposure was compared either in LPS or HS context. Although no significant, a modest increase was observed in Stx2 + LPS condition while a decrease was detected in Stx2 + HS one. A sharper synergic effect was observed in Stx2 + LPS and Stx2 + HS as compared to LPS and HS, respectively. Surprisingly, Stx2 + LPS + HS showed an attenuated effect (**Figure 4C**, dashed violet and green lines). Finally, $BrdU^+$ nuclei quantification corroborated that MTT findings were associated with metabolic activity (Gerlier and Thomasset, 1986) rather than cell viability (**Figure 4D**).

Subcellular Presence and Distribution of Stx2 Receptor Gb3 Depend on Culture Contexts

Gb3 presence and subcellular distribution were determined by ICC. Depending on MG cell culture context, Gb3 expression showed three clearly distinguishable distribution patterns: perinuclear in Control, vesicular in LPS and on the cell membrane in HS (**Figure 5**, double red arrows, single red arrow, and red arrowhead, respectively). In turn, LPS + HS showed Gb3 vesicular and cell surface coexistence (**Figure 5**, single red arrow and red arrowhead).

MG cell incubation with Stx2 alone rendered double immunofluorescence, which indicates that there is a Stx2 uptake

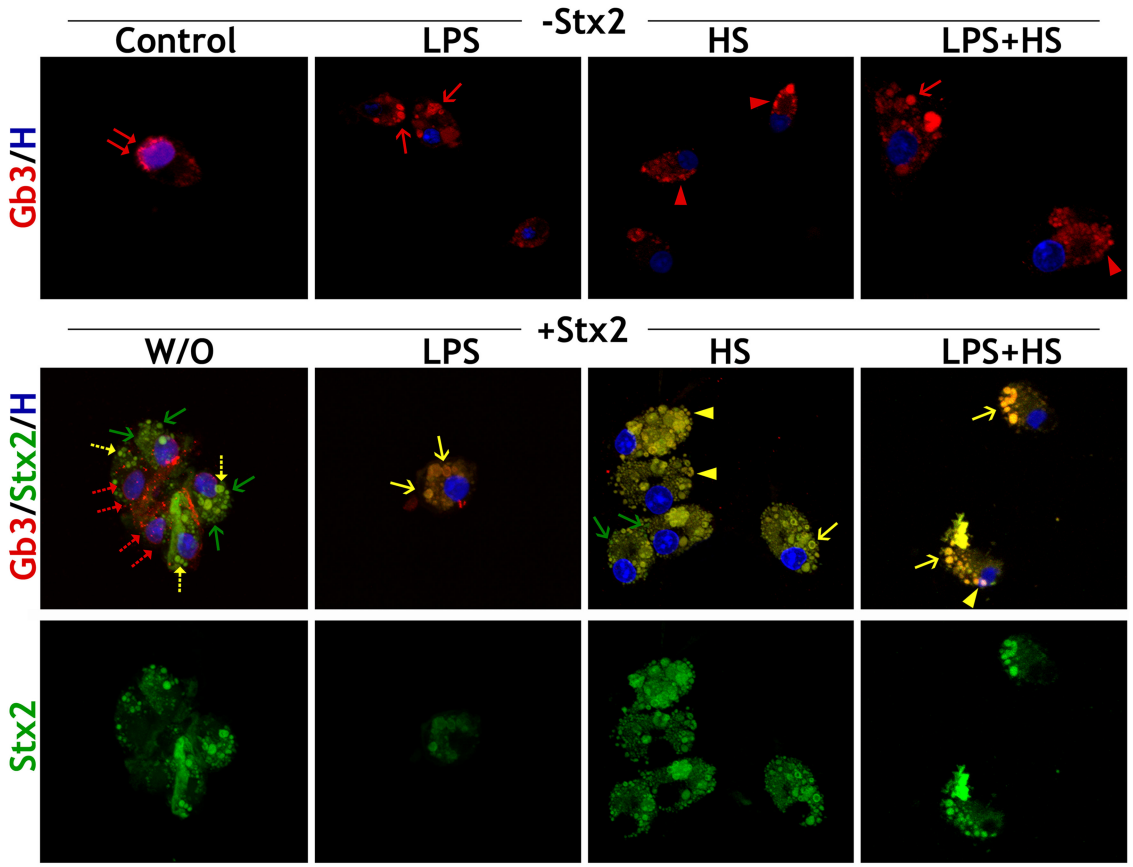

FIGURE 5 | MG cell Gb3 distribution pattern. Stx2 and Gb3 detection by ICC in different culture contexts (LPS, HS, LPS + HS), Control and Stx2 100 ng/ml incubations W/O and with contexts. Merge of Gb3/Stx2/Hoechst labeling. Double red arrows: perinuclear location of Gb3; single red arrows: vesicle location of Gb3; red arrowheads: membrane location of Gb3; single green arrows: toxin vesicles without Gb3; single yellow arrows: vesicle location of Stx2 + Gb3; yellow arrowheads: membrane location of Stx2 + Gb3. Dotted-arrows represent specific distribution reductions. $n = 4$, replicates = 3.

that seems to be independent of Gb3 binding (**Figure 5**, single green arrow) along with a Gb3-dependent uptake depicted by a few double immunofluorescence vesicles (**Figure 5**, single yellow dotted-arrow). In addition, Gb3 perinuclear distribution was reduced upon Stx2 exposure (**Figure 5**, double red dotted-arrow) in comparison with Control condition. In contrast, the Gb3 canonical pathway underlay most of the Stx2 uptake in LPS, HS, and LPS + HS, as double immunolabeling matched the specific pattern characterizing each context: only large vesicular arrangement for LPS condition, clusters localized in nearby cell surface for HS condition and a combination of both patterns when LPS and HS were applied (**Figure 5**, single yellow arrow and arrowheads).

MG Cells Behave Similarly Upon Stx2 and Stx2B Exposure

As part of the Stx family, Stx2 has an AB5 structure in which a single subunit A is associated with five subunits B. Subunit A represents the catalytic activity while the B-pentamer (Stx2B) is the binding site of the Stx2-Gb3 receptor (Fraser et al., 2004). Recombinant Stx2B (Parma et al., 2011) was used to compare its biological effects on MG cells with the Stx2 one. Iba1 expression levels equally increased in both Stx2- and Stx2B-incubated MG cells, with or W/O context. Once again, MG cell responsiveness was significantly more evident when cultures were exposed to Stx2B and LPS, HS, or LPS + HS (**Figure 6A**, left panel). Environmental cues tuned up Stx2B uptake in the same manner as for Stx2; accordingly Stx2B uptake quantification showed significant increments when cultures were exposed to Stx2B and LPS, HS, or LPS + HS contexts. Interestingly, no significant differences were observed comparing Stx2 and Stx2B in the same context (**Figure 6A**, right panel). Gb3 distribution pattern in the presence of Stx2B was similar to that observed in the presence of Stx2, both with and W/O context conditions (**Figure 6A**, lower panel). However, Stx2B MTT score was significantly lower than that of Stx2 incubation W/O context. In addition, when MG cells were incubated with Stx2B in LPS and HS, MTT values showed a diminishing tendency as compared to Stx2 incubation in the same contexts, reaching a significant decrease in LPS + HS (**Figure 6B**). Finally, BrdU incorporation (**Figure 6C**) and Trypan blue assays (data not shown) showed non-significant differences between groups.

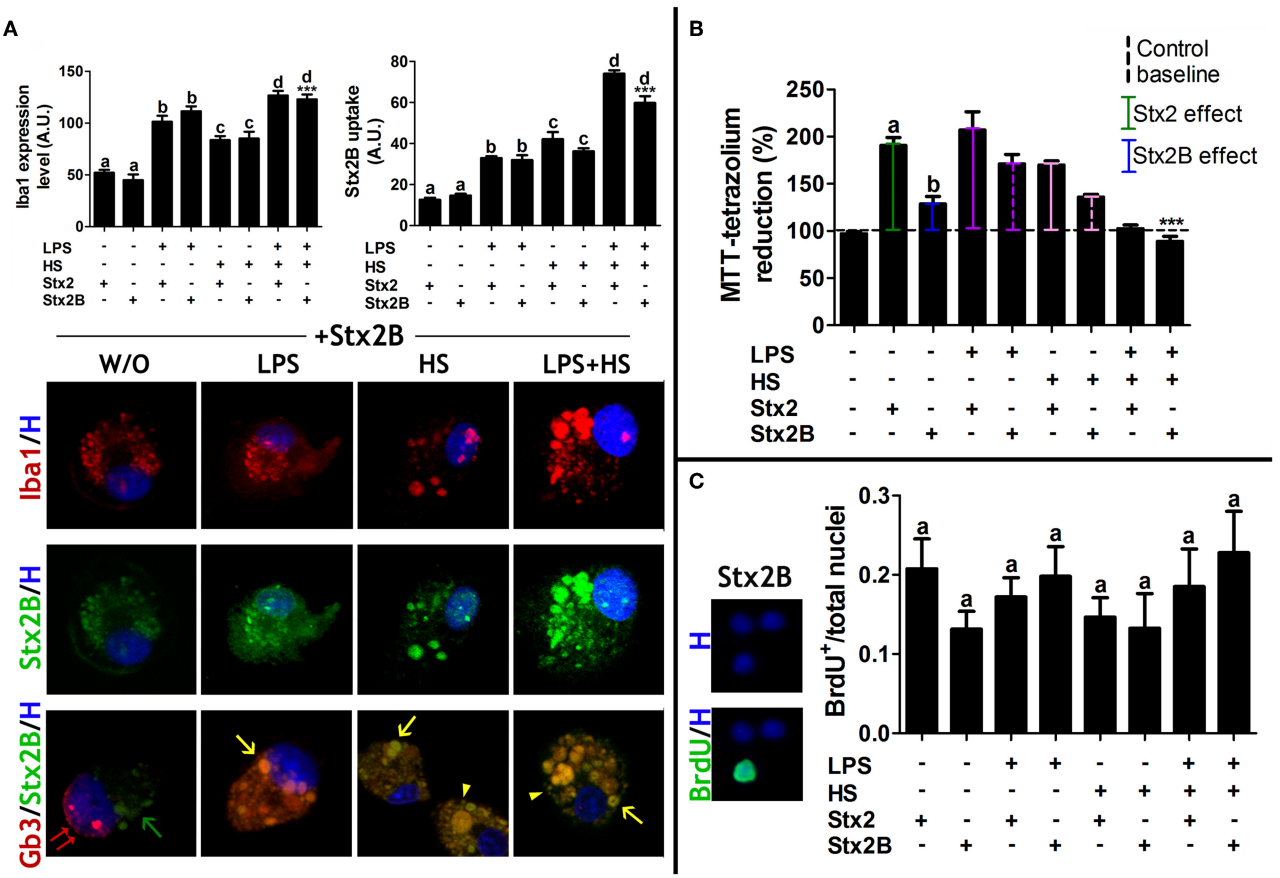

FIGURE 6 | MG cell responsiveness and Stx2B uptake. **(A)** Iba1 expression level and Stx2B uptake quantifications in MG cell cultures. Lower images: merge of Gb3/Stx2B/Hoechst labeling. Double red arrows: perinuclear location of Gb3; single green arrows: toxin vesicles without Gb3; single yellow arrows: vesicle location of Stx2B + Gb3; yellow arrowheads: membrane location of Stx2 + Gb3. Significant differences are indicated by different letters comparing Stx2 and Stx2B in the same context (a: W/O context, b: LPS, c: HS, d: LPS + HS; $p < 0.05$). Significant differences in comparison with Stx2B, Stx2B + LPS and Stx2B + HS (***$p < 0.001$). Bonferroni's *post-hoc* test; $n = 4$; replicates = 4. **(B)** MTT assay. Significant differences between Stx2 and Stx2B (a and b, $p < 0.05$). Newman-Keuls's *post-hoc* test; $n = 5$; replicates = 12. **(C)** BrdU-positive nuclei quantification showed no significant differences across contexts. Bonferroni's *post-hoc* test; $n = 4$; replicates = 3.

MG Cell Phagocytic Profile Is Independent of Stx2 Catalytic Subunit

MG cell activity was described through a phagocytosis assay. MG cells were incubated 15, 30, and 60 min with FITC-yeast conjugated in order to determine the phagocytic kinetics and the saturation point. Comparing Control and context conditions, differences in the maximum phagocytized yeast were most evident after 30 min incubation (**Figure 7A**). Following 30 min incubation, the frequency distribution in the number of phagocytized yeast/cell showed that all treatments increased in comparison with Control, being LPS condition the higher one. In addition, both Stx2 and Stx2B incubations increased the number of phagocytized yeast/cell in comparison with Control group but showed similar results to each other (**Figure 7B**). The phagocytic index showed that toxin incubation alone seem to have no profound effect on phagocytic efficiency. Remarkably, context challenges strongly tuned up toxin, holo, and B-subunit, effects by increasing MG cell phagocytic efficiency, as more MG cells/field were actively engaged in the process. Interestingly, the increase triggered by LPS on Stx2 effect was attenuated when HS was combined with them (**Figure 7C**).

MG Cell Pro-Inflammatory Profile Is Positively Dependent on Stx2 Incubation and Challenged Culture Contexts

Cytokine profiles were evaluated either by WB, to detect cytokine expression levels on cellular fractions (**Figure 8A**), or by ELISA, to determine cytokine release on culture supernatants (**Figure 8B**). As expected, the LPS context showed a pro-inflammatory profile, increasing IL1β and IFNγ synthesis and release. Stx2 and Stx2B incubation W/O context also increased IL1β synthesis and release, whereas only Stx2 increased IFNγ release. IFNγ synthesis was undetectable under Stx2 or Stx2B exposure (data not shown). Interestingly, Stx2 + LPS exhibited a synergic effect on IL1β expression levels, but both IL1β and IFNγ release showed no significant differences with Stx2 alone. HS increased IL1β and IFNγ release in comparison with Control, although the cytokine pro-inflammatory profiles triggered by

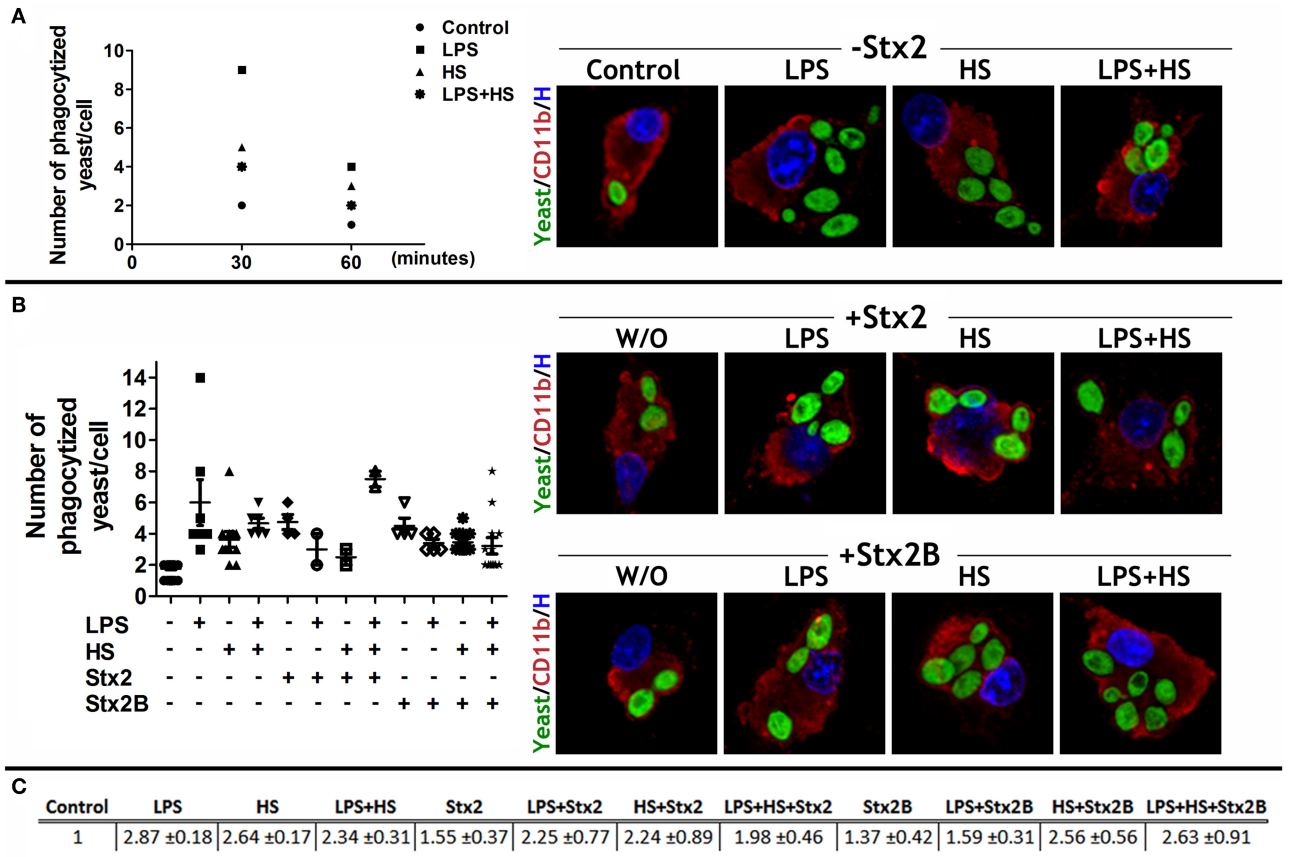

C

Control	LPS	HS	LPS+HS	Stx2	LPS+Stx2	HS+Stx2	LPS+HS+Stx2	Stx2B	LPS+Stx2B	HS+Stx2B	LPS+HS+Stx2B
1	2.87 ±0.18	2.64 ±0.17	2.34 ±0.31	1.55 ±0.37	2.25 ±0.77	2.24 ±0.89	1.98 ±0.46	1.37 ±0.42	1.59 ±0.31	2.56 ±0.56	2.63 ±0.91

FIGURE 7 | MG cell phagocytic profile. **(A)** The phagocytic kinetics was determined in MG cells cultured in LPS, HS, and LPS + HS contexts by incubating them with FITC-yeast conjugated for 15, 30, and 60 min. Fifteen-min incubation was not sufficient to bring about significant differences across treatments but 30 min incubation displayed stark differences. **(B)** MG cells challenged with Stx2 or Stx2B and specific culture context were incubated for 30 min with FITC-yeast. Data are expressed either as the number of phagocytized yeast/cell or **(C)** as a phagocytic index ($p < 0.05$). Bonferroni's *post-hoc* test; $n = 4$; replicates = 4.

LPS and Stx2 exposures were attenuated when HS was combined with them. None of the treatments tested showed detectable levels of anti-inflammatory cytokines IL10 and IL6 (data not shown).

DISCUSSION

MG cells, with a mesodermal/mesenchymal developmental origin, are considered CNS resident macrophages. MG cells constitute the most reliable environmental sensors in the brain and "resting" MG cells status seems somewhat a misnomer since they stand for a continuous sensing state. Upon the detection of a variety of CNS dysfunctions, MG cells undergo a complex, multistage activation process that converts them into an activated status (Kettenmann et al., 2011). Pathogenesis of CNS during the acute phase of HUS is known to correlate with brain-blood-barrier disruption, neuronal disturbances and astrogliosis (Pinto et al., 2017), although less is known so far about MG cell behavior and their role in the events observed in these CNS complications.

The present work explored the capacity of MG cells to uptake different concentrations of Stx2 and Stx2B in different contexts: HS, LPS, and LPS + HS. In addition, the Gb3 canonical pathway for holotoxin uptake was analyzed comparing the biological response of MG cells to either Stx2 or Stx2B. Finally, MG cell activation, metabolic activity, phagocytic profile, and cytokine release were further analyzed in the different contexts.

MG cell sensitivity, described by intracellular Stx2 quantification, was much higher in HS than in LPS. Moreover, MG cells were so sensitive in HS that low toxin concentrations brought about Stx2 uptake. Interestingly, MG cell responsiveness depicted by activated MG marker Iba1 expression was increased in the three contexts evaluated upon Stx2 exposure. As reflected by the expression of Iba1, Stx2, and also Stx2B succeeded in activating MG cells in all contexts. However, this activated state only coincided with increased metabolic activity rather than proliferative status when these cells were treated with Stx2 in LPS, but not when MG cells where incubated with Stx2B in the same context. In addition, pro-inflammatory cytokine expression levels were equally increased by Stx2 and Stx2B incubations, although their release seemed to be dependent on the holotoxin effect. Therefore, it can be inferred that metabolic activity and cytokine release depend on the holotoxin, where the catalytic and

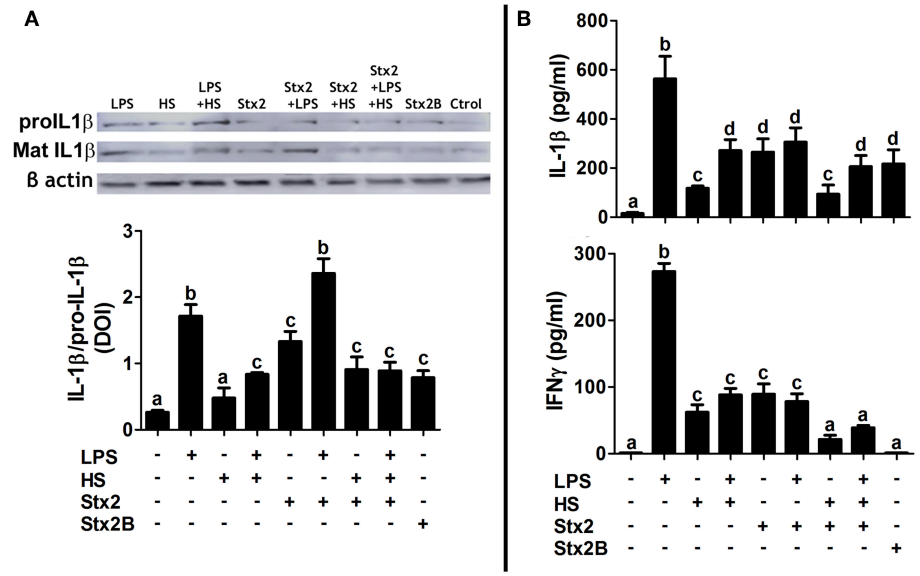

FIGURE 8 | MG cell cytokine profile. **(A)** IL1β expression levels quantified by WB on cellular fractions. Pro IL1β: IL1β not active. Mat IL1β: cleaved and active IL1β. Data are expressed as mean IOD ± SEM relative to β-actin detection. **(B)** ELISA on culture supernatants to quantify IL1β and IFNγ release. Significant differences are expressed as different letters (a–d, $p < 0.01$). Dunnett's multiple comparison *post-hoc* test; $n = 3$; replicates = 2.

binding subunit—Stx2B—are integrated. On the other hand, our results confirm that B-pentamer is responsible for Stx2 uptake in MG cells, noting that environmental cues modified Stx2B effect in the same manner as for Stx2.

In being reactive to Stx2, MG cells could play a pivotal role in inflammatory mechanisms underlying cellular damage associated with neurological dysfunctions. In fact, previous work has demonstrated the role of MG cells in system homeostasis through a physiological balance of pro-inflammatory and anti-inflammatory profiles (Sirerol-Piquer et al., 2019); thus, a shift toward a pro-inflammatory profile correlates with physiological and system damage. Under the present acute experimental conditions, toxin incubation triggered a pro-inflammatory profile in terms of IL1β and IFNγ synthesis and release, with a sharper effect when the catalytic subunit was present. In addition, environmental cues tuned up Stx2 effect: on the one hand, LPS context increased pro-inflammatory cytokine synthesis. On the other hand, HS treatment softened MG cells activation, even though a pro-inflammatory profile remains. It is worth mentioning that the two techniques used to determine cytokine synthesis and release, WB and ELISA, respectively, show different threshold sensitivity, the latter allowing for easy detection of cytokines on supernatants as compared to the corresponding protein product. Bearing in mind that IFNγ concentrations were under 300pg/ml, it is reasonable to infer that its synthesis was undetectable by WB.

The present work also demonstrates, for the first time, that MG cells exhibit both a Gb3-independent and Gb3 canonical pathway for Stx2 uptake. Our results seem to be in line with Johannes review (Johannes, 2017), which reported toxin clustering on the plasma membrane as well as receptor binding and intracellular trafficking by endocytic carriers for the Gb3 canonical pathway. Stx2 has been seen associated with clathrin-coated pits (Sandvig et al., 1989) but, even though clathrin function was proficiently inhibited, a 75% of Shiga toxin uptake remained intact (Lauvrak et al., 2004). In addition, the present results agree and elaborate on those obtained by Griener et al. (2007), where human neutrophils exhibited Gb3-independent Stx2 uptake, murine neutrophils showed the classical Gb3-dependent Stx2 uptake, and MG cells showed both Stx2 uptake pathways. A recent work by Brigotti et al. (2018) has beautifully confirmed that toll-like receptor 4 (TLR4) is mainly responsible for Stx2 interaction on neutrophil membrane. TLRs are receptors expressed by cells with an innate immune profile, such as MG cells, which are stimulated by pathogen-associated molecular patterns (PAMPs), including LPS. Most importantly, LPS/TLR4 signaling triggers the expression of pro-inflammatory cytokines (Lu et al., 2008). This pathway has been proved that MG cell activation underlies neuro-degenerative mechanisms (Jiang et al., 2016) and even linked CNS effects and systemic inflammation (Zhou et al., 2019). Bearing this in mind, we observed that Gb3-independent Stx2 uptake was no longer detectable in LPS context.

MG cells are specialists in phagocytosis, and the current work shows an increase in their phagocytic efficiency upon toxin exposure. Moreover, as Stx2B also yielded phagocytic properties, phagocytosis appeared to be independent of the Stx2A catalytic subunit. Environmental conditions, by themselves, have positively changed MG cells phagocytic performance and also emphasized toxin effect, Stx2 and Stx2B, since MG cell engagement to a phagocytic profile was increased when LPS was applied. On the contrary, HS treatment attenuated MG cells phagocytic profile when combine with LPS. Phagocytic

status is not only an activated MG cell feature but also a spillover effect to regulate system homeostasis, conferring MG cells a neuroprotective function through dying cells clearance, preventing pro-inflammatory and neurotoxic molecules events (Hamzei Taj et al., 2016; Wolf et al., 2017; Janda et al., 2018). It has been showed that MG cells phagocytosis impairment worsens Alzheimer Disease pathology (Noda and Suzumura, 2012). In this regards, previous results have revealed cellular deleterious effects by STEC and LPS actions, the presence of Stx2 in abnormal-phenotype neurons and neuronal damage which correlate with MG cells reactivity (Goldstein et al., 2007; Pinto et al., 2018; Berdasco et al., 2019). Former and present results build up one another showing that phagocytic MG cells correlated either with MG cells clearance function of Stx2-induced debris or Stx2 direct effect.

Several report shave established that cell nuclei can display diverse morphologies which correlate with functions and specific cell processes, for example, chromatin remodeling correlating with neutrophil activation steps (Carvalho et al., 2015). Interestingly, nuclear reshaping has been observed in macrophages in response not only to environmental conditions but also to *Bacillus anthracis* edema toxin (Trescos et al., 2015), although macrophage functionality was unaltered. Mosser and Edwards (2008) established a link between nucleus remodeling with an increase cellular plasticity to change between roles since readily deformable nucleus facilitates transcriptional regulation (Skinner and Johnson, 2017). To our knowledge, no similar data have been reported thus far on MG cells. Worth highlighting, irregular nuclei morphology in the current work was observed only when MG cells were incubated with Stx2 in challenged culture conditions.

ETs have been recently recognized as a defense mechanism in several types of innate immune cells and have been described in eosinophils (Yousefi et al., 2012; Geering et al., 2013), neutrophil—NETs (Clark et al., 2007; Yipp et al., 2012) and macrophages—METs (Liu et al., 2014; Kalsum et al., 2017). An intriguing discovery was that both NETs and METs formation overlapped with intact functional cells, hence called vital ETs (Yousefi et al., 2009), which gives ETs a protective rather than a harmful role (Malachowa et al., 2016). In this scenario, ET-LS observed in MG cells upon specific STEC cues demonstrated the feasibility of this particular cell behavior occurrence in MG cells, as far as we know, described for the first time. Last but not least, and even if we are well aware that this cytological observation should be complemented by additional assessments in order to determine ET-LS molecular nature, our data provide novel insights into the matter and thus worth digging into.

In the light of the events observed in this work, it is easily conceivable that Stx2, LPS, and HS effects on MG cell behavior drive STEC consequences in the CNS. Worth pointing out, that Stx2 incubation does not only reflect a physiological feature of STEC infection but also a baseline over the course of the disease when compared to LPS, HS, and LPS + HS. LPS and HS challenges were used to mimic inflammatory reaction and fever, respectively, being the latter a pathophysiological feature which commonly occurs during HUS-associated encephalopathy. Shimizu et al. (2012) have reported high levels of the endogenous pyrogen TNFα in patients with acute encephalopathy during the HUS phase but physiological ones in the absence of encephalopathy during the HUS phase. In addition, the inflammatory profile triggered by STEC in the gut and then replicated in the CNS by MG cells has been mimicked through the LPS context. On early stages of STEC infection, Stx2 had a direct effect on MG cells, as they were capable of toxin uptake. Stx2 itself, increased MG cells responsiveness, metabolic activity, and pro-inflammatory profile. Later on the physiopathology, environmental cues, particularly LPS challenged, increased both MG cells sensitivity, and responsiveness together with an increase of metabolic activity and phagocytic and pro-inflammatory profiles, over and above Stx2 effect. In addition, upon specific STEC cues, MG cells seems to develop nucleus remodeling and ETs like structures, which could be associated with a plastic and adaptive behavior. As HUS phase moves forward, and features gathered, MG cells behavior exhibited some interesting features attributable only to HS context—fever. In this regards, MG cells increased their sensitivity, as they responded even to low toxin concentrations. This observation correlates with HS effect on Gb3 pattern distribution: by changing Gb3 perinuclear distribution to a clustering localization in nearby the cell surface, even in Stx2 absence, the receptor availability was increased and consequently, cell competence to toxin uptake too. In addition, MG cells metabolic activity and pro-inflammatory profile were attenuated. More important, MG cell phagocytosis was also softened. This fact might well be read as an impairment in MG cells capacity to restore system homeostasis, leading toward HUS-associated encephalopathy.

These findings underscore MG cells pivotal role in inflammatory processes observed in clinical HUS encephalopathies and make inroads into the development of future therapeutic strategies which deserve further investigation.

DATA AVAILABILITY STATEMENT

The raw data supporting the conclusions of this manuscript will be made available by the authors, without undue reservation, to any qualified researcher.

ETHICS STATEMENT

The animal study was reviewed and approved by Institutional Review Board at Buenos Aires University Council of Animal Care and in accordance with the National Institutes of Health Guide for the Care and Use of Laboratory Animals. Animal protocols were approved by the School of Medicine Committee on Ethics and Animal Research (CICUAL Number: 046/2017).

AUTHOR'S NOTE

Hemolytic Uremic Syndrome is an illness caused by bacterium enterohemhorragic *Escherichia coli*, orally acquired by the

ingestion of contaminated food or water or direct transmission. Once inside the gut, this bacterium releases a toxin called Shiga, which is responsible for tissue bleeding and renal failure. Shiga toxin also produces encephalopathies, but little is known about how it leads to neuronal death and whether other brain cells participate in the process. For these reasons, we decided to explore Shiga toxin effects on a particular cell type called microglia. Although less famous than neurons, microglial cells have a crucial role in inflammatory processes inside the brain and are thus probably responsible for the severity of encephalopathies. Our experiments are *in vitro*, which means that we started from a whole rat brain to finally isolate microglial cells and maintain them in a specific culture medium for several days. We then modified culture medium, by adding Shiga toxin for example, and observed that microglial cells have a specific path to incorporate the toxin. Once this happens, these cells increase their metabolism and phagocytic capacity, thus favoring inflammation. These findings make novel inroads in the development of therapeutic strategies with a focus on microglial cells.

AUTHOR CONTRIBUTIONS

CB, JG, and MR-S conceived the experiments. CB and MR-S designed and performed the experiments. MD performed the cytokine expression levels assays. CB, JG, and MR-S analyzed the data. MR-S and JG wrote the paper.

FUNDING

This work was supported by Agencia Nacional de Promoción Científica y Tecnológica (ANPCyT) (PICT-2016-1175) and Universidad de Buenos Aires (UBACyT) (20020160100135BA), Argentina.

ACKNOWLEDGMENTS

The authors were especially grateful to Dr. Alipio Pinto for his helpful insights as well as his willingness to participate in the open discussion of the present work. Stx2B and anti-Stx2 were a generous gift from Dr. Mariano Enrique Fernandez-Miyakawa. We were also grateful to María Marta Rancez for her special dedication and technical assistance.

REFERENCES

Alconcher, L. F., Coccia, P. A., Suarez, A. D. C., Monteverde, M. L., Perez, Y. G. M. G., Carlopio, P. M., et al. (2018). Hyponatremia: a new predictor of mortality in patients with Shiga toxin-producing *Escherichia coli* hemolytic uremic syndrome. *Pediatr. Nephrol.* 33, 1791–1798. doi: 10.1007/s00467-018-3991-6

Ashkenazi, S., Yuhas, Y., Even-Tov, S., Kaminsky, E., and Danon, Y. L. (1994). The effect of shiga toxin and sonicates of *Shigella* isolates from children with neurologic manifestation on neuroblastoma cell lines. *Isr. J. Med. Sci.* 30, 604–610.

Bekri, S., Lidove, O., Jaussaud, R., Knebelmann, B., and Barbey, F. (2006). The role of ceramide trihexoside (globotriaosylceramide) in the diagnosis and follow-up of the efficacy of treatment of Fabry disease: a review of the literature. *Cardiovasc. Hematol. Agents Med. Chem.* 4, 289–297. doi: 10.2174/187152506778520718

Berdasco, C., Pinto, A., Calabro, V., Arenas, D., Cangelosi, A., Geoghegan, P., et al. (2019). Shiga toxin 2 from enterohemorrhagic *Escherichia coli* induces reactive glial cells and neurovascular disarrangements including edema and lipid peroxidation in the murine brain hippocampus. *J. Biomed. Sci.* 26:16. doi: 10.1186/s12929-019-0509-x

Boccoli, J., Loidl, C. F., Lopez-Costa, J. J., Creydt, V. P., Ibarra, C., and Goldstein, J. (2008). Intracerebroventricular administration of Shiga toxin type 2 altered the expression levels of neuronal nitric oxide synthase and glial fibrillary acidic protein in rat brains. *Brain Res.* 1230, 320–333. doi: 10.1016/j.brainres.2008.07.052

Brigotti, M., Arfilli, V., Carnicelli, D., Ricci, F., Tazzari, P. L., Ardissino, G., et al. (2018). Soluble toll-like receptor 4 impairs the interaction of Shiga toxin 2a with human serum amyloid p component. *Toxins* 10:E379. doi: 10.3390/toxins10090379

Carvalho, L. O., Aquino, E. N., Neves, A. C., and Fontes, W. (2015). The neutrophil nucleus and its role in neutrophilic function. *J. Cell. Biochem.* 116, 1831–1836. doi: 10.1002/jcb.25124

Clark, S. R., Ma, A. C., Tavener, S. A., McDonald, B., Goodarzi, Z., Kelly, M. M., et al. (2007). Platelet TLR4 activates neutrophil extracellular traps to ensnare bacteria in septic blood. *Nat. Med.* 13, 463–469. doi: 10.1038/nm1565

de Vellis, J., and Cole, R. (2012). Preparation of mixed glial cultures from postnatal rat brain. *Methods Mol. Biol.* 814, 49–59. doi: 10.1007/978-1-61779-452-0_4

Fraser, M. E., Fujinaga, M., Cherney, M. M., Melton-Celsa, A. R., Twiddy, E. M., O'Brien, A. D., et al. (2004). Structure of Shiga toxin type 2 (Stx2) from *Escherichia coli* O157:H7. *J. Biol. Chem.* 279, 27511–27517. doi: 10.1074/jbc.M401939200

Geering, B., Stoeckle, C., Conus, S., and Simon, H. U. (2013). Living and dying for inflammation: neutrophils, eosinophils, basophils. *Trends Immunol.* 34, 398–409. doi: 10.1016/j.it.2013.04.002

Gerlier, D., and Thomasset, N. (1986). Use of MTT colorimetric assay to measure cell activation. *J. Immunol. Methods* 94, 57–63. doi: 10.1016/0022-1759(86)90215-2

Gianantonio, C. A., Vitacco, M., Mendilaharzu, F., Gallo, G. E., and Sojo, E. T. (1973). The hemolytic-uremic syndrome. *Nephron* 11, 174–192. doi: 10.1159/000180229

Goldstein, J., Loidl, C. F., Creydt, V. P., Boccoli, J., and Ibarra, C. (2007). Intracerebroventricular administration of Shiga toxin type 2 induces striatal neuronal death and glial alterations: an ultrastructural study. *Brain Res.* 1161, 106–115. doi: 10.1016/j.brainres.2007.05.067

Griener, T. P., Mulvey, G. L., Marcato, P., and Armstrong, G. D. (2007). Differential binding of Shiga toxin 2 to human and murine neutrophils. *J Med Microbiol.* 56(Pt 11), 1423–1430. doi: 10.1099/jmm.0.47282-0

Hamzei Taj, S., Kho, W., Aswendt, M., Collmann, F. M., Green, C., Adamczak, J., et al. (2016). Dynamic modulation of microglia/macrophage polarization by miR-124 after focal cerebral ischemia. *J. Neuroimmune Pharmacol.* 11, 733–748. doi: 10.1007/s11481-016-9700-y

Imai, Y., Ibata, I., Ito, D., Ohsawa, K., and Kohsaka, S. (1996). A novel gene iba1 in the major histocompatibility complex class III region encoding an EF hand protein expressed in a monocytic lineage. *Biochem. Biophys. Res. Commun.* 224, 855–862. doi: 10.1006/bbrc.1996.1112

Janda, E., Boi, L., and Carta, A. R. (2018). Microglial phagocytosis and its regulation: a therapeutic target in Parkinson's disease? *Front. Mol. Neurosci.* 11:144. doi: 10.3389/fnmol.2018.00144

Jiang, L., Xu, F., He, W., Chen, L., Zhong, H., Wu, Y., et al. (2016). CD200Fc reduces TLR4-mediated inflammatory responses in LPS-induced rat primary microglial cells via inhibition of the NF-κB pathway. *Inflamm. Res.* 65, 521–532. doi: 10.1007/s00011-016-0932-3

Johannes, L. (2017). Shiga toxin-a model for glycolipid-dependent and lectin-driven endocytosis. *Toxins* 9:E340. doi: 10.3390/toxins9110340

Johannes, L., and Decaudin, D. (2005). Protein toxins: intracellular trafficking for targeted therapy. *Gene Ther.* 12, 1360–1368. doi: 10.1038/sj.gt.3302557

Kalsum, S., Braian, C., Koeken, V., Raffetseder, J., Lindroth, M., van Crevel, R., et al. (2017). The cording phenotype of mycobacterium tuberculosis induces

the formation of extracellular traps in human macrophages. *Front. Cell. Infect. Microbiol.* 7:278. doi: 10.3389/fcimb.2017.00278

Karmali, M. A. (2004). Infection by Shiga toxin-producing *Escherichia coli*: an overview. *Mol. Biotechnol.* 26, 117–122. doi: 10.1385/MB:26:2:117

Kavaliauskiene, S., Dyve Lingelem, A. B., Skotland, T., and Sandvig, K. (2017). Protection against Shiga toxins. *Toxins* 9:44. doi: 10.3390/toxins9020044

Kettenmann, H., Hanisch, U. K., Noda, M., and Verkhratsky, A. (2011). Physiology of microglia. *Physiol. Rev.* 91, 461–553. doi: 10.1152/physrev.00011.2010

Landoni, V. I., de Campos-Nebel, M., Schierloh, P., Calatayud, C., Fernandez, G. C., Ramos, M. V., et al. (2010). Shiga toxin 1-induced inflammatory response in lipopolysaccharide-sensitized astrocytes is mediated by endogenous tumor necrosis factor alpha. *Infect. Immun.* 78, 1193–1201. doi: 10.1128/IAI.00932-09

Lauvrak, S. U., Torgersen, M. L., and Sandvig, K. (2004). Efficient endosome-to-Golgi transport of Shiga toxin is dependent on dynamin and clathrin. *J Cell Sci.* 117(Pt 11), 2321–2331. doi: 10.1242/jcs.01081

Liu, P., Wu, X., Liao, C., Liu, X., Du, J., Shi, H., et al. (2014). *Escherichia coli* and *Candida albicans* induced macrophage extracellular trap-like structures with limited microbicidal activity. *PLoS ONE* 9:e90042. doi: 10.1371/journal.pone.0090042

Louise, C. B., and Obrig, T. G. (1992). Shiga toxin-associated hemolytic uremic syndrome: combined cytotoxic effects of Shiga toxin and lipopolysaccharide (endotoxin) on human vascular endothelial cells *in vitro*. *Infect. Immun.* 60, 1536–1543.

Lu, Y. C., Yeh, W. C., and Ohashi, P. S. (2008). LPS/TLR4 signal transduction pathway. *Cytokine* 42, 145–151. doi: 10.1016/j.cyto.2008.01.006

Malachowa, N., Kobayashi, S. D., Quinn, M. T., and DeLeo, F. R. (2016). NET confusion. *Front. Immunol.* 7:259. doi: 10.3389/fimmu.2016.00259

Melton-Celsa, A. R. (2014). Shiga toxin (Stx) classification, structure, and function. *Microbiol Spectr* 2:EHEC-0024-2013. doi: 10.1128/microbiolspec.EHEC-0024-2013

Mosmann, T. (1983). Rapid colorimetric assay for cellular growth and survival: application to proliferation and cytotoxicity assays. *J. Immunol. Methods* 65, 55–63. doi: 10.1016/0022-1759(83)90303-4

Mosser, D. M., and Edwards, J. P. (2008). Exploring the full spectrum of macrophage activation. *Nat. Rev. Immunol.* 8, 958–969. doi: 10.1038/nri2448

Noda, M., and Suzumura, A. (2012). Sweepers in the CNS: microglial migration and phagocytosis in the alzheimer disease pathogenesis. *Int. J. Alzheimers. Dis.* 2012:891087. doi: 10.1155/2012/891087

Obata, F. (2010). Influence of *Escherichia coli* Shiga toxin on the mammalian central nervous system. *Adv. Appl. Microbiol.* 71, 1–19. doi: 10.1016/S0065-2164(10)71001-7

Parma, Y. R., Chacana, P. A., Roge, A., Kahl, A., Cangelosi, A., Geoghegan, P., et al. (2011). Antibodies anti-Shiga toxin 2 B subunit from chicken egg yolk: isolation, purification and neutralization efficacy. *Toxicon* 58, 380–388. doi: 10.1016/j.toxicon.2011.07.009

Pinto, A., Berdasco, C., Arenas-Mosquera, D., Cangelosi, A., Geoghegan, P. A., Nunez, M. C., et al. (2018). Anti-inflammatory agents reduce microglial response, demyelinating process and neuronal toxin uptake in a model of encephalopathy produced by Shiga toxin 2. *Int. J. Med. Microbiol.* 308, 1036–1042. doi: 10.1016/j.ijmm.2018.09.007

Pinto, A., Cangelosi, A., Geoghegan, P. A., and Goldstein, J. (2017). Dexamethasone prevents motor deficits and neurovascular damage produced by Shiga toxin 2 and lipopolysaccharide in the mouse striatum. *Neuroscience* 344, 25–38. doi: 10.1016/j.neuroscience.2016.12.036

Pinto, A., Jacobsen, M., Geoghegan, P. A., Cangelosi, A., Cejudo, M. L., Tironi-Farinati, C., et al. (2013). Dexamethasone rescues neurovascular unit integrity from cell damage caused by systemic administration of Shiga toxin 2 and lipopolysaccharide in mice motor cortex. *PLoS ONE* 8:e70020. doi: 10.1371/journal.pone.0070020

Rosato-Siri, M. V., Marziali, L., Guitart, M. E., Badaracco, M. E., Puntel, M., Pitossi, F., et al. (2018). Iron availability compromises not only oligodendrocytes but also astrocytes and microglial cells. *Mol. Neurobiol.* 55, 1068–1081. doi: 10.1007/s12035-016-0369-2

Sandvig, K., Olsnes, S., Brown, J. E., Petersen, O. W., and van Deurs, B. (1989). Endocytosisfrom coated pits of Shiga toxin: a glycolipid-binding protein from *Shigella* dysenteriae 1. *J. Cell Biol.* 108, 1331–1343. doi: 10.1083/jcb.108.4.1331

Sandvig, K., and van Deurs, B. (2005). Delivery into cells: lessons learned from plant and bacterial toxins. *Gene Ther.* 12, 865–872. doi: 10.1038/sj.gt.3302525

Sasaki, Y., Ohsawa, K., Kanazawa, H., Kohsaka, S., and Imai, Y. (2001). Iba1 is an actin-cross-linking protein in macrophages/microglia. *Biochem. Biophys. Res. Commun.* 286, 292–297. doi: 10.1006/bbrc.2001.5388

Shimizu, M., Kuroda, M., Sakashita, N., Konishi, M., Kaneda, H., Igarashi, N., et al. (2012). Cytokine profiles of patients with enterohemorrhagic *Escherichia coli* O111-induced hemolytic-uremic syndrome. *Cytokine* 60, 694–700. doi: 10.1016/j.cyto.2012.07.038

Siegler, R. L. (1994). Spectrum of extrarenal involvement in postdiarrheal hemolytic-uremic syndrome. *J. Pediatr.* 125, 511–518. doi: 10.1016/S0022-3476(94)70001-X

Sirerol-Piquer, M. S., Belenguer, G., Morante-Redolat, J. M., Duart-Abadia, P., Perez-Villalba, A., and Farinas, I. (2019). Physiological interactions between microglia and neural stem cells in the adult subependymal niche. *Neuroscience.* 405, 77–91. doi: 10.1016/j.neuroscience.2019.01.009

Skinner, B. M., and Johnson, E. E. (2017). Nuclear morphologies: their diversity and functional relevance. *Chromosoma* 126, 195–212. doi: 10.1007/s00412-016-0614-5

Sugimoto, N., Toma, T., Shimizu, M., Kuroda, M., Wada, T., and Yachie, A. (2014). Shiga toxin-2 enhances heat-shock-induced apoptotic cell death in cultured and primary glial cells. *Cell Biol. Toxicol.* 30, 289–299. doi: 10.1007/s10565-014-9286-1

Tironi-Farinati, C., Loidl, C. F., Boccoli, J., Parma, Y., Fernandez-Miyakawa, M. E., and Goldstein, J. (2010). Intracerebroventricular Shiga toxin 2 increases the expression of its receptor globotriaosylceramide and causes dendritic abnormalities. *J. Neuroimmunol.* 222, 48–61. doi: 10.1016/j.jneuroim.2010.03.001

Trescos, Y., Tessier, E., Rougeaux, C., Goossens, P. L., and Tournier, J. N. (2015). Micropatterned macrophage analysis reveals global cytoskeleton constraints induced by *Bacillus anthracis* edema toxin. *Infect. Immun.* 83, 3114–3125. doi: 10.1128/IAI.00479-15

Wolf, S. A., Boddeke, H. W., and Kettenmann, H. (2017). Microglia in physiology and disease. *Annu. Rev. Physiol.* 79, 619–643. doi: 10.1146/annurev-physiol-022516-034406

Xing, B., Bachstetter, A. D., and Van Eldik, L. J. (2011). Microglial p38α MAPK is critical for LPS-induced neuron degeneration, through a mechanism involving TNFα. *Mol. Neurodegener.* 6:84. doi: 10.1186/1750-1326-6-84

Yipp, B. G., Petri, B., Salina, D., Jenne, C. N., Scott, B. N., Zbytnuik, L. D., et al. (2012). Infection-induced NETosis is a dynamic process involving neutrophil multitasking *in vivo*. *Nat. Med.* 18, 1386–1393. doi: 10.1038/nm.2847

Yousefi, S., Mihalache, C., Kozlowski, E., Schmid, I., and Simon, H. U. (2009). Viable neutrophils release mitochondrial DNA to form neutrophil extracellular traps. *Cell Death Differ.* 16, 1438–1444. doi: 10.1038/cdd.2009.96

Yousefi, S., Simon, D., and Simon, H. U. (2012). Eosinophil extracellular DNA traps: molecular mechanisms and potential roles in disease. *Curr. Opin. Immunol.* 24, 736–739. doi: 10.1016/j.coi.2012.08.010

Zhou, J., Yu, W., Zhang, M., Tian, X., Li, Y., and Lu, Y. (2019). Imbalance of microglial TLR4/TREM2 in LPS-treated APP/PS1 transgenic mice: a potential link between Alzheimer's disease and systemic inflammation. *Neurochem. Res.* 44, 1138–1151. doi: 10.1007/s11064-019-02748-x

Conflict of Interest: The authors declare that the research was conducted in the absence of any commercial or financial relationships that could be construed as a potential conflict of interest.

frontiers in Cellular and Infection Microbiology

REVIEW
published: 06 March 2020
doi: 10.3389/fcimb.2020.00091

Secretion and Delivery of Intestinal Pathogenic *Escherichia coli* Virulence Factors via Outer Membrane Vesicles

Christian Rueter[1]* *and Martina Bielaszewska*[2,3]

[1] Center for Molecular Biology of Inflammation (ZMBE), Institute of Infectiology, University of Muenster, Münster, Germany, [2] National Institute of Public Health, Reference Laboratory for E. coli and Shigellae, Prague, Czechia, [3] Institute for Hygiene, University Hospital of Muenster, University of Muenster, Münster, Germany

Outer membrane vesicles (OMVs) are nanoscale proteoliposomes secreted from the cell envelope of all Gram-negative bacteria. Originally considered as an artifact of the cell wall, OMVs are now recognized as a general secretion system, which serves to improve the fitness of bacteria and facilitate bacterial interactions in polymicrobial communities as well as interactions between the microbe and the host. In general, OMVs are released in increased amounts from pathogenic bacteria and have been found to harbor much of the contents of the parental bacterium. They mainly encompass components of the outer membrane and the periplasm including various virulence factors such as toxins, adhesins, and immunomodulatory molecules. Numerous studies have clearly shown that the delivery of toxins and other virulence factors via OMVs essentially influences their interactions with host cells. Here, we review the OMV-mediated intracellular deployment of toxins and other virulence factors with a special focus on intestinal pathogenic *Escherichia coli*. Especially, OMVs ubiquitously produced and secreted by enterohemorrhagic *E. coli* (EHEC) appear as a highly advanced mechanism for secretion and simultaneous, coordinated and direct delivery of bacterial virulence factors into host cells. OMV-associated virulence factors are not only stabilized by the association with OMVs, but can also often target previously unknown target structures and perform novel activities. The toxins are released by OMVs in their active forms and are transported via cell sorting processes to their specific cell compartments, where they can develop their detrimental effects. OMVs can be considered as bacterial "long distance weapons" that attack host tissues and help bacterial pathogens to establish the colonization of their biological niche(s), impair host cell function, and modulate the defense of the host. Thus, OMVs contribute significantly to the virulence of the pathogenic bacteria.

Keywords: outer membrane vesicles, intestinal pathogenic *Escherichia coli,* EHEC, ETEC, virulence factors, toxins

OPEN ACCESS

Edited by:
Tânia Aparecida Tardelli Gomes, Federal University of São Paulo, Brazil

Reviewed by:
Toru Tobe, Osaka University, Japan
Sivapriya Kailasan Vanaja, University of Connecticut, United States

***Correspondence:**
Christian Rueter
rueterc@uni-muenster.de

Specialty section:
This article was submitted to Bacteria and Host, a section of the journal Frontiers in Cellular and Infection Microbiology

Received: *13 December 2019*
Accepted: *21 February 2020*
Published: *06 March 2020*

Citation:
Rueter C and Bielaszewska M (2020) Secretion and Delivery of Intestinal Pathogenic Escherichia coli Virulence Factors via Outer Membrane Vesicles. Front. Cell. Infect. Microbiol. 10:91. doi: 10.3389/fcimb.2020.00091

INTRODUCTION

Outer membrane vesicles (OMVs) are nanoscale proteoliposomes secreted from the cell envelope of all Gram-negative bacteria (Amano et al., 2010; Ellis and Kuehn, 2010; Kulp and Kuehn, 2010; O'Donoghue and Krachler, 2016). They are produced by a controlled blebbing of the bacterial outer membrane due to the envelope disturbances via different mechanisms

(Kulp and Kuehn, 2010; Schwechheimer and Kuehn, 2015; Elhenawy et al., 2016; Roier et al., 2016; Toyofuku et al., 2019). As a result, OMVs are surrounded by a single membrane bilayer and contain mostly components of the bacterial outer membrane (outer membrane proteins, lipopolysaccharide, phospholipids, peptidoglycan) and the periplasm (periplasmic proteins) (Kulp and Kuehn, 2010; Schwechheimer and Kuehn, 2015; Toyofuku et al., 2019). Originally considered an artifact of the cell wall, OMVs are now recognized as a general secretion system (Guerrero-Mandujano et al., 2017), which serves to improve the fitness of bacteria and facilitate interactions between cells in the context of mixed bacterial communities and between host and microbe (Ellis and Kuehn, 2010; Kulp and Kuehn, 2010; MacDonald and Kuehn, 2012; Haurat et al., 2015). The release of membrane vesicles is an ubiquitous process and was observed among a wide range of bacteria. Not only pathogenic bacteria such as for example *Vibrio cholerae*, *Campylobacter jejuni, Helicobacter pylori, Aggregatibacter actinomycetemcomitans, Pseudomonas aeruginosa*, *Moraxella catarrhalis, Stenotrophomonas maltophilia, Acinetobacter baumannii*, *Shigella flexneri*, *Salmonella enterica* serovar Typhimurium, enterotoxigenic *Escherichia coli* (ETEC), enterohemorrhagic *E. coli* (EHEC), adherent-invasive *E. coli*, and extraintestinal pathogenic *E. coli*, but also non-pathogenic bacteria such as *E. coli* Nissle 1917, shed membrane vesicles during growth (Kadurugamuwa and Beveridge, 1995, 1997; Wai et al., 1995, 2003; Horstman and Kuehn, 2000, 2002; Kesty et al., 2004; Balsalobre et al., 2006; Kouokam et al., 2006; Bomberger et al., 2009; Lindmark et al., 2009; Ellis and Kuehn, 2010; Rolhion et al., 2010; Chatterjee and Chaudhuri, 2011; Rumbo et al., 2011; Schaar et al., 2011; Rompikuntal et al., 2012, 2015; Guidi et al., 2013; Kunsmann et al., 2015; Elhenawy et al., 2016; Bielaszewska et al., 2017; Chatterjee et al., 2017; Devos et al., 2017; Fabrega et al., 2017; Svennerholm et al., 2017; Wang et al., 2019).

OMVs typically have a diameter of 20–250 nm and are released during all growth phases and under all environmental conditions (Ellis and Kuehn, 2010; Bonnington and Kuehn, 2014). OMVs protect their molecular biological content against the external environment and can transport their cargo over long distances (Bomberger et al., 2009; Bonnington and Kuehn, 2014). The cargo may either be present as a solute in the vesicle lumen or be associated with or integrated into the vesicle membrane (Horstman and Kuehn, 2000; Kesty et al., 2004; Bomberger et al., 2009; Lindmark et al., 2009; Bielaszewska et al., 2013, 2017; Kunsmann et al., 2015; **Figures 1A,B**I,II). OMVs carry both bacterial toxins (Horstman and Kuehn, 2000; Wai et al., 2003; Kesty et al., 2004; Balsalobre et al., 2006; Kouokam et al., 2006; Aldick et al., 2009; Ellis and Kuehn, 2010; Chatterjee and Chaudhuri, 2011; Rompikuntal et al., 2012; Guidi et al., 2013; Kunsmann et al., 2015; Bielaszewska et al., 2017) and other virulence factors such as adhesins, invasins, outer membrane proteins, lipopolysaccharide (LPS), flagellin, and proteases (Kadurugamuwa and Beveridge, 1995; Bomberger et al., 2009; Ellis and Kuehn, 2010; Rolhion et al., 2010; Kunsmann et al., 2015; Rompikuntal et al., 2015; Vanaja et al., 2016; Bielaszewska et al., 2017). Secretion of OMVs is generally considered to be an adaptive response to environmental stress and often occurs during infection when the bacteria are exposed to the host's defense mechanisms (MacDonald and Kuehn, 2012; Orench-Rivera and Kuehn, 2016; Bauwens et al., 2017b). In the presence of antimicrobial peptides or bacteriophages, increased production of membrane vesicles correlates with improved fitness and increased survival (Manning and Kuehn, 2011; Duperthuy et al., 2013). For example, EHEC enhances the secretion of outer membrane protease OmpT-loaded OMVs during infection and thereby blocks bacterial cell attack by human antibacterial peptide cathelicidin LL-37 (Urashima et al., 2017).

In general, OMVs are released in increased amounts from pathogenic bacteria, suggesting that OMV secretion is an additional virulence mechanism of pathogens (Horstman and Kuehn, 2000; Ellis and Kuehn, 2010). OMVs can take on both defensive and offensive tasks during infection (MacDonald and Kuehn, 2012). Defensively, they can be used to sequester antibiotics, bacteriophages, and antibodies, bind or degrade antimicrobial peptides, as well as bait antigens to distract the immune system (Manning and Kuehn, 2011; MacDonald and Kuehn, 2012; Duperthuy et al., 2013; O'Donoghue and Krachler, 2016; Urashima et al., 2017; Reyes-Robles et al., 2018). The potential of OMVs as offensive weapons is evident in their ability to deliver virulence factors into host cells (**Figure 1B**III) (Kesty et al., 2004; Tan et al., 2007; Bomberger et al., 2009; Amano et al., 2010; Ellis and Kuehn, 2010; Kulp and Kuehn, 2010; Schaar et al., 2011; Rompikuntal et al., 2012; Bielaszewska et al., 2013, 2017; Kunsmann et al., 2015; O'Donoghue and Krachler, 2016; Rüter et al., 2018) as well as to induce sepsis, sepsis-associated cardiomyopathy or disseminated intravascular coagulation in the absence of intact bacterial cells (Park et al., 2010; Shah et al., 2012; Svennerholm et al., 2017; Wang et al., 2019). The OMV-associated LPS does not only appear to be effective through the extracellular Toll-like receptor (TLR) 4 (Kunsmann et al., 2015; Bielaszewska et al., 2018; Wang et al., 2019) or TLR2 (Schaar et al., 2011), as OMV-bound LPS can also activate the non-canonical inflammasome signaling pathway intracellularly after uptake of the OMVs into the target cells (Vanaja et al., 2016). The uptake of OMV occurs either by phagocytosis or by classic endocytosis (Kesty et al., 2004; Bielaszewska et al., 2013, 2017; Rewatkar et al., 2015; O'Donoghue and Krachler, 2016), whereupon the virulence factors differentially separate during the intracellular transport of the OMVs and can develop their toxic activities (Bielaszewska et al., 2017). Many "well-known" virulence factors and toxins have been identified that use OMVs as an alternative secretory pathway. However, some toxins, such as EHEC cytolysin ClyA, EHEC cytolethal distending toxin V, ETEC heat-labile enterotoxin (LT), *Shigella* enterotoxin 1 (ShET1), and *C. jejuni* cytolethal distending toxin, seem to use OMVs exclusively as a secretory pathway (Horstman and Kuehn, 2000, 2002; Wai et al., 2003; Kesty et al., 2004; Lindmark et al., 2009; Kunsmann et al., 2015; O'Donoghue and Krachler, 2016; Bielaszewska et al., 2017). Beyond their'canonical' functions, the packaging of virulence factors into or onto OMVs concentrates and increases the stability of virulence factors, allows a differential intracellular release of toxins and other virulence factors, targets specific virulence factors to distinct organelles in the host cell,

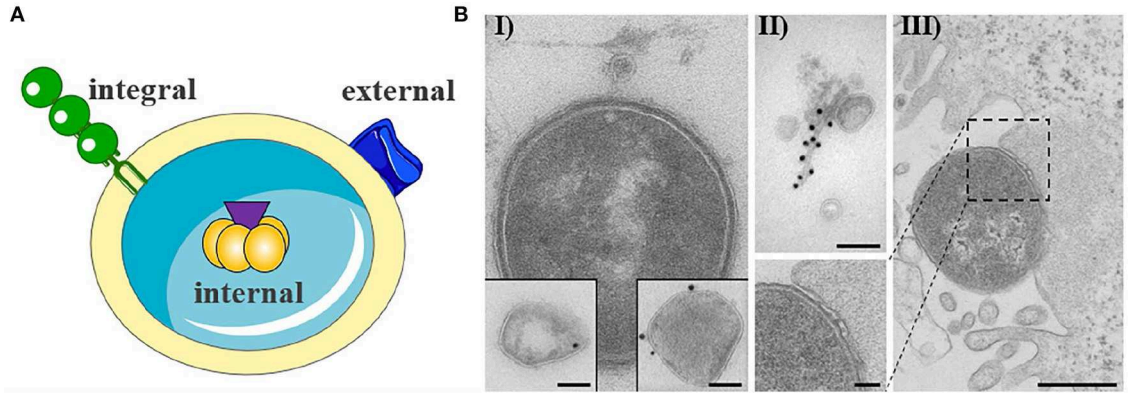

FIGURE 1 | Outer membrane vesicle from gram negative bacteria. **(A)** Schematic representation of OMV with cargo. The cargo may either be present as a solute in the vesicle lumen (internal) or be associated with (external) or integrated into the vesicle membrane (integral). The figure was produced using Servier Medical Art. **(B)** Exemplary electron microscopy pictures of outer membrane vesicles (based on Bielaszewska et al., 2013, 2017). (I) OMV released from the entero-hemorrhaghic *E. coli*. Virulence factors can either be internal (immunogold labeling of Stx2a, left inset) or associated (immunogold labeling of EHEC-Hly, right inset) with OMVs (scale bar 100 nm). (II) OMVs are often associated with flagelin (immunogold labeling of flagellin, scale bar 100 nm). (III) Bacteria are also able to release OMVs to host cells during infection (scale bar 500 nm).

which can broaden or change their functions, and allows their transport for long distances (Aldick et al., 2009; Bomberger et al., 2009; Kulp and Kuehn, 2010; Bielaszewska et al., 2013, 2017; Vanaja et al., 2016; Rüter et al., 2018).

BIOGENESIS OF OMVS

Different mechanisms for OMV biogenesis have been described so far. One mechanism proposes the temporary reduction or relocation of covalent linkages of proteins between the outer membrane (OM) and the peptidoglycan (PG). At the site of local decrease in overall crosslinks, the OM has to grow fast and finally bud off (Schwechheimer and Kuehn, 2015). This model was supported by a study in which mutants lacking OmpA and thus harboring a lower number of crosslinks between OM and PG, revealed an increased OMV production (Kulp and Kuehn, 2010). Another model of OMV biogenesis includes the accumulation of misfolded proteins or envelope components such as PG fragments in the periplasm (Schwechheimer and Kuehn, 2015). Local assembly of these components might be able to induce a periplasmic turgor pressure on the OM. As a consequence, the OM protrudes, encapsulates undesirable components, and pinches off. The accumulation of proteins or envelope components at a specific area in the periplasm might be further attracted by a depletion of covalent crosslinks between the OM and PG (Kulp and Kuehn, 2010). Another mechanism of OMV biogenesis is based on a species- specific *P. aeruginosa* model. The signaling molecule Pseudomonas quinolone signal (PQS) was shown to influence and modify the membrane curvature (Roier et al., 2016). PQS can be inserted into the OM and is able to bind to LPS. This leads to the loss of linkages between the OM and PG and induces periplasmic turgor pressure. Due to binding of positively charged components and reduction of Mg^{2+} and Ca^{2+} salt bridges, anionic repulsions between LPS molecules increase causing the OM to pinch off (Schwechheimer and Kuehn, 2015; Jan, 2017). Another promising mechanism of OMV biogenesis is more general and might be conserved among different bacterial species. The model includes a regulated ABC transport system for phospholipids which is spanned from the OM to the cytoplasmic membrane (Roier et al., 2016). The gene cluster *yrb* (*yrbB-yrbE*) as well as the lipoprotein VacJ have been shown to be part of the system. Maintaining the lipid asymmetry in the OM, it regulates the retrograde transport from the OM to the inner membrane avoiding accumulation of phospholipids. Roier et al. (2016) showed by deletion or reduced expression of the transporter that the OMV production was increased and phospholipids assembled close to the OM. Moreover, under iron-limited conditions the transport system was downregulated dependent on the ferric uptake regulator (Fur) suggesting that increased OMV production is regulated indirectly by Fur and the phospholipid transporter (Roier et al., 2016).

INCREASED OMV PRODUCTION AS A BACTERIAL STRESS RESPONSE

Larger amounts of membrane vesicle release has been broadly observed related to stress response of bacteria. Nutrient scarcity, iron limitation, oxidative stress, hydrogen peroxide as well as a low pH induced the release of OMVs in high amounts (Schwechheimer and Kuehn, 2015; Orench-Rivera and Kuehn, 2016; Bauwens et al., 2017b). OMVs seem to provide resistance and dispose defensive mechanisms against environmental stressors (MacDonald and Kuehn, 2012; Orench-Rivera and Kuehn, 2016). Furthermore, OMVs seem to facilitate adaptation to a challenging environment and increase the chance of bacterial survival (Duperthuy et al., 2013; Bauwens et al., 2017b; Urashima et al., 2017). Stressors can be of physical, chemical or biological nature. Temperature as a stressor has often been described. Higher temperature can lead

to denaturation or misfolding of proteins which results in accumulation in the periplasmic space (Guerrero-Mandujano et al., 2017). The outer membrane further becomes more fluid by higher temperature which promotes protrusion and OMV production (Kulp and Kuehn, 2010). In contrast, a reduction in temperature leads to an increased OMV release in the cold-adapted bacterium *Shewanella livingstonensis*, the soil bacterium *Serratia marcescens* and the pathogen *Bartonella henselae* (Schwechheimer and Kuehn, 2015). Increased vesicle production can also occur after treatment with antimicrobials such as the ciprofloxacin, polymyxin B, gentamicin, or beta-lactam antibiotics (Kadurugamuwa and Beveridge, 1995, 1997; Manning and Kuehn, 2011; MacDonald and Kuehn, 2012; Maredia et al., 2012; Bauwens et al., 2017a; Devos et al., 2017). Interestingly, on the one hand, vesicles are able to carry resistance determinants, either a resistance gene or a respective degradative enzyme, to prevent damage of the bacterial cell (Ciofu et al., 2000; Rumbo et al., 2011; Fulsundar et al., 2014; Schaar et al., 2014; Chattopadhyay and Jagannadham, 2015; Stentz et al., 2015; Devos et al., 2016; González et al., 2016; Chatterjee et al., 2017; Domingues and Nielsen, 2017; Kim et al., 2018). On the other hand, OMV-mediated absorption and subsequent inactivation or degradation of antimicrobials of the surrounding environment has been demonstrated (Manning and Kuehn, 2011; Duperthuy et al., 2013; Orench-Rivera and Kuehn, 2016; Guerrero-Mandujano et al., 2017; Urashima et al., 2017). Last-mentioned, vesicle production can be increased after bacteriophage infection. By exposure of receptors on the vesicle surface, the T4-phage was bound and inactivated (Manning and Kuehn, 2011). Phage-particles were encapsulated and this prevented damage of the bacterial cell (Manning and Kuehn, 2011; Guerrero-Mandujano et al., 2017). Increased OMV production provides many advantages against environmental stressors not only *in vitro* but also in the human host as demonstrated by significantly upregulated vesiculation in EHEC under simulated human intestinal conditions and in the human intestine (Bauwens et al., 2017b).

It is worth mentioning that membrane vesicles produced under particular environmental stress may not result from the outer membrane blebbing typical for the formation of OMVs, but arise by different mechanisms and thus differ from OMVs by their composition and presumably by their functions. Specifically, the outer-inner membrane vesicles (OIMVs) recently identified in several genera of Gram-negative bacteria including pathogens such as *Neisseria gonorrhea*, *Pseudomonas aeruginosa*, and *Acinetobacter baumannii* (Pérez-Cruz et al., 2013, 2015) are characterized by a double membrane bilayer derived from the outer and the inner membrane, respectively. Due to their origin, OIMVs carry, besides membrane components, also cytoplasmic components including DNA (Pérez-Cruz et al., 2015; Toyofuku et al., 2019) and has been thus proposed as major vesicles type involved in the DNA transfer (Toyofuku et al., 2019). OIMVs have been suggested to result from an explosive cell lysis triggered by a phage-derived endolysin that degrades the cell wall peptidoglycan (Turnbull et al., 2016); by reassembling of fragments of the outer and inner membrane of the lysed cells OIMVs arise, whereas reassembling of outer membrane fragments gives rise to so called explosive OMVs (EOMVs) (Turnbull et al., 2016; Toyofuku et al., 2019). The observation of OIMVs and EOMVs formation after bacterial treatment with SOS response-triggering agents such as ciprofloxacin and mitomycin C (Turnbull et al., 2016; Devos et al., 2017) which also induce temperate bacteriophages including those encoding endolysin (Turnbull et al., 2016; Devos et al., 2017) suggests that formation of these vesicles results from phage-mediated cell lysis triggered by the SOS response (Toyofuku et al., 2019).

OMVS AS AN ALTERNATIVE SECRETION SYSTEM: TYPE-0 SECRETION SYSTEM

Besides the well-established secretion-systems 1-6, OMVs have been recently considered as a new independent type-0 secretion system (T0SS) (Guerrero-Mandujano et al., 2017). OMVs not only secrete misfolded proteins or toxic products as described above, but they are also able to transport different types of macromolecules. Because of the lipophilic structure of OMVs, secretion of lipids, hydrophobic and insoluble proteins is facilitated (Guerrero-Mandujano et al., 2017). Moreover, the bilayered envelope of OMVs provides protection against physical and chemical influences as well as enzymatic degradation. OMVs provide unique advantages against other secretion systems by transporting proteins in high concentrations and delivering them to target destinations over long distances (Bomberger et al., 2009; Kulp and Kuehn, 2010; Guerrero-Mandujano et al., 2017). Many studies have reported that the cargo of OMVs is selectively packaged and certain molecules are enriched or excluded (Kesty and Kuehn, 2004; Schwechheimer and Kuehn, 2015). The delivery of bacterial effector proteins by OMVs into host cells seems to be a crucial aspect for pathogens (**Figure 1B**III). In this regard, several investigations have demonstrated that budded portions of outer membrane material are shed also *in vivo*: vesicles produced by *H. pylori* were found in human gastric epithelium biopsies (Fiocca et al., 1999), and outer membrane protein–LPS complexes have been found in the sera of patients and rats with sepsis caused by *Enterobacteriaceae* (Hellman et al., 2000), in the plasma and the cerebrospinal fluid of patients with N*eisseria meningitidis* sepsis and meningitis, respectively (Stephens et al., 1982; Namork and Brandtzaeg, 2002), and in the nasal mucosa of a patient with sinusitis caused by *M. catarrhalis* (Tan et al., 2007). Vesicles from pathogenic strains such as *Pseudomonas aeruginosa, H. pylori, A. actinomycetemcomitans, C. jejuni, S. enterica*, *V. cholera*, and pathogenic *E. coli* contain active virulence factors, such as proteases, pro-inflammatory proteins, LPS, and toxins (Kadurugamuwa and Beveridge, 1995, 1997; Kolling and Matthews, 1999; Horstman and Kuehn, 2000; Keenan and Allardyce, 2000; Kato et al., 2002; Wai et al., 2003; Kesty et al., 2004; Kouokam et al., 2006; Lindmark et al., 2009; Ellis and Kuehn, 2010; Kaparakis et al., 2010; Chatterjee and Chaudhuri, 2011; Schaar et al., 2011; Rompikuntal et al., 2012, 2015; Bielaszewska et al., 2013, 2017, 2018; Guidi et al., 2013; Elluri et al., 2014; Thay et al., 2014; Kunsmann et al., 2015). However, the molecular mechanism of virulence factor delivery

via vesicles has been unclear. In addition to their production during infection, the key role of OMVs in bacterial virulence is supported by their ability to mimic in animal models diseases caused by the parental pathogens (Kim et al., 2011; Shah et al., 2012; Svennerholm et al., 2017), and to induce protective immune responses (Roy et al., 2011; Leitner et al., 2015; Roier et al., 2016; Liu et al., 2017).

OMV-ASSOCIATED TOXINS AND OTHER VIRULENCE FACTORS FROM INTESTINAL PATHOGENIC *ESCHERICHIA COLI*

Intestinal pathogenic *E. coli* such as ETEC and EHEC produce OMVs under laboratory conditions as well as during infection (Wai et al., 1995; Kolling and Matthews, 1999; Horstman and Kuehn, 2000; Yokoyama et al., 2000; Kesty et al., 2004; Aldick et al., 2009; Ellis and Kuehn, 2010; Bielaszewska et al., 2013, 2017; Kunsmann et al., 2015; Bauwens et al., 2017b). Vesicles may contribute to the bacterial pathogenicity by serving as vehicles for toxin delivery into host cells (Kesty et al., 2004; Bielaszewska et al., 2013, 2017) as well as by inducing an inflammatory response, in particular secretion of interleukin 8 (IL-8) from intestinal epithelial cells (Kunsmann et al., 2015; Bielaszewska et al., 2018). Most vesicle proteins were resistant to dissociation, suggesting they were integral, or internal (Bielaszewska et al., 2013, 2017). In some cases, virulence factors can also be tightly attached to the vesicle surface (Bielaszewska et al., 2013; Kunsmann et al., 2015). **Table 1** shows an overview of virulence factors associated with OMVs from pathogenic *E. coli*, which will be discussed in the following text separately for the OMV-mediated delivery of toxins and other virulence factors from ETEC and EHEC.

OMV-MEDIATED DELIVERY OF TOXINS AND OTHER VIRULENCE FACTORS FROM ETEC

ETEC are leading causes of traveler's diarrhea and childhood diarrhea in developing countries (Fleckenstein and Kuhlmann, 2019). The OMV association of the heat-labile enterotoxin (LT), one of the major virulence factors of these strains which disrupts electrolyte balance in the gut epithelium (Mirhoseini et al., 2018), has been demonstrated by several groups (Wai et al., 1995; Horstman and Kuehn, 2000). The toxin is located both inside and on the external of OMVs (Horstman and Kuehn, 2000, 2002) and is biologically active as demonstrated by the ability of LT-carrying OMVs to elicit typical morphological changes on Y1 cells (Horstman and Kuehn, 2000; Kesty et al., 2004). According to the proposed model for LT secretion from ETEC and its interaction with host cells (Horstman and Kuehn, 2002), LT binds, after its secretion from the bacteria via the general secretion pathway, to the bacterial outer membrane via interaction of LT-B subunit with LPS. Subsequently, LT is released from the bacterial cells by budding of OMVs, which contain LT both inside and on the external surface bound to LPS. The external LT binds, via interaction of another site of its B subunit, with GM_1 cell receptor, tethering thus the vesicle to the host cell (Horstman and Kuehn, 2002). The cellular binding of LT-carrying OMVs to their target cells is thus dependent on the OMV-associated toxin, as has also been reported for OMV-associated cholera toxin of *V. cholerae* (Chatterjee and Chaudhuri, 2011). Cellular binding of LT-carrying OMVs leads to their internalization via lipid rafts and caveolin-dependent endocytosis and internalized vesicles accumulate in a non-acidified compartment of the host cell (Kesty et al., 2004). The pathogenetic role of ETEC OMVs during infection is supported by their increased production *in vivo* (Ellis and Kuehn, 2010) and by their ability to induce immune responses to OMV-associated LT and other virulence proteins such as autotransporter TibA, EtpA adhesin and a novel extracytoplasmic protein CexE (**Table 1**) (Roy et al., 2010, 2011) which protect against ETEC colonization in a mouse model (Roy et al., 2011; Leitner et al., 2015).

OMV-MEDIATED DELIVERY OF TOXINS AND OTHER VIRULENCE FACTORS FROM EHEC

EHEC are worldwide causes of diarrhea and its severe extraintestinal complication, the hemolytic uremic syndrome (HUS) (Karch et al., 2005; Tarr et al., 2005). EHEC OMVs contain Shiga toxins (Stx) (**Table 1**; Kolling and Matthews, 1999; Yokoyama et al., 2000; Kunsmann et al., 2015; Bielaszewska et al., 2017), the major EHEC virulence factors involved in the pathogenesis of HUS, which is a thrombotic microangiopathy resulting from Stx-mediated injury of microvascular endothelium, in particular in the renal glomeruli but also in the brain (Zoja et al., 2010; Karpman et al., 2017). Besides Stx, EHEC OMVs also carry other EHEC toxins which injure microvascular endothelium and may thus play roles in the pathogenesis of HUS such as the cytolethal distending toxin V (CdtV) and EHEC hemolysin (EHEC-Hly), as well as flagellin (Aldick et al., 2009; Bielaszewska et al., 2013, 2017; Kunsmann et al., 2015; **Table 1**). Whereas Stx, EHEC-Hly, and flagellin also exist as free extracellular proteins (Kunsmann et al., 2015; Bielaszewska et al., 2017), CdtV is exclusively secreted via OMVs (Bielaszewska et al., 2017). Studies of interactions of EHEC OMVs and OMV-associated virulence factors with human intestinal epithelial and microvascular endothelial cells, which are the major targets during EHEC infection demonstrated that OMVs with their toxin cargoes are taken up by cells via dynamin-dependent endocytosis (Bielaszewska et al., 2013, 2017) and transported to early and late endosomes (Bielaszewska et al., 2013, 2017) (**Figure 2**). Here, OMV-associated toxins or their biologically active subunits separate from OMVs and are trafficked, using different pathways, to their cellular targets including ribosomes (Stx2a A subunit), the nucleus (CdtV B subunit), and mitochondria (EHEC-Hly) (Bielaszewska et al., 2013, 2017) (**Figure 2**). By analyzing biological consequences of OMV-mediated delivery of virulence factors into host cells, we demonstrated that EHEC OMVs that carried Stx2a, CdtV, and EHEC-Hly caused G2 cell cycle arrest followed by apoptosis in human intestinal epithelial and microvascular endothelial cells (Bielaszewska et al., 2013, 2017). CdtV, specifically its B

TABLE 1 | Overview of virulence factors associated with OMVs from intestinal pathogenic *E. coli*.

Type of pathogenic *E. coli*	OMV associated virulence factor	Function	Association with OMV	Vesicle formation	References
Enterotoxigenic *E. coli*	Heat labile enterotoxin (LT)	Cytotoxicity	Internal and external	Blebbing	Horstman and Kuehn, 2000, 2002
(ETEC)					Kesty et al., 2004
	EtpA	T-Cell stimulating Protein/Adhesin	Not determined	Not determined	Roy et al., 2010
	CexE	Adhesin	Not determined	Not determined	Roy et al., 2011
	TibA	Autotransport/Adhesin	Not determined	Not determined	Roy et al., 2010
	Flagellin	Not determined	External	Not determined	Roy et al., 2010
Enterohemorrhagic *E. coli*	Shiga toxin 1	Cytotoxicity, Apoptosis	Not determined	Not determined	Yokoyama et al., 2000
(EHEC)	Shiga toxin 2	Cytotoxicity, Apoptosis	Internal	Blebbing	Kolling and Matthews, 1999
	Cytolysin A (ClyA)	Cytotoxicity	Not determined	Blebbing	Wai et al., 2003
	Shigella enterotoxin 1 (ShET1)	Unknown	Internal	Blebbing	Kunsmann et al., 2015
	EHEC hemolysin	Apoptosis	External	Blebbing	Bielaszewska et al., 2013, 2017
	Cytolethal distending toxin V	Cell cycle arrest, apoptosis	Internal	Blebbing	Bielaszewska et al., 2017
	Flagellin	Proinflammatory (IL-8 secretion)	External	Blebbing	Kunsmann et al., 2015
	Outer membrane protease OmpT	Protection against antimicrobial Peptides	Internal	Not determined	Urashima et al., 2017
	Lipopolysaccharide	Proinflammatory (IL-8 secretion)	Integral	Blebbing	Kunsmann et al., 2015

Information on vesicle formation and association of virulence factors are based on electron microscopy. Formation of vesicles and the proportions of different vesicle types in the culture, even of the same bacterium might differ dependent on culture conditions.

subunit, which possesses the DNase-like activity, was the OMV component responsible for the G2 arrest, whereas all of the OMV-delivered toxins contributed to apoptosis (Bielaszewska et al., 2013, 2017). A detailed analysis of the mechanism of apoptosis caused by OMV-delivered EHEC-Hly demonstrated that after its translocation from late endosomes/lysosomes to the mitochondria, EHEC-Hly causes permeabilization of the inner and outer mitochondrial membranes, which leads to the decrease of the mitochondrial membrane potential, release of cytochrome C from the mitochondria to the cytoplasm, and, as a consequence, activation of caspase-9, the initiator caspase of the intrinsic apoptotic pathway. Subsequent activation of the effector caspase-3 via caspase-9 triggers the apoptotic cell death (Bielaszewska et al., 2013). The failure of OMVs that lacked the EHEC toxins to cause the G2 arrest and apoptosis indicates that the OMV-delivered toxins accounted for the OMV-mediated biological effects (Bielaszewska et al., 2013, 2017). Importantly, the report by Kim et al. (2011) that EHEC O157 OMVs carrying Stx2a, the major EHEC virulence factor, elicited a HUS-like disease in a mouse model supports the hypothesis that OMV-mediated secretion and delivery of EHEC toxins into host cells *in vivo* essentially contribute to the pathogenesis of EHEC infection.

Besides their endothelial cytotoxicity, EHEC OMVs induce secretion of IL-8 from human intestinal epithelial cells (Kunsmann et al., 2015; Bielaszewska et al., 2018), which may also have pathogenetic implications since proinflammatory cytokines play multiple roles in the pathogenesis of HUS (Zoja et al., 2010; Karpman et al., 2017). A deeper analysis of OMV-mediated IL-8 production demonstrated that flagellin and LPS are the key IL-8-inducing components of EHEC OMVs, and that flagellin-mediated signaling via TLR5, and LPS-mediated signaling via TLR4/MD-2 complex, followed by activation of the nuclear factor NF-κB, are the major pathways underlying IL-8 production (Kunsmann et al., 2015; Bielaszewska et al., 2018). The identification of EHEC OMVs as carriers for major EHEC virulence factors and powerful tools for their intracellular delivery and endothelial injury, combined with the proinflammatory and immunomodulatory activities of OMVs, allow to consider these nanostructures as novel virulence tools of EHEC which may play roles in the pathogenesis of EHEC-mediated diseases, in particular of HUS. This is further supported by a significantly increased EHEC OMV production under simulated human intestinal conditions and in the human intestine (Bauwens et al., 2017b). In contrast to ETEC OMVs where OMV-associated LT mediates the OMV interaction with the host cell via its interaction with GM_1 (Horstman and Kuehn, 2002), the cellular uptake of EHEC OMVs is independent on OMV-associated virulence factors (Bielaszewska et al., 2017) and the cell receptor(s) for OMVs as well as their detailed internalization mechanism(s) remain unknown.

OUTLOOK

The roles of ETEC and EHEC OMVs as carriers for virulence factors and tools for their delivery into the host cells, together with OMV abilities to elicit immune responses against the major virulence proteins lead to attempts to exploit OMVs as vaccine candidates. OMVs are promising

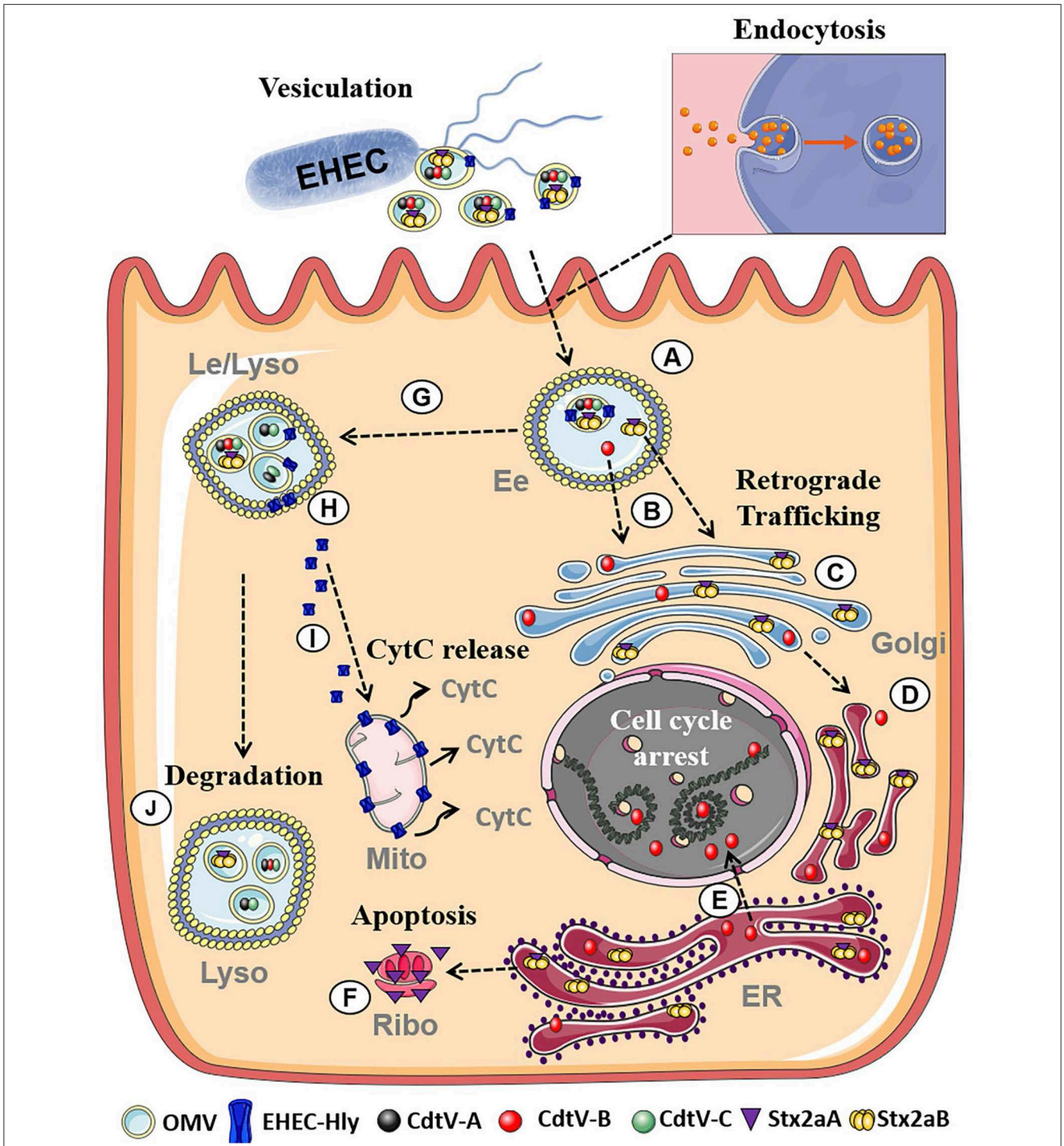

FIGURE 2 | Summary of intracellular trafficking of EHEC O157 OMVs and OMV-delivered toxins (based on Bielaszewska et al., 2013, 2017). After uptake via dynamin-dependent endocytosis, O157 OMVs carrying the toxin cocktail enter the endosomal compartments of target cells **(A)**. Stx2a holotoxin and CdtV-B subunit separate from OMVs in early endosomes **(B)** and are retrogradely transported to the Golgi complex **(C)** and the endoplasmic reticulum **(D)**. From the endoplasmic reticulum, CdtV-B is translocated to the nucleus to target DNA and cause cell-cycle arrest **(E)**, and Stx2a A1 catalytic fragment to the cytosol to reach ribosomes and induce apoptosis **(F)**. CdtV-A and CdtV-C subunits and EHEC-Hly are sorted with OMVs to late endosomes/lysosomes **(G)**. Here EHEC-Hly separates from OMVs, escapes from the lysosomes **(H)**, and is transported to the mitochondria where it causes release of cytochrome C **(I)**. CdtV-A and CdtV-C remain OMV-associated and are degraded with OMVs in lysosomes **(J)**. Moreover, residual subsets of CdtV-B and Stx2a, which did not separate from OMVs in early endosomes, are sorted with OMVs to lysosomes for degradation. Figure was taken from Bielaszewska et al. (2017) and modified using Servier Medical Art. (Ee, Early endosomes; Le, Late endosomes; Lyso, Lysosomes; Golgi, Golgi Apparatus, ER, Endoplasmatic reticulum; Ribo, Ribosome; Mito, Mitochondria, CytC, Cytochrome C).

components of vaccines since they combine the antigen and adjuvant in a single formulation. A vaccine based on OMVs of a major EHEC serotype O157:H7 was found to protect against EHEC-mediated pathology in a mouse model and to be immunogenic in calves (Fingermann et al., 2018). These initial studies suggest that EHEC-derived OMVs have a potential for the formulation of both human and veterinary vaccines. However, further studies are needed to determine immunogenicity and protective efficacy of OMVs from other major EHEC serotypes associated with HUS (Karch et al., 2005), identify OMV components involved in the immune responses and mechanisms underlying OMV-elicited protective immunity.

The progress of development of OMV-based ETEC vaccines is more advanced than in EHEC. ETEC OMVs contain both confirmed and probable ETEC virulence factors (**Table 1**), which are highly immunogenic (Roy et al., 2010, 2011). Several studies with differently prepared OMVs from various strains demonstrated the immunogenic as well as protective effects of such vaccines in animal models (Roy et al., 2011; Leitner et al., 2015; Hays et al., 2018). Moreover, a combined OMV-based vaccine against ETEC and *V. cholerae* has been developed and shown to successfully protect against both pathogens (Leitner et al., 2015). However, a lot of additional work remains to be done before OMV-based vaccines against EHEC and ETEC infections can be used in clinical studies as it is already the case for vaccines against *Neisseria meningitidis* and *Neisseria gonorrhoeae* infections (Marsay et al., 2015; Petousis-Harris et al., 2017).

AUTHOR CONTRIBUTIONS

All authors listed have made a substantial, direct and intellectual contribution to the work, and approved it for publication.

FUNDING

The work in the laboratory of the authors has been supported by grants of the Deutsche Forschungsgemeinschaft (DFG) (DFG RU 1884/2-1, DFG RU 1884/3-1, CRC1009 TP B03, and B04), and NIH (RO1 1R56AR072594-01A1).

ACKNOWLEDGMENTS

We apologize to all our colleagues whose excellent contributions to this important topic could not be considered due to space limitations. We are grateful to Lilo Greune (Institute of Infectiology, Center for Molecular Biology of Inflammation—ZMBE, University of Munster) for support of exemplary electron microscopy pictures of OMVs shown in **Figure 1**. We like to thank all the past and present members of the Institute of Infectiology—ZMBE, and the Institute for Hygiene for their valuable contributions.

REFERENCES

Aldick, T., Bielaszewska, M., Uhlin, B. E., Humpf, H. U., Wai, S. N., and Karch, H. (2009). Vesicular stabilization and activity augmentation of enterohaemorrhagic *Escherichia coli* haemolysin. *Mol. Microbiol.* 71, 1496–1508. doi: 10.1111/j.1365-2958.2009.06618.x

Amano, A., Takeuchi, H., and Furuta, N. (2010). Outer membrane vesicles function as offensive weapons in host-parasite interactions. *Microbes Infect.* 12, 791–798. doi: 10.1016/j.micinf.2010.05.008

Balsalobre, C., Silván, J. M., Berglund, S., Mizunoe, Y., Uhlin, B. E., and Wai, S. N. (2006). Release of the type I secreted alpha-haemolysin via outer membrane vesicles from *Escherichia coli*. *Mol. Microbiol.* 59, 99–112. doi: 10.1111/j.1365-2958.2005.04938.x

Bauwens, A., Kunsmann, L., Karch, H., Mellmann, A., and Bielaszewska, M. (2017a). Antibiotic-mediated modulations of outer membrane vesicles in enterohemorrhagic *Escherichia coli* O104:H4 and O157:H7. *Antimicrob. Agents Chemother.* 61:e00937–17. doi: 10.1128/AAC.00937-17

Bauwens, A., Kunsmann, L., Marejkova, M., Zhang, W., Karch, H., Bielaszewska, M., et al. (2017b). Intrahost milieu modulates production of outer membrane vesicles, vesicle-associated Shiga toxin 2a and cytotoxicity in *Escherichia coli* O157:H7 and O104:H4. *Environ. Microbiol. Rep.* 9, 626–634. doi: 10.1111/1758-2229.12562

Bielaszewska, M., Marejkova, M., Bauwens, A., Kunsmann-Prokscha, L., Mellmann, A., and Karch, H. (2018). Enterohemorrhagic *Escherichia coli* O157 outer membrane vesicles induce interleukin 8 production in human intestinal epithelial cells by signaling via Toll-like receptors TLR4 and TLR5 and activation of the nuclear factor NF-kappa B. *Inter. J. Med. Microbiol.* 308, 882–889. doi: 10.1016/j.ijmm.2018.06.004

Bielaszewska, M., Rüter, C., Bauwens, A., Greune, L., Jarosch, K. A., Steil, D., et al. (2017). Host cell interactions of outer membrane vesicle-associated virulence factors of enterohemorrhagic *Escherichia coli* O157: intracellular delivery, trafficking and mechanisms of cell injury. *PLoS Pathog.* 13:e1006159. doi: 10.1371/journal.ppat.1006159

Bielaszewska, M., Rüter, C., Kunsmann, L., Greune, L., Bauwens, A., Zhang, W., et al. (2013). Enterohemorrhagic *Escherichia coli* hemolysin employs outer membrane vesicles to target mitochondria and cause endothelial and epithelial apoptosis. *PLoS Pathog.* 9:e1003797. doi: 10.1371/journal.ppat.1003797

Bomberger, J. M., MacEachran, D. P., Coutermarsh, B. A., Ye, S. Y., O'Toole, G. A., and Stanton, B. A. (2009). Long-distance delivery of bacterial virulence factors by *Pseudomonas aeruginosa* outer membrane vesicles. *PLoS Pathog.* 5:e1000382. doi: 10.1371/journal.ppat.1000382

Bonnington, K. E., and Kuehn, M. J. (2014). Protein selection and export via outer membrane vesicles. *Biochim. Biophys. Acta Mol. Cell Res.* 1843, 1612–1619. doi: 10.1016/j.bbamcr.2013.12.011

Chatterjee, D., and Chaudhuri, K. (2011). Association of cholera toxin with *Vibrio cholerae* outer membrane vesicles which are internalized by human intestinal epithelial cells. *FEBS Lett.* 585, 1357–1362. doi: 10.1016/j.febslet.2011.04.017

Chatterjee, S., Mondal, A., Mitra, S., and Basu, S. (2017). *Acinetobacter baumannii* transfers the bla_{NDM-1} gene via outer membrane vesicles. *J. Antimicrob. Chemother.* 72, 2201–2207. doi: 10.1093/jac/dkx131

Chattopadhyay, M. K., and Jagannadham, M. V. (2015). Vesicles-mediated resistance to antibiotics in bacteria. *Front. Microbiol.* 6:974. doi: 10.3389/fmicb.2015.00974

Ciofu, O., Beveridge, T. J., Kadurugamuwa, J., Walther-Rasmussen, J., and Høiby, N. (2000). Chromosomal beta-lactamase is packaged into membrane vesicles and secreted from *Pseudomonas aeruginosa*. *J. Antimicrob. Chemother.* 45, 9–13. doi: 10.1093/jac/45.1.9

Devos, S., Stremersch, S., Raemdonck, K., Braeckmans, K., and Devreese, B. (2016). Intra- and interspecies effects of outer membrane vesicles from *Stenotrophomonas maltophilia* on beta-lactam resistance. *Antimicrob. Agents Chemother.* 60, 2516–2518. doi: 10.1128/AAC.02171-15

Devos, S., Van Putte, W., Vitse, J., Van Driessche, G., Stremersch, S., Van Den Broek, W., et al. (2017). Membrane vesicle secretion and prophage induction in multidrug-resistant *Stenotrophomonas maltophilia* in response to ciprofloxacin stress. *Environ. Microbiol.* 19, 3930–3937. doi: 10.1111/1462-2920.13793

Domingues, S., and Nielsen, K. M. (2017). Membrane vesicles and horizontal gene transfer in prokaryotes. *Curr. Opin. Microbiol.* 38, 16–21. doi: 10.1016/j.mib.2017.03.012

Duperthuy, M., Sjöström, A. E., Sabharwal, D., Damghani, F., Uhlin, B. E., and Wai, S. N. (2013). Role of the vibrio cholerae matrix protein Bap1 in cross-resistance to antimicrobial peptides. *PLoS Pathog.* 9:e1003620. doi: 10.1371/journal.ppat.1003620

Elhenawy, W., Bording-Jorgensen, M., Valguarnera, E., Haurat, M. F., Wine, E., and Feldman, M. F. (2016). LPS remodeling triggers formation of outer membrane vesicles in *Salmonella*. *mBio* 7:e00940–16. doi: 10.1128/mBio.00940-16

Ellis, T. N., and Kuehn, M. J. (2010). Virulence and immunomodulatory roles of bacterial outer membrane vesicles. *Microbiol. Mol. Biol. Rev.* 74, 81–94. doi: 10.1128/MMBR.00031-09

Elluri, S., Enow, C., Vdovikova, S., Rompikuntal, P. K., Dongre, M., Carlsson, S., et al. (2014). Outer membrane vesicles mediate transport of biologically active *Vibrio cholerae* cytolysin (VCC) from *V. cholerae strains*. *PLoS ONE* 9:e106731. doi: 10.1371/journal.pone.0106731

Fabrega, M. J., Rodriguez-Nogales, A., Garrido-Mesa, J., Algieri, F., Badia, J., Gimenez, R., et al. (2017). Intestinal anti-inflammatory effects of outer membrane vesicles from *Escherichia coli* Nissle 1917 in DSS-experimental colitis in mice. *Front. Microbiol.* 8:1274. doi: 10.3389/fmicb.2017.01274

Fingermann, M., Avila, L., De Marco, M. B., Vazquez, L., Di Biase, D. N., Muller, A. V., et al. (2018). OMV-based vaccine formulations against Shiga toxin producing *Escherichia coli* strains are both protective in mice and immunogenic in calves. *Hum. Vaccin. Immunother.* 14, 2208–2213. doi: 10.1080/21645515.2018.1490381

Fiocca, R., Necchi, V., Sommi, P., Ricci, V., Telford, J., Cover, T. L., et al. (1999). Release of *Helicobacter pylori* vacuolating cytotoxin by both a specific secretion pathway and budding of outer membrane vesicles. uptake of released toxin and vesicles by gastric epithelium. *J. Pathol.* 188, 220–226. doi: 10.1002/(SICI)1096-9896(199906)188:2<220::AID-PATH307>3.0.CO;2-C

Fleckenstein, J. M., and Kuhlmann, F. M. (2019). Enterotoxigenic *Escherichia coli* Infections. *Curr. Infect. Dis. Rep.* 21:9. doi: 10.1007/s11908-019-0665-x

Fulsundar, S., Harms, K., Flaten, G. E., Johnsen, P. J., Chopade, B. A., and Nielsen, K. M. (2014). Gene transfer potential of outer membrane vesicles of *Acinetobacter baylyi* and effects of stress on vesiculation. *Appl. Environ. Microbiol.* 80, 3469–3483. doi: 10.1128/AEM.04248-13

González, L. J., Bahr, G., Nakashige, T. G., Nolan, E. M., Bonomo, R. A., and Vila, A. J. (2016). Membrane anchoring stabilizes and favors secretion of New Delhi metallo-β-lactamase. *Nat. Chem. Biol.* 12, 516–522. doi: 10.1038/nchembio.2083

Guerrero-Mandujano, A., Hernandez-Cortez, C., Ibarra, J. A., and Castro-Escarpulli, G. (2017). The outer membrane vesicles: secretion system type zero. *Traffic* 18, 425–432. doi: 10.1111/tra.12488

Guidi, R., Levi, L., Rouf, S. F., Puiac, S., Rhen, M., and Frisan, T. (2013). *Salmonella enterica* delivers its genotoxin through outer membrane vesicles secreted from infected cells. *Cell. Microbiol.* 15, 2034–2050. doi: 10.1111/cmi.12172

Haurat, M. F., Elhenawy, W., and Feldman, M. F. (2015). Prokaryotic membrane vesicles: new insights on biogenesis and biological roles. *Biol. Chem.* 396, 95–109. doi: 10.1515/hsz-2014-0183

Hays, M. P., Houben, D., Yang, Y., Luirink, J., and Hardwidge, P. R. (2018). Immunization with Skp delivered on outer membrane vesicles protects mice against enterotoxigenic *Escherichia coli* challenge. *Front. Cell. Infect. Microbiol.* 8:132. doi: 10.3389/fcimb.2018.00132

Hellman, J., Loiselle, P. M., Zanzot, E. M., Allaire, J. E., Tehan, M. M., Boyle, L. A., et al. (2000). Release of gram-negative outer-membrane proteins into human serum and septic rat blood and their interactions with immunoglobulin in antiserum to *Escherichia coli* J5. *J. Infect. Dis.* 181, 1034–1043. doi: 10.1086/315302

Horstman, A. L., and Kuehn, M. J. (2000). Enterotoxigenic *Escherichia coli* secretes active heat-labile enterotoxin via outer membrane vesicles. *J. Biol. Chem.* 275, 12489–12496. doi: 10.1074/jbc.275.17.12489

Horstman, A. L., and Kuehn, M. J. (2002). Bacterial surface association of heat-labile enterotoxin through lipopolysaccharide after secretion via the general secretory pathway. *J. Biol. Chem.* 277, 32538–32545. doi: 10.1074/jbc.M203740200

Jan, A. T. (2017). Outer Membrane Vesicles (OMVs) of gram-negative bacteria. *a* perspective update. *Front. Microbiol.* 8:1053. doi: 10.3389/fmicb.2017.01053

Kadurugamuwa, J. L., and Beveridge, T. J. (1995). Virulence factors are released from *Pseudomonas-aeruginosa* in association with membrane-vesicles during normal growth and exposure to gentamicin - A novel mechanism of enzyme-secretion. *J. Bacteriol.* 177, 3998–4008. doi: 10.1128/JB.177.14.3998-4008.1995

Kadurugamuwa, J. L., and Beveridge, T. J. (1997). Natural release of virulence factors in membrane vesicles by *Pseudomonas aeruginosa* and the effect of aminoglycoside antibiotics on their release. *J. Antimicrob. Chemother.* 40, 615–621. doi: 10.1093/jac/40.5.615

Kaparakis, M., Turnbull, L., Carneiro, L., Firth, S., Coleman, H. A., Parkington, H. C., et al. (2010). Bacterial membrane vesicles deliver peptidoglycan to NOD1 in epithelial cells. *Cell. Microbiol.* 12, 372–385. doi: 10.1111/j.1462-5822.2009.01404.x

Karch, H., Tarr, P. I., and Bielaszewska, M. (2005). Enterohaemorrhagic *Escherichia coli* in human medicine. *Inter. J. Med. Microbiol.* 295, 405–418. doi: 10.1016/j.ijmm.2005.06.009

Karpman, D., Loos, S., Tati, R., and Arvidsson, I. (2017). Haemolytic uraemic syndrome. *J. Inter. Med.* 281, 123–148. doi: 10.1111/joim.12546

Kato, S., Kowashi, Y., and Demuth, D. R. (2002). Outer membrane-like vesicles secreted by *Actinobacillus actinomycetemcomitans* are enriched in leukotoxin. *Microb. Pathog.* 32, 1–13. doi: 10.1006/mpat.2001.0474

Keenan, J. I., and Allardyce, R. A. (2000). Iron influences the expression of *Helicobacter pylori* outer membrane vesicle-associated virulence factors. *Eur. J. Gastroenterol. Hepatol.* 12, 1267–1273. doi: 10.1097/00042737-200012120-00002

Kesty, N. C., and Kuehn, M. J. (2004). Incorporation of heterologous outer membrane and periplasmic proteins into *Escherichia coli* outer membrane vesicles. *J. Biol. Chem.* 279, 2069–2076. doi: 10.1074/jbc.M307628200

Kesty, N. C., Mason, K. M., Reedy, M., Miller, S. E., and Kuehn, M. J. (2004). Enterotoxigenic escherichia coli vesicles target toxin delivery into mammalian cells. *EMBO J.* 23, 4538–4549. doi: 10.1038/sj.emboj.7600471

Kim, S. H., Lee, Y. H., Lee, S. H., Lee, S. R., Huh, J. W., Kim, S. U., et al. (2011). Mouse model for hemolytic uremic syndrome induced by outer membrane vesicles of *Escherichia coli* O157:H7. *FEMS Immunol. Med. Microbiol.* 63, 427–434. doi: 10.1111/j.1574-695X.2011.00869.x

Kim, S. W., Park, S. B., Im, S. P., Lee, J. S., Jung, J. W., Gong, T. W., et al. (2018). Outer membrane vesicles from β-lactam-resistant *Escherichia coli* enable the survival of β-lactam-susceptible *E. coli* in the presence *of β*-lactam antibiotics. *Sci. Rep.* 8:5402. doi: 10.1038/s41598-018-23656-0

Kolling, G. L., and Matthews, K. R. (1999). Export of virulence genes and shiga toxin by membrane vesicles of *Escherichia coli* O157:H7. *Appl. Environ. Microbiol.* 65, 1843–1848. doi: 10.1128/AEM.65.5.1843-1848.1999

Kouokam, J. C., Wai, S. N., Fallman, M., Dobrindt, U., Hacker, J., and Uhlin, B. E. (2006). Active cytotoxic necrotizing factor 1 associated with outer membrane vesicles from uropathogenic *Escherichia coli*. *Infect. Immunity* 74, 2022–2030. doi: 10.1128/IAI.74.4.2022-2030.2006

Kulp, A., and Kuehn, M. J. (2010). Biological functions and biogenesis of secreted bacterial outer membrane vesicles. *Annu. Rev. Microbiol.* 64, 163–184. doi: 10.1146/annurev.micro.091208.073413

Kunsmann, L., Rüter, C., Bauwens, A., Greune, L., Gluder, M., Kemper, B., et al. (2015). Virulence from vesicles: novel mechanisms of host cell injury by *Escherichia coli* O104:H4 outbreak strain. *Sci. Rep.* 5:13252. doi: 10.1038/srep13252

Leitner, D. R., Lichtenegger, S., Temel, P., Zingl, F. G., Ratzberger, D., Roier, S., et al. (2015). A combined vaccine approach against *Vibrio cholerae* and ETEC based on outer membrane vesicles. *Front. Microbiol.* 6:823. doi: 10.3389/fmicb.2015.00823

Lindmark, B., Rompikuntal, P. K., Vaitkevicius, K., Song, T. Y., Mizunoe, Y., Uhlin, B. E., et al. (2009). Outer membrane vesicle-mediated release of cytolethal distending toxin (CDT) from *Campylobacter jejuni*. *BMC Microbiol.* 9:220. doi: 10.1186/1471-2180-9-220

Liu, Q., Yi, J., Liang, K., and Zhang, X. M. (2017). *Salmonella* Choleraesuis outer membrane vesicles: proteomics and immunogenicity. *J. Basic Microbiol.* 57, 852–861. doi: 10.1002/jobm.201700153

MacDonald, I. A., and Kuehn, M. J. (2012). Offense and defense: microbial membrane vesicles play both ways. *Res. Microbiol.* 163, 607–618. doi: 10.1016/j.resmic.2012.10.020

Manning, A. J., and Kuehn, M. J. (2011). Contribution of bacterial outer membrane vesicles to innate bacterial defense. *BMC Microbiol.* 11:258. doi: 10.1186/1471-2180-11-258

Maredia, R., Devineni, N., Lentz, P., Dallo, S. F., Yu, J. J., Guentzel, N., et al. (2012). Vesiculation from *Pseudomonas aeruginosa* under SOS. *Sci. World J.* 2012:402919. doi: 10.1100/2012/402919

Marsay, L., Dold, C., Green, C. A., Rollier, C. S., Norheim, G., Sadarangani, M., et al. (2015). A novel meningococcal outer membrane vesicle vaccine with constitutive expression of FetA: a phase I clinical trial. *J. Infect.* 71, 326–337. doi: 10.1016/j.jinf.2015.05.006

Mirhoseini, A., Amani, J., and Nazarian, S. (2018). Review on pathogenicity mechanism of enterotoxigenic *Escherichia coli* and vaccines against it. *Microb. Pathog.* 117, 162–169. doi: 10.1016/j.micpath.2018.02.032

Namork, E., and Brandtzaeg, P. (2002). Fatal meningococcal septicaemia with "blebbing" meningococcus. *Lancet* 360, 1741–1741. doi: 10.1016/S0140-6736(02)11721-1

O'Donoghue, E. J., and Krachler, A. M. (2016). Mechanisms of outer membrane vesicle entry into host cells. *Cell. Microbiol.* 18, 1508–1517. doi: 10.1111/cmi.12655

Orench-Rivera, N., and Kuehn, M. J. (2016). Environmentally controlled bacterial vesicle-mediated export. *Cell. Microbiol.* 18, 1525–1536. doi: 10.1111/cmi.12676

Park, K. S., Choi, K. H., Kim, Y. S., Hong, B. S., Kim, O. Y., Kim, J. H., et al. (2010). Outer membrane vesicles derived from *Escherichia coli* induce systemic inflammatory response syndrome. *PLoS ONE* 5:e11334. doi: 10.1371/journal.pone.0011334

Pérez-Cruz, C., Carrión, O., Delgado, L., Martinez, G., López-Iglesias, C., and Mercade, E. (2013). New type of outer membrane vesicle produced by the Gram-negative bacterium Shewanella vesiculosa M7T: implications for DNA content. *Appl. Environ. Microbiol.* 79, 1874–1881. doi: 10.1128/AEM.03657-12

Pérez-Cruz, C., Delgado, L., López-Iglesias, C., and Mercade, E. (2015). Outer-inner membrane vesicles naturally secreted by gram-negative pathogenic bacteria. *PLoS ONE* 10:e0116896. doi: 10.1371/journal.pone.0116896

Petousis-Harris, H., Paynter, J., Morgan, J., Saxton, P., McArdle, B., Goodyear-Smith, F., et al. (2017). Effectiveness of a group B outer membrane vesicle meningococcal vaccine against gonorrhoea in New Zealand: a retrospective case-control study. *Lancet* 390, 1603–1610. doi: 10.1016/S0140-6736(17)31449-6

Rewatkar, P. V., Parton, R. G., Parekh, H. S., and Parat, M. O. (2015). Are caveolae a cellular entry route for non-viral therapeutic delivery systems? *Adv. Drug Deliv. Rev.* 91, 92–108. doi: 10.1016/j.addr.2015.01.003

Reyes-Robles, T., Dillard, R. S., Cairns, L. S., Silva-Valenzuela, C. A., Housman, M., Ali, A., et al. (2018). *Vibrio cholerae* outer membrane vesicles inhibit bacteriophage infection. *J. Bacteriol.* 200:e00792–17. doi: 10.1128/JB.00792-17

Roier, S., Zingl, F. G., Cakar, F., and Schild, S. (2016). Bacterial outer membrane vesicle biogenesis: a new mechanism and its implications. *Microb. Cell.* 3, 257–259. doi: 10.15698/mic2016.06.508

Rolhion, N., Barnich, N., Bringer, M. A., Glasser, A. L., Ranc, J., Hébuterne, X., et al. (2010). Abnormally expressed ER stress response chaperone Gp96 in CD favours adherent-invasive escherichia coli invasion. *Gut* 59, 1355–1362. doi: 10.1136/gut.2010.207456

Rompikuntal, P. K., Thay, B., Khan, M. K., Alanko, J., Penttinen, A. M., Asikainen, S., et al. (2012). Perinuclear localization of internalized outer membrane vesicles carrying active cytolethal distending toxin from *Aggregatibacter actinomycetemcomitans*. *Infect. Immunity* 80, 31–42. doi: 10.1128/IAI.06069-11

Rompikuntal, P. K., Vdovikova, S., Duperthuy, M., Johnson, T. L., Ahlund, M., Lundmark, R., et al. (2015). Outer membrane vesicle-mediated export of processed PrtV protease from *Vibrio cholerae*. *PLoS ONE* 10:e0134098. doi: 10.1371/journal.pone.0134098

Roy, K., Bartels, S., Qadri, F., and Fleckenstein, J. M. (2010). Enterotoxigenic *Escherichia coli* elicits immune responses to multiple surface proteins. *Infect. Immunity* 78, 3027–3035. doi: 10.1128/IAI.00264-10

Roy, K., Hamilton, D. J., Munson, G. P., and Fleckenstein, J. M. (2011). Outer membrane vesicles induce immune responses to virulence proteins and protect against colonization by enterotoxigenic *Escherichia coli*. *Clin. Vaccine Immunol.* 18, 1803–1808. doi: 10.1128/CVI.05217-11

Rumbo, C., Fernández-Moreira, E., Merino, M., Poza, M., Mendez, J. A., Soares, N. C., et al. (2011). Horizontal transfer of the OXA-24 carbapenemase gene via outer membrane vesicles: a new mechanism of dissemination of carbapenem resistance genes in *Acinetobacter baumannii*. *Antimicrob. Agents Chemother.* 55, 3084–3090. doi: 10.1128/AAC.00929-10

Rüter, C., Lubos, M. L., Norkowski, S., and Schmidt, M. A. (2018). All in-Multiple parallel strategies for intracellular delivery by bacterial pathogens. *Inter. J. Med. Microbiol.* 308, 872–881. doi: 10.1016/j.ijmm.2018.06.007

Schaar, V., de Vries, S. P. W., Vidakovics, M., Bootsma, H. J., Larsson, L., Hermans, P. W. M., et al. (2011). Multicomponent *Moraxella catarrhalis* outer membrane vesicles induce an inflammatory response and are internalized by human epithelial cells. *Cell. Microbiol.* 13, 432–449. doi: 10.1111/j.1462-5822.2010.01546.x

Schaar, V., Uddback, I., Nordstrom, T., and Riesbeck, K. (2014). Group a streptococci are protected from amoxicillin-mediated killing by vesicles containing beta-lactamase derived from *Haemophilus influenzae*. *J. Antimicrob. Chemother.* 69, 117–120. doi: 10.1093/jac/dkt307

Schwechheimer, C., and Kuehn, M. J. (2015). Outer-membrane vesicles from gram-negative bacteria: biogenesis and functions. *Nat. Rev. Microbiol.* 13, 605–619. doi: 10.1038/nrmicro3525

Shah, B., Sullivan, C. J., Lonergan, N. E., Stanley, S., Soult, M. C., and Britt, L. D. (2012). Circulating bacterial membrane cesicles cause sepsis in rats. *Shock* 37, 621–628. doi: 10.1097/SHK.0b013e318250de5d

Stentz, R., Horn, N., Cross, K., Salt, L., Brearley, C., Livermore, D. M., et al. (2015). Cephalosporinases associated with outer membrane vesicles released by *Bacteroides* spp. protect gut pathogens and commensals against beta-lactam antibiotics. *J. Antimicrob. Chemother.* 70, 701–709. doi: 10.1093/jac/dku466

Stephens, D. S., Edwards, K. M., Morris, F., and McGee, Z. A. (1982). Pili and outer-membrane appendages on *Neisseria meningitidis* in the cerebrosinal-fluid of an infant. *J. Infect. Dis.* 146, 568–568. doi: 10.1093/infdis/146.4.568

Svennerholm, K., Park, K. S., Wikstrom, J., Lasser, C., Crescitelli, R., Shelke, G. V., et al. (2017). *Escherichia coli* outer membrane vesicles can contribute to sepsis induced cardiac dysfunction. *Sci. Rep.* 7:17434. doi: 10.1038/s41598-017-16363-9

Tan, T. T., Morgelin, M., Forsgren, A., and Riesbeck, K. (2007). *Haemophilus influenzae* survival during complement-mediated attacks is promoted by *Moraxella catarrhalis* outer membrane vesicles. *Inter. J. Antimicrob. Agents* 29, S206–S206. doi: 10.1016/S0924-8579(07)70656-8

Tarr, P. I., Gordon, C. A., and Chandler, W. L. (2005). Shiga-toxin-producing *Escherichia coli* and haemolytic uraemic syndrome. *Lancet* 365, 1073–1086. doi: 10.1016/S0140-6736(05)74232-X

Thay, B., Damm, A., Kufer, T. A., Wai, S. N., and Oscarsson, J. (2014). *Aggregatibacter actinomycetemcomitans* outer membrane vesicles are internalized in human host cells and trigger NOD1- and NOD2-dependent NF-kappa B activation. *Infect. Immunity* 82, 4034–4046. doi: 10.1128/IAI.01980-14

Toyofuku, M., Nomura, N., and Eberl, L. (2019). Types and origins of bacterial membrane vesicles. *Nat. Rev. Microbiol.* 17, 13–24. doi: 10.1038/s41579-018-0112-2

Turnbull, L., Toyofuku, M., Hynen, A. L., Kurosawa, M., Pessi, G., Petty, N. K., et al. (2016). Explosive cell lysis as a mechanism for the biogenesis of bacterial membrane vesicles and biofilms. *Nat. Commun.* 7:11220. doi: 10.1038/ncomms11220

Urashima, A., Sanou, A., Yen, H., and Tobe, T. (2017). Enterohaemorrhagic escherichia coli produces outer membrane vesicles as an active defence system against antimicrobial peptide LL-37. *Cell. Microbiol.* 19:e12758. doi: 10.1111/cmi.12758

Vanaja, S. K., Russo, A. J., Behl, B., Banerjee, I., Yankova, M., Deshmukh, S. D., et al. (2016). Bacterial outer membrane vesicles mediate cytosolic localization of LPS and caspase-11 activation. *Cell* 165, 1106–1119. doi: 10.1016/j.cell.2016.04.015

Wai, S. N., Lindmark, B., Soderblom, T., Takade, A., Westermark, M., Oscarsson, J., et al. (2003). Vesicle-mediated export and assembly of pore-forming oligomers of the enterobacterial ClyA cytotoxin. *Cell* 115, 25–35. doi: 10.1016/S0092-8674(03)00754-2

Wai, S. N., Takade, A., and Amako, K. (1995). The release of outer-membrane vesicles from the strains of enterotoxigenic *Escherichia coli*. *Microbiol. Immunol.* 39, 451–456. doi: 10.1111/j.1348-0421.1995.tb02228.x

Wang, E. H., Liu, Y. K., Qiu, X. H., Tang, Y. T., Wang, H. D., Xiao, X. Z., et al. (2019). Bacteria-released outer membrane vesicles promote

disseminated intravascular coagulation. *Thromb. Res.* 178, 26–33. doi: 10.1016/j.thromres.2019.03.019

Yokoyama, K., Horii, T., Yamashino, T., Hashikawa, S., Barua, S., Hasegawa, T., et al. (2000). Production of shiga toxin by *Escherichia coli* measured with reference to the membrane vesicle-associated toxins. *FEMS Microbiol. Lett.* 192, 139–144. doi: 10.1111/j.1574-6968.2000.tb09372.x

Zoja, C., Buelli, S., and Morigi, M. (2010). Shiga toxin-associated hemolytic uremic syndrome: pathophysiology of endothelial dysfunction. *Pediatr. Nephrol.* 25, 2231–2240. doi: 10.1007/s00467-010-1522-1

Conflict of Interest: The authors declare that the research was conducted in the absence of any commercial or financial relationships that could be construed as a potential conflict of interest.

frontiers in Cellular and Infection Microbiology

ORIGINAL RESEARCH
published: 24 March 2020
doi: 10.3389/fcimb.2020.00125

High Prevalence of ST131 Subclades C2-*H*30Rx and C1-M27 Among Extended-Spectrum β-Lactamase-Producing *Escherichia coli* Causing Human Extraintestinal Infections in Patients From Two Hospitals of Spain and France During 2015

Saskia-Camille Flament-Simon[1,2], *Vanesa García*[1,2], *Marion Duprilot*[3,4], *Noémie Mayer*[3], *María Pilar Alonso*[2,5], *Isidro García-Meniño*[1,2], *Jesús E. Blanco*[1,2], *Miguel Blanco*[1,2], *Marie-Hélène Nicolas-Chanoine*[3,4] *and Jorge Blanco*[1,2]*

[1] *Laboratorio de Referencia de E. coli (LREC), Departamento de Microbioloxía e Parasitoloxía, Facultade de Veterinaria, Universidade de Santiago de Compostela (USC), Lugo, Spain,* [2] *Grupo Escherichia coli, Instituto de Investigación Sanitaria de Santiago de Compostela (IDIS), Santiago, Spain,* [3] *Service de Microbiologie, Hôpital Beaujon, AP-HP, Clichy, France,* [4] *INSERM and University Paris Diderot, IAME, UMR 1137, Paris, France,* [5] *Unidade de Microbioloxía, Hospital Universitario Lucus Augusti (HULA), Lugo, Spain*

The present study was carried out to evaluate the prevalence of sequence type 131 (ST131) among 188 extended-spectrum β-lactamase-producing *Escherichia coli* (ESBL-EC) collected in 2015 in Lucus Augusti University hospital (Lugo, Spain) and AP-HP Beaujon hospital (Clichy, France) with regard to other STs and to characterize, the types of ESBL produced, serotypes, virulence factor (VF)-encoding genes and the ST131 clades and subclades. ST131 was detected in 33 (39.1%) and 46 (47.9%) of the isolates in Lucus Augusti and Beaujon, respectively. The 109 remaining isolates displayed 57 other STs, the following STs being displayed by at least three isolates: ST10 (8 isolates), ST23 (3), ST38 (4), ST58 (3), ST88 (5), ST95 (4), ST167 (3), ST354 (5), ST361 (3), ST410 (6), ST648 (4), ST744 (3), and ST1615 (6). ST354, ST410, and ST1615 were significantly ($P < 0.05$) more frequent in Lucus Augusti (5.4%, 6.5%, and 6.5%) than in Beaujon (0% for the three STs). The new globally emerging clone ST1193 among extraintestinal clinical ESBL-EC was identified in one isolate from France and one from Spain. CTX-M-15 was the commonest ESBL detected in the two hospitals (44.6% in Lucus Augusti and 50.0% in Beaujon). CTX-M-14 was significantly ($P = 0.0003$) more frequent in Lucus Augusti (31.5%) than in Beaujon (10.4%), whereas CTX-M-1 (20.8 vs. 7.6%; $P = 0.008$) and CTX-M-27 (15.6 vs. 6.5%; $P = 0.0389$) were more frequent in Beaujon than in Lucus Augusti. The ST131 isolates showed a higher virulence score (mean 13.367) compared with the non-ST131 isolates (mean 7.661) ($P < 0.001$). Among the 79 ST131 isolates, most of them (52; 65.8%) belonged to subclade C2 (also known as subclone

OPEN ACCESS

Edited by:
Roxane M. Piazza, Butantan Institute, Brazil

Reviewed by:
Luchang Zhu, Houston Methodist Research Institute, United States
Terezinha Knöbl, University of São Paulo, Brazil

***Correspondence:**
Jorge Blanco
jorge.blanco@usc.es

Specialty section:
This article was submitted to Molecular Bacterial Pathogenesis, a section of the journal Frontiers in Cellular and Infection Microbiology

Received: *13 December 2019*
Accepted: *06 March 2020*
Published: *24 March 2020*

Citation:
Flament-Simon S-C, García V, Duprilot M, Mayer N, Alonso MP, García-Meniño I, Blanco JE, Blanco M, Nicolas-Chanoine M-H and Blanco J (2020) High Prevalence of ST131 Subclades C2-H30Rx and C1-M27 Among Extended-Spectrum β-Lactamase-Producing Escherichia coli Causing Human Extraintestinal Infections in Patients From Two Hospitals of Spain and France During 2015. Front. Cell. Infect. Microbiol. 10:125. doi: 10.3389/fcimb.2020.00125

*H*30Rx) followed by those belonging to subclade C1 (cluster C1-M27: 16 isolates, 20.3%; cluster non-C1-M27: 6 isolates, 7.6%) and clade A (4 isolates; 5.1%). The C2 subclade isolates showed a higher VF-encoding gene score (mean 14.250) compared with the C1-M27 cluster isolates (mean 10.875) ($P < 0.001$). In conclusion, this study highlights the epidemiological differences between the ESBL-EC isolated from two hospitals of France and Spain obtain in 2015 and reports, for the first time, the presence of clone ST1193 in Spain.

Keywords: β-lactamases, CTX-M, *E. coli*, ESBL, ExPEC, resistance, ST131, ST1193

INTRODUCTION

Extended-spectrum β-lactamase-producing *Escherichia coli* (ESBL-EC) is an important cause of urinary tract and bloodstream infections, as well as other types of human extraintestinal infections (Arnaud et al., 2015; Mamani et al., 2019). The main sequence type (ST) responsible for the global increase in ESBL-EC is, without a doubt, ST131 (Nicolas-Chanoine et al., 2008, 2014). This pandemic high-risk clone has numerous virulence factor (VF)-encoding genes (Blanco et al., 2013). Whole-genome sequencing (WGS) analysis had revealed that ST131 consists of three different clades (A, B, and C) characterized by different alleles of the *fimH* gene that is implicated in the colonization abilities, i.e., *fimH*41, *fimH*22, and *fimH*30, respectively (Petty et al., 2014; Ben Zakour et al., 2016). Subclade C2 (also known as subclone *H*30Rx) associated with the production of CTX-M-15 seems to be the most expanded and successful ST131 sublineage (Banerjee et al., 2013; Price et al., 2013; Dahbi et al., 2014; Peirano et al., 2014; Sauget et al., 2016). However, cluster C1-M27 that belongs to subclade C1 and produces CTX-M-27 has recently expanded, first in Japan (Matsumura et al., 2016, 2017), then in other countries (Thailand, Australia, Canada, USA, France, Italy, Germany, The Netherlands and Spain) (Blanc et al., 2014; Birgy et al., 2016; Bevan et al., 2017; Merino et al., 2018; Peirano and Pitout, 2019). The other STs frequently found among ESBL-EC are ST10, ST38, ST405, ST410, ST648, and ST1193 (Brisse et al., 2012; Naseer et al., 2012; Peirano et al., 2012; Izdebski et al., 2013; Peirano and Pitout, 2019). Besides there are notable differences with regard to the ESBL-EC epidemiology according to the countries, including, sometimes, the emergence of new lineages. Thus, a new clade of ST131 associated with the production of the CTX-M-101 enzyme and the *fimH*27 allele has recently been identified in *E. coli* responsible for bacteremia in Denmark (Roer et al., 2017).

The present study was carried out to evaluate the prevalence of clone ST131 among ESBL-EC collected in 2015 in Lucus Augusti University hospital (Lugo, Spain) and AP-HP Beaujon hospital (Clichy, France) with regard to the other STs and to characterize the types of ESBL produced, the serotypes, and the VF-encoding genes as well as the clades and the subclades of the ST131 isolates. This study allowed us to highlight the ESBL-EC epidemiological differences in the two hospitals and to report, for the first time, the presence of the new emerging global clone ST1193 among the ESBL-EC clinical isolates from Spain.

This study was presented in part at the 29th European Congress of Clinical Microbiology and Infectious Diseases, Amsterdam, 13–16 April 2019 (Flament-Simon et al., 2019).

MATERIALS AND METHODS

In this study, 188 non-duplicate (one isolate per patient) ESBL-EC isolated in 2015 in Spain (92 from Lucus Augusti hospital in Lugo) and in France (96 from Beaujon hospital in Clichy) were characterized. They comprised 139 isolates from urine, 25 from blood, seven from bile, and 17 from various other sources.

The following characters were determined as previously described: serotypes using all available O (O1 to O181) and H (H1 to H56) antisera (Guinée et al., 1981), ESBL types (TEM, SHV, and CTX-M enzymes) (Leflon-Guibout et al., 2004), phylogenetic groups (A, B1, B2, C, D, E, F) (Clermont et al., 2013), STs of Achtman scheme (Wirth et al., 2006), clonotypes (*fumC* and *fimH* genes) (Weissman et al., 2012), and VF-encoding genes (Mamani et al., 2019). Isolates were classified as extraintestinal pathogenic *E. coli* (ExPEC) (Johnson et al., 2015) if positive for ≥2 of 5 markers, including *papAH* and/or *papC*, *sfa/focDE*, *afa/draBC*, *kpsM II*, and *iutA*, as uropathogenic *E. coli* (UPEC) (Spurbeck et al., 2012) if positive for ≥3 of 4 markers, including *chuA*, *fyuA*, *vat*, and *yfcV*, and as avian pathogenic *E. coli* (APEC) (Johnson et al., 2008) if positive for ≥4 of 5 markers (*hlyF*, *iutA*, *iroN*, *iss,* and *ompT*). The virotypes A to F were assigned according to the scheme developed by Dahbi et al. (2014). The ST131 clades (A, B, C), subclade C2 (also known as subclone *H*30Rx) and the two clusters of subclade C1 (C1-M27 and the non-C1-M27) were stablished using the PCR assay recently developed by Matsumura et al. (2017).

All the *P*-values were calculated using the Fisher's exact test, except for the comparison of the means that was performed using the one-way ANOVA test. $P < 0.05$ were considered statistically significant.

RESULTS

Types of ESBL Enzymes

A total of 89 (47.3%) isolates were positive for CTX-M-15, 39 (20.7%) for CTX-M-14, 27 (14.4%) for CTX-M-1, 21 (11.2%) for CTX-M-27, 11 (5.9%) for SHV-12, two (1.1%) for CTX-M-32 and one (0.5%) for CTX-M-55. CTX-M-15 was the commonest ESBL detected in the two hospitals (44.6% in Lucus Augusti and

50.0% in Beaujon). CTX-M-14 was significantly ($P = 0.0003$) more frequent in Lucus Augusti (31.5%) than in Beaujon (10.4%), whereas CTX-M-1 (20.8 vs. 7.6%; $P = 0.008$) and CTX-M-27 (15.6 vs. 6.5%; $P = 0.0389$) were more frequent in Beaujon than in Lucus Augusti (**Table 1**).

Phylogenetic Groups

The most frequent phylogenetic group was B2 (50.5%), followed by A (14.4%), C (11.7%), B1 (9.6%), F (6.9%), E (5.3%), and D (1.6%). Phylogenetic groups A, C and F were found more frequently among Lucus Augusti isolates, while phylogenetic group B2 was more frequent among Beaujon isolates ($P < 0.05$) (**Table 1**).

Among CTX-M-15 and CTX-M-27-producing isolates, the most frequent phylogenetic group was B2, while among those producing CTX-M-1, CTX-M-14, and SHV-12, the most frequent phylogenetic groups were B1, C, and F, respectively (**Table 2**).

Sequence Types

ST131 was detected in 33 (39.1%) and 46 (47.9%) of isolates in Lucus Augusti and Beaujon, respectively. The 109 remaining isolates displayed 57 different STs and the following STs displayed at least three isolates: ST10 (8 isolates), ST23 (3), ST38 (4), ST58 (3), ST88 (5), ST95 (4), ST167 (3), ST354 (5), ST361 (3), ST410 (6), ST648 (4), ST744 (3), and ST1615 (6). ST354, ST410, and ST1615 were significantly ($P < 0.05$) more frequent in Lucus Augusti (5.4, 6.5, and 6.5%) than in Beaujon (0% for the three STs) (**Tables 1**, **2**). The new emerging global clone ST1193 was identified in one isolate from France and one from Spain. The majority (121 of 188; 64.4%) of ESBL-EC isolates belonged to only three clonal complexes: CC10 (19 isolates), CC23 (22 isolates) and CC131 (80 isolates) (**Table S1**).

Clonotypes, Clades and Subclades of ST131 Isolates

The 79 ST131 isolates were distributed in three clonotypes: CH40-30 (73 isolates), CH40-35 (2), CH40-41 (4) (**Table 1**). Subclade C2 (also known as subclone *H*30Rx) was the commonest subclade detected among the 79 ST131 isolates (52 isolates; 65.8%), followed by cluster C1-M27 (16 isolates; 20.3%), cluster non-C1-M27 (6 isolates; 7.6%), and clade A (4 isolates; 5.1%). The 52 C2 subclade isolates were positive for CTX-M-15, whereas the 16 C1-M27 isolates were positive for CTX-M-27. Five non-C1-M27 isolates of C1 subclade were positive for CTX-M-15 and one for CTX-M-14. The four isolates belonging to clade A were positive for CTX-M-1 (2), CTX-M-15 (1), and CTX-M-27 (1).

Clones

A total of 71 clones (defined by the association of phylogroup, clonotype and ST) were identified among the 188 ESBL-EC with 23 of them including at least two isolates and only five at least five isolates: A-CH11-54-ST10 (6 isolates), B2-CH40-30-ST131 (73), C-CH4-24-ST410 (6), C-CH263-32-ST1615 (6), and F-CH88-58-ST354 (5) (**Table 3**).

TABLE 1 | Characteristics of 188 ESBL-EC isolated from extraintestinal infections.

Characteristic	No. (%) of isolates		*P*-value
	Lucus augusti hospital, Spain ($n = 92$)	Beaujon hospital, France ($n = 96$)	
ESBL enzyme			
CTX-M-1	7 (7.6)	**20 (20.8)**	0.008
CTX-M-14	**29 (31.5)**	10 (10.4)	0.0003
CTX-M-15	41 (44.6)	48 (50.0)	
CTX-M-27	6 (6.5)	**15 (15.6)**	0.0389
CTX-M-32	2 (2.2)	0	
CTX-M-55	0	1 (1.0)	
SHV-12	8 (8.7)	3 (3.1)	
Phylogenetic group			
A	**18 (19.6)**	9 (9.4)	0.0367
B1	7 (7.6)	11 (11.5)	
B2	38 (41.3)	**57 (59.4)**	0.0097
C	**16 (17.4)**	6 (6.3)	0.0151
D	1 (1.1)	2 (2.1)	
E	2 (2.2)	8 (8.3)	
F	**10 (10.9)**	3 (3.1)	0.0341
ST131			
Total	33 (39.1)	46 (47.9)	
Clade A	1 (1.1)	3 (3.1)	
Subclade C1	5 (5.4)	11 (11.5)	
Cluster C1-M27			
Subclade C1 Cluster non-C1-M27	0	**6 (6.3)**	0.0164
Subclade C2	27 (29.3)	25 (26.0)	
Clade-Not typeable	0	1 (1.0)	
Clonotype CH40-30	30 (32.6)	43 (44.8)	
Clonotype CH40-35	2 (2.2)	0	
Clonotype CH40-41	1 (1.1)	3 (3.1)	
Virotype A	**7 (7.6)**	1 (1.0)	0.0280
Virotype C1	1 (1.1)	1 (1.0)	
Virotype C2	10 (10.9)	15 (15.6)	
Virotype C3	0	2 (2.1)	
Virotype E	10 (10.9)	8 (8.3)	
Virotype F	3 (3.3)	**11 (11.5)**	0.0293
Virotype A-like	1 (1.1)	6 (6.3)	
Virotype E-like	1 (1.1)	0	
Virotype-not typeable	1 (1.1)	2 (2.1)	
Other ST[a]			
ST10	6 (6.5)	2 (2.1)	
ST23	1 (1.1)	2 (2.1)	
ST38	0	4 (4.2)	
ST58	2 (2.2)	1 (1.0)	
ST88	1 (1.1)	4 (4.2)	
ST95	0	4 (4.2)	
ST167	2 (2.2)	1 (1.0)	
ST354	**5 (5.4)**	0	0.0265
ST361	2 (2.2)	1 (1.0)	
ST410	**6 (6.5)**	0	0.0126
ST648	3 (3.3)	1 (1.0)	
ST744	1 (1.1)	2 (2.1)	
ST1615	**6 (6.5)**	0	0.0126

[a] *Represented by at least 3 isolated.*

Significant differences are indicated in bold.

TABLE 2 | Phylogenetic groups and sequence types according to ESBL enzymes.

ESBL enzyme (no. of isolates)	Phylogenetic groups	Sequence types
CTX-M-1 (27)	A (3), B1 (11), B2 (3), C (6), D (1), E (2), F (1)	ST10 (1), ST23 (2), ST34 (1), ST58 (1), ST69 (1), **ST88** (3), ST90 (1), ST131 (2), ST155 (1), ST162 (1), ST205 (1), ST224 (1), ST453 (2), ST1266 (1), ST1431 (1), ST2067 (1), ST2558 (1), ST2766 (1), ST3778 (1), ST8152 (1), ST new 2-6057like (1), ST new 3-1268like (1)
CTX-M-14 (39)	A (8), B1 (4), B2 (10), C (11), E (2), F (4)	**ST10** (4), ST12 (1), ST59 (1), ST73 (1), ST88 (2), ST93 (1), ST95 (2), ST131 (1), **ST167** (3), **ST354** (3), ST357 (1), ST362 (1), ST404 (2), ST405 (1), **ST410** (3), ST448 (1), ST602 (1), ST1154 (1), ST1193 (1), **ST1615** (6), ST5528 (1), ST10328 (1)
CTX-M-15 (89)	A (11), B2 (64), C (4), D (2), E (4), F (4)	ST4 (1), ST34 (1), ST38 (2), ST44 (1), ST69 (1), ST90 (1), ST95 (2), ST127 (1), **ST131** (59), ST141 (1), ST358 (1), **ST361** (3), ST405 (1), **ST410** (3), ST540 (1), **ST648** (4), ST744 (2), ST1284 (1), ST2279 (1), ST3075 (1), ST5214 (1)
CTX-M-27 (21)	B2 (18), C (1), E (2),	**ST131** (17), ST38 (2), ST90 (1), ST1193 (1)
CTX-M-32 (2)	B1 (2)	ST58 (2)
CTX-M-55 (1)	A (1)	ST744 (1)
SHV-12 (11)	A (4), B1 (1), C (1), F (5)	ST10 (2), ST23 (1), ST117 (1), ST156 (1), ST354 (2), ST1485 (1), ST3778 (1), ST new 1-10 like (2)

The most frequent STs are indicated in bold.

TABLE 3 | ESBL enzymes, serotypes and ExPEC, UPEC and APEC status according to the clones including at least two isolates.

Clones (no. of isolates from Spain and France)	ESBL enzymes	Serotypes	ExPEC	UPEC	APEC
A-CH11-54-ST10 (5/1)	CTX-M-14 (4), SHV-12 (2)	O6:HNM (1), O101:HNT (2), ONT:HNM (3)	0	0	2
A-CH11-negative-ST167 (2/1)	CTX-M-14 (3)	O101:HNM (2), O101:H25 (1)	1	0	0
A-CH11-54-ST744 (1/2)	CTX-M-15 (2), CTX-M-55 (1)	ONT:H9 (1), ONT:HNM (2)	0	0	0
A-CH99-54-ST361 (2/1)	CTX-M-15 (3)	O9:HNM (3)	0	0	0
B1-CH4-32-ST58 (1/1)	CTX-M-1 (1), CTX-M-32 (1)	O9:H25 (1), ONT:HNM (1)	1	0	2
B1-CH6-31-ST453 (0/2)	CTX-M-1 (2)	O23:HNM (1), ONT:HNM (1)	0	0	1
B2-CH38-15-ST95 (0/2)	CTX-M-14 (2)	O18:H7 (2)	2	2	2
B2-CH38-294-ST95 (0/2)	CTX-M-15 (2)	O18:H7 (2)	2	2	2
B2-CH40-30-ST131 (30/43)	CTX-M-15 (56), CTX-M-27 (16), CTX-M-14 (1)	O25:H4 (69), O14:H4 (1), ONT:H4 (3)	68	73	0
B2-CH40-35-ST131 (2/0)	CTX-M-15 (2)	O25:H4 (2)	2	2	0
B2-CH40-41-ST131 (1/3)	CTX-M-1 (2), CTX-M-15 (1), CTX-M-27 (1)	O16:H5 (3), O153:H5 (1)	3	2	0
B2-CH14-27-ST404 (1/1)	CTX-M-14 (2)	O75:HNM (2)	2	2	0
B2-CH14-64-ST1193 (1/1)	CTX-M-14 (1), CTX-M-27 (1)	O75:HNM (2)	2	2	0
C-CH4-35-ST23 (1/2)	CTX-M-1 (2), SHV-12 (1)	O55:H9 (1), O78:HNM (2)	1	0	2
C-CH4-41-ST88 (0/2)	CTX-M-1 (1), CTX-M-14 (1)	O8:HNM (1), O86:HNT (1)	2	0	0
C-CH4-303-ST88 (0/2)	CTX-M-1 (2)	O9:H17 (2)	2	0	2
C-CH4-142-ST90 (2/0)	CTX-M-1 (1), CTX-M-15 and CTX-M-27 (1)	O8:H9 (2)	0	0	0
C-CH4-24-ST410 (6/0)	CTX-M-14 (3), CTX-M-15 (3)	O9:HNM (2), O20:H9 (3), ONT:HNM (1)	0	0	0
C-CH263-32-ST1615 (6/0)	CTX-M-14 (6)	O11:H9 (3), O153:H9 (1), ONT:H9 (2)	0	0	0
E-CH26-negative-ST38 (0/3)	CTX-M-15 (1), CTX-M-27 (2)	O86:H18 (3)	3	0	0
E-CH37-27-ST405 (1/1)	CTX-M-14 (1), CTX-M-15 (1)	O102:H4 (1), O102:HNM (1)	0	0	0
F-CH88-58-ST354 (5/0)	CTX-M-14 (3), SHV-12 (2)	O1:H34 (1), O1:HNM (1), O11:H4 (2), O153:HNT (1)	1	2	0
F-CH4-171-ST648 (2/0)	CTX-M-15 (2)	O45:H45 (2)	0	0	0

Serotypes

The 188 ESBL-EC isolates belonged to 30 O serogroups and expressed 17 different H antigens, but 71 of the 79 ST131 isolates belonged to serotype O25:H4. The other prevalent serotypes were: O9:HNM (three ST361 isolates), O11:H9 (three ST1615 isolates), O16:H5 (three ST131 isolates), O18:H7 (four ST95 isolates), O20:H9 (three ST410 isolates), O75:HNM (two ST404 and two ST1193 isolates of clonal complex 14), and O86:H18 (three ST38 isolates). The H4 and H5 flagellar antigens were associated with ST131, the H7 with ST95, the H9 with ST10, ST744, and four STs of the clonal complex 23 (ST23, ST90, ST410, ST1615), the H18 with ST38 and ST69, and the H6 and the H45 antigens with ST648 (**Table 3** and **Table S1**).

Virulence Factor (VF)-Encoding Genes

Of the 188 ESBL-EC isolates, 57.4% were classified as ExPEC, 52.7% as UPEC and 12.8% as APEC. The prevalence of ExPEC (92.4 vs. 32.1%) ($P < 0.001$) and UPEC (97.5 vs. 20.2%) (P

< 0.001) status were higher within ST131 isolates than within non-ST131 isolates. In contrast, the prevalence of APEC (0 vs. 22%) status was higher among non-ST131 isolates ($P < 0.001$) (**Table 4**).

The ST131 isolates showed a higher VF-encoding gene score (mean 13.367) compared with the non-ST131 isolates (mean 7.661) ($P < 0.001$). However, four isolates belonging to clones B2-CH38-15-ST95 and B2-CH38-294-ST95 were those with the highest number of virulence genes (mean 21.000).

Nineteen VF-encoding genes (*papAH, papC, papEF, afa/draBC*, *yfcV*, *sat*, *cnf1*, *hlyA, iucD*, *iutA*, *fyuA*, *chuA*, *kpsM II*, *kpsM II-K2*, *kpsM II-K5*, *traT, malX*, *usp,* and *ompT*) were significantly associated with ST131 isolates, whereas that 10 (*fimAv*$_{MT78}$, *sfa/focDE*, *hlyF*, *tsh, vat*, *iroN*, *kpsM II-K1*, *cvaC*, *iss, and ibeA*) were significantly associated with non-ST131 isolates.

The C2 subclade isolates showed a higher virulence score (mean 14.250) compared with C1-M27 isolates (mean 10.875) ($P < 0.001$). The genes *papAH, papC, papEF, cnf1, and hlyA* were associated with the C2 subclade isolates.

The most prevalent virotypes identified in ST131 isolates were A (8 isolates), C2 (25), E (18) and F (14) and a new virotype similar to A (virotype A-like) displayed by seven isolates. Further, a second new virotype similar to E (virotype E-like) was found in one isolate (**Table S1**). The virotype A was found more frequently among Lucus Augusti isolates ($P = 0.0280$), while virotype F was more frequent among Beaujon isolates ($P = 0.0293$).

DISCUSSION

The management of urinary tract and bloodstream infections due to *E. coli* has been complicated by the emergence of multidrug-resistance, especially of that related to the expansion of high-risk clones such as ST131 (Nicolas-Chanoine et al., 2008; de Toro et al., 2017). Since 2006, the prevalence of ESBL-EC among *E. coli* causing bacteremia has raised in Lucus Augusti hospital. This increase has been due to the spread of the multidrug-resistant ST131 subclade C2 associated with the production of CTX-M-15. Thus, the number of ESBL-EC isolates increased from 1.0% during 2000–2005 to 5.5% during 2006–2011. While during the first period 0% of the ESBL-EC isolates belonged to subclade C2, during the second period this subclone represented 39.8% (Mamani et al., 2019). A similar situation has been reported in France in different hospitals (Brisse et al., 2012; Sauget et al., 2016) and worldwide (Peirano et al., 2012).

The main change with respect to previous studies conducted at the Lucus Augusti hospital, is the emergence of isolates producing CTX-M-27. Indeed, this enzyme was not produced by any of the 105 ESBL-EC isolates recovered from extraintestinal infections between 2006 and 2007 (Blanco et al., 2009) and by any of the 92 ESBL-EC bloodstream isolates collected from 2001 to 2011 (Mamani et al., 2019) and only by one of 47 ST131 ESBL-EC isolated from urinary tract infections in 2012 (Dahbi et al., 2013). Furthermore, the CTX-M-27 was only detected in one of the 44 Spanish hospitals analyzed in a study carried out in 2006 Díaz et al. (2010), in one of 94 clinical ESBL-EC collected during 2008 in Vall d'Hebron hospital of Barcelona (Coelho et al., 2011), and in none of the 92 ESBL-EC obtained in eight Spanish hospitals during 2010 and 2011 (Merino et al., 2016). In the present study, CTX-M-27 was significantly more frequent in Beaujon (15.6%) than in Lucus Augusti (6.5%). However, the Beaujon's CTX-M-27 percentage appeared as remarkably higher than those found before 2014 (4.5–5.4%) in other 19 hospitals located as Beaujon in the Paris area (Robin et al., 2017; Surgers et al., 2019). Inversely, this percentage was closer to that found between 2014 and 2017 in 24 pediatric centers located in six French regions, i.e., 12.4% among 251 ESBL-EC isolated from febrile urinary tract infections (FUTIs) (Birgy et al., 2020). In addition, it has to be noted that CTX-M-27-producing isolates had already been found in 2012 in the feces of children in day care centers (DDCs) in France (Blanc et al., 2014) and also in feces of patients hospitalized in Madrid during a European survey conducted between 2014 and 2015 (Merino et al., 2018).

The increased prevalence of the CTX-M-27 in the two hospitals enrolled in the present study was mainly due to the expansion of cluster C1-M27 since 17 of the 21 positive CTX-M-27 isolates belonged to this cluster. The four remaining isolates belonged to three different STs, including ST38 (2 isolates), ST90 and ST1193. In the FUTI study, Birgy et al. (2020) also showed that their 31 CTX-M-27-producing isolates mostly belonged to cluster C1-M27 (10 isolates) and ST38 (8 isolates), and also that two belonged to ST1193.

The two ST1193 isolates identified in the present study belonged to clonotype CH14-64 and serotype O75:HNM and were positive for CTX-M-14 (the isolate from Spain) and CTX-M-27 (the isolate from France). As far as we know, this is the first report of the new emerging global clone ST1193 among clinical ESBL-EC isolates from Spain. Inversely, the ST1193 has already been described in France and shown producing either CTX-M-15 or CTX-M-27 in the pediatric FUTIs study (Birgy et al., 2020) and CTX-M-14 among the fecal isolates obtained from children in DCCs in France (Blanc et al., 2014). ST1193 has also been detected in two of 243 third-generation-cephalosporin-resistant *E. coli* isolates obtained from patients with bloodstream infection in Denmark during 2015 (Roer et al., 2018), in three of 51 clinical ESBL-EC isolated in Germany during 2015 and 2016 (Valenza et al., 2019) and in 11 of 225 cefotaxime-resistant *E. coli* isolated from UTIs in South-West England during 2017 and 2018 (Findlay et al., 2019). ST 1193 is currently much more expanded in China (Xia et al., 2014; Wu et al., 2017) and the USA (Johnson et al., 2019; Tchesnokova et al., 2019).

Despite the emergence of ST1193 and ST131 cluster C1-M27, it is clear that ST131 subclade C2 associated to CTX-M-15 remains the most prevalent sublineage among ESBL-EC in the two hospitals studied here, as it is the case in most of the European hospitals (Merino et al., 2016; Sauget et al., 2016; Roer et al., 2018; Findlay et al., 2019; Valenza et al., 2019; Birgy et al., 2020). The C2 subclade isolates showed a higher virulence score (mean 14.250) compared with the subclade C1-M27 ST131 isolates (mean 10.875) ($P < 0.001$) and non-ST131 isolates (mean 7.661) ($P < 0.001$). Interestingly, the *papAH, papC, papEF, cnf1,* and *hlyA* genes were associated with the C2 subclade isolates, which mostly displayed the vitotypes A, A-like, C2, E and F. The virotype A-like is new and differs

TABLE 4 | Virulence factor-encoding genes in the studied 188 isolates and according to ST131 lineage.

Genes	No. (%) of isolates					*P*-value[a]	*P*-value[a]
	Total (*n* = 188)	ST131 Cluster C1-M27 (*n* = 16)	ST131 Subclade C2 (*n* = 52)	ST131 (*n* = 79)	Non-ST131 (*n* = 109)	C1-M27 vs. C2	ST131 vs. non-ST131
Adhesin							
fimH	180 (95.7)	16 (100)	52 (100)	79 (100)	101 (92.7)		
$fimAv_{MT78}$	27 (14.4)	0	0	0	**27 (24.8)**		<0.00001
papAH	50 (26.6)	0	**30 (57.7)**	**31 (39.2)**	19 (17.4)	<0.00001	0.0008
papC	51 (27.1)	0	**30 (57.7)**	**31 (39.2)**	20 (18.3)	<0.00001	0.0013
papEF	52 (27.7)	0	**31 (59.6)**	**32 (40.5)**	20 (18.3)	<0.00001	0.0007
sfa/focDE	10 (5.3)	0	0	0	**10 (9.2)**		0.0036
afa/draBC	20 (10.6)	0	10 (19.2)	**15 (19.0)**	5 (4.6)		0.0018
yfcV	104 (55.3)	16 (100)	52 (100)	**77 (97.5)**	27 (24.8)		<0.00001
Toxin							
sat	82 (43.6)	15 (93.8)	50 (96.2)	**74 (93.7)**	8 (7.3)		<0.00001
cnf1	25 (13.3)	0	**17 (32.7)**	**18 (22.8)**	7 (6.4)	0.0049	<0.00001
hlyA	25 (13.3)	0	**17 (32.7)**	**18 (22.8)**	7 (6.4)	0.0049	<0.00001
hlyF	31 (16.5)	0	0	0	**31 (28.4)**		<0.00001
cdtB	5 (2.7)	0	1 (1.9)	1 (1.3)	4 (3.7)		
tsh	12 (6.4)	0	0	0	**12 (11)**		0.0011
vat	17 (9)	0	0	0	**17 (15.6)**		0.00005
Iron uptake							
iucD	132 (70.2	15 (93.8)	50 (96.2)	**74 (93.7)**	58 (53.2)		<0.00001
iutA	134 (71.3)	15 (93.8)	50 (96.2)	**74 (93.7)**	60 (55)		<0.00001
iroN	32 (17)	0	0	0	**32 (29.4)**		<0.00001
fyuA	128 (68.1)	16 (100)	52 (100)	**79 (100)**	49 (45)		<0.00001
chuA	121 (64.4)	16 (100)	52 (100)	**79 (100)**	42 (38.5)		<0.00001
Capsule							
kpsM II	106 (56.4)	15 (93.8)	49 (94.2)	**73 (92.4)**	33 (30.3)		<0.00001
kpsM II-K2	13 (6.9)	0	7 (13.5)	**11 (13.9)**	2 (1.8)		0.0015
kpsM II-K5	83 (44.1)	15 (93.8)	42 (80.8)	**62 (78.5)**	21 (19.3)		<0.00001
neuC-K1	10 (5.3)	0	0	0	**10 (9.2)**		0.0036
kpsM III	2 (1.1)	0	0	0	2 (1.8)		
Miscellaneous							
cvaC	21 (11.2)	0	0	0	**21 (19.3)**		<0.00001
iss	23 (12.2)	0	0	0	**23 (21.1)**		<0.00001
traT	139 (73.9)	13 (81.3)	42 (80.8)	**64 (81)**	75 (68.8)		0.0422
ibeA	12 (6.4)	0	0	0	**12 (11)**		0.0011
malX	113 (60.1)	16 (100)	52 (100)	**79 (100)**	34 (31.2)		<0.00001
usp	101 (53.7)	16 (100)	52 (100)	**79 (100)**	22 (20.2)		<0.00001
ompT	126 (67)	16 (100)	52 (100)	**79 (100)**	47 (43.1)		<0.00001
ExPEC status	108 (57.4)	15 (93.8)	50 (96.2)	**73 (92.4)**	35 (32.1)		<0.00001
UPEC status	99 (52.7)	16 (100)	52 (100)	**77 (97.5)**	22 (20.2)		<0.00001
APEC status	24 (12.8)	0	0	**0**	**24 (22)**		<0.00001

[a] *P-values (by Fisher's exact test) are shown where P < 0.05.*
Significant differences are indicated in bold.

from the virotype A in the type of capsular *kpsM II* gene that is *K*5 instead of *K*2 (Dahbi et al., 2014). In future studies, it would be very interesting to determine the whole genome sequence of the C2 subclade isolates belonging to the new virotype A-like.

Of note, four isolates belonging to clones B2-CH38-15-ST95 and B2-CH38-294-ST95 were those with the highest number of VF-encoding genes (mean 21.000). These four UTI isolates were classified as APEC and could be of avian origin and foodborne pathogens (Vincent et al., 2010; Singer, 2015; Liu et al., 2018).

ST95 is one of the most frequently ST identified among *E. coli* causing human extraintestinal infections, but it is rarely producer of ESBL enzymes (Kallonen et al., 2017). Nevertheless, recently Birgy et al. (2020) detected nine ST95 isolates among 251 ESBL-EC from pediatric FUTIs. The combination of so many virulence genes and resistance-encoding genes in this successful ST is very worrying.

CONCLUSIONS

Despite the enormous genetic diversity observed in our ESBL-EC collection (71 clones amongst 188 ESBL-EC), it can be concluded that the majority of the isolates belong to only three clonal complexes (CC10, CC23, and CC131) and that ST131 subclade C2 associated with the production of CTX-M-15 remains the most prevalent *E. coli* lineage among the ESBL-EC isolates identified in the studied Spanish and French hospitals.

DATA AVAILABILITY STATEMENT

All datasets generated for this study are included in the article/**Supplementary Material**.

AUTHOR CONTRIBUTIONS

S-CF-S, VG, MD, NM, MA, IG-M, JEB, and MB undertook the laboratory work. M-HN-C and JB conceived the concept for the paper and designed the experiments. All authors provided critical input, contributed to the writing of the manuscript, and have approved the final version.

FUNDING

This study was supported by projects: PI16/01477 from Plan Estatal de I+D+I 2013–2016, Instituto de Salud Carlos III (ISCIII), Subdirección General de Evaluación y Fomento de la Investigación, Ministerio de Economía y Competitividad (Gobierno de España) and Fondo Europeo de Desarrollo Regional (FEDER); and ED431C2017/57 from the Consellería de Cultura, Educación e Ordenación Universitaria (Xunta de Galicia), and FEDER.

ACKNOWLEDGMENTS

S-CF-S acknowledges the FPU programme for her grant (FPU15/02644) from the Secretaría General de Universidades, Spanish Ministerio de Educación, Cultura y Deporte. VG and IG-M acknowledge the Consellería de Cultura, Educación e Ordenación Universitaria, Xunta de Galicia for her postdoctoral grant (ED481B2018/018) and his predoctoral grant (ED481A-2015/149), respectively.

SUPPLEMENTARY MATERIAL

The Supplementary Material for this article can be found online at: https://www.frontiersin.org/articles/10.3389/fcimb.2020.00125/full#supplementary-material

Table S1 | Characteristics of 188 extended-spectrum β-lactamase-producing *Escherichia coli* (ESBL-EC) collected in 2015 in Lucus Augusti University hospital (Lugo, Spain) and AP-HP Beaujon hospital (Clichy, France).

REFERENCES

Arnaud, I., Maugat, S., Jarlier, V., Astagneau, P., and RAISIN/multidrug resistance study group (2015). Ongoing increasing temporal and geographical trends of the incidence of extended-spectrum beta-lactamase-producing *Enterobacteriaceae* infections in France, 2009 to 2013. *Euro. Surveill.* 20:30014. doi: 10.2807/1560-7917.ES.2015.20.36.30014

Banerjee, R., Robicsek, A., Kuskowski, M. A., Porter, S., Johnston, B. D., Sokurenko, E., et al. (2013). Molecular epidemiology of *Escherichia coli* sequence type 131 and its H30 and H30-Rx subclones among extended-spectrum-β-lactamase-positive and -negative *E. coli* clinical isolates from the Chicago Region, 2007 to 2010. *Antimicrob. Agents Chemother.* 57, 6385–6388. doi: 10.1128/AAC.01604-13

Ben Zakour, N. L., Alsheikh-Hussain, A. S., Ashcroft, M. M., Khanh Nhu, N. T., Roberts, L. W., Stanton-Cook, M., et al. (2016). Sequential acquisition of virulence and fluoroquinolone resistance has shaped the evolution of *Escherichia coli* ST131. *MBio* 7:e00347-16. doi: 10.1128/mBio.00347-16

Bevan, E. R., Jones, A. M., and Hawkey, P. M. (2017). Global epidemiology of CTX-M β-lactamases: temporal and geographical shifts in genotype. *J. Antimicrob. Chemother.* 72, 2145–2155. doi: 10.1093/jac/dkx146

Birgy, A, Levy, C., Bidet, P., Thollot, F., Derkx, V., Béchet, S., et al. (2016) ESBL-producing Escherichia coli ST131 versus non-ST131: evolution and risk factors of carriage among French children in the community between 2010 and 2015. *J. Antimicrob. Chemother.* 71, 2949–2956. doi: 10.1093/jac/dkw219

Birgy, A., Madhi, F., Jung, C., Levy, C., Cointe, A., Bidet, P., et al. (2020). Diversity and trends in population structure of ESBL-producing *Enterobacteriaceae* in febrile urinary tract infections in children in France from 2014 to 2017. *J. Antimicrob. Chemother.* 75, 96–105. doi: 10.1093/jac/dkz423

Blanc, V., Leflon-Guibout, V., Blanco, J., Haenni, M., Madec, J. Y., and Rafignon, G. (2014). Prevalence of day-care centre children (France) with faecal CTX-M-producing *Escherichia coli* comprising O25b:H4 and O16:H5 ST131 strains. *J. Antimicrob. Chemother.* 69, 1231–1237. doi: 10.1093/jac/dkt519

Blanco, J., Mora, A., Mamani, R., López, C., Blanco, M., Dahbi, G., et al. (2013). Four main virotypes among extended-spectrum-β-lactamase-producing isolates of *Escherichia coli* O25b:H4-B2-ST131: bacterial, epidemiological, and clinical characteristics. *J. Clin. Microbiol.* 51, 3358–3367. doi: 10.1128/JCM.01555-13

Blanco, M., Alonso, M. P., Nicolas-Chanoine, M. H., Dahbi, G., Mora, A., Blanco, J. E., et al. (2009). Molecular epidemiology of *Escherichia coli* producing extended-spectrum β-lactamases in Lugo (Spain): dissemination of clone O25b:H4-ST131 producing CTX-M-15. *J. Antimicrob. Chemother.* 63, 1135–1141. doi: 10.1093/jac/dkp122

Brisse, S., Diancourt, L., Laouénan, C., Vigan, M., Caro, V., Arlet, G., et al. (2012). Phylogenetic distribution of CTX-M- and non-extended-spectrum-β-lactamase-producing *Escherichia coli* isolates: group B2 isolates, except clone ST131, rarely produce CTX-M enzymes. *J. Clin. Microbiol.* 50, 2974–2981. doi: 10.1128/JCM.00919-12

Clermont, O., Christenson, J. K., Denamur, E., and Gordon, D. M. (2013). The clermont *Escherichia coli* phylo-typing method revisited: improvement of specificity and detection of new phylo-groups. *Environ. Microbiol. Rep.* 5, 58–65. doi: 10.1111/1758-2229.12019

Coelho, A., Mora, A., Mamani, R., López, C., González-López, J. J., Larrosa, M. N., et al. (2011). Spread of *Escherichia coli* O25b:H4-B2-ST131 producing CTX-M-15 and SHV-12 with high virulence gene content in Barcelona (Spain). *J. Antimicrob. Chemother.* 66, 517–526. doi: 10.1093/jac/dkq491

Dahbi, G., Mora, A., López, C., Alonso, M. P., Mamani, R., Marzoa, J., et al. (2013). Emergence of new variants of ST131 clonal group among extraintestinal pathogenic *Escherichia coli* producing extended-spectrum β-lactamases. *Int. J. Antimicrob. Agents* 42, 347–351. doi: 10.1016/j.ijantimicag.2013.06.017

Dahbi, G., Mora, A., Mamani, R., López, C., Alonso, M. P., Marzoa, J., et al. (2014). Molecular epidemiology and virulence of *Escherichia coli* O16:H5-ST131: comparison with H30 and H30-Rx subclones of O25b:H4-ST131. *Int. J. Med. Microbiol.* 304, 1247–1257. doi: 10.1016/j.ijmm.2014.10.002

de Toro, M., Fernández, J., García, V., Mora, A., Blanco, J., and de la Cruz, F., et al. (2017). Whole genome sequencing, molecular typing and *in vivo* virulence of OXA-48-producing *Escherichia coli* isolates including ST131 H30-Rx, H22 and H41 subclones. *Sci. Rep.* 21:2103. doi: 10.1038/s41598-017-12015-0

Díaz, M.A., Hernández-Bello, J.R., Rodríguez-Baño, J., Martínez-Martínez, L., Calvo, J., Blanco, J., et al. (2010) Diversity of Escherichia coli strains producing extended-spectrum beta-lactamases in Spain: second nationwide study. *J. Clin. Microbiol.* 48, 2840–2845. doi: 10.1128/JCM.02147-09

Findlay, J., Gould, V. C., North, P., Bowker, K. E., Williams, M. O., MacGowan, A. P., et al. (2019). Characterization of cefotaxime-resistant urinary *Escherichia coli* from primary care in South-West England 2017-18. *J. Antimicrob. Chemother.* 75, 65–71. doi: 10.1101/701383

Flament-Simon, S. C., García, V., Duprilot, M., Mayer, N., Alonso, M. P., García-Meniño, I., et al. (2019). "High prevalence of ST131 subclades C2 and C1-M27 producing CTX-M-15 and CTX-M-27, respectively, among ESBL-producing *Escherichia coli* causing extraintestinal infections in Spain and France during 2015," in *29th European Congress of Clinical Microbiology and Infectious Diseases*, (Amsterdam).

Guinée, P. A. M., Jansen, W. H., Wadström, T., and Sellwood, R. (1981). "*Escherichia coli* associated with neonatal diarrhoea in piglets and calves," in *Laboratory Diagnosis in Neoanatal Calf and Pig Diarrhoea. Current Topics in Veterinary and Animal Science*, eds P. W. de Leeuw and P. A. M. Guinée (Leiden: Martinus Nijhoff Publishers), 126–162.

Izdebski, R., Baraniak, A., Fiett, J., Adler, A., Kazma, M., Salomon, J., et al. (2013). Clonal structure, extended-spectrum β-lactamases, and acquired AmpC-type cephalosporinases of *Escherichia coli* populations colonizing patients in rehabilitation centers in four countries. *Antimicrob. Agents Chemother.* 57, 309–316. doi: 10.1128/AAC.01656-12

Johnson, J. R., Johnston, B. D., Porter, S. B., Clabots, C., Bender, T. L., Thuras, P., et al. (2019). Rapid emergence, subsidence, and molecular detection of *Escherichia coli* sequence type 1193-*fimH64*, a new disseminated multidrug-resistant commensal and extraintestinal pathogen. *J. Clin. Microbiol.* 57:e01664-18. doi: 10.1128/JCM.01664-18

Johnson, J. R., Porter, S., Johnston, B., Kuskowski, M. A., Spurbeck, R. R., Mobley, H. L., et al. (2015). Host characteristics and bacterial traits predict experimental virulence for *Escherichia coli* bloodstream isolates from patients with urosepsis. *Open Forum Infect. Dis.* 2:ofv083. doi: 10.1093/ofid/ofv083

Johnson, T. J., Wannemuehler, Y., Doetkott, C., Johnson, S. J., Rosenberger, S. C., and Nolan, L. K. (2008). Identification of minimal predictors of avian pathogenic *Escherichia coli* virulence for use as a rapid diagnostic tool. *J. Clin. Microbiol.* 46, 3987–3996. doi: 10.1128/JCM.00816-08

Kallonen, T., Brodrick, H. J., Harris, S. R., Corander, J., Brown, N. M., Martin, V., et al. (2017). Systematic longitudinal survey of invasive *Escherichia coli* in England demonstrates a stable population structure only transiently disturbed by the emergence of ST131. *Genome Res.* 27, 1437–1449. doi: 10.1101/gr.216606.116

Leflon-Guibout, V., Jurand, C., Bonacorsi, S., Espinasse, F., Guelfi, M. C., Duportail, F., et al. (2004). Emergence and spread of three clonally related virulent isolates of CTX-M-15-producing *Escherichia coli* with variable resistance to aminoglycosides and tetracycline in a French geriatric hospital. *Antimicrob. Agents Chemother.* 48, 3736–3742. doi: 10.1128/AAC.48.10.3736-3742.2004

Liu, C. M., Stegger, M., Aziz, M., Johnson, T. J., Waits, K., Nordstrom, L., et al. (2018). *Escherichia coli* ST131-*H*22 as a foodborne uropathogen. *MBio* 9:e00470-18. doi: 10.1128/mBio.00470-18

Mamani, R., Flament-Simon, S. C., García, V., Mora, A., Alonso, M. P., López, C., et al. (2019). Sequence types, clonotypes, serotypes, and virotypes of extended-spectrum β-lactamase-producing *Escherichia coli* causing bacteraemia in a Spanish hospital over a 12-year period (2000 to 2011). *Front. Microbiol.* 10:1530. doi: 10.3389/fmicb.2019.01530

Matsumura, Y., Pitout, J. D., Gomi, R., Matsuda, T., Noguchi, T., Yamamoto, M., et al. (2016). Global *Escherichia coli* sequence type 131 clade with $bla_{CTX-M-27}$ gene. *Emerg. Infect. Dis.* 22, 1900–1907. doi: 10.3201/eid2211.160519

Matsumura, Y., Pitout, J. D. D., Peirano, G., DeVinney, R., Noguchi, T., Yamamoto, M., et al. (2017). Rapid identification of different *Escherichia coli* sequence type 131 clades. *Antimicrob. Agents Chemother.* 61:e00179-17. doi: 10.1128/AAC.00179-17

Merino, I., Hernández-García, M., Turrientes, M. C., Pérez-Viso, B., López-Fresneña, N., Diaz-Agero, C., et al. (2018). Emergence of ESBL-producing *Escherichia coli* ST131-C1-M27 clade colonizing patients in Europe. *J. Antimicrob. Chemother.* 73, 2973–2980. doi: 10.1093/jac/dky296

Merino, I., Shaw, E., Horcajada, J. P., Cercenado, E., Mirelis, B., Pallarés, M. A., et al. (2016). CTX-M-15-H30Rx-ST131 subclone is one of the main causes of healthcare-associated ESBL-producing *Escherichia coli* bacteraemia of urinary origin in Spain. *J. Antimicrob. Chemother.* 71, 2125–2130. doi: 10.1093/jac/dkw133

Naseer, U., Olsson-Liljequist, B. E., Woodford, N., Dhanji, H., Cantón, R., Sundsfjord, A., et al. (2012). Multi-locus variable number of tandem repeat analysis for rapid and accurate typing of virulent multidrug resistant *Escherichia coli* clones. *PLoS ONE* 7:e41232. doi: 10.1371/journal.pone.0041232

Nicolas-Chanoine, M. H., Bertrand, X., and Madec, J. Y. (2014). *Escherichia coli* ST131, an intriguing clonal group. *Clin. Microbiol. Rev.* 27, 543–574. doi: 10.1128/CMR.00125-13

Nicolas-Chanoine, M. H., Blanco, J., Leflon-Guibout, V., Demarty, R., Alonso, M. P., Caniça, M. M., et al. (2008). Intercontinental emergence of *Escherichia coli* clone O25:H4-ST131 producing CTX-M-15. *J. Antimicrob. Chemother.* 61, 273–281. doi: 10.1093/jac/dkm464

Peirano, G., and Pitout, J. D. D. (2019). Extended-spectrum β-lactamase-producing *Enterobacteriaceae*: update on molecular epidemiology and treatment options. *Drugs* 79, 1529–1541. doi: 10.1007/s40265-019-01180-3

Peirano, G., van der Bij, A. K., Freeman, J. L., Poirel, L., Nordmann, P., Costello, M., et al. (2014). Characteristics of *Escherichia coli* sequence type 131 isolates that produce extended-spectrum β-lactamases: global distribution of the *H*30-Rx sublineage. *Antimicrob. Agents Chemother.* 58, 3762–3767. doi: 10.1128/AAC.02428-14

Peirano, G., van der Bij, A. K., Gregson, D. B., and Pitout, J. D. (2012). Molecular epidemiology over an 11-year period (2000 to 2010) of extended-spectrum β-lactamase-producing *Escherichia coli* causing bacteremia in a centralized Canadian region. *J. Clin. Microbiol.* 50, 294–299. doi: 10.1128/JCM.06025-11

Petty, N. K., Ben Zakour, N. L., Stanton-Cook, M., Skippington, E., Totsika, M., and Forde, B. M. (2014). Global dissemination of a multidrug resistant *Escherichia coli* clone. *Proc. Natl. Acad. Sci. U.S.A.* 111, 5694–5699. doi: 10.1073/pnas.1322678111

Price, L. B., Johnson, J. R., Aziz, M., Clabots, C., Johnston, B., Tchesnokova, V., et al. (2013). The epidemic of extended-spectrum-β-lactamase-producing *Escherichia coli* ST131 is driven by a single highly pathogenic subclone, H30-Rx. *MBio* 4:e00377-13. doi: 10.1128/mBio.00377-13

Robin, F., Beyrouthy, R., Bonacorsi, S., Aissa, N., Bret, L., Brieu, N., et al. (2017). Inventory of extended-spectrum-β-lactamase-producing *Enterobacteriaceae* in France as assessed by a multicenter study. *Antimicrob. Agents Chemother.* 61:e01911-16. doi: 10.1128/AAC.01911-16

Roer, L., Hansen, F., Thomsen, M. C. F., Knudsen, J. D., Hansen, D. S., Wang, M., et al. (2017). WGS-based surveillance of third-generation cephalosporin-resistant *Escherichia coli* from bloodstream infections in Denmark. *J. Antimicrob. Chemother.* 72, 1922–1929. doi: 10.1093/jac/dkx092

Roer, L., Johannesen, T. B., Hansen, F., Stegger, M., Tchesnokova, V., Sokurenko, E., et al. (2018). CHTyper, a web tool for subtyping of extraintestinal pathogenic *Escherichia coli* based on the *fumC* and *fimH* alleles. *J. Clin. Microbiol.* 56:e00063-18. doi: 10.1128/JCM.00063-18

Sauget, M., Cholley, P., Vannier, A., Thouverez, M., Nicolas-Chanoine, M. H., Hocquet, D., et al. (2016). Trends of extended-spectrum β-lactamase-producing *Escherichia coli* sequence type 131 and its *H*30 subclone in a French hospital over a 15-year period. *Int. J. Antimicrob. Agents.* 48, 744–747. doi: 10.1016/j.ijantimicag.2016.09.023

Singer, R. S. (2015). Urinary tract infections attributed to diverse ExPEC strains in food animals: evidence and data gaps. *Front. Microbiol.* 6:28. doi: 10.3389/fmicb.2015.00028

Spurbeck, R. R., Dinh, P. C. Jr., Walk, S. T., Stapleton, A. E., Hooton, T. M., Nolan, L. K., et al. (2012). *Escherichia coli* isolates that carry vat, fyuA, chuA, and yfcV efficiently colonize the urinary tract. *Infect. Immun.* 80, 4115–4122. doi: 10.1128/IAI.00752-12

Surgers, L., Boersma, P., Girard, P. M., Homor, A., Geneste, D., Arlet, G., et al. (2019). Molecular epidemiology of ESBL-producing *E. coli* and *K. pneumoniae*: establishing virulence clusters. *Infect. Drug Resist.* 12, 119–127. doi: 10.2147/IDR.S179134

Tchesnokova, V. L., Rechkina, E., Larson, L., Ferrier, K., Weaver, J. L., Schroeder, D. W., et al. (2019). Rapid and extensive expansion in the United States of a new multidrug-resistant *Escherichia coli* clonal group, sequence type 1193. *Clin. Infect. Dis.* 68, 334–337. doi: 10.1093/cid/ciy525

Valenza, G., Werner, M., Eisenberger, D., Nickel, S., Lehner-Reindl, V., Höller, C., et al. (2019). First report of the new emerging global clone ST1193 among clinical isolates of extended-spectrum β-lactamase (ESBL)-producing *Escherichia coli* from Germany. *J. Glob. Antimicrob. Resist.* 17, 305–308. doi: 10.1016/j.jgar.2019.01.014

Vincent, C., Boerlin, P., Daignault, D., Dozois, C.M., Dutil, L., Galanakis, C., et al. (2010). Food reservoir for Escherichia coli causing urinary tract infections. *Emerg. Infect. Dis.* 16, 88–95. doi: 10.3201/eid1601.091118

Weissman, S. J., Johnson, J. R., Tchesnokova, V., Billig, M., Dykhuizen, D., Riddell, K., et al. (2012). High-resolution two-locus clonal typing of extraintestinal pathogenic *Escherichia coli*. *Appl. Environ. Microbiol.* 78, 1353–1360. doi: 10.1128/AEM.06663-11

Wirth, T., Falush, D., Lan, R., Colles, F., Mensa, P., Wieler, L. H., et al. (2006). Sex and virulence in *Escherichia coli*: an evolutionary perspective. *Mol. Microbiol.* 60, 1136–1151. doi: 10.1111/j.1365-2958.2006.05172.x

Wu, J., Lan, F., Lu, Y., He, Q., and Li, B. (2017). Molecular characteristics of ST1193 clone among phylogenetic group B2 non-ST131 fluoroquinolone-resistant *Escherichia coli*. *Front. Microbiol.* 8:2294. doi: 10.3389/fmicb.2017.02294

Xia, S., Fan, X., Huang, Z., Xia, L., Xiao, M., Chen, R., et al. (2014). Dominance of CTX-M-type extended-spectrum β-lactamase (ESBL)-producing *Escherichia coli* isolated from patients with community-onset and hospital-onset infection in China. *PLoS ONE* 9:e100707. doi: 10.1371/journal.pone.0100707

Conflict of Interest: The authors declare that the research was conducted in the absence of any commercial or financial relationships that could be construed as a potential conflict of interest.

frontiers in Cellular and Infection Microbiology

ORIGINAL RESEARCH
published: 22 April 2020
doi: 10.3389/fcimb.2020.00144

Analysis of the Virulence Profile and Phenotypic Features of Typical and Atypical Enteroaggregative *Escherichia coli* (EAEC) Isolated From Diarrheal Patients in Brazil

*Regiane C. B. Dias[1], Rodrigo H. S. Tanabe[1], Melissa A. Vieira[1], Maria C. Cergole-Novella[2], Luís F. dos Santos[3], Tânia A. T. Gomes[4], Waldir P. Elias[5] and Rodrigo T. Hernandes[1]**

[1] Universidade Estadual Paulista (UNESP), Instituto de Biociências, São Paulo, Brazil, [2] Laboratório Regional de Santo André, Instituto Adolfo Lutz, São Paulo, Brazil, [3] Centro de Bacteriologia, Instituto Adolfo Lutz, São Paulo, Brazil, [4] Departamento de Microbiologia, Imunologia e Parasitologia, Universidade Federal de São Paulo- Escola Paulista de Medicina (UNIFESP-EPM), São Paulo, Brazil, [5] Laboratório de Bacteriologia, Instituto Butantan, São Paulo, Brazil

OPEN ACCESS

Edited by:
Guoquan Zhang, The University of Texas at San Antonio, United States

Reviewed by:
George P. Munson, University of Miami, United States
Jorge Blanco, University of Santiago de Compostela, Spain

***Correspondence:**
Rodrigo T. Hernandes
rt.hernandes@unesp.br

Specialty section:
This article was submitted to Molecular Bacterial Pathogenesis, a section of the journal Frontiers in Cellular and Infection Microbiology

Received: *06 February 2020*
Accepted: *19 March 2020*
Published: *22 April 2020*

Citation:
Dias RCB, Tanabe RHS, Vieira MA, Cergole-Novella MC, dos Santos LF, Gomes TAT, Elias WP and Hernandes RT (2020) Analysis of the Virulence Profile and Phenotypic Features of Typical and Atypical Enteroaggregative Escherichia coli (EAEC) Isolated From Diarrheal Patients in Brazil. Front. Cell. Infect. Microbiol. 10:144. doi: 10.3389/fcimb.2020.00144

Enteroaggregative *Escherichia coli* (EAEC) is an important agent of acute and persistent diarrhea in children and adults worldwide. Here we report a characterization of 220 EAEC isolates, 88.2% (194/220) of which were typical and 11.8% (26/220) were atypical, obtained from diarrheal patients during seven years (2010-2016) of epidemiological surveillance in Brazil. The majority of the isolates were assigned to phylogroups A (44.1%, 97/220) or B1 (21.4%, 47/220). The aggregative adherence (AA) pattern was detected in 92.7% (204/220) of the isolates, with six of them exhibiting AA concomitantly with a chain-like adherence pattern; and *agg5A* and *agg4A* were the most common adhesin-encoding genes, which were equally detected in 14.5% (32/220) of the isolates. Each of 12 virulence factor-encoding genes (*agg4A*, *agg5A*, *pic*, *aap*, *aaiA*, *aaiC*, *aaiG*, *orf3*, *aar*, *air*, *capU,* and *shf*) were statistically associated with typical EAEC ($P < 0.05$). The genes encoding the newly described aggregate-forming pili (AFP) searched (*afpB*, *afpD*, *afpP*, and *afpA2*), and/or its regulator (*afpR*), were exclusively detected in atypical EAEC (57.7%, 15/26), and showed a significant association with this subgroup of EAEC ($P < 0.001$). In conclusion, we presented an extensive characterization of the EAEC circulating in the Brazilian settings and identified the *afp* genes as putative markers for increasing the efficiency of atypical EAEC diagnosis.

Keywords: EAEC, virulence factors, diarrhea, diagnosis, antimicrobial resistance

INTRODUCTION

Enteroaggregative *Escherichia coli* (EAEC) is one of the six diarrheagenic *E. coli* (DEC) pathotypes, which is defined as *E. coli* isolates that produce the aggregative adherence pattern (AA) on cultured epithelial cells (HeLa and/or HEp-2) *in vitro* (Nataro and Kaper, 1998; Kaper et al., 2004; Croxen et al., 2013). The AA pattern is characterized by a bacterial arrangement that resembles stacked bricks on both epithelial cells and the coverslip (Nataro et al., 1987). EAEC is a cause of diarrheal disease in children and adults, living in both developing and developed countries, and are associated

with cases of persistent diarrhea and diarrheal outbreaks worldwide (Huang et al., 2006; Estrada-Garcia and Navarro-Garcia, 2012; Hebbelstrup Jensen et al., 2014), besides the fact that EAEC can also be isolated from asymptomatic subjects (Gioppo et al., 2000; Araujo et al., 2007; Lima et al., 2013, 2019a; Dias et al., 2016; Durand et al., 2016).

Previous studies have shown that EAEC isolates can be identified in several serotypes (Zamboni et al., 2004; Boisen et al., 2012; Lima et al., 2019b), and are distributed across the four main *E. coli* phylogroups (A, B1, B2, and D) (França et al., 2013; Imuta et al., 2016). Moreover, high rates of resistance to ampicillin and trimethoprim-sulphamethoxazole, but not to quinolones, have been observed (Aslani et al., 2011; Ikumapayi et al., 2017).

The pathogenicity of EAEC is characterized by the colonization of the intestinal epithelium, followed by the production and secretion of enterotoxins and cytotoxins, which result in secretory diarrhea (Nataro and Kaper, 1998). The establishment of the AA pattern has been associated with the presence of five distinct aggregative adherence fimbriae (AAF/I-AAF/V) (Nataro et al., 1992; Czeczulin et al., 1997; Bernier et al., 2002; Boisen et al., 2008; Jønsson et al., 2015), which belong to the chaperone-usher subclass, as well as afimbrial adhesins (Monteiro-Neto et al., 2003; Bhargava et al., 2009). Very recently, a type IV pilus, termed aggregate-forming pili (AFP), encoded by genes located in the *afp* operon, was identified to be responsible for the establishment of the AA pattern by a hybrid EAEC/STEC (Shiga-toxin producing *E. coli*) isolate of serotype O23:H8, that lacks the AAFs described so far (Lang et al., 2018).

Once adhered to the intestinal epithelium, EAEC produces several enterotoxins and cytotoxins, which include: the enteroaggregative *E. coli* heat-stable enterotoxin (EAST-1), encoded by the *astA* gene, the plasmid-encoded toxin (Pet), the protein involved in colonization (Pic), and autotransporter proteases such as SigA and SepA, which were initially described in *Shigella flexneri*. Another important virulence factor associated with the pathogenicity of EAEC is the protein dispersin (Aap), which facilitates bacterial dispersion in the intestinal epithelium (Sheikh et al., 2002). Dispersin secretion occurs via an ATP-binding cassette (ABC) transporter system, encoded by a cluster of five genes (*aatPABCD*) located in the aggregative adherence plasmid (pAA). The *aatA* gene, which corresponds to the former EAEC probe CVD432, is one the most used target for EAEC identification nowadays (Baudry et al., 1990; Nishi et al., 2003; Lozer et al., 2013).

The AggR protein, encoded by the *aggR* gene located in the pAA, is a global virulence regulator, which activates the expression of several plasmidial and chromosomal virulence factor-encoding genes in the EAEC 042 prototype strain, such as the AAFs, as well as a chromosomal pathogenicity island (PAI), termed *aaiA-aaiP*, which encodes a Type VI Secretion System (T6SS) (Dudley et al., 2006; Morin et al., 2013). Some studies employed genes of the *aaiA-aaiP* operon, such as *aaiA*, *aaiC,* and *aaiG*, as an additional chromosomal marker to enhance the efficiency of EAEC diagnosis (Lima et al., 2013; Andrade et al., 2014; Havt et al., 2017; Hebbelstrup Jensen et al., 2018). Based on the presence of the *aggR* gene, EAEC isolates can be subgrouped into typical ($aggR^+$) and atypical ($aggR^-$) (Kaper et al., 2004).

Moreover, other potential virulence factor-encoding genes that may contribute to the pathogenicity of EAEC isolates, such as *aar* (AggR-activated regulator), *shf* (which encodes a protein involved in biofilm formation initially identified in *Shigella flexneri*), *air* (Enteroaggregative immunoglobulin repeat protein), and *capU* (which encodes a homologous hexosyltransferase) have been described (Czeczulin et al., 1999; Sheikh et al., 2006; Santiago et al., 2017).

The goal of this study was to better understand the diversity of typical and atypical EAEC isolates, obtained from diarrheal patients in Brazil, regarding the somatic (O) and flagellar (H) antigens determination (serotypes), phylogenetic classification, presence of 25 virulence factors-encoding genes (e.g., adhesins, toxins, secreted proteases, type VI secretion system), adherence pattern produced on HeLa cells, and the susceptibility to 11 distinct antimicrobial drugs.

MATERIALS AND METHODS

Enteroaggregative *Escherichia coli* (EAEC) Isolates Used in This Study

A total of 220 EAEC isolates, obtained from stool samples of sporadic cases of diarrhea occurred in Brazil, were included in this study. Of note, 203 EAEC isolates were obtained over 6-years of active epidemiological surveillance (2011–2016), performed at the Instituto Adolfo Lutz (IAL), a public health laboratory and the Brazilian reference center for diarrheagenic *E. coli* identification, as previously published (Ori et al., 2019), as well as 17 EAEC isolates, obtained during the year of 2010, at the same Institute.

In this study, EAEC was defined as *E. coli* isolates that possess the *aatA* gene (former CVD432 probe), and typical and atypical EAEC were differentiated based on the presence of the *aggR* gene in the former group (Kaper et al., 2004).

Serotyping

The somatic (O) and flagellar (H) antigens from 203 EAEC isolates, obtained from 2011 to 2016, were determined in our previous epidemiological surveillance study (Ori et al., 2019). In the 17 remaining EAEC isolates, obtained during the year of 2010, the O and H antigens were determined by standard agglutination tests, with O (O1–O181) and H (H1–H56) antisera produced at Instituto Adolfo Lutz, São Paulo, Brazil (Ewing, 1986).

Phylogroup classification

The classification of the 220 EAEC isolates studied into distinct phylogroups (A, B1, B2, C, D, E, and F) and *Escherichia* clades were performed using the quadruplex Polymerase Chain Reaction (PCR) method as previously described by Clermont et al. (2013). Subsequently, EAEC isolates classified in the phylogroup B2, with the following genotype: $arpA^-$, $chuA^+$, $yjaA^-$, and $TspE4^+$, and all isolates assigned in the phylogroup F were tested in an additional Triplex PCR, using primers and PCR conditions as recently described (Clermont et al., 2019), in order to confirm these isolates as B2 and F or to reclassify them in the phylogroup G.

Detection of Virulence Factor-Encoding Genes

The presence or absence of the EAEC diagnosis markers *aatA* and *aggR* was confirmed in all 220 isolates, and subsequently, these isolates were tested for the presence of genes encoding for: adhesins (*aggA*, *aafA*, *agg3A*, *agg4A*, *agg5A*, *afpB*, *afpD*, *afpP*, *afpA2*, *afpR*, and *eibG*), toxins (*pic*, *pet*, *astA*, *sigA*, and *sepA*) and other virulence factors (*aap*, *aaiA*, *aaiC*, *aaiG*, *orf3*, *aar*, *air*, *capU*, and *shf*), by PCR DNA amplification. PCR was performed using GoTaq Green Master Mix (Promega, Madison, WI, USA) with 0.34 μM of each of the primers. All primer sequences and PCR assay conditions used for the detection of virulence genes are described in the references cited in **Table S1**. PCR products were subjected to agarose gel electrophoresis, prepared with Tris-borate-EDTA (TBE) buffer, and visualized with SYBR Safe DNA Gel Stain (Invitrogen, CA, USA).

Antimicrobial Susceptibility Test

Antimicrobial susceptibility assays were performed following the recommendations of the Clinical and Laboratory Standards Institute (CLSI, 2018), using the disk diffusion method on Mueller-Hinton agar (OXOID, UK). The antimicrobial drugs tested were: ampicillin (AMP; 10 μg), amoxicillin-clavulanic acid (AMC; 20/10 μg), cefazolin (CFZ; 30 μg), cefuroxime (CFX; 30 μg), cefotaxime (CTX; 30 μg), cefepime (CPM; 30 μg), imipenem (IPM; 10 μg), gentamicin (GEN; 10 μg), tobramycin (TOB; 10 μg), ciprofloxacin (CIP; 5 μg), and trimetoprim-sulfamethoxazole (SUT, 1.25/23.75 μg). The *E. coli* ATCC 25922 was used as quality control, and the commercial disks were obtained from Cefar Diagnóstica Ltda (SP, Brazil). EAEC multidrug-resistant was defined by the detection of isolates resistant to three or more classes of antibiotics tested (Magiorakos et al., 2012; Chattaway et al., 2017).

Adherence Assays

The adherence patterns of the EAEC isolates was evaluated in HeLa cells as previously described (Cravioto et al., 1979), with some modifications. Cells were cultured in DMEM (Dulbecco's Modified Eagle Medium—high glucose; Sigma-Aldrich; St. Louis, MO, USA), supplemented with 10% fetal bovine serum (Gibco; Grand Island, New York, USA), with 1% antibiotic (Penicillin-Streptomycin, Sigma; St. Louis, MO, USA) in 5% CO_2 at 37°C. For the adherence assay, ∼1 × 10^5 cells were cultivated in a 24-well microplate, using the same medium described above and containing glass coverslips in each well of the microplate, for 48 h until reaching a confluence of ∼80%. Then, the cells were washed three times with phosphate-buffered saline (PBS, pH 7.4), 1.0 mL of DMEM, supplemented with 2% fetal bovine serum and 1% D-mannose (Sigma, Saint Louis, MO, USA) was added, the cells were infected with 20 μL of an overnight bacterial suspension in LB broth (containing ∼10^8 CFU/mL), and the adherence assay was performed in 5% CO_2 at 37°C. After 3 h of incubation, the infected cells were washed six times with PBS and then fixed with methanol (Dinâmica, SP, Brazil) and stained

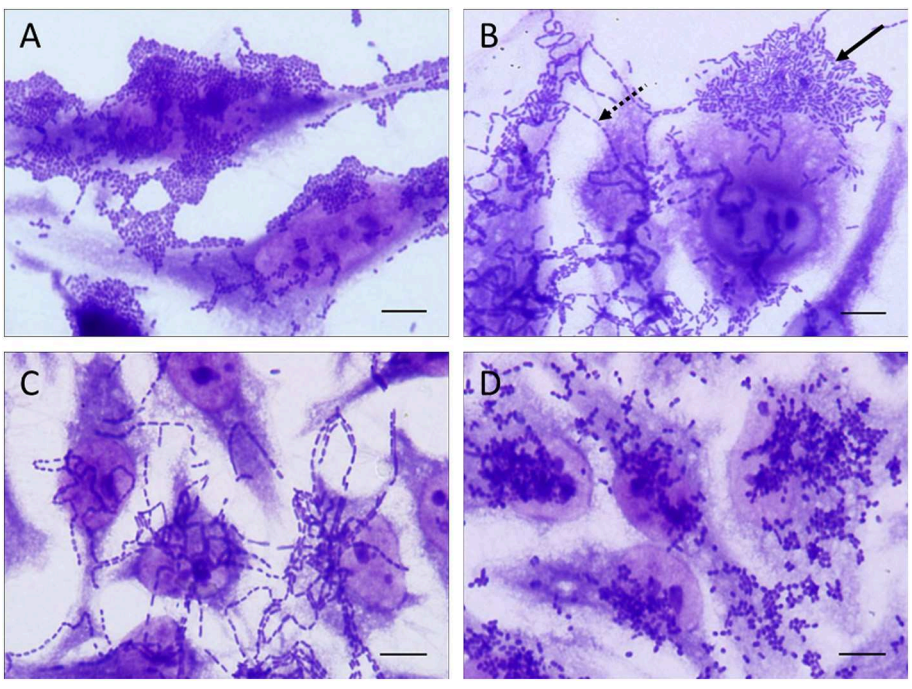

FIGURE 1 | Representative images of the distinct patterns of adherence exhibited by the EAEC isolates studied in adherence assays performed with HeLa cells. The adherence patterns are illustrated as follow: **(A)** aggregative adherence pattern, **(B)** aggregative adherence pattern (solid arrow) occurring concomitantly with the chain-like adherence (dashed arrow), **(C)** chain-like adherence pattern, and **(D)** diffuse adherence pattern. All the adherence patterns illustrated in this picture were observed in adherence assays performed with 3 h of infection. Scale bar = 10 μm.

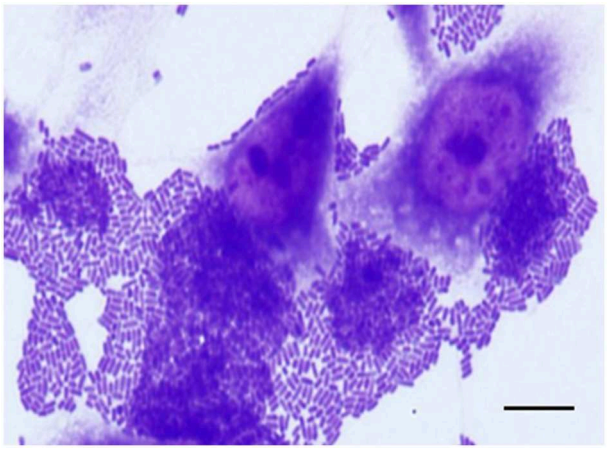

FIGURE 2 | Aggregative adherence (AA) pattern exhibited by an atypical EAEC (*aatA*$^{+}$/*aggR*$^{-}$) isolate (IAL 6006) that harbored the *afp* operon. Note the bacterial stacked brick-like arrangement, characteristic of the AA pattern, on both epithelial cells and coverslip surfaces detected in adherence assay performed with 3 h of infection. Scale bar = 10 μm.

with May-Grünwald (Sigma; St. Louis, MO, USA) and Giemsa (Dinâmica, SP, Brazil) for identification of the adherence pattern by light microscopy analyzes. When the EAEC isolates did not adhere to the epithelial cells or the adherence pattern could not be defined, the adherence assay was repeated in a 6 h bacteria-cell interaction assay, with a washing step after 3 h of incubation, as previously described (Rodrigues et al., 1996), stained with May-Grünwald/Giemsa and then observed by light microscopy. To eliminate potential bias in the adherence pattern classification, each slide was analyzed by three distinct blinded examiners, both to define the adherence pattern exhibited by each EAEC isolate, as well as to select the representative images to be included in **Figures 1**, **2**. In cases of divergence among the three examiners, the EAEC isolate was submitted to a new adherence assay and reevaluated in a blinded-manner until a consensus was obtained.

Statistical Analyses

Differences observed between typical and atypical EAEC were investigated using a Chi-square with Yates' correction or two-tailed Fisher's exact test, as appropriate, and a significance level of 5% ($P < 0.05$) was adopted to consider the differences statistically significant.

RESULTS

The majority of the diarrheal patients, from which the EAEC isolates were obtained, were children up to five-years-old (62.7%, 138/220) and from the São Paulo State (66.8%, 147/220), besides EAEC isolates that were obtained from other Brazilian States, such as Minas Gerais (18.6%, 41/220) and Santa Catarina (14.5%, 32/220) (**Table S2**). We detected 194 typical (88.2%, 194/220) and 26 (11.8%, 26/220) atypical EAEC (**Table 1**), and observed that 56.8% (125/220) were classified in 39 distinct serogroups, besides the occurrence of O non-typeable (19.5%, 43/220) and rough (23.6%, 52/220) isolates (**Table S3**). Regarding the serotypes, O15:H2 (4.5%; 10/220), O175:H28 (4.5%; 10/220), O73:H1 (4.1%; 9/220), O153:H2 (3.6%; 8/220), and O21:H2 (3.2%; 7/220) were the most frequent ones, and exclusively detected in the typical EAEC subgroup (**Table S3**). The classification of the EAEC isolates in the distinct *E. coli* phylogroups, demonstrated that EAEC were assigned mainly in the phylogroups A (44.1%, 97/220), B1 (21.4%, 47/220), D (13.2%, 29/220), and E (10.0%, 22/220) (**Table 2**), and the number of atypical EAEC identified in the phylogroup A was significantly higher than typical (65.4 vs. 41.2%), with this difference being statistically significant ($P < 0.05$). Moreover, 2.3% (5/220) of the EAEC isolates studied,

TABLE 1 | Occurrence of virulence factor-encoding genes in typical and atypical EAEC isolates.

Genes investigated	No. (%) of isolates			*P*-value[c,d]
	Typical EAEC (*n* = 194)	Atypical EAEC (*n* = 26)	Total (*n* = 220)	
Adhesins				
aggA	6 (3.1)	0	6 (2.7)	NS[d]
aafA	18 (9.3)	0	18 (8.2)	NS[d]
agg3A	22 (11.3)	0	22 (10.0)	NS[d]
agg4A[a]	32 (16.5)	0	32 (14.5)	0.032[d]
agg5A[a]	32 (16.5)	0	32 (14.5)	0.032[d]
afpB[b]	0	14 (53.8)	14 (6.4)	<0.0001[d]
afpD[b]	0	14 (53.8)	14 (6.4)	<0.0001[d]
afpP[b]	0	14 (53.8)	14 (6.4)	<0.0001[d]
afpA2[b]	0	10 (38.5)	10 (4.5)	<0.0001[d]
afpR[b]	0	14 (53.8)	14 (6.4)	<0.0001[d]
eibG	1 (0.5)	0	1 (0.5)	NS[d]
Toxins				
pic[a]	123 (63.4)	4 (15.4)	127 (57.7)	<0.0001[c]
pet	20 (10.3)	0	20 (9.1)	NS[d]
astA	76 (39.2)	13 (50.0)	89 (40.5)	NS[c]
sigA	18 (9.3)	0	18 (8.2)	NS[d]
sepA	34 (17.5)	4 (15.4)	38 (17.3)	NS[d]
Other				
aap[a]	192 (99.0)	18 (69.2)	210 (95.5)	<0.0001[d]
aaiA[a]	141 (72.7)	12 (46.2)	153 (69.5)	0.011[c]
aaiC[a]	121 (62.4)	3 (11.5)	124 (56.4)	<0.0001[c]
aaiG[a]	133 (68.6)	5 (19.2)	138 (62.7)	<0.0001[c]
orf3[a]	192 (99.0)	5 (19.2)	197 (89.5)	<0.0001[d]
aar[a]	172 (88.7)	8 (30.8)	180 (81.8)	<0.0001[d]
air[a]	59 (30.4)	1 (3.8)	60 (27.3)	0.009[c]
capU[a]	93 (47.9)	5 (19.2)	98 (44.5)	0.011[c]
shf[a]	88 (45.4)	4 (15.4)	92 (41.8)	0.007[c]

[a] *Virulence genes significantly more prevalent in typical EAEC than in atypical EAEC (P < 0.05).*

[b] *Virulence genes significantly more prevalent in atypical EAEC than in typical EAEC (P < 0.0001).*

[c,d] *Differences observed between typical and atypical EAEC were tested by using Chi-square test with Yates correlation (c) or two-tailed Fisher's exact test (d), as appropriate. NS: The difference between typical and atypical EAEC was considered not significant.*

TABLE 2 | Classification of the typical and atypical EAEC isolates in the distinct *E. coli* phylogroups.

E. coli phylogroup	Typical EAEC (*n* = 194)	Atypical EAEC (*n* = 26)	Total (*n* = 220)	*P*-value
A	80 (41.2)[a]	17 (65.4)[a]	97 (44.1)	0.034[b]
B1	42 (21.6)	5 (19.2)	47 (21.4)	NS[b]
B2	7 (3.6)	0	7 (3.2)	NS[c]
C	4 (2.1)	0	4 (1.8)	NS[c]
D	28 (14.4)	1 (3.8)	29 (13.2)	NS[c]
E	22 (11.3)	0	22 (10.0)	NS[c]
G	5 (2.6)	0	5 (2.3)	NS[c]
Unknown	6 (3.1)	3 (11.5)	9 (4.1)	NS[c]

[a]*Statistically significant difference was observed between the two EAEC groups studied (P < 0.05).*

[b,c]*Differences observed between typical and atypical EAEC were tested by using Chi-square test with Yates correlation (b) or two-tailed Fisher's exact test (c), as appropriate. NS: The difference between typical and atypical EAEC was considered not significant.*

TABLE 3 | Occurrence of the *aai* operon genes in typical and atypical EAEC isolates.

aai operon genes	*N*° (%) of EAEC isolates		
	Typical EAEC (*n* = 194)	Atypical EAEC (*n* = 26)	Total (*n* = 220)
aaiA, *aaiC*, *aaiG*	119 (61.3)	3 (11.5)	122 (55.5)
aaiA, *aaiC*	2 (1.0)	0	2 (0.9)
aaiA, *aaiG*	14 (7.2)	2 (7.7)	16 (7.3)
aaiA	6 (3.1)	7 (26.9)	13 (5.9)
None	53 (27.3)	14 (53.8)	67 (30.5)

serotypes O73:H1 (3 isolates) and O15:H18 (2 isolates), were identified in the newly described phylogroup G (**Table 2**).

We also investigated the occurrence of 25 virulence genes encoding adhesins, toxins, secreted proteases, and T6SS (**Table 1**). Genes encoding the major subunit of the five distinct AAFs were exclusively detected in typical EAEC, with *agg4A* (16.5%, 32/194) and *agg5A* (16.5%, 32/194) being the most frequent ones (**Table 1**). Interestingly, genes encoding proteins associated with the biogenesis of the newly described AFP adhesin (*afpB*, *afpD*, *afpP*, and *afpA2*) and/or its regulator (*afpR*) were exclusively detected in atypical EAEC (57.7%, 15/26), showing a statistical association with this subgroup ($P < 0.0001$). Typical EAEC harbored all five genes encoding for toxins investigated in this study, such as *pic*, *pet*, *astA*, *sigA,* and *sepA*, while atypical EAEC isolates lacked the *pet* and *sigA* genes. Furthermore, *pic* was significantly more frequent in typical than atypical EAEC (63.4 vs. 15.4%, $P < 0.0001$). Additionally, the genes encoding for dispersin (*aap*), T6SS (*aaiA*, *aaiC,* and *aaiG*) and five other putative virulence factors (*orf3*, *aar*, *air*, *capU,* and *shf*) were detected in typical and atypical, despite their statistical association with the former group (**Table 1**). The genes encoding the T6SS investigated here (*aaiA*, *aaiC,* and *aaiG*) were detected in 69.5% (153/220) of the EAEC isolates studied, with the concomitant occurrence of the three genes being the most common genotype (55.5%, 122/220) detected (**Table 3**). Besides the aforementioned combination, the *aaiA* gene was observed in association with *aaiG* (7.3%, 16/220), *aaiC* (0.9%, 2/220), or not associated with these two genes (5.9%, 13/220) (**Table 3**).

The AA pattern was detected in 92.7% (204/220) of the isolates (**Table 4**). In 75.9% (167/220) of them, the AA pattern was detected after 3 h of bacteria-cell interaction (**Figure 1A**), while in 14.1% (31/220) this phenotype was detected using more prolonged periods of incubation (6 h) (**Table 4**). Curiously, six EAEC isolates (2.7%, 6/220) produced AA concomitantly with long-chain aggregates of bacteria adhered to both HeLa cell surfaces and coverslip (**Figure 1B**), which is characteristic of an adherence pattern termed chain-like adhesion (CLA). We also observed that 1.4% (3/220) and 0.9% (2/220) of the EAEC isolates produced CLA (**Figure 1C**) or the diffuse adherence (DA) patterns (**Figure 1D**), respectively. EAEC isolates exhibiting an undefined (UND) adherence (1.4%, 3/220) or unable to adhere to HeLa cells (3.6%, 8/220), even using more prolonged periods of bacteria-cell interaction, were observed (**Table 4**). The majority of the typical EAEC isolates (82.4%, 89/108) that harbored one or more of the adhesin-encoding genes investigated were able to produce the AA pattern within 3 h of assay, and the only EAEC that harbored the *eibG* gene produced CLA (**Table 4**). Interestingly, two typical EAEC isolates harbored the *agg3A* concomitantly with the *agg5A*, and both the isolates were able to produce the AA pattern (**Table 4**). Among the 26 atypical EAEC, 76.9% (20/26) produced AA, besides isolates exhibiting UND adherence (7.7%, 2/26), or non-adherent (NA) (15.4%, 4/26) (**Table 4**). Taken into consideration the 14 afp^+ EAEC isolates, 85.7% (12/14) produced AA, while the other two isolates (14.3%, 2/14) were NA (**Table 4**). The isolate IAL 5749 that harbored only the regulator-encoding gene (*afpR*), but lacked the genes from the *afp* operon investigated, produced a UND adherence pattern to HeLa cells (**Table 4**).

Considering the novelty of the association of the genes of the *afp* operon and/or its regulator (*afpR*) with atypical EAEC, we compiled the main features of these 15 EAEC isolates in **Table 5**. Most of them were identified in the phylogroup A (80.0%, 12/15) and produced AA in 3 h assay (73.3%, 11/15) (**Figure 2**), even though they were heterogeneous regarding the serotype, and virulence profile exhibited (**Table 5**).

Among the 11 antimicrobial drugs tested, non-susceptible typical EAEC isolates were observed for ampicillin, amoxicillin/clavulanic acid, cefazolin, gentamicin, tobramycin, ciprofloxacin, and trimethoprim/sulfamethoxazole, with the highest resistance rates observed for ampicillin (52.6%, 102/194), and trimethoprim/sulfamethoxazole (33.5%, 65/194) (**Table 6**). Non-susceptible atypical EAEC were observed only for ampicillin (19.2%, 5/26) and trimethoprim/sulfamethoxazole (19.2%, 5/26) (**Table 6**). Multidrug resistance phenotype was observed only in two (1.0%, 2/194) of the typical and in none of the atypical EAEC isolates studied (**Table S4**).

DISCUSSION

The importance of EAEC as an etiological agent of diarrheal diseases has been reinforced in the last decade (Boisen et al., 2012;

TABLE 4 | Correlation of adhesin-encoding genes and adherence patterns detected in the typical and atypical EAEC isolates studied.

Adhesin-encoding genes investigated	No. of EAEC isolates	No. (%) of EAEC exhibiting distinct adherence patterns on HeLa cells[a]							
		AA		DA		AA/CLA	CLA	UND	NA
		3 h	6 h	3 h	6 h	3 h	3 h	6 h	6 h
Typical EAEC (Total)	**194**	**154 (79.4)**	**24 (12.4)**	**1 (0.5)**	**1 (0.5)**	**6 (3.1)**	**3 (1.5)**	**1 (0.5)**	**4 (2.1)**
aagA	6	6 (100.0)	0	0	0	0	0	0	0
aafA	18	18 (100.0)	0	0	0	0	0	0	0
agg3A	20	18 (90.0)	1 (5.0)	0	0	0	0	1 (5.0)	0
agg4A	31	17 (54.8)	7 (22.6)	0	0	4 (12.9)	2 (6.5)	0	1 (3.2)
agg5A	30	29 (96.7)	1 (3.3)	0	0	0	0	0	0
agg3A+ agg5A	2	1 (50.0)	1 (50.0)	0	0	0	0	0	0
agg4A+eibG	1	0	0	0	0	0	1 (100.0)	0	0
None	86	65 (75.6)	14 (16.3)	1 (1.2)	1 (1.2)	2 (2.3)	0	0	3 (3.5)
Atypical EAEC (Total)	**26**	**13 (50.0)**	**7 (26.9)**	**0**	**0**	**0**	**0**	**2 (7.7)**	**4 (15.4)**
afp operon	14	11 (78.6)	1 (7.1)	0	0	0	0	0	2 (14.3)
afpR	1[b]	0	0	0	0	0	0	1 (100.0)	0
None	11	2 (18.2)	6 (54.5)	0	0	0	0	1 (9.1)	2 (18.2)
TOTAL	**220**	**167 (75.9)**	**31 (14.1)**	**1 (0.5)**	**1 (0.5)**	**6 (2.7)**	**3 (1.4)**	**3 (1.4)**	**8 (3.6)**

[a] *AA, aggregative adherence pattern; CLA, chain-like adherence pattern; AA/CLA, AA observed concomitant with CLA; DA, diffuse adherence pattern; NA, non-adherent EAEC isolates; UND, EAEC isolates exibithing undefined adherence, characterized by the occurrence of few bacteria randomly attached on the HeLa cells surface.*
[b] *EAEC isolate (IAL 5749) that harbored the afpR gene, but lacked the genes from the afp operon investigated (**Table 5**).*

TABLE 5 | Phenotypic and molecular features of atypical EAEC harboring the *afp* operon gene.

Atypical EAEC identification	Phylogroup	Serotype	Adherence pattern		*afp* operon				*afpR*	Virulence factor-encoding genes
			3 h	6 h	*afpB*	*afpD*	*afpP*	*afpA2*		
IAL 5700	A	OR:H33	AA	-	+	+	+	+	+	*aatA*
IAL 5742	Unknown	OR:H45	AA	-	+	+	+	+	+	*aatA, aap*, *aaiA*
IAL 5744	A	ONT:H-	NA	NA	+	+	+	+	+	*aatA, astA*, *aap*, *aaiA*
IAL 5749	B1	OR:H35	NA	UND	-	-	-	-	+	*aatA, aaiA*
IAL 5826	B1	OR:H35	AA	-	+	+	+	+	+	*aatA, aaiA*, *aar*
IAL 5823	A	ONT:H32	AA	-	+	+	+	+	-	*aatA, aap*, *capU*, *shf*
IAL 5846	A	OR:H33	AA	-	+	+	+	+	+	*aatA, aap*, *orf3*, *aar*
IAL 5852	A	O80:H10	AA	-	+	+	+	-	+	*aatA, astA*, *aap*, *aaiA*, *orf3*, *aar*
IAL 5854	A	O80:H10	AA	-	+	+	+	-	+	*aatA, astA*, *aap*, *orf3*
IAL 5892	A	OR:H-	AA	-	+	+	+	+	+	*aatA, astA*, aap, *aaiA*, *capU*
IAL 5898	A	O55:H25	NA	NA	+	+	+	+	+	*aatA*
IAL 5901	A	OR:H10	AA	-	+	+	+	-	+	*aatA, astA*, *aap*
IAL 5911	A	O55:H25	AA	-	+	+	+	+	+	*aatA, aap*
IAL 6001	A	OR:H10	UND	AA	+	+	+	-	+	*aatA, astA*, *aap*
IAL 6006	A	ONT:H32	AA	-	+	+	+	+	+	*aatA, aap, capU*, *shf*

Lima et al., 2013; Durand et al., 2016; Chattaway et al., 2017; Ori et al., 2019). However, some questions remain to be addressed, such as the use of the adherence pattern as the gold standard for diagnosis, how to identify truly pathogenic isolates in this heterogeneous group of isolates, and which would be the best molecular markers to improve the diagnosis of EAEC, mainly atypical EAEC.

Several of the virulence factor-encoding genes investigated here were statistically more frequent among typical EAEC, which is not surprising since the majority of these genes were identified, and functionally characterized, in the typical EAEC prototype strain 042 (Harrington et al., 2006; Chaudhuri et al., 2010; Hebbelstrup Jensen et al., 2014). Similar findings were also observed by other Brazilian authors that compared typical and atypical EAEC isolates, especially with the *pic*, *aap*, *shf,* and *agg4A* genes being more frequent among the typical EAEC isolates (Andrade et al., 2017; Taborda et al., 2018; Guerrieri et al., 2019).

TABLE 6 | Antimicrobial susceptibility of the EAEC isolates studied.

Antimicrobial drugs tested[a]	Typical EAEC ($n = 194$)[b]			Atypical EAEC ($n = 26$)[b]		
	S	I	R	S	I	R
AMP	92 (47.4)	0	102 (52.6)	21 (80.8)	0	5 (19.2)
AMC	187 (96.4)	6 (3.1)	1 (0.5)	26 (100.0)	0	0
CFZ	159 (82.0)	28 (14.4)	7 (3.6)	24 (92.3)	2 (7.7)	0
CTX	194 (100.0)	0	0	26 (100.0)	0	0
CPM	194 (100.0)	0	0	26 (100.0)	0	0
CFX	194 (100.0)	0	0	26 (100.0)	0	0
IPM	194 (100.0)	0	0	26 (100.0)	0	0
GEN	187 (96.4)	2 (1.0)	5 (2.6)	26 (100.0)	0	0
TOB	190 (97.9)	3 (1.5)	1 (0.5)	26 (100.0)	0	0
CIP	193 (99.5)	0	1 (0.5)	26 (100.0)	0	0
SUT	129 (66.5)	0	65 (33.5)	21 (80.8)	0	5 (19.2)

[a]*Ampicillin (AMP, 10 μg), amoxicillin-clavulanic acid (AMC, 20/10μg), cefazolin (CFZ, 30 μg), cefuroxime (CFX, 30 μg), cefotaxime (CTX, 30 μg), cefepime (CPM, 30 μg), imipenem (IPM, 10 μg), gentamicin (GEN, 10 μg), tobramycin (TOB, 10 μg), ciprofloxacin (CIP, 5 μg), trimetoprim-sulfamethoxazole (SUT, 1.25 / 23.75 μg).*

[b]*Antibiogram interpretation: S, susceptible; I, intermediate; R, resistant.*

Case-control studies, performed in distinct geographic regions, have been able to demonstrate the association of some genes encoding virulence factors with diarrheal disease. *pic*, which encodes a protein with hemagglutinin and mucinolytic activity *in vitro* (Henderson et al., 1999), was statistically more frequent among diarrheal Peruvian children than in healthy subjects (Durand et al., 2016), as well as *sepA*, encoding an autotransporter protease originally described in *Shigella* spp., was associated with diarrhea in children from Bamako, Mali (Boisen et al., 2012). A case-control study performed in Northeastern Brazil demonstrated the association of *pet* (Plasmid-encoded toxin) and *aafA* (AAF/II fimbrial subunit) with diarrhea (Lima et al., 2013). Moreover, the occurrence of typical EAEC, harboring concomitantly *aatA* and *aaiC*, was more frequent among malnourished than in nourished children (Havt et al., 2017), thus reinforcing the need for greater attention to asymptomatic infections by this pathogen.

In typical EAEC the establishment of the AA pattern is mediated by five distinct AAFs (Jønsson et al., 2017a), and the occurrence of genes associated with the biogenesis of AAF/I-AAF/IV has already been reported among Brazilian EAEC isolates, with their frequency varying according to the geographic regions studied (Elias et al., 1999; Zamboni et al., 2004; Lima et al., 2013; Guerrieri et al., 2019). However, the occurrence of Brazilian EAEC isolates harboring the *agg5A*, alone or concomitantly with *agg3A*, is described for the first time in this study. A study performed with Danish EAEC isolates identified six harboring the major pilin subunits from both AAF/III (*agg3A*) and AAF/V (*agg5A*), with these genes located in a novel pAA variant (Jønsson et al., 2017b).

Recently, Lang and coworkers described a new fimbria, termed aggregate-forming pili (AFP), in a hybrid EAEC/STEC isolate of serotype O23:H8 (Lang et al., 2018). The genes responsible for the biogenesis of AFP have ∼52% of nucleotide identity with the genes responsible for encoding the bundle-forming pili (BFP), a type IV pilus that mediates the localized adherence (LA) phenotype of typical enteropathogenic *E. coli* on epithelial cells surface (Scaletsky et al., 1984; Girón et al., 1991; Donnenberg et al., 1992). The *afp* and *bfp* operons have a similar gene organization (Tobe et al., 1999; Lang et al., 2018), despite the presence of an additional *afpA2* gene, that is not required for AFP biogenesis (Lang et al., 2018). The deletion of the complete *afp* operon, *afpA* and *afpR* genes (encoding an AraC-like regulator), but not *afpA2*, led to the loss of fimbriae production and drastically reduced the ability of the EAEC/STEC isolate in adhering to epithelial cells *in vitro* (Lang et al., 2018).

Using an NCBI nucleotide BLAST analysis with the *afp* operon genes as a query sequence, Lang et al. (2018) identified 17 *afp*-positive *E. coli* isolates, which were also positive for EAEC markers, such as *aatA* and *aap*, but lacking *aggR*, which is a genotype of atypical EAEC. This observation motived us to deeply investigate the occurrence of the *afp* genes in other EAEC isolates, including both typical and atypical. To the best of our knowledge, this is the first study to demonstrate the association of genes from the *afp* operon, as well as, a gene encoding its regulator (*afpR*) with the atypical EAEC subgroup, thus providing a new putative molecular marker to increase the diagnostic efficiency of this pathogen.

Moreover, some of the isolates classified as typical EAEC ($aatA^+/aggR^+$) produced the CLA or DA patterns on HeLa cells (3 and 2 isolates, respectively), similar to the observed in previous studies that compared adherence pattern and molecular markers of the distinct DEC pathotypes (Gomes et al., 1998; Gioppo et al., 2000; Scaletsky et al., 2002; Spano et al., 2017). A Brazilian study demonstrated that *E. coli* isolates exhibiting CLA on epithelial cells harbored genes commonly used as a marker of the EAEC pathotype, i.e., *aatA* and *aggR*, as well as virulence factor-encoding genes, such as *pet*, *astA*, and *aggC* (Gioppo et al., 2000). These data demonstrate that the EAEC definition is still ambiguous since *E. coli* isolates producing the AA pattern on HeLa cells could be devoid of EAEC molecular markers of this pathotype, as well as *E. coli* positive for such genes could produce adherence patterns distinct from AA. We believe that further studies using whole-genome sequencing analysis, in combination with phenotypic features of the EAEC isolates and clinical information of the patients could provide greater accuracy to the molecular markers necessary for the EAEC diagnosis, as well as, in the identification of truly pathogenic isolates.

In conclusion, although we have characterized the EAEC isolates studied in terms of phylogroups, serotypes, adherence patterns, and genes that encode virulence factors, the main message of this study is the association of the aggregate-forming pili (AFP)-encoding genes with the atypical EAEC subgroup. Our study showed that the *afp* operon was found only in *E. coli* isolates that carry the *aatA* gene, but are devoid of the genes encoding the EAEC virulence regulator and the aggregative adherence fimbriae ($aatA^+/aggR^-$/AAFs$^-$), thus providing a novel putative marker for increasing the efficiency of atypical EAEC diagnosis.

DATA AVAILABILITY STATEMENT

All datasets generated for this study are included in the article/**Supplementary Material**.

ETHICS STATEMENT

This study was analyzed and approved by the Botucatu Medical School Ethical Committee for human experimentation (CAAE 09994419.6.1001.5411). Written and informed consent from the participants was not required as approved by the aforementioned Ethics Committee.

AUTHOR CONTRIBUTIONS

RH, LS, and WE conceptualized the study. RD, LS, RH, and WE contributed to the formal analysis. RH and RD were responsible for the funding acquisition. RD, RT, MV, MC-N, LS, TG, WE, and RH carried out the investigation. RD, RT, MV, and MC-N worked on the methodology. RH, RD, and LS helped with the project administration. RH, LS, TG, and WE supervised the study. RH, LS, TG, and WE validated the study. RD and RH wrote the original draft. RD, RT, MV, MC-N, LS, TG, WE, and RH reviewed and edited the manuscript.

FUNDING

This study was financed in part by the Coordenação de Aperfeiçoamento de Pessoal de Nível Superior - Brasil (CAPES) - Finance Code 001 and CAPES/PROEX 0708/2018.

ACKNOWLEDGMENTS

The authors thank Cefar Diagnóstica Ltda for providing the antimicrobial drug disks used in this study.

SUPPLEMENTARY MATERIAL

The Supplementary Material for this article can be found online at: https://www.frontiersin.org/articles/10.3389/fcimb.2020.00144/full#supplementary-material

REFERENCES

Andrade, F. B., Abreu, A. G., Nunes, K. O., Gomes, T. A., Piazza, R. M., and Elias, W. P. (2017). Distribution of serine protease autotransporters of *Enterobacteriaceae* in typical and atypical enteroaggregative *Escherichia coli*. *Infect. Genet. Evol.* 50, 83–86. doi: 10.1016/j.meegid.2017.02.018

Andrade, F. B., Gomes, T. A., and Elias, W. P. (2014). A sensitive and specific molecular tool for detection of both typical and atypical enteroaggregative *Escherichia coli*. *J. Microbiol. Methods.* 106, 16–18. doi: 10.1016/j.mimet.2014.07.030

Araujo, J. M., Tabarelli, G. F., Aranda, K. R., Fabbricotti, S. H., Fagundes-Neto, U., Mendes, C. M., et al. (2007). Typical enteroaggregative and atypical enteropathogenic types of *Escherichia coli* are the most prevalent diarrhea-associated pathotypes among Brazilian children. *J. Clin. Microbiol.* 45, 3396–3399. doi: 10.1128/JCM.00084-07

Aslani, M. M., Alikhani, M. Y., Zavari, A., Yousefi, R., and Zamani, A. R. (2011). Characterization of enteroaggregative *Escherichia coli* (EAEC) clinical isolates and their antibiotic resistance pattern. *Int. J. Infect. Dis.* 15, e136–e139. doi: 10.1016/j.ijid.2010.10.002

Baudry, B., Savarino, S. J., Vial, P., Kaper, J. B., and Levine, M. M. (1990). A sensitive and specific DNA probe to identify enteroaggregative *Escherichia coli*, a recently discovered diarrheal pathogen. *J. Infect. Dis.* 161, 1249–1251. doi: 10.1093/infdis/161.6.1249

Bernier, C., Gounon, P., and Le Bouguénec, C. (2002). Identification of an aggregative adhesion fimbria (AAF) type III-encoding operon in enteroaggregative *Escherichia coli* as a sensitive probe for detecting the AAF-encoding operon family. *Infect Immun.* 70, 4302–4311.doi: 10.1128/iai.70.8.4302–4311.2002

Bhargava, S., Johnson, B. B., Hwang, J., Harris, T. A.,George, A. S., Muir, A., et al. (2009). Heat-resistant agglutinin 1 is an accessory enteroaggregative *Escherichia coli* colonization factor. *J. Bacteriol.* 191, 4934–4942. doi: 10.1128/JB.01831-08

Boisen, N., Scheutz, F., Rasko, D. A., Redman, J. C., Persson, S., Simon, J., et al. (2012). Genomic characterization of enteroaggregative *Escherichia coli* from children in Mali. *J. Infect. Dis.* 205, 431–444. doi: 10.1093/infdis/jir757

Boisen, N., Struve, C., Scheutz, F., Krogfelt, K. A., and Nataro, J. P. (2008). New adhesin of enteroaggregative *Escherichia coli* related to the Afa/Dr/AAF family. *Infect. Immun.* 76, 3281–3292.doi: 10.1128/IAI.01646–07

Chattaway, M. A., Day, M., Mtwale, J., White, E., Rogers, J., Day, M., et al. (2017). Clonality, virulence and antimicrobial resistance of enteroaggregative *Escherichia coli* from Mirzapur, Bangladesh. *J. Med. Microbiol.* 66, 1429–1435. doi: 10.1099/jmm.0.000594

Chaudhuri, R. R., Sebaihia, M., Hobman, J. L., Webber, M. A., Leyton, D. L., Goldberg, M. D., et al. (2010). Complete genome sequence and comparative metabolic profiling of the prototypical enteroaggregative *Escherichia coli* strain 042. *PLoS ONE* 5:e8801. doi: 10.1371/journal.pone.0008801

Clermont, O., Christenson, J. K., Denamur, E., and Gordon, D. M. (2013). The Clermont *Escherichia coli* phylo-typing method revisited: improvement of specificity and detection of new phylo-groups. *Environ. Microbiol.* 5, 58–65.doi: 10.1111/1758–2229.12019

Clermont, O., Dixit, O. V. A., Vangchhia, B., Condamine, B., Dion, S., Bridier-Nahmias, A., et al. (2019). Characterization and rapid identification of phylogroup G in *Escherichia coli*, a lineage with high virulence and antibiotic resistance potential. *Environ. Microbiol.* 21, 3107–3117. doi: 10.1111/1462-2920.14713

CLSI (2018). *Performance Standards for Antimicrobial Susceptibility Testing. CLSI Supplement M100, 28th edn*. Wayne, PA: Clinical and Laboratory Standards Institute.

Cravioto, A., Gross, R. J., Scotland, S. M., and Rowe, B. (1979). An adhesive factor found in strains of *Escherichia coli* belonging to the traditional infantile enteropathogenic serotypes. *Curr. Microbiol.* 3, 95–99.doi: 10.1007/BF02602439

Croxen, M. A., Law, R. J., Scholz, R., Keeney, K. M., Wlodarska, M., and Finlay, B. B. (2013). Recent advances in understanding enteric pathogenic *Escherichia coli*. *Clin. Microbiol. Rev.* 26, 822–880.doi: 10.1128/CMR.00022–13

Czeczulin, J. R., Balepur, S., Hicks, S., Phillips, A., Hall, R., Kothary, M. H., et al. (1997). Aggregative adherence fímbria II, a second fimbrial antigen mediating aggregative adherence in enteroaggregative *Escherichia coli*. *Infect. Immun.* 65, 4135–4145. doi: 10.1128/IAI.65.10.4135-4145.1997

Czeczulin, J. R., Whittam, T. S., Henderson, I. R., Navarro-Garcia, F., and Nataro, J. P. (1999). Phylogenetic analysis of enteroaggregative and diffusely adherent *Escherichia coli*. *Infect. Immun.* 67, 2692–2699. doi: 10.1128/IAI.67.6.2692-2699.1999

Dias, R. C. B., Dos Santos, B. C., Dos Santos, L. F., Vieira, M. A., Yamatogi, R. S., Mondelli, A. L., et al. (2016). Diarrheagenic *Escherichia coli* pathotypes investigation revealed atypical enteropathogenic *E. coli* as putative emerging diarrheal agents in children living in Botucatu, São Paulo State, Brazil. *APMIS.* 124, 299–308. doi: 10.1111/apm.12501

Donnenberg, M. S., Girón, J. A., Nataro, J. P., and Kaper, J. B. (1992). A plasmid-encoded type IV fimbrial gene of enteropathogenic *Escherichia coli* associated with localized adherence. *Mol. Microbiol.* 6, 3427–3437. doi: 10.1111/j.1365-2958.1992.tb02210.x

Dudley, E. G., Thomson, N. R., Parkhill, J., Morin, N. P., and Nataro, J. P. (2006). Proteomic and microarray characterization of the AggR regulon identifies a pheU pathogenicity island in enteroaggregative *Escherichia coli*. *Mol. Microbiol.* 61, 1267–1282. doi: 10.1111/j.1365–2958.2006.05281.x

Durand, D., Contreras, C. A., Mosquito, S., Ruíz, J., Cleary, T. G., and Ochoa, T. J. (2016). *pic* gene of enteroaggregative *Escherichia coli* and its association with diarrhea in Peruvian children. *Pathog. Dis.* 74:e54. doi: 10.1093/femspd/ftw054

Elias, W. P., Suzart, S., Trabulsi, L. R., Nataro, J. P., and Gomes, T. A. (1999). Distribution of *aggA* and *aafA* gene sequences among *Escherichia coli* isolates with genotypic or phenotypic characteristics, or both, of enteroaggregative *E. coli*. *J. Med. Microbiol.* 48, 597–599. doi: 10.1099/00222615–48-6–597

Estrada-Garcia, T., and Navarro-Garcia, F. (2012). Enteroaggregative *Escherichia coli* pathotype: a genetically heterogeneous emerging foodborne enteropathogen. *FEMS Immunol. Med. Microbiol.* 66, 281–298. doi: 10.1111/j.1574-695X.2012.01008.x

Ewing, W. H. (1986). *Edwards and Ewing's Identification of Enterobacteriaceae, 4th Edn*. New York, NY: Elsevier Science Publishing.

França, F. L., Wells, T. J., Browning, D. F., Nogueira, R. T., Sarges, F. S., Pereira, A. C., et al. (2013). Genotypic and phenotypic characterisation of enteroaggregative *Escherichia coli* from children in Rio de Janeiro, Brazil. *PLoS ONE* 8:e69971. doi: 10.1371/journal.pone.0069971

Gioppo, N. M., Elias, W. P. Jr., Vidotto, M. C., Linhares, R. E.,Saridakis, H. O., Gomes, T. A., et al. (2000). Prevalence of HEp-2 cell-adherent *Escherichia coli* and characterisation of enteroaggregative *E. coli* and chain-like adherent *E. coli* isolated from children with and without diarrhoea, in Londrina, Brazil. *FEMS Microbiol. Lett.* 190, 293–298. doi: 10.1111/j.1574-6968.2000.tb09301.x

Girón, J. A., Ho, A. S., and Schoolnik, G. K. (1991). An inducible bundle-forming pilus of enteropathogenic *Escherichia coli*. *Science* 254, 710–713. doi: 10.1126/science.1683004

Gomes, T. A., Vieira, M. A., Abe, C. M., Rodrigues, D., Griffin, P. M., and Ramos, S. R. (1998). Adherence patterns and adherence-related DNA sequences in *Escherichia coli* isolates from children with and without diarrhea in São Paulo city, Brazil. *J. Clin. Microbiol.* 36, 3609–3613. doi: 10.1128/JCM.36.12.3609-3613.1998

Guerrieri, C. G., Monfardini, M. V., Silva, E. A., Bueno de Freitas, L., Schuenck, R. P., and Spano, L. C. (2019). Wide genetic heterogeneity and low antimicrobial resistance of enteroaggregative *Escherichia coli* isolates from several rural communities. *J. Med. Microbiol.* 69, 96–103. doi: 10.1099/jmm.0.001120

Harrington, S. M., Dudley, E. G., and Nataro, J. P. (2006). Pathogenesis of enteroaggregative *Escherichia coli* infection. *FEMS Microbiol. Lett.* 254, 12–18. doi: 10.1111/j.1574-6968.2005.00005.x

Havt, A., Lima, I. F., Medeiros, P. H., Clementino, M. A., Santos, A. K., Amaral, M. S., et al. (2017). Prevalence and virulence gene profiling of enteroaggregative *Escherichia coli* in malnourished and nourished Brazilian children. *Diagn. Microbiol. Infect. Dis.* 89, 98–105. doi: 10.1016/j.diagmicrobio.2017.06.024

Hebbelstrup Jensen, B., Adler Sørensen, C., Hebbelstrup Rye Rasmussen, S., Rejkjær Holm, D., Friis-Møller, A., Engberg, J., et al. (2018). Characterization of diarrheagenic enteroaggregative *Escherichia coli* in Danish adults-antibiotic treatment does not reduce duration of diarrhea. *Front. Cell. Infect. Microbiol.* 8:306. doi: 10.3389/fcimb.2018.00306

Hebbelstrup Jensen, B., Olsen, K. E., Struve, C., Krogfelt, K. A., and Petersen, A. M. (2014). Epidemiology and clinical manifestations of enteroaggregative *Escherichia coli*. *Clin. Microbiol. Rev.* 27, 614–630. doi: 10.1128/CMR.00112–13

Henderson, I. R., Hicks, S., Navarro-Garcia, F., Elias, W. P., Philips, A. D., and Nataro, J. P. (1999). Involvement of the enteroaggregative *Escherichia coli* plasmid-encoded toxin in causing human intestinal damage. *Infect. Immun.* 67, 5338–5344. doi: 10.1128/IAI.67.10.5338-5344.1999

Huang, D. B., Nataro, J. P., DuPont, H. L., Kamat, P. P., Mhatre, A. D., Okhuysen, P. C., et al. (2006). Enteroaggregative *Escherichia coli* is a cause of acute diarrheal illness: a meta-analysis. *Clin. Infect. Dis.* 43, 556–563. doi: 10.1086/505869

Ikumapayi, U. N., Boisen, N., Hossain, M. J., Betts, M., Lamin, M., Saha, D., et al. (2017). Identification of subsets of enteroaggregative *Escherichia coli* associated with diarrheal disease among under 5 years of age children from rural Gambia. *Am. J. Trop. Med. Hyg.* 97, 997–1004. doi: 10.4269/ajtmh.16-0705

Imuta, N., Ooka, T., Seto, K., Kawahara, R., and Koriyama, T., Kojyo, et al. (2016). Phylogenetic analysis of enteroaggregative *Escherichia coli* (EAEC) isolates from japan reveals emergence of CTX-M-14-producing EAEC O25:H4 clones related to sequence type 131. *J. Clin. Microbiol.* 54, 2128–2134. doi: 10.1128/JCM.00711-16

Jønsson, R., Liu, B., Struve, C., Yang, Y., Jørgensen, R., Xu, Y., et al. (2017a). Structural and functional studies of *Escherichia coli* aggregative adherence fimbriae (AAF/V) reveal a deficiency in extracellular matrix binding. *Biochim. Biophys. Acta.* 1865: 304–311. doi: 10.1016/j.bbapap.2016.11.017

Jønsson, R., Struve, C., Boisen, N., Mateiu, R. M., Santiago, A. E., Jenssen, H., et al. (2015). Novel aggregative adherence fimbria variant of enteroaggregative *Escherichia coli*. *Infect. Immun.* 83, 1396–1405. doi: 10.1128/IAI.02820-14

Jønsson, R., Struve, C., Boll, E. J., Boisen, N., Joensen, K. G., Sørensen, C. A., et al. (2017b). A novel pAA virulence plasmid encoding toxins and two distinct variants of the fimbriae of enteroaggregative *Escherichia coli*. *Front. Microbiol.* 8:263. doi: 10.3389/fmicb.2017.00263

Kaper, J. B., Nataro, J. P., and Mobley, H. L. (2004). Pathogenic *Escherichia coli*. *Nat. Rev. Microbiol.* 2, 123–140. doi: 10.1038/nrmicro818

Lang, C., Fruth, A., Holland, G., Laue, M., Mühlen, S., Dersch, P., et al. (2018). Novel type of pilus associated with a Shiga-toxigenic *E. coli* hybrid pathovar conveys aggregative adherence and bacterial virulence. *Emerg. Microbes. Infect.* 7:203. doi: 10.1038/s41426-018-0209-8

Lima, A. A. M., Oliveira, D. B., Quetz, J. S., Havt, A., Prata, M. M. G., Lima, I. F. N., et al. (2019a). Etiology and severity of diarrheal diseases in infants at the semiarid region of Brazil: a case-control study. *PLoS Negl. Trop. Dis.* 13:e0007154. doi: 10.1371/journal.pntd.0007154

Lima, F. M., de Paulo Daurelio, F., Mucci, E. R., Ahagon, C. M., Dos Santos Carmo, A. M., Eterovic, A., et al. (2019b). Epidemiology and genetic screening of diarrheagenic *Escherichia coli* among symptomatic and asymptomatic children. *J. Med. Microbiol.* 68, 1033–1041. doi: 10.1099/jmm.0.001020

Lima, I. F., Boisen, N., Quetz Jda, S., Havt, A., de Carvalho, E. B., Soares, A. M., et al. (2013). Prevalence of enteroaggregative *Escherichia coli* and its virulence-related genes in a case-control study among children from north-eastern Brazil. *J. Med. Microbiol.* 62, 683–693. doi: 10.1099/jmm.0.054262–0

Lozer, D. M., Souza, T. B., Monfardini, M. V., Vicentini, F., Kitagawa, S. S., Scaletsky, I. C. A., et al. (2013). Genotypic and phenotypic analysis of diarrheagenic *Escherichia coli* strains isolated from Brazilian children living in low socioeconomic level communities. *BMC Infect. Dis.* 13:418. doi: 10.1186/1471-2334-13-418

Magiorakos, A. P., Srinivasan, A., Carey, R. B., Carmeli, Y., Falagas, M. E., Giske, C. G., et al. (2012). Multidrug-resistant, extensively drug-resistant and pandrug-resistant bacteria: an international expert proposal for interim standard definitions for acquired resistance. *Clin. Microbiol. Infect.* 18, 268–281. doi: 10.1111/j.1469-0691.2011.03570.x

Monteiro-Neto, V., Bando, S. Y., Moreira-Filho, C. A., and Girón, J. A. (2003). Characterization of an outer membrane protein associated with haemagglutination and adhesive properties of enteroaggregative *Escherichia coli* O111:H12. *Cell. Microbiol.* 5, 533–547. doi: 10.1046/j.1462–5822.2003.00299.x

Morin, N., Santiago, A. E., Ernst, R. K., Guillot, S. J., and Nataro, J. P. (2013). Characterization of the AggR regulon in enteroaggregative *Escherichia coli*. *Infect. Immun.* 81, 122–132. doi: 10.1128/IAI.00676–12

Nataro, J. P., Deng, Y., Maneval, D. R., German, A. L., Martin, W. C., and Levine, M. M. (1992). Aggregative adherence fimbriae I of enteroaggregative *Escherichia coli* mediate adherence to HEp-2 cells and hemagglutination of human erythrocytes. *Infect. Immun.* 60, 2297–2304. doi: 10.1128/IAI.60.6.2297-2304.1992

Nataro, J. P., and Kaper, J. B. (1998). Diarrheagenic *Escherichia coli*. *Clin. Microbiol. Rev.* 11, 142–201. doi: 10.1128/CMR.11.1.142

Nataro, J. P., Kaper, J. B., Robins-Browne, R., Prado, V., Vial, P., and Levine, M. M. (1987). Patterns of adherence of diarrheagenic *Escherichia coli* to HEp-2 cells. *Pediatr. Infect. Dis. J.* 6, 829–831. doi: 10.1097/00006454-198709000-00008

Nishi, J., Sheikh, J., Mizuguchi, K., Luisi, B., Burland, V., Boutin, A., et al. (2003). The export of coat protein from enteroaggregative *Escherichia coli* by a specific ATP-binding cassette transporter system. *J. Biol. Chem.* 278, 45680–45689. doi: 10.1074/jbc.M306413200

Ori, E. L., Takagi, E. H., Andrade, T. S., Miguel, B. T., Cergole-Novella, M. C., Guth, B. E. C., et al. (2019). Diarrhoeagenic *Escherichia coli* and *Escherichia albertii* in Brazil: pathotypes and serotypes over a 6-year period of surveillance. *Epidemiol. Infect*. 147, 1–9. doi: 10.1017/S0950268818002595

Rodrigues, J., Scaletsky, I. C., Campos, L. C., Gomes, T. A., Whittam, T. S., and Trabulsi, L. R. (1996). Clonal structure and virulence factors in strains of *Escherichia coli* of the classic serogroup O55. *Infect. Immun*. 64, 2680–2686. doi: 10.1128/IAI.64.7.2680-2686.1996

Santiago, A. E., Yan, M. B., Hazen, T. H., Sauder, B., Meza-Segura, M., Rasko, D. A., et al. (2017). The AraC Negative Regulator family modulates the activity of histone-like proteins in pathogenic bacteria. *PLoS Pathog*. 13:e1006545. doi: 10.1371/journal.ppat.1006545

Scaletsky, I. C., Fabbricotti, S. H., Aranda, K. R., Morais, M. B., and Fagundes-Neto, U. (2002). Comparison of DNA hybridization and PCR assays for detection of putative pathogenic enteroadherent *Escherichia coli. J. Clin. Microbiol*. 40, 1254–1258. doi: 10.1128/JCM.40.4.1254-1258.2002

Scaletsky, I. C., Silva, M. L., and Trabulsi, L. R. (1984). Distinctive patterns of adherence of enteropathogenic *Escherichia coli* to HeLa cells. *Infect. Immun*. 45, 534–536. doi: 10.1128/IAI.45.2.534-536.1984

Sheikh, J., Czeczulin, J. R., Harrington, S., Hicks, S., Henderson, I. R., Le Bouguénec, C., et al. (2002). A novel dispersin protein in enteroaggregative *Escherichia coli. J. Clin. Invest*. 110, 1329–1337. doi: 10.1172/JCI16172

Sheikh, J., Dudley, E. G., Sui, B., Tamboura, B., Suleman, A., and Nataro, J. P. (2006). EilA, a HilA-like regulator in enteroaggregative *Escherichia coli. Mol. Microbiol*. 61, 338–350. doi: 10.1111/j.1365-2958.2006.05234.x

Spano, L. C., Cunha, K. F., Monfardini, M. V., Fonseca, R. C. B., and Scaletsky, I. C. A. (2017). High prevalence of diarrheagenic *Escherichia coli* carrying toxin-encoding genes isolated from children and adults in southeastern Brazil. *BMC Infect. Dis*. 17:773. doi: 10.1186/s12879-017-2872-0

Taborda, R. L. M., Silva, L. A. D., Orlandi, P. P., Batista, F. S., Rodrigues, R. S., and Matos, N. B. (2018). Characterization of enteroaggregative *Escherichia coli* among diarrheal children in western brazilian amazon. *Arq. Gastroenterol*. 55, 390–396. doi: 10.1590/s0004-2803.201800000-84

Tobe, T., Hayashi, T., Han, C. G., Schoolnik, G. K., Ohtsubo, E., and Sasakawa, C. (1999). Complete DNA sequence and structural analysis of the enteropathogenic *Escherichia coli* adherence factor plasmid. *Infect. Immun*. 67, 5455–5462. doi: 10.1128/IAI.67.10.5455-5462.1999

Zamboni, A., Fabbricotti, S. H., Fagundes-Neto, U., and Scaletsky, I. C. (2004). Enteroaggregative *Escherichia coli* virulence factors are found to be associated with infantile diarrhea in Brazil. *J. Clin. Microbiol*.4 1058–1063. doi: 10.1128/JCM.42.3.1058-1063.2004

Conflict of Interest: The authors declare that the research was conducted in the absence of any commercial or financial relationships that could be construed as a potential conflict of interest.

frontiers in Cellular and Infection Microbiology

ORIGINAL RESEARCH
published: 05 May 2020
doi: 10.3389/fcimb.2020.00195

In silico Analyses of Core Proteins and Putative Effector and Immunity Proteins for T6SS in Enterohemorrhagic *E. coli*

*Jaime Vazquez-Lopez and Fernando Navarro-Garcia**

Department of Cell Biology, Centro de Investigación y de Estudios Avanzados del IPN (CINVESTAV-IPN), Mexico City, Mexico

Shiga-toxin-producing *Escherichia coli* (STEC) has become an important pathogen that can cause diarrhea, hemorrhagic colitis and hemolytic uremic syndrome (HUS) in humans. Recent reports show that the type VI secretion system (T6SS) from EHEC is required to produce infection in a murine model and its expression has been related to a higher prevalence of HUS. In this work, we use bioinformatics analyses to identify the core genes of the T6SS and compared the differences between these components among the two published genomes for EHEC O157:H7 strain EDL933. Prototype strain EDL933 was further compared with other O157:H7 genomes. Unlike other typical T6SS effectors found in *E. coli*, we identified that there are several *rhs* family genes in EHEC, which could serve as T6SS effectors. *In-silico* and PCR analyses of the differences between *rhs* genes in the two existing genomes, allowed us to determine that the most recently published genome is more reliable to study the *rhs* genes. Analyzing the putative tridimensional structure of Rhs proteins, as well as the motifs found in their C-terminal end, allowed us to predict their possible functions. A phylogenetic analysis showed that the orphan *rhs* genes are more closely related between them than the *rhs* genes belonging to *vgrG* islands and that they are divided into three clades. Analyses of the downstream region of the *rhs* genes for identifying hypothetical immunity proteins showed that every gene has an associated small ORF (129-609 nucleotides). These genes could serve as immunity proteins as they had several interaction motifs as well as structural homology with other known immunity proteins. Our findings highlight the relevance of the T6SS in EHEC as well as the possible function of the Rhs effectors of EHEC O157:H7 during pathogenesis and bacterial competition, and the identification of novel effectors for the T6SS using a structural approach.

Keywords: enterohemorrhagic *E. coli*, type 6 secretion system, effector proteins, Rhs, bacterial competition, pathogenesis

OPEN ACCESS

Edited by:
Roxane M. Piazza, Butantan Institute, Brazil

Reviewed by:
Fernanda Fernandes Dos Santos, Federal University of São Paulo, Brazil
Matthew L. Nilles, University of North Dakota, United States
Felipe Del Canto, University of Chile, Chile

****Correspondence:***
Fernando Navarro-Garcia
fnavarro@cell.cinvestav.mx

Specialty section:
This article was submitted to Molecular Bacterial Pathogenesis, a section of the journal Frontiers in Cellular and Infection Microbiology

Received: *28 January 2020*
Accepted: *14 April 2020*
Published: *05 May 2020*

Citation:
Vazquez-Lopez J and Navarro-Garcia F (2020) In silico Analyses of Core Proteins and Putative Effector and Immunity Proteins for T6SS in Enterohemorrhagic E. coli. Front. Cell. Infect. Microbiol. 10:195. doi: 10.3389/fcimb.2020.00195

INTRODUCTION

Shiga-toxin-producing *Escherichia coli* (STEC) bacteria, including enterohemorrhagic *E. coli* (EHEC), are intestinal pathogens responsible for diseases such as enterohemorrhagic colitis and hemolytic uremic syndrome (HUS). HUS is a serious complication that may cause renal failure and heart damage, resulting in death in 10% of the affected (Croxen et al., 2013). Antibiotic treatment

against STEC infection increases HUS risk (Wong et al., 2000), and EHEC infectious dose is under 50 CFU (Tilden Jr et al., 1996), thus placing STEC as an important health risk for epidemic diseases. Cows are the principal STEC reservoir, in which the bacteria live as a commensal and do not cause infection, along with vegetables irrigated with contaminated waters, which have caused important outbreaks (Frank et al., 2011). Nowadays EHEC serotype O157:H7 and the hybrid strain between an enteroaggregative *E. coli* and STEC (EAEC/STEC O104:H4) are the most commonly associated strains to epidemic outbreaks (Yang et al., 2017). On one hand, EHEC O157:H7 has a locus of enterocyte effacement (LEE), which encodes a type 3 secretion system (T3SS) used for injecting effectors that subvert the cell physiology, causing the characteristic attaching and effacing (A/E) lesions (Schmidt, 2010). On the other hand, EAEC/STEC O104:H4 has the aggregative adherence fimbriae like AAFI as well as multiple antibiotic resistance genes (Rohde et al., 2011; Navarro-Garcia, 2014). Even if both serotypes have a different origin and have few virulence factors in common, both have the *stx2* gene, which encodes the Shiga toxin 2. The presence of this toxin in both genomes is probably due to horizontal gene transfer from a O157:H7 strain to EAEC strain 55989, the presumptive parental strain of EAEC/STEC O104:H4 (Rohde et al., 2011).

Both EHEC EDL933, an O157:H7 serotype used as a reference strain, and EAEC/STEC O104:H4, encode a type VI secretion system (T6SS) (Journet and Cascales, 2016), a nanomachine comprised from 13 *core* elements that make up for four defined structures: a membrane complex formed by TssJLM that attaches the T6SS to the inner membrane and makes the intermembrane pore; a baseplate comprised by TssEFGHK that connects the tail to the membrane complex and helps with the T6SS disassembly once it has contracted; a tail made up of stacked Hcp hexamers with a spike formed by a VgrG trimer; and a contractile sheath comprised by TssBC, which expel the Hcp tail to the exterior of the bacterial cell, while TssA regulates the T6SS assembly and contraction (Navarro-Garcia et al., 2019; Schneider et al., 2019). The core components are grouped in a genomic island and present homology with some of the components of the T4 bacteriophage machinery (Pukatzki et al., 2007; Leiman et al., 2009). The T6SS punctures other cell membranes, which can be from eukaryotic or prokaryotic organisms, and injects effectors directly into the cytoplasm that mediate bacterial competition and pathogenesis (Ma and Mekalanos, 2010; Basler et al., 2013). Effectors are usually classified into three families: (i) phospholipases that degrade the plasma membrane; (ii) murein-hydrolases and amidases that attack the cell wall; and (iii) nucleases which target DNA or RNA. The genes encoding those effectors are usually part of a bicistronic operon that also encodes an immunity protein, which binds to the effector protein and prevents autointoxication (Bingle et al., 2008). Finally, there are other effectors with non-canonical activities, including ADP ribosylation, ion chelation or even actin crosslinking (Lien and Lai, 2017).

Wan et al. (2017) have already shown that the T6SS of EHEC strain EDL933 is functional in an isogenic mutant for the master regulatory protein H-NS, and showed that EHEC can translocate KatN, a catalase effector, into the macrophage upon phagocytosis. KatN neutralizes iROs present in the phagosome, thus avoiding bacterial killing. Wan et al. (2017) also showed that T6SS is essential to cause disease in a murine model, as isogenic mutants for *clpv* were unable to provoke death in the infected mice. ClpV is an ATPase that is essential for T6SS function by recycling the sheath components (Douzi et al., 2016). Nonetheless, mice death was independent of KatN, implying that other effectors acting as virulence factors in EHEC strain EDL933. Recently, Rhs family proteins have been associated with interbacterial competition in several STEC strains. Rhs family proteins are known for containing RHS repeats (recombination hotspot), often contain a PAAR domain that interacts with VgrG proteins (Bondage et al., 2016), and also have a C-terminal region with a nuclease, protease or deaminase activity (Ma et al., 2017b). In this work, we explore the differences between the T6SS genes and the putative effectors in two published genomes of EHEC O157:H7 strain EDL933 (Perna et al., 2001; Latif et al., 2014). Using bioinformatics analyses we could identify both the core genes of the T6SS as well as several putative effectors, and we provide evidence that the most-recently published genome (Latif et al., 2014) better represents the T6SS components and effectors. Additionally, analyzing sequence motifs and the modeled structure we identified several putative Rhs effectors, as well as the associated putative immunity proteins for each Rhs.

METHODS

Strains Used in This Study

EHEC strain EDL933 was kindly provided by Dr. Jose Luis Puente (Riley et al., 1983; Arenas-Hernández et al., 2014). The genomes bioinformatics comparison was made from EHEC strain EDL933 ATCC 700727 in the genome of Perna et al. (2001) (GenBank accession number: AE005174.2) and the genome of Latif et al. (2014) (GenBank accession number: CP008957.1). *E. coli* strain HB101 was obtained from ATCC 33694. The strains were grown overnight in LB plates with 1.5% agar at 37°C.

Bioinformatics Analyses

Motif searching for putative T6SS effectors was performed using the PROSITE, NCBI-CDD and Pfam databases (Marchler-Bauer et al., 2010; Sigrist et al., 2012; Finn et al., 2013) with the GenomeNet search engine. An *e-value* cutoff score of 0.01 was used. The tridimensional models were calculated using I-TASSER software (Yang and Zhang, 2015). For the analyses of the possible effector activity of the Rhs proteins, only the C-terminal end of each protein was modeled. The search for T6SS islands was performed using MacSyDB (Abby et al., 2016) and SecReT6 (Li et al., 2015). Relationship analyses between different Rhs proteins was conducted using STRING version 11 (Szklarczyk et al., 2019). Prediction of signal sequences was made using SignalIP (Juncker et al., 2003). Evolutionary analyses were conducted in MEGA X (Kumar et al., 2018) from the nucleotide sequences form the genome published by Latif et al. (2014), using the Maximum Likelihood method and Tamura-Nei model (Tamura and Nei, 1993). The tree presented is the consensus of 100 bootstrap repetitions (Felsenstein, 1985).

Primer Designing and Amplification for *rhsA* and *rhsC* Genes in EHEC Strain EDL933 DNA

Three primers were designed using Primer BLAST (Ye et al., 2012). The forward primer was designed to aligning with the *rhsA* gene in both genomes (*z5014* and *EDL933_4854*), while a genome-specific reverse primer was designed for each published genome (Perna et al., 2001; Latif et al., 2014). The sequence of the forward primer was 5′-CGCTATCTTTACGAC CCGCT-3′. The primer rhsA1R with the sequence 5′-GGC AAGGGGAATGGTCTAGG-3′ was complementary with the *rhsA* gene (*locus z5014*) according to Perna et al. (2001), whereas the primer rhsA2R with the sequence 5′-GATGTG GGGGTACCATGCC-3′ was complementary to the *rhsA* gene (locus *EDL933_4854*) according to Latif et al. (2014). For the amplification of the *rhsC* gene (*locus z0847*), the primers rhsAF and rhsCR (sequence 5′-TAGGCGGTTTGTTGGGTC TC-3′) were used. The optimal aligning temperature for all the combinations were experimentally obtained by PCR using a temperature gradient and a final primer concentration of 0.4 μM. The expected product was 800 bp for rhsA1R primer and 875 bp for rhsA2R, while a fragment of 832 bp fragment was expected for rhsCR. Chromosomal DNA from EHEC strain EDL933 was used as template. After PCR, the products were separated in a 1.5% agarose gel and then stained with ethidium bromide.

RESULTS AND DISCUSSION

In-silico Analysis of the T6SS Island in EHEC Strain EDL933

Three distinct families of T6SS exist, which differ in their genetic organization as well as in the homology of their components (T6SS-1, T6SS-2 and T6SS-3) (Journet and Cascales, 2016). T6SS-1 and T6SS-3 have been associated with bacterial competition as well as with the invasive capacity of certain *E. coli* pathotypes, while T6SS-2 is commonly found in intestinal strains, including STECs like EHEC EDL933 and EAEC/STEC O104:H4 (Journet and Cascales, 2016). Wan et al. (2017) described the T6SS island in EHEC strain EDL933 using the genome published by Perna et al. (2001), which was obtained via shotgun sequencing as described by Mahillon et al. (1998). However, recent reports of structural proteins and the publication of a gapless genome without ambiguities for EHEC strain EDL933 using PacBio and Ilumina sequencing (Latif et al., 2014) allowed us to perform a deeper analysis of the genetic island (**Figure 1A**). We found that the island encodes the 13 core components of the T6SS (TssA, TssBC, TssEFGHK, TssJLM, Hcp, and VgrG), which appears to be divided into two general operons: the first one (named here structural operon) would be codified on the complementary DNA strand and would contain both the baseplate components (TssEFGHK) and the membrane complex components (TssJLM). Besides, this operon includes two hcp genes (*tssD*, loci *z0247,* and *z0264*) and a *tssC* gene, an essential component of the T6SS sheath. Analyzing the genomes from O157:H7 strains in GenBank, we found that 137 strains out of 145 possessed the T6SS-2 structural genes and only 8 did not (strains 09BKT002497, 121, 262, 611, EC10, EC4024, GZ-021210/cattle, and ZAP430). No significant similarity with T6SS-1 or T6SS-3 structural genes from EAEC 042, a reference strain for these T6SS families, was found in O157:H7 genomes. The second operon (named here *vgrG* operon) would be on the main DNA strand containing a group of genes that encode the tail components such as another *hcp* gene (*z0266*) and a *vgrG* gene (*tssI*, *z0267*). Additionally, in this operon, we found two genes downstream *vgrG*, and one of them encodes an Rhs family protein with a PAAR domain (*z0268*). Interestingly, both the *rhs* family gene and the gene directly downstream (*z0269*) were not found in every T6SS-2 islands, such as EAEC 042, EAEC 55989, or EAEC/STEC O104:H4, as previously reported (Journet and Cascales, 2016). This suggests that this pair of genes encode a T6SS effector as well as its associated immunity protein. Finally, *z0268* and *z0269* were found only in 66 EHEC O157:H7 strains from the lineage I and were absent in 79 strains from lineage II (Zhang et al., 2007).

One particularity of the T6SS island in EHEC strain EDL933 is that it contains three homologs of *hcp* genes (*z0247*, *z0264* and *z0266*) (Wan et al., 2017), so we decided to further analyze them. *hcp1* (*z0247*) is not recognized as an ORF in Latif et al. (2014), even though that region is 100% identical to Perna et al. (2001). This might be because there is a little overlapping between the 5' end of locus *z0247* and 3' end of locus *z0249*, so perhaps the region in this latter analysis was not properly recognized by the annotation software, RAST. For *hcp2* (*z0264*), it has already been shown that EHEC*Δhns*, an isogenic mutant for the master regulatory protein H-NS repressing the T6SS expression in several bacteria, secretes the Hcp2 protein to the supernatant (Wan et al., 2017). However, upon inspecting the motifs found in the protein, we found a PF05591 motif, which may be found both in Hcp2 and TssB. Remarkably, the island reported by Wan et al. (2017) lacks the *tssB* gene, an essential component of the T6SS (Zhang et al., 2014). Our analyses using MacsyDB and SecReT6 (Li et al., 2015; Abby et al., 2016) suggested that the gene is not *hcp* but *tssB*, but experimental data is required to completely clarify the identity of this gene. Finally, none of the three *hcp* genes belongs to the Hcp-ET family reported by Ma et al. (2017a), and no known effector domains fused with the Hcp core were found that might participate during pathogenesis or interbacterial competition in EHEC strain EDL933.

Furthermore, *tssA* gene (*z0251*) is half as long as the reported genes in other strains, and after inspecting the region between the loci *z0251* and *z0252* (Perna et al., 2001), we found that the gene seems to be interrupted, as a missing cytosine in the 249,998th nucleotide producing a stop codon. In fact, in the genome published by Latif et al. (2014), the segment containing z0251 and z0252 is recognized as a single pseudogene, even though this region is 100% identical as in the genome published by Perna et al. (2001). Being TssA an essential protein for the T6SS function, it would be odd that the gene was mutated, especially when the functionality of the T6SS has already been confirmed in this strain (Wan et al., 2017). Interestingly, Zoued et al. (2016) demonstrated that both N-terminal and C-terminal regions of TssA interact with different components of the T6SS, and it is possible that, even if the gene is divided in two,

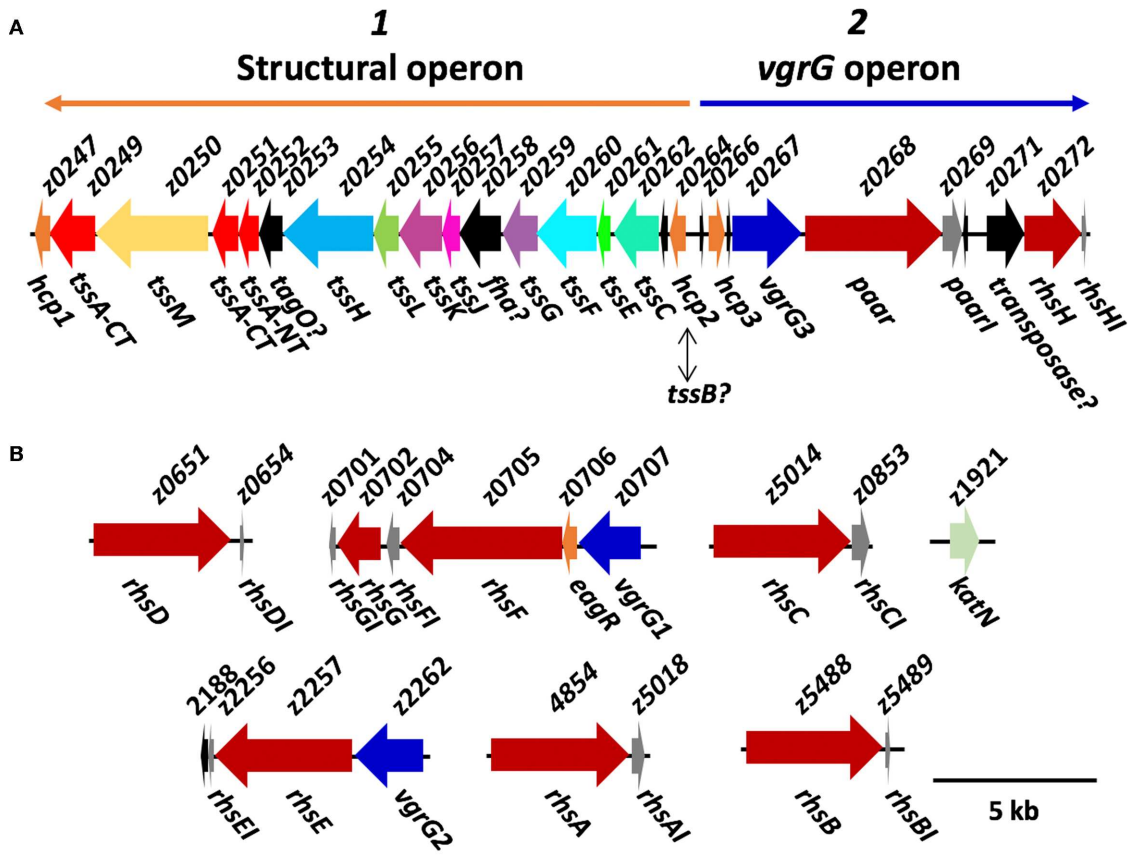

FIGURE 1 | Diagram of the organization of T6SS genes in EHEC strain EDL933. **(A)** Organization of the T6SS island components, in which the genes of unknown function are shown in black. Orange and blue arrows are showing the localization of the putative operon 1 and 2 in the island (named here structural and *vgrG* operons). **(B)** Putative T6SS effectors. The *rhs* genes found in EHEC strain EDL933 are shown in red, and the *vgrG* homologs are shown in blue. KatN, the only confirmed T6SS effector to date is shown in green, while the immunity proteins are shown in gray. This diagram was constructed based on CP008957 genome published by Latif et al. (2014), and the genes only found in this genome lack the z-prefix.

both regions could properly oligomerize and perform TssA function during T6SS biogenesis. About a third of the O157:H7 strains we analyzed showed the same single-nucleotide deletion, while the rest encoded a full length TssA protein. Additionally, *z0249* also encodes a protein of the cluster of differentiation 3515 (COG3515) that would also correspond to the C-terminal fraction of TssA, although the identity between Z0251 and Z0249 is rather low (41.67% and 7% of query cover). The TssA C-terminal region forms dodecamers, suggesting that the gene could be duplicated on the genome, but the low homology could imply that both loci perform different activities during T6SS biogenesis and/or function.

Outside of the T6SS island, we found two islands that encode VgrG proteins (*vgrG* islands, **Figure 1B**), which Uchida et al. (2013) renamed *vgrG1* (*z0707*) and *vgrG2* (*z2262*), while the locus *z0267* inside the T6SS island was named *vgrG3*. Interestingly, downstream of *vgrG1*, we found an hypothetical protein with a domain of unknown function 1795 (DUF1795), which has been found to interact with Rhs and VgrG proteins in *Serratia marcescens* (Alcoforado Diniz et al., 2015), and is essential for T6SS-mediated translocation of Rhs proteins in several STECs (Ma et al., 2017b). The three VgrG proteins have ≥90% amino acid identity and resemble other VgrG proteins of the T6SS-2. Interestingly, the same 8 STEC O157:H7 strains that were negative for structural genes were also negative for *vgrG* genes, while the other possessed at least one *vgrG* homolog in their genome, having up to five copies of *vgrG*.

Several T6SS effectors are VgrG proteins that have a C-terminal extension with enzymatic activity (Ma and Mekalanos, 2010; Suarez et al., 2010; Brooks et al., 2013; Sana et al., 2015). However, none of the VgrG homologs in EHEC O157:H7 strains had a known effector domain in its C-terminal, though we found that the C-terminal region was highly divergent while the N-terminal region was conserved. T6SS-translocated proteins are carried by VgrG proteins, and those effectors usually interact with the C-terminal region of VgrG (Hachani et al., 2014; Whitney et al., 2014). Thereby, we postulate that the three different VgrG proteins present in EHEC O157:H7 strains carry different effectors to the prey cell.

Wan et al. (2017) already demonstrated that T6SS in EHEC EDL933 is functional in an *hns* isogenic mutant and that it can translocate the KatN catalase upon macrophage phagocytosis, thus neutralizing the iROs in the phagosome and avoiding bacterial death. They also showed that the T6SS is essential to cause disease in a murine model, as the isogenic *clpV* mutants were unable to provoke death in mice. Nonetheless, mice death was independent of *katN*, so there must be other unidentified effectors that could contribute to EHEC strain EDL933 pathogenesis.

Identification of Putative Effectors Using a Bioinformatics Approach

Each T6SS family has characteristic effectors according to its own functionality, and even if we could not find a single O157:H7 strain with a T6SS-1 or T6SS-3, we decided to look for effectors of any T6SS family in EHEC O157:H7 trying to determine the role of the secretion system. The commonly reported T6SS effectors in *E. coli* were not found in the genomes of EHEC O157:H7 available to date. EHEC O157:H7 lacks the effectors of the VT1-VT5 families described previously (Ma et al., 2018), as well as effectors with DUF2169, DUF4123 or DUF2345 domains. Proteins with the characteristic GXSXG or HXKXXXXD motifs were also absent (Lien and Lai, 2017). On the other hand, after identifying a PAAR domain-containing protein in the T6SS island of EHEC strain EDL933, we looked for other PAAR domain-containing proteins in EHEC strain EDL933 genome and found seven genes that encode these proteins. PAAR proteins have been found in T6SS-associated effectors in *Pseudomonas aeruginosa* and *Vibrio cholerae* (Shneider et al., 2013), in EHEC strain EDL933, they also contained RHS (Recombination Hotspot) repeats, so they were classified as Rhs family proteins. In recent years, several T6SS-effectors related to Rhs proteins have been described in UPEC and STEC strains (Poole et al., 2011; Ma et al., 2017b), as well as in other species such as *P. aeruginosa* and *S. marcescens* (Kung et al., 2012; Diniz and Coulthurst, 2015). By using the I-TASSER software, we modeled the tridimensional structure of Z0268 (PAAR) and found that this protein resembled a shell-like structure built up by β-sheets that enclose a C-terminal region with enzymatic activity (**Figure 2A**). The N-terminal and central region of PAAR-Rhs proteins is present in both Gram-negative and Gram-positive bacteria, and there are even homologous proteins in eukaryotes, known as teneurins. The structure of the extracellular domain of teneurins is similar to Rhs proteins, and their presence in eukaryotes was probably due to horizontal gene transfer (Jackson et al., 2018). Teneurins bind to latrophilins and mediate cell-cell adhesion (Cruz-Ortega and Boucard, 2019), while the Rhs proteins in bacteria seem to mediate intercellular competition (Koskiniemi et al., 2013).

The C-terminal region of Rhs proteins frequently share homology with several bacterial toxins and the studied Rhs effectors usually fall into the canonical categories (nucleases, lipases, and murein-hydrolases). Ma et al. (2017b) showed that the PAAR domain was required for the translocation of Rhs proteins via T6SS. The PAAR domain interacts with the C-terminal end of VgrG for its transport to the cytoplasm of the prey cell, where the Rhs C-terminal exerts its functional role (Busby et al., 2013; Shneider et al., 2013).

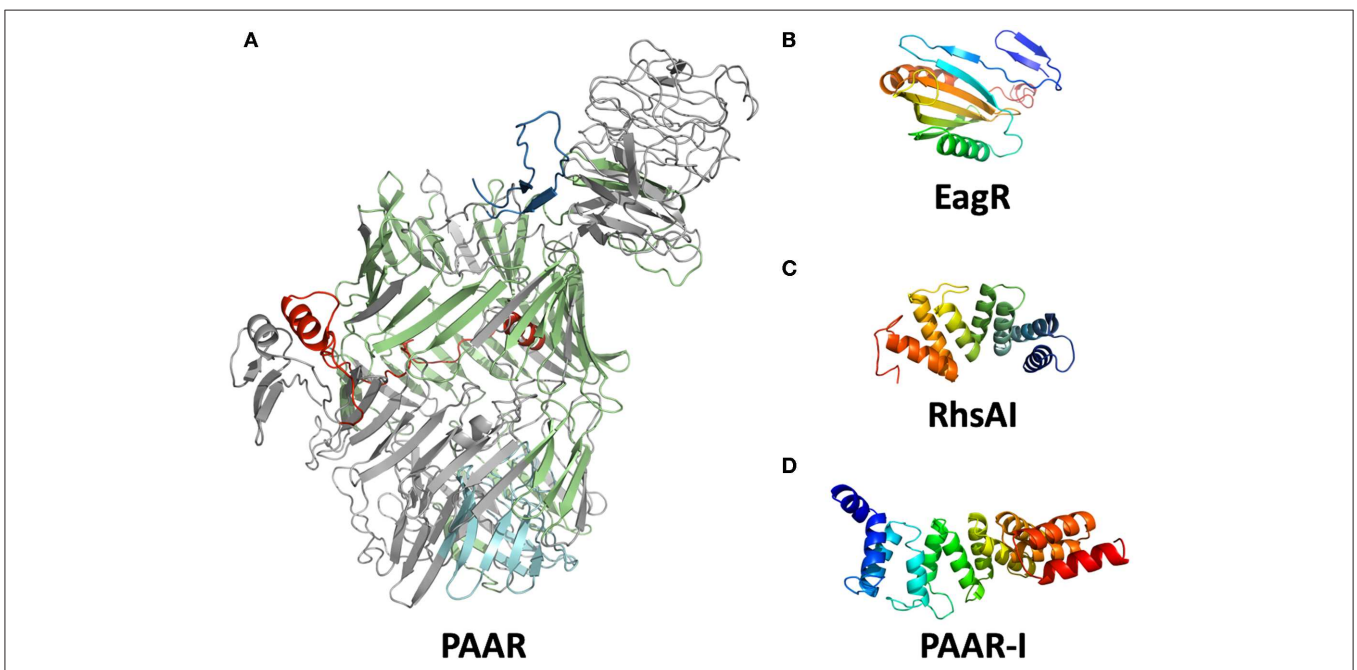

FIGURE 2 | Modeled structures of T6SS associated proteins in EHEC. Structure modeling was performed using I-TASSER software. **(A)** Putative structure of PAAR (locus *z0267*). The PAAR domain is shown in red; RHS repeats (15) are shown in green; amino acid kinase is shown in cyan. The TM-score for this modeling is 0.968 with Teneurin 2 (pdb: 6fb3A). **(B)** Putative conformation of EagR (locus *z0706*). **(C)** Putative structure of RhsA-I. **(D)** The structural model of PAAR-I (locus *z0268*).

TABLE 1 | Comparison between Rhs proteins from two available genomes in EHEC EDL933.

Proposed name	Loci from Perna et al.	GenBank ID	Loci from Latif et al.	Genbank ID	Notes
RhsA	*z5014*	AAG58737	*EDL933_4854*	AIG70995	Fused with *z5017*
RhsB	*z5488*	AAG59133	*z5488*	AIG71408	99.7% Identical
RhsC	*z0847*	AAG55021	*z0847*	AIG66972	Fused with *z0851*
RhsD	*z0651*	AAG54854	*z0651*	AIG66789	100% Identical
RhsE	*z2257*	AAG56314	*z2257*	AIG68376	*z2257-z2261* are fused
	z2259	AAG56315	*z2259*		
	z2261	AAG56316	*z2261*		
RhsF	*z0705*	AAG54900	*z0705*	AIG66446	100% Identical
RhsG	*z0702*	AAG54898	*z0702*	AIG66832	100% Identical
RhsH	*z0272*	AAG54539	*z0272*	AIG66830	100% Identical
PAAR	*z0268*	AAG54536	*z0268*	AIG66450	100% Identical

In EHEC strain EDL933, we found several genes of the Rhs family, but these genes differ between both available genomes; 9 loci (Latif et al., 2014) vs. 11 loci (Perna et al., 2001) (**Table 1**). Although *z2488*, *z0651*, *z0268*, *z0272*, *z2257,* and *z0705* genes were identical in both genomes, we found several important differences. In the first genome published, for example, locus *z5014* encodes an Rhs protein with a PAAR motif that we identified as a putative DNAse domain in its C-terminal end, while in the genome published by Latif et al. (2014), this C-terminal end was not a DNAse and contained the sequence corresponding to locus *z5017* (**Figures 3A,B**). We also found that the protein encoded by locus *z5014* had different C-terminal regions, whereas locus *z2257* from Latif et al. (2014) genome contained regions from loci *z2256, z2257,* and *z2259* (**Table 1**), as there were 20 gaps and 42 mismatches between this region in both genomes. A possible reason for these discrepancies is that the genome published by Perna et al. (2001) might have assembly mistakes in the regions that encode Rhs proteins due to their size and the presence of multiple homologs in the genome. In fact, upon analysis of *rhs* genes in EHEC O157:H7 strain Sakai, we found that they were practically identical to those in EHEC strain EDL933 according to the genome published by Latif et al. (2014), both in the number of loci as in their sequences, including the C-terminal encoding region.

To test which of the two published genomes represented better the *rhs* genes in EHEC strain EDL933, we decided to amplify a region of an *rhs* gene present in EHEC EDL933 that should correspond to the same sequence in the different genomes reported; in Perna et al. (2001), it would be the locus *z5014* and in Latif et al. (2014) the locus *EDL933_4854*. Locus *z5014* from the genome published by Perna et al. (2001) contains a 3′ end that does not correspond to any other sequence from the genome published by Latif et al. (2014), while in this latter genome the locus *z5017* is fused to the 3′region of *z5014*, here named *EDL933_4854* (**Figure 3A**). Thus, we designed a forward primer (rhsAF) that could serve for both genomes, as well as a reverse primer (rhsA1R) specific for the 3′region of *z5014* in Perna et al. (2001) that would produce an 800 bp amplicon. We also designed another reverse primer (rhsA2R) that aligned with locus *z5017* from Perna et al. (2001) and locus *EDL933_4854* from Latif et al. (2014), which would produce a 2.6 kb long amplicon and an 875 bp long amplicon, respectively (**Figure 3A**). The reverse primer designed for the genome published by Perna et al. (2001) (rhsA1R) did not amplify the expected DNA fragment (800 bp) in EHEC EDL933 (**Figure 3B**), while the reverse primer for the genome published by Latif et al. (2014) (rhsA2R), amplified the 875 bp fragment from EHEC strain EDL933. To test if the reverse primer designed for the genome published by Perna et al. (2001) was reliable, we used *E. coli* strain HB101 as a positive control, since this strain has an *rhs* gene identical to the locus *z5014* reported by Perna et al. (2001). The amplification of an 800 bp fragment only in strain HB101 using rhsA1R primer (**Figure 3B**) suggested that EHEC EDL933 does not harbor the sequence reported by Perna et al. (2001). Using the same strategy (see **Figure 3A**), we analyzed the *rhsC* gene region, another chromosomal region with differences between both genomes. The region of the *rhsC* gene was amplified using the rhsAF primer and a specific primer (rhsCR) that would give a 2.7 kb fragment for the genome of Perna et al. (2001) and a 832 bp fragment for the genome of Latif et al. (2014). Similar to *rhsA*, a fragment of 832 bp was obtained both in EHEC ELD933 as in *E. coli* strain HB101, while the 2.6 kb fragment was not obtained in any strains. In conclusion, the genome published by Latif et al. (2014) better represents the *rhs* genes in EHEC strain EDL933, so we recommend using this genome in posterior analyses. In this genome, we found 9 genes of the *rhs* family, of which 7 are long (>4 kb) and have a PAAR domain, while the two remaining are relatively small (<1 kb) and do not have a PAAR domain. Because the locus *ELD933_4854* was similar to the *rhsA* gene from *E. coli* strain K-12, we named this gene as *rhsA,* named the other loci as *rhsB-H* according to their sequence similarity with genes in *E. coli* K-12, and named *paar* the *rhs* gene that is encoded inside the T6SS island to differentiate it from the others.

Once we determined which genome was better for the study of the Rhs family proteins, we wanted to elucidate the possible role of each protein, so we analyzed the C-terminal end of each Rhs looking for functional domains, and for effectors structural homology using I-TASSER software. We first analyzed the RhsA protein (locus *EDL933_4854*) and did not find any known motif, but after modeling its structure with I-TASSER we found that the C-terminal region had structural similarity with the toxin-A of *Clostridium difficile*, a toxin that inactivates GTP-binding proteins such as Rho, Rac, and Cdc42 (Voth et al., 2019) (pdb: 3HO6, TM-score: 0.73). The C-terminal end of RhsB (*z5488*) was structurally similar with the human proteasome 26S lid, which recognizes ubiquitinated proteins (Schweitzer et al., 2016) (pdb: 5l4kV, TM-score: 0.694), though we found

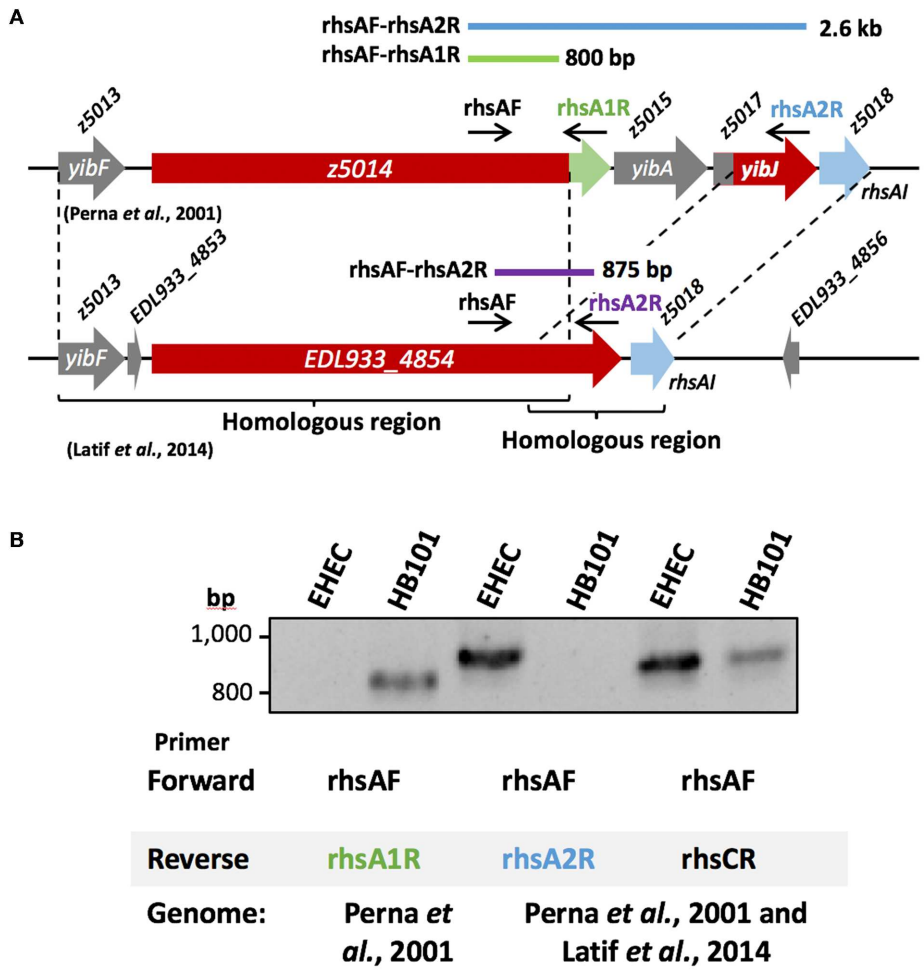

FIGURE 3 | Gene amplification of rhsA in EHEC strain EDL933. **(A)** Diagram of the region between loci *z5013* and *z5018* according to Perna et al. (2001) and according to Latif et al. (2014). The *rhs* gene (red) has a different C-terminal end in each genome, harboring a DNAse domain (green) in and the sequence corresponding to locus *z5017* (red). **(B)** The 800 bp amplicon for *rhsA* gene (locus *z5014*) was not generated in EHEC strain EDL933 using the primer pair rhsAF-rhsA1R designed for the gene according to Perna et al. (2001). *E. coli* strain HB101 was used as a positive control for these primers (rhsAF-rhsA1R), which generated an 800 bp amplicon. Whereas, when the primer pair rhsAF-rhsA2R designed based on Perna et al. (2001) and Latif et al. (2014) was used, the expected 2.6 kb fragment was not obtained, but the 875 bp was, as expected from the genome from Latif et al. (2014). By using a specific primer (rhsCR) for *rhsC*, a 832 bp fragment was obtained, as expected from the genome of Latif et al. (2014), while the 2.7 kb fragment from the genome of Perna et al. (2001) was not obtained neither in EHEC EDL933 nor in *E. coli* strain HB101. A 63°C temperature was used for **(B)**. The PCR products were separated in an 1.5% agarose gel and stained using ethidium bromide.

a DUF4329 motif (PF05593, *e-value*: $5x10^{-13}$) that according to Ma et al. (2017b) is an RNase domain. The C-terminal end of RhsC (*z5014*) had structural similarity with VipE protein of *Legionella pneumophila*, a protein that inhibits the vesicular traffic in yeast (Shohdy et al., 2005) (pdb: 4qn8A, TM-score: 0.574). The C-terminal region of RhsD (*z0651*) was structurally homologous with the human serum amyloid A1 protein (Lu et al., 2014) (pdb: 4ip8A, TM-score: 0.623), which participates in the inflammatory response, chemotaxis and opsonization upon binding with several integrins and G protein-coupled receptors (GPCRs) (Niemi et al., 2011). The C-terminal end of RhsE (*z2257*) had structural homology with the RsaA protein of *Caulobacter crescentus* (Bharat et al., 2017) (pdb: 5n8pA, TM-score: 0.71), as well as the adhesin PfbA of *Streptococcus pneumoniae* (Suits and Boraston, 2013) (pdb: 3zpp, TM-score: 0.647). Both RsaA and PfbA are present in the S-layer of bacteria and could serve as adhesins. Finally, the C-terminal end of PAAR (*z0268*) presented homology with the cysteine-protease domain of the RtxA toxin of *V. cholerae* (Prochazkova et al., 2009) (pdb: 3fzyA, TM-score: 0.681), a toxin that crosslinks actin and actively participates during the pathogenesis of *V. cholerae*. Nonetheless, the C-terminal end did not have a RTX motif nor the actin cross-linking domain normally found in the RtxA toxin (Boardman et al., 2007) (**Table 2**).

TABLE 2 | Putative function of Rhs effectors in EHEC strain EDL933.

Locus	Domain homolog	TM-score	Homolog function
EDL933_4854 (rhsA)	Toxin A from *C. difficile*	0.73	Small-GTPase inhibition (like Rho and Rac)
z5488 (rhsB)	Proteasome lid 26S	0.694	Protein ubiquitination
z5014 (rhsC)	VipE	0.574	Vesicular-traffic inhibition
z0651 (rhsD)	human serum amyloid A1 protein	0.623	Chemotaxis, inflammatory response
z2257 (rhsE)	RsaA from *Caulobacter crescentus*	0.71	S-layer Adhesin
z0268 (paar)	Toxin RtxA from *V. cholerae*	0.681	Cysteine protease, actin-crosslinking
z0705 (rhsF)	Capsid protein from betanodavirus	0.863	Capsid protein

RhsF protein (*z0705*) did not harbor any apparent motif, but the structural modeling showed that the C-terminal end resembled the structure of capsid proteins present in viruses such as betanodavirus (pdb: 3jbmA, TM-score: 0.863) or Orsay-like virus (pdb: 4nwvA, TM-score: 0.825). Just downstream of the *rhsF* gene, we found another *rhs* gene (*rhsG*, locus *z0702*). RhsG protein had a metallopeptidase-4 domain (PF15640, *e-value*: 1×10^{-32}), which has already been described in a similar STEC strain (Ma et al., 2017b), but lacked the PAAR domain in EHEC strain EDL933 and it seems to be interrupted (this region is identical in both published genomes). The presence of a C-terminal region similar to capsid proteins has not been reported previously, and upon inspecting the 3′ region of the *rhsF* gene and the linker sequence between *rhsF* and *rhsG,* we found that both sequences shared similarity with Pithovirus LCDPAC02. This suggests that the *rhsG* gene was originally fused with *rhsF*, but a viral sequence was inserted in this region and separated the gene. It is unclear if the C-terminal of the RhsF protein has a function related to interbacterial competition or pathogenesis. To corroborate the predicted functions of the Rhs proteins as T6SS effectors, a translocation assay is needed, and this becomes complicated due to the current difficulty to activate the T6SS *in vitro*. As there are several methodologies to achieve expression of the T6SS *in vitro* (Gueguen and Cascales, 2013; Miyata et al., 2013; Wan et al., 2017), co-expression of the Rhs proteins and the T6SS components needs to be achieved to properly investigate their function. Heterologous expression can help to study the effector function, and murine infection models with isogenic mutants for these genes could help to establish the importance of the Rhs proteins during intestine colonization and pathogenesis.

The genes *rhsE, rhsF,* and *paar* were located downstream of a distinct *vgrG* gene (**Figure 1**), suggesting that these Rhs proteins are translocated by a its specific VgrG protein. On the other hand, *rhsA, rhsB, rhsC,* and *rhsD* were orphan genes that did not belong to a *vgrG* island, so presumably, they can be translocated by any VgrG protein. If each VgrG protein translocates specific Rhs proteins, then it would be logical to think that the *rhs* genes are divided in three categories according to the number of *vgrG* genes in EHEC EDL933. Using phylogenetic analysis, we found that *rhs* genes were indeed divided into three clades (**Figure 4**). The first clade grouped *rhsA, rhsB,* and *rhsC* genes being the last two more closely related. The second clade contained *rhsD, rhsE,* and *paar* genes, being the latter one more dissimilar of them. Finally, *rhsF* gene was clearly different from the others, being the only member of its clade. While *rhsF* is adjacent to *vgrG1*, it would seem that VgrG1 translocates RhsF, however, both *rhsE* and *paar* are in the same clade and are adjacent to *vgrG2* and *vgrG3*. Besides, the first clade containing *rhsA, rhsB,* and *rhsC* did not include any *rhs* gene encoded around a *vgrG* island, so it is unclear which VgrG protein, if any, translocates these proteins. Ma et al. (2017b) claimed that, in STEC, the *rhs* genes encoded in the vicinity of the EagR chaperone are phylogenetically distinct from the orphan genes (*rhs* genes not encoded in an *eagR* island), which is consistent in EHEC EDL933, as *eagR* was directly upstream of the *rhsF* gene, the less conserved gene in EHEC EDL933. When we modeled the structure of EagR (locus *z0706*) (**Figure 2B**), we found that the protein resembles PA0094 (TM-score: 0.888) from *P. aeruginosa*, whose crystal structure was obtained by Osipiuk et al. (unpublished, pdb: 1TU1). PA0094 acts as a chaperone for the Tse6 (PA0093), a PAAR-domain containing protein that also has a Ntox46 domain with nuclease activity. The high structural homology between PA0094 and EagR suggests that the EagR protein also functions as a chaperone for RhsF in EHEC EDL933. Nevertheless, because of the absence of a known motif in RhsF C-terminus, more studies are needed to determine if this island and its encoded proteins are indeed functional.

We have found that *rhs* genes are widely distributed among bacteria through data base analyses. By searching all EHEC O157:H7 genomes in GenBank, we found that there are some strains having up to 11 of these genes. Other studies have already classified PAAR-Rhs proteins as T6SS effectors, being mostly nucleases or peptidases (Koskiniemi et al., 2013; Ma et al., 2017b). The RNAse motif present in Z5014 from the genome published by Perna et al. (2001) (PF15606) is not present in other Rhs proteins from O157:H7 strains, suggesting that this motif is not present in EHEC O157:H7. However, in EHEC O157:H7 strains there are 9 PAAR-Rhs proteins with a DUF4329 that has a RNase activity, including RhsB from EDL933 as showed above ($e \leq 0.01$). Interestingly, 7 PAAR-Rhs proteins in EHEC O157:H7 strains contain a serum amyloid A protein motif in their C-terminal region (PF00277; $e \leq 0.01$). As we discussed earlier, this motif could play a role in the immunological response but experimental evidences are required. Though we found 26 Rhs proteins with metallopeptidase-4 domain in EHEC O157:H7 strains, none had a PAAR domain that would identify them as T6SS effectors. Finally, 11 PAAR-Rhs proteins contained an amino acid kinase motif (AAK, cd04259) in their C-terminal, which is commonly found in proteins related to lysine and aspartate metabolism. Proteins with this activity could phosphorylate prey proteins and change their behavior, thus contributing to the bacterium survival and/or pathogenesis. However, EHEC O157:H7 strain EDL933 does not possess this interesting motif.

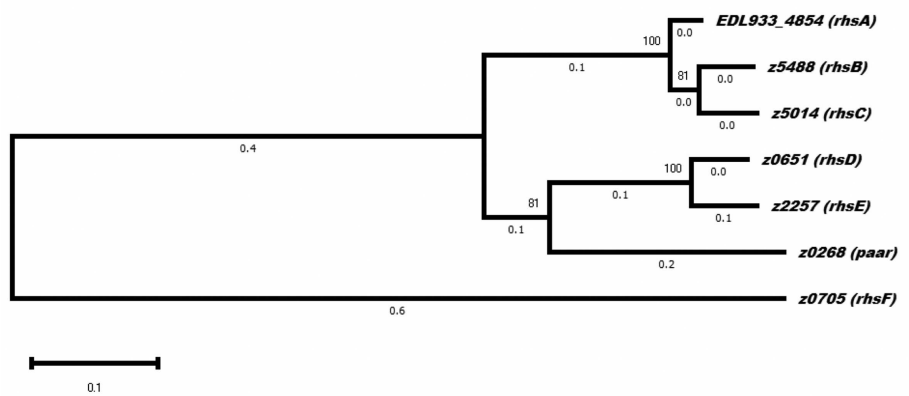

FIGURE 4 | Evolutionary analysis of *rhs* genes in EHEC strain EDL933. The phylogenetic tree shows three distinct clades, of which the one containing *rhsF* is the one that diverged first. Two of the genes encoded in a *vgrG* island are in the same clade (*rhsE* and *paar*), while *rhsA*. *rhsB* and *rhsC* did not belong to a neighborhood containing other T6SS genes. The evolutionary history was inferred by using the Maximum Likelihood method and Tamura-Nei model. The tree with the highest log likelihood (-23369.81) is shown. The percentage of trees in which the associated taxa clustered together is shown next to the branches. Evolutionary analyses were conducted in MEGA X (Kumar et al., 2018).

Immunity/Effector Rhs Pairs in EHEC Strain EDL933

Antibacterial effectors translocated via T6SS are usually encoded by a bicistronic operon containing genes for an effector and its respective immunity protein, whose function is to inhibit the activity of this effector. These immunity proteins are useful to avoid autointoxication and to guard off attacks of sister cells. When we analyzed the region downstream of the *rhs* genes, we found that all of them contain a relatively small ORF (129-609 nucleotides) that could act as the immunity gene for each Rhs. Just as the C-terminal ends are highly divergent, these related immunity proteins are also poorly conserved, suggesting that an immunity protein is only able to inhibit the action of its related effector, as demonstrated for *Dickeya dadantii* strain 3937 (Koskiniemi et al., 2013). To know if the genes downstream *rhs* genes encoded immunity proteins, we decided to look for protein-protein interaction motifs as well as structural modeling of the putative proteins to search structural homologs in the same fashion as we did for the C-terminal end of the Rhs proteins.

Locus *z5018* would encode for the putative immunity protein of RhsA, a 132 amino acid protein that we named RhsAI. In this protein, we found tetratricopeptide repeats (TPR; *e-value*: 1×10^{-5}) and Sel-1-like repeats (SLR; *e-value*: 4×10^{-5}). TPR and SLR motifs belong to the Sel-1 superfamily, whose members usually act as molecular adaptors between proteins both in prokaryotes and eukaryotes (Mittl and Schneider-Brachert, 2007). Recently, the crystal structure of two immunity proteins for T6SS effectors was obtained from *P. aeruginosa* (PA5088 and PA5087), and these structures harbor SLR repeats that directly interact and inhibit phospholipase D effectors (Yang et al., 2016). Nonetheless, PA5087 and PA5088 SLR motifs only possessed 35.06 and 28.99% identity with RhsAI, respectively. Through modeling RhsAI structure using I-TASSER (**Figure 2C**), we found that it shares structural homology with the protein C5321 from Uropathogenic *E. coli* (UPEC) strain CFT071 (TM-score: 0.899, pdb: 4BWR). Urosev et al. (2013) described C5321 as a potential model for vaccine-development against ExPEC, but did not provide any more information about the protein function in UPEC. We did not find any known T6SS effector in the vicinity of *c5321* in UPEC, nor any *rhs* gene, so it seems unlikely that this protein acts as an immunity protein in UPEC. Nonetheless, it could be possible that *c5321* is an orphan immunity gene and that the presence of this gene might protect UPEC from RhsA of EHEC, or other T6SS effectors in gram-negative bacteria. RhsAI also possesses structural homology with the protein LpnE from *Legionella pneumophila* (TM-score: 0.899, pdb: 6dehA). LpnE interacts with the Oculocerebrorenal syndrome of Lowe (OCRL) protein in eukaryotic cells (Voth et al., 2019), which is a Inositol-polyphosphate 5-phosphatase. This similarity was interesting because the PA5088 immunity protein (which has structural homology with RhsAI) also interacts with a phosphatase effector, suggesting that RhsA might have a phosphatase activity, and phosphatases have been implicated in antibacterial activity, pathogenesis, or even both (Jiang et al., 2014). Finally, RhsAI had also structural homology with the protein Suppressor of lin-12-like protein 1 (SEL1L), a murine protein that can oligomerize, something that is also necessary for some immunity proteins to inhibit T6SS-associated effectors (Yang et al., 2018).

The putative immunity protein for RhsB only contained 57 amino acids (locus *z5489*), and upon sequence analysis, we found two interesting motifs. The first one is from the family PF07114 including the transmembrane protein 126 (TMEM126A/B, *e-value*: 0.022), which suggests its possible location in the cell, although the *e-value* is high, it is on the edge. In humans, TMEM126B participates in the construction of the mitochondrial respiratory complex I (Andrews et al., 2013). The membrane location should be congruent with the predicted function of RhsB as ubiquitin-receptor, as we predicted above using structural modeling, and the TMEM family have a variety of functions in eukaryotes, participating in phospholipid

scrambling, ion transport and regulation of other membrane proteins (Pedemonte and Galietta, 2014). On the other hand, RhsBI also contained a dsRNA-binding domain found in the Dead-end protein homolog-1 (DND1) protein (*e-value*: 0.087). Both motifs have a high *e-value*, meaning that RhsB shares poor homology with those proteins, so the function of the RhsBI protein remains unclear until experimental evidence. However, it is worth to mention that DND1 is a RNA-binding protein, and it is known to protect eukaryotic mRNA from miRNAs, so the RhsBI protein could have a protective effect from mRNA degradation from the RNase motif DUF4329 present in RhsB, as we discussed earlier.

For RhsCI (locus *z0853*) and RhsDI (locus *z0654*) there was a TPR motif and a TIGR03373 motif, respectively, but both had high *e-values* (0.21 and 0.35), suggesting that there is no sequence similarity between these proteins and the consensus sequence. STRING analyses suggest that the *rhsC-D* genes are often in the same neighborhood as their cognate immunity genes, but there is no evidence of co-expression or interaction for any Rhs protein with their associated immunity protein.

Locus *EDL933_2188* would encode the immunity protein of RhsE, and the protein encoded was of 61 amino acids that bear a lipoprotein signal peptide according to the software SignalP (Juncker et al., 2003), indicating that the immunity protein is probably anchored to the bacterial internal membrane. As we mentioned earlier, RhsE protein possessed structural homology with RsaA protein, present in the S-layer. S-layer located proteins (SLPs) are involved in several activities, such as cell-wall biogenesis, cell division, and swimming. Besides, SLPs have been involved in pathogenesis, altering the immune response of the host and promoting bacterial adhesion to host cells (Fagan and Fairweather, 2014). This signal peptide might lead to the translocation of RhsEI to the periplasm, suggesting that RhsEI binds to RhsE in the outer membrane, where RhsE would normally act. Dong et al. (2013) have shown that Tai3, the immunity protein for the amidase effector Tae3 in *Ralstonia picketti*, also harbors a signal sequence. In the S-layer, the C-terminal end of RhsE could damage the plasma membrane or the cell-wall of other bacteria, and the immunity protein would be on the membrane to avoid cell death provoked by RhsE in sister cells. Additionally, RhsEI possessed another motif (PF16855) present in small proteins of the viral external capsid (*e-value:* 0.072), though the high *e-value* indicates poor homology with the consensus sequence of PF16855.

Finally, the candidate for the PAAR-I protein (locus *z0269*) was 203 amino acid long, larger than other putative immunity proteins. We identified 7 SLR/TPR motifs, as previously mentioned, are motifs found in immunity proteins. Upon analysis of the putative tridimensional structure of PAARI by I-TASSER, we found that the immunity protein resembled the *Helicobacter* cysteine-rich protein C (TM-score: 0.928, pdb: 1OUV) (**Figure 2D**). Although the exact role of this protein is still unknown, it seems to participate during cell-wall biogenesis. Besides, patients infected with *H. pylori* usually bear high antibody titers against this protein. Lüthy et al. (2004) demonstrated that the structural conformation of the *Helicobacter* cysteine-rich protein C resembles the Hsp60/Hsp70, which provides more evidence of the possible chaperone activity of PAARI. Finally, the presence of loci *z0268* and *z0267* is specific to a specific lineage of O157:H7 that includes EHEC EDL933 and EHEC Sakai, as previously reported (Zhang et al., 2007).

Small Rhs proteins were also part of bicistronic operons, and we named them RhsH (*z0272*) and RhsG (*z0702*). Both effectors were part of an island that also contained another *rhs* gene. RhsG seems to be the former C-terminal region of RhsF that was probably divided when a viral sequence was inserted, as we mentioned above. Since these proteins were 444 and 586 amino acids in length, compared to the >1,400 amino acids of other Rhs proteins, their genes were probably part of a larger former gene. The putative immunity proteins for RhsG and RhsH were also small (69 and 56 amino acids respectively) and did not have a clear structural homolog. The absence of the PAAR motif in both proteins suggests that these proteins are not secreted via T6SS, and the small size and poor structural homology of the putative immunity proteins suggest that their genes are actually pseudogenes.

The immunity proteins protect the bacteria from sister cells attacks when the effectors modulate antibacterial competition. Interestingly, Wan et al. (2017) have shown that EHECΔ*hns* does not have a bactericidal activity, suggesting that the Rhs proteins do not have a toxic effect on other bacteria, although *rhs* gene expression was not measured. As we show here, several effector-immunity proteins seem to be related to the cell membrane and cell-wall biogenesis, so more studies are necessary to elucidate the function of the T6SS both in bacterial competition and during pathogenesis. It is also possible that the putative immunity proteins described have a different function than predicted, maybe as chaperones like EagR.

CONCLUSIONS

The two existing genome sequences exhibit critical differences among the Rhs proteins, and as demonstrated experimentally and bioinformatically we suggest using the genome published by Latif et al. (2014) to study the Rhs proteins in EHEC strain EDL933. Upon analysis of the core components of the T6SS island, we found that the TssA gene seems to be split in two, but these two proteins should still be able to perform their function, as the functionality of the T6SS has been demonstrated by Wan et al. (2017). Although EHEC strain EDL933 lacks the commonly found T6SS effectors in *E. coli*, many *rhs* genes appear to serve as T6SS effectors. Using a structural homology approach, we postulate that RhsA may interact with small GTPases such as Rho and Rac; RhsB could interfere in the protein ubiquitination; RhsC might participate in the vesicular traffic; RhsD could auto-aggregate; RhsE might act as an S-layer adhesin; and PAAR could act as a cysteine protease. Finally, RhsF would not have any function due to a viral DNA sequence inserted on the 3′ end of the gene, which separated the former metallopeptidase into RhsF and RhsG. Additionally, we did not find direct *in silico* information supporting EHEC strain ELD933 is involved in bacterial competition, as suggested by Wan et al. (2017). The role of Rhs proteins during pathogenesis

or bacterial competition requires experimental support. The exact role of T6SS and its effectors in EHEC and other STECs might provide new strategies to fight diseases caused by those pathogens.

DATA AVAILABILITY STATEMENT

Publicly available datasets were analyzed in this study. This data can be found here: AE005174.2, CP008957.1.

AUTHOR CONTRIBUTIONS

JV-L and FN-G participated in the design of the study, data analysis and writing of the manuscript. JV-L carried out the PCR experiments. Both authors read and approved the final manuscript.

FUNDING

FN-G was supported by a Conacyt grant (501212).

REFERENCES

Abby, S. S., Cury, J., Guglielmini, J., Néron, B., Touchon, M., and Rocha, E. P. (2016). Identification of protein secretion systems in bacterial genomes. *Sci. Rep.* 6:23080. doi: 10.1038/srep23080

Alcoforado Diniz, J., Liu, Y. C., and Coulthurst, S. J. (2015). Molecular weaponry: diverse effectors delivered by the type VI secretion system. *Cell. Microbiol.* 17, 1742–1751. doi: 10.1111/cmi.12532

Andrews, B., Carroll, J., Ding, S., Fearnley, I. M., and Walker, J. E. (2013). Assembly factors for the membrane arm of human complex I. *Proc. Natl. Acad. Sci. U.S.A.* 110, 18934–18939. doi: 10.1073/pnas.1319247110

Arenas-Hernández, M. M., Rojas-López, M., Medrano-López, A., Nuñez-Reza, K. J., Puente, J. L., Martínez-Laguna, Y., et al. (2014). Environmental regulation of the long polar fimbriae 2 of enterohemorrhagic Escherichia coli O157: H7. *FEMS Microbiol. Lett.* 357, 105–114. doi: 10.1111/1574-6968.12513

Basler, M., Ho, B., and Mekalanos, J. (2013). Tit-for-tat: type VI secretion system counterattack during bacterial cell-cell interactions. *Cell* 152, 884–894. doi: 10.1016/j.cell.2013.01.042

Bharat, T. A., Kureisaite-Ciziene, D., Hardy, G. G., Ellen, W. Y., Devant, J. M., Hagen, W. J., et al. (2017). Structure of the hexagonal surface layer on Caulobacter crescentus cells. *Nature Microbiol.* 2:17059. doi: 10.1038/nmicrobiol.2017.59

Bingle, L. E., Bailey, C. M., and Pallen, M. J. (2008). Type VI secretion: a beginner's guide. *Curr. Opin. Microbiol.* 11, 3–8. doi: 10.1016/j.mib.2008.01.006

Boardman, B. K., Meehan, B. M., and Satchell, K. J. F. (2007). Growth phase regulation of Vibrio cholerae RTX toxin export. *J. Bacteriol.* 189, 1827–1835. doi: 10.1128/JB.01766-06

Bondage, D. D., Lin, J.-S., Ma, L.-S., Kuo, C.-H., and Lai, E.-M. (2016). VgrG C-terminus confers the type VI effector transport specificity and is required for binding with PAAR and adaptor-effector complex. *Proc. Natl. Acad. Sci. U.S.A.* 113, E3931–E3940. doi: 10.1073/pnas.1600428113

Brooks, T. M., Unterweger, D., Bachmann, V., Kostiuk, B., and Pukatzki, S. (2013). Lytic activity of the vibrio cholerae type VI secretion toxin VgrG-3 is inhibited by the antitoxin TsaB. *J. Biol. Chem.* 288, 7618–7625. doi: 10.1074/jbc.M112.436725

Busby, J. N., Panjikar, S., Landsberg, M. J., Hurst, M. R., and Lott, J. S. (2013). The BC component of ABC toxins is an RHS-repeat-containing protein encapsulation device. *Nature* 501, 547. doi: 10.1038/nature12465

Croxen, M. A., Law, R. J., Scholz, R., Keeney, K. M., Wlodarska, M., and Finlay, B. B. (2013). Recent advances in understanding enteric pathogenic Escherichia coli. *Clin. Microbiol. Rev.* 26, 822–880. doi: 10.1128/CMR.00022-13

Cruz-Ortega, J. S., and Boucard, A. A. (2019). Actin cytoskeleton remodeling defines a distinct cellular function for adhesion G protein-coupled receptors ADGRL/latrophilins 1, 2 and 3. *Biol. Open* 8:bio039826. *doi: 10.1242/bio.039826*

Diniz, J. A., and Coulthurst, S. J. (2015). Intraspecies competition in Serratia marcescens is mediated by type VI-secreted Rhs effectors and a conserved effector-associated accessory protein. *J. Bacteriol.* 197, 2350–2360. doi: 10.1128/JB.00199-15

Dong, C., Zhang, H., Gao, Z.-Q., Wang, W.-J., She, Z., Liu, G.-F., et al. (2013). Structural insights into the inhibition of type VI effector Tae3 by its immunity protein Tai3. *Biochem. J.* 454, 59–68. doi: 10.1042/BJ20130193

Douzi, B., Brunet, Y. R., Spinelli, S., Lensi, V., Legrand, P., Blangy, S., et al. (2016). Structure and specificity of the Type VI secretion system ClpV-TssC interaction in enteroaggregative Escherichia coli. *Sci. Rep.* 6, 1–13. doi: 10.1038/srep34405

Fagan, R. P., and Fairweather, N. F. (2014). Biogenesis and functions of bacterial S-layers. *Nat. Rev. Microbiol.* 12, 211–222. doi: 10.1038/nrmicro3213

Felsenstein, J. (1985). Confidence limits on phylogenies: an approach using the bootstrap. *Evolution* 39, 783–791. doi: 10.1111/j.1558-5646.1985.tb00420.x

Finn, R. D., Bateman, A., Clements, J., Coggill, P., Eberhardt, R. Y., Eddy, S. R., et al. (2013). Pfam: the protein families database. *Nucleic Acids Res.* 42, D222–D230. doi: 10.1093/nar/gkt1223

Frank, C., Werber, D., Cramer, J. P., Askar, M., Faber, M., ander Heiden, M., et al. (2011). Epidemic profile of shiga-toxin-producing Escherichia coli O104: H4 outbreak in Germany. *New Engl. J. Med.* 365, 1771–1780. doi: 10.1056/NEJMoa1106483

Gueguen, E., and Cascales, E. (2013). Promoter swapping unveils the role of the citrobacter rodentium CTS1 type VI secretion system in interbacterial competition. *Appl. Environ. Microbiol.* 79, 32–38. doi: 10.1128/AEM.02504-12

Hachani, A., Allsopp, L. P., Oduko, Y., and Filloux, A. (2014). The VgrG proteins are "a la carte" delivery systems for bacterial type VI effectors. *J. Biol. Chem.* 289, 17872–17884. doi: 10.1074/jbc.M114.563429

Jackson, V. A., Meijer, D. H., Carrasquero, M., van Bezouwen, L. S., Lowe, E. D., Kleanthous, C., et al. (2018). Structures of teneurin adhesion receptors reveal an ancient fold for cell-cell interaction. *Nat. Commun.* 9:1079. doi: 10.1038/s41467-018-03460-0

Jiang, F., Waterfield, N. R., Yang, J., Yang, G., and Jin, Q. (2014). A pseudomonas aeruginosa type VI secretion phospholipase D effector targets both prokaryotic and eukaryotic cells. *Cell Host Microbe* 15, 600–610. doi: 10.1016/j.chom.2014.04.010

Journet, L., and Cascales, E. (2016). The type VI secretion system in Escherichia coli and related *species. EcoSal. Plus* 7:1–20. doi: 10.1128/ecosalplus.ESP-0009-2015

Juncker, A. S., Willenbrock, H., Von Heijne, G., Brunak, S., Nielsen, H., and Krogh, A. (2003). Prediction of lipoprotein signal peptides in Gram-negative bacteria. *Protein Sci.* 12, 1652–1662. doi: 10.1110/ps.0303703

Koskiniemi, S., Lamoureux, J. G., Nikolakakis, K. C., t'Kint de Roodenbeke, C., Kaplan, M. D., Low, D. A., et al. (2013). Rhs proteins from diverse bacteria mediate intercellular competition. *Proc. Natl. Acad. Sci. U.S.A.* 110, 7032–7037. doi: 10.1073/pnas.1300627110

Kumar, S., Stecher, G., Li, M., Knyaz, C., and Tamura, K. (2018). MEGA X: molecular evolutionary genetics analysis across computing platforms. *Mol. Biol. Evolut.* 35, 1547–1549. doi: 10.1093/molbev/msy096

Kung, V. L., Khare, S., Stehlik, C., Bacon, E. M., Hughes, A. J., and Hauser, A. R. (2012). An rhs gene of Pseudomonas aeruginosa encodes a virulence protein that activates the inflammasome. *Proc. Natl. Acad. Sci. U.S.A.* 109, 1275–1280. doi: 10.1073/pnas.1109285109

Latif, H., Li, H. J., Charusanti, P., Palsson, B. O., and Aziz, R. K. (2014). A Gapless, unambiguous genome sequence of the enterohemorrhagic Escherichia coli O157:H7 strain EDL933. *Genome Announc.* 2:e00821-14. doi: 10.1128/genomeA.00821-14

Leiman, P. G., Basler, M., Ramagopal, U. A., Bonanno, J. B., Sauder, J. M., Pukatzki, S., et al. (2009). Type VI secretion apparatus and phage tail-associated protein complexes share a common evolutionary origin.

Proc. Natl. Acad. Sci. U.S.A. 106, 4154–4159. doi: 10.1073/pnas.0813360106

Li, J., Yao, Y., Xu, H. H., Hao, L., Deng, Z., Rajakumar, K., et al. (2015). SecReT6: a web-based resource for type VI secretion systems found in bacteria. *Environ. Microbiol.* 17, 2196–2202. doi: 10.1111/1462-2920.12794

Lien, Y.-W., and Lai, E.-M. (2017). Type VI secretion effectors: methodologies and biology. *Front. Cell. Infect. Microbiol.* 7:254. doi: 10.3389/fcimb.2017.00254

Lu, J., Yu, Y., Zhu, I., Cheng, Y., and Sun, P. D. (2014). Structural mechanism of serum amyloid A-mediated inflammatory amyloidosis. *Proc. Natl Acad. Sci. U.S.A.* 111, 5189–5194. doi: 10.1073/pnas.1322357111

Lüthy, L., Grütter, M. G., and Mittl, P. R. (2004). The crystal structure of helicobacter cysteine-rich protein C at 2.0 Å resolution: similar peptide-binding sites in TPR and SEL1-like repeat proteins. *J. Mol. Biol.* 340, 829–841. doi: 10.1016/j.jmb.2004.04.055

Ma, A. T., and Mekalanos, J. J. (2010). *In vivo* actin cross-linking induced by Vibrio cholerae type VI secretion system is associated with intestinal inflammation. *Proc. Natl. Acad. Sci. U.S.A.* 107, 4365–4370. doi: 10.1073/pnas.0915156107

Ma, J., Pan, Z., Huang, J., Sun, M., Lu, C., and Yao, H. (2017a). The hcp proteins fused with diverse extended-toxin domains represent a novel pattern of antibacterial effectors in type VI secretion systems. *Virulence* 8, 1189–1202. doi: 10.1080/21505594.2017.1279374

Ma, J., Sun, M., Dong, W., Pan, Z., Lu, C., and Yao, H. (2017b). PAAR-Rhs proteins harbor various C-terminal toxins to diversify the antibacterial pathways of type VI secretion systems. *Environ. Microbiol.* 19, 345–360. doi: 10.1111/1462-2920.13621

Ma, J., Sun, M., Pan, Z., Song, W., Lu, C., and Yao, H. (2018). Three hcp homologs with divergent extended loop regions exhibit different functions in avian pathogenic Escherichia coli. *Emerg. Microbes Infect.* 7, 1–13. doi: 10.1038/s41426-018-0042-0

Mahillon, J., Kirkpatrick, H. A., Kijenski, H. L., Bloch, C. A., Rode, C. K., Mayhew, G. F., et al. (1998). Subdivision of the Escherichia coli K-12 genome for sequencing: manipulation and DNA sequence of transposable elements introducing unique restriction sites. *Gene* 223, 47–54. doi: 10.1016/S0378-1119(98)00365-5

Marchler-Bauer, A., Lu, S., Anderson, J. B., Chitsaz, F., Derbyshire, M. K., DeWeese-Scott, C., et al. (2010). CDD: a Conserved Domain Database for the functional annotation of proteins. *Nucleic Acids Res.* 39(Suppl. 1), D225–D229. *doi: 10.1093/nar/gkq1189*

Mittl, P. R., and Schneider-Brachert, W. (2007). Sel1-like repeat proteins in signal transduction. *Cell. Signal.* 19, 20–31. doi: 10.1016/j.cellsig.2006.05.034

Miyata, S. T., Bachmann, V., and Pukatzki, S. (2013). Type VI secretion system regulation as a consequence of evolutionary pressure. *J. Med. Microbiol.* 62, 663–676. doi: 10.1099/jmm.0.053983-0

Navarro-Garcia, F. (2014). Escherichia coli O104:H4 pathogenesis: an enteroaggregative E. *coli/shiga toxin-producing E. coli explosive cocktail of high virulence. Microbiol. Spectr.* 2:1–19. doi: 10.1128/microbiolspec.EHEC-0008-2013

Navarro-Garcia, F., Ruiz-Perez, F., Cataldi, A. A., and Larzabal, M. (2019). Type VI secretion system in pathogenic escherichia coli: structure, role in virulence and acquisition. *Front. Microbiol.* 10:1965. doi: 10.3389/fmicb.2019.01965

Niemi, K., Teiril,ä, L., Lappalainen, J., Rajamäki, K., Baumann, M. H., Öörni, K., et al. (2011). Serum amyloid A activates the NLRP3 inflammasome via P2X7 receptor and a cathepsin B-sensitive pathway. *J. Immunol.* 186, 6119–6128. doi: 10.4049/jimmunol.1002843

Pedemonte, N., and Galietta, L. J. (2014). Structure and function of TMEM16 proteins (anoctamins). *Physiol. Rev.* 94, 419–459. doi: 10.1152/physrev.00039.2011

Perna, N. T., Plunkett, G. 3rd, Burland, V., Mau, B., Glasner, J. D., Rose, D. J., et al. (2001). Genome sequence of enterohaemorrhagic Escherichia coli O157:H7. *Nature* 409, 529–533. doi: 10.1038/35054089

Poole, S. J., Diner, E. J., Aoki, S. K., Braaten, B. A., de Roodenbeke, C., t'K., Low, D. A., et al. (2011). Identification of functional toxin/immunity genes linked to contact-dependent growth inhibition (CDI) and rearrangement hotspot (Rhs) systems. *PLoS Genet.* 7:e1002217. doi: 10.1371/journal.pgen.1002217

Prochazkova, K., Shuvalova, L. A., Minasov, G., Voburka, Z., Anderson, W. F., and Satchell, K. J. (2009). Structural and molecular mechanism for autoprocessing of MARTX toxin of vibrio cholerae at multiple sites. *J. Biol. Chem.* 284, 26557–26568. doi: 10.1074/jbc.M109.025510

Pukatzki, S., Ma, A. T., Revel, A. T., Sturtevant, D., and Mekalanos, J. J. (2007). Type VI secretion system translocates a phage tail spike-like protein into target cells where it cross-links actin. *Proc. Natl. Acad. Sci. U.S.A.* 104, 15508–15513. doi: 10.1073/pnas.0706532104

Riley, L. W., Remis, R. S., Helgerson, S. D., McGee, H. B., Wells, J. G., Davis, B. R., et al. (1983). Hemorrhagic colitis associated with a rare Escherichia coli serotype. *New Engl. J. Med.* 308, 681–685. doi: 10.1056/NEJM198303243081203

Rohde, H., Qin, J., Cui, Y., Li, D., Loman, N. J., Hentschke, M., et al. (2011). Open-source genomic analysis of Shiga-toxin-producing E. coli O104: H4. *New Engl. J. Med.* 365, 718–724. doi: 10.1056/NEJMoa1107643

Sana, T. G., Baumann, C., Merdes, A., Soscia, C., Rattei, T., Hachani, A., et al. (2015). Internalization of Pseudomonas aeruginosa strain PAO1 into epithelial cells is promoted by interaction of a T6SS effector with the microtubule network. *MBio* 6, e00712–00715. doi: 10.1128/mBio.00712-15

Schmidt, M. A. (2010). LEEways: tales of EPEC, ATEC and EHEC. *Cell. Microbiol.* 12, 1544–1552. doi: 10.1111/j.1462-5822.2010.01518.x

Schneider, J. P., Nazarov, S., Adaixo, R., Liuzzo, M., Ringel, P. D., Stahlberg, H., et al. (2019). Diverse roles of TssA-like proteins in the assembly of bacterial type VI secretion systems. *EMBO J.* 38:e100825. doi: 10.15252/embj.2018100825

Schweitzer, A., Aufderheide, A., Rudack, T., Beck, F., Pfeifer, G., Plitzko, J. M., et al. (2016). Structure of the human 26S proteasome at a resolution of 3.9 Å. *Proc. Natl. Acad. Sci. U.S.A.* 113, 7816–7821. doi: 10.1073/pnas.1608050113

Shneider, M. M., Buth, S. A., Ho, B. T., Basler, M., Mekalanos, J. J., and Leiman, P. G. (2013). PAAR-repeat proteins sharpen and diversify the type VI secretion system spike. *Nature* 500, 350–353. doi: 10.1038/nature12453

Shohdy, N., Efe, J. A., Emr, S. D., and Shuman, H. A. (2005). Pathogen effector protein screening in yeast identifies Legionella factors that interfere with membrane trafficking. *Proc. Natl. Acad. Sci. U.S.A.* 102, 4866–4871. doi: 10.1073/pnas.0501315102

Sigrist, C. J., De Castro, E., Cerutti, L., Cuche, B. A., Hulo, N., Bridge, A., et al. (2012). New and continuing developments at PROSITE. *Nucleic Acids Res.* 41, D344–D347. doi: 10.1093/nar/gks1067

Suarez, G., Sierra, J., Erova, T., Sha, J., Horneman, A., and Chopra, A. (2010). A type VI secretion system effector protein, VgrG1, from Aeromonas hydrophila that induces host cell toxicity by ADP ribosylation of actin. *J. Bacteriol.* 192, 155–168. doi: 10.1128/JB.01260-09

Suits, M. D., and Boraston, A. B. (2013). Structure of the streptococcus pneumoniae surface protein and adhesin PfbA. *PloS ONE* 8:e67190. doi: 10.1371/journal.pone.0067190

Szklarczyk, D., Gable, A. L., Lyon, D., Junge, A., Wyder, S., Huerta-Cepas, J., et al. (2019). STRING v11: protein-protein association networks with increased coverage, supporting functional discovery in genome-wide experimental datasets. *Nucleic Acids Res.* 47, D607–D613. doi: 10.1093/nar/gky1131

Tamura, K., and Nei, M. (1993). Estimation of the number of nucleotide substitutions in the control region of mitochondrial DNA in humans and chimpanzees. *Mol. Biol. Evolut.* 10, 512–526.

Tilden Jr, J., Young, W., McNamara, A.-M., Custer, C., Boesel, B., Lambert-Fair, M. A., et al. (1996). A new route of transmission for Escherichia coli: infection from dry fermented salami. *Am. J. Public Health* 86, 1142–1145. doi: 10.2105/AJPH.86.8_Pt_1.1142

Uchida, K., Leiman, P. G., Arisaka, F., and Kanamaru, S. (2013). Structure and properties of the C-terminal β-helical domain of VgrG protein from Escherichia coli O157. *J. Biochem.* 155, 173–182. doi: 10.1093/jb/mvt109

Urosev, D., Ferrer-Navarro, M., Pastorello, I., Cartocci, E., Costenaro, L., Zhulenkovs, D., et al. (2013). Crystal structure of c5321: a protective antigen present in uropathogenic Escherichia coli strains displaying an SLR fold. *BMC Struc. Biol.* 13:19. doi: 10.1186/1472-6807-13-19

Voth, K. A., Chung, I. Y. W., van Straaten, K., Li, L., Boniecki, M. T., and Cygler, M. (2019). The structure of Legionella effector protein LpnE provides insights into its interaction with Oculocerebrorenal syndrome of Lowe (OCRL) protein. *FEBS J.* 286, 710–725. doi: 10.1111/febs.14710

Wan, B., Zhang, Q., Ni, J., Li, S., Wen, D., Li, J., et al. (2017). Type VI secretion system contributes to Enterohemorrhagic Escherichia coli virulence by secreting catalase against host reactive oxygen species (ROS). *PLoS Pathogens* 13:e1006246. doi: 10.1371/journal.ppat.1006246

Whitney, J. C., Beck, C. M., Goo, Y. A., Russell, A. B., Harding, B. N., De Leon, J. A., et al. (2014). Genetically distinct pathways guide effector export through the type VI secretion system. *Mol. Microbiol.* 92, 529–542. doi: 10.1111/mmi.12571

Wong, C. S., Jelacic, S., Habeeb, R. L., Watkins, S. L., and Tarr, P. I. (2000). The risk of the hemolytic-uremic syndrome after antibiotic treatment of Escherichia coli O157: H7 infections. *New Engl. J. Med.* 342, 1930–1936. doi: 10.1056/NEJM200006293422601

Yang, J., and Zhang, Y. (2015). I-TASSER server: new development for protein structure and function predictions. *Nucleic Acids Res.* 43, W174–W181. doi: 10.1093/nar/gkv342

Yang, S.-C., Lin, C.-H., Aljuffali, I. A., and Fang, J.-Y. (2017). Current pathogenic Escherichia coli foodborne outbreak cases and therapy development. *Arch. Microbiol.* 199, 811–825. doi: 10.1007/s00203-017-1393-y

Yang, X., Long, M., and Shen, X. (2018). Effector-immunity pairs provide the T6SS nanomachine its offensive and defensive capabilities. *Molecules* 23:1009. doi: 10.3390/molecules23051009

Yang, X. Y., Li, Z. Q., She, Z., Geng, Z., Xu, J. H., Gao, Z. Q., et al. (2016). Structural analysis of Pseudomonas aeruginosa H3-T6SS immunity proteins. *FEBS Lett.* 590, 2787–2796. doi: 10.1002/1873-3468.12291

Ye, J., Coulouris, G., Zaretskaya, I., Cutcutache, I., Rozen, S., and Madden, T. L. (2012). Primer-BLAST: a tool to design target-specific primers for polymerase chain reaction. *BMC Bioinform.* 13:134. doi: 10.1186/1471-2105-13-134

Zhang, L., Xu, J., Xu, J., Zhang, H., He, L., and Feng, J. (2014). TssB is essential for virulence and required for type VI secretion system in Ralstonia solanacearum. *Microb. Pathogen.* 74, 1–7. doi: 10.1016/j.micpath.2014.06.006

Zhang, Y., Laing, C., Steele, M., Ziebell, K., Johnson, R., Benson, A. K., et al. (2007). Genome evolution in major Escherichia coli O157: H7 lineages. *BMC genomics* 8:121. doi: 10.1186/1471-2164-8-121

Zoued, A., Durand, E., Brunet, Y. R., Spinelli, S., Douzi, B., Guzzo, M., et al. (2016). Priming and polymerization of a bacterial contractile tail structure. *Nature* 531, 59. doi: 10.1038/nature17182

Conflict of Interest: The authors declare that the research was conducted in the absence of any commercial or financial relationships that could be construed as a potential conflict of interest.

frontiers in Cellular and Infection Microbiology

REVIEW
published: 06 May 2020
doi: 10.3389/fcimb.2020.00169

Treatment Strategies for Infections With Shiga Toxin-Producing *Escherichia coli*

Sabrina Mühlen[1,2] *and Petra Dersch*[1,2]*

[1] Institute for Infectiology, University of Münster, Münster, Germany, [2] German Center for Infection Research (DZIF), Associated Site University of Münster, Münster, Germany

Infections with Shiga toxin-producing *Escherichia coli* (STEC) cause outbreaks of severe diarrheal disease in children and the elderly around the world. The severe complications associated with toxin production and release range from bloody diarrhea and hemorrhagic colitis to hemolytic-uremic syndrome, kidney failure, and neurological issues. As the use of antibiotics for treatment of the infection has long been controversial due to reports that antibiotics may increase the production of Shiga toxin, the recommended therapy today is mainly supportive. In recent years, a variety of alternative treatment approaches such as monoclonal antibodies or antisera directed against Shiga toxin, toxin receptor analogs, and several vaccination strategies have been developed and evaluated *in vitro* and in animal models. A few strategies have progressed to the clinical trial phase. Here, we review the current understanding of and the progress made in the development of treatment options against STEC infections and discuss their potential.

Keywords: STEC, Shiga toxin, antibiotics, antibodies, vaccines

OPEN ACCESS

Edited by:
Tânia Aparecida Tardelli Gomes, Federal University of São Paulo, Brazil

Reviewed by:
Marina Sandra Palermo, Consejo Nacional de Investigaciones Científicas y Técnicas (CONICET), Argentina
Vernon L. Tesh, Texas A&M University, United States

***Correspondence:**
Petra Dersch
petra.dersch@uni-muenster.de

Specialty section:
This article was submitted to Bacteria and Host, a section of the journal Frontiers in Cellular and Infection Microbiology

Received: *10 February 2020*
Accepted: *31 March 2020*
Published: *06 May 2020*

Citation:
Mühlen S and Dersch P (2020) Treatment Strategies for Infections With Shiga Toxin-Producing Escherichia coli. Front. Cell. Infect. Microbiol. 10:169. doi: 10.3389/fcimb.2020.00169

INTRODUCTION

Shiga-toxin producing (enterohemorrhagic) *Escherichia coli* (STEC/EHEC) are a major cause of severe gastrointestinal disease in industrialized countries and a major public health problem with most frequent and severe infections linked to serotype O157:H7 (Kaper and O'Brien, 2014). The bacteria are commonly transmitted through ingestion of contaminated food such as undercooked meat, particularly beef products, cross-contaminated raw vegetables, sprouts, and seeds (Caprioli et al., 2014).

The resulting disease ranges in intensity from watery diarrhea or hemorrhagic colitis to the life-threatening hemolytic uremic syndrome (HUS) leading to kidney failure and neurological episodes (Nataro and Kaper, 1998). Upon ingestion, EHEC resides in the intestinal tract and adheres to the gut epithelium of the distal ileum and colon. Initial binding is promoted by fimbriae, which, in EHEC infections (e.g., by EHEC O157:H7, O126, O103, O45, O111, O121, O145), is followed by the injection of effector proteins (Esp proteins) via a filamentous type III secretion system (T3SS) (Donnenberg and Kaper, 1992; Garmendia et al., 2005; Gaytan et al., 2016). Injection of the translocated intimin receptor (Tir), which integrates into the host cell plasma membrane and interacts with the bacterial outer membrane protein intimin, initiates bacterial attachment to the host cell and effacement of the brush border microvilli. The interaction between intimin and Tir leads to intimate attachment of the bacteria and initiates actin polymerization and subsequent formation of attaching and effacing (A/E) lesions (Kenny et al., 1997). The genes encoding Tir,

intimin, and the T3SS are localized on the chromosomal "locus of enterocyte effacement" (LEE) pathogenicity island. Notably, this island is missing from LEE-negative STEC and from the unusual HUS-inducing *E. coli* strain EAHEC of serotype O104:H4, which is responsible for the major outbreak in Germany and parts of Europe in 2011. This latter strain is similar to enteroaggregative *E. coli* (EAEC) (Bielaszewska et al., 2011; Mellmann et al., 2011).

While the HUS-inducing strains belong to a variety of *E. coli* pathovars, their main discerning trait is the production of at least one of two genetically distinct Shiga toxins, named Stx1 and Stx2. Four subtypes of Stx1 (Stx1a, Stx1c, Stx1d, Stx1e) and seven subtypes of Stx2 (Stx2a-g) have been identified, of which especially the Stx2 variants Stx2a and Stx2c are commonly associated with HUS development in humans (Melton-Celsa, 2014). Both types of Shiga toxins are AB_5 toxins that bind to the glycosphingolipids globotriaosylceramide (Gb3, CD77) and, to a lesser extent, globotetraosylceramide (Gb4) (Legros et al., 2018), which are found on a variety of human cells, such as glomerular and brain endothelial cells. The Stx toxins result in the arrest of protein translation and, ultimately, cell death (Melton-Celsa, 2014). The systemic consequences of intoxication are vascular dysfunction and thrombus formation, which lead to HUS. The genes encoding for Stx are located in the late region of a lambdoid phage, which adds additional complications to treatment options. As several antibiotics, especially those belonging to the quinolone family were shown to be potent inducers of the bacterial SOS response, which initiates the production and release of phages from the bacteria, treatment of STEC infections with antibiotics is generally not advised (Kakoullis et al., 2019). To date, there are no protective measures or therapies against STEC infections. Current treatment of STEC infections is solely supportive and includes rehydration therapy, and, where necessary, dialysis. However, over the past years, new therapeutic approaches and novel, promising strategies to manage the infection and the ensuing disease have been developed. These are outlined in this review.

ANTIBODY THERAPY

Stx-Targeted Antibodies

Antibodies are valuable therapeutics. As Stx-specific antibodies can completely neutralize the cytotoxicity of the toxin in cell culture and protect animals from developing Stx-induced symptoms when administered shortly after infection (Cheng et al., 2013), effective Stx-targeting antibodies are a suitable option for human therapy (**Figure 1A**).

Mohawk et al. (2010) investigated the ability of polyclonal Stx2-neutralizing antibodies from rabbits to protect mice from lethal infection with the Stx2a-producing *E. coli* O157:H7 strain 86-24. The administration of the rabbit serum did not reduce the initial colonization of mice with EHEC 86-24, but it decreased the bacterial burden after 3–5 days and increased animal survival.

Bovine colostrum preparations harboring high titers of Stx1 and Stx2 antibodies were used to treat mice infected with *E. coli* O157:H7. This efficiently inhibited bacterial attachment, colonization, and growth (Funatogawa et al., 2002). Although the frequency of stool excretion was reduced, the presence of the bacterial toxin was not notably affected (Kuribayashi et al., 2006; Seita et al., 2013). Furthermore, colostral IgG against Shiga toxin and bovine lactoferrin completely prevented lethality of *E. coli* O157:H7 in a weaned mouse model (Albanese et al., 2018). In addition, an early study in children showed that bovine colostrum is well-tolerated, reduced the frequency of loose stools, and eliminated bacterial infection (Huppertz et al., 1999).

Another interesting concept for this strategy is the production of recombinant antibodies or even secretory antibodies specific for Stx by transgenic plants (e.g., thale grass—*Arabidopsis thaliana*) (Nakanishi et al., 2013, 2017), a concept that may be transferred to other plants, providing the possibility of an edible therapy.

Promising tools are also Stx-targeting humanized antibodies. Humanized antibodies were established by an exchange of the regions within the antigen-binding variable domains, which react with the antigen of the human IgG molecule with equivalent regions of the murine Stx-specific Mab (Nakao et al., 1999) to produce TMA-15 (Urtoxazumab) (Yamagami et al., 2001; Kimura et al., 2002). TMA-15 was shown to protect mice from a lethal challenge with STEC if given within 24 h of infection (Yamagami et al., 2001), while it was also able to reduce brain lesions and death in a gnotobiotic piglet model (Moxley et al., 2017). When tested in healthy adults or pediatric patients with a confirmed STEC infection, intravenous application of TMA-15 (Urtoxazumab) was found to be well-tolerated and safe (Lopez et al., 2010).

Chimeric murine-human MAbs (cαStx1/cαStx2) comprising the variable regions of the murine Stx1 (B-subunit) or Stx2 (A-subunit)-neutralizing antibodies 13C4 and 11E10 (Strockbine et al., 1985; Perera et al., 1988) fused to the light chain of human IgG1 were found to neutralize Stxs in mice (Bitzan et al., 2009). In addition, they were well–tolerated in healthy human volunteers when given as a single dose either separate or in combination (Dowling et al., 2005; Bitzan et al., 2009). Unfortunately, the efficacies of hybrid antibodies were often found to be lower compared to the murine parent antibodies (Tzipori et al., 2004). Another concern of chimeric MAbs is that they still retain murine IgG elements that could trigger antibody formation by treated patients. With this in mind, HuMAbs have been engineered, which encode the human heavy- and light-chain IgG genes, leading to the formation of human antibodies in response to immunization with an antigen, e.g., Stx1 or Stx2 [e.g., 5A4 (Stx1) and 5C12 (Stx2)] (Mukherjee et al., 2002a,b; Sheoran et al., 2005). These resulted in prolonged survival of mice in a Stx1 toxicosis model (Mukherjee et al., 2002b) and higher survival of gnotobiotic piglets when treated 48 h after challenge with an Stx2a-producing STEC strain (Sheoran et al., 2005). Interestingly, when piglets were infected with an Stx1- and Stx2-producing strain, only administration of 5C12 (αStx2) was protective (Jeong et al., 2010).

Another promising approach used hetero-multimeric camelid toxin-neutralizing agents containing two linked heavy-chain-only antibody V_H domains that neutralize Stx1 or Stx2 co-administered with an antitag MAb—an "effector Ab"—that indirectly decorates each toxin with four Ab molecules in cell-based and *in vivo* mouse models (Tremblay et al., 2013). The

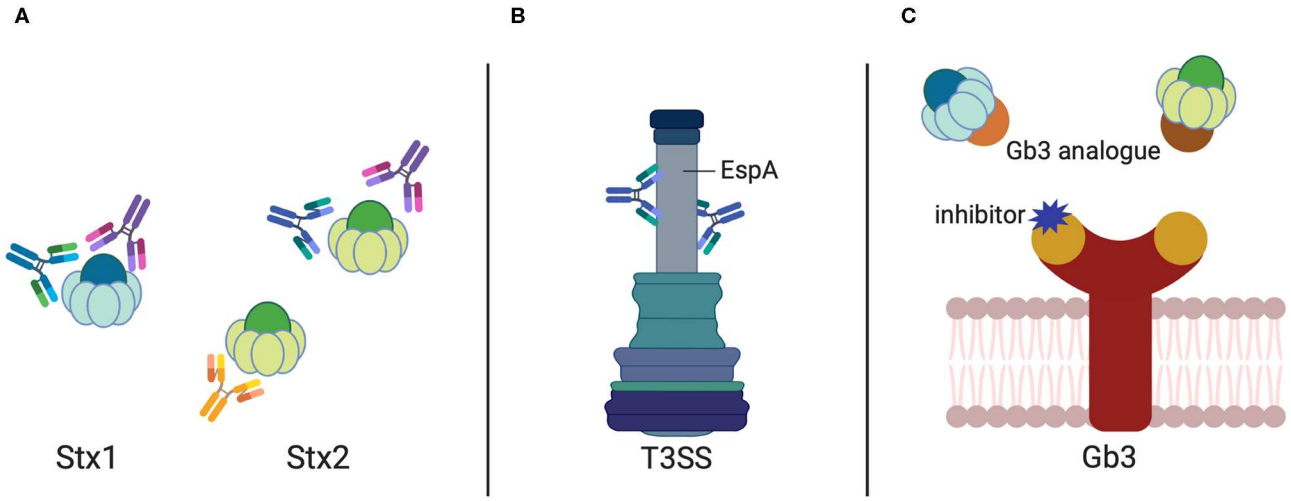

FIGURE 1 | Antibodies and Gb3 analogs against STEC-induced diseases. Antibody targets in STEC treatment include **(A)** the Shiga toxins (Stx1 and Stx2) and **(B)** the sheath component EspA of the *E. coli* Type-3-Secretion System. **(C)** Analogs to the Stx receptor Gb3 harboring the Stx binding domains (given in brown and orange) sequestering Stx1 and Stx2. Inhibitors blocking the Stx binding site of the Gb3 receptor are illustrated in purple.

effector antibody binds to multiple epitope tags engineered into the VHH-based toxin-neutralizing agent. When the toxin-neutralizing agent interacts with separate sites of the Stx toxins, and each, in turn, binds to two or more effector Abs through the tags, the Stxs become decorated with sufficient Abs to prevent all symptoms of Stx1 and Stx2 intoxication and protect mice from Stx lethality (Tremblay et al., 2013). Moreover, camelid antibodies, which are special as they only contain heavy chains, have been produced that target the Stx2 B-subunit. These antibodies decreased Shiga toxicity when injected into mice and were proposed as an alternative treatment for HUS sequelae (Mejias et al., 2016). Moreover, Luz et al. have produced recombinant antibody fragments that specifically bind to and neutralize Stx2 *in vitro* (Luz et al., 2015). They further showed that mice were protected from challenge with a lethal dose of Stx2 after pre-incubation of the toxin with the antibody fragment FabC11:Stx2 (Luz et al., 2018).

A combined antibody–antibiotic (e.g., tigecycline) treatment scheme that was found to eliminate the toxicity from STEC (Skinner et al., 2015) may help to eliminate bacteria in addition to inhibiting Shiga-toxin mediated disease, decreasing the probability of transmission to others due to continued bacterial carriage and excretion.

Evaluation of the different antibody therapies against HUS, mostly in piglets and mice, showed that they mainly differ in their protective efficacy and/or their specificity to Stx variants, whereby the A-subunit specific antibodies were better neutralizers than their B-subunit specific counterparts (Tzipori et al., 2004). A very critical point for passive immunization with Stx antibodies that has to be considered for successful therapy is the time point and dosage of antibody administration. Studies using piglets or mice demonstrated that administration of the Stx2-specific HuAbs 5C12 or TMA-15 protected the animals 48 or 24 h after infection, respectively. However, when TMA-15 was used as treatment 48 h after infection, no protection was observed (Yamagami et al., 2001). This indicated that infected patients might be protected against the development of HUS when the antibodies are given shortly after the onset of diarrhea (Orth et al., 2008). However, as mice and piglets do not develop either bloody diarrhea or HUS, results describing a protective effect of Stx-specific antibodies cannot easily be transferred to humans. Moreover, knowledge about the time when the Stxs enter the bloodstream and the Stx levels in the blood and infected tissues is scarce.

Effector- or Intimin-Targeted Antibodies

The *E. coli* secreted effector protein EspA forms the filamentous sheath of the T3SS, which aids in the transportation of the bacterial effectors into the host cells and elicits a protective immune response. A MAb (1H10) was identified to recognize the linear, conserved, and protective epitope Lys100-Val120 on the surface of EspA (Yu et al., 2011) (**Figure 1B**). This EspA-specific MAb was shown to inhibit EHEC-induced actin polymerization *in vitro* and conferred protection against EHEC, e.g., reduced their colonization efficiency in mice (Yu et al., 2011), which could be exploited for the development of epitope-based vaccine and MAb-based therapy. In addition, a camelid single-domain antibody (nanobody), TD4, which specifically recognized the Tir domain overlapping with the binding site of the adhesin intimin, was able to inhibit EHEC attachment and intimin-induced clustering of Tir, and reduced the colonization of EHEC on the human colonic mucosa (Ruano-Gallego et al., 2019).

HuMAb Against Complement Component 5 (C5): Eculizumab

Eculizumab is a recombinantly produced HuMAb against the complement component 5 (C5). Binding of the antibody to C5 results in the inhibition of complement activation. Originally not devised for the treatment of STEC-induced HUS,

Eculizumab was initially trialed in patients with severe STEC-HUS during the outbreak in northern Europe in 2011, as Shiga toxin had been shown to mediate complement activation (Orth et al., 2009; Morigi et al., 2011; Noris et al., 2012; Karpman and Tati, 2016) reviewed in Buelli et al. (2019), which, in turn, negatively affects renal health. Unfortunately, the results obtained for the use of Eculizumab in STEC-HUS were inconsistent. While most studies reported no benefit on renal and extrarenal outcomes (Kielstein et al., 2012; Loos et al., 2012, 2017; Menne et al., 2012), other publications reported a beneficial effect of Eculizumab treatment in pediatric cases (Lapeyraque et al., 2011) or fewer severely infected patients (Delmas et al., 2014). This indicated that the early use of Eculizumab in children with HUS may be beneficial. However, a more recent study evaluating the short and intermediate outcome of Eculizumab treatment, including 18 children with STEC-HUS in a single-center matched cohort study did not reveal a benefit of Eculizumab on renal and extrarenal outcomes (Monet-Didailler et al., 2019). It has been discussed that the delay between HUS diagnosis and Eculizumab administration could affect patient recovery (Keenswijk et al., 2017). It was also suggested that Eculizumab might improve potential neurological outcomes (Pape et al., 2015; Monet-Didailler et al., 2019).

TOXIN RECEPTOR ANALOGS

The Stxs, once released from the bacterial cell, spread through the body and target cells (Lingwood et al., 1987), which express the Gb3 receptor on their cell surface, such as renal glomerular and brain endothelial cells. Binding of Stxs to the Gb3 receptors is based on the multivalent interaction of the five B-subunits with the trisaccharide moiety of Gb3. Therefore, interfering with receptor binding by using receptor analogs to probe for free toxin in the gut or the circulation is a promising approach to reduce Stx-mediated disease. Over the last decade or so, a variety of strategies have been employed to produce (i) inhibitors of the Stx receptor Gb3 to prevent Stx binding and uptake, and (ii) Stx-neutralizing Gb3 analogs (Macconnachie and Todd, 2004; Serna and Boedeker, 2008; Rahal et al., 2015; Kavaliauskiene et al., 2017) (**Figure 1C**).

SYNSORB Pk

Synsorb Pk was one of the first and certainly a promising Stx receptor analog. It consists of silicon dioxide particles (diatomaceous earth) with covalently linked trisaccharides that functioned as an orally administered Stx adsorbent. SYNSORB Pk was tested in a large multicenter trial including 145 children diagnosed with STEC-induced HUS (Trachtman et al., 2003). Unfortunately, however, no treatment benefit could be observed. There were no significant differences in the number of deaths or incidence of extrarenal complications and no reduction in the need for dialysis was observed. Likely reasons for the observed failure are that (i) the agent was administered too late, (ii) the Stx toxins are mostly cell-associated and not free-floating, and (iii) the Stx binding capacity of monomeric SYNSORB Pk is substantially lower than that of Gb3 polymers.

Starfish and Daisy

Starfish is an oligovalent, water-soluble carbohydrate ligand with a sub-nanomolar inhibitory activity designed based on the crystal structure of the Stx1 B-subunit (Kitov et al., 2000). The *in vitro* inhibitory activity is very high as the two trisaccharide receptors at the tip of a 5-spacer arm engage all five Stx1 B-subunits. Daisy is a Gb3 analog (αGal(1,4)βGal) from the same group that developed Starfish, which was shown to protect mice from Stx1- and Stx2-mediated disease by subcutaneous administration (Mulvey et al., 2003).

SUPER TWIG (1) and (2)

Nishikawa and colleagues (Nishikawa et al., 2002, 2005) designed a series of carbosilane dendrimers carrying various numbers of terminal Gb3 moieties to bind Shiga toxin in the bloodstream before it reaches target cells expressing the receptor. The SUPER TWIG Gb3 analogs bound Stx1 and Stx2 with high affinity, prevented Stx uptake into host cells, induced phagocytosis of Stx by macrophages, and protected mice from a fatal challenge with EHEC.

Acrylamide Polymers With Gb3 Trisaccharides

Watanabe et al. (2004) constructed acrylamide polymers of Gb3 as toxin absorbent in the gut that bound both Stx1 and Stx2 with a very high affinity [e.g., it interacted with a higher affinity to the Stx B subunit than SUPER TWIG (1)]. They further showed that the oral administration of these polymers was able to protect mice that had been orally challenged with a fatal dose of STEC, whereby the toxin content in serum samples in the treated infected mice was significantly reduced. This protection was observed even if the polymers were administered after colonization.

Phage-Display Generated Stx-Neutralizing Peptides

Three peptides that bind to Gb3 receptor have been developed using phage-display (PC7-2, P12-26, and PC7-30). They efficiently competed with the Stx for binding and inhibited Stx-triggered cell toxicity. Peptide PC7-30 further inhibited Stx1-induced lethality in EHEC-infected animals, indicating that this peptide might be useful to prevent STEC-triggered diseases such as HUS (Bernedo-Navarro et al., 2014).

Bacteria Expressing Gb3 Analogs

In addition to previous attempts, *E. coli* strains and probiotics can be engineered to express Gb3 receptor mimics on their surface (Paton et al., 2000; Asahara et al., 2004; Hostetter et al., 2014). They absorb and neutralize Stx1, Stx2, Stx2c, and Stx2d *in vitro* and oral administration of Gb3 analog-expressing bacteria protected mice from fatal challenge with different highly virulent STEC strains.

Nanoparticles Displaying Stx Ligands

Kulkarni et al. (2010) established glycan-encapsulated gold nanoparticles that allowed multivalent display of glycans, e.g., the glycan Pk trisaccharide, which preferentially interacts with Stx.

The coated nanoparticles neutralized Stx1 and Stx2, but not all variants in a Vero cell toxicity assay.

Gb3 Inhibitors

Inhibitors that interfere with the synthesis of the Stx receptor Gb3 are also attractive targets. The agent C-9 is a specific inhibitor of glucosylceramide synthase that downregulates the expression of Gb3, limiting the amount of receptor displayed on the surface of cells (Silberstein et al., 2011). C-9 addition to human kidney cells in a tissue culture model decreased Stx2-mediated tissue damage. Furthermore, administration of C-9 in a rat model decreased mortality by about 50% and significantly diminished toxin-mediated tubular necrosis and damage to goblet cells. In addition, PDMP, a ceramide analog shown to inhibit the synthesis of GlcCer and affect the composition of glycosphingolipids, reduced Stx binding and uptake and blocked initial transport of the toxin into the Golgi apparatus (Raa et al., 2009). It was also discovered that the glucose analog 2-fluoro-2-deoxy-D-glucose (FDG) reduced cellular uptake of Gb3 levels by 50%, likely by inhibiting precursor formation of Gb3 synthesis, and resulted in a decrease in Stx binding (Kavaliauskiene et al., 2015, 2016).

Intracellular Interference With Shiga Toxins

Not only Stx binding and uptake, but also its intracellular targeting from early endosomes to the Golgi apparatus and the endoplasmic reticulum (ER) can be inhibited by certain cell-permeable agents. One such substance is chloroquine, a weak base that can diffuse across membranes and accumulate in acidic compartments. Chloroquine treatment protected HEp-2 cells from Stx-mediated cytotoxicity, most likely by interfering with the translocation of the StxA subunit into the cytosol (Dyve Lingelem et al., 2012; Kavaliauskiene et al., 2017). The Retro-1 and−2 substances were shown to inhibit the retrograde transport of Stx1B from the endosomes to the Golgi apparatus, and it has been assumed that this could be mediated by the relocalization of the SNARE proteins syntaxin 5 and 6 (Noel et al., 2013; Kavaliauskiene et al., 2017). Later, it has been shown by Secher et al. (2015) that Retro-2 was able to protect mice against the toxic effects of Stx. Recently, a drug delivery system using Retro-2-loaded nanoglobules has been developed, which increased the solubility of the inhibitor and might enable a more successful therapeutic approach inhibiting the transport of Stx (Gandhi et al., 2019). Moreover, two other substances, Ac-PPP-tet and TVP, which also interfere with intracellular Stx trafficking, have been tested in animal models and were found to successfully prevent Stx2 intoxication (Watanabe-Takahashi et al., 2010; Stearns-Kurosawa et al., 2011).

VACCINATION STRATEGIES

Toxin-Based Vaccines

Stx is the main virulence factor associated with the potency of STEC-mediated disease pathology. It is released from the bacterial cell and exposed to the host immune system and has, therefore, long been considered one of the most prudent targets for vaccine strategy. Once released from the bacterial cell, Stx can be detected in the intestinal lumen and its target cells in the kidney and brain (Clements et al., 2012). Hence, immune cells primed to recognize Stx by prior vaccination can interfere and respond to the toxin as it travels from the site of release to the distal organs and eliminate it before it reaches its targets (**Figure 2A**). Of Stx1, Stx2, and the different varieties of each of these subtypes, Stx2 has been at the center of a greater number of vaccination approaches as it is commonly associated with more severe disease outcomes in humans, such as the development of HUS. Several vaccination strategies have been developed and tested that are solely toxin-based. With the active site of Stx known, inactive derivatives of the toxin are easy to make, and present safe alternatives for application. Several different studies showed that vaccination of animals with purified inactive Stx derivatives induced the production of neutralizing antibodies against the respective toxin and protected the animals from toxemia or limited shedding or disease after challenge (Gordon et al., 1992; Acheson et al., 1996; Konadu et al., 1999; Marcato et al., 2001, 2005; Ishikawa et al., 2003; Kerner et al., 2015; Schmidt et al., 2018). In addition to vaccines based on the inactive toxin, hybrid subunit vaccine approaches have been tested as the development of a vaccine, which may induce neutralizing antibodies against not only one but both types of Stx, would be ideal.

Vaccination with a hybrid toxin consisting of an inactive Stx2 A-subunit fused to the native Stx1 B-subunit was able to produce neutralizing antibodies against both Stx1 and Stx2. Mice immunized with this toxin were protected from subsequent lethal challenge with either Stx1 or Stx2, or both toxins (Smith et al., 2006).

Injection with a purified fusion protein consisting of the B-subunits of Stx subtypes 1 and 2 (Stx2B-Stx1B; short 2S) generated neutralizing antibodies against both Stxs and increased survival of mice after a challenge with *E. coli* O157:H7 lysates (Gao et al., 2009). Interestingly, the protective effects of the vaccine were stronger with the Stx2B-Stx1B-subunit fusion than when separate B-subunits were used for immunization (Gao et al., 2009).

Moreover, a fusion protein comprising the B-subunit of Stx1 and the inactive A-subunit of Stx2 (Stx2Am-Stx1) was constructed. Immunization with this protein resulted in a strong induction of neutralizing antibodies against both types of Shiga toxin and increased the survival rate of mice after challenge with *E. coli* O157:H7 lysates (Cai et al., 2011). A vector-based DNA vaccine encoding the C-terminal 32 amino acids of the Stx2 A-subunit and the complete B subunit (pStx2ΔAB) also produced neutralizing antibodies against both Stx2 subunits. It further decreased the mortality of mice after lethal challenge with Stx2 (Bentancor et al., 2009).

Intranasal immunization with the Stx2 B-subunit in combination with a mutant of heat-labile toxin induced neutralizing antibodies against both Stx1 and Stx2 *in vivo* and protected mice against fatal disease. Interestingly, immunization of mice with the B-subunit of Stx1 only protected against subsequent challenge with Stx1 (Tsuji et al., 2008). A fusion of the Stx B-subunit to the B-subunit of heat-labile toxin has also been assessed for toxin subtype 2e. Here, the ability of the fusion protein to induce neutralizing antibody production was much

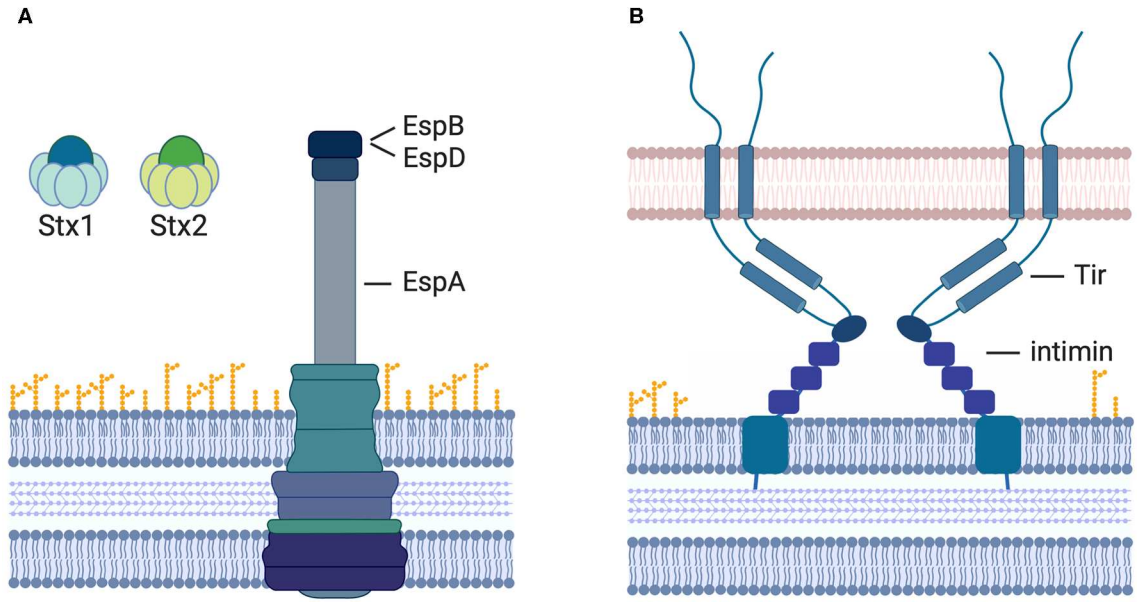

FIGURE 2 | Vaccination strategies to prevent STEC-induced diseases. Currently assessed vaccine targets include **(A)** the A-and B-subunits of Stx1 and Stx2, the T3SS components EspA (sheath) and EspB (pore complex), as well as **(B)** the bacterial outer membrane protein intimin and its T3-translocated receptor Tir.

higher than for the Stx2 B-subunit alone. Furthermore, mice that had been immunized with the Stx2eB-LTB fusion protein were protected against challenge with a lethal dose of toxin (Ran et al., 2008).

In another study, the B subunit of Stx2 was fused with *Brucella* lumazine synthase, a protein that forms a dimer of pentamers thereby creating a scaffold for the presentation of the Stx. The resulting fusion protein induced a lasting immune response in mice after three vaccinations and vaccinated mice were protected from intravenous challenge with Stx2. Furthermore, antibodies isolated from vaccinated mice neutralized Stx2 as well as its variants. In addition, weaned mice inoculated with the immune sera were protected against oral infection with EHEC (Mejias et al., 2013).

Vaccine Approaches Based on LEE-Encoded Proteins

While Stx is produced by all strains that are classed as STEC, only some STEC strains encode the locus of enterocyte effacement pathogenicity island (LEE), which encodes for the T3SS. Therefore, the use of T3-secreted proteins in vaccine approaches is valid but limits the specificity of the vaccines to LEE-positive STEC strains. As the most common EHEC strains including those of the O157:H7 serotype are LEE-positive, the T3-S protein-based approaches will target many of the most common serotypes. However, they do not affect other pathotypes such as the O104:H4 strain, which caused the outbreak in Germany in 2011.

Only a few of the T3-secreted proteins can be used as targets for vaccination strategies, however, as most are translocated from the bacterial cell directly into the host cell cytoplasm and are never exposed to the surrounding environment. A few proteins including EspA, EspB (**Figure 2A**), Tir, and intimin (**Figure 2B**) are exposed on the outside of the cell at times as antibodies to these proteins are detectable in humans after an EHEC infection (Li et al., 2000; Asper et al., 2011). These proteins have been assessed as targets for vaccination strategies. The translocated intimin receptor (Tir) inserts into the host cell membrane upon translocation. Its surface-exposed receptor domain then interacts with the bacterial outer membrane protein intimin to induce intimate attachment of the bacteria to the host cell surface.

Furthermore, protein components of the T3 secretion system such as the sheath protein EspA, as well as EspB and EspD, the proteins required for forming a pore in the host cell membrane, have also been assessed for their immunogenicity (Loureiro et al., 1998; Martinez et al., 1999; Asper et al., 2011; Guirro et al., 2013). Most T3-secreted protein-based vaccines have been assessed using the intranasal immunization route. This vaccination approach promises a needle-free application and has, so far, yielded promising results.

Subcutaneous and intranasal immunization of mice with T3-secreted proteins showed that while subcutaneous injection was unable to raise an immune response, intranasal vaccination induced the production of anti-Tir and EspA antibodies. This reduced *E. coli* O157:H7 shedding after infection (Babiuk et al., 2008). Subcutaneous and intranasal immunization with purified Tir showed similar results. Mice immunized intranasally produced neutralizing antibodies, which resulted in reduced fecal shedding of *E. coli* O157:H7 after infection and increased animal survival (Fan et al., 2012). Intranasal immunization of mice with a purified fusion protein consisting of EspB and the C-terminus

of intimin induced neutralizing antibodies against both EspB and intimin and antisera of immunized mice had promising anti-hemolytic effects *in vitro* (Cataldi et al., 2008).

A recombinant fusion protein of EspA, intimin, and Tir (EIT) was created and used for immunization of mice. Subcutaneous or oral immunization of mice with the EIT protein resulted in a significant decrease of bacterial colonization and shedding after challenge with EHEC O157:H7 and an increase in anti-EIT IgG and IgA (Amani et al., 2010). In a follow-up study, rEIT was linked to chitosan and used for either intranasal electrospray (Doavi et al., 2016) or oral (Khanifar et al., 2019a) immunization of mice. Intranasal and oral administration both induced specific immune responses and reduced bacterial shedding after challenge with *E. coli* O157:H7 (Doavi et al., 2016). Oral administration additionally helped protect mice against *E. coli* O157 challenge and reduced damage (Khanifar et al., 2019a). An additional approach was made by encapsulating EIT together with the B-subunit of Stx2 (Khanifar et al., 2019b). Mice were subcutaneously or orally immunized and either infected with *E. coli* O157:H7 or challenged with a fatal dose of Stx2. While the former mice showed reduced colonization and bacterial shedding, the latter showed increased survival (Khanifar et al., 2019b). A shortened variant of the EIT fusion protein consisting of only EspA and intimin (EI) was recombinantly expressed and its immunogenicity was assessed after subcutaneous injection with two subcutaneous boosters and a third booster that was administered i.p. (Rad et al., 2013). This fusion protein, too, induced an immune response and decreased bacterial shedding and histopathological changes in the intestine after challenge (Rad et al., 2013).

In addition, the immunogenicity and protective efficacy of a DNA vaccine against a truncated version of the EHEC factor for adherence-1 (Efa-1'; the homolog of LifA in EPEC and *C. rodentium*) was evaluated in mice. Intranasal immunization with plasmid DNA induced efa-1-specific immune responses and protected mice from subsequent challenge with *E. coli* O157:H7 (Riquelme-Neira et al., 2015).

Peptide-based approaches to vaccination include the KT-12 peptide, which is based on a predicted B-cell epitope of intimin conjugated to adjuvant (Wan et al., 2011) and the synthetic peptides CoilA and CoilB, which interact with EspA (Larzabal et al., 2013). KT-12, when used for intranasal immunization, induced the production of neutralizing antibodies and protected mice from challenge with *E. coli* O157:H7 (Wan et al., 2011). Immunization of mice with CoilA and CoilB was shown to block intestinal damage in mice infected with *C. rodentium* (Larzabal et al., 2013).

A fusion of EspA, the C-terminus of intimin and the B-subunit of Stx2 (EIS), was constructed and assessed for its ability to induce the production of neutralizing antibodies. Indeed, antibodies against all three components of the fusion protein were detected, and immunized mice were protected from challenge with *E. coli* O157:H7 or lysates thereof (Gu et al., 2009). Fusion of the processed, active form of the Stx2A-subunit (Stx2A1) to the N-terminus of EspA induced the production of neutralizing antibodies in immunized mice (Cheng et al., 2009) and a fusion of the B-subunits of Stx1, Stx2, to a truncated version of intimin resulted in increased immune responses and protection of mice after a fatal challenge with *E. coli* O157:H7 (Gao et al., 2011).

Intranasal immunization with a novel EspA-Tir fusion protein (EspA-Tir-M; designating that the middle domain of Tir was used) showed high levels of neutralizing antibodies while subcutaneous vaccination had little effect. Additionally, intranasal immunization increased the survival of mice from subsequent challenge with *E. coli* O157:H7 and reduced organ damage (Lin et al., 2017b).

BACTERIA-BASED VACCINES

Attenuated or Vaccine Strains

Several vaccination approaches use non-pathogenic bacteria or bacterial vaccine strains as delivery vehicles and to increase immunogenicity. These approaches include genetically modified EHEC, EPEC, and *Salmonella* strains as well as probiotic strains such as *Lactococcus lactis* and *Lactobacillus acidophilus*.

A non-pathogenic variant of the EHEC O157:H7 86-24 strain was created by deletion of both the gene encoding the transcriptional regulator of the LEE (*ler*) and the *stx* gene. These deletions completely abolished cytotoxicity *in vitro* when compared to EHEC EDL933. A derivative of this strain that expresses the inactive forms of Stx1 and Stx2 from a plasmid also showed highly diminished cytotoxicity *in vitro*. Injection with either *stx/ler* deletion mutant or the respective Stx1/Stx2-expressing strain reduced the colonization of *E. coli* O157:H7 after infection of mice. Furthermore, if mice were immunized when pregnant, they passed the immunity on to their offspring, which were protected against *E. coli* O157:H7 infection (Liu et al., 2009).

Enteropathogenic *E. coli* (EPEC) also presents a vaccine alternative for EHEC as it is less pathogenic and shares the LEE pathogenicity island-encoded virulence genes. Immunization with EPEC raised neutralizing antibodies against EspB and intimin and conferred some protection against an EHEC infection. Vaccinated mice showed only mild disease phenotypes such as slight intestinal damage, while no kidney pathology could be detected (Calderon Toledo et al., 2011).

Immunization of mice with a *Salmonella* Typhimurium vaccine strain expressing an inactive Stx2 variant consisting of the A2- and B-subunit of Stx2 (Stx2ΔAB) resulted in efficient colonization of the Peyer's patches and production of neutralizing antibodies. Serum collected from immunized mice was able to neutralize Stx2-mediated toxicity *in vitro*. However, there was only minimal protection observed when mice were challenged with a lethal dose of Stx2, and no protective effect was seen for kidney health (Rojas et al., 2010).

Additionally, another group constructed a *Salmonella* Typhimurium strain expressing intimin, which was used to immunize mice orally (Oliveira et al., 2012). This immunization resulted in a significant increase in the levels of serum IgG and fecal IgA and reduced fecal shedding after an *E. coli* O157:H7 infection (Oliveira et al., 2012). A boost vaccination 2 weeks after the initial immunization led to continuously high colonization levels of the vaccine strain and dissemination into the underlying tissues such as Peyer's patches and spleen (Oliveira et al.,

2012). Oral immunization of mice with attenuated *Salmonella* expressing a hybrid protein consisting of EspA in combination with the C-terminus of intimin and the Stx2 B-subunit (EIS, also see above) raised neutralizing antibodies against the respective proteins and protected mice from a lethal challenge with EHEC for more than 70 days. This period could be extended by a subcutaneous boost with purified EIS (Gu et al., 2011).

Inoculation of mice with a recombinant *Mycobacterium bovis* BCG (rBCG) vaccine, which was modified to express the Stx2 B-subunit, induced the production of neutralizing antibodies against Stx2. Two high-dose intraperitoneal immunizations resulted in decreased colonization and increased survival after fatal challenge with a STEC strain (Fujii et al., 2012).

The probiotic lactic acid bacterium *Lactococcus lactis* is considered a safe vaccine vehicle. Use of a *L. lactis* strain expressing the Stx2 A1-subunit (the A-subunit missing the 15 C-terminal amino acids) for the immunization of mice resulted in increased levels of fecal and serum IgA. Immunized animals had significantly reduced intestinal and kidney damage. Furthermore, immunized mice showed increased survival after challenge with a lethal dose of Shiga toxin isolated from either *E. coli* O157:H7 or *Shigella dysenteriae* (Sreerohini et al., 2019).

L. lactis expressing the T3-secreted protein EspB did not yield neutralizing antibodies when used to infect mice. After an i.p. boost with recombinant EspB, however, specific IgG and IgA levels increased (Ahmed et al., 2013). In a follow-up study, the *L. lactis* was modified to secrete EspB after expression, which resulted in an increased production of neutralizing antibodies. Also, mice immunized with this version of the EspB-expressing *L. lactis* were protected against *E. coli* O157:H7 colonization (Ahmed et al., 2014). An *L. lactis* strain expressing the EspA protein has also been designed. However, this strain has so far only been used for the production of recombinant EspA, as described above. Here, too, a system to either display the protein at the cell surface or secrete it from the cell will probably be needed but may be worthwhile (Luan et al., 2010). A recombinant *L. lactis* strain that displays the Stx1 B-subunit via albumin binding domains (single-domain non-immunoglobulin scaffolds) on the bacterial cell surface was recently designed by Zadravec et al. (2016). ELISA and FACS analysis confirmed the ability of this strain to bind Stx1. The immunogenicity and safety of this strain and its ability to protect against challenge were, however, not yet tested in animals.

Lastly, a recombinant *Lactobacillus acidophilus* variant expressing EspA and the Tir central domain (EspA-Tir-M) inhibited A/E lesions formation by EHEC O157:H7 after pre-incubation *in vitro*. Oral immunization of mice induced the production of specific and systemic neutralizing antibodies and reduced EHEC O157:H7 colonization. It also inhibited intestinal A/E lesions and toxin-mediated organ damage (Lin et al., 2017a).

Bacterial Ghosts

Bacterial ghosts (BGs) remain when bacteria are treated with viral E protein. This protein forms tubes across the bacterial cell membrane releasing the cytoplasm of the bacteria into the surroundings. What remains are bacterial ghosts, empty membranes with intact bacterial morphology and cell surface structures. Because of this, bacterial ghosts are highly immunogenic. Moreover, due to the ubiquitous process used to create them, bacterial ghosts can be produced from whichever strain is desirable (Lubitz et al., 2009; Hajam et al., 2017).

E. coli O157:H7 N°CIP 105282 encode Stx1 and Stx2. BGs were produced from this strain by combining treatment with viral E protein to remove the cytoplasm and addition of staphylococcal nuclease A to degrade pathogenic DNA. Oral immunization of mice induced a specific immune response and mice were protected from a subsequent challenge with an EHEC strain (Mayr et al., 2005). When oral immunization was followed by an oral boost on day 28, antibody production increased, resulting in even better survival (Mayr et al., 2005). A later study showed that a single rectal inoculation of mice with these BGs led to the production of neutralizing antibodies that completely protected mice from infection with a lethal dose of bacteria without requiring a boost (Mayr et al., 2012).

The use of *E. coli* O157:H7 (EDL933) bacterial ghosts yielded similar results. Here, too, an increase in neutralizing antibodies and protection was observed after a boost (Cai et al., 2010). When the BGs were modified to display an inactive Stx2A–Stx1B fusion (Stx2Am–Stx1B) on the cell surface, a stronger induction of neutralizing antibodies was observed, which correlated with better survival and reduced organ damage upon challenge with EHEC. Furthermore, bacterial ghosts displaying the Stx2Am–Stx1B on the surface performed better than those that did not, suggesting that the combination of surface antigens such as intimin in combination with the toxin resulted in even better immune responses (Cai et al., 2015).

Outer Membrane Vesicles

Outer membrane vesicles (OMVs) are nanoparticles that are released by many Gram-negative bacteria including *E. coli*. Their major component is bacterial LPS, making them highly immunogenic. Modified OMVs from Shiga toxin A-subunit-deficient *E. coli* O157:H7 were prepared and tested by eyedrop application for their activity against HUS development. Mice received a boost after 2 weeks, and subsequent intraperitoneal challenge with wild-type OMVs was carried out 4 weeks after the initial immunization. The vaccinated mice were shown to be protected from the lethality usually observed upon challenge with wildtype OMVs (Choi et al., 2014). Immunization with chemically inactivated OMVs obtained from a virulent *E. coli* O157 strain was also effective in the murine infection model. Here, mice were immunized subcutaneously on days 0 and 21 and received an intraperitoneal challenge with concentrated cell supernatants 2 weeks after application of second immunization. While 90% of control mice died by day seven post-challenge, all immunized mice survived (Fingermann et al., 2018).

Plant-Based Vaccines

Plant-based vaccines have been trialed with the idea that they can easily be used for oral vaccination.

Toxin-Targeted Plant-Based Vaccines

The inactive A-subunit of Stx2 was produced by expression in a tobacco plant cell line (NT-1). Subsequent immunization of mice by feeding or by parenteral immunization with an oral boost resulted in increased Stx2 IgA and IgG levels. It was able to protect mice from a lethal challenge with an EHEC strain. Sera of immunized mice further neutralized toxicity *in vitro* (Wen et al., 2006). For the treatment of porcine edema disease, which is a severe and often fatal disease in pigs that is also mediated by Stx (in this case subtype Stx2e), Hamabata et al. have recently developed *stx2eB*-transgenic lettuce for immunization. Infection of piglets with STEC after oral vaccination by feeding the lettuce showed decreased levels of pathogenesis in lettuce-fed piglets (Hamabata et al., 2019).

Virulence Protein-Targeted Vaccines

The immunization capacity of plant-codon optimized intimin expressed in the NT-1 tobacco cell line was also assessed by either i.p. injection of purified protein, feeding of transgenic plant cells, or a combination thereof. Here, mice immunized by injection and boosted by feeding developed neutralizing antibodies against intimin and reduced the time of bacterial shedding after challenge with *E. coli* O157:H7 (Judge et al., 2004). In another approach, chimeric protein composed of the LEE-encoded proteins EspA, intimin, and Tir (named EIT and further described above) was codon-optimized for expression in tobacco and canola plants. Using this plant-based expression strategy, recombinant EIT was prepared, and immune responses in mice were assessed after parenteral and oral immunization as well as after a combination. Here, a combination of subcutaneous injection and oral gavage yielded the highest immune responses and resulted in significantly reduced fecal shedding of *E. coli* O157:H7 after challenge (Amani et al., 2011).

INHIBITORS

Pyocins

R(rod)-type pyocins are bacterial structures that have developed from phages and show a high similarity to bacteriophage tails. R-type pyocins bind to the core polysaccharides in the outer membrane of bacteria via specific receptor binding proteins, resulting in selective targeting of certain bacteria. The LPS recognition induces contraction of the phage-like tail and puncturing of the bacterial cell envelope, leading to loss of bacterial membrane potential and subsequent cell death. This mechanism is best described for *Pseudomonas aeruginosa*, which use pyocins to target competitors. However, by designing hybrid proteins that possess the receptor binding proteins or tail fibers of known bacteriophages, the specificity of the pyocins can be changed (Kim et al., 2019). An EHEC O157:H7 specific pyocin (AvR2-V10) developed by Scholl et al. was able to specifically recognize and degrade O157 LPS and kill *E. coli* O157:H7 without inducing Stx expression (Scholl et al., 2009). A new version of this pyocin (AvR2-10.3) was tested *in vivo* in a rabbit EHEC infection model. Here, reduced diarrhea colonization and bacterial shedding, as well as less intestinal damage, were observed (Ritchie et al., 2011). Furthermore, Scholl et al. identified an O104-specific bacteriophage tail protein and showed that fusion of this protein to the pyocin tail fiber resulted in specific targeting and killing of O104 strains by the pyocin (AvR2-104.1) (Scholl et al., 2012), showing that this approach is promising for a variety of different serotypes.

ALTERNATIVE APPROACHES USING ANTIMICROBIAL AGENTS

Probiotics

Management of STEC-mediated diseases including HUS onset (curative or preventive) by probiotics has also recently been addressed in many studies. The administration of certain probiotics to humans or reservoir animals may reduce colonization and carriage of STEC, which will prevent and/or reduce the risk of infection and transmission of the pathogenic bacteria (Sargeant et al., 2007; Corr et al., 2009). Protective and beneficial capabilities of probiotics have been described in several studies in which probiotics have been applied prior to an STEC infection of cultured cells or in mice (recently reviewed in detail by (Eaton et al., 2011; Mogna et al., 2012; Chen et al., 2013; Kakisu et al., 2013; Rund et al., 2013; Cordonnier et al., 2017; Giordano et al., 2019)). Significant inhibitory effects against the growth of STEC have been demonstrated for several *Lactobacillus* strains (*L. rhamnosus* LR04, LR06, *L. delbrueckii, L. pentosus, L. fermentum, L. crispatus, L. plantarum, L. lactis, L. kefir, L. gasseri* CCDM215, *L. accidophila* CCDM149, *L. helveticus* KLDS, *L. casei, L. paracasei* NZU101), *E. coli* Nissle, *Enterococcus faecium* YF5, *Enterococcus faecalis* (Symbioflor), *Bifidobacterium longum,* and others. Moreover, use of direct-fed microbiota was found to reduce shedding of *E. coli* O157:H7 in cattle (Peterson et al., 2007; Callaway et al., 2009; Rahal et al., 2015; Wisener et al., 2015; Giordano et al., 2019). The success seems to depend on the probiotic strain(s), immunomodulation of the host, and their metabolism and ability to modify the local milieu, e.g., by the production of short chain acids, such as lactate, butyrate, and acetate (Ogawa et al., 2001; Takahashi et al., 2004; Carey et al., 2008; Fukuda et al., 2011), or/and occupy similar niches in the intestinal tract in which they compete for adhesion to the gut epithelium and nutrients. In fact, recent studies demonstrated that the efficiency of colonization of the different gut section by intestinal pathogens is dependent on the composition of the microbiota (Baumler and Sperandio, 2016; Litvak et al., 2019).

Despite the observed beneficial effects in animals, it is very difficult to extrapolate the data to humans, considering that the beneficial ratio of probiotic to pathogen varied from 1:1 to $1:10^5$ colony forming units (CFU). Furthermore, it remains unclear how and when the probiotic should be administered.

Phages

Another upcoming potential measure to prevent infectious bacterial diseases is phage therapy, i.e., the application of lytic phages to kill and decrease the number of pathogens in food, animal reservoirs, or patients. One of the first attempts to eliminate STEC from animals (e.g., mice, sheep, and cattle) and food was performed with bacteriophages (e.g., the T-even bacteriophage CEV1, rV5, WV8, WV7, wV11, e11/2, and e4/1c),

which have the potential to lyse *E. coli* O:157:H7 (Raya et al., 2006; Sheng et al., 2006; Abuladze et al., 2008; Rivas et al., 2010; Stanford et al., 2010). To date, a large variety of phages have been isolated and shown to be highly effective in the killing of STEC strains *in vitro*, but the application of individual bacteriophages *in vivo* seemed less promising, likely due to the fact that bacterial access of the phages in the gut is reduced, or the intestinal environment is disadvantageous for phage survival and/or replication (Niu et al., 2009; Dini et al., 2016; Sabouri et al., 2017; Wang et al., 2017; Safwat-Mohamed et al., 2018). However, more recently, use of certain phages and phage cocktails including multiple STEC-specific phages for oral or rectal administration to ruminants or for spraying on fruits and vegetables has shown the potential of phage therapy to reduce STEC carriage in domestic animals (Niu et al., 2009; Dini et al., 2016; Sabouri et al., 2017; Wang et al., 2017; Safwat-Mohamed et al., 2018).

Antibiotics

Early studies investigating the effect of antibiotics in the treatment of STEC infections have suggested that antibiotics induce the bacterial SOS response, resulting in an increase of Shiga toxin production and release (O'Brien et al., 1984; Muhldorfer et al., 1996; Kimmitt et al., 2000). This has raised concerns that antibiotics may increase the risk of HUS development (Zimmerhackl, 2000; Panos et al., 2006; Kakoullis et al., 2019), and therefore, their use during STEC infections has been contraindicated. However, not all studies were able to confirm Stx induction or an increase in the amount of HUS incidences in response to antibiotics. Furthermore, the effects of antibiotics on *stx* expression vary greatly and are dependent on the antibiotic class, the antibiotic concentration, the respective STEC strain, as well as the Stx subtype (Walterspiel et al., 1992; Grif et al., 1998; Kimmitt et al., 2000; Ochoa et al., 2007; Pedersen et al., 2008; Zhang et al., 2009; McGannon et al., 2010; Bielaszewska et al., 2012; Nassar et al., 2013). While the results obtained from some antibiotic classes, such as β-lactams, are conflicting (Yoh et al., 1997, 1999; Grif et al., 1998; Yoshimura et al., 1999; McGannon et al., 2010; Muhlen et al., 2020), ansamycins and chloramphenicol consistently yielded promising results in *in vitro* studies (Kimmitt et al., 2000; Ochoa et al., 2007; McGannon et al., 2010; Kakoullis et al., 2019; Muhlen et al., 2020) while fluoroquinolones were regularly associated with toxin induction (Zhang et al., 2000; Hiramatsu et al., 2003; Bielaszewska et al., 2012; Berger et al., 2019; Muhlen et al., 2020).

Some animal studies used to mimic STEC- or Stx-mediated disease in response to antibiotic treatment confirmed previous *in vitro* results, while others were contradicting the *in vitro* data (Zhang et al., 2000, 2009; Rahal et al., 2011a; Zangari et al., 2014; Kakoullis et al., 2019). Interestingly, the *in vivo* studies confirmed a detrimental effect of fluoroquinolone antibiotics (Zhang et al., 2000; Hiramatsu et al., 2003; Muhlen et al., 2020) and a reduction of disease pathology when animals were treated with rifamycin antibiotics (Rahal et al., 2011a,b; Muhlen et al., 2020).

As studies using antibiotics that inhibit transcription or translation, such as rifamycins, have regularly been shown to inhibit Stx production *in vitro* and *in vivo* (Rahal et al., 2011a,b; Corogeanu et al., 2012; Fadlallah et al., 2015; Berger et al., 2019; Muhlen et al., 2020) even after pre-treatment with fluoroquinolone ciprofloxacin (Berger et al., 2019), this opens up the possibility of a potential treatment regimen for STEC infection using antibiotics combination therapy consisting of a transcriptional inhibitor supplied in advance of or simultaneously with an antibiotic such as ciprofloxacin, which efficiently clears the bacterial infection.

Natural Products

Several studies have tested natural products for their ability to reduce or prevent Stx-induced cell or tissue damage in cell cultures *in vitro* or in animal infection models. An inhibition of cytotoxicity of Stx of *E. coli* O:157:H7 was found for white carob tree (*Prosopsis alba*) and *Ziziphus mistol* extracts (Pellarin et al., 2013) and for Ellagitannin from the Aleppo oak (*Quercus infectoria*) (Voravuthikunchai et al., 2012). Moreover, bacterial products such as lactic acid, linoleic acid, (Pittman et al., 2012), green tea extracts (Isogai et al., 1998, 2001), fruit juices (Nogueira et al., 2003), and other plant products (Takemasa et al., 2009; Lacombe et al., 2010; Lee and Stein, 2011; Sheng et al., 2016; Sewlikar and D'Souza, 2017; Patel et al., 2018) have been shown to have a beneficial effect on STEC-infected cells and animals alone or in combination of other agents, e.g., antibiotics.

CONCLUSIONS

Although almost four decades have passed since the first clinical human HUS case (Centers for Disease Control, 1982) and the incidence of HUS increases, a generally accepted and successful therapy for STEC-induced HUS in patients is still missing. Nevertheless, a number of promising approaches and clinical studies employing different strategies have been performed. Here, we have reviewed therapeutic strategies including Stx toxin receptor analogs, Stx-specific antibodies, and alternative antimicrobial agents. For some, a beneficial effect has been reported, although the outcome seems to depend on multiple factors, e.g., the dose of the agent, the STEC isolate/strain, the Stx variants, the time point of administration, the route of application, the severity of the infection/symptoms, and the type of agent. Another important problem is that our information about the concentration, activity, and the precise localization of the toxins during the course of the infection is still scarce. Further studies examining these issues and testing the efficacy of Stx-inhibiting agents according to gained knowledge from these experiments are required to select the most successful regimens that could then be assessed in clinical trials. As none of the current animal models mimic EHEC infections and HUS development in humans, clinical trials and cohort studies are urgently needed to evaluate whether newly developed treatment strategies are effective. In this context, it should also be mentioned that early detection of an EHEC infection is crucial for the success of most newly developed therapeutics. Thus, the development of fast and reliable diagnostic tools to screen for Stx is also of utter importance. Moreover, a vaccination strategy for humans, but also for cattle limiting STEC carriage in their reservoirs would be of great benefit for public health.

What is the current situation of possible therapies and vaccines? While many different treatment strategies have been employed in order to develop a therapeutic or prophylactic treatment against STEC-induced disease, few have, to date, progressed past Phase II trials. Several approaches including monoclonal antibodies, receptor analogs such as Synsorb Pk, or the use of Eculizumab looked promising, but when evaluated systematically or in Phase III trials showed little evidence of success. The disadvantage of monomeric antibodies may likely be that the Stx receptor forms polymers, thus leaving Stx docking spaces available. Newly developed antibodies and neutralizing peptides therefore aim at providing multimeric recognition sites to capture as many receptor-binding sites as possible. These have, however, yet to be tested in clinical trials.

Vaccine approaches face other difficulties. While STEC infections are an important cause for diarrhea disease and especially dangerous as they can lead to HUS and systemic complications, the total amount of STEC infections is rather low. Therefore, a prophylactic vaccine may only be of interest for countries in which these infections are endemic. In general, while phase II clinical trials can be carried out, the availability of patients with STEC infections for phase III trials is limited. Furthermore, these infections will vary in the infection-causing strain and Stx subtype, both of which need to be controlled in a clinical trial. Also, the time of presentation at the physician or in hospital will most likely be after the onset of bloody diarrhea or late stages of watery diarrhea, making an early intervention difficult.

AUTHOR CONTRIBUTIONS

All authors listed have made an equal, substantial, direct and intellectual contribution to the work, and approved it for publication.

FUNDING

The work on potential novel therapeutic strategies of STEC infections by the authors is supported by the German Center of Infection Research (DZIF).

ACKNOWLEDGMENTS

We thank M. Fenner and U. Dobrindt for helpful discussion.

REFERENCES

Abuladze, T., Li, M., Menetrez, M. Y., Dean, T., Senecal, A., and Sulakvelidze, A. (2008). Bacteriophages reduce experimental contamination of hard surfaces, tomato, spinach, broccoli, and ground beef by *Escherichia coli* O157:H7. *Appl. Environ. Microbiol.* 74, 6230–6238. doi: 10.1128/AEM.01465-08

Acheson, D. W., Levine, M. M., Kaper, J. B., and Keusch, G. T. (1996). Protective immunity to shiga-like toxin I following oral immunization with shiga-like toxin I B-subunit-producing *Vibrio cholerae* CVD 103-HgR. *Infect. Immun.* 64, 355–357. doi: 10.1128/IAI.64.1.355-357.1996

Ahmed, B., Loos, M., Vanrompay, D., and Cox, E. (2013). Mucosal priming of the murine immune system against enterohemorrhagic *Escherichia coli* O157:H7 using *Lactococcus lactis* expressing the type III secretion system protein EspB. *Vet. Immunol. Immunopathol.* 152, 141–145. doi: 10.1016/j.vetimm.2012.09.019

Ahmed, B., Loos, M., Vanrompay, D., and Cox, E. (2014). Oral immunization with *Lactococcus lactis*-expressing EspB induces protective immune responses against *Escherichia coli* O157:H7 in a murine model of colonization. *Vaccine* 32, 3909–3916. doi: 10.1016/j.vaccine.2014.05.054

Albanese, A., Sacerdoti, F., Seyahian, E. A., Amaral, M. M., Fiorentino, G., Fernandez Brando, R., et al. (2018). Immunization of pregnant cows with shiga toxin-2 induces high levels of specific colostral antibodies and lactoferrin able to neutralize *E. coli* O157:H7 pathogenicity. *Vaccine* 36, 1728–1735. doi: 10.1016/j.vaccine.2018.02.060

Amani, J., Mousavi, S. L., Rafati, S., and Salmanian, A. H. (2011). Immunogenicity of a plant-derived edible chimeric EspA, intimin and tir of *Escherichia coli* O157:H7 in mice. *Plant Sci.* 180, 620–627. doi: 10.1016/j.plantsci.2011.01.004

Amani, J., Salmanian, A. H., Rafati, S., and Mousavi, S. L. (2010). Immunogenic properties of chimeric protein from espA, eae and tir genes of *Escherichia coli* O157:H7. *Vaccine* 28, 6923–6929. doi: 10.1016/j.vaccine.2010.07.061

Asahara, T., Shimizu, K., Nomoto, K., Hamabata, T., Ozawa, A., and Takeda, Y. (2004). Probiotic bifidobacteria protect mice from lethal infection with shiga toxin-producing *Escherichia coli* O157:H7. *Infect. Immun.* 72, 2240–2247. doi: 10.1128/IAI.72.4.2240-2247.2004

Asper, D. J., Karmali, M. A., Townsend, H., Rogan, D., and Potter, A. A. (2011). Serological response of shiga toxin-producing *Escherichia coli* type III secreted proteins in sera from vaccinated rabbits, naturally infected cattle, and humans. *Clin. Vaccine Immunol.* 18, 1052–1057. doi: 10.1128/CVI.00068-11

Babiuk, S., Asper, D. J., Rogan, D., Mutwiri, G. K., and Potter, A. A. (2008). Subcutaneous and intranasal immunization with type III secreted proteins can prevent colonization and shedding of *Escherichia coli* O157:H7 in mice. *Microb. Pathog.* 45, 7–11. doi: 10.1016/j.micpath.2008.01.005

Baumler, A. J., and Sperandio, V. (2016). Interactions between the microbiota and pathogenic bacteria in the gut. *Nature* 535, 85–93. doi: 10.1038/nature18849

Bentancor, L. V., Bilen, M., Brando, R. J., Ramos, M. V., Ferreira, L. C., Ghiringhelli, P. D., et al. (2009). A DNA vaccine encoding the enterohemorragic *Escherichia coli* shiga-like toxin 2 A2 and B subunits confers protective immunity to shiga toxin challenge in the murine model. *Clin. Vaccine Immunol.* 16, 712–718. doi: 10.1128/CVI.00328-08

Berger, M., Aijaz, I., Berger, P., Dobrindt, U., and Koudelka, G. (2019). Transcriptional and translational inhibitors block SOS response and shiga toxin expression in enterohemorrhagic *Escherichia coli*. *Sci. Rep.* 9:18777. doi: 10.1038/s41598-019-55332-2

Bernedo-Navarro, R. A., Miyachiro, M. M., Da Silva, M. J., Reis, C. F., Conceicao, R. A., Gatti, M. S., et al. (2014). Peptides derived from phage display libraries as potential neutralizers of shiga toxin-induced cytotoxicity *in vitro* and *in vivo*. *J. Appl. Microbiol.* 116, 1322–1333. doi: 10.1111/jam.12451

Bielaszewska, M., Idelevich, E. A., Zhang, W., Bauwens, A., Schaumburg, F., Mellmann, A., et al. (2012). Effects of antibiotics on shiga toxin 2 production and bacteriophage induction by epidemic *Escherichia coli* O104:H4 strain. *Antimicrob. Agents Chemother.* 56, 3277–3282. doi: 10.1128/AAC.06315-11

Bielaszewska, M., Mellmann, A., Zhang, W., Kock, R., Fruth, A., Bauwens, A., et al. (2011). Characterisation of the *Escherichia coli* strain associated with an outbreak of haemolytic uraemic syndrome in Germany, 2011: a microbiological study. *Lancet Infect. Dis.* 11, 671–676. doi: 10.1016/S1473-3099(11)70165-7

Bitzan, M., Poole, R., Mehran, M., Sicard, E., Brockus, C., Thuning-Roberson, C., et al. (2009). Safety and pharmacokinetics of chimeric anti-shiga toxin 1 and anti-shiga toxin 2 monoclonal antibodies in healthy volunteers. *Antimicrob. Agents Chemother.* 53, 3081–3087. doi: 10.1128/AAC.01661-08

Buelli, S., Zoja, C., Remuzzi, G., and Morigi, M. (2019). Complement activation contributes to the pathophysiology of shiga toxin-associated hemolytic uremic syndrome. *Microorganisms* 7:15. doi: 10.3390/microorganisms7010015

Cai, K., Gao, X., Li, T., Hou, X., Wang, Q., Liu, H., et al. (2010). Intragastric immunization of mice with enterohemorrhagic *Escherichia coli* O157:H7 bacterial ghosts reduces mortality and shedding and induces a Th2-type dominated mixed immune response. *Can. J. Microbiol.* 56, 389–398. doi: 10.1139/W10-025

Cai, K., Gao, X., Li, T., Wang, Q., Hou, X., Tu, W., et al. (2011). Enhanced immunogenicity of a novel Stx2Am-Stx1B fusion protein in a mice model of enterohemorrhagic *Escherichia coli* O157:H7 infection. *Vaccine* 29, 946–952. doi: 10.1016/j.vaccine.2010.11.035

Cai, K., Tu, W., Liu, Y., Li, T., and Wang, H. (2015). Novel fusion antigen displayed-bacterial ghosts vaccine candidate against infection of *Escherichia coli* O157:H7. *Sci. Rep.* 5:17479. doi: 10.1038/srep17479

Calderon Toledo, C., Arvidsson, I., and Karpman, D. (2011). Cross-reactive protection against enterohemorrhagic *Escherichia coli* infection by enteropathogenic *E. coli* in a mouse model. *Infect. Immun.* 79, 2224–2233. doi: 10.1128/IAI.01024-10

Callaway, T. R., Carr, M. A., Edrington, T. S., Anderson, R. C., and Nisbet, D. J. (2009). Diet, *Escherichia coli* O157:H7, and cattle: a review after 10 years. *Curr. Issues Mol. Biol.* 11, 67–79.

Caprioli, A., Scavia, G., and Morabito, S. (2014). Public health microbiology of shiga toxin-producing *Escherichia coli*. *Microbiol. Spectr.* 2. doi: 10.1128/microbiolspec.EHEC-0014-2013

Carey, C. M., Kostrzynska, M., Ojha, S., and Thompson, S. (2008). The effect of probiotics and organic acids on shiga-toxin 2 gene expression in enterohemorrhagic *Escherichia coli* O157:H7. *J. Microbiol Methods* 73, 125–132. doi: 10.1016/j.mimet.2008.01.014

Cataldi, A., Yevsa, T., Vilte, D. A., Schulze, K., Castro-Parodi, M., Larzabal, M., et al. (2008). Efficient immune responses against Intimin and EspB of enterohaemorragic *Escherichia coli* after intranasal vaccination using the TLR2/6 agonist MALP-2 as adjuvant. *Vaccine* 26, 5662–5667. doi: 10.1016/j.vaccine.2008.07.027

Chen, Y. P., Lee, T. Y., Hong, W. S., Hsieh, H. H., and Chen, M. J. (2013). Effects of Lactobacillus kefiranofaciens M1 isolated from kefir grains on enterohemorrhagic *Escherichia coli* infection using mouse and intestinal cell models. *J. Dairy Sci.* 96, 7467–7477. doi: 10.3168/jds.2013-7015

Cheng, L. W., Henderson, T. D., Patfield, S., Stanker, L. H., and He, X. (2013). Mouse *in vivo* neutralization of *Escherichia coli* shiga toxin 2 with monoclonal antibodies. *Toxins* 5, 1845–1858. doi: 10.3390/toxins5101845

Cheng, Y., Feng, Y., Luo, P., Gu, J., Yu, S., Zhang, W. J., et al. (2009). Fusion expression and immunogenicity of EHEC EspA-Stx2Al protein: implications for the vaccine development. *J. Microbiol.* 47, 498–505. doi: 10.1007/s12275-009-0116-8

Choi, K. S., Kim, S. H., Kim, E. D., Lee, S. H., Han, S. J., Yoon, S., et al. (2014). Protection from hemolytic uremic syndrome by eyedrop vaccination with modified enterohemorrhagic *E. coli* outer membrane vesicles. *PLoS ONE* 9:e100229. doi: 10.1371/journal.pone.0100229

Clements, A., Young, J. C., Constantinou, N., and Frankel, G. (2012). Infection strategies of enteric pathogenic *Escherichia coli*. *Gut Microbes* 3, 71–87. doi: 10.4161/gmic.19182

Control, C. F. D. (1982). Isolation of E. coli O157:H7 from sporadic cases of hemorrhagic colitis - United States. *MMWR* 31, 580–585.

Cordonnier, C., Thevenot, J., Etienne-Mesmin, L., Alric, M., Livrelli, V., and Blanquet-Diot, S. (2017). Probiotic and enterohemorrhagic *Escherichia coli*: an effective strategy against a deadly enemy? *Crit. Rev. Microbiol.* 43, 116–132. doi: 10.1080/1040841X.2016.1185602

Corogeanu, D., Willmes, R., Wolke, M., Plum, G., Utermohlen, O., and Kronke, M. (2012). Therapeutic concentrations of antibiotics inhibit shiga toxin release from enterohemorrhagic *E. coli* O104:H4 from the 2011 German outbreak. *BMC Microbiol.* 12:160. doi: 10.1186/1471-2180-12-160

Corr, S. C., Hill, C., and Gahan, C. G. (2009). Understanding the mechanisms by which probiotics inhibit gastrointestinal pathogens. *Adv. Food Nutr. Res.* 56, 1–15. doi: 10.1016/S1043-4526(08)00601-3

Delmas, Y., Vendrely, B., Clouzeau, B., Bachir, H., Bui, H. N., Lacraz, A., et al. (2014). Outbreak of *Escherichia coli* O104:H4 haemolytic uraemic syndrome in France: outcome with eculizumab. *Nephrol. Dial Transplant.* 29, 565–572. doi: 10.1093/ndt/gft470

Dini, C., Bolla, P. A., and De Urraza, P. J. (2016). Treatment of *in vitro* enterohemorrhagic *Escherichia coli* infection using phage and probiotics. *J. Appl. Microbiol.* 121, 78–88. doi: 10.1111/jam.13124

Doavi, T., Mousavi, S. L., Kamali, M., Amani, J., and Fasihi Ramandi, M. (2016). Chitosan-based intranasal vaccine against *Escherichia coli* O157:H7. *Iran Biomed. J.* 20, 97–108. doi: 10.7508/ibj.2016.02.005

Donnenberg, M. S., and Kaper, J. B. (1992). Enteropathogenic *Escherichia coli*. *Infect. Immun.* 60, 3953–3961. doi: 10.1128/IAI.60.10.3953-3961.1992

Dowling, T. C., Chavaillaz, P. A., Young, D. G., Melton-Celsa, A., O'Brien, A., Thuning-Roberson, C., et al. (2005). Phase 1 safety and pharmacokinetic study of chimeric murine-human monoclonal antibody c alpha Stx2 administered intravenously to healthy adult volunteers. *Antimicrob. Agents Chemother.* 49, 1808–1812. doi: 10.1128/AAC.49.5.1808-1812.2005

Dyve Lingelem, A. B., Bergan, J., and Sandvig, K. (2012). Inhibitors of intravesicular acidification protect against shiga toxin in a pH-independent manner. *Traffic* 13, 443–454. doi: 10.1111/j.1600-0854.2011.01319.x

Eaton, K. A., Honkala, A., Auchtung, T. A., and Britton, R. A. (2011). Probiotic *Lactobacillus reuteri* ameliorates disease due to enterohemorrhagic *Escherichia coli* in germfree mice. *Infect. Immun.* 79, 185–191. doi: 10.1128/IAI.00880-10

Fadlallah, S. M., Rahal, E. A., Sabra, A., Kissoyan, K. A., and Matar, G. M. (2015). Effect of rifampicin and gentamicin on shiga toxin 2 expression level and the SOS response in *Escherichia coli* O104:H4. *Foodborne Pathog. Dis.* 12, 47–55. doi: 10.1089/fpd.2014.1824

Fan, H. Y., Wang, L., Luo, J., and Long, B. G. (2012). Protection against *Escherichia coli* O157:H7 challenge by immunization of mice with purified tir proteins. *Mol. Biol. Rep.* 39, 989–997. doi: 10.1007/s11033-011-0824-0

Fingermann, M., Avila, L., De Marco, M. B., Vazquez, L., Di Biase, D. N., Muller, A. V., et al. (2018). OMV-based vaccine formulations against shiga toxin producing *Escherichia coli* strains are both protective in mice and immunogenic in calves. *Hum. Vaccine Immunother.* 14, 2208–2213. doi: 10.1080/21645515.2018.1490381

Fujii, J., Naito, M., Yutsudo, T., Matsumoto, S., Heatherly, D. P., Yamada, T., et al. (2012). Protection by a recombinant mycobacterium bovis bacillus calmette-guerin vaccine expressing shiga toxin 2 B subunit against shiga toxin-producing *Escherichia coli* in mice. *Clin. Vaccine Immunol.* 19, 1932–1937. doi: 10.1128/CVI.00473-12

Fukuda, S., Toh, H., Hase, K., Oshima, K., Nakanishi, Y., Yoshimura, K., et al. (2011). Bifidobacteria can protect from enteropathogenic infection through production of acetate. *Nature* 469, 543–547. doi: 10.1038/nature09646

Funatogawa, K., Ide, T., Kirikae, F., Saruta, K., Nakano, M., and Kirikae, T. (2002). Use of immunoglobulin enriched bovine colostrum against oral challenge with enterohaemorrhagic *Escherichia coli* O157:H7 in mice. *Microbiol. Immunol.* 46, 761–766. doi: 10.1111/j.1348-0421.2002.tb02761.x

Gandhi, T., Patki, M., Kong, J., Koya, J., Yoganathan, S., Reznik, S., et al. (2019). Development of an arginine anchored nanoglobule with retrograde trafficking inhibitor (Retro-2) for the treatment of an enterohemorrhagic *Escherichia coli* outbreak. *Mol. Pharm.* 16, 4405–4415. doi: 10.1021/acs.molpharmaceut.9b00727

Gao, X., Cai, K., Li, T., Wang, Q., Hou, X., Tian, R., et al. (2011). Novel fusion protein protects against adherence and toxicity of enterohemorrhagic *Escherichia coli* O157:H7 in mice. *Vaccine* 29, 6656–6663. doi: 10.1016/j.vaccine.2011.06.106

Gao, X., Cai, K., Shi, J., Liu, H., Hou, X., Tu, W., et al. (2009). Immunogenicity of a novel Stx2B-Stx1B fusion protein in a mice model of Enterohemorrhagic *Escherichia coli* O157:H7 infection. *Vaccine* 27, 2070–2076. doi: 10.1016/j.vaccine.2009.01.115

Garmendia, J., Frankel, G., and Crepin, V. F. (2005). Enteropathogenic and enterohemorrhagic *Escherichia coli* infections: translocation, translocation, translocation. *Infect. Immun.* 73, 2573–2585. doi: 10.1128/IAI.73.5.2573-2585.2005

Gaytan, M. O., Martinez-Santos, V. I., Soto, E., and Gonzalez-Pedrajo, B. (2016). Type three secretion system in attaching and effacing pathogens. *Front. Cell Infect. Microbiol.* 6:129. doi: 10.3389/fcimb.2016.00129

Giordano, M., Baldassarre, M. E., Palmieri, V., Torres, D. D., Carbone, V., Santangelo, L., et al. (2019). Management of STEC Gastroenteritis: is there a role for probiotics? *Int. J. Environ. Res. Public Health* 16:1649. doi: 10.3390/ijerph16091649

Gordon, V. M., Whipp, S. C., Moon, H. W., O'Brien, A. D., and Samuel, J. E. (1992). An enzymatic mutant of shiga-like toxin II variant is a vaccine candidate for edema disease of swine. *Infect. Immun.* 60, 485–490. doi: 10.1128/IAI.60.2.485-490.1992

Grif, K., Dierich, M. P., Karch, H., and Allerberger, F. (1998). Strain-specific differences in the amount of shiga toxin released from enterohemorrhagic *Escherichia coli* O157 following exposure to subinhibitory concentrations of antimicrobial agents. *Eur. J. Clin. Microbiol. Infect. Dis.* 17, 761–766. doi: 10.1007/s100960050181

Gu, J., Liu, Y., Yu, S., Wang, H., Wang, Q., Yi, Y., et al. (2009). Enterohemorrhagic *Escherichia coli* trivalent recombinant vaccine containing EspA, intimin and Stx2 induces strong humoral immune response and confers protection in mice. *Microbes Infect.* 11, 835–841. doi: 10.1016/j.micinf.2009.04.024

Gu, J., Ning, Y., Wang, H., Xiao, D., Tang, B., Luo, P., et al. (2011). Vaccination of attenuated EIS-producing Salmonella induces protective immunity against enterohemorrhagic *Escherichia coli* in mice. *Vaccine* 29, 7395–7403. doi: 10.1016/j.vaccine.2011.07.069

Guirro, M., De Souza, R. L., Piazza, R. M., and Guth, B. E. (2013). Antibodies to intimin and *Escherichia coli*-secreted proteins EspA and EspB in sera of Brazilian children with hemolytic uremic syndrome and healthy controls. *Vet Immunol. Immunopathol.* 152, 121–125. doi: 10.1016/j.vetimm.2012.09.016

Hajam, I. A., Dar, P. A., Won, G., and Lee, J. H. (2017). Bacterial ghosts as adjuvants: mechanisms and potential. *Vet. Res.* 48:37. doi: 10.1186/s13567-017-0442-5

Hamabata, T., Sato, T., Takita, E., Matsui, T., Imaoka, T., Nakanishi, N., et al. (2019). shiga toxin 2eB-transgenic lettuce vaccine is effective in protecting weaned piglets from edema disease caused by shiga toxin-producing *Escherichia coli* infection. *Anim. Sci. J.* 90, 1460–1467. doi: 10.1111/asj.13292

Hiramatsu, K., Murakami, J., Kishi, K., Hirata, N., Yamasaki, T., Kadota, J., et al. (2003). Treatment with rokitamycin suppresses the lethality in a murine model of *Escherichia coli* O157:H7 infection. *Int. J. Antimicrob. Agents* 21, 471–477. doi: 10.1016/S0924-8579(03)00007-4

Hostetter, S. J., Helgerson, A. F., Paton, J. C., Paton, A. W., and Cornick, N. A. (2014). Therapeutic use of a receptor mimic probiotic reduces intestinal shiga toxin levels in a piglet model of hemolytic uremic syndrome. *BMC Res. Notes* 7:331. doi: 10.1186/1756-0500-7-331

Huppertz, H. I., Rutkowski, S., Busch, D. H., Eisebit, R., Lissner, R., and Karch, H. (1999). Bovine colostrum ameliorates diarrhea in infection with diarrheagenic *Escherichia coli*, shiga toxin-producing *E. coli,* and *E. coli* expressing intimin and hemolysin. *J. Pediatr. Gastroenterol. Nutr.* 29, 452–456. doi: 10.1097/00005176-199910000-00015

Ishikawa, S., Kawahara, K., Kagami, Y., Isshiki, Y., Kaneko, A., Matsui, H., et al. (2003). Protection against shiga toxin 1 challenge by immunization of mice with purified mutant shiga toxin 1. *Infect. Immun.* 71, 3235–3239. doi: 10.1128/IAI.71.6.3235-3239.2003

Isogai, E., Isogai, H., Hirose, K., Hayashi, S., and Oguma, K. (2001). *In vivo* synergy between green tea extract and levofloxacin against enterohemorrhagic *Escherichia coli* O157 infection. *Curr. Microbiol.* 42, 248–251. doi: 10.1007/s0028403357

Isogai, E., Isogai, H., Takeshi, K., and Nishikawa, T. (1998). Protective effect of Japanese green tea extract on gnotobiotic mice infected with an *Escherichia coli* O157:H7 strain. *Microbiol. Immunol.* 42, 125–128. doi: 10.1111/j.1348-0421.1998.tb02260.x

Jeong, K. I., Tzipori, S., and Sheoran, A. S. (2010). Shiga toxin 2-specific but not shiga toxin 1-specific human monoclonal antibody protects piglets challenged with enterohemorrhagic *Escherichia coli* producing shiga toxin 1 and shiga toxin 2. *J. Infect. Dis.* 201, 1081–1083. doi: 10.1086/651198

Judge, N. A., Mason, H. S., and O'Brien, A. D. (2004). Plant cell-based intimin vaccine given orally to mice primed with intimin reduces time of *Escherichia coli* O157:H7 shedding in feces. *Infect. Iimmun.* 72, 168–175. doi: 10.1128/IAI.72.1.168-175.2004

Kakisu, E., Abraham, A. G., Farinati, C. T., Ibarra, C., and De Antoni, G. L. (2013). *Lactobacillus plantarum* isolated from kefir protects vero cells from cytotoxicity by type-II shiga toxin from *Escherichia coli* O157:H7. *J. Dairy Res.* 80, 64–71. doi: 10.1017/S0022029912000659

Kakoullis, L., Papachristodoulou, E., Chra, P., and Panos, G. (2019). shiga toxin-induced haemolytic uraemic syndrome and the role of antibiotics: a global overview. *J. Infect.* 79, 75–94. doi: 10.1016/j.jinf.2019.05.018

Kaper, J. B., and O'Brien, A. D. (2014). Overview and historical perspectives. *Microbiol. Spectr* 2. doi: 10.1128/microbiolspec.EHEC-0028-2014

Karpman, D., and Tati, R. (2016). Complement contributes to the pathogenesis of shiga toxin-associated hemolytic uremic syndrome. *Kidney Int.* 90, 726–729. doi: 10.1016/j.kint.2016.07.002

Kavaliauskiene, S., Dyve Lingelem, A. B., Skotland, T., and Sandvig, K. (2017). Protection against shiga Toxins. *Toxins* 9:44. doi: 10.3390/toxins9020044

Kavaliauskiene, S., Skotland, T., Sylvanne, T., Simolin, H., Klokk, T. I., Torgersen, M. L., et al. (2015). Novel actions of 2-deoxy-D-glucose: protection against shiga toxins and changes in cellular lipids. *Biochem J.* 470, 23–37. doi: 10.1042/BJ20141562

Kavaliauskiene, S., Torgersen, M. L., Lingelem, A. B., Klokk, T. I., Lintonen, T., Simolin, H., et al. (2016). Cellular effects of fluorodeoxyglucose: global changes in the lipidome and alteration in intracellular transport. *Oncotarget* 7, 79885–79900. doi: 10.18632/oncotarget.13089

Keenswijk, W., Vanmassenhove, J., Raes, A., Dhont, E., and Vande Walle, J. (2017). Blood urea nitrogen to serum creatinine ratio is an accurate predictor of outcome in diarrhea-associated hemolytic uremic syndrome, a preliminary study. *Eur. J. Pediatr.* 176, 355–360. doi: 10.1007/s00431-016-2846-z

Kenny, B., Devinney, R., Stein, M., Reinscheid, D. J., Frey, E. A., and Finlay, B. B. (1997). Enteropathogenic *E. coli* (EPEC) transfers its receptor for intimate adherence into mammalian cells. *Cell* 91, 511–520. doi: 10.1016/S0092-8674(00)80437-7

Kerner, K., Bridger, P. S., Kopf, G., Frohlich, J., Barth, S., Willems, H., et al. (2015). Evaluation of biological safety *in vitro* and immunogenicity *in vivo* of recombinant *Escherichia coli* shiga toxoids as candidate vaccines in cattle. *Vet. Res.* 46:38. doi: 10.1186/s13567-015-0175-2

Khanifar, J., Hosseini, R. H., Kazemi, R., Ramandi, M. F., Amani, J., and Salmanian, A. H. (2019a). Prevention of EHEC infection by chitosan nano-structure coupled with synthetic recombinant antigen. *J. Microbiol. Methods* 157, 100–107. doi: 10.1016/j.mimet.2019.01.002

Khanifar, J., Salmanian, A. H., Haji Hosseini, R., Amani, J., and Kazemi, R. (2019b). Chitosan nano-structure loaded with recombinant *E. coli* O157:H7 antigens as a vaccine candidate can effectively increase immunization capacity. *Artif. Cells Nanomed. Biotechnol.* 47, 2593–2604. doi: 10.1080/21691401.2019.1629947

Kielstein, J. T., Beutel, G., Fleig, S., Steinhoff, J., Meyer, T. N., Hafer, C., et al. (2012). Best supportive care and therapeutic plasma exchange with or without eculizumab in shiga-toxin-producing *E. coli* O104:H4 induced haemolytic-uraemic syndrome: an analysis of the German STEC-HUS registry. *Nephrol. Dial Transplant.* 27, 3807–3815. doi: 10.1093/ndt/gfs394

Kim, B. O., Kim, E. S., Yoo, Y. J., Bae, H. W., Chung, I. Y., and Cho, Y. H. (2019). Phage-derived antibacterials: harnessing the simplicity, plasticity, and diversity of phages. *Viruses* 11, 268. doi: 10.3390/v11030268

Kimmitt, P. T., Harwood, C. R., and Barer, M. R. (2000). Toxin gene expression by shiga toxin-producing *Escherichia coli*: the role of antibiotics and the bacterial SOS response. *Emerg. Infect. Dis.* 6, 458–465. doi: 10.3201/eid0605.000503

Kimura, T., Co, M. S., Vasquez, M., Wei, S., Xu, H., Tani, S., et al. (2002). Development of humanized monoclonal antibody TMA-15 which neutralizes shiga toxin 2. *Hybrid Hybridomics* 21, 161–168. doi: 10.1089/153685902760173872

Kitov, P. I., Sadowska, J. M., Mulvey, G., Armstrong, G. D., Ling, H., Pannu, N. S., et al. (2000). shiga-like toxins are neutralized by tailored multivalent carbohydrate ligands. *Nature* 403, 669–672. doi: 10.1038/35001095

Konadu, E., Donohue-Rolfe, A., Calderwood, S. B., Pozsgay, V., Shiloach, J., Robbins, J. B., et al. (1999). Syntheses and immunologic properties of *Escherichia coli* O157 O-specific polysaccharide and shiga toxin 1 B subunit conjugates in mice. *Infect. Immun.* 67, 6191–6193. doi: 10.1128/IAI.67.11.6191-6193.1999

Kulkarni, A. A., Weiss, A. A., and Iyer, S. S. (2010). Glycan-based high-affinity ligands for toxins and pathogen receptors. *Med. Res. Rev.* 30, 327–393. doi: 10.1002/med.20196

Kuribayashi, T., Seita, T., Fukuyama, M., Furuhata, K., Honda, M., Matsumoto, M., et al. (2006). Neutralizing activity of bovine colostral antibody against verotoxin derived from enterohemorrhagic *Escherichia coli* O157:H7 in mice. *J. Infect. Chemother.* 12, 251–256. doi: 10.1007/s10156-006-0470-Y

Lacombe, A., Wu, V. C., Tyler, S., and Edwards, K. (2010). Antimicrobial action of the American cranberry constituents; phenolics, anthocyanins, and organic

acids, against *Escherichia coli* O157:H7. *Int J. Food Microbiol.* 139, 102–107. doi: 10.1016/j.ijfoodmicro.2010.01.035

Lapeyraque, A. L., Malina, M., Fremeaux-Bacchi, V., Boppel, T., Kirschfink, M., Oualha, M., et al. (2011). Eculizumab in severe shiga-toxin-associated HUS. *New Engl. J. Med.* 364, 2561–2563. doi: 10.1056/NEJMc1100859

Larzabal, M., Zotta, E., Ibarra, C., Rabinovitz, B. C., Vilte, D. A., Mercado, E. C., et al. (2013). Effect of coiled-coil peptides on the function of the type III secretion system-dependent activity of enterohemorragic *Escherichia coli* O157:H7 and citrobacter rodentium. *Int. J. Med. Microbiol.* 303, 9–15. doi: 10.1016/j.ijmm.2012.12.001

Lee, J. H., and Stein, B. D. (2011). Antimicrobial activity of a combination of mume fructus, schizandrae fructus, and coptidis rhizoma on enterohemorrhagic *Escherichia coli* O26, O111, and O157 and its effect on shiga toxin releases. *Foodborne Pathog. Dis.* 8, 643–646. doi: 10.1089/fpd.2010.0710

Legros, N., Pohlentz, G., Steil, D., and Muthing, J. (2018). shiga toxin-glycosphingolipid interaction: status quo of research with focus on primary human brain and kidney endothelial cells. *Int. J. Med. Microbiol.* 308, 1073–1084. doi: 10.1016/j.ijmm.2018.09.003

Li, Y., Frey, E., Mackenzie, A. M., and Finlay, B. B. (2000). Human response to *Escherichia coli* O157:H7 infection: antibodies to secreted virulence factors. *Infect. Immun.* 68, 5090–5095. doi: 10.1128/IAI.68.9.5090-5095.2000

Lin, R., Zhang, Y., Long, B., Li, Y., Wu, Y., Duan, S., et al. (2017a). Oral immunization with recombinant *Lactobacillus acidophilus* expressing espA-Tir-M confers protection against enterohemorrhagic *Escherichia coli* O157:H7 challenge in mice. *Front. Microbiol.* 8:417. doi: 10.3389/fmicb.2017.00417

Lin, R., Zhu, B., Zhang, Y., Bai, Y., Zhi, F., Long, B., et al. (2017b). Intranasal immunization with novel EspA-Tir-M fusion protein induces protective immunity against enterohemorrhagic *Escherichia coli* O157:H7 challenge in mice. *Microb. Pathog.* 105, 19–24. doi: 10.1016/j.micpath.2017.01.062

Lingwood, C. A., Law, H., Richardson, S., Petric, M., Brunton, J. L., De Grandis, S., et al. (1987). Glycolipid binding of purified and recombinant *Escherichia coli* produced verotoxin *in vitro*. *J. Biol. Chem.* 262, 8834–8839.

Litvak, Y., Mon, K. K. Z., Nguyen, H., Chanthavixay, G., Liou, M., Velazquez, E. M., et al. (2019). Commensal enterobacteriaceae protect against salmonella colonization through oxygen competition. *Cell Host. Microbe* 25, 128–139 e125. doi: 10.1016/j.chom.2018.12.003

Liu, J., Sun, Y., Feng, S., Zhu, L., Guo, X., and Qi, C. (2009). Towards an attenuated enterohemorrhagic *Escherichia coli* O157:H7 vaccine characterized by a deleted ler gene and containing apathogenic shiga toxins. *Vaccine* 27, 5929–5935. doi: 10.1016/j.vaccine.2009.07.097

Loos, S., Ahlenstiel, T., Kranz, B., Staude, H., Pape, L., Hartel, C., et al. (2012). An outbreak of shiga toxin-producing *Escherichia coli* O104:H4 hemolytic uremic syndrome in Germany: presentation and short-term outcome in children. *Clin. Infect. Dis.* 55, 753–759. doi: 10.1093/cid/cis531

Loos, S., Aulbert, W., Hoppe, B., Ahlenstiel-Grunow, T., Kranz, B., Wahl, C., et al. (2017). Intermediate follow-up of pediatric patients with hemolytic uremic syndrome during the 2011 outbreak caused by *E. coli* O104:H4. *Clin. Infect. Dis.* 64, 1637–1643. doi: 10.1093/cid/cix218

Lopez, E. L., Contrini, M. M., Glatstein, E., Gonzalez Ayala, S., Santoro, R., Allende, D., et al. (2010). Safety and pharmacokinetics of urtoxazumab, a humanized monoclonal antibody, against shiga-like toxin 2 in healthy adults and in pediatric patients infected with shiga-like toxin-producing *Escherichia coli*. *Antimicrob. Agents Chemother.* 54, 239–243. doi: 10.1128/AAC.00343-09

Loureiro, I., Frankel, G., Adu-Bobie, J., Dougan, G., Trabulsi, L. R., and Carneiro-Sampaio, M. M. (1998). Human colostrum contains IgA antibodies reactive to enteropathogenic *Escherichia coli* virulence-associated proteins: intimin, BfpA, EspA, and EspB. *J. Pediatr. Gastroenterol. Nutr.* 27, 166–171. doi: 10.1097/00005176-199808000-00007

Luan, J., Zhuang, Z., Liu, Y., Yun, K., Chen, M., and Wang, P. G. (2010). Expression of EspA in *Lactococcus lactis* NZ9000 and the detection of its immune effect *in vivo* and *vitro*. *Immunopharmacol. Immunotoxicol.* 32, 133–140. doi: 10.3109/08923970903207083

Lubitz, P., Mayr, U. B., and Lubitz, W. (2009). Applications of bacterial ghosts in biomedicine. *Adv. Exp. Med. Biol.* 655, 159–170. doi: 10.1007/978-1-4419-1132-2_12

Luz, D., Amaral, M. M., Sacerdoti, F., Bernal, A. M., Quintilio, W., Moro, A. M., et al. (2018). Human recombinant fab fragment neutralizes shiga toxin type 2 cytotoxic effects *in vitro* and *in vivo*. *Toxins* 10:508. doi: 10.3390/toxins10120508

Luz, D., Chen, G., Maranhao, A. Q., Rocha, L. B., Sidhu, S., and Piazza, R. M. (2015). Development and characterization of recombinant antibody fragments that recognize and neutralize *in vitro* Stx2 toxin from shiga toxin-producing *Escherichia coli*. *PLoS ONE* 10:e0120481. doi: 10.1371/journal.pone.0120481

Macconnachie, A. A., and Todd, W. T. (2004). Potential therapeutic agents for the prevention and treatment of haemolytic uraemic syndrome in shiga toxin producing *Escherichia coli* infection. *Curr. Opin. Infect. Dis.* 17, 479–482. doi: 10.1097/00001432-200410000-00013

Marcato, P., Griener, T. P., Mulvey, G. L., and Armstrong, G. D. (2005). Recombinant shiga toxin B-subunit-keyhole limpet hemocyanin conjugate vaccine protects mice from shigatoxemia. *Infect. Immun.* 73, 6523–6529. doi: 10.1128/IAI.73.10.6523-6529.2005

Marcato, P., Mulvey, G., Read, R. J., Vander Helm, K., Nation, P. N., and Armstrong, G. D. (2001). Immunoprophylactic potential of cloned shiga toxin 2 B subunit. *J. Infect. Dis.* 183, 435–443. doi: 10.1086/318080

Martinez, M. B., Taddei, C. R., Ruiz-Tagle, A., Trabulsi, L. R., and Giron, J. A. (1999). Antibody response of children with enteropathogenic *Escherichia coli* infection to the bundle-forming pilus and locus of enterocyte effacement-encoded virulence determinants. *J. Infect. Dis.* 179, 269–274. doi: 10.1086/314549

Mayr, U. B., Haller, C., Haidinger, W., Atrasheuskaya, A., Bukin, E., Lubitz, W., et al. (2005). Bacterial ghosts as an oral vaccine: a single dose of *Escherichia coli* O157:H7 bacterial ghosts protects mice against lethal challenge. *Infect. Immun.* 73, 4810–4817. doi: 10.1128/IAI.73.8.4810-4817.2005

Mayr, U. B., Kudela, P., Atrasheuskaya, A., Bukin, E., Ignatyev, G., and Lubitz, W. (2012). Rectal single dose immunization of mice with *Escherichia coli* O157:H7 bacterial ghosts induces efficient humoral and cellular immune responses and protects against the lethal heterologous challenge. *Microb. Biotechnol.* 5, 283–294. doi: 10.1111/j.1751-7915.2011.00316.x

McGannon, C. M., Fuller, C. A., and Weiss, A. A. (2010). Different classes of antibiotics differentially influence shiga toxin production. *Antimicrob. Agents Chemother.* 54, 3790–3798. doi: 10.1128/AAC.01783-09

Mejias, M. P., Ghersi, G., Craig, P. O., Panek, C. A., Bentancor, L. V., Baschkier, A., et al. (2013). Immunization with a chimera consisting of the B subunit of shiga toxin type 2 and brucella lumazine synthase confers total protection against shiga toxins in mice. *J. Immunol.* 191, 2403–2411. doi: 10.4049/jimmunol.1300999

Mejias, M. P., Hiriart, Y., Lauche, C., Fernandez-Brando, R. J., Pardo, R., Bruballa, A., et al. (2016). Development of camelid single chain antibodies against shiga toxin type 2 (Stx2) with therapeutic potential against Hemolytic Uremic Syndrome (HUS). *Sci. Rep.* 6:24913. doi: 10.1038/srep24913

Mellmann, A., Harmsen, D., Cummings, C. A., Zentz, E. B., Leopold, S. R., Rico, A., et al. (2011). Prospective genomic characterization of the German enterohemorrhagic *Escherichia coli* O104:H4 outbreak by rapid next generation sequencing technology. *PLoS ONE* 6:e22751. doi: 10.1371/journal.pone.0022751

Melton-Celsa, A. R. (2014). Shiga toxin (Stx) classification, structure, and function. *Microbiol Spectr* 2:EHEC-0024-2013. doi: 10.1128/microbiolspec.EHEC-0024-2013

Menne, J., Nitschke, M., Stingele, R., Abu-Tair, M., Beneke, J., Bramstedt, J., et al. (2012). Validation of treatment strategies for enterohaemorrhagic *Escherichia coli* O104:H4 induced haemolytic uraemic syndrome: case-control study. *BMJ* 345:e4565. doi: 10.1136/bmj.e4565

Mogna, L., Del Piano, M., Deidda, F., Nicola, S., Soattini, L., Debiaggi, R., et al. (2012). Assessment of the *in vitro* inhibitory activity of specific probiotic bacteria against different *Escherichia coli* strains. *J. Clin. Gastroenterol.* 46, S29–32. doi: 10.1097/MCG.0b013e31826852b7

Mohawk, K. L., Melton-Celsa, A. R., Robinson, C. M., and O'Brien, A. D. (2010). Neutralizing antibodies to shiga toxin type 2 (Stx2) reduce colonization of mice by Stx2-expressing *Escherichia coli* O157:H7. *Vaccine* 28, 4777–4785. doi: 10.1016/j.vaccine.2010.04.099

Monet-Didailler, C., Chevallier, A., Godron-Dubrasquet, A., Allard, L., Delmas, Y., Contin-Bordes, C., et al. (2019). Outcome of children with shiga toxin-associated haemolytic uraemic syndrome treated with eculizumab: a matched cohort study. *Nephrol. Dial Transplant.* 14:gfz158. doi: 10.1093/ndt/gfz158

Morigi, M., Galbusera, M., Gastoldi, S., Locatelli, M., Buelli, S., Pezzotta, A., et al. (2011). Alternative pathway activation of complement by shiga toxin promotes exuberant C3a formation that triggers microvascular thrombosis. *J. Immunol.* 187, 172–180. doi: 10.4049/jimmunol.1100491

Moxley, R. A., Francis, D. H., Tamura, M., Marx, D. B., Santiago-Mateo, K., and Zhao, M. (2017). Efficacy of urtoxazumab (TMA-15 Humanized monoclonal antibody specific for shiga toxin 2) against post-diarrheal neurological sequelae caused by *Escherichia coli* O157:H7 infection in the neonatal gnotobiotic piglet model. *Toxins* 9:49. doi: 10.3390/toxins9020049

Muhldorfer, I., Hacker, J., Keusch, G. T., Acheson, D. W., Tschape, H., Kane, A. V., et al. (1996). Regulation of the shiga-like toxin II operon in Escherichia coli. *Infect. Immun.* 64, 495–502. doi: 10.1128/IAI.64.2.495-502.1996

Muhlen, S., Ramming, I., Pils, M. C., Koeppel, M., Glaser, J., Leong, J., et al. (2020). Identification of antibiotics that diminish disease in a murine model of enterohemorrhagic *Escherichia coli* infection. *Antimicrob. Agents Chemother.* 64. doi: 10.1128/AAC.02159-19

Mukherjee, J., Chios, K., Fishwild, D., Hudson, D., O'donnell, S., Rich, S. M., et al. (2002a). Human Stx2-specific monoclonal antibodies prevent systemic complications of *Escherichia coli* O157:H7 infection. *Infect. Immun.* 70, 612–619. doi: 10.1128/IAI.70.2.612-619.2002

Mukherjee, J., Chios, K., Fishwild, D., Hudson, D., O'donnell, S., Rich, S. M., et al. (2002b). Production and characterization of protective human antibodies against shiga toxin 1. *Infect. Immun.* 70, 5896–5899. doi: 10.1128/IAI.70.10.5896-5899.2002

Mulvey, G. L., Marcato, P., Kitov, P. I., Sadowska, J., Bundle, D. R., and Armstrong, G. D. (2003). Assessment in mice of the therapeutic potential of tailored, multivalent shiga toxin carbohydrate ligands. *J. Infect. Dis.* 187, 640–649. doi: 10.1086/373996

Nakanishi, K., Morikane, S., Ichikawa, S., Kurohane, K., Niwa, Y., Akimoto, Y., et al. (2017). Protection of human colon cells from shiga toxin by plant-based recombinant secretory IgA. *Sci. Rep.* 7:45843. doi: 10.1038/srep45843

Nakanishi, K., Narimatsu, S., Ichikawa, S., Tobisawa, Y., Kurohane, K., Niwa, Y., et al. (2013). Production of hybrid-IgG/IgA plantibodies with neutralizing activity against shiga toxin 1. *PLoS ONE* 8:e80712. doi: 10.1371/journal.pone.0080712

Nakao, H., Kiyokawa, N., Fujimoto, J., Yamasaki, S., and Takeda, T. (1999). Monoclonal antibody to shiga toxin 2 which blocks receptor binding and neutralizes cytotoxicity. *Infect. Immun.* 67, 5717–5722. doi: 10.1128/IAI.67.11.5717-5722.1999

Nassar, F. J., Rahal, E. A., Sabra, A., and Matar, G. M. (2013). Effects of subinhibitory concentrations of antimicrobial agents on *Escherichia coli* O157:H7 shiga toxin release and role of the SOS response. *Foodborne Pathog. Dis.* 10, 805–812. doi: 10.1089/fpd.2013.1510

Nataro, J. P., and Kaper, J. B. (1998). Diarrheagenic *Escherichia coli*. *Clin. Microbiol. Rev.* 11, 142–201. doi: 10.1128/CMR.11.1.142

Nishikawa, K., Matsuoka, K., Kita, E., Okabe, N., Mizuguchi, M., Hino, K., et al. (2002). A therapeutic agent with oriented carbohydrates for treatment of infections by shiga toxin-producing *Escherichia coli* O157:H7. *Proc. Natl. Acad. Sci. U.S.A.* 99, 7669–7674. doi: 10.1073/pnas.112058999

Nishikawa, K., Matsuoka, K., Watanabe, M., Igai, K., Hino, K., Hatano, K., et al. (2005). Identification of the optimal structure required for a shiga toxin neutralizer with oriented carbohydrates to function in the circulation. *J. Infect. Dis.* 191, 2097–2105. doi: 10.1086/430388

Niu, Y. D., Johnson, R. P., Xu, Y., Mcallister, T. A., Sharma, R., Louie, M., et al. (2009). Host range and lytic capability of four bacteriophages against bovine and clinical human isolates of shiga toxin-producing *Escherichia coli* O157:H7. *J. Appl. Microbiol.* 107, 646–656. doi: 10.1111/j.1365-2672.2009.04231.x

Noel, R., Gupta, N., Pons, V., Goudet, A., Garcia-Castillo, M. D., Michau, A., et al. (2013). N-methyldihydroquinazolinone derivatives of retro-2 with enhanced efficacy against shiga toxin. *J. Med. Chem.* 56, 3404–3413. doi: 10.1021/jm4002346

Nogueira, M. C., Oyarzabal, O. A., and Gombas, D. E. (2003). Inactivation of *Escherichia coli* O157:H7, *Listeria monocytogenes,* and Salmonella in cranberry, lemon, and lime juice concentrates. *J. Food Prot.* 66, 1637–1641. doi: 10.4315/0362-028X-66.9.1637

Noris, M., Mescia, F., and Remuzzi, G. (2012). STEC-HUS, atypical HUS and TTP are all diseases of complement activation. *Nat. Rev. Nephrol.* 8, 622–633. doi: 10.1038/nrneph.2012.195

O'Brien, A. D., Newland, J. W., Miller, S. F., Holmes, R. K., Smith, H. W., and Formal, S. B. (1984). Shiga-like toxin-converting phages from *Escherichia coli* strains that cause hemorrhagic colitis or infantile diarrhea. *Science* 226, 694–696. doi: 10.1126/science.6387911

Ochoa, T. J., Chen, J., Walker, C. M., Gonzales, E., and Cleary, T. G. (2007). Rifaximin does not induce toxin production or phage-mediated lysis of shiga toxin-producing Escherichia coli. *Antimicrob. Agents Chemother.* 51, 2837–2841. doi: 10.1128/AAC.01397-06

Ogawa, M., Shimizu, K., Nomoto, K., Tanaka, R., Hamabata, T., Yamasaki, S., et al. (2001). Inhibition of *in vitro* growth of shiga toxin-producing *Escherichia coli* O157:H7 by probiotic Lactobacillus strains due to production of lactic acid. *Int. J. Food Microbiol.* 68, 135–140. doi: 10.1016/S0168-1605(01)00465-2

Oliveira, A. F., Cardoso, S. A., Almeida, F. B., De Oliveira, L. L., Pitondo-Silva, A., Soares, S. G., et al. (2012). Oral immunization with attenuated salmonella vaccine expressing *Escherichia coli* O157:H7 intimin gamma triggers both systemic and mucosal humoral immunity in mice. *Microbiol. Immunol.* 56, 513–522. doi: 10.1111/j.1348-0421.2012.00477.x

Orth, D., Grif, K., Zimmerhackl, L. B., and Wurzner, R. (2008). Prevention and treatment of enterohemorrhagic *Escherichia coli* infections in humans. *Expert. Rev. Anti. Infect. Ther.* 6, 101–108. doi: 10.1586/14787210.6.1.101

Orth, D., Khan, A. B., Naim, A., Grif, K., Brockmeyer, J., Karch, H., et al. (2009). Shiga toxin activates complement and binds factor H: evidence for an active role of complement in hemolytic uremic syndrome. *J. Immunol.* 182, 6394–6400. doi: 10.4049/jimmunol.0900151

Panos, G. Z., Betsi, G. I., and Falagas, M. E. (2006). Systematic review: are antibiotics detrimental or beneficial for the treatment of patients with *Escherichia coli* O157:H7 infection? *Aliment Pharmacol. Ther.* 24, 731–742. doi: 10.1111/j.1365-2036.2006.03036.x

Pape, L., Hartmann, H., Bange, F. C., Suerbaum, S., Bueltmann, E., and Ahlenstiel-Grunow, T. (2015). Eculizumab in typical Hemolytic Uremic Syndrome (HUS) With neurological involvement. *Medicine* 94:e1000. doi: 10.1097/MD.0000000000001000

Patel, J., Keelara, S., and Green, J. (2018). Inactivation of *Escherichia coli* O157:H7 and salmonella on fresh herbs by plant essential oils. *Foodborne Pathog. Dis.* 15, 332–338. doi: 10.1089/fpd.2017.2377

Paton, A. W., Morona, R., and Paton, J. C. (2000). A new biological agent for treatment of shiga toxigenic *Escherichia coli* infections and dysentery in humans. *Nat. Med.* 6, 265–270. doi: 10.1038/73111

Pedersen, M. G., Hansen, C., Riise, E., Persson, S., and Olsen, K. E. (2008). Subtype-specific suppression of shiga toxin 2 released from *Escherichia coli* upon exposure to protein synthesis inhibitors. *J. Clin. Microbiol.* 46, 2987–2991. doi: 10.1128/JCM.00871-08

Pellarin, M. G., Albrecht, C., Rojas, M. J., Aguilar, J. J., Konigheim, B. S., Paraje, M. G., et al. (2013). Inhibition of cytotoxicity of shiga toxin of *Escherichia coli* O157:H7 on vero cells by prosopis alba griseb (fabaceae) and ziziphus mistol griseb (rhamnaceae) extracts. *J. Food Prot.* 76, 1733–1739. doi: 10.4315/0362-028X.JFP-13-087

Perera, L. P., Marques, L. R., and O'Brien, A. D. (1988). Isolation and characterization of monoclonal antibodies to shiga-like toxin II of enterohemorrhagic *Escherichia coli* and use of the monoclonal antibodies in a colony enzyme-linked immunosorbent assay. *J. Clin. Microbiol.* 26, 2127–2131. doi: 10.1128/JCM.26.10.2127-2131.1988

Peterson, R. E., Klopfenstein, T. J., Erickson, G. E., Folmer, J., Hinkley, S., Moxley, R. A., et al. (2007). Effect of *Lactobacillus acidophilus* strain NP51 on *Escherichia coli* O157:H7 fecal shedding and finishing performance in beef feedlot cattle. *J. Food Prot* 70, 287–291. doi: 10.4315/0362-028X-70.2.287

Pittman, C. I., Geornaras, I., Woerner, D. R., Nightingale, K. K., Sofos, J. N., Goodridge, L., et al. (2012). Evaluation of lactic acid as an initial and secondary subprimal intervention for *Escherichia coli* O157:H7, non-O157 shiga toxin-producing *E. coli*, and a nonpathogenic *E. coli* surrogate for *E. coli* O157:H7. *J. Food. Prot.* 75, 1701–1708. doi: 10.4315/0362-028X.JFP-11-520

Raa, H., Grimmer, S., Schwudke, D., Bergan, J., Walchli, S., Skotland, T., et al. (2009). Glycosphingolipid requirements for endosome-to-Golgi transport of shiga toxin. *Traffic* 10, 868–882. doi: 10.1111/j.1600-0854.2009.00919.x

Rad, H. S., Mousavi, S. L., Rasooli, I., Amani, J., and Nadooshan, M. R. (2013). EspA-Intimin chimeric protein, a candidate vaccine against *Escherichia coli* O157:H7. *Iran J. Microbiol.* 5, 244–251.

Rahal, E. A., Fadlallah, S. M., Nassar, F. J., Kazzi, N., and Matar, G. M. (2015). Approaches to treatment of emerging shiga toxin-producing *Escherichia coli* infections highlighting the O104:H4 serotype. *Front. Cell Infect. Microbiol.* 5:24. doi: 10.3389/fcimb.2015.00024

Rahal, E. A., Kazzi, N., Kanbar, A., Abdelnoor, A. M., and Matar, G. M. (2011a). Role of rifampicin in limiting *Escherichia coli* O157:H7 shiga-like toxin expression and enhancement of survival of infected BALB/c mice. Int *J. Antimicrob. Agents* 37, 135–139. doi: 10.1016/j.ijantimicag.2010.10.009

Rahal, E. A., Kazzi, N., Sabra, A., Abdelnoor, A. M., and Matar, G. M. (2011b). Decrease in shiga toxin expression using a minimal inhibitory concentration of rifampicin followed by bactericidal gentamicin treatment enhances survival of *Escherichia coli* O157:H7-infected BALB/c mice. *Ann. Clin. Microbiol. Antimicrob.* 10:34. doi: 10.1186/1476-0711-10-34

Ran, X. Q., Wang, H. Z., Liu, J. J., Li, S., and Wang, J. F. (2008). The immunogenicity of fusion protein linking the carboxyl terminus of the B subunit of shiga toxin 2 to the B subunit of *E. coli* heat-labile enterotoxin. *Vet. Microbiol.* 127, 209–215. doi: 10.1016/j.vetmic.2007.08.021

Raya, R. R., Varey, P., Oot, R. A., Dyen, M. R., Callaway, T. R., Edrington, T. S., et al. (2006). Isolation and characterization of a new T-even bacteriophage, CEV1, and determination of its potential to reduce *Escherichia coli* O157:H7 levels in sheep. *Appl. Environ. Microbiol.* 72, 6405–6410. doi: 10.1128/AEM.03011-05

Riquelme-Neira, R., Rivera, A., Saez, D., Fernandez, P., Osorio, G., Del Canto, F., et al. (2015). Vaccination with DNA Encoding truncated enterohemorrhagic *Escherichia coli* (EHEC) Factor for adherence-1 Gene (efa-1') Confers protective immunity to mice infected with *E. coli* O157:H7. *Front. Cell Infect. Microbiol.* 5:104. doi: 10.3389/fcimb.2015.00104

Ritchie, J. M., Greenwich, J. L., Davis, B. M., Bronson, R. T., Gebhart, D., Williams, S. R., et al. (2011). An *Escherichia coli* O157-specific engineered pyocin prevents and ameliorates infection by *E. coli* O157:H7 in an animal model of diarrheal disease. *Antimicrob. Agents Chemother.* 55, 5469–5474. doi: 10.1128/AAC.05031-11

Rivas, L., Coffey, B., Mcauliffe, O., Mcdonnell, M. J., Burgess, C. M., Coffey, A., et al. (2010). *In vivo* and *ex vivo* evaluations of bacteriophages e11/2 and e4/1c for use in the control of *Escherichia coli* O157:H7. *Appl. Environ. Microbiol.* 76, 7210–7216. doi: 10.1128/AEM.01530-10

Rojas, R. L., Gomes, P. A., Bentancor, L. V., Sbrogio-Almeida, M. E., Costa, S. O., Massis, L. M., et al. (2010). Salmonella enterica serovar typhimurium vaccine strains expressing a nontoxic shiga-like toxin 2 derivative induce partial protective immunity to the toxin expressed by enterohemorrhagic *Escherichia coli*. *Clin. Vaccine Immunol.* 17, 529–536. doi: 10.1128/CVI.00495-09

Ruano-Gallego, D., Yara, D. A., Di Ianni, L., Frankel, G., Schuller, S., and Fernandez, L. A. (2019). A nanobody targeting the translocated intimin receptor inhibits the attachment of enterohemorrhagic *E. coli* to human colonic mucosa. *PLoS Pathog.* 15:e1008031. doi: 10.1371/journal.ppat.1008031

Rund, S. A., Rohde, H., Sonnenborn, U., and Oelschlaeger, T. A. (2013). Antagonistic effects of probiotic *Escherichia coli* nissle 1917 on EHEC strains of serotype O104:H4 and O157:H7. *Int. J. Med. Microbiol.* 303, 1–8. doi: 10.1016/j.ijmm.2012.11.006

Sabouri, S., Sepehrizadeh, Z., Amirpour-Rostami, S., and Skurnik, M. (2017). A minireview on the *in vitro* and *in vivo* experiments with anti-*Escherichia coli* O157:H7 phages as potential biocontrol and phage therapy agents. *Int. J. Food Microbiol.* 243, 52–57. doi: 10.1016/j.ijfoodmicro.2016.12.004

Safwat-Mohamed, D., Farouk-Ahmed, E., Mohamed-Mahmoud, A., Abd El-Baky, R. M., and John, J. (2018). Isolation and evaluation of cocktail phages for the control of multidrug-resistant *Escherichia coli* serotype O104: H4 and *E. coli* O157: H7 isolates causing diarrhea. *FEMS Microbiol. Lett.* 365:fnx275. doi: 10.1093/femsle/fnx275

Sargeant, J. M., Amezcua, M. R., Rajic, A., and Waddell, L. (2007). Pre-harvest interventions to reduce the shedding of *E. coli* O157 in the faeces of weaned domestic ruminants: a systematic review. *Zoonoses Public Health* 54, 260–277. doi: 10.1111/j.1863-2378.2007.01059.x

Schmidt, N., Barth, S. A., Frahm, J., Meyer, U., Danicke, S., Geue, L., et al. (2018). Decreased STEC shedding by cattle following passive and active vaccination based on recombinant *Escherichia coli* shiga toxoids. *Vet. Res.* 49:28. doi: 10.1186/s13567-018-0523-0

Scholl, D., Cooley, M., Williams, S. R., Gebhart, D., Martin, D., Bates, A., and Mandrell, R. (2009). An engineered R-type pyocin is a highly specific and sensitive bactericidal agent for the food-borne pathogen *Escherichia coli* O157:H7. *Antimicrob. Agents Chemother.* 53, 3074–3080. doi: 10.1128/AAC.01660-08

Scholl, D., Gebhart, D., Williams, S. R., Bates, A., and Mandrell, R. (2012). Genome sequence of *E. coli* O104:H4 leads to rapid development of a targeted antimicrobial agent against this emerging pathogen. *PLoS ONE* 7:e33637. doi: 10.1371/journal.pone.0033637

Secher, T., Shima, A., Hinsinger, K., Cintrat, J. C., Johannes, L., Barbier, J., et al. (2015). Retrograde trafficking inhibitor of shiga toxins reduces morbidity and mortality of mice infected with enterohemorrhagic *Escherichia coli*. *Antimicrob. Agents Chemother.* 59, 5010–5013. doi: 10.1128/AAC.00455-15

Seita, T., Kuribayashi, T., Honjo, T., and Yamamoto, S. (2013). Comparison of efficacies of bovine immune colostral antibody and each immunoglobulin class against verotoxin 2, flagellum and somatic cells of *Escherichia coli* O157:H7 in mice. *J. Microbiol. Immunol. Infect.* 46, 73–79. doi: 10.1016/j.jmii.2012.01.002

Serna, A. T., and Boedeker, E. C. (2008). Pathogenesis and treatment of shiga toxin-producing *Escherichia coli* infections. *Curr. Opin. Gastroenterol.* 24, 38–47. doi: 10.1097/MOG.0b013e3282f2dfb8

Sewlikar, S., and D'Souza, D. H. (2017). Antimicrobial effects of quillaja saponaria extract against *Escherichia coli* O157:H7 and the emerging non-o157 shiga toxin-producing *E. coli*. *J. Food Sci.* 82, 1171–1177. doi: 10.1111/1750-3841.13697

Sheng, H., Knecht, H. J., Kudva, I. T., and Hovde, C. J. (2006). Application of bacteriophages to control intestinal *Escherichia coli* O157:H7 levels in ruminants. *Appl. Environ. Microbiol.* 72, 5359–5366. doi: 10.1128/AEM.00099-06

Sheng, L., Olsen, S. A., Hu, J., Yue, W., Means, W. J., and Zhu, M. J. (2016). Inhibitory effects of grape seed extract on growth, quorum sensing, and virulence factors of CDC "top-six" non-O157 shiga toxin producing *E. coli*. *Int. J. Food Microbiol.* 229, 24–32. doi: 10.1016/j.ijfoodmicro.2016.04.001

Sheoran, A. S., Chapman-Bonofiglio, S., Harvey, B. R., Mukherjee, J., Georgiou, G., Donohue-Rolfe, A., et al. (2005). Human antibody against shiga toxin 2 administered to piglets after the onset of diarrhea due to *Escherichia coli* O157:H7 prevents fatal systemic complications. *Infect. Immun.* 73, 4607–4613. doi: 10.1128/IAI.73.8.4607-4613.2005

Silberstein, C., Lucero, M. S., Zotta, E., Copeland, D. P., Lingyun, L., Repetto, H. A., et al. (2011). A glucosylceramide synthase inhibitor protects rats against the cytotoxic effects of shiga toxin 2. *Pediatr. Res.* 69, 390–394. doi: 10.1203/PDR.0b013e318211dd57

Skinner, C., Zhang, G., Patfield, S., and He, X. (2015). An *in vitro* combined antibiotic-antibody treatment eliminates toxicity from shiga toxin-producing *Escherichia coli*. *Antimicrob. Agents Chemother.* 59, 5435–5444. doi: 10.1128/AAC.00763-15

Smith, M. J., Teel, L. D., Carvalho, H. M., Melton-Celsa, A. R., and O'Brien, A. D. (2006). Development of a hybrid shiga holotoxoid vaccine to elicit heterologous protection against shiga toxins types 1 and 2. *Vaccine* 24, 4122–4129. doi: 10.1016/j.vaccine.2006.02.035

Sreerohini, S., Balakrishna, K., and Parida, M. (2019). Oral immunization of mice with lactococcus lactis expressing shiga toxin truncate confers enhanced protection against shiga toxins of *Escherichia coli* O157:H7 and Shigella dysenteriae. *APMIS* 127, 671–680. doi: 10.1111/apm.12983

Stanford, K., Mcallister, T. A., Niu, Y. D., Stephens, T. P., Mazzocco, A., Waddell, T. E., et al. (2010). Oral delivery systems for encapsulated bacteriophages targeted at *Escherichia coli* O157:H7 in feedlot cattle. *J. Food Prot.* 73, 1304–1312. doi: 10.4315/0362-028X-73.7.1304

Stearns-Kurosawa, D. J., Collins, V., Freeman, S., Debord, D., Nishikawa, K., Oh, S. Y., et al. (2011). Rescue from lethal shiga toxin 2-induced renal failure with a cell-permeable peptide. *Pediatr. Nephrol.* 26, 2031–2039. doi: 10.1007/s00467-011-1913-y

Strockbine, N. A., Marques, L. R., Holmes, R. K., and O'Brien, A. D. (1985). Characterization of monoclonal antibodies against shiga-like toxin from *Escherichia coli*. *Infect. Immun.* 50, 695–700. doi: 10.1128/IAI.50.3.695-700.1985

Takahashi, M., Taguchi, H., Yamaguchi, H., Osaki, T., Komatsu, A., and Kamiya, S. (2004). The effect of probiotic treatment with clostridium butyricum on enterohemorrhagic *Escherichia coli* O157:H7 infection in mice. *FEMS Immunol. Med. Microbiol.* 41, 219–226. doi: 10.1016/j.femsim.2004.03.010

Takemasa, N., Ohnishi, S., Tsuji, M., Shikata, T., and Yokoigawa, K. (2009). Screening and analysis of spices with ability to suppress verocytotoxin

production by *Escherichia coli* O157. *J. Food Sci.* 74, M461–466. doi: 10.1111/j.1750-3841.2009.01326.x

Trachtman, H., Cnaan, A., Christen, E., Gibbs, K., Zhao, S., Acheson, D. W., et al. (2003). Effect of an oral shiga toxin-binding agent on diarrhea-associated hemolytic uremic syndrome in children: a randomized controlled trial. *JAMA* 290, 1337–1344. doi: 10.1001/jama.290.10.1337

Tremblay, J. M., Mukherjee, J., Leysath, C. E., Debatis, M., Ofori, K., Baldwin, K., et al. (2013). A single VHH-based toxin-neutralizing agent and an effector antibody protect mice against challenge with shiga toxins 1 and 2. *Infect. Immun.* 81, 4592–4603. doi: 10.1128/IAI.01033-13

Tsuji, T., Shimizu, T., Sasaki, K., Tsukamoto, K., Arimitsu, H., Ochi, S., et al. (2008). A nasal vaccine comprising B-subunit derivative of shiga toxin 2 for cross-protection against shiga toxin types 1 and 2. *Vaccine* 26, 2092–2099. doi: 10.1016/j.vaccine.2008.02.034

Tzipori, S., Sheoran, A., Akiyoshi, D., Donohue-Rolfe, A., and Trachtman, H. (2004). Antibody therapy in the management of shiga toxin-induced hemolytic uremic syndrome. *Clin. Microbiol. Rev.* 17, 926–941, table of contents. doi: 10.1128/CMR.17.4.926-941.2004

Voravuthikunchai, S. P., Suwalak, S., and Mitranan, W. (2012). Ellagitannin from quercus infectoria eradicates intestinal colonization and prevents renal injuries in mice infected with *Escherichia coli* O157 : H7. *J. Med. Microbiol.* 61, 1366–1372. doi: 10.1099/jmm.0.044495-0

Walterspiel, J. N., Ashkenazi, S., Morrow, A. L., and Cleary, T. G. (1992). Effect of subinhibitory concentrations of antibiotics on extracellular shiga-like toxin I. *Infection* 20, 25–29. doi: 10.1007/BF01704889

Wan, C. S., Zhou, Y., Yu, Y., Peng, L. J., Zhao, W., and Zheng, X. L. (2011). B-cell epitope KT-12 of enterohemorrhagic *Escherichia coli* O157:H7: a novel peptide vaccine candidate. *Microbiol. Immunol.* 55, 247–253. doi: 10.1111/j.1348-0421.2011.00316.x

Wang, L., Qu, K., Li, X., Cao, Z., Wang, X., Li, Z., et al. (2017). Use of bacteriophages to control *Escherichia coli* O157:H7 in domestic ruminants, meat products, and fruits and vegetables. *Foodborne Pathog. Dis.* 14, 483–493. doi: 10.1089/fpd.2016.2266

Watanabe, M., Matsuoka, K., Kita, E., Igai, K., Higashi, N., Miyagawa, A., et al. (2004). Oral therapeutic agents with highly clustered globotriose for treatment of shiga toxigenic *Escherichia coli* infections. *J. Infect. Dis.* 189, 360–368. doi: 10.1086/381124

Watanabe-Takahashi, M., Sato, T., Dohi, T., Noguchi, N., Kano, F., Murata, M., et al. (2010). An orally applicable shiga toxin neutralizer functions in the intestine to inhibit the intracellular transport of the toxin. *Infect. Immun.* 78, 177–183. doi: 10.1128/IAI.01022-09

Wen, S. X., Teel, L. D., Judge, N. A., and O'Brien, A. D. (2006). A plant-based oral vaccine to protect against systemic intoxication by shiga toxin type 2. *Proc. Natl. Acad. Sci. U.S.A.* 103, 7082–7087. doi: 10.1073/pnas.0510843103

Wisener, L. V., Sargeant, J. M., O'connor, A. M., Faires, M. C., and Glass-Kaastra, S. K. (2015). The use of direct-fed microbials to reduce shedding of *Escherichia coli* O157 in beef cattle: a systematic review and meta-analysis. *Zoonoses Public Health* 62, 75–89. doi: 10.1111/zph.12112

Yamagami, S., Motoki, M., Kimura, T., Izumi, H., Takeda, T., Katsuura, Y., and Matsumoto, Y. (2001). Efficacy of postinfection treatment with anti-shiga toxin (Stx) 2 humanized monoclonal antibody TMA-15 in mice lethally challenged with Stx-producing *Escherichia coli*. *J. Infect. Dis.* 184, 738–742. doi: 10.1086/323082

Yoh, M., Frimpong, E. K., and Honda, T. (1997). Effect of antimicrobial agents, especially fosfomycin, on the production and release of Vero toxin by enterohaemorrhagic *Escherichia coli* O157:H7. *FEMS Immunol. Med. Microbiol.* 19, 57–64. doi: 10.1111/j.1574-695X.1997.tb01072.x

Yoh, M., Frimpong, E. K., Voravuthikunchai, S. P., and Honda, T. (1999). Effect of subinhibitory concentrations of antimicrobial agents (quinolones and macrolide) on the production of verotoxin by enterohemorrhagic *Escherichia coli* O157:H7. *Can J. Microbiol.* 45, 732–739. doi: 10.1139/w99-069

Yoshimura, K., Fujii, J., Taniguchi, H., and Yoshida, S. (1999). Chemotherapy for enterohemorrhagic *Escherichia coli* O157:H infection in a mouse model. *FEMS Immunol. Med. Microbiol.* 26, 101–108. doi: 10.1111/j.1574-695X.1999.tb01376.x

Yu, S., Gu, J., Wang, H. G., Wang, Q. X., Luo, P., Wu, C., et al. (2011). Identification of a novel linear epitope on EspA from enterohemorrhagic *E. coli* using a neutralizing and protective monoclonal antibody. *Clin. Immunol.* 138, 77–84. doi: 10.1016/j.clim.2010.09.009

Zadravec, P., Mareckova, L., Petrokova, H., Hodnik, V., Perisic Nanut, M., Anderluh, G., et al. (2016). Development of recombinant lactococcus lactis displaying albumin-binding domain variants against shiga toxin 1 B Subunit. *PLoS ONE* 11:e0162625. doi: 10.1371/journal.pone.0162625

Zangari, T., Melton-Celsa, A. R., Panda, A., Smith, M. A., Tatarov, I., De Tolla, L., et al. (2014). Enhanced virulence of the *Escherichia coli* O157:H7 spinach-associated outbreak strain in two animal models is associated with higher levels of Stx2 production after induction with ciprofloxacin. *Infect. Immun.* 82, 4968–4977. doi: 10.1128/IAI.02361-14

Zhang, Q., Donohue-Rolfe, A., Krautz-Peterson, G., Sevo, M., Parry, N., Abeijon, C., et al. (2009). Gnotobiotic piglet infection model for evaluating the safe use of antibiotics against *Escherichia coli* O157:H7 infection. *J. Infect. Dis.* 199, 486–493. doi: 10.1086/596509

Zhang, X., Mcdaniel, A. D., Wolf, L. E., Keusch, G. T., Waldor, M. K., and Acheson, D. W. (2000). Quinolone antibiotics induce shiga toxin-encoding bacteriophages, toxin production, and death in mice. *J. Infect. Dis.* 181, 664–670. doi: 10.1086/315239

Zimmerhackl, L. B. (2000). *E. coli,* antibiotics, and the hemolytic-uremic syndrome. *New Engl. J. Med.* 342, 1990–1991. doi: 10.1056/NEJM200006293422611

Conflict of Interest: The authors declare that the research was conducted in the absence of any commercial or financial relationships that could be construed as a potential conflict of interest.

frontiers in Cellular and Infection Microbiology

ORIGINAL RESEARCH
published: 03 June 2020
doi: 10.3389/fcimb.2020.00260

Tracing Back the Evolutionary Route of Enteroinvasive *Escherichia coli* (EIEC) and *Shigella* Through the Example of the Highly Pathogenic O96:H19 EIEC Clone

Valeria Michelacci[1], Rosangela Tozzoli[1], Silvia Arancia[1], Alfio D'Angelo[1], Arianna Boni[1], Arnold Knijn[1], Gianni Prosseda[2], David R. Greig[3], Claire Jenkins[3], Teresa Camou[4], Alfredo Sirok[4], Armando Navarro[5], Felipe Schelotto[6], Gustavo Varela[6] and Stefano Morabito[1]*

[1] Department of Food Safety, Nutrition and Veterinary Public Health, Istituto Superiore di Sanità, Rome, Italy, [2] Department of Biology and Biotechnology "Charles Darwin", Università Sapienza di Roma, Rome, Italy, [3] Gastrointestinal Bacteria Reference Unit (GBRU), Public Health England, E. coli, Shigella, Yersinia and Vibrio Reference Service, National Infection Service, London, United Kingdom, [4] Departamento de Laboratorios, Ministerio de Salud Pública, Montevideo, Uruguay, [5] Public Health Department, Medicine Faculty, Universidad Nacional Autónoma de Mexico (UNAM), Mexico City, Mexico, [6] Departamento de Bacteriología y Virología, Facultad de Medicina, Instituto de Higiene, Universidad de la República, Montevideo, Uruguay

OPEN ACCESS

Edited by:
Tânia Aparecida Tardelli Gomes, Federal University of São Paulo, Brazil

Reviewed by:
Rosa Maria Silva, Federal University of São Paulo, Brazil
Ulrich Dobrindt, University of Münster, Germany

***Correspondence:**
Valeria Michelacci
valeria.michelacci@iss.it

Specialty section:
This article was submitted to Molecular Bacterial Pathogenesis, a section of the journal Frontiers in Cellular and Infection Microbiology

Received: *22 January 2020*
Accepted: *04 May 2020*
Published: *03 June 2020*

Citation:
Michelacci V, Tozzoli R, Arancia S, D'Angelo A, Boni A, Knijn A, Prosseda G, Greig DR, Jenkins C, Camou T, Sirok A, Navarro A, Schelotto F, Varela G and Morabito S (2020) Tracing Back the Evolutionary Route of Enteroinvasive Escherichia coli (EIEC) and Shigella Through the Example of the Highly Pathogenic O96:H19 EIEC Clone. Front. Cell. Infect. Microbiol. 10:260. doi: 10.3389/fcimb.2020.00260

Enteroinvasive *Escherichia coli* (EIEC) cause intestinal illness through the same pathogenic mechanism used by *Shigella* spp. The latter species can be typed through genomic and phenotypic methods used for *E. coli* and have been proposed for reclassification within *E. coli* species. Recently the first appearance of a highly pathogenic EIEC O96:H19 was described in Europe as the causative agent of two large outbreaks that occurred in Italy and in the United Kingdom. In contrast to *Shigella* spp and to the majority of EIEC strains, EIEC O96:H19 fermented lactose, lacked pathoadaptive mutations, and showed good fitness in extracellular environment, similarly to non-pathogenic *E. coli,* suggesting they have emerged following acquisition of the invasion plasmid by a non-pathogenic *E. coli*. Here we describe the whole genome comparison of two EIEC O96:H19 strains isolated from severe cases of diarrhea in Uruguay in 2014 with the sequences of EIEC O96:H19 available in the public domain. The phylogenetic comparison grouped all the O96:H19 strains in a single cluster, while reference EIEC strains branched into different clades with *Shigella* strains occupying apical positions. The comparison of the virulence plasmids showed the presence of a complete conjugation region in at least one O96:H19 EIEC. Reverse Transcriptase Real Time PCR experiments confirmed in this strain the expression of the pilin-encoding gene and conjugation experiments suggested its ability to mobilize an accessory plasmid in a recipient strain. Noteworthy, the *tra* region was comprised between two reversely oriented IS*600* elements, which were also found as remnants in another EIEC O96:H19 plasmid lacking the *tra locus*. We hypothesize that an IS-mediated recombination mechanism may have caused the loss of the conjugation region commonly observed in EIEC and *Shigella* virulence plasmids. The results of this study support the hypothesis of EIEC

originating from non-pathogenic *E. coli* through the acquisition of the virulence plasmid via conjugation. Remarkably, this study showed the ability of a circulating EIEC strain to mobilize plasmids through conjugation, suggesting a mechanism for the emergence of novel EIEC clones.

Keywords: EIEC, phylogenomics, conjugation, evolution, emerging clones

INTRODUCTION

Enteroinvasive *Escherichia coli* (EIEC) cause disease in humans, characterized by abdominal cramps, bloody and mucous diarrhea (van den Beld and Reubsaet, 2012). EIEC are able to invade and multiply in the human colonic epithelial cells analogously to the mechanism used by *Shigella* spp (Nataro and Kaper, 1998; Lan et al., 2004), making it difficult to differentiate between the disease caused by the two microorganisms. The main virulence genes of EIEC and *Shigella* are harbored on a large virulence plasmid termed pINV. These include the *mxi* and *spa* genes encoding a type three secretion system (T3SS) as well as the *ipaB*, *ipaC*, *ipaD*, and *icsA* genes encoding effectors necessary to invade and disseminate into the host cells (Pasqua et al., 2017). The transmission of the infection occurs *via* the fecal-oral route and the incidence of EIEC and *Shigella* infections is higher in geographical areas where there is less or no access to safe drinking water, health services, or electricity. However, infection may also occur by the ingestion of contaminated food or water. During the last decade an increase in the number of cases of EIEC infections has been observed in Europe, with two large outbreaks, suspected to be linked to the consumption of contaminated food, occurred in Italy and in the United Kingdom between 2012 (Escher et al., 2014) and 2014 (Newitt et al., 2016). The strains responsible for both the outbreaks belonged to the O96:H19 serotype and sequence type 99 (ST-99), which had never been described as EIEC before 2012. A third isolate sharing the same characteristics was also identified as the cause of a sporadic case of EIEC infection occurred in Spain in 2013, confirming the circulation of such clone in Europe (Michelacci et al., 2016).

The genomic characterization of these three strains enabled the detection of an IncFII plasmid larger than 200 kbp, resembling the invasion plasmid of EIEC and *Shigella* and harboring the virulence genes essential for intracellular localization and spread, but in a genomic background different from that of reference EIEC and *Shigella* strains (Michelacci et al., 2016). This led to the hypothesis that O96:H19 EIEC clone might have emerged after the acquisition of the virulence plasmid by an *E. coli* with the phenotypic and biochemical properties of a commensal *E. coli* strain (Michelacci et al., 2016).

In the present study, we report the description of two O96:H19 EIEC strains isolated from two patients in Uruguay in 2014 and describe the genomic comparison of their chromosome and plasmids with those of the O96:H19 EIEC strains isolated in Europe. Our data support the hypothesis that this EIEC clone may have emerged and spread thanks to pINV mobilization through conjugation and provide evidence that at least one of the EIEC O96:H19 studied possessed a complete conjugation region in the pINV and displayed a functional plasmid mobilization machinery.

MATERIALS AND METHODS

Bacterial Strains and Genomes

Two EIEC strains from Uruguay were included in this study: the strains V48 and V73 were isolated from fecal samples of an 18 month-old girl with bloody diarrhea and of a 14 year-old girl with fever, vomiting, abdominal pain, bloody diarrhea and shock in April and October 2014, respectively. The latter strain was isolated form a case part of a foodborne outbreak and there was no epidemiological link between the two cases (Peirano et al., 2018).

Genomes of EIEC O96:H19 available in the public domain were included in the comparative analyses. These included those of strains EF432, 152661 and CNM-2113/13, isolated during EIEC outbreaks occurring in Italy (Escher et al., 2014; Michelacci et al., 2016) and the UK (Michelacci et al., 2016; Newitt et al., 2016) and from a sporadic case in Spain, respectively (Michelacci et al., 2016), and the genomes of four other EIEC O96:H19 strains described in a previous study on EIEC circulating in the United Kingdom (details in **Supplementary Table 1**) (Cowley et al., 2018). The presence of the *ipaH* genetic marker of EIEC and *Shigella* was confirmed by PCR (Luscher and Altwegg, 1994) or *in silico* in all the *E. coli* strains included in the study.

The *E. coli* K12 strain CSH26 Nal^r (Sorensen et al., 2003), showing resistance to nalidixic acid and sensitivity to streptomycin and sulfamethoxazole, was used as recipient strain in conjugation experiments with donor EF432 strain.

Genomes from reference EIEC and *Shigella* strains as well as from EIEC strains recently described to circulate in the UK and belonging to different serotypes (Cowley et al., 2018) were retrieved from international databases and analyzed to give context to the phylogenetic comparison (details in **Supplementary Table 1**).

DNA Extraction and Sequencing

The total DNA of the strains V48, V73, and CNM-2113/13 was extracted from two ml of overnight bacterial cultures with the GRS Genomic DNA kit (GRISP, Porto, Portugal) and sequenced on an Ion Torrent S5 platform (Life Technologies, Carlsbad, USA). In detail, 400 bp fragments libraries were prepared by using the NEBNext® Fast DNA Fragmentation & Library Prep Set for Ion Torrent (New England Biolabs, Ipswich, Massachusetts, USA). The template preparation and sequencing run were performed with the ION 520/530 KIT-OT2 following the manufacturer's instructions for 400 bp DNA libraries on ION 530 chips.

The genome of the 152661 strain from the outbreak in the UK, already sequenced through Illumina technology for routine surveillance of *E. coli* and *Shigella* by Public Health England (**Supplementary Table 1**), was re-sequenced using a MinION system (Oxford Nanopore Technologies Ltd, Oxford, UK), producing long reads, with the aim of closing the complete sequence of the chromosome and the plasmids harbored by this strain.

In detail, total genomic DNA of 152661 strain was extracted using the Wizard Genomic DNA Purification kit (Promega, Madison, WI, USA) with significant modifications from manufacturer's instructions including no vortexing steps, double incubation and elution times and pre-chilling of 70% ethanol and 99% isopropanol before use. Library preparation was performed using the SQK-RBK004 (rapid) library preparation kit (Oxford Nanopore Technologies Ltd, Oxford, UK) according to manufacturer's instructions. The sequencing library was loaded onto a FLO-MIN106 R9.4.1 flow cell and sequenced on the MinION for 24 h.

The sequencing data generated during this project has been uploaded to the EMBL-ENA sequence database in the study with accession number PRJEB35723 and at NCBI Bioproject with Acc. No. PRJNA315192 (details in **Supplementary Table 1**).

Bioinformatics Analysis

Basic Analyses: Trimming and Assembly

The bioinformatics analyses of Illumina and Ion Torrent data were performed through the ARIES instance of the Galaxy bioinformatics framework (https://www.iss.it/site/aries) as previously described (Michelacci et al., 2016). Briefly, FastQC was used for quality check and "FastQ Positional and Quality Trimming" (Cuccuru et al., 2014) for trimming the raw reads. The contigs were assembled from Illumina and Ion Torrent trimmed data using SPADES version 3.12.0 (Bankevich et al., 2012), followed by the tool "Filter SPAdes repeats" Galaxy Version 1.0.1 (https://github.com/phac-nml/galaxy_tools/). Default parameters were applied in the two steps.

As for the sample 152661, the data deriving from Illumina and Nanopore sequencing platforms were integrated. In detail, data produced from the MinION in a raw FAST5 format was basecalled and de-multiplexed using Albacore V2.3.3 (Oxford Nanopore Technologies, ONT) and Deepbinner v0.2.0 (Wick et al., 2018) to obtain sample-specific files in FASTQ format. Run metrics were generated using Nanoplot v1.8.1 (De Coster et al., 2018). The barcode and y-adapter were trimmed and chimeric reads split using Porechop v0.2.4[1]. Finally, the trimmed reads were filtered using Filtlong v0.1.1 with the following parameters: min length = 1,000, keep percent = 90 and target bases = 550 Mbp, to generate ∼100x coverage with the longest and highest quality reads[2].

Trimmed ONT FASTQ files were assembled using Canu v1.7 (Koren et al., 2017) and the filtered ONT FASTQ files were assembled using both Unicycler v0.4.2 (Wick et al., 2017) with the following parameters: min_fasta_length=1000, mode=normal. The assembly showing the highest N50 and lowest number of contigs, with an assembly size comprised between 5.3 and 6.0 Mbp, were used for the following analyses. Polishing of the assemblies was performed in a three-step process, firstly using Nanopolish v0.11.1 (Loman et al., 2015) with both the trimmed ONT FASTQs and FAST5s files accounting for methylation using the –methylation-aware=dcm and –min-candidate-frequency=0.5.

Secondly, Pilon v1.22 (Walker et al., 2014) was applied with Illumina FASTQ reads (Acc. No. SRR4181492) as the query dataset with the use of BWA v0.7.17 (Li and Durbin, 2010) and Samtools v1.7 (Li et al., 2009). Finally, Racon v1.2.1 (Vaser et al., 2017) also using BWA v0.7.17 (Li and Durbin, 2010) and Samtools v1.7 (Li et al., 2009) was used with the Illumina reads for two cycles to produce a final assembly for each of the samples. The chromosome from the assembly was re-circularized and closed and re-orientated to start at the *dnaA* gene, as in the reference sequence of K12 *E. coli* MG1655 strain (Acc. No. NC_000913), using the –fixstart parameter in circlator v1.5.5 (Hunt et al., 2015).

The completely assembled sequence of 152661 resulting from this process was used as such for chromosome and plasmids comparison, strain characterization and phylogenetic analysis, as described later.

WGS Analysis for Strain Characterization, Chromosome, and Plasmids Comparison and Phylogenetic Analysis

The WGS analyses for strain characterization and typing were performed through ARIES webserver (https://www.iss.it/site/aries). Multi Locus Sequence Typing (MLST) was inferred from the trimmed Illumina and Ion Torrent reads using the SRST2 tool (Inouye et al., 2014) and applying the scheme developed by Wirth and colleagues (Wirth et al., 2006). The "*E. coli* Serotyper" tool (Galaxy Version 1.1) was used with default parameters to interrogate the database of reference sequences for the determination of the serotypes (Joensen et al., 2015). The virulence genes typical of EIEC and *Shigella* were searched in the genome sequences as previously described Michelacci et al. (2016). Moreover, the assembled sequences of the EIEC O96:H19 strains were tested for the presence of virulence genes typical of other pathotypes of *E. coli* (Joensen et al., 2014) performing blastn analysis, using the threshold of minimum 90% of sequence identity and 80% of gene coverage.

The complete list of Accession Numbers of the sequences included in the comparison analysis is provided in **Supplementary Table 1**.

The Prokka tool (Seemann, 2014) was used for the functional annotation of the assembled sequences, using the *E. coli* specific gene database. Blast Ring Image Generator (BRIG) software v0.95 (Alikhan et al., 2011) was used with default parameters to compare the completely assembled sequences of the chromosome and virulence plasmid of the EIEC strains from Italy (EF432) (Pettengill et al., 2015a) used as reference sequences, with those of the other EIEC O96:H19 considered in this study. This analysis also included the completely assembled sequence of the largest plasmid of strain 152661 (Acc. No. CP046677).

[1] *Porechop*. https://github.com/rrwick/Porechop
[2] *Filtlong*. https://github.com/rrwick/Filtlong

The presence of pathoadaptive mutations in *cadA, cadB, cadC, speG, nadA*, and *nadB* was investigated and the sequences of *speA, speB, speC, speD, speE*, and *speF* genes verified as previously described (Michelacci et al., 2016) through the use of MAUVE software (suggested development snapshot 2015-02-26) (Rissman et al., 2009).

The detection of genetic elements involved in conjugation and the design of the maps of the closed plasmids were performed through the OriT Finder tool available online (http://202.120.12.134/oriTfinder/oriTfinder.html) with default parameters by uploading the annotated Genbank files produced with the Prokka software. MAUVE software (Rissman et al., 2009) was used for a deeper comparison of the conjugative regions in a set of plasmid sequences selected on the basis of the results of the BRIG analysis. The ISfinder webserver (https://www-is.biotoul.fr) (Siguier et al., 2006) was used to characterize and compare the insertion elements identified at the two sides of the conjugation region of pINV from strain EF432.

The core genome MLST (cgMLST) comparison was performed with the chewBBACA tool version 2.0.13 (Silva et al., 2018) with default parameters and used the database developed by EnteroBase (https://enterobase.warwick.ac.uk/) and curated in the framework of INNUENDO project, comprising the analysis of 2360 *loci* (Llarena et al., 2018) to call the alleles. The Minimum Spanning Tree was generated by analyzing the allelic matrix on the PHYLOViZ online web-based tool (Ribeiro-Goncalves et al., 2016).

Analysis of the Expression of *traA* Pilin-Encoding Gene

RNA was extracted from one ml of overnight cultures of the strain EF432 grown at 30° and 37°C using the Norgen RNA/Protein Purification Kit (Norgen Biotek, Thorold, ON, Canada). In detail, 1 μg of extracted RNA was used for DNA removal and retro-transcription with the QuantiTect Reverse Transcription (Qiagen, Germantown, MD, USA). Two μl of the cDNA solutions were used in Real Time PCR reactions targeting *traA* gene, encoding the pilin, in 40 cycles of a two steps thermal profile (15 s at 95°C and 1 min at 55°C) using the following primers and probes: traA_FWD: AGTGATCCCGGTTGCTGTTT; traA_REV: GTACATGACTGCACCGACCA; traA_probe: CTTCTGCTGGTAAAGGCACG. The efficiency of the reaction was evaluated by using serial dilution (10^{-1},10^{-2}, 10^{-3}, and 10^{-4}) of a 11.3 ng/μl DNA preparation purified from an overnight culture of EF432 strain as template in the same amplification run. The reactions were duplexed with reagents targeting *gapA* reference housekeeping gene, as previously described (Fitzmaurice et al., 2004). A negative control reaction was performed using non-retrotranscribed RNA. The efficiency, R^2 and M values of the *traA* gene amplification were compared to those of the reaction targeting *gapA* gene.

Bacterial Conjugation

Overnight cultures of donor strain EF432 and recipient strain CSH26 Nal^r were diluted 1:10 in TSB and refreshed for 1.5 h. Two ml of each culture were mixed and incubated for 3 h at 37°C without shaking. The selective marker for the recipient strain was nalidixic acid, as EF432 was proved to be susceptible to its presence in growth media. As no selection markers were found on pINV, CongoRed was used as differential additive in combination with nalidixic acid, due to its ability to identify *E. coli* strains harboring pINV plasmid as red colonies (Maurelli et al., 1984). One hundred μl of undiluted conjugation mix and 10^{-1}, 10^{-2}, and 10^{-3} serial dilutions were then plated and incubated at 37°C on two different media: CongoRed TSA plates supplied with 10 μg/ml of nalidixic acid and LB plates containing 10 μg/ml of nalidixic acid and 10 μg/ml of streptomycin. The colonies obtained on the latter were then streaked on LB plates containing 10 μg/ml of sulfamethoxazole for confirming the presence of the resistance plasmid of strain EF432.

RESULTS

Genomic Characterization of O96:H19 EIEC Strains Isolated From Uruguay

The genomic sequences of the V48 and V73 strains isolated in Uruguay were assembled in 141 and 139 contigs with N50 values of 113,473 and 103,437 bp, respectively. *In silico* typing confirmed the O96:H19 serotype and assigned to the strains the ST-99, the same Sequence Type identified in the already described O96:H19 EIEC (Michelacci et al., 2016). The virulence gene content and the presence of pathoadaptive mutations was investigated in the strains from Uruguay and compared to the same information obtained from the whole genome sequences of all the EIEC O96:H19 strains included in the study.

The results of the identification of the virulence genes typical of EIEC and *Shigella* are shown in **Supplementary Table 2**. All the strains showed the same virulence gene asset already described for the O96:H19 isolated in Europe (Michelacci et al., 2016). A major exception was the strain identified with the Acc. No. SRR4786227 among the selected UK strains, which showed a peculiar asset of plasmid-borne virulence genes. In particular, the presence of the genes *ipaH*, *ospG, virA*, and *virF* and the absence of the region known as "entry region," encoding the T3SS and its effectors were observed. On the other hand, the absence of *ospG* virulence gene was identified in two of these (Acc. No. SRR3578973 and SRR3578582), while in remaining one (Acc. No. SRR3578770) *ospG* gene was present, but the genes *virA* and *icsA* were lacking.

The detection of virulence genes of pathogenic *E. coli* other than EIEC allowed identifying the presence of *lpfA* and *capU* genes in all the O96:H19 strains. In particular, in the completely assembled sequences available of strains EF432 and 152661, *lpfA* gene was found on the chromosome while *capU* was detected in the virulence plasmid pINV.

The analysis of pathoadaptive mutations highlighted their absence in all the strains tested.

The comparison of the chromosomes of all the O96:H19 strains investigated is presented in **Supplementary Figure 1**, and showed a similar structure in all the genomes investigated. Nevertheless, some short fragments resulted only present in the sequence of the completely assembled chromosomes of

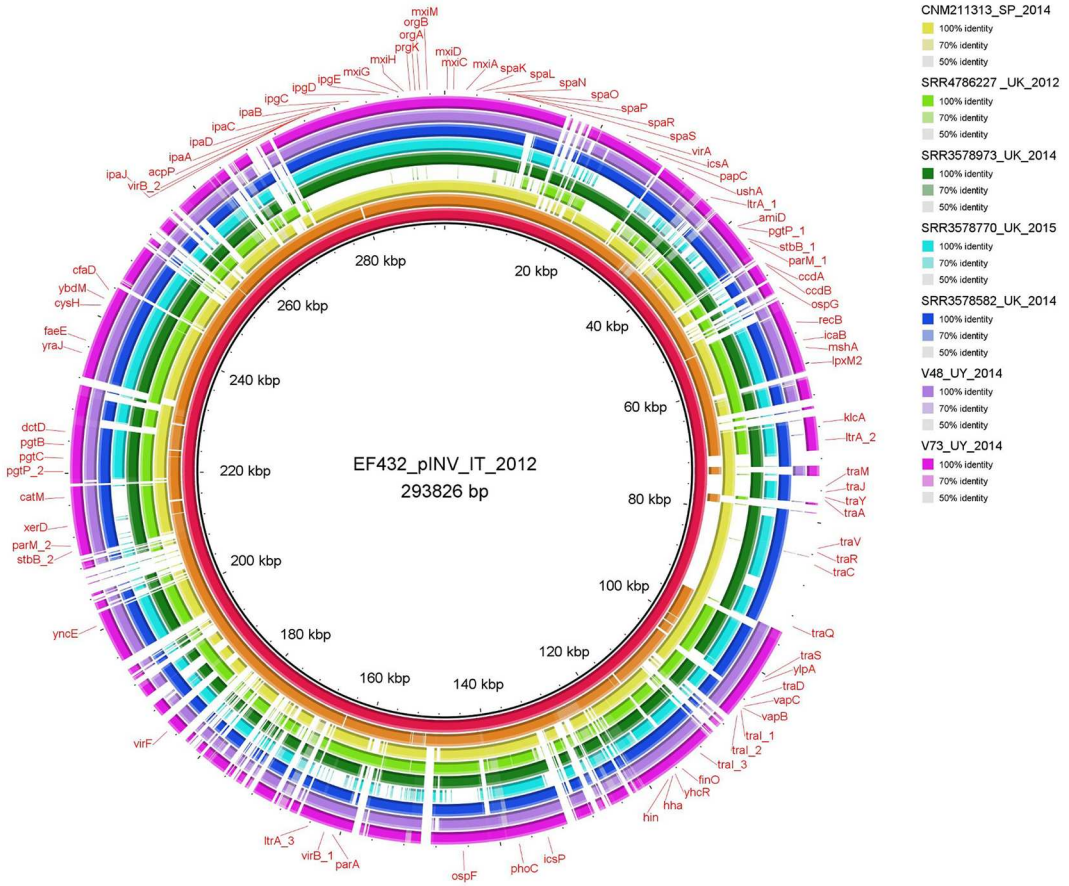

FIGURE 1 | Comparison of invasion plasmids of O96:H19 EIEC strains. The completely assembled pINV from EF432 strain (inner circle, red color) responsible of the outbreak occurred in Italy in 2012 was used as reference for alignment and gene annotation.

strains EF432 and 152661, mainly representing regions harboring prophages and encoding tRNAs and rRNAs. The complete list of these regions differentially present in the genomes, together with the encoded functions derived from annotation is presented in **Supplementary Table 3**.

Comparison of the Invasion Plasmids

The comparison of the sequences of invasion plasmids showed the absence of the region comprising *tra* genes in four of the nine O96:H19 strains assayed. The same region was instead present in the sequence of the invasion plasmid of the EIEC O96:H19 strain EF432 isolated in Italy (**Figure 1**). In detail, the sequences of pINV of the strains V48, V73, 152661 and that of the strain with the Acc. No. SRR4786227 completely lacked these genetic *loci*. Conversely, the strain from Spain CNM-2113/13 and three of the other isolates from the UK showed the presence of this *locus*, although apparently lacking some genetic fragments in the region (**Figure 1**).

Interestingly, a fragment longer than 30 kbp, corresponding to the "entry region" encoding the T3SS and its effectors, was absent from the plasmid of SRR4786227 strain, confirming the virulotyping results.

Mobilization Analysis of the Invasion Plasmids of O96:H19 EIEC Strains

In order to investigate the possibility to mobilize the pINV by the EIEC O96:H19 strain harboring the complete conjugative region, a detailed search of the presence of the genetic elements involved in conjugation was performed in the sequence of the plasmids of strain EF432. In addition, a transcription assay on pilin-encoding gene *traA* and a conjugation assay among EF432 and a recipient strain were also carried out.

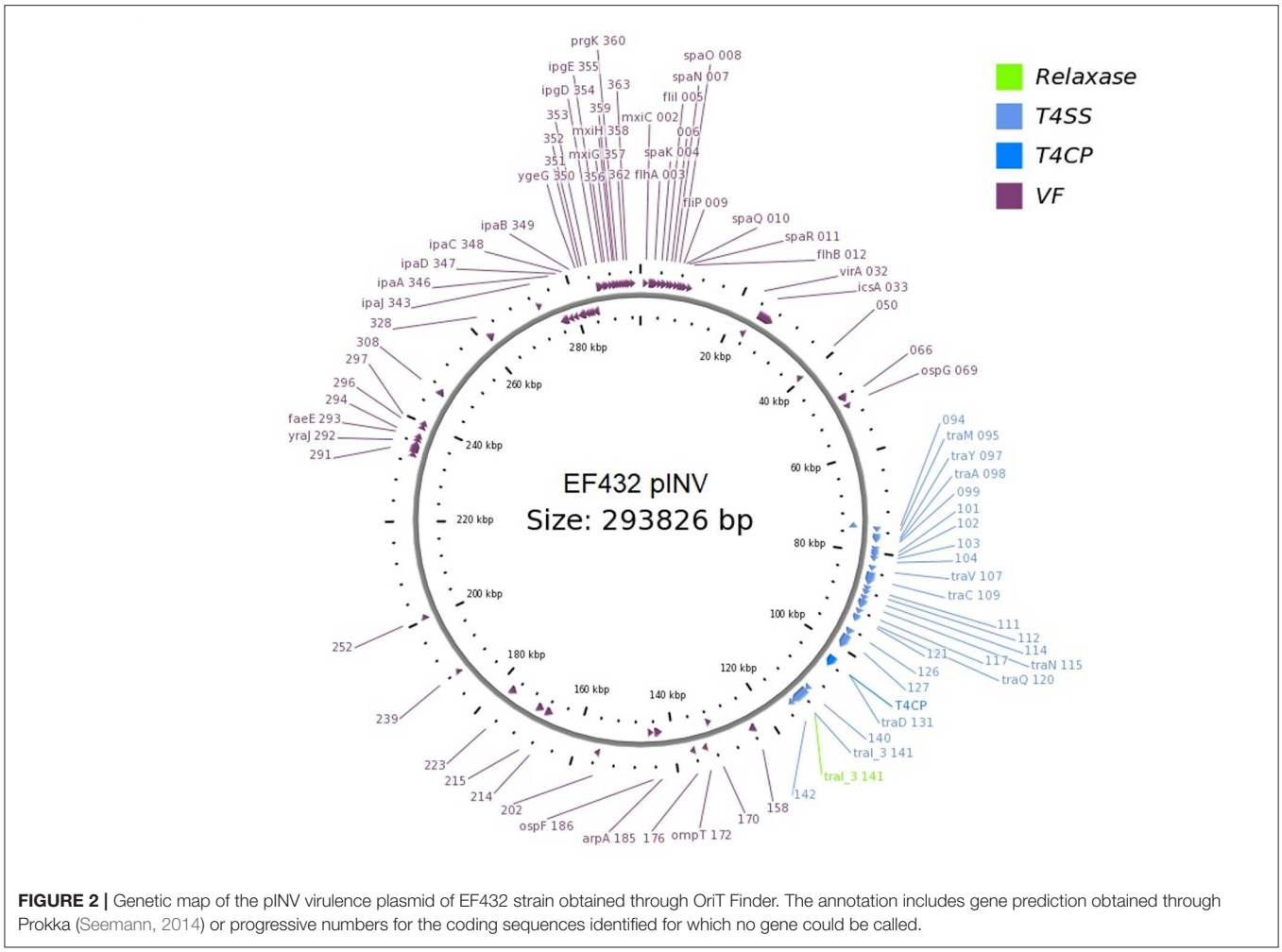

FIGURE 2 | Genetic map of the pINV virulence plasmid of EF432 strain obtained through OriT Finder. The annotation includes gene prediction obtained through Prokka (Seemann, 2014) or progressive numbers for the coding sequences identified for which no gene could be called.

Analysis of the Presence of Conjugation-Related Genetic Elements

The presence of genetic *loci* involved in plasmid transfer through conjugation was initially investigated on the closed sequences of the plasmids of strains EF432 and 152661 (Pettengill et al., 2015a). The maps of pINV plasmids from the two strains are reported in **Figures 2**, **3**, while the maps of the accessory plasmids found in the same strains and harboring resistance genes (named pRES hereafter), are included as **Supplementary Figures 2**, **3**. The complete list of the features involved in conjugation resulting from these analyses is reported in **Table 1**, showing the presence of the complete asset of conjugation-related regions only on pINV plasmid from EF432 strain ($pINV_{EF432}$). In particular, pINV from EF432 harbored genes encoding the relaxase and type IV coupling protein (T4CP), two essential components of the ssDNA conjugation machinery, and a region of about 41 kbp encoding the Type Four Secretion System (T4SS). The pRES plasmid harbored in the same strain, possessed part of the conjugative features but lacked the T4SS gene cluster (**Table 1**). On the other hand, either the pINV or the pRES plasmids present in the strain 152661 lacked the origin of transfer (*oriT*), and the T4SS gene cluster region present on this pINV consisted of 16 kbp only (**Table 1**). A deeper analysis showed the presence of two identical and inverted copies of a 1258 bp-long IS*600* element in the *tra* region (positions 72898- 74161 and 95672-94409, Acc. No. CP011417) in $pINV_{EF432}$. The same region was lacking in pINV of 152661 ($pINV_{152661}$), but remnants of IS*600* elements (1121/1199 nucleotidic identity, 46 gaps) were found in the corresponding positions (**Figure 4**).

The same analysis was performed to compare the *tra* region of $pINV_{EF432}$ with those partially found in the pINV of other four isolates. The results, reported in **Supplementary Figure 4**, showed a complete panel of *tra* genes only in the pINV of strain CNM-2113/13. The *traD* gene encoding the T4CP was instead absent from the remaining three plasmids. Additionally, the genes *traN* and *traI* were absent in the pINV sequence of strain SRR3578770. Finally, the presence of different short insertion elements in all the strains but CNM-2113/13 was observed (**Supplementary Figure 4**).

Transcription Assay of Pilin-Encoding Gene *traA* in EF432 Strain

A reverse transcriptase Real Time PCR expression assay was deployed to verify the transcription of *traA* gene, encoding the main component of the conjugative pilus, present in $pINV_{EF432}$. The results showed that the *traA* gene was transcribed

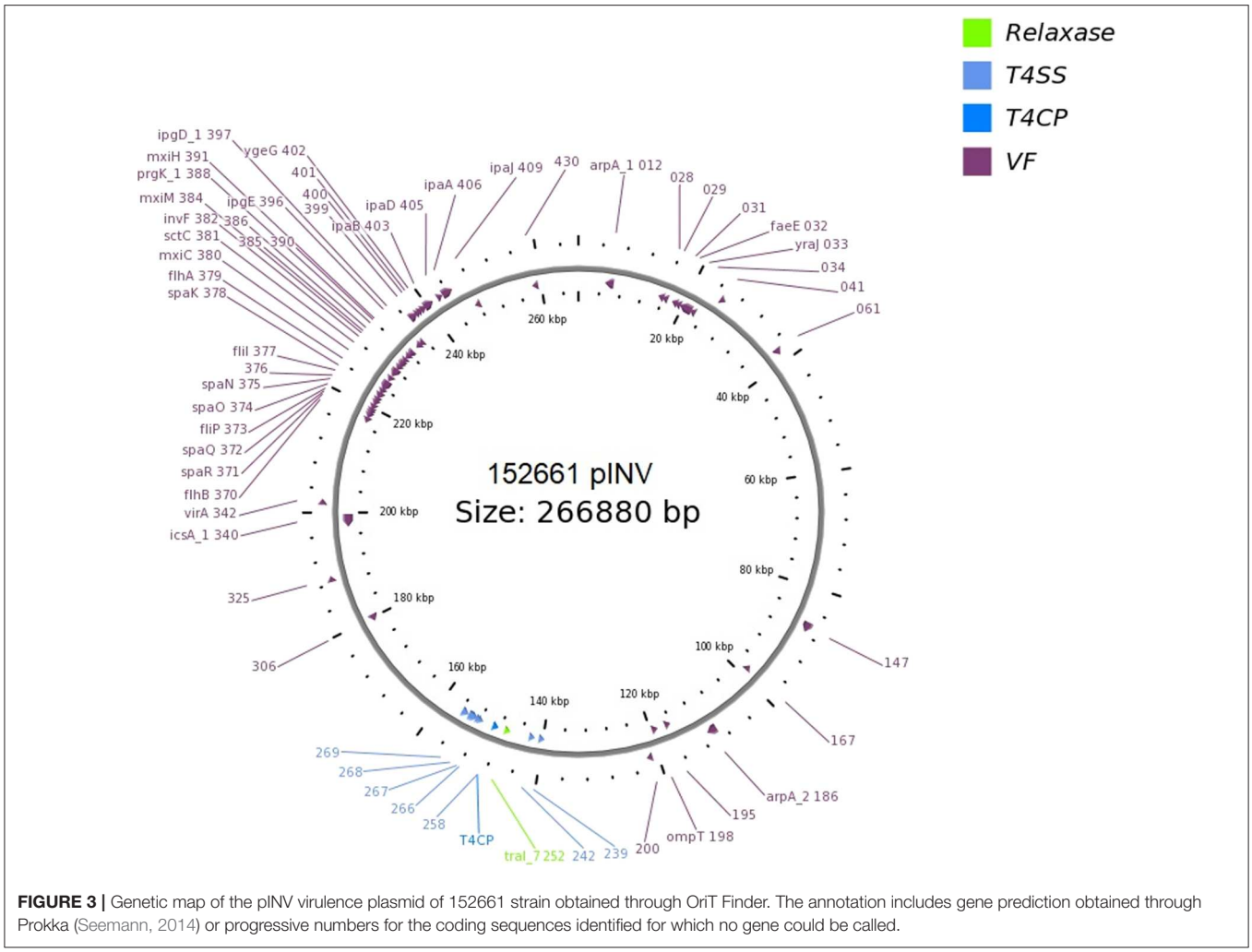

FIGURE 3 | Genetic map of the pINV virulence plasmid of 152661 strain obtained through OriT Finder. The annotation includes gene prediction obtained through Prokka (Seemann, 2014) or progressive numbers for the coding sequences identified for which no gene could be called.

TABLE 1 | Analysis of the presence of conjugation-related genetic elements in the closed sequences of the plasmids of the O96:H19 strains EF432 and 152661.

Strain and plasmid	Feature encoded	Location
EF432 pINV	*oriT* region	74839..74924 (–)
293826 bp	Relaxase	110756..114385 (+)
(Acc. No. CP011417)	T4CP	102213..104438 (+)
	T4SS gene cluster	74272..115151
EF432 pRES	Relaxase	01885..7155 (–)
47606 bp	T4CP	07155..9443 (–)
(Acc. No. CP011418)		
152661 pINV	Relaxase	146372..147019 (–)
266880 bp	T4CP	0148908..149147 (–)
(Acc. No. CP046677.1)	T4SS gene cluster	139934..155870
152661 pRES	Relaxase	018019..23289 (+)
48742 bp	T4CP	015758..18019 (+)
(Acc. No. CP046678.1)		

in both the growth conditions used (incubation at 30° and 37°C), even if at lower levels than the housekeeping *gapA* gene (**Table 2**). The efficiency results of the reactions targeting *traA* and the housekeeping gene *gapA*, used as control, were comparable.

Conjugation Between Donor EF432 Strain and Recipient CSH26NaI *E. coli* K12 Strain

Conjugation experiments between donor strain EF432 and the recipient *E. coli* K12 strain CSH26 Nal^r were performed to assess the ability of the strain EF432 to transfer one or both the pINV and pRES plasmids to the recipient strain. No red transconjugant colonies were identified on TSA plates supplemented with nalidixic acid and Congo Red. PCR screening for the presence of *ipaH* gene in a selection of 200 colonies also resulted negative. This was in line with the lack of red colonies observed, as the presence of pINV plasmid is associated with red color on plates containing Congo Red (Sakai et al., 1986). Nevertheless, when the conjugation mixture was plated on LB media supplemented with streptomycin, one colony was detected, which was proven to be also resistant to sulphametoxazole and negative to *ipaH* gene in PCR, resembling a trans-conjugative colony of CSH26 Nal^r which got the accessory plasmid harboring the resistance genes to the two antimicrobials present in EF432 strain.

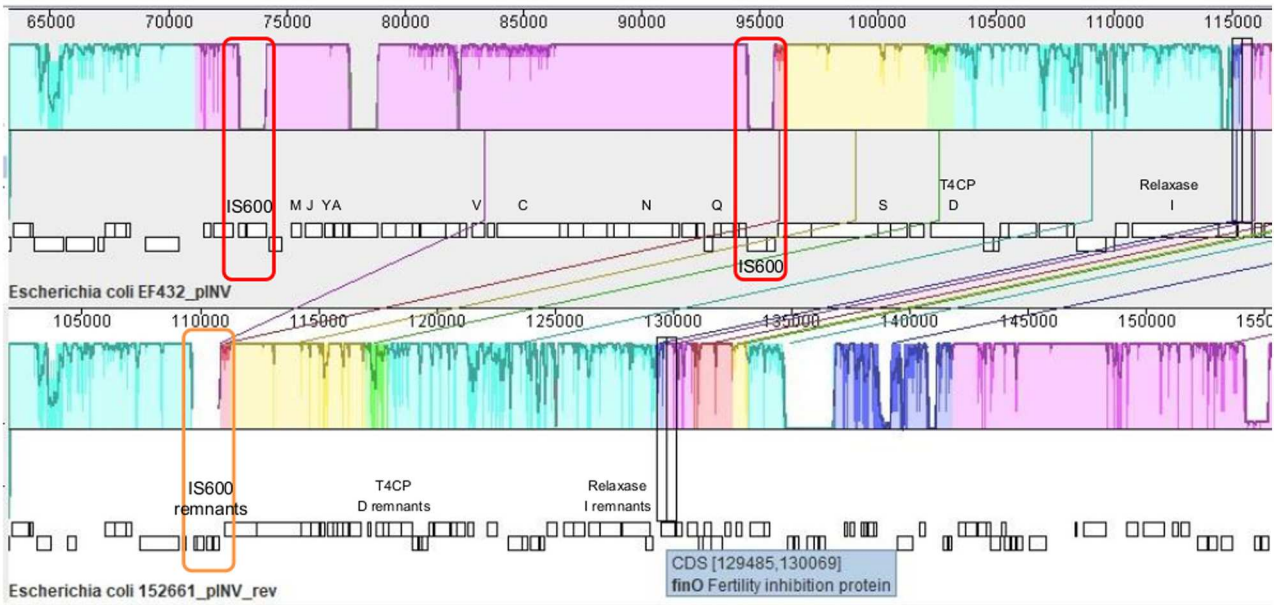

FIGURE 4 | Alignment of *tra* regions in pINV of EF432 strain, used as reference, and pINV of 152661, produced with MAUVE tool (Rissman et al., 2009). Conserved segments that appear to be internally free from big genome rearrangements are visualized as colored blocks. A decrease in percentage of sequence identity is represented as a decrease in coloring. The genetic organization is represented under each sequence, with *tra* genes indicated with the corresponding letters (*traMJYAVCNQSDI*) and T4CP and Relaxase-encoding genes highlighted for their encoded function. The red boxes indicate the two identical and inverted copies of an IS*600* element in the reference, while the orange box highlights the IS*600* remnant in the corresponding region of pINV in 152661 strain.

TABLE 2 | Results of the reverse transcription real time PCR expression assay for *traA* and *gapA* genes.

	mean Ct *traA*	Std. Dev. Ct *traA*	mean Ct *gapA*	Std. Dev. Ct *gapA*
cDNA 30	28.71	0.21	22.06	0.42
cDNA 37	27.59	0.11	25.14	0.30
DNA 2,25 ng/reaction	18.57	0.27	21.26	0.26
DNA 2,25 × 10^{-1} ng/reaction	22.66	0.30	24.96	0.41
DNA 2,25 × 10^{-2} ng/reaction	25.42	0.12	28.26	0.28
DNA 2,25 × 10^{-3} ng/reaction	28.65	0.20	31.76	0.93

Phylogenetic Analysis of EIEC O96:H19 Strains in Comparison With Reference EIEC and *Shigella* Strains

A whole genome comparison of the population of EIEC O96:H19 genomes studied was performed using cgMLST. The strains included were the EIEC strains isolated in Uruguay and EIEC strains belonging to the serotype O96:H19, including those isolated in the outbreaks occurred in Italy and the UK, the strain isolated in Spain and isolates described in a previous study on EIEC strains isolated from UK residents (Cowley et al., 2018). Moreover, EIEC strains representative of all the serotypes detected during the same study (Cowley et al., 2018) were included in the analysis for comparative purposes, as well as the 4608 and 6.81 EIEC reference strains and genomes from different *Shigella* species (**Supplementary Table 1**). The statistics of this analysis are reported in **Supplementary Table 4**, while the minimum spanning tree is shown in **Figure 5**. It is important to note that, with the only exception of the 6.81 reference EIEC strain whose published sequence showed the lowest quality, for all the other genomes alleles could be called for almost all the *loci* included in the cgMLST scheme used (**Supplementary Table 4**). The figure shows colors based on the detected Sequence Type. The O96:H19 strains, all belonging to ST-99, formed a homogeneous cluster. Two separate branches, one comprising only EIEC strains belonging to ST-6 and the second including all the other STs comprising all the *Shigella* and EIEC reference strains, segregated far apart from each other in terms of allelic distances and from the cluster of O96:H19 strains. Noteworthy, all *Shigella* strains occupied terminal positions, branching from one single EIEC strain typed as O28ac:H7 and showing the highest number of allelic distances from O96:H19 cluster.

DISCUSSION

The acquisition of genetic elements through horizontal gene transfer represents a major genetic mechanism driving the radiation of pathogenic *Escherichia coli* into different groups. Besides, the loss of genetic functions that are not required or

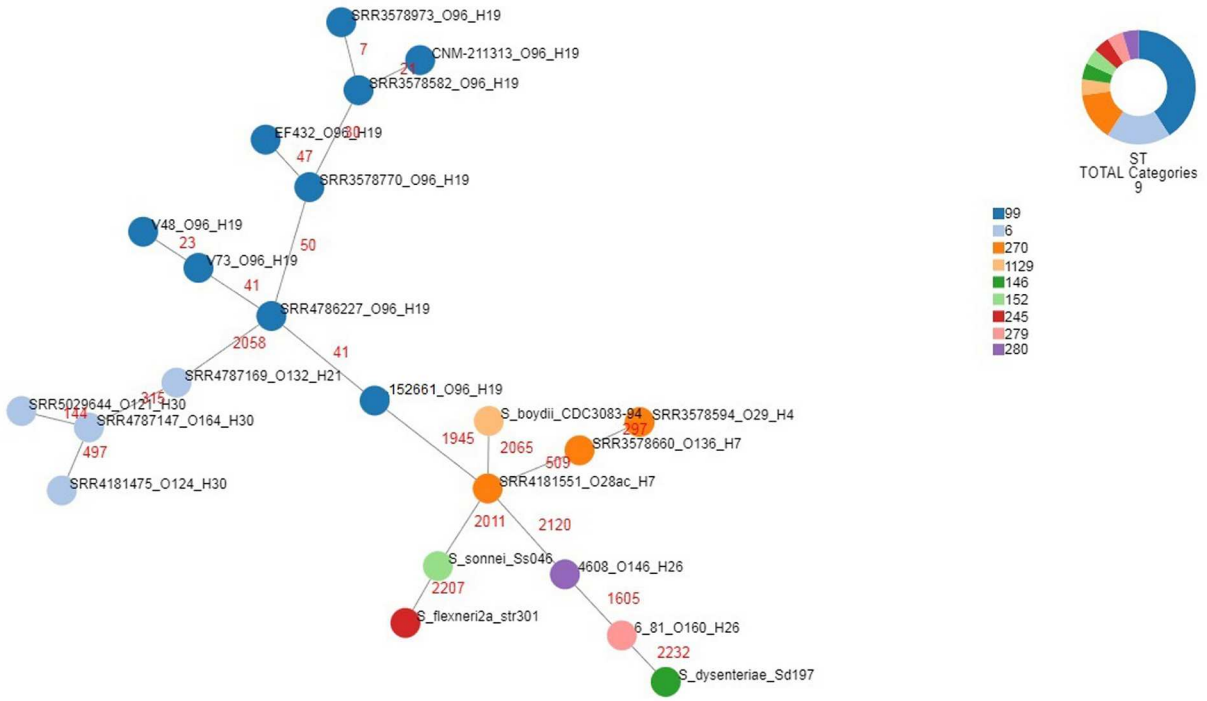

FIGURE 5 | Phylogenomic analysis of EIEC and *Shigella* strains through cgMLST. For EIEC isolates, the strains identifiers include the strain name and the O and H antigens, each separated by underscores. For *Shigella* isolates, the strains identifiers comprise the species and the strain name. The different colors categorize the Sequence Types derived for the corresponding strains, as detailed in the legend. The numbers in red indicate the number of allelic differences identified for each link.

could even have an adverse effect on the life of the bacterial pathogen offers additional advantages to certain pathogenic *E. coli* populations. Among diarrheagenic *E. coli*, Enteroinvasive *E. coli* (EIEC) are able to invade and replicate into the epithelial cells in the colon of the human host, with the same mechanism exerted by *Shigella* spp. (Pasqua et al., 2017). The key genetic event characterizing the evolution of EIEC and *Shigella* consisted in the acquisition of the pINV virulence plasmid, which harbors the majority of genes involved in the invasion mechanism, in combination with the accumulation of pathoadaptive mutations in anti-virulence *loci*, which has been extensively demonstrated either in EIEC or *Shigella* strains (Pasqua et al., 2017).

A novel EIEC O96:H19, emerging in Europe as a foodborne pathogen associated with outbreaks and sporadic cases, showed peculiar characteristics, such as lactose fermentation, motility, and lack of pathoadaptive mutations (Michelacci et al., 2016).

In the present paper we investigated the hypothesis of the emergence of such clone following an event of acquisition of the pINV plasmid by a non-pathogenic *E. coli* and studied its ability to exchange genetic material via conjugation. Additionally, we describe the characterization of EIEC O96:H19 strains isolated from two severe cases of infections occurred in Uruguay in 2014 (Peirano et al., 2018). The isolates from South America showed the absence in their genomes of pathoadaptive mutations and of chromosomal virulence genes usually found in EIEC and *Shigella*, while showed the presence of *gsp* genes, encoding a Type 2 Secretion System, also described in non-pathogenic *E. coli* (Stathopoulos et al., 2000). After the first description of EIEC O96:H19 (Michelacci et al., 2016), the whole genome sequences of other EIEC strains isolated in the UK were made available, including several O96:H19 isolates (Cowley et al., 2018). Four of these latter genomes were included in the present work and their comparison with the genomes of the other EIEC strains studied allowed to observe in one strain (Acc. No. SRR4786227) the lack of the complete "entry region"of the pINV virulence plasmids of EIEC and *Shigella,* which usually harbors the *ipa-mxi-spa locus* (Pasqua et al., 2017) (**Figure 1** and **Supplementary Table 2**). The loss of such region had already been described in spontaneous avirulent isolates of *Shigella flexnerii* (Venkatesan et al., 2001). It is interesting to note that in both cases, the deletion also included the region encompassing *virA* and *icsA* genes, not physically linked to the "entry region," but still pivotal for the pathogenesis of *Shigella* and EIEC. While it is not possible to determine if such regions were lost or had never been acquired, in another EIEC O96:H19 strain (Acc. No. SRR3578770) the region including *virA* and *icsA* was absent from the plasmid, in presence of a complete "entry region" (**Figure 1** and **Supplementary Table 2**). This finding provides the first evidence, to the best of our knowledge, that the two regions can be acquired or lost in separate events. Moreover, the absence of *ospG* observed in two strains (Acc. No. SRR3578973 and SRR3578582), proving instead positive either for the "entry region" or the *virA-icsA* region, appeared in contrast with the previous hypothesis of co-acquisition of these *loci* (Buchrieser et al., 2000). Even if it is not

possible to exclude that the absence of *ospG* gene in one of the strains could derive from a specific deletion event, its presence in the other, lacking the "entry region" and the *virA-icsA locus* (SRR4786227), suggests instead that the acquisition of *ospG locus* could have derived from an independent acquisition event.

Despite the absence of some EIEC virulence genes in many of the O96:H19 strains isolated in UK, it should be considered that they were all isolated from hospitalized or community cases of gastrointestinal disease (Cowley et al., 2018). In this respect, the reported presence of multiple transposons and insertion elements in pINV plasmids of EIEC and *Shigella* (Pasqua et al., 2017), together with previous reports of spontaneous loss of the "entry region" from pINV plasmids resulting in avirulent strains (Venkatesan et al., 2001), suggest that the loss of such virulence region in SRR4786227 could have occurred during isolation and subculturing of the strain.

The presence of the two virulence genes *capU* and *lpfA* in the EIEC O96:H19 strains, encoding an hexosyltransferase of Enteroaggregative *E coli* and rarely identified in *S. flexnerii* strains (Fujiyama et al., 2008; Ikumapayi et al., 2017) and the main subunit of the long polar fimbriae, frequently present in Shiga-toxin producing *E. coli* (STEC) and rarely identified in EIEC (Toma et al., 2006), respectively, may not be enough to explain the association of the strain lacking the "entry region" with gastrointestinal illness. Nevertheless, the conserved presence of these two genes suggests a role for their products in the virulence of EIEC O96:H19. Their function in the specific context of EIEC pathogenesis would necessitate further investigation.

The comparison of the virulence plasmids of the EIEC O96:H19 strains carried out in this study also highlighted the presence of a complete conjugation region in pINV of EF432 and CNM-2113/13 strains and a nearly complete region in other strains analyzed (namely SRR3578973, SRR3578770, and SRR3578582) (**Figures 1**, **2**, **4** and **Supplementary Figure 4**). This region is completely lacking in pINV from reference EIEC and *Shigella* strains (Pasqua et al., 2017). The production of the completely closed sequences of the chromosomes and the plasmids of the strains EF432 and 152661 allowed a deeper investigation of the region involved in conjugation both in the pINV and in the accessory plasmid harboring resistance genes (pRES) found in the two strains (**Figures 2**, **3**, **Supplementary Figures 2**, **3** and **Table 1**). This analysis confirmed the presence of the whole set of *loci* involved in conjugation only in pINV from the EF432 strain, supporting the hypothesis that this plasmid may be capable of transferring to other *E. coli* strains through conjugation. The observation of active transcription of the *traA* pilin-coding gene through Real Time PCR and the result of conjugation experiments suggesting the transfer of the accessory pRES plasmid to a recipient strain strengthened such a hypothesis. As a matter of fact, the pRES plasmid of EF432 carried the genes conferring resistance to streptomycin and sulfametoxazole, which could have both been transferred to the *E. coli* K12 CSH26 Nal^r used as recipient in the conjugation experiments. On the other hand, the pRES of this strain was negative for the *tra* genes involved in conjugation and, as such, could have been moved by exploiting an *in trans*-encoded conjugation machinery, which was, in our system, harbored on the $pINV_{EF432}$. The lack of identification of CSH26 Nal^r transconjugant strains which acquired the $pINV_{EF432}$ could be explained by the very low conjugation frequency ($<10^{-7}$) previously reported for pINV plasmids of *Shigella* strains (Sansonetti et al., 1981), in association with the lack of a selective marker on $pINV_{EF432}$. Further work involving different strategies such as tagging the plasmid with the insertion of an antimicrobial resistance gene cassette would ease the recovery of transconjugant clones confirming its capacity of self-mobilization through conjugation.

Altogether, these results are strongly indicative of the presence of a functional conjugation system at least in one O96:H19 EIEC strain, EF432. A similar system could also be present in the genome of the strain CNM-2113/13. Unfortunately, the sequence of this strain was not available as a closed genome and the fragmented contigs did not allow to completely characterize the *tra locus* on the plasmid (**Supplementary Figure 4**). The finding of the identification of two inverted copies of IS*600*, belonging to IS*3* family, at the two sides of the region of $pINV_{EF432}$ encoding conjugative elements and the presence of remnants of a similar IS*600* sequence in the corresponding region of the $pINV_{152261}$ (**Figure 4**) suggested that a recombination event between these two copies could have led to the deletion of the DNA stretch of about 23 kbp, resulting in a plasmid with a defective conjugation region in the latter strain. This mechanism could be part of the stabilization process of the pINV in EIEC O96:H19, resulting in progressive loss of conjugation ability, as reported for *Shigella* species (Johnson and Nolan, 2009). Nevertheless, the identification of other insertion elements and of inversions in the *tra* region of other O96:H19 strains analyzed suggests that multiple events could contribute to the inactivation of the *locus* and the resulting stabilization of the plasmid. Similarly, the observation of a mosaic virulence genes asset in the pINV of several EIEC O96:H19, together with a variable pattern in the presence of the conjugation region, supports the recent emergence of the EIEC O96:H19 clone and could be related with the activation of mobile genetic elements on the plasmid.

In order to visualize the phylogenetic relationships among the EIEC O96:H19 strains, an analysis was conducted using the core genome Multi Locus Sequence Typing, including reference EIEC and *Shigella* strains for comparison (**Figure 5**). A low number of allelic differences was observed among the different EIEC O96:H19 strains, which confirmed their recent evolution. This was also supported by the low variability in the chromosome structure as observed in the whole genome comparison performed by BRIG analysis (**Supplementary Figure 1**) and by the identification of prophages in the majority of the differing regions.

The apical positions occupied by all the *Shigella* strains in the minimum spanning tree, which shows these strains branching from typical EIEC strains belonging to Sequence Types 270, 279 and 280 (**Figure 5**), support the reclassification of *Shigella* into the *E. coli* species (Pettengill et al., 2015b) and are in line with the high specialization of such strains for living as intracellular pathogens. It is also interesting to note that all the EIEC strains belonging to ST-6 formed a separate branch, supporting the

previous hypothesis of a separate evolution for this EIEC clone (Michelacci et al., 2016).

Altogether, the results of this study demonstrate that the circulation of the highly virulent O96:H19 EIEC clone is not restricted to Europe and provide evidences for its recent emergence showing still active evolution mechanisms.

Noteworthy, the retention by some of the O96:H19 EIEC strains of the genetic *locus* encoding a functional conjugation machinery adds strong evidence to the hypothesis of the emergence of novel EIEC clones through the acquisition of the pINV plasmid by commensal or environmental *E. coli* strains via conjugation. As a matter of fact, EIEC O96:H19 display, besides the presence of the pINV plasmid, good growing abilities and capacity of mobilization outside the cells (Michelacci et al., 2016).

It cannot be excluded that such a clone could have been circulating even before its first description during the 2012 outbreak (Escher et al., 2014), and that it remained undetected due to its peculiar characteristics. As a matter of fact, in routine diagnosis, the identification of EIEC and *Shigella* usually relies on the isolation of colonies lacking lactose fermentation, lysine decarboxylase activity and motility.

Notably, a foodborne outbreak caused by a novel O8:H19 EIEC clone was also reported in North Carolina in 2018, representing the first confirmed outbreak of EIEC infections in the United States in 47 years, and the first report of EIEC serotype O8:H19 (Herzig et al., 2019), confirming the importance of preparedness in the detection of the EIEC pathotype. Further work should be carried out to explore the possibility that other EIEC types, including the mentioned O8:H19, may possess hybrid characteristics encompassing the ability of striving outside a eukaryotic cell and the presence of pINV, thus demonstrating the evolutionary pathway connecting the *E. coli* genomic continuum and *Shigella* strains.

DATA AVAILABILITY STATEMENT

The datasets generated and used for this study can be found in the EMBL-European Nucleotide Archive Study with Acc. No. PRJEB35723 and at NCBI Bioproject with Acc. No. PRJNA315192. All the details about the Acc. No. of each sequencing run and of additional samples included in the study are listed in **Supplementary Table 1**.

AUTHOR CONTRIBUTIONS

VM conceived the experimental design and drafted the manuscript. RT contributed in the scientific discussion and particularly in the design of the conjugation and Real Time PCR experiments. AD'A performed the bioinformatics analyses on ARIES webserver. SA and AB prepared and checked the bacterial cultures and performed the Real Time PCR experiments. AK installed the ARIES server for the bioinformatic analyses and installed the tools for the data analysis. GP contributed in the discussion and provided the CSH26Nal strain for conjugation. DG and CJ took care of the Nanopore sequencing and data analysis at PHE and provided the strain from the United Kingdom, TC, AS, AN, FS, and GV provided and characterized the strains from Uruguay (in detail TC and AS made the initial characterization. GV and FS made the complete identification, including detection of the *ipaH* gene. AN performed the serotyping of both isolates). SM contributed in the scientific discussion and thoroughly revised the manuscript. Finally, all the authors approved the manuscript to be published.

FUNDING

The Oxford Nanopore sequencing was supported by the National Institute for Health Research Health Protection Research Unit in Gastrointestinal Infections. CJ and DG are affiliated to the National Institute for Health Research Health Protection Research Unit (NIHR HPRU) in Gastrointestinal Infections at the University of Liverpool in partnership with PHE, in collaboration with the University of East Anglia, the University of Oxford and the Quadram Institute of Food Research. CJ and DG are based at PHE. The views expressed are those of the authors and not necessarily those of the National Health Service, the NIHR, the Department of Health or PHE.

ACKNOWLEDGMENTS

We wish to thank Dr. Marco Crescenzi, Fiorella Ciaffoni, and Manuela Marra from the ISS Core Facilities Technical-Scientific Service for the Next Generation Sequencing through the Ion Torrent S5 platform.

SUPPLEMENTARY MATERIAL

The Supplementary Material for this article can be found online at: https://www.frontiersin.org/articles/10.3389/fcimb.2020.00260/full#supplementary-material

Supplementary Tables 1, 2, 3 and 4 include, respectively: the list of strains used in this study, with accession numbers; virulotyping results of O96:H19 EIEC strains; regions of difference identified among chromosomes of O96:H19 strains; and the statistics of cgMLST analysis.

Supplementary Figures 1, 2, 3 and 4 illustrate, respectively: BRIG alignment among chromosomes of O96:H19 strains; genetic map of pRES from EF432; genetic map of pRES from 152661; alignment of *tra* regions in pINV of EF432 and of the strains harboring at least a part of the region.

REFERENCES

Alikhan, N. F., Petty, N. K., Ben Zakour, N. L., and Beatson, S. A. (2011). BLAST ring image generator (BRIG): simple prokaryote genome comparisons. *BMC Genom.* 12:402. doi: 10.1186/1471-2164-12402

Bankevich, A., Nurk, S., Antipov, D., Gurevich, A. A., Dvorkin, M., Kulikov, A. S., et al. (2012). SPAdes: a new genome assembly algorithm and its applications to single-cell sequencing. *J. Computat. Biol.* 19, 455–477. doi: 10.1089/cmb.2012.0021

Buchrieser, C., Glaser, P., Rusniok, C., Nedjari, H., D'Hauteville, H., Kunst, F., et al. (2000). The virulence plasmid pWR100 and the repertoire of proteins

secreted by the type III secretion apparatus of *Shigella flexneri*. *Mol. Microbiol.* 38, 760–771. doi: 10.1046/j.1365-2958.2000.02179.x

Cowley, L. A., Oresegun, D. R., Chattaway, M. A., Dallman, T. J., and Jenkins, C. (2018). Phylogenetic comparison of enteroinvasive *Escherichia coli* isolated from cases of diarrhoeal disease in England, 2005–2016. *J. Med. Microbiol.* 67, 884–888. doi: 10.1099/jmm.0.000739

Cuccuru, G., Orsini, M., Pinna, A., Sbardellati, A., Soranzo, N., Travaglione, A., et al. (2014). Orione, a web-based framework for NGS analysis in microbiology. *Bioinformatics* 30, 1928–1929. doi: 10.1093/bioinformatics/btu135

De Coster, W., D'Hert, S., Schultz, D. T., Cruts, M., and Van Broeckhoven, C. (2018). NanoPack: visualizing and processing long-read sequencing data. *Bioinformatics* 34, 2666–2669. doi: 10.1093/bioinformatics/bty149

Escher, M., Scavia, G., Morabito, S., Tozzoli, R., Maugliani, A., Cantoni, S., et al. (2014). A severe foodborne outbreak of diarrhoea linked to a canteen in Italy caused by enteroinvasive Escherichia coli, an uncommon agent. *Epidemiol. Infect.* 142, 2559–2566. doi: 10.1017/S0950268814000181

Fitzmaurice, J., Glennon, M., Duffy, G., Sheridan, J. J., Carroll, C., and Maher, M. (2004). Application of real-time PCR and RT-PCR assays for the detection and quantitation of VT 1 and VT 2 toxin genes in *E. coli* O157:H7. *Mol. Cell Probes.* 18, 123–32. doi: 10.1016/j.mcp.2003.10.004

Fujiyama, R., Nishi, J., Imuta, N., Tokuda, K., Manago, K., and Kawano, Y. (2008). The shf gene of a *Shigella flexneri* homologue on the virulent plasmid pAA2 of enteroaggregative *Escherichia coli* 042 is required for firm biofilm formation. *Curr Microbiol.* 56, 474–480. doi: 10.1007/s00284-008-9115-y

Herzig, C. T. A., Fleischauer, A. T., Lackey, B., Lee, N., Lawson, T., Moore, Z. S., et al. (2019). Notes from the field: enteroinvasive *Escherichia coli* outbreak associated with a potluck party - North Carolina, June-July 2018. *MMWR Morb. Mortal. Wkly Rep.* 68, 183–184. doi: 10.15585/mmwr.mm6807a5

Hunt, M., Silva, N. D., Otto, T. D., Parkhill, J., Keane, J. A., and Harris, S. R. (2015). Circlator: automated circularization of genome assemblies using long sequencing reads. *Genome Biol.* 16:294. doi: 10.1186/s13059-015-0849-0

Ikumapayi, U. N., Boisen, N., Hossain, M. J., Betts, M., Lamin, M., Saha, D., et al. (2017). Identification of subsets of enteroaggregative *Escherichia coli* associated with diarrheal disease among under 5 years of age children from Rural Gambia. *Am. J. Trop Med. Hygiene* 97, 997–1004. doi: 10.4269/ajtmh.16-0705

Inouye, M., Dashnow, H., Raven, L. A., Schultz, M. B., Pope, B. J., Tomita, T., et al. (2014). SRST2: rapid genomic surveillance for public health and hospital microbiology labs. *Genome Med.* 6:90. doi: 10.1186/s13073-014-0090-6

Joensen, K. G., Scheutz, F., Lund, O., Hasman, H., Kaas, R. S., Nielsen, E. M., et al. (2014). Real-time whole-genome sequencing for routine typing, surveillance, and outbreak detection of verotoxigenic *Escherichia coli*. *J. Clin. Microbiol.* 52, 1501–1510. doi: 10.1128/JCM.03617-13

Joensen, K. G., Tetzschner, A. M., Iguchi, A., Aarestrup, F. M., and Scheutz, F. (2015). Rapid and easy *in silico* serotyping of escherichia coli isolates by use of whole-genome sequencing data. *J. Clin. Microbiol.* 53, 2410–2426. doi: 10.1128/JCM.00008-15

Johnson, T. J., and Nolan, L. K. (2009). Pathogenomics of the virulence plasmids of *Escherichia coli*. *Microbiol. Mol. Biol. Rev.* 73, 750–774. doi: 10.1128/MMBR.00015-09

Koren, S., Walenz, B. P., Berlin, K., Miller, J. R., Bergman, N. H., and Phillippy, A. M. (2017). Canu: scalable and accurate long-read assembly via adaptive k-mer weighting and repeat separation. *Genome Res.* 27, 722–736. doi: 10.1101/gr.215087.116

Lan, R., Alles, M. C., Donohoe, K., Martinez, M. B., and Reeves, P. R. (2004). Molecular evolutionary relationships of enteroinvasive *Escherichia coli* and Shigella spp. *Infect Immun.* 72, 5080–5088. doi: 10.1128/IAI.72.9.5080-5088.2004

Li, H., and Durbin, R. (2010). Fast and accurate long-read alignment with burrows-wheeler transform. *Bioinformatics* 26, 589–595. doi: 10.1093/bioinformatics/btp698

Li, H., Handsaker, B., Wysoker, A., Fennell, T., Ruan, J., Homer, N., et al. (2009). The sequence alignment/map format and SAMtools. *Bioinformatics* 25, 2078–2079. doi: 10.1093/bioinformatics/btp352

Llarena, A. K. R., Silva, D. N., Halkilahti, J., Machado, M. P., and Da Silva, M. S. (2018). INNUENDO: a cross-sectoral platform for the integration ofgenomics in the surveillance of food-borne pathogens. *External Sci. Rep.* 15:5123. doi: 10.2903/sp.efsa.2018.EN-1498

Loman, N. J., Quick, J., and Simpson, J. T. (2015). A complete bacterial genome assembled de novo using only nanopore sequencing data. *Nat. Methods* 12, 733–735. doi: 10.1038/nmeth.3444

Luscher, D., and Altwegg, M. (1994). Detection of shigellae, enteroinvasive and enterotoxigenic Escherichia coli using the polymerase chain reaction (PCR) in patients returning from tropical countries. *Mol. Cell Probes* 8, 285–290. doi: 10.1006/mcpr.1994.1040

Maurelli, A. T., Blackmon, B., and Curtiss, R. III. (1984). Loss of pigmentation in *Shigella flexneri* 2a is correlated with loss of virulence and virulence-associated plasmid. *Infect. Immun.* 43, 397–401. doi: 10.1128/IAI.43.1.397-401.1984

Michelacci, V., Prosseda, G., Maugliani, A., Tozzoli, R., Sanchez, S., Herrera-Leon, S., et al. (2016). Characterization of an emergent clone of enteroinvasive *Escherichia coli* circulating in Europe. *Clin. Microbiolo. Infect.* 22:e11–9. doi: 10.1016/j.cmi.2015.10.025

Nataro, J. P., and Kaper, J. B. (1998). Diarrheagenic *Escherichia coli*. *Clin. Microbiol. Rev.* 11, 142–201. doi: 10.1128/CMR.11.1.142

Newitt, S., MacGregor, V., Robbins, V., Bayliss, L., Chattaway, M. A., Dallman, T., et al. (2016). Two linked enteroinvasive *Escherichia coli* outbreaks, Nottingham, UK, June 2014. *Emerg. Infect. Dis.* 22, 1178–1184. doi: 10.3201/eid2207.152080

Pasqua, M., Michelacci, V., Di Martino, M. L., Tozzoli, R., Grossi, M., Colonna, B., et al. (2017). The intriguing evolutionary journey of enteroinvasive *E. coli* (EIEC) toward pathogenicity. *Front. Microbiol.* 8:2390. doi: 10.3389/fmicb.2017.02390

Peirano, V., Bianco, M. N., Navarro, A., Schelotto, F., and Varela, G. (2018). Diarrheagenic *Escherichia coli* associated with acute gastroenteritis in children from Soriano, Uruguay. *Can. J. Infect. Dis. Med. Microbiol.* 2018:8387218. doi: 10.1155/2018/8387218

Pettengill, E. A., Hoffmann, M., Binet, R., Roberts, R. J., Payne, J., Allard, M., et al. (2015a). Complete genome sequence of enteroinvasive *Escherichia coli* O96:H19 associated with a severe foodborne outbreak. *Genome Announc.* 3:e00883–15. doi: 10.1128/genomeA.00883-15

Pettengill, E. A., Pettengill, J. B., and Binet, R. (2015b). Phylogenetic analyses of shigella and enteroinvasive escherichia coli for the identification of molecular epidemiological markers: whole-genome comparative analysis does not support distinct genera designation. *Front. Microbiol.* 6:1573. doi: 10.3389/fmicb.2015.01573

Ribeiro-Goncalves, B., Francisco, A. P., Vaz, C., Ramirez, M., and Carrico, J. A. (2016). PHYLOViZ Online: web-based tool for visualization, phylogenetic inference, analysis and sharing of minimum spanning trees. *Nucleic Acids Res.* 44, W246–W251. doi: 10.1093/nar/gkw359

Rissman, A. I., Mau, B., Biehl, B. S., Darling, A. E., Glasner, J. D., and Perna, N. T. (2009). Reordering contigs of draft genomes using the Mauve aligner. *Bioinformatics* 25, 2071–2073. doi: 10.1093/bioinformatics/btp356

Sakai, T., Sasakawa, C., Makino, S., Kamata, K., and Yoshikawa, M. (1986). Molecular cloning of a genetic determinant for Congo red binding ability which is essential for the virulence of Shigella flexneri. *Infect. Immun.* 51, 476–482. doi: 10.1128/IAI.51.2.476-482.1986

Sansonetti, P. J., Kopecko, D. J., and Formal, S. B. (1981). Shigella sonnei plasmids: evidence that a large plasmid is necessary for virulence. *Infect. Immun.* 34, 75–83. doi: 10.1128/IAI.34.1.75-83.1981

Seemann, T. (2014). Prokka: rapid prokaryotic genome annotation. *Bioinformatics* 30, 2068–2069. doi: 10.1093/bioinformatics/btu153

Siguier, P., Perochon, J., Lestrade, L., Mahillon, J., and Chandler, M. (2006). ISfinder: the reference centre for bacterial insertion sequences. *Nucleic Acids Res.* 34:D32–6. doi: 10.1093/nar/gkj014

Silva, M., Machado, M. P., Silva, D. N., Rossi, M., Moran-Gilad, J., Santos, S., et al. (2018). chewBBACA: a complete suite for gene-by-gene schema creation and strain identification. *Microb Genom.* 4:e000166. doi: 10.1101/173146

Sorensen, A. H., Hansen, L. H., Johannesen, E., and Sorensen, S. J. (2003). Conjugative plasmid conferring resistance to olaquindox. *Antimicrob. Agents Chemother.* 47, 798–799. doi: 10.1128/AAC.47.2.798-799.2003

Stathopoulos, C., Hendrixson, D. R., Thanassi, D. G., Hultgren, S. J., St Geme, J. W., and Curtiss, R. III. (2000). Secretion of virulence determinants by the general secretory pathway in gram-negative pathogens: an evolving story. *Microbes Infect.* 2, 1061–1072. doi: 10.1016/S1286-4579(00)01260-0

Toma, C., Higa, N., Iyoda, S., Rivas, M., and Iwanaga, M. (2006). The long polar fimbriae genes identified in Shiga toxin-producing *Escherichia coli* are present

in other diarrheagenic *E. coli* and in the standard *E. coli* collection of reference (ECOR) strains. *Res. Microbiol.* 157, 153–161. doi: 10.1016/j.resmic.2005.06.009

van den Beld, M. J., and Reubsaet, F. A. (2012). Differentiation between Shigella, enteroinvasive *Escherichia coli* (EIEC) and noninvasive *Escherichia coli*. *Eur. J. Clin. Microbiol. Infect. Dis.* 31, 899–904. doi: 10.1007/s10096-011-1395-7

Vaser, R., Sovic, I., Nagarajan, N., and Sikic, M. (2017). Fast and accurate *de novo* genome assembly from long uncorrected reads. *Genome Res.* 27, 737–746. doi: 10.1101/gr.214270.116

Venkatesan, M. M., Goldberg, M. B., Rose, D. J., Grotbeck, E. J., Burland, V., and Blattner, F. R. (2001). Complete DNA sequence and analysis of the large virulence plasmid of *Shigella flexneri*. *Infect. Immun.* 69, 3271–3285. doi: 10.1128/IAI.69.5.3271-3285.2001

Walker, B. J., Abeel, T., Shea, T., Priest, M., Abouelliel, A., Sakthikumar, S., et al. (2014). Pilon: an integrated tool for comprehensive microbial variant detection and genome assembly improvement. *PLoS ONE* 9:e112963. doi: 10.1371/journal.pone.0112963

Wick, R. R., Judd, L. M., Gorrie, C. L., and Holt, K. E. (2017). Unicycler: resolving bacterial genome assemblies from short and long sequencing reads. *PLoS Comput. Biol.* 13:e1005595. doi: 10.1371/journal.pcbi.1005595

Wick, R. R., Judd, L. M., and Holt, K. E. (2018). Deepbinner: demultiplexing barcoded oxford nanopore reads with deep convolutional neural networks. *PLoS Comput. Biol.* 14:e1006583. doi: 10.1371/journal.pcbi.1006583

Wirth, T., Falush, D., Lan, R., Colles, F., Mensa, P., Wieler, L. H., et al. (2006). Sex and virulence in *Escherichia coli*: an evolutionary perspective. *Mol Microbiol.* 60, 1136–1151. doi: 10.1111/j.1365-2958.2006.05172.x

Conflict of Interest: The authors declare that the research was conducted in the absence of any commercial or financial relationships that could be construed as a potential conflict of interest.

frontiers in Cellular and Infection Microbiology

ORIGINAL RESEARCH
published: 26 June 2020
doi: 10.3389/fcimb.2020.00299

The Vacuolating Autotransporter Toxin (Vat) of *Escherichia coli* Causes Cell Cytoskeleton Changes and Produces Non-lysosomal Vacuole Formation in Bladder Epithelial Cells

Juan Manuel Díaz[1], *Charles M. Dozois*[2], *Francisco Javier Avelar-González*[3], *Eduardo Hernández-Cuellar*[1], *Pravil Pokharel*[2], *Alfredo Salazar de Santiago*[1] *and Alma Lilian Guerrero-Barrera*[1]*

[1] *Departamento de Morfología, Universidad Autónoma de Aguascalientes (UAA), Aguascalientes, Mexico,* [2] *Institut National de Recherche Scientifique (INRS)-Centre Armand-Fappier Santé Biotechnologie, Laval, QC, Canada,* [3] *Departamento de Fisiología y Farmacología, Universidad Autónoma de Aguascalientes (UAA), Aguascalientes, Mexico*

OPEN ACCESS

Edited by:
Ulrich Dobrindt,
University of Münster, Germany

Reviewed by:
Lee-Ann H. Allen,
The University of Iowa, United States
Alain L. Servin,
Institut National de la Santé et de la Recherche Médicale (INSERM), France

***Correspondence:**
Alma Lilian Guerrero-Barrera
alguerre@correo.uaa.mx

Specialty section:
This article was submitted to Bacteria and Host, a section of the journal Frontiers in Cellular and Infection Microbiology

Received: *09 November 2019*
Accepted: *19 May 2020*
Published: *26 June 2020*

Citation:
Díaz JM, Dozois CM, Avelar-González FJ, Hernández-Cuellar E, Pokharel P, de Santiago AS and Guerrero-Barrera AL (2020) The Vacuolating Autotransporter Toxin (Vat) of Escherichia coli Causes Cell Cytoskeleton Changes and Produces Non-lysosomal Vacuole Formation in Bladder Epithelial Cells. Front. Cell. Infect. Microbiol. 10:299. doi: 10.3389/fcimb.2020.00299

Urinary tract infections (UTIs) affect more than 150 million people, with a cost of over 3.5 billion dollars, each year. *Escherichia coli* is associated with 70–80% of UTIs. Uropathogenic *E. coli* (UPEC) has virulence factors including adhesins, siderophores, and toxins that damage host cells. Vacuolating autotransporter toxin (Vat) is a member of serine protease autotransporter proteins of *Enterobacteriaceae* (SPATEs) present in some uropathogenic *E. coli* (UPEC) strains. Vat has been identified in 20–36% of UPEC and is present in almost 68% of urosepsis isolates. However, the mechanism of action of Vat on host cells is not well-known. Thus, in this study the effect of Vat in a urothelium model of bladder cells was investigated. Several toxin concentrations were tested for different time periods, resulting in 15–47% of cellular damage as measured by the LDH assay. Vat induced vacuole formation on the urothelium model in a time-dependent manner. Vat treatment showed loss of the intercellular contacts on the bladder cell monolayer, observed by Scanning Electron Microscopy. This was also shown using antibodies against ZO-1 and occludin by immunofluorescence. Additionally, changes in permeability of the epithelial monolayer was demonstrated with a fluorescence-based permeability assay. Cellular damage was also evaluated by the identification of cytoskeletal changes produced by Vat. Thus, after Vat treatment, cells presented F-actin distribution changes and loss of stress fibers in comparison with control cells. Vat also modified tubulin, but it was not found to affect Arp3 distribution. In order to find the nature of the vacuoles generated by Vat, the Lysotracker deep red fluorescent dye for the detection of acidic organelles was used. Cells treated with Vat showed generation of some vacuoles without acidic content. An *ex vivo* experiment with mouse bladder exposed to Vat demonstrated

loss of integrity of the urothelium. In conclusion, Vat induced cellular damage, vacuole formation, and urothelial barrier dysregulation of bladder epithelial cells. Further studies are needed to elucidate the role of these vacuoles induced by Vat and their relationship with the pathogenesis of urinary tract infection.

Keywords: urinary tract infection, *Escherichia coli,* virulence factors, vat, cell damage, vacuoles, cytoskeleton, cell junctions

INTRODUCTION

Urinary tract infections (UTIs) are a public health problem that affects more than 150 million people, with an estimated cost of over 3.5 billion dollars each year (Flores-Mireles et al., 2015). For the development of the disease, several risk factors exist such as diabetes, vaginal infections, sexual activity, presence of a urinary catheter, neurological disease, immunosuppression, and kidney transplantation (Foxman, 2003; Nielubowicz and Mobley, 2010).

UTIs are caused mainly by bacteria, but sometimes can be provoked by yeast or other fungi. The most frequent cause of UTIs is uropathogenic *Escherichia coli* (UPEC), with a prevalence of 70 to 80% worldwide (Flores-Mireles et al., 2015; Ramírez-Castillo et al., 2018). *Escherichia coli* is typically found in the gastrointestinal tract as part of the microbiota, and certain commensal *E. coli* strains residing in the gut have the potential to cause UTIs. The difference between purely commensal *E. coli* strains and UPEC is the presence of certain virulence factors in the pathogenic strains (Terlizzi et al., 2017). UPEC has the capacity to attach, colonize and invade the urinary tract through production of several virulence factors including adhesins, siderophores, capsular polysaccharides and the production of toxins (Kaper et al., 2004; Crépin et al., 2012; López-Banda et al., 2014).

One of the virulence factors identified in some UPEC is the Vacuolating autotransporter toxin (Vat), which is a member of the serine protease autotransporter proteins of *Enterobacteriaceae* (SPATEs). The Vat toxin is a ∼110 kDa secreted protein exported by the Type Va secretion system and belongs to the class II cytotoxic SPATEs (Henderson and Nataro, 2001; Dutta et al., 2002; Nichols et al., 2016). The *vat* gene has been identified in both avian pathogenic *E. coli* (APEC) and UPEC strains. It has been shown to generate the formation of vacuoles in chicken embryo fibroblasts and contribute to the development of cellulitis in chickens (Parreira and Gyles, 2003). Although the mechanism of action of Vat and its implication in the development of UTIs is not entirely known, the gene sequences encoding the toxin were detected in 36% of UPEC strains (Ramírez-Castillo et al., 2018). In a different study, the *vat* gene was found in patients with cystitis (57.9%), pyelonephritis (59.3%), prostatitis (72.4%) and septicemia (64.7%) (Parham et al., 2005; Spurbeck et al., 2012; Nichols et al., 2016). Also, our group recently published the prevalence of *vat* genes in UPEC from Guadeloupe (Habouria et al., 2019) where *vat* sequences were found in 333 isolates (48.7%) of the UTI strains. Despite the fact that Vat is one of the most prevalent SPATEs in UPEC, the mechanism of action and specific activity of this protein during urinary infection has not been determined (Welch, 2016).

The bladder epithelial cell is an *in vitro* cell culture model extensively studied because of the interaction of these cells during the pathogenesis of infection (McLellan and Hunstad, 2016). The urothelium plays a significant role as a barrier against biotic and abiotic agents, and disruption of this barrier may lead to urinary tract disease (Parsons, 2007). The characteristics of the urothelial wall are mainly imparted by the integrity of the bladder cells. Interestingly, enteroaggregative and enteropathogenic *Escherichia coli* induce epithelial cell damage that involves virulence factors such as SPATEs (Gates and Peifer, 2005; Khurana, 2006; Windoffer et al., 2011; Sanchez-Villamil et al., 2019). Thus, the objective of this study was to determine the effects of the vacuolating autotransporter toxin, Vat, from *Escherichia coli* on human epithelial bladder cells, in order to elucidate the mechanism of action of this toxin, and to serve as a basis for a more detailed study of this virulence factor, serving as a precedent of its function *in vivo*.

MATERIALS AND METHODS

Bacterial Strains and Cell Culture

The *vat* autotransporter encoding gene was amplified by PCR using specific primers (Forward: TATTGGATCCTCCGCTCTGAACCGCCACGC; Reverse: CAAGCTTCGTAATCAGATAATCGCAGC) from pathogenic *E. coli* strain QT598 (Genbank accession QDB64244.1) (Habouria et al., 2019), which with the exception of a single Arg_{534} to His_{534} substitution is identical to Vat (c0393) from UPEC strain CFT073. PCR products contained 15 bp extensions homologous to the pUCmT multi-cloning site. Linearized pUCmT digested with *Xho*I and *BamHI* was used to clone inserts by fusion reaction with the Quick-fusion cloning kit (Biotool, #B2261). The plasmid clones were transformed into *E. coli* DH5α then into *E. coli* BL21 for protein production (Habouria et al., 2019). The model to test the cytotoxicity of Vat was performed with human urinary bladder epithelial cell line ATCC 5637 (American Type Culture Collection HTB-9). The cells were maintained in RPMI 1640 (Sigma-Aldrich, #R7509) supplemented with 10% heat-inactivated fetal calf serum (Invitrogen, #16000044) without antibiotics.

Vat Production and Concentration

Escherichia coli BL21 (pUCmT::*vat*) was grown in 200 ml of Lennox Broth (LB) medium with ampicillin (100 μg/ml) overnight (37°C/100 rpm). The culture was centrifuged (2,370 × g for 10 min at 4°C) and the supernatant filtered through a 0.22 μm membrane filter (Corning Inc, # R7509) (Salvadori et al., 2001). The protein from the sterile supernatant was

concentrated through a 50 kDa centrifugal filter unit (Millipore, #UFC905024) by centrifugation (2,370 × g for 10 min at 4°C). Quantification of the protein was determined by Bradford assay, and the absorbance was measured at 595 nm, using a microplate reader (Bio-Rad, #028007). To determine the concentration of the protein the measurements were overlapped with a standard linear curve. The protein was visualized using Coomassie blue staining (**Figure 1**) after separation by sodium dodecyl sulfate-polyacrylamide gel electrophoresis (SDS-PAGE) (Dutta et al., 2002).

Cytotoxic Effect of Vat Toxin Measured by Lactate Dehydrogenase Release Assay

Confluent cultures of the 5637 cell line were grown in 96-well plates and were treated with different Vat concentrations from the concentrated supernatant sample (5, 25, 50, 75, 100 μg/ml) in a final volume of 100 μl of RPMI per well, and incubated at different times (3, 6, 12, and 24 h) (Dutta et al., 2002). Parreira and Gyles, 2003). The culture supernatant from *E. coli* BL21 containing the empty vector (pUCmT) was added volume/volume as a negative control to compare to bladder cells exposed to Vat supernatant. Cell damage was determined by lactate dehydrogenase (LDH) release using the LDH-Cytotoxicity Assay Kit II (Biovision, #K313) according to the manufacturer's instructions; the absorbance was measured at an optical density of 495 nm using a microplate reader (Fanizza et al., 2009). The background control (RPMI 1640-medium only) and the lysis control (treatment with Triton X-100) (Sigma, #T8787) were used (Peidaee et al., 2013). All the samples were tested by triplicate ($n = 3$). The results were obtained and analyzed statistically using Dunnett's multiple comparisons tests.

Evaluation of Vacuole Formation in Bladder Cells Following Exposure to Vat

The concentrated supernatant of the toxin was tested to determine the effect on bladder cells *in vitro* as reported previously for the effect of Vat on chicken fibroblast cell culture (Parreira and Gyles, 2003). The 5637-bladder cell line was grown in 8-well Lab-Tek chambers (Nunc, #Z734853) until ∼60% confluence. The monolayers were exposed to 50 μg/ml of the Vat toxin per well with a total volume of 300 μl RPMI 1640 and incubated for 0.5, 1, 3, 6, and 12 h at 37°C with 5% CO_2 (Greune et al., 2009; Habouria et al., 2019). After incubation, the cells were washed three times with PBS and stained with Giemsa dye (Hu et al., 2015). Vacuole formation was observed by optical microscope (Zeiss, Primo star). A random semiquantitative analysis of the images of the vacuolated cells per well was done, and the results were statistically analyzed using a one-way ANOVA multiple comparisons test.

Evaluation of Changes on Epithelial Bladder Cell Junctions Induced by Vat

Cultures of bladder cells were grown in 8-well Lab-Tek II chamber slides until reaching 100% confluence. The cultures were exposed to 50 μg/ml of Vat for 6 h, 12 h and 24 h; supernatant from a clone containing the empty vector was used as a negative control. The integrity of the urothelial monolayer was observed by Scanning Electron Microscopy. After exposure to Vat for different time points, samples were fixed with 2.5% Glutaraldehyde for 24 h, after that, the samples were dehydrated using increasing concentrations of ethanol (60, 70, 80, 90, 96, and 100%), incubating for 10 min in each step. At the end, the samples were dried at 37°C/5% CO_2 for 12 h (Nordestgaard and Rostgaard, 1985). The slide was covered with 100 Å of gold, using Denton Vacuum Desk II. Images were obtained and analyzed under JEOL JSM 5900LV, Scanning Electron Microscope.

The cell-cell distribution of ZO-1 and Occludin, tight junction molecules, were analyzed by immunofluorescence, using the same toxin exposition protocol as described above. Epithelial cells were fixed with 3.7% formaldehyde. After washing with PBS, the cells were permeabilized with 0.1% Triton X-100 for 5 min and then incubated with blocking solution, PBS / 5% BSA for 30 min. To label ZO-1 and Occludin, it was used a primary antibody Anti-ZO-1 (Abcam, #ab221547) and Anti-Occludin (Abcam, #ab216327) respectively, incubating for 2 h at 37°C. Secondary antibody anti-rabbit conjugated with Alexa fluor 488 for ZO-1 (Sigma-Aldrich, #SAB4600387) and Alexa fluor 594 (ThermoFisher, #A-11012) for Occludin. The samples were incubated for 2 h at 37°C. Then, samples were mounted with ProLong Gold (Invitrogen, # P36930) antifade reagent (Bercier et al., 2018). Images were obtained using a confocal microscope (Zeiss, LSM700) with Zen Black software (2012).

Fluorescence-Based Permeability Assay

Permeability changes following exposure of the bladder cell monolayer with Vat, were evaluated by a paracellular permeability assay using FITC-Dextran 4 (FD4) (Sigma-Aldrich, #60842-46-8) according to the method of Bercier et al. (2018). Briefly, 5637 Bladder cells were seeded and incubated until 100% confluence on Transwell polyester membrane cell culture inserts (Sigma-Aldrich, #CLS3472). The Basolateral space was filled with 300 μl PBS at the start the experiment. The apical chamber was filled with 300 μl of RPMI containing 50 μl/ml of Vat and 1 mg/ml of FD-4. The control was established using the empty vector supernatant in the same amount of cell media and FD4. The permeability measurement was made at 6, 12, and 24 h using a FP-8000 Series Fluorometer. The numeric results were interpreted as Relative Fluorescent Units (Bercier et al., 2018). All the experiments were performed by triplicate and the data analyzed statistically using two-way ANOVA comparisons tests.

Evaluation of Cell Damage and Cytoskeletal Changes Caused by Exposure to Vat

The F-actin, α-tubulin and Arp3 protein distribution changes produced following Vat treatment were evaluated using bladder cell cultures. Cell monolayers were cultured in 8-well Lab-Tek chambers until 60% confluency was reached and cells were then incubated with 50 μg of the Vat protein for 6 h; as a control to rule out a possible LPS effect on samples, cells were incubated with the toxin simultaneously with 50 μg/ml of polymyxin B

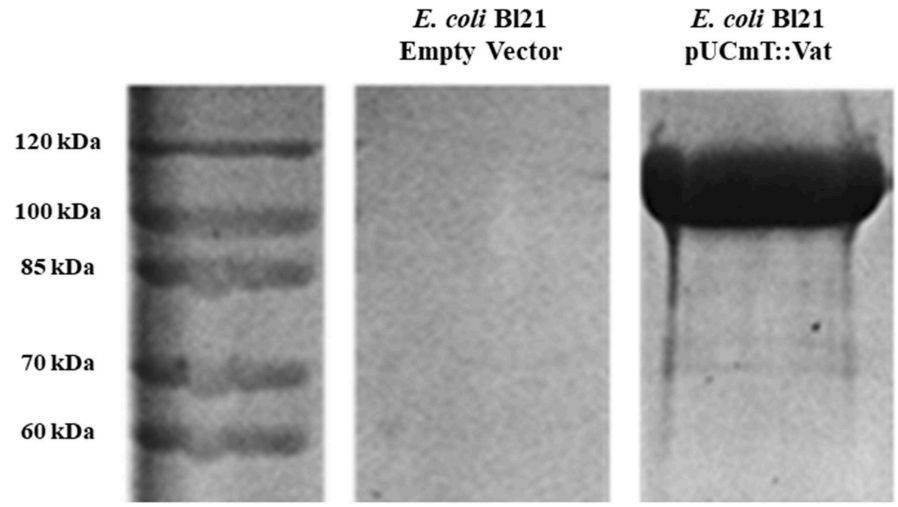

FIGURE 1 | Overexpression of Vat protein detected by SDS-PAGE. The filtered supernatants from overnight cultures of *E. coli* BL21 (pUCmT::vat) and *E. coli* BL21 empty vector were concentrated by Amicon filter units and the protein from the supernatant was migrated next to a protein marker (10–200 kDa). The gel was stained with Coomassie Blue.

(InvivoGen, #1405-20-5) (Tsuzuki et al., 2001; Lu et al., 2017). Cells incubated with 50 μg/ml of heat-inactivated Vat at 95°C for 20 min provided another control (Salvadori et al., 2001; Simon et al., 2018). After incubation, the cells were washed three times with PBS and were fixed.

F-Actin labeling was done by permeabilizing the samples and incubating with Alexa Fluor 488 phalloidin (Invitrogen, #A12379) at 37°C, during 60 min (Guerrero-Barrera et al., 1996). To observe the effect on α-tubulin after Vat incubation, samples were permeabilized and blocked as described above. To label tubulin in cells, anti-α-Tubulin (Sigma, #T5168) at 10 μg/ml was used as the primary antibody and incubated for 2 h at 37°C. This was followed by incubation with a secondary antibody conjugated with Alexa fluor 488 for 2 h at 37°C. The samples were mounted (Invitrogen, # P36930) and images were obtained by confocal microscope.

Labeling of Acidic Organelles in Bladder Cells After Exposure to Vat

Samples were processed for fluorescence detection of acidic organelles with Lysotracker Deep Red staining (Thermo Fisher, # L12492) (Chen et al., 2015; Magryś et al., 2018). Bladder cells plated on 8-well glass slides were treated with 50 μg/ml of Vat for 6 h. After incubation, cells were washed three time with PBS and were exposed to 300 μl of RPMI added with Lysotracker Deep Red reagent at 10 nM. After 1 h of incubation at 37°C, samples were washed and mounted with Prolong Gold prior to analysis by confocal microscopy (Nagahama et al., 2011).

Ex vivo Culture of Murine Urinary Bladder Exposed to Vat

The animal protocol for this study was approved by the animal ethics committee of the Autonomous University of Aguascalientes, México in accordance with the NIH ethical program. Eight BALB/c female mice were sedated and euthanized to obtain by midline laparotomy urinary bladders. The procedure was developed under sterile conditions (Durnin et al., 2018; Gabella, 2019). In 12-well plates (Corning, #3513) the bladders were placed in RPMI 1640 supplemented with 100 μg/mL streptomycin, 100 U/mL penicillin, 50 mg/L gentamicin. The tissues were exposed to 25, 50, and 100 μg of Vat toxin and incubated for 24 or 48 h at 37°C in 5% CO_2. The control tissue was incubated for 48 h with supernatant from a clone containing the empty vector. Another control used was simply RPMI 1640 medium for 48 h in order to observe possible changes in the tissue during the cell culture time period (Kannan and Baseman, 2006). Formalin-fixed bladders were dehydrated and cleared automatically with a Histokinette (Leica, #TP1020). Next, the tissues were embedded in paraffin and 5 μm thick sections were obtained (Kim et al., 2010; Najafzadeh et al., 2011). Tissues were stained with hematoxylin and eosin (Prophet et al., 1995) and observed under an optical microscope with a 40X objective (Zeiss, Primo star).

Statistical Methods

GraphPad Prism 8.0 was the software used to evaluate the quantitative data in this study. Dunnett's multiple comparisons tests were used to analyze the presence of statistically significant differences ($P \leq 0.05$) between the cells exposed to empty vector supernatant or following exposure to different concentrations of Vat for the LDH release assay. One-way ANOVA, and the multiple comparisons test was used to evaluate the quantity of vacuolated cells per field generated depending on the exposure time to Vat. Two-way ANOVA was used for statistical comparisons of samples from the fluorescence-based cell permeability assay.

RESULTS

Cytotoxic Effect of Vat Toxin Measured by Lactate Dehydrogenase Release Assay

LDH release from cells to the extracellular media is considered an indicator of cell membrane integrity damage (Fanizza et al., 2009; Radin et al., 2011). Vat treatment of bladder cells with different toxin concentrations (5, 25, 50, 75, 100 μg/ml) at different times (3, 6, 12, and 24 h) showed statistically significant differences in comparison with the *E. coli* empty vector supernatant treatment ($P \leq 0.05$) (**Figure 2**). LDH released to the media was dependent on the time of exposure and concentration of Vat.

Vacuole Formation in Bladder Cells Exposed to Vat

The bladder cells exposed to Vat during 6 h showed vacuole formation that increased in numbers with the time of exposition (**Figure 3A**). There were no vacuoles observed following exposure to toxin for 0.5 or 1 h. Statistically significant vacuole production (**Supplementary Image 1**) was found after 3 h of exposure to the toxin (**Figure 3B**).

Evaluation of Changes to Epithelial Cell Junctions Following Exposure to Vat

Scanning Electronic Microscopy analysis of the bladder cell monolayer, showed increased spacing between cells when it was exposed to Vat, as well as changes in cell morphology (**Figure 4**). After 6 h of treatment, these spaces appeared in the monolayer when compared to the control cells. This damage increased with time of exposure and resembled alterations between cell-cell junctions. In order to characterize cellular alterations due to Vat, the localization of two important tight junction molecules, ZO-1 and Occludin, were evaluated. Vat induced discontinuities in the pattern of distribution of both ZO-1 and Occludin in bladder epithelial cells following 12 and 24 h of treatment (**Figure 4**).

Fluorescence-Based Permeability Assay for Epithelial Bladder Monolayer Cell Culture Treated With Vat Toxin

Changes in monolayer integrity were confirmed by the permeability assay. The quantification of FD4 fluorescence in the supernatants of basolateral transwell chambers showed a significative difference in permeability at 12 and 24 h of toxin exposure with respect to the control (**Figure 5**). The fluorescence increased by ∼2-fold from 12 to 24 h of exposure.

Evaluation of Cell Damage Induced by Vat Through Cytoskeletal Changes

Bladder cell cultures exposed to Vat were analyzed for alterations of the cytoskeleton components actin and tubulin by confocal microscopy. After 6 h of exposure to Vat toxin, cells labeled with phalloidin, revealed changes in F-actin distribution with a diffuse pattern (**Figure 6B**) resulting in round cell shape, loss of integrity of stress fibers, and disruption of cell-cell interactions. In the control cells treated with the empty vector supernatant, the F-actin cytoskeleton was intact with well-defined stress fibers distributed along with the cytoplasm (**Figure 6A**). In control cells, tubulin showed mainly a peripheral distribution and a normal cell shape (**Figure 6C**). When cells were treated with Vat toxin, this pattern changed, and tubulin was more diffuse at the cell surface, and correlated with the altered morphology of the cells (**Figure 6D**). Toxin activity was validated using control samples, testing the cells with heat-inactivated toxin and by the addition of polymyxin B to inhibit any potential cellular changes that might be caused by traces of LPS present in the culture supernatants (**Supplementary Image 2**).

Labeling of Acidic Organelles After Exposure to Vat

Acidic organelles were found using Lysotracker Deep Red. **Figure 7** shows cells after 12 h of Vat treatment (**Figure 7B**),

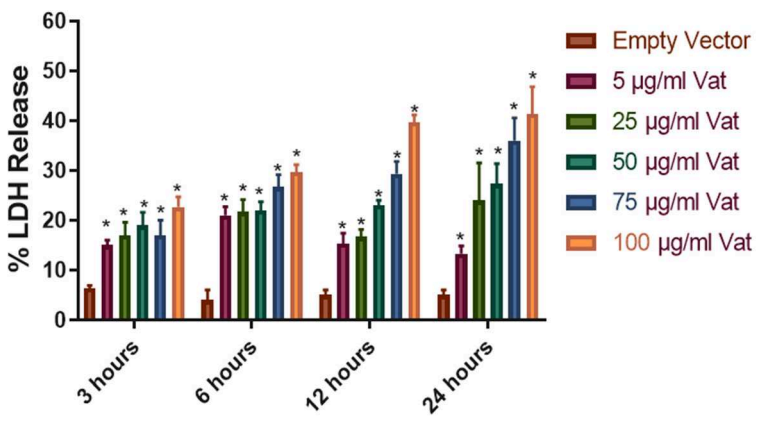

FIGURE 2 | Cellular damage provoked by Vat toxin measured by LDH release. Cells from human urinary bladder cell line 5,637 were exposed during 3, 6, 12, and 24 h to 5, 25, 50, 75, and 100 μg/ml of Vat toxin. As a control supernatant from the empty vector was used. After incubation, LDH in the cell culture supernatant was measured. All toxin concentrations showed statistically significant differences compared to the control in a dose- and time-dependent manner. The percentage of cell damage after toxin exposure resulted in 15 to 47% LDH release (*$p \leq 0.05$, two-way ANOVA, Dunnett's test).

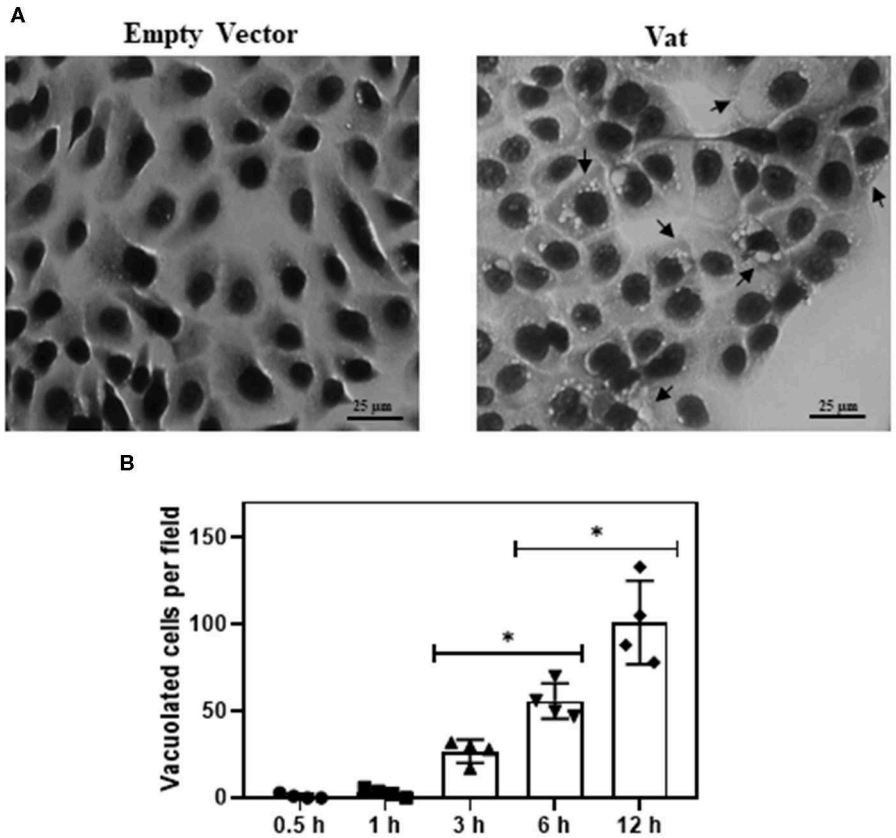

FIGURE 3 | Effect of Vat in human urinary bladder cells 5637 at different time of exposition **(A)** Control cells exposed to empty vector for 6 h, showing normal cell shape and distribution on the monolayer. The cells incubated for 6 h with 50 μg/ml of Vat toxin, exhibit cytoplasmic vacuole formation (black arrows). **(B)** Plotted results of the vacuole formation showed a significative difference between 3 to 6 h and 6 to 12 h. (*$p \leq 0.05$, ANOVA, Dunnett's).

with the distribution of acidic organelles. A merged image combining bright field and fluorescence (**Figure 7C**) identifies cells containing multiple vacuoles that are not fluorescent (white arrows), whereas acidic organelles are shown with black arrows. **Supplementary Image 3** shows that acidic organelles are also produced by control cells. By contrast the vacuoles produced by Vat are not labeled with Lysotracker.

Ex vivo Culture of Murine Urinary Bladder Tissue Exposed to Vat

Bladder tissues exposed to different concentrations of Vat for 24 and 48 h showed partial cell desquamation of the urothelial cells (Black arrow) in comparison with the controls. This effect was dependent on toxin concentration (**Figure 8**). With 25 μg/ml of toxin at 24 h (**Figure 7C**), the most superficial urothelial cells showed exfoliation from the underlying tissue. Treatment with 50 μg/ml of Vat for 24 h (**Figure 8D**) caused extended changes in epithelial cell integrity, affecting deeper stratum. Higher concentrations of Vat resulted in a thinner urothelium in comparison with other samples, this suggests that Vat caused a loss of normal integrity of the epithelial cell barrier. Also, Vat treatment showed an alteration of the urinary bladder lamina propria. After 48 h of incubation with 25 μg/ml of Vat, the transitional epithelium was absent and the lamina propria was loose and disorganized (**Figure 8F**). Treatment with 50 μg/ml of toxin increased damage to the lamina propria, resulting in loss of the normal bladder structure (**Figure 8G**). Similar results were observed with 100 μg/ml of Vat at 48 h (**Figure 8H**). Tissue changes were compared with bladder exposed to supernatant from bacteria containing only the empty vector or only with RPMI 1640 cell culture medium for 48 h in order to validate the *ex vivo* experiments and the action of Vat toxin on tissues (**Figures 8A,B**).

Discussion

Exposure of bladder cells to the Vacuolating autotransporter toxin caused vacuole formation, and these changes resembled cytological changes observed previously in avian cell models (Parreira and Gyles, 2003; Nichols et al., 2016). Also, cell rounding of the bladder cells and the alteration in cell-cell contact could result in the loss of integrity of the urothelial barrier. This epithelial disruption has also been observed with another vacuolating toxin, VacA, from *Helicobacter pylori* (Tombola et al., 1999; de Bernard et al., 2004; Bercier et al., 2018).

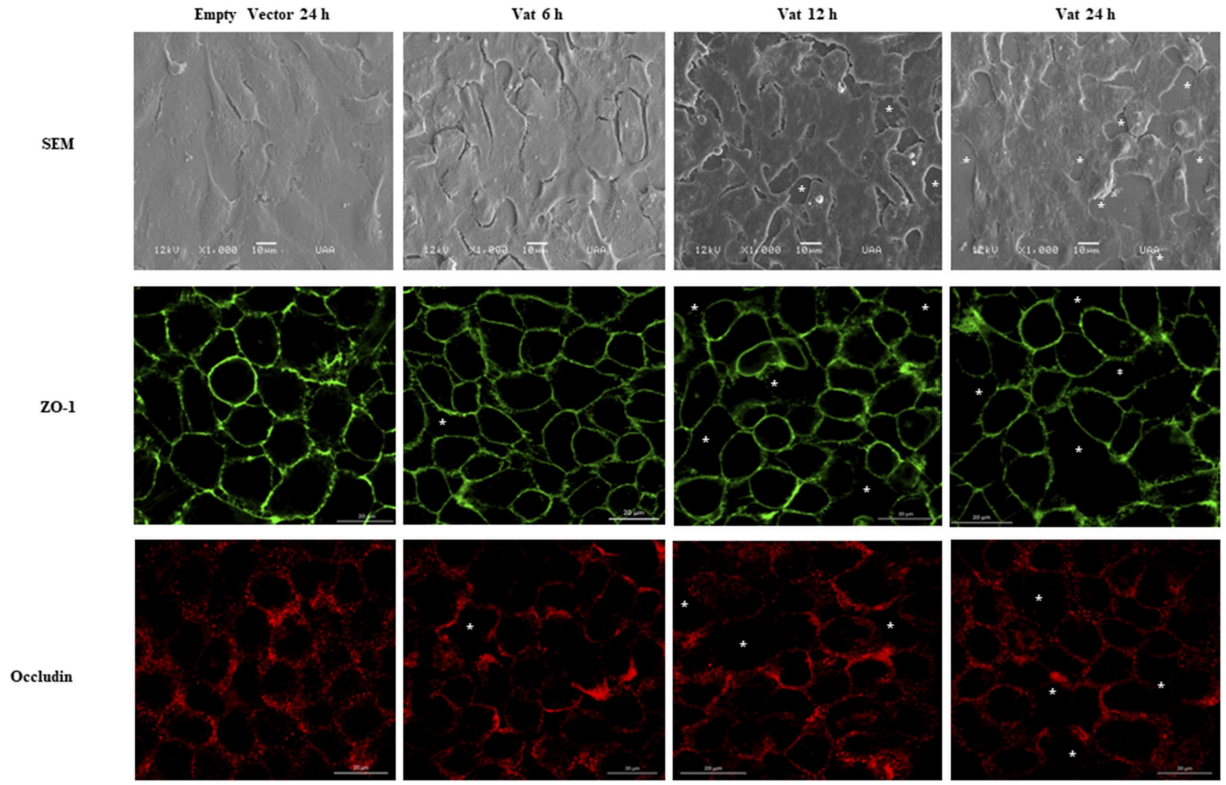

FIGURE 4 | Modification of cell junctions of the bladder urothelial monolayer after incubation with Vat. Analysis by scanning electron microscopy revealed loss of integrity of the cell monolayer (White asterisks) starting at 6 h. The changes in the monolayer are more visible at 12 and 24 h after exposure to the toxin in comparison to the control. The immunofluorescence labeling of ZO-1 and Occludin proteins show cell junction disruption in the cell monolayer.

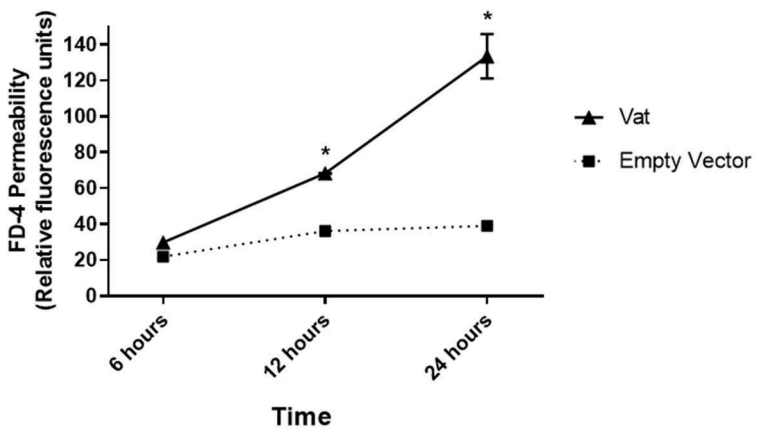

FIGURE 5 | Fluorescence-based permeability assay of a bladder epithelial cell monolayer treated with Vat toxin. The quantitative method showed changes in the permeability of the monolayer exposed to the toxin. Comparison between the Vat toxin and the empty vector control supernatant had statistically significant differences at 6 and 12 h of incubation (*$p \leq 0.05$, two-way ANOVA).

Lactate Dehydrogenase (LDH) is a cytoplasmic enzyme that is released into the extracellular medium when cell membrane integrity is compromised. Time of exposure and dose effect on cytotoxic activity of Vat was assessed by LDH release and suggests that a high concentration and exposure time of at least 6 h was required to achieve a high level (>50%) of cytotoxicity for bladder cells *in vitro*. These results in comparison to other bacterial toxins from *Escherichia coli*, *Helicobacter pylori* and *Clostridioides difficile* toxin (Grossmann et al., 2000; Roberts et al., 2001; Radin et al., 2011), suggest that Vat likely plays a subtle role in the pathogenesis of UTIs (Roberts et al., 2001; Peterson et al., 2009).

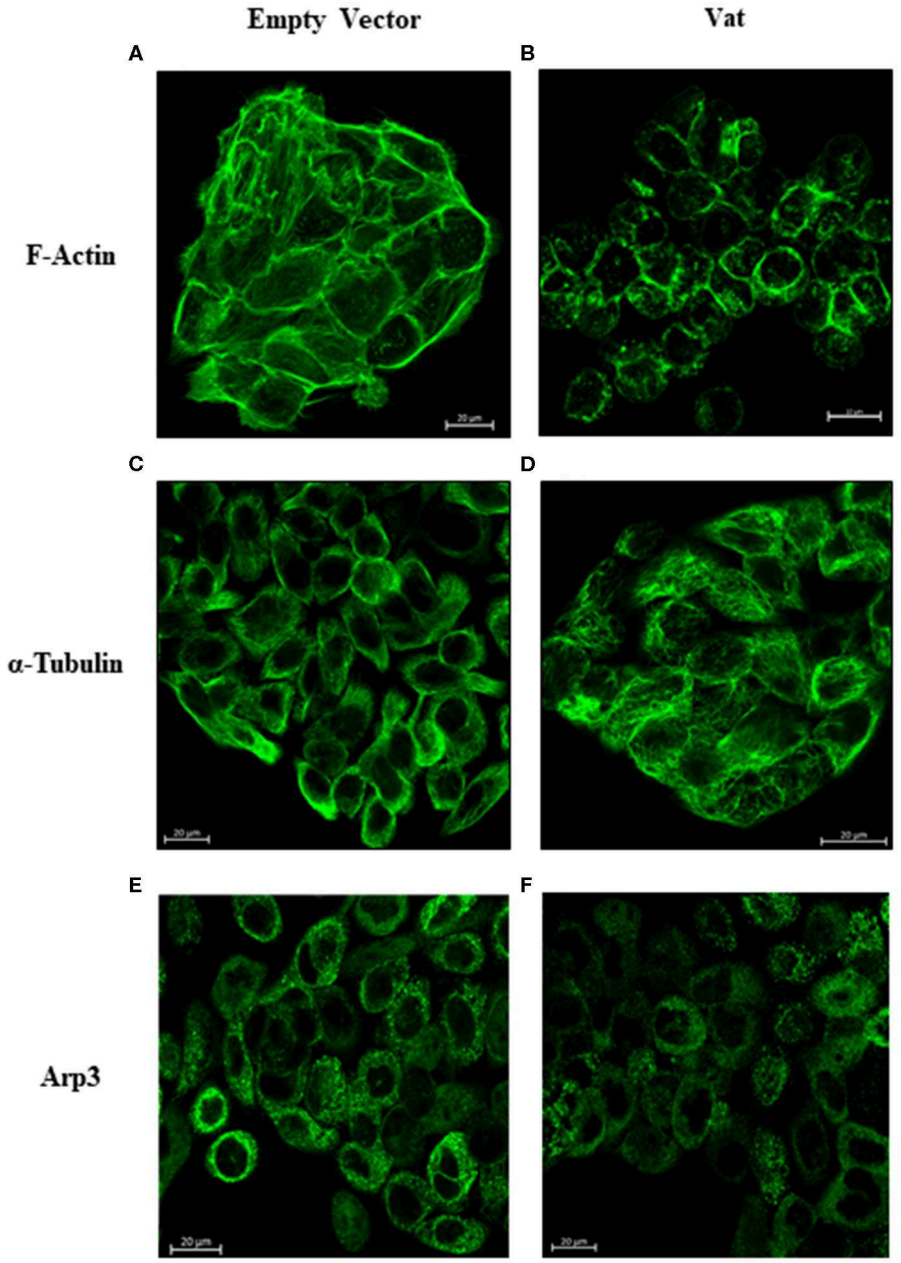

FIGURE 6 | Changes in the distribution of F-actin, α-Tubulin, and Arp3 cytoskeletal proteins detected after Vat treatment of bladder cells observed by confocal microscopy. The negative control cells **(A)** showed a normal distribution of actin stress fibers with a normal cell shape and appearance. After exposure to Vat **(B)** the cells acquired a rounded shape with loss of the cytoplasmic actin stress fibers. Normal tubulin distribution was observed in the control cells **(C)** with its presence throughout the cell. Once cells were exposed to Vat **(D)** the distribution of tubulin was altered. Arp3 demonstrated a cytoplasmic dotted distribution **(E)** on the untreated cells, and there was no evident change in Arp3 distribution when cells were treated with Vat **(F)**.

Cell damage can also be evaluated through cytoskeletal changes such as distribution of F-actin and tubulin that have an effect on cell morphology and cell-cell association. Alfaro-Aco and Petry (2015) have proposed that actin and tubulin cytoskeleton components play a critical role in cytoprotection, intercellular junction maintenance, shape definition and intracellular vesicular transport (Tang et al., 2014; Gefen and Weihs, 2015; Tran and Ten Hagen, 2017). Damage to these cytoskeletal components, as observed after the exposure to Vat, affects the normal cell distribution and morphology *in vitro*. The alteration and redistribution of F-actin and α-tubulin in the cytoskeleton correlated with the morphological changes in cells, a decrease in monolayer integrity and the desquamation of cells from the substrate, a phenomenon similar to what occurs

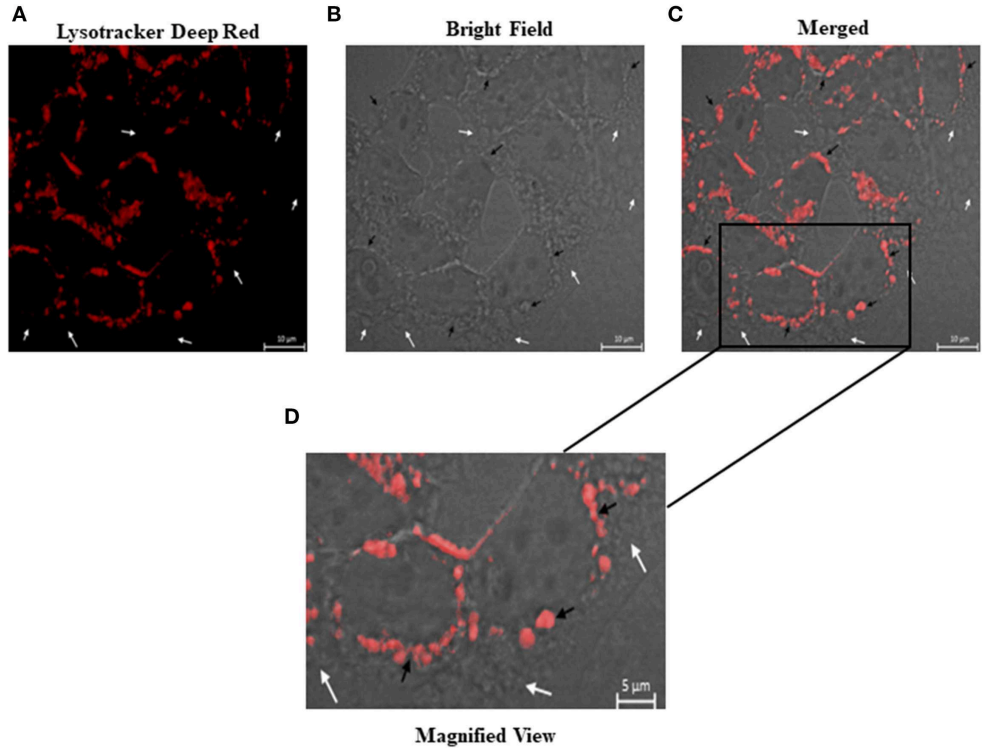

FIGURE 7 | Characterization of the vacuoles produced in bladder epithelial cells after treatment with Vat. After 12 h of Vat exposure, samples were labeled with Lysotracker deep red to identify acidic organelles **(A–C)**. The vacuoles that incorporated Lysotracker reagent (Black arrows) show a red color. Some other vacuoles were identified in the samples which did not have an acidic content (White arrows) **(C,D)**.

following exposure of cells to other SPATEs (Dautin, 2010; Liévin-Le Moal et al., 2011; Glotfelty et al., 2014; Gasic and Mitchison, 2019).

Vacuole formation within mammalian cells affects cell homeostasis. A variety of secreted bacterial toxins can induce vacuole production in cells with different functions in its pathogenesis in the host (Lee et al., 2015; Shubin et al., 2016; Magryś et al., 2018). In order to determine the nature of the vacuoles generated by the Vat toxin, the presence of acidic organelles was determined in bladder cells. The results obtained in this study by the overlaying of fluorescence confocal microscopy and bright field image, reveals acidic content in some vacuoles generated by Vat as well as others vacuoles with non-acidic characteristics inside of them (Nagahama et al., 2011; Chen et al., 2015). The non-lysosomal nature of some vacuoles in bladder cells treated with Vat is of interest and merits further investigation (Appelqvist et al., 2013; Ram and Ramakrishna, 2014; Shubin et al., 2016).

Finally, our *ex vivo* experiment suggests that Vat can induce detachment of epithelial cells comprising the urothelium of the bladder, possibly as a direct effect of the toxin on the adhesion molecules of the cell surface or due to an indirect effect caused by changes in the morphology of the cells as a consequence of alterations to the cytoskeleton. Further, the lamina propia underlying the urothelium of the bladder was affected by Vat at the highest concentration. This suggests that some connective tissue molecules may be targeted by the toxin. Proteolytic activity of Vat has been shown to exhibit an elastase-like activity (Habouria et al., 2019). This result is in agreement with our *in vitro* experiments in which we observed the loss of intercellular contacts of cells from the monolayer and in its integrity showed with the permeability assay.

In conclusion, the effect of the vacuolating autotransporter toxin from *Escherichia coli* was investigated by using a bladder epithelial cell model. Cytotoxicity of Vat was dose-dependent and suggested that Vat most likely acts as a cytopathic toxin that alters bladder cell function with a limited degree of cell death. Vat caused vacuole formation on bladder cells similar to the cytopathic effects that were previously reported following exposure of avian cells to *E. coli* culture supernatants containing Vat. Also, the Vat toxin caused alterations on cell junctions, affecting monolayer integrity, causing redistribution of tight junction proteins and increasing urothelial cell permeability. Furthermore, redistribution of actin and tubulin in bladder epithelial cells occurred simultaneously with morphological changes on cells. In addition, our results suggest that some vacuoles on epithelial cells induced by Vat have not acidic content. Finally, our *ex vivo* experiments on murine bladder demonstrated that Vat caused alterations of the urothelium and lamina propria of the bladder. It will be of future interest to

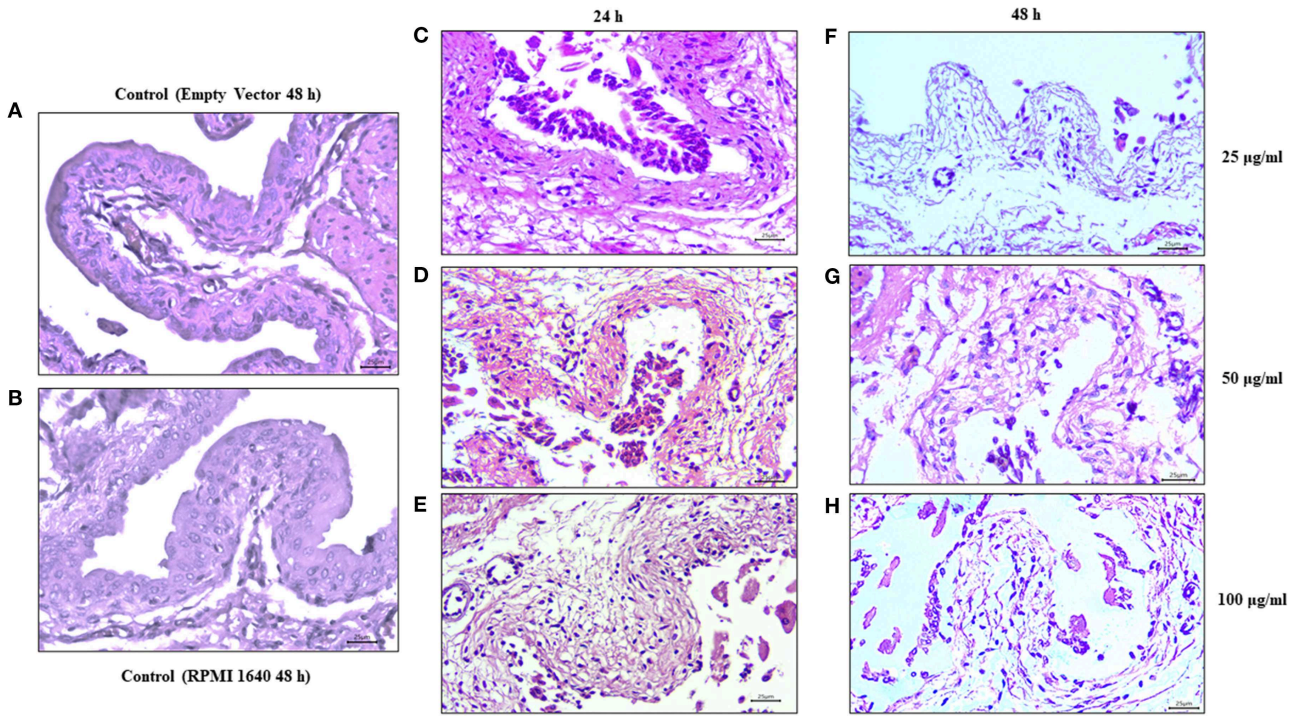

FIGURE 8 | Effect of Vat on urinary bladder tissues. Mouse urinary bladders were incubated *ex vivo* with 25, 50, and 100 µg/ml of Vat toxin supernatant for 24 h or for 48 h. After 24 h of Vat treatment **(C–E)**, detachment of the urothelium from the underlying connective tissue was observed (Black arrows). This effect was dependent on the toxin concentration. After 48 h of incubation, alterations in the lamina propria (Black asterisk) were visible on bladder samples with a loose and disorganized connective tissue **(F–H)**. Those changes were compared with bladders exposed to the empty vector supernatant and the control containing only RPMI 1640 medium **(A,B)**.

investigate whether Vat targets an adhesion molecule on the epithelial cell surface or a specific component of the lamina propria. As well, characterization of the composition of the vacuoles induced by Vat may provide further evidence of how this toxin contributes to the pathogenesis of UTIs caused by UPEC.

DATA AVAILABILITY STATEMENT

All datasets generated for this study are included in the article/**Supplementary Material**.

ETHICS STATEMENT

This study was reviewed and approved by the ethics committee for the use of animals in the teaching and research of The Autonomous University of Aguascalientes.

AUTHOR CONTRIBUTIONS

JD was the primary author of the manuscript. CD and PP contributed to optimization of protein production and revision of the manuscript. FA-G provided expertise in statistical analysis. EH-C advised for the planning and design of some experiments. AS contributed to the development of experimental work. AG-B proposed the line of research and was responsible for major funding of the project.

FUNDING

This work was funded through the support of CONACyT scholarship (572462). Universidad Autonoma de Aguascalientes, Mexico Award number: PIBT16-3 to ALGB. The project was supported by Special Resource UAA for Research 2017 and 2018, as well as Fonds de recherche du Québec–Nature et technologies (FRQ-NT) and the Centre de recherche en infectiologie porcine et avicole (CRIPA) that provided an international internship, #264179, to JMDV. CD was funded by NSERC Discovery grant 2019-06642.

ACKNOWLEDGMENTS

We thank Dr. Josée Harel and Dr. Cécile Crost for their support and guidance on the cooperative funding through the CRIPA FRQ-NT funded internship program. We thank Adriana Cecilia Moreno Flores for technical assistance with confocal microscopy, also to Sébastien Houle and Fabiola Galindo Guerrero for their technical assistance.

SUPPLEMENTARY MATERIAL

The Supplementary Material for this article can be found online at: https://www.frontiersin.org/articles/10.3389/fcimb.2020.00299/full#supplementary-material

Supplementary Image 1 | Kinetics of vacuole formation induced by Vat toxin on human urinary bladder cell line 5,637. Kinetics of vacuole formation (Black arrows) showed cytoplasmic vacuoles after 3 h of toxin exposure, with vacuole formation increasing over time.

Supplementary Image 2 | Distribution of F-actin, α-Tubulin, and Arp3 cytoskeletal proteins detected after treatment of bladder epithelial cells with Vat observed by confocal microscopy. The negative control cells **(A)** show a normal distribution of actin stress fibers with a homogeneous pattern. A similar pattern was observed in samples exposed to 50 μg of heat-inactivated Vat toxin **(B)**. After exposure to Vat **(C)**, the cells acquired a rounded shape with a loss of the cytoplasmic actin stress fibers. This effect was also observed in cells treated with Vat together with polymyxin B **(D)**. Tubulin was distributed throughout the cell in control cells **(E)** with its presence throughout the cell. Cells incubated with the toxin after heat inactivation have a similar tubulin pattern as those treated with the empty vector supernatant **(F)**. Once cells were exposed to Vat **(G)**, the tubulin pattern showed cytoplasmic rearrangement resembling the morphological changes in cell shape **(H)**. The presence of Polymyxin B in the cell culture did not alter the effect of the toxin on cells. Arp3 had a cytoplasmic dotted distribution **(I)** in untreated control cells. This was also the case with cells exposed to the inactivated toxin **(J)**. Cells after treatment with Vat **(K)** with or without polymyxin B **(L)**, showed a homogeneous cytoplasmic distribution of Arp3 in contrast to the control cells.

Supplementary Image 3 | Characterization of the vacuoles in bladder epithelial cells treated with Vat. After exposure to Vat toxin, cells were stained with Lysotracker deep red and visualized. Vacuoles with acidic content (Black arrows) with a perinuclear distribution were observed and other vacuoles without lysotracker staining were also observed (White arrows). The samples exposed to supernatant from bacteria contain the empty vector did not produce vacuoles (Bright-field microscopy), and the slight lysotracker staining may indicate a basal level of lysosomes in these cells.

REFERENCES

Alfaro-Aco, R., and Petry, S. (2015). Building the microtubule cytoskeleton piece by piece. *J. Biol. Chem.* 290, 17154–17162. doi: 10.1074/jbc.R115.638452

Appelqvist, H., Wäster, P., Kågedal, K., and Öllinger, K. (2013). The lysosome: from waste bag to potential therapeutic target. *J. Mol. Cell Biol.* 5, 214–226. doi: 10.1093/jmcb/mjt022

Bercier, P., Gottschalk, M., and Grenier, D. (2018). Effects of actinobacillus pleuropneumoniae on barrier function and inflammatory response of pig tracheal epithelial cells. *Pathog. Dis.* 77:fty079. doi: 10.1093/femspd/fty079

Chen, X., Bi, Y., Wang, T., Li, P., Yan, X., Hou, S., et al. (2015). Lysosomal targeting with stable and sensitive fluorescent probes (superior lysoprobes): applications for lysosome labeling and tracking during apoptosis. *Sci. Rep.* 5:9004. doi: 10.1038/srep09004

Crépin, S., Houle, S., Charbonneau, M., Mourez, M., Harel, J., and Dozois, C. (2012). Decreased expression of type 1 fimbriae by apstmutant of uropathogenic *Escherichia coli* reduces urinary tract infection. *Infect. Immun.* 80, 2802–2815. doi: 10.1128/IAI.00162-12

Dautin, N. (2010). Serine protease autotransporters of enterobacteriaceae (SPATEs): biogenesis and function. *Toxins* 2, 1179–1206. doi: 10.3390/toxins2061179

de Bernard, M., Cappon, A., Del Giudice, G., Rappuoli, R., and Montecucco, C. (2004). The multiple cellular activities of the VacA cytotoxin of Helicobacter pylori. *Int. J. Med. Microbiol.* 293, 589–597. doi: 10.1078/1438-4221-00299

Durnin, L., Kwok, B., Kukadia, P., McAvera, R., Corrigan, R., Ward, S., et al. (2018). An *ex vivo* bladder model with detrusor smooth muscle removed to analyse biologically active mediators released from the suburothelium. *J. Physiol.* 597, 1467–1485. doi: 10.1113/JP276924

Dutta, P. R., Cappello, R., Navarro-García, F., and Nataro, J. P. (2002). Functional comparison of serine protease autotransporters of Enterobacteriaceae. *Infect. Immun.* 70, 7105–7113. doi: 10.1128/iai.70.12.7105-7113.2002

Fanizza, C., Fresegna, A., Maiello, R., Paba, E., and Cavallo, D. (2009). Evaluation of cytotoxic concentration-time response in A549 cells exposed to respirableα-quartz. *J. Appl. Toxicol.* 29, 537–544. doi: 10.1002/jat.1440

Flores-Mireles, A., Walker, J., Caparon, M., and Hultgren, S. (2015). Urinary tract infections: epidemiology, mechanisms of infection and treatment options. *Nat. Rev. Microbiol.* 13, 269–284. doi: 10.1038/nrmicro3432

Foxman, B. (2003). Epidemiology of urinary tract infections: incidence, morbidity, and economic costs. *Dis. Month* 49, 53–70. doi: 10.1067/mda.2003.7

Gabella, G. (2019). Lamina propria: the connective tissue of rat urinary bladder mucosa. *Neurourol. Urodyn.* 38, 2093–2103. doi: 10.1002/nau.24085

Gasic, I., and Mitchison, T. (2019). Autoregulation and repair in microtubule homeostasis. *Curr. Opin. Cell Biol.* 56, 80–87. doi: 10.1016/j.ceb.2018.10.003

Gates, J., and Peifer, M. (2005). Can 1000 reviews be wrong? Actin, α-catenin, and adherens junctions. *Cell* 123, 769–772. doi: 10.1016/j.cell.2005.11.009

Gefen, A., and Weihs, D. (2015). Mechanical cytoprotection: a review of cytoskeleton-protection approaches for cells. *J. Biomech.* 49, 1321–1329. doi: 10.1016/j.jbiomech.2015.10.030

Glotfelty, L., Zahs, A., Iancu, C., Shen, L., and Hecht, G. (2014). Microtubules are required for efficient epithelial tight junction homeostasis and restoration. *Am. J. Physiol. Cell Physiol.* 307, C245–C254. doi: 10.1152/ajpcell.00336.2013

Greune, L., Kemper, B., Dobrindt, U., Geelen, J., Kim, K., Schmidt, M., et al. (2009). Vacuolisation of human microvascular endothelial cells by enterohaemorrhagic *Escherichia coli*. *Thromb. Haemost.* 102, 1080–1092. doi: 10.1160/TH09-07-0499

Grossmann, E., Longo, W., Kaminski, D., Smith, G., Murphy, C., Durham, R., et al. (2000). Clostridium difficile toxin: cytoskeletal changes and lactate dehydrogenase release in hepatocytes. *J. Surg. Res.* 88, 165–172. doi: 10.1006/jsre.1999.5736

Guerrero-Barrera, A., Garcia-Cuellar, C., Villalba, J., Segura-Nieto, M., Gomez-Lojero, C., Reyes, M., et al. (1996). Actin-related proteins in anabaena spp. and *Escherichia coli*. *Microbiology* 142, 1133–1140. doi: 10.1099/13500872-142-5-1133

Habouria, H., Pokharel, P., Maris, S., Garénaux, A., Bessaiah, H., Houle, S., et al. (2019). Three new serine-protease autotransporters of Enterobacteriaceae (SPATEs) from extra-intestinal pathogenic *Escherichia coli* and combined role of SPATEs for cytotoxicity and colonization of the mouse kidney. *Virulence* 10, 568–587. doi: 10.1080/21505594.2019.1624102

Henderson, I., and Nataro, J. (2001). Virulence functions of autotransporter proteins. *Infect. Immun.* 69, 1231–1243. doi: 10.1128/IAI.69.3.1231-1243.2001

Hu, X., Laguerre, V., Packert, D., Nakasone, A., and Moscinski, L. (2015). A simple and efficient method for preparing cell slides and staining without using cytocentrifuge and cytoclips. *Int. J. Cell Biol.* 2015, 1–4. doi: 10.1155/2015/813216

Kannan, T. R., and Baseman, J. B. (2006). ADP-ribosylating and vacuolating cytotoxin of *Mycoplasma pneumoniae* represents unique virulence determinant among bacterial pathogens. *Proc. Natl. Acad. Sci. U. S. A.* 103, 6724–6729. doi: 10.1073/pnas.0510644103

Kaper, J., Nataro, J., and Mobley, H. (2004). Pathogenic *Escherichia coli*. *Nat. Rev. Microbiol.* 2, 123–140. doi: 10.1038/nrmicro818

Khurana, S. (2006). *Aspects of the Cytoskeleton, Vol 37*. Burlington: Elsevier.

Kim, S., Song, S., Ahn, K., Kwon, D., Park, K., and Ryu, S. (2010). Changes in aquaporin 1 expression in rat urinary bladder after partial bladder outlet obstruction: preliminary report. *Korean J. Urol.* 51:281. doi: 10.4111/kju.2010.51.4.281

Lee, J.-H., McBrayer, M. K., Wolfe, D. M., Haslett, L. J., Kumar, A., Sato, Y., et al. (2015). Presenilin 1 maintains lysosomal Ca2+ homeostasis via TRPML1 by Regulating vATPase-Mediated lysosome acidification. *Cell Rep.* 12, 1430–1444.

Liévin-Le Moal, V., Comenge, Y., Ruby, V., Amsellem, R., Nicolas, V., and Servin, A. (2011). Secreted autotransporter toxin (Sat) triggers autophagy in

epithelial cells that relies on cell detachment. *Cell. Microbiol.* 13, 992–1013. doi: 10.1111/j.1462-5822.2011.01595.x

López-Banda, D., Carrillo-Casas, E., Leyva-Leyva, M., Orozco-Hoyuela, G., Manjarrez-Hernández, Á., Arroyo-Escalante, S., et al. (2014). Identification of virulence factors genes inescherichia coliisolates from women with urinary tract infection in Mexico. *BioMed. Res. Int.* 2014, 1–10. doi: 10.1155/2014/959206

Lu, X. X., Jiang, Y. F., Li, H., Ou, Y. Y., Zhang, Z. D., DI, H. Y., et al. (2017). Polymyxin B as an inhibitor of lipopolysaccharides contamination of herb crude polysaccharides in mononuclear cells. *Chin. J. Nat. Med.* 15, 487–494. doi: 10.1016/S1875-5364(17)30074-2

Magryś, A., Deryło, K., Bogut, A., Olender, A., and Tchórzewski, M. (2018). Intraphagolysosomal conditions predispose to *Staphylococcus epidermidis* small colony variants persistence in macrophages. *PLoS ONE* 13:e0207312. doi: 10.1371/journal.pone.0207312

McLellan, L., and Hunstad, D. (2016). Urinary tract infection: pathogenesis and outlook. *Trends Mol. Med.* 22, 946–957. doi: 10.1016/j.molmed.2016.09.003

Nagahama, M., Itohayashi, Y., Hara, H., Higashihara, M., Fukatani, Y., Takagishi, T., et al. (2011). Cellular vacuolation induced by clostridium perfringens epsilon-toxin. *FEBS J.* 278, 3395–3407. doi: 10.1111/j.1742-4658.2011.08263.x

Najafzadeh, H., Masoodi, A., Rezaie, A., and Mehrzadi, S. (2011). Comparison of the effect of vanadium and deferoxamine on acetaminophen toxicity in rats. *Indian J. Pharmacol.* 43, 429–432. doi: 10.4103/0253-7613.83115

Nichols, K., Totsika, M., Moriel, D., Lo, A., Yang, J., Wurpel, D., et al. (2016). Molecular characterization of the vacuolating autotransporter toxin in uropathogenic *Escherichia coli*. *J. Bacteriol.* 198, 1487–1498. doi: 10.1128/JB.00791-15

Nielubowicz, G., and Mobley, H. (2010). Host–pathogen interactions in urinary tract infection. *Nat. Rev. Urol.* 7, 430–441. doi: 10.1038/nrurol.2010.101

Nordestgaard, B., and Rostgaard, J. (1985). Critical-point drying versus freeze drying for scanning electron microscopy: a quantitative and qualitative study on isolated hepatocytes. *J. Microsc.* 137, 189–207. doi: 10.1111/j.1365-2818.1985.tb02577.x

Parham, N., Pollard, S., Desvaux, M., Scott-Tucker, A., Liu, C., Fivian, A., et al. (2005). Distribution of the serine protease autotransporters of the enterobacteriaceae among extraintestinal clinical isolates of *Escherichia coli*. *J. Clin. Microbiol.* 43, 4076–4082. doi: 10.1128/JCM.43.8.4076-4082.2005

Parreira, V., and Gyles, C. (2003). A novel pathogenicity island integrated adjacent to the thrW tRNA gene of avian pathogenic *Escherichia coli* encodes a vacuolating autotransporter toxin. *Infect. Immun.* 71, 5087–5096. doi: 10.1128/IAI.71.9.5087-5096.2003

Parsons, C. (2007). The role of the urinary epithelium in the pathogenesis of interstitial cystitis/prostatitis/urethritis. *Urology* 69, S9–S16. doi: 10.1016/j.urology.2006.03.084

Peidaee, P., Almansour, N., Shukla, R., and Pirogova, E. (2013). The cytotoxic effects of low intensity visible and infrared light on human breast cancer (MCF7) cells. *Comput. Struct. Biotechnol. J.* 6:e201303015. doi: 10.5936/csbj.201303015

Peterson, D., Collier, J., Katterman, M., Turner, R., and Riley, M. (2009). Cytotoxicity of bacterial-derived toxins to immortal lung epithelial and macrophage cells. *Appl. Biochem. Biotechnol.* 160, 751–763. doi: 10.1007/s12010-009-8526-y

Prophet, E., Mills, B., Arrington, J., and Sobin, L. (1995). *Laboratory Methods in Histotechnology*. Washington: American Registry of Pathology.

Radin, J., González-Rivera, C., Ivie, S., McClain, M., and Cover, T. (2011). Helicobacter pylori VacA induces programmed necrosis in gastric epithelial cells. *Infect. Immun.* 79, 2535–2543. doi: 10.1128/IAI.01370-10

Ram, B. M., and Ramakrishna, G. (2014). Endoplasmic reticulum vacuolation and unfolded protein response leading to paraptosis like cell death in cyclosporine A treated cancer cervix cells is mediated by cyclophilin B inhibition. *Biochim. Biophys. Acta* 1843, 2497–2512. doi: 10.1016/j.bbamcr.2014.06.020

Ramírez-Castillo, F., Moreno-Flores, A., Avelar-González, F., Márquez-Díaz, F., Harel, J., and Guerrero-Barrera, A. (2018). An evaluation of multidrug-resistant *Escherichia coli* isolates in urinary tract infections from aguascalientes, Mexico: cross-sectional study. *Ann. Clin. Microbiol. Antimicrob.* 17:34. doi: 10.1186/s12941-018-0286-5

Roberts, P., Davis, K., Garstka, W., and Bhunia, A. (2001). Lactate dehydrogenase release assay from Vero cells to distinguish verotoxin producing *Escherichia coli* from non-verotoxin producing strains. *J. Microbiol. Methods* 43, 171–181. doi: 10.1016/S0167-7012(00)00222-0

Salvadori, M., Yano, T., Carvalho, H., Parreira, V., and Gyles, C. (2001). Vacuolating cytotoxin produced by avian pathogenic *Escherichia coli*. *Avian Dis.* 45, 43–51. doi: 10.2307/1593010

Sanchez-Villamil, J., Navarro-Garcia, F., Castillo-Romero, A., Gutierrez-Gutierrez, F., Tapia, D., and Tapia-Pastrana, G. (2019). Curcumin blocks cytotoxicity of enteroaggregative and enteropathogenic *Escherichia coli* by blocking pet and EspC proteolytic release from bacterial outer membrane. *Front. Cell. Infect. Microbiol.* 9:334. doi: 10.3389/fcimb.2019.00334

Shubin, A. V., Demidyuk, I. V., Komissarov, A. A., Rafieva, L. M., and Kostrov, S. V. (2016). Cytoplasmic vacuolization in cell death and survival. *Oncotarget* 7, 55863–55889. doi: 10.18632/oncotarget.10150

Simon, J., Müller, J., Ghazaryan, A., Morsbach, S., Mailänder, V., and Landfester, K. (2018). Protein denaturation caused by heat inactivation detrimentally affects biomolecular corona formation and cellular uptake. *Nanoscale* 10, 21096–21105. doi: 10.1039/C8NR07424K

Spurbeck, R., Dinh, P., Walk, S., Stapleton, A., Hooton, T., Nolan, L., et al. (2012). *Escherichia coli* isolates that carryvat, fyuA, chuA, andyfcV efficiently colonize the urinary tract. *Infect. Immun.* 80, 4115–4122. doi: 10.1128/IAI.00752-12

Tang, E., Mok, K., Lee, W., and Cheng, C. (2014). EB1 regulates tubulin and actin cytoskeletal networks at the sertoli cell blood-testis barrier in male rats: an *in vitro* study. *Endocrinology* 156, 680–693. doi: 10.1210/en.2014-1720

Terlizzi, M., Gribaudo, G., and Maffei, M. (2017). UroPathogenic *Escherichia coli* (UPEC) infections: virulence factors, bladder responses, antibiotic, and non-antibiotic antimicrobial strategies. *Front. Microbiol.* 8:1566. doi: 10.3389/fmicb.2017.01566

Tombola, F., Carlesso, C., Szabò, I., de Bernard, M., Reyrat, J., Telford, J., et al. (1999). Helicobacter pylori vacuolating toxin forms anion-selective channels in planar lipid bilayers: possible implications for the mechanism of cellular vacuolation. *Biophys. J.* 76, 1401–1409. doi: 10.1016/S0006-3495(99)77301-7

Tran, D., and Ten Hagen, K. (2017). Real-time insights into regulated exocytosis. *J. Cell Sci.* 130, 1355–1363. doi: 10.1242/jcs.193425

Tsuzuki, H., Tani, T., Ueyama, H., and Kodama, M. (2001). Lipopolysaccharide: neutralization by polymyxin B shuts down the signaling pathway of nuclear factor κB in peripheral blood mononuclear cells, even during activation. *J. Surg. Res.* 100, 127–134. doi: 10.1006/jsre.2001.6227

Welch, R. (2016). Uropathogenic *Escherichia coli*-associated exotoxins. *Microbiol. Spectr.* 4. doi: 10.1128/microbiolspec.UTI-0011-2012

Windoffer, R., Beil, M., Magin, T., and Leube, R. (2011). Cytoskeleton in motion: the dynamics of keratin intermediate filaments in epithelia. *J. Cell Biol.* 194, 669–678. doi: 10.1083/jcb.201008095

Conflict of Interest: The authors declare that the research was conducted in the absence of any commercial or financial relationships that could be construed as a potential conflict of interest.

frontiers in Cellular and Infection Microbiology

BRIEF RESEARCH REPORT
published: 30 June 2020
doi: 10.3389/fcimb.2020.00319

Comparison of the Gut Microbiota Between *Pulsatilla* Decoction and Levofloxacin Hydrochloride Therapy on *Escherichia coli* Infection

Xiaoye Liu [1,2,3], Shangwen He [1], Qiuyue Li [1], Xiang Mu [1], Ge Hu [1] and Hong Dong [1]**

[1] Beijing Traditional Chinese Veterinary Engineering Center and Beijing Key Laboratory of Traditional Chinese Veterinary Medicine, Beijing University of Agriculture, Beijing, China, [2] Department of Mechanics and Engineering Science, College of Engineering, Academy for Advanced Interdisciplinary Studies, and Beijing Advanced Innovation Center for Engineering Science and Emerging Technology, College of Engineering, Peking University, Beijing, China, [3] Beijing Advanced Innovation Center for Food Nutrition and Human Health, College of Veterinary Medicine, China Agricultural University, Beijing, China

OPEN ACCESS

Edited by:
Tânia Aparecida Tardelli Gomes, Federal University of São Paulo, Brazil

Reviewed by:
Yao Wang, Northwest A&F University, China
Don Thushara Galbadage, Biola University, United States

***Correspondence:**
Xiaoye Liu
xiaoyeliu@pku.edu.cn
Hong Dong
donghongbua@163.com

Specialty section:
This article was submitted to Bacteria and Host, a section of the journal Frontiers in Cellular and Infection Microbiology

Received: *20 February 2020*
Accepted: *26 May 2020*
Published: *30 June 2020*

Citation:
Liu X, He S, Li Q, Mu X, Hu G and Dong H (2020) Comparison of the Gut Microbiota Between Pulsatilla Decoction and Levofloxacin Hydrochloride Therapy on Escherichia coli Infection. Front. Cell. Infect. Microbiol. 10:319. doi: 10.3389/fcimb.2020.00319

Gut microbiota serves as a critical indicator for gut health during treatment of pathogenic bacterial infection. Both *Pulsatilla* Decoction (abbreviated to PD, a traditional Chinese medicine compound) and Levofloxacin Hydrochloride (LVX) were known to have therapeutic effects to intestinal infectious disease. However, the changes of gut microbiota after PD or LVX treatment remain unclear. Herein, this work aimed to investigate the changes of intestinal flora after PD or LVX therapy of *Escherichia coli* infection in rats. Results revealed that PD exhibited a valid therapeutic approach for *E. coli* infection via the intestinal protection, as well as the inhibited release of IL-8 and ICAM-1. Besides, PD was beneficial to rebuild the gut microbiota via restoring *Bacteroidetes* spp in the composition of the gut microbiota. Comparatively, LVX treatment promoted the infection and ravaged gut microbiota by significantly decreasing Bacteroidetes and increasing Firmicutes. These findings not only highlight the mechanism of Chinese herbal formula, but extend the application of PD as veterinary medicine, feed additive and pre-mixing agent for improving the production of animal derived foods.

Keywords: *Pulsatilla* Decoction, Levofloxacin Hydrochloride, *Escherichia coli*, infection, gut microbiota

INTRODUCTION

Gut microbiota plays a fundamental role in providing the colonization resistance of intestinal tissues against the exogenous pathogenic bacteria (Baumler and Sperandio, 2016). When it comes to infectious diseases, the problem emerged as antibiotics, especially the broad-spectrum ones cannot distinguish the intestinal beneficial bacteria from the exogenous harmful bacteria (Blaser, 2016; Lange et al., 2016). Many previous reports showed that antibiotic treatments altered the composition of intestinal microbiota, resulting in an increased risk of many other illnesses (Blaser, 2011; Angelucci et al., 2019; Dierikx et al., 2020; Zwittink et al., 2020). For instance, intestinal inflammation that is tightly linked with altered gut microbiota might be triggered by antibiotic treatment (Belkaid and Hand, 2014; Slager et al., 2014; Becattini et al., 2016). Moreover, frequent exposure of the pathogenic bacteria to antibiotics could lead to the antibiotic resistance crisis

(Ventola, 2015; Yelin and Kishony, 2018). Worse still, most recent researches revealed that the drug-resistant pathogens could further promote the spread of resistant plasmid in gut and then induce secondary infection (Bakkeren et al., 2019; Wu et al., 2020).

Traditional Chinese medicine (TCM) includes diverse Chinese herbs with low toxicity and less resistance, which has gradually developed into a group of natural antimicrobial agents (Li et al., 2019; Huang et al., 2020). Noticeably, *Astragalus*, *Berberine* and many other herbs, which are compositional in many Chinese herbal formulations, have not only the antibacterial but also the anti-inflammatory effects (Auyeung et al., 2016; Ma et al., 2018; Zhang et al., 2019). *Pulsatilla* Decoction (PD) is a classic TCM compound for the treatment of heat and dysentery (Hua et al., 2020). PD consists of four classical herbs of *Radix Pulsatillae*, *Rhizoma Coptidis*, *Cortex Phellodendri,* and *Cortex Fraxini*, which contains various antibacterial and anti-inflammatory ingredients (Hu et al., 2009; Yang et al., 2018). In modern medicine, PD is also proved to have a good curative effect on bacterial diarrhea and inflammatory bowel diseases (Wang et al., 2016; Yang et al., 2018; Hua et al., 2019, 2020). As most Chinese herbal compounds were oral administration, there was a large chance for them to interact with intestinal microbes (Li et al., 2019; Huang et al., 2020). However, unlike the systemically studied inhibitory effect of PD on pathogenic bacteria in gut, little is known about the influence of PD treatment on gut microbiota. Therefore, in this paper, we carefully investigated the gut microbiota changes after antibiotic or TCM compound treatment on *Escherichia coli* induced infection (**Figure 1**). As shown in **Figure 1A**, we chose Levofloxacin Hydrochloride (LVX) as the antibiotic group, which belonged to quinolones with a broad spectrum of antibacterial effect against most Enterobacteriaceae bacteria (Perez-Pitarch et al., 2017). And PD was selected as the TCM compound group to make a comparison on the treatment of *E. coli* infection and the changes of rat intestinal microbiota. We believe our work will benefit to understand the pharmacological action of PD, and its applications of guarantee the intestinal health on the animal source food.

RESULTS

PD Treatment Prevented the Intestinal Damage Induced by *Escherichia coli* Infection

The integrity of intestine indicated intestinal homeostasis and the health of epithelial barrier (Dupaul-Chicoine et al., 2010; Konig et al., 2016). Therefore, we firstly compared the intestinal tissue under PD or LVX treatment of *E. coli* infection by a HE staining assay. We found that *E. coli* infection led to mucosa lamina propria coagulation necrosis, focal necrosis with inflammatory cell infiltration and mucosa lamina propria with congestion (**Figure 2A**), suggesting that the infection was proceeding. Compared with *E. coli* treated rats, oral supplementations of LVX led to infection-mucosa lamina propria with inflammatory cellular infiltrates, while PD had almost no damage on intestinal tissue (**Figures 2B,C**). Additionally, in accordance with the previous study which showed that PD effectively inhibited the expression of proinflammatory cytokines including IL-1beta, IL-6, and TNF-alpha (Hu et al., 2009), PD treatment also decreased IL-8 and ICAM-1 induced by *E. coli* infection in our work (**Figure 2D**).

LVX Reduced the Overall Abundances of Intestinal Microbiota

To analyze the changes of gut microbiota abundances under PD or LVX treatment, we firstly performed high throughput sequencing on the V3-V4 hypervariable region of bacteria *16S rRNA* gene with Illumina MiSeq to show the microbial composition. Then a total of 764838 valid reads were obtained from the 24 samples with an average of 30593 reads per sample. The good's coverage of all samples was 0.9977 ± 0.0007%, indicating that the *16S rRNA* sequences represented the majority of bacteria in the samples of this study. Rarefaction curves indicated that the most diversity of the bacteria had been covered (**Figure 3A**). Rand-Abundance curves showed that the abundance had been presented (**Figure 3B**). Weighted Unifrac principal component analysis (PCA) revealed that the gut microbiota structure changed significantly in response to different administration. Furthermore, The first principal component (PC1) distinctly separated LVX treatment from other treatments (**Figure 3C**). Further hierarchical cluster analysis revealed that the robust differences in LVX treatment compare to normal saline (NS) treatment and PD treatment (**Figure 3D**). Heatmap images also pointed out that the difference of LVX treatment from other treatments (**Figure 4**). Especially, PD treatment did not change the major component of intestine microbiota.

PD Treatment Protected *Bacteroidales* spp and Did Not Facilitate the Relative Abundance of *Clostridiales* spp and *Lactobacillales* spp

To further understand the difference of PD and LVX treatment on gut microbiota. We used the illumina sequencing assay to analyze the microbiota. We observed four major phyla including Firmicutes, Bacteroidetes, Proteobacteria, and Verrucomicrobia in all treatments (**Figure 5A**). Bacteroidetes abundance was mostly distributed on NS (75.85 ± 3.08) and PD (60.26 ± 2.97) treatment. While oral supplementations of LVX had dramatically decreased the relative abundance of Bacteroidetes (0.17 ± 0.08), and increased firmicutes abundance (98.06 ± 1.02). These tendencies were more obvious than those of *E. coli* infection without any treatments (Firmicutes, 58.53 ± 3.98; Bacteroidetes, 37.71 ± 4.651). The ratio of Firmicutes and Bacteroidetes population is critical for intestinal integrity (Chen et al., 2016), the downregulation of this ratio by LVX might be the main reason for the gut microbiota changes (**Figure 5B**).

Alternations of gut microbiota in all treatments were in an order of Bacteroidales > Clostridiales > Lactobacillales

Abbreviations: *E. coli*, *Escherichia coli*; PD, *Pulsatilla* Decoction; LVX, Levofloxacin Hydrochloride.

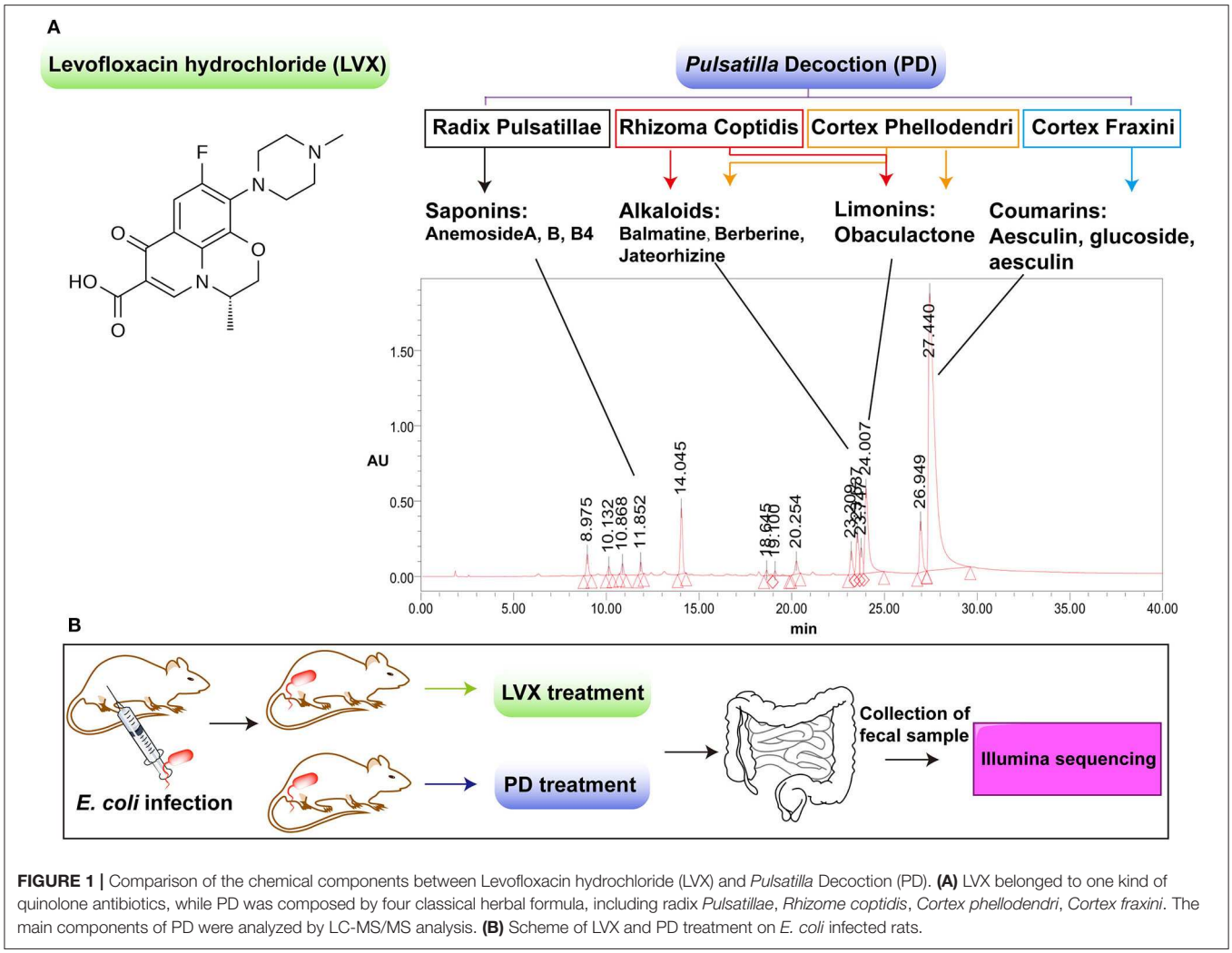

FIGURE 1 | Comparison of the chemical components between Levofloxacin hydrochloride (LVX) and *Pulsatilla* Decoction (PD). **(A)** LVX belonged to one kind of quinolone antibiotics, while PD was composed by four classical herbal formula, including radix *Pulsatillae*, *Rhizome coptidis*, *Cortex phellodendri*, *Cortex fraxini*. The main components of PD were analyzed by LC-MS/MS analysis. **(B)** Scheme of LVX and PD treatment on *E. coli* infected rats.

(**Figure 6A**). As shown, Bacteroidales was most abundant in NS (75.84 ± 3.09) and PD (60.26 ± 2.97) treatments, followed by Clostridiales (16.00 ± 2.13 and 24.09 ± 2.91), and Lactobacillales (5.40 ± 1.592) and (3.61 ± 1.46). Oral administrations of LVX had a significant impact on gut microbiota composition, indicated by that the relative abundance of Bacteroidales (0.17 ± 0.08) was nearly absent, while that of Lactobacillales (40.99 ± 4.78) and Clostridiales (52.46 ± 3.89) were increased compared with other treatments. Clostridiales was also abundant in *E. coli* infection (58.53 ± 3.98), and Lactobacillales was 1.31%, while Bacteroidetes (37.70 ± 4.65) was less than NS or PD treatment. Oral administrations of Levofloxacin hydrochloride reduced the relative abundance of Bacteroidales, but increased that of Clostridiales or Lactobacillales compared with normal and PD treatments. Intraperitoneal injection of *E. coli* also reduced the relative abundance of Bacteroidales and increased Clostridiales compared with NS and PD treatment.

We further compared the difference of microbiota distribution at the genus level in four treatment. As shown in **Figures 6B–D**, the proportion of Bacteroides, Prevotella and Lactobacillales were increasingly different in four treatments. Prevotella belonging to Bacteroidales was most abundant in normal treatments (66.38 ± 4.092). Bacteroides belonging to Bacteroidales was most abundant in PD treatments (32.92 ± 7.44). Lactobacillus belonging to Lactobacillales was mostly enriched in LVX treatments (35.73 ± 5.32). In contrast, Prevotella and Bacteroides were nearly absent in LVX treatment.

DISCUSSION

Among the intestinal microbial population, Bacteroidetes and Firmicutes accounted for 90% of the total gut microbiota (Pascale et al., 2019). Our results showed that abundances of two phylum in NS model, LVX and PD treatment were 99.22, 96.24, 98.23, 95.04%, respectively. It was evidential that a lower Bacteroidetes/Firmicutes ratio (B/F ratio) reflected phylum-wide increase in Firmicutes and/or reduction in Bacteroidetes, which were related to many diseases, such as obesity (Pascale et al., 2019), colon

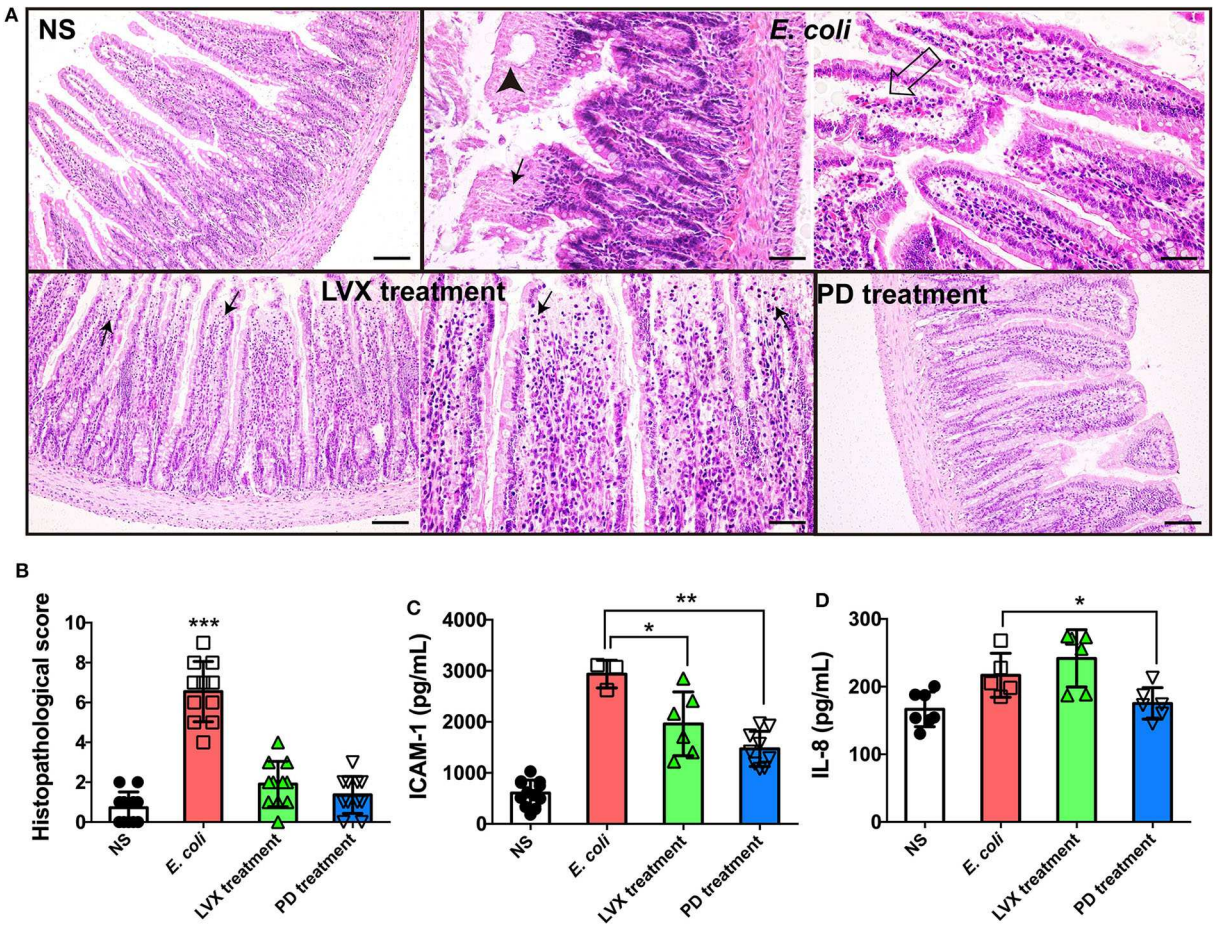

FIGURE 2 | PD treatment triggered less intestinal injury comparing to LVX treatment. **(A)** HE staining of intestine under PD or LVX treatment of *E. coli* infection. Rats were infected with *E. coli* O_{101} (1×10^{11} cfu/kg) for 3 days. Rats treated with normal saline (NS) as an uninfected group. Then the infected rats were received oral administration of PD or LVX. Arrowhead showed coagulation necrosis, while empty arrow showed mucosa lamina propria with congestion. Black arrows pointed to focal necrosis with inflammatory cell infiltration. Scar bar = 100 μm. **(B)** The pathological scores of the intestine presented the severity of intestine pathological lesions. **(C,D)** LVX treatment increased IL-8 and ICAM-1 release. Values represented the mean ± SD (*$P < 0.05$, **$P < 0.01$, ***$P < 0.001$, $n = 10$).

cancer (Zhu et al., 2014) and immunosuppression (Xu and Zhang, 2015). B/F ratio might also serve as an index to evaluate the imbalance of gut microbiota from various illnesses. In our study, we confirmed *E. coli* infection can disrupt the B/F ratio. Treatment with PD resulted in a considerable increase in the relative abundance of Bacteriodetes and the B/F ratio (1.732), comparing to the *E. coli* group (0.644) or antibiotic Levofloxacin hydrochloride groups (0.002). Furthermore, the B/F ratio of 3.245 in normal rats was consistent with the previous researches (Gu et al., 2013). Previous studies had also suggested that the imbalance in the ratio of intestinal bacteria played a vital role in the development of obesity with induction of systemic inflammation, and acceleration of fat deposition (John and Mullin, 2016). *E. coli* colonized in GI tract could release toxins and inflammation cytokines, causing breakdown of the tight junctional complexes between the intestinal epithelial cells and disruption channel regulation. They led to an influx of water and ions into the intestinal lumen, causing infection (Viggiano et al., 2015). Our study suggested that oral administration of PD significantly decreased the level of proinflammatory IL-8, ICAM-1 and improved intestinal histopathology injurie in comparison with the *E. coli* group. Although antibiotic Levofloxacin hydrochloride also decreased the level of proinflammatory ICAM-1 and improved intestinal histopathology injurie in comparison with the *E. coli* group, the level of IL-8 was elevated. After replenishing PD, the levels of serum proinflammatory IL-8 and intestinal histopathology injurie recovered to the normal level in the *E. coli* -infected group, indicating that the symptoms of intestine were improved. As a broad-spectrum antibiotic, Levofloxacin hydrochloride treatment broadly killed bacterial populations, such as Bacteroidetes, leading to the disturbed intestinal microbiota. Therefore, the corresponding effect of treating infection was inferior to that of PD. In the previous study, the reduced Bacteroidetes and Firmicutes, combined with the increased Proteobacteria caused antibiotic-induced imbalances

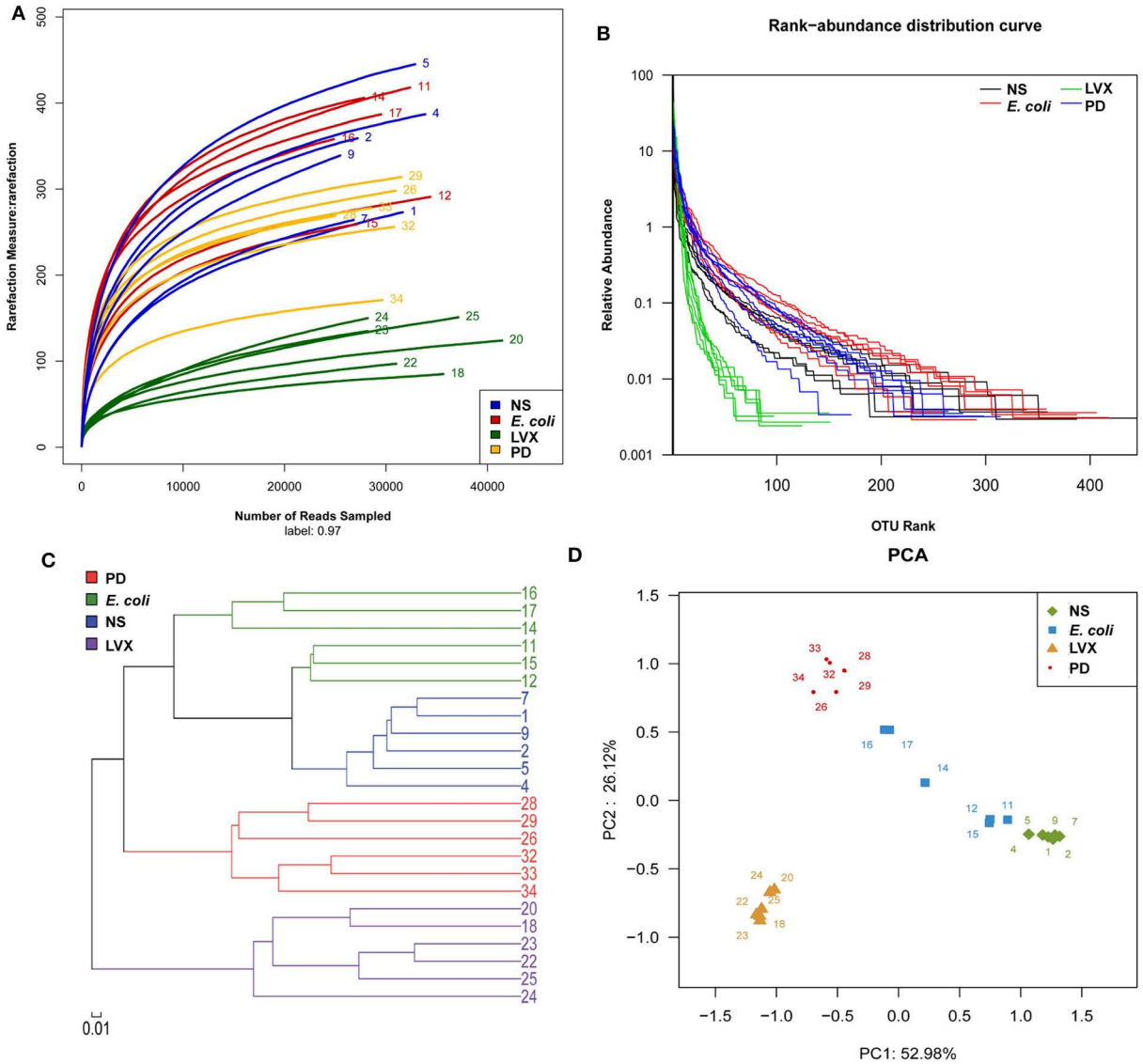

FIGURE 3 | Overall structural and modulation of gut microbiota after PD or LVX treatment. **(A)** The richness and diversity of rats' fecal microbiota among four groups. Rarefaction curves were used to estimate richness (at a 97% similarity level) of rats' fecal microbiota. **(B)** Rank abundance curve was used to estimate the abundance and evenness. **(C)** Difference and similarity of microbial communities among four groups revealed by Weighted Uniface principal component analysis (PCA). **(D)** Hierarchical cluster analysis.

in gut microbiota, which aggravated cholesterol accumulation and liver injuries in rats fed with a high-cholesterol diet (Hu et al., 2015). Bacteroidetes was known to promote the catabolism of plant cell wall (Spence et al., 2006) and the increased abundance of Bacteroidetes might ameliorate the intestinal mucosal barrier function and ultimately enhanced the innate immune responses (Sonnenburg et al., 2005). These results indicated that PD, which could regulate the distribution of the intestinal flora through increasing and/or restoring the B/F ratio, played an essential role in combating *E. coli*-induced infection.

At order level, the compositions of four bacterial populations were dominated by three orders: Lactobacillales (L), Clostridiales (C), Bacteroidales (B). Lactobacillales and Clostridiales belonged to Firmicutes. Bacteroidales belonged to Bacteroidetes. The major difference lied in the ratio of Bacteroidales /Lactobacillales+ Clostridiale: B/L+C (normal groups) = 3.54, B/L+C (model groups) = 0.65, B/L+C (LH groups) = 0.001, B/L+C (PD groups) = 2.17, which was consistent with the results at phylum level. Antibiotics also broadly reduced Bacteroidales and increased Lactobacillales and Clostridiales compared with normal rats. Obviously, Clostridiales was highly presented in both model and antibiotic group. Treatment with *Pulsatilla* Decoction could reduce the relative abundance of Clostridiales. *Clostridium difficile* (Abu Faddan et al., 2016),

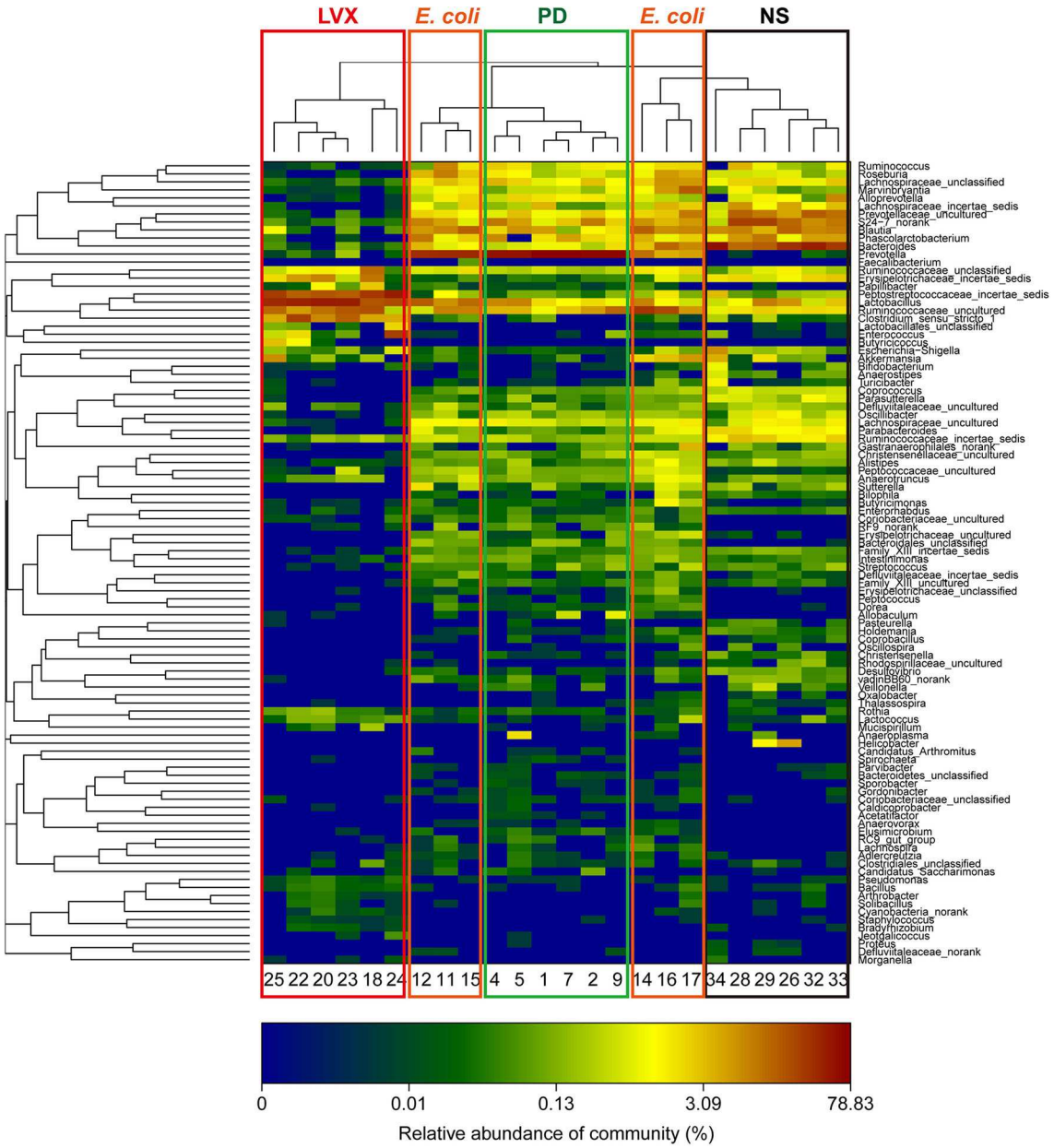

FIGURE 4 | Heatmap of hierarchy cluster indicated the amount of genus in feces. Colors reflect relative abundance from low (blue) to high (red).

a species belonging to order Clostridiales, produced multiple toxins which might produce infection and inflammation. These results suggested that *Pulsatilla* Decoction could modulate the distribution of the intestinal flora in order level to alleviate infection. In fact, Chinese herbal medicine compound has no direct antibacterial effect *in vitro* but enhances the antibacterial effect *in vivo* by mobilizing innate immunity. As report showed, among 30 Chinese herbs, only Scutellaria barbata had the 100% antibacterial activity *in vitro* (Tsai et al., 2018). Actually, Chinese herbs, such as Astragali Radix are benefit for intestinal bacterial conversion (Zhou et al., 2012). Both Chinese herbs and the gut microbiota had the regulation of innate immunity (Wójcik et al., 2009; Wang et al., 2019). Therefore, Chinese herbs rarely has a direct antibacterial ability, but it can rely on inhibiting bacterial growth proteins to inhibit infection (Si et al., 2016) or enhance the regulatory factors that promote innate immunity to achieve antibacterial effect (Ma et al., 2013, 2018; Si et al., 2016; Wang et al., 2016; Yang et al., 2018; Pascale et al., 2019). Consisting with the long-term research of our labs that the integrity of barrier cells such as epithelial cells and endothelial cells contributed to the bactericidal function of immune cells such as neutrophils (Liu et al., 2016). The

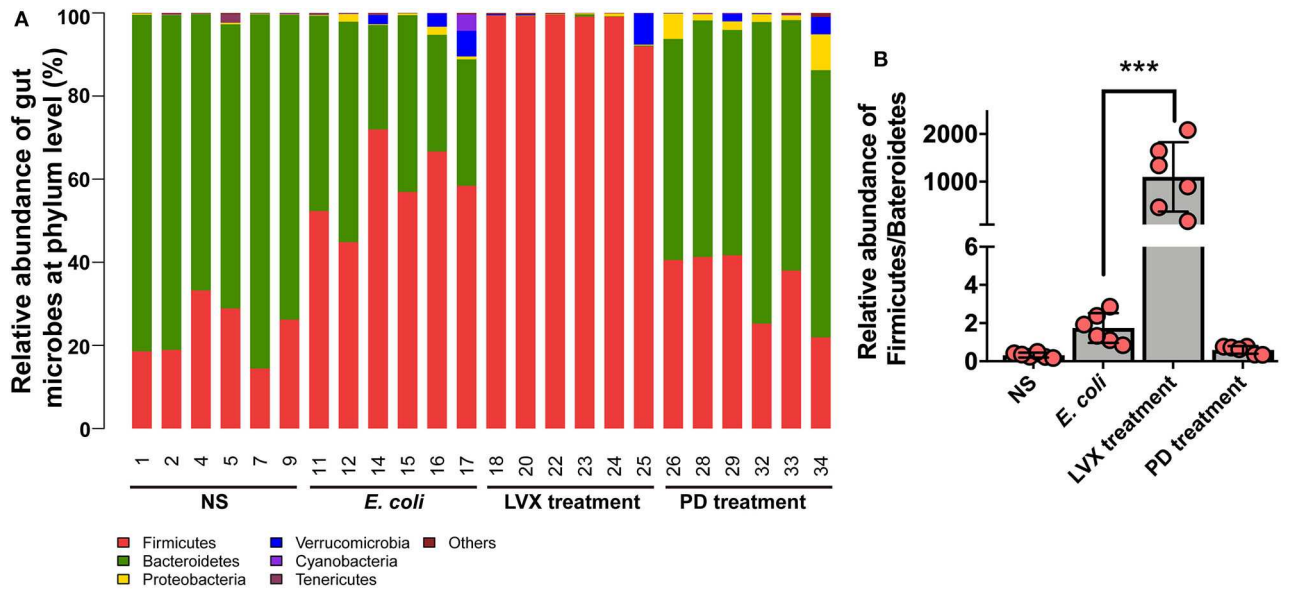

FIGURE 5 | Microbial composition of PD or LVX treatment at the phylum level. **(A)** Distribution of bacterial taxa under PD or LVX treatment at the phylum level. Sequences that could not be classified into any known group were designated as "unclassified". **(B)** Relative abundance of Firmicutes/Bacteroidetes under PD or LVX treatment. Date showed the mean ± SD (***$P < 0.001$, $n = 6$).

traditional Chinese medicine compound promotes the innate immune and antibacterial effect by protecting the integrity of such barrier cells.

CONCLUSION

Our work compared the difference on gut microbiota in *E. coli* infected rats after PD or LVX treatments. PD protected the intestinal tissue and regulated the balance of gut microbiota via restoring the composition of the gut microbiota in *Bacteroidetes* spp. In contrast, LVX treatment leaded the intestinal tissue damage, as well as ravaged gut microbiota by significantly decreasing Bacteroidetes and increasing Firmicutes. This work provided experimental data for the study of the mechanism of Chinese medicine prescription in the treatment of bacterial infection. It was also emphasized that the important role of intestinal flora in the prevention and therapy of bacterial infection.

METHODS AND MATERIALS

Animals

Specific pathogen-free male Sprague Dawley Rat (190–210 g) were supplied by Vital River Laboratory Animal Technology (Beijing, China). Rats were kept at a temperature of 22 °C and 12-h light/dark cycle environment for at least 1 week before use, and fed on the same batch of standard laboratory diet to minimize the variation of environmental factors. The present study was approved by the Institutional Animal Care and Use Committee of the Academy of Military Medical Sciences (Beijing, China; approval no. SYXK2014-0002). All animal care and experimental procedures were conducted according to the Chinese Laboratory Animals' Welfare and Ethics guidelines.

Preparation of *Pulsatilla* Decoction (PD) Extract Powder

PD consisted of four herbs including Radix Pulsatillae (60 g), Rhizoma Coptidis (30 g), Cortex Phellodendri (45 g), and Cortex Fraxini (60 g). All those herbs were purchased from Tong Ren Tang Medicinal Materials Company (Beijing, China), which was authenticated by professor Pengyue Li from Beijing university of Chinese medicine. Voucher specimens with specific storage code were well-deposited at Beijing university of Chinese medicine. PD were extracted twice with boiling water (1:10 and then 1:8, w/v) for 1 h. The water extracts were combined, concentrated in vacuum into 2 g/mL, and then stored at 4°C until use. Chromatographic fingerprint analysis on PD could be found in our previous study.

Infection and Therapy

Rats were infected by intraperitoneal injection of *E. coli* O_{101} (China Institute of Veterinary Drugs Control, O101: K91, K88, 1×10^{11} cfu/kg) for three consecutive days. Meanwhile, 10 rats were randomly selected for each group, which were subject to the treatment with isovolumetric normal saline (NS) as negative control, oral absorption of PD (7.5 g/kg) or levofloxacin hydrochloride (LVX, Sangjing Pharmachceutical co., LTD, 100 mg/kg, mimicing the human dose of 500 mg/day), respectively. Another three consecutive days were employed as therapeutic schedule of infected rats, respectively. Blood samples were collected before sacrifice. Serums of rats were selected by centrifugation at 3,000 r/min for 10 min at 4°C. Fresh fecal

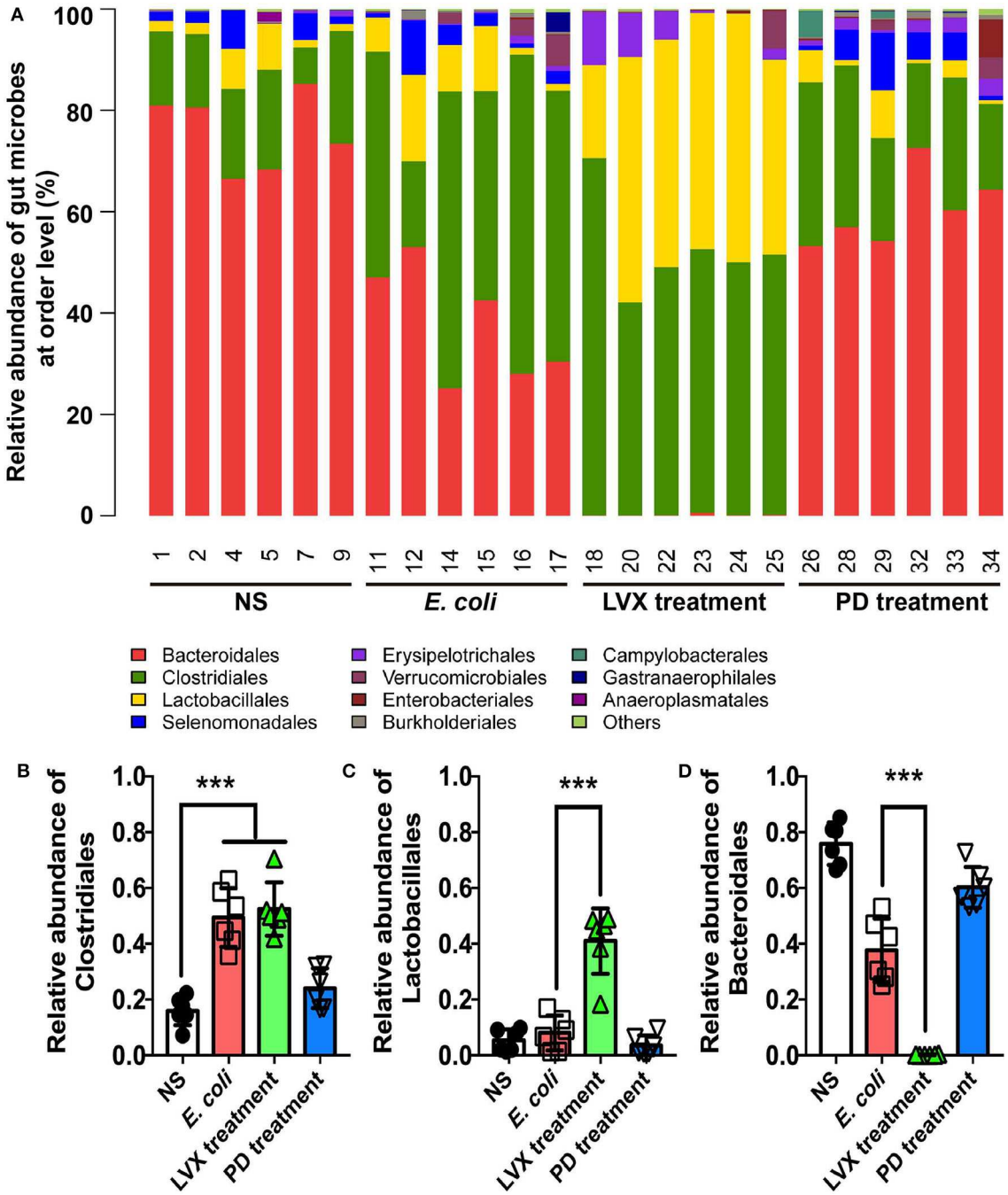

FIGURE 6 | Comparison of main genera in intestine between PD and LVX treatment. **(A)** Distribution of bacterial taxa under PD or LVX treatment at the order level. **(B)** Relative abundance of *Bacteroidales*, *Lactobacillales,* and *Clostridiales* under PD or LVX treatment. Results showed the mean ± SD (***$P < 0.001$, $n = 6$).

samples were collected at the day of sacrifice and then kept at −80°C.

Histopathological Analysis

Intestine samples were fixed in 4% paraformaldehyde. The jejunum of small intestine was selected prepared for hematoxylin and eosin staining (HE staining). Olympus microscope (Olympus Optical Co., Ltd.) was used to observe and score the histopathological changes as previous methods (Han et al., 2014). Each group contained 10 rats and all samples for pathological analysis were blindly selected.

ELISA

Cytokines IL-8 and ICAM-1 (ENZO life sciences) were detected by enzyme-linked immunosorbent assay (ELISA) according to the manufacturer's instructions.

DNA Extraction, PCR Amplification and Illumina Sequencing

After PD and LVX treatments for 3 days, fresh fecal samples from random selected 6 rats were collected individually. Then these samples were frozen immediately in liquid nitrogen and stored at −80°C for further analysis. Total DNA was extracted from fecal samples by using the E.Z.N.A.® Soil DNA Kit (Omega Bio-tek, Norcross, GA, USA) according to the manufacturer's protocol. The variable regions V3-V4 of the 16S rRNA were amplified. Equimolar concentrations of purified PCR products were pooled and paired-end sequenced (2 × 300 bp) on an Illumina MiSeq platform (Illumina Inc., San Diego, CA, USA).

Sequences data were subject to bioinformatic analysis. Operational taxonomic Units (OTUs) were using UPARSE software (version 7.1) (http://drive5.com/uparse/). The 16S rRNA sequences of *E. coli* O_{101} to compare and distinguish foreign *E. coli* from the local *E. coli* in gut. OTUs that reached 97% similarity were used for Good's coverage and rarefaction curve analysis (Schloss et al., 2011). Through the classification operation, the sequences were divided into many groups according to their similarities, and a group was an OTU. According to different similarity levels, all sequences could be divided into OTUs, and biological information statistical analysis was usually performed on OTUs at 97% similarity levels. Community structure comparisons with Principal Component Analysis (PCA) were based on weighted UniFrac distance. Hierarchical cluster analysis, Rank-Abundance and heatmap were generated according to R software package (http://www.R-project.org) (Wang et al., 2012).

Statistical Analysis

Data were expressed as means ± standard deviation (SD) and analyzed by using GraphPad Prism 8 software. The criterion of significance was conducted using unpaired *t*-test by one-way ANOVA. At least 10 rats were involved in every group for animal experiments. All experiments were performed on no <3 biological replicates. All animals were used for analysis unless the mice died.

DATA AVAILABILITY STATEMENT

The datasets generated for this study are available on request to the corresponding author.

ETHICS STATEMENT

The experimental protocols and all animals were approved by the Genentech Institutional Animal Care and Use Committee at the Beijing University of Agriculture (SYXK, 2015-0004) and China Agricultural University (SYXK, 2016-0008).

AUTHOR CONTRIBUTIONS

HD conceived the project. XL and HD did for the research design. XL, SH, and QL performed the experiments. XL, SH, GH, and HD did data analysis. GH and XM carried out the histopathological analysis. XL, GH, and HD wrote the manuscript. All authors read and approved the manuscript.

FUNDING

This work was supported by the National Natural Science Foundation of China (31572558, 31272144), Beijing municipal commission of science and technology: scientific and technological support for major and urgent tasks in urban areas (Z181100009818007), and the Profession scientific research special item of agricultural public welfare, Ministry of Agriculture, China (201403051-10).

ACKNOWLEDGMENTS

We would like to great appreciate XM for kindly providing the 5 traditional Chinese medicine prescription ingredient extraction platform. We also thank Mrs. Xiangwan Sun and Mr. Xin Wang for the animal data analysis. We would also like to thank Dr. Xing Su for language revision.

REFERENCES

Abu Faddan, N. H., Aly, S. A., and Abou Faddan, H. H. (2016). Nosocomial *Clostridium difficile*-associated diarrhoea in assiut university children's hospital, Egypt. *Paediatr. Int. Child Health* 36, 39–44. doi: 10.1179/2046905514Y.0000000167

Angelucci, F., Cechova, K., Amlerova, J., and Hort, J. (2019). Antibiotics, gut microbiota, and Alzheimer's disease. *J. Neuroinflammation* 16:108. doi: 10.1186/s12974-019-1494-4

Auyeung, K. K., Han, Q. B., and Ko, J. K. (2016). *Astragalus membranaceus*: a review of its protection against inflammation and gastrointestinal cancers. *Am. J. Chin. Med.* 44, 1–22. doi: 10.1142/S0192415X16500014

Bakkeren, E., Huisman, J. S., Fattinger, S. A., Hausmann, A., Furter, M., Egli, A., et al. (2019). *Salmonella* persisters promote the spread of antibiotic resistance plasmids in the gut. *Nature* 573, 276–280. doi: 10.1038/s41586-019-1521-8

Baumler, A. J., and Sperandio, V. (2016). Interactions between the microbiota and pathogenic bacteria in the gut. *Nature* 535, 85–93. doi: 10.1038/nature18849

Becattini, S., Taur, Y., and Pamer, E. G. (2016). Antibiotic-induced changes in the intestinal microbiota and disease. *Trends Mol. Med.* 22, 458–478. doi: 10.1016/j.molmed.2016.04.003

Belkaid, Y., and Hand, T. W. (2014). Role of the microbiota in immunity and inflammation. *Cell* 157, 121–141. doi: 10.1016/j.cell.2014.03.011

Blaser, M. (2011). Antibiotic overuse: stop the killing of beneficial bacteria. *Nature* 476, 393–394. doi: 10.1038/476393a

Blaser, M. J. (2016). Antibiotic use and its consequences for the normal microbiome. *Science* 352, 544–545. doi: 10.1126/science.aad9358

Chen, S., Cheng, H., Wyckoff, K. N., and He, Q. (2016). Linkages of firmicutes and bacteroidetes populations to methanogenic process performance. *J. Ind. Microbiol. Biotechnol.* 43, 771–781. doi: 10.1007/s10295-016-1760-8

Dierikx, T. H., Visser, D. H., Benninga, M. A., Van Kaam, A., De Boer, N. K. H., De Vries, R., et al. (2020). The influence of prenatal and intrapartum antibiotics on intestinal microbiota colonisation in infants: a systematic review. *J. Infect.* doi: 10.1016/j.jinf.2020.05.002. [Epub ahead of print].

Dupaul-Chicoine, J., Yeretssian, G., Doiron, K., Bergstrom, K. S., Mcintire, C. R., Leblanc, P. M., et al. (2010). Control of intestinal homeostasis, colitis, and colitis-associated colorectal cancer by the inflammatory caspases. *Immunity* 32, 367–378. doi: 10.1016/j.immuni.2010.02.012

Gu, S., Chen, D., Zhang, J. N., Lv, X., Wang, K., Duan, L. P., et al. (2013). Bacterial community mapping of the mouse gastrointestinal tract. *PLoS ONE* 8:e74957. doi: 10.1371/journal.pone.0074957

Han, D., Hu, Y., Li, L., Tian, H., Chen, Z., Wang, L., et al. (2014). Highly pathogenic porcine reproductive and respiratory syndrome virus infection results in acute lung injury of the infected pigs. *Vet. Microbiol.* 169, 135–146. doi: 10.1016/j.vetmic.2013.12.022

Hu, X., Wang, T., Liang, S., Li, W., Wu, X., and Jin, F. (2015). Antibiotic-induced imbalances in gut microbiota aggravates cholesterol accumulation and liver injuries in rats fed a high-cholesterol diet. *Appl. Microbiol. Biotechnol.* 99, 9111–9122. doi: 10.1007/s00253-015-6753-4

Hu, Y., Chen, X., Duan, H., Hu, Y., and Mu, X. (2009). *Pulsatilla* decoction and its active ingredients inhibit secretion of NO, ET-1, TNF-alpha, and IL-1 alpha in LPS-induced rat intestinal microvascular endothelial cells. *Cell. Biochem. Funct.* 27, 284–288. doi: 10.1002/cbf.1570

Hua, Y. L., Ma, Q., Li, W., Zhang, X. S., Cheng, X. H., Jia, Y. Q., et al. (2019). Metabolomics analysis of *Pulsatilla* decoction on treatment of wetness-heat-induced diarrhea in rats based on UPLC-Q/TOF-MS/MS. *Biomed. Chromatogr.* 33:e4629. doi: 10.1002/bmc.4629

Hua, Y. L., Ma, Q., Zhang, X. S., Jia, Y. Q., Peng, X. T., Yao, W. L., et al. (2020). *Pulsatilla* decoction can treat the dampness-heat diarrhea rat model by regulating glycerinphospholipid metabolism based lipidomics approach. *Front. Pharmacol.* 11:197. doi: 10.3389/fphar.2020.00197

Huang, X., Wang, P., Li, T., Tian, X., Guo, W., Xu, B., et al. (2020). Self-assemblies based on traditional medicine berberine and cinnamic acid for adhesion-induced inhibition multidrug-resistant *Staphylococcus aureus*. *ACS Appl. Mater. Interfaces* 12, 227–237. doi: 10.1021/acsami.9b17722

John, G. K., and Mullin, G. E. (2016). The gut microbiome and obesity. *Curr. Oncol. Rep.* 18:45. doi: 10.1007/s11912-016-0528-7

Konig, J., Wells, J., Cani, P. D., Garcia-Rodenas, C. L., Macdonald, T., Mercenier, A., et al. (2016). Human intestinal barrier function in health and disease. *Clin. Transl. Gastroenterol.* 7:e196. doi: 10.1038/ctg.2016.54

Lange, K., Buerger, M., Stallmach, A., and Bruns, T. (2016). Effects of antibiotics on gut microbiota. *Dig. Dis.* 34, 260–268. doi: 10.1159/000443360

Li, T., Wang, P., Guo, W., Huang, X., Tian, X., Wu, G., et al. (2019). Natural berberine-based Chinese herb medicine assembled nanostructures with modified antibacterial application. *ACS Nano* 13, 6770–6781. doi: 10.1021/acsnano.9b01346

Liu, X., Dong, H., Wang, M., Gao, Y., Zhang, T., Hu, G., et al. (2016). IL-1alpha-induced microvascular endothelial cells promote neutrophil killing by increasing MMP-9 concentration and lysozyme activity. *Immunol. Res.* 64, 133–142. doi: 10.1007/s12026-015-8731-4

Ma, H. D., Deng, Y. R., Tian, Z., and Lian, Z. X. (2013). Traditional Chinese medicine and immune regulation. *Clin. Rev. Allergy Immunol.* 44, 229–241. doi: 10.1007/s12016-012-8332-0

Ma, X., Chen, Z., Wang, L., Wang, G., Wang, Z., Dong, X., et al. (2018). The pathogenesis of diabetes mellitus by oxidative stress and inflammation: its inhibition by berberine. *Front. Pharmacol.* 9:782. doi: 10.3389/fphar.2018.00782

Pascale, A., Marchesi, N., Govoni, S., Coppola, A., and Gazzaruso, C. (2019). The role of gut microbiota in obesity, diabetes mellitus, and effect of metformin: new insights into old diseases. *Curr. Opin. Pharmacol.* 49, 1–5. doi: 10.1016/j.coph.2019.03.011

Perez-Pitarch, A., Guglieri-Lopez, B., Nacher, A., Merino, V., and Merino-Sanjuan, M. (2017). Levofloxacin effect on erlotinib absorption. Evaluation of the interaction in undernutrition situations through population pharmacokinetic analysis in rats. *Biopharm. Drug Dispos.* 38, 315–325. doi: 10.1002/bdd.2065

Schloss, P. D., Gevers, D., and Westcott, S. L. (2011). Reducing the effects of PCR amplification and sequencing artifacts on 16S rRNA-based studies. *PLoS ONE* 6:e27310. doi: 10.1371/journal.pone.0027310

Si, L., Li, P., Liu, X., and Luo, L. (2016). Chinese herb medicine against sortase a catalyzed transformations, a key role in gram-positive bacterial infection progress. *J. Enzyme Inhib. Med. Chem.* 31, 184–196. doi: 10.1080/14756366.2016.1178639

Slager, J., Kjos, M., Attaiech, L., and Veening, J. W. (2014). Antibiotic-induced replication stress triggers bacterial competence by increasing gene dosage near the origin. *Cell* 157, 395–406. doi: 10.1016/j.cell.2014.01.068

Sonnenburg, J. L., Xu, J., Leip, D. D., Chen, C. H., Westover, B. P., Weatherford, J., et al. (2005). Glycan foraging *in vivo* by an intestine-adapted bacterial symbiont. *Science* 307, 1955–1959. doi: 10.1126/science.1109051

Spence, C., Wells, W. G., and Smith, C. J. (2006). Characterization of the primary starch utilization operon in the obligate anaerobe bacteroides fragilis: regulation by carbon source and oxygen. *J. Bacteriol.* 188, 4663–4672. doi: 10.1128/JB.00125-06

Tsai, C. C., Lin, C. S., Hsu, C. R., Chang, C. M., Chang, I. W., Lin, L. W., et al. (2018). Using the Chinese herb scutellaria barbata against extensively drug-resistant *Acinetobacter baumannii* infections: *in vitro* and *in vivo* studies. *BMC Complement Altern. Med.* 18:96. doi: 10.1186/s12906-018-2151-7

Ventola, C. L. (2015). The antibiotic resistance crisis: part 1: causes and threats. *P T* 40, 277–283. doi: 10.1016/S0194-5998(97)80284-7

Viggiano, D., Ianiro, G., Vanella, G., Bibbo, S., Bruno, G., Simeone, G., et al. (2015). Gut barrier in health and disease: focus on childhood. *Eur. Rev. Med. Pharmacol. Sci.* 19, 1077–1085.

Wang, C., Liu, H., Mu, G., Lu, S., Wang, D., Jiang, H., et al. (2019). Effects of traditional Chinese medicines on immunity and culturable gut microflora to oncorhynchus masou. *Fish Shellfish Immunol.* 93, 322–327. doi: 10.1016/j.fsi.2019.07.071

Wang, X., Fan, F., and Cao, Q. (2016). Modified *Pulsatilla* decoction attenuates oxazolone-induced colitis in mice through suppression of inflammation and epithelial barrier disruption. *Mol. Med. Rep.* 14, 1173–1179. doi: 10.3892/mmr.2016.5358

Wang, Y., Sheng, H. F., He, Y., Wu, J. Y., Jiang, Y. X., Tam, N. F., et al. (2012). Comparison of the levels of bacterial diversity in freshwater, intertidal wetland, and marine sediments by using millions of illumina tags. *Appl. Environ. Microbiol.* 78, 8264–8271. doi: 10.1128/AEM.01821-12

Wójcik, R., Siwicki, A. K., Skopinska-Rózewska, E., Wasiutynski, A., Sommer, E., and Furmanowa, M. (2009). The effect of Chinese medicinal herb rhodiola kirilowii extracts on cellular immunity in mice and rats. *Pol. J. Vet. Sci.* 12, 399–405. doi: 10.1080/00480169.2009.64736

Wu, H., Ma, Y., Peng, X., Qiu, W., Kong, L., Ren, B., et al. (2020). Antibiotic-induced dysbiosis of the rat oral and gut microbiota and resistance to *Salmonella*. *Arch. Oral. Biol.* 114:104730. doi: 10.1016/j.archoralbio.2020.104730

Xu, X., and Zhang, X. (2015). Effects of cyclophosphamide on immune system and gut microbiota in mice. *Microbiol. Res.* 171, 97–106. doi: 10.1016/j.micres.2014.11.002

Yang, L., Wu, H., Qiu, W., Guo, L., Du, X., Yu, Q., et al. (2018). *Pulsatilla* decoction inhibits Candida albicans proliferation and adhesion in a mouse model of vulvovaginal candidiasis via the Dectin-1 signaling pathway. *J. Ethnopharmacol.* 223, 51–62. doi: 10.1016/j.jep.2018.05.018

Yelin, I., and Kishony, R. (2018). Antibiotic resistance. *Cell* 172, 1136–1136.e1131. doi: 10.1016/j.cell.2018.02.018

Zhang, W., Xu, J. H., Yu, T., and Chen, Q. K. (2019). Effects of berberine and metformin on intestinal inflammation and gut microbiome composition *in vivo*/*vitro* mice. *Biomed. Pharmacother.* 118:109131. doi: 10.1016/j.biopha.2019.109131

Zhou, R. N., Song, Y. L., Ruan, J. Q., Wang, Y. T., and Yan, R. (2012). Pharmacokinetic evidence on the contribution of intestinal bacterial

conversion to beneficial effects of astragaloside IV, a marker compound of astragali radix, in traditional oral use of the herb. *Drug Metab. Pharmacokinet.* 27, 586–597. doi: 10.2133/dmpk.DMPK-11-RG-160

Zhu, Q., Jin, Z., Wu, W., Gao, R., Guo, B., Gao, Z., et al. (2014). Analysis of the intestinal lumen microbiota in an animal model of colorectal cancer. *PLoS ONE* 9:e90849. doi: 10.1371/journal.pone.0090849

Zwittink, R. D., Van Zoeren-Grobben, D., Renes, I. B., Van Lingen, R. A., Norbruis, O. F., Martin, R., et al. (2020). Dynamics of the bacterial gut microbiota in preterm and term infants after intravenous amoxicillin/ceftazidime treatment. *BMC Pediatr.* 20:195. doi: 10.1186/s12887-020-02067-z

Conflict of Interest: The authors declare that the research was conducted in the absence of any commercial or financial relationships that could be construed as a potential conflict of interest.

frontiers in Cellular and Infection Microbiology

MINI REVIEW
published: 15 July 2020
doi: 10.3389/fcimb.2020.00339

Diversity of Hybrid- and Hetero-Pathogenic *Escherichia coli* and Their Potential Implication in More Severe Diseases

Ana Carolina de Mello Santos, Fernanda Fernandes Santos*†, Rosa Maria Silva and Tânia Aparecida Tardelli Gomes*

Disciplina de Microbiologia, Departamento de Microbiologia, Imunologia e Parasitologia, Escola Paulista de Medicina, Universidade Federal de São Paulo, São Paulo, Brazil

OPEN ACCESS

Edited by:
John M. Leong, Tufts University School of Medicine, United States

Reviewed by:
Shannon D. Manning, Michigan State University, United States
Sivapriya Kailasan Vanaja, University of Connecticut, United States

***Correspondence:**
Ana Carolina de Mello Santos
carolina.mello@unifesp.br
Fernanda Fernandes Santos
ff.santos@unifesp.br

†Present address:
Fernanda Fernandes Santos, Laboratório ALERTA, Disciplina de Infectologia, Departamento de Medicina, Escola Paulista de Medicina, Universidade Federal de São Paulo, São Paulo, Brazil

Specialty section:
This article was submitted to Bacteria and Host, a section of the journal Frontiers in Cellular and Infection Microbiology

Received: *04 February 2020*
Accepted: *04 June 2020*
Published: *15 July 2020*

Citation:
Santos ACM, Santos FF, Silva RM and Gomes TAT (2020) Diversity of Hybrid- and Hetero-Pathogenic Escherichia coli and Their Potential Implication in More Severe Diseases. Front. Cell. Infect. Microbiol. 10:339. doi: 10.3389/fcimb.2020.00339

Although extraintestinal pathogenic *Escherichia coli* (ExPEC) are designated by their isolation site and grouped based on the type of host and the disease they cause, most diarrheagenic *E. coli* (DEC) are subdivided into several pathotypes based on the presence of specific virulence traits directly related to disease development. This scenario of a well-categorized *E. coli* collapsed after the German outbreak of 2011, caused by one strain bearing the virulence factors of two different DEC pathotypes (enteroaggregative *E. coli* and Shiga toxin-producing *E. coli*). Since the outbreak, many studies have shown that this phenomenon is more frequent than previously realized. Therefore, the terms hybrid- and hetero-pathogenic *E. coli* have been coined to describe new combinations of virulence factors among the classic *E. coli* pathotypes. In this review, we provide an overview of these classifications and highlight the *E. coli* genomic plasticity that results in some mixed *E. coli* pathotypes displaying novel pathogenic strategies, which lead to a new symptomatology related to *E. coli* diseases. In addition, as the capacity for genome interrogation has grown in the last few years, it is clear that genes encoding some virulence factors, such as Shiga toxin, are found among different *E. coli* pathotypes to which they have not traditionally been associated, perhaps foreshowing their emergence in new and severe outbreaks caused by such hybrid strains. Therefore, further studies regarding hetero-pathogenic and hybrid-pathogenic *E. coli* isolates are necessary to better understand and control the spread of these pathogens.

Keywords: *Escherichia coli*, intestinal infection, extraintestinal infection, hybrid, hetero-pathogenic, pathotypes, ExPEC, DEC

INTRODUCTION

Escherichia coli is a gram-negative, facultative anaerobic rod, which produces catalase but not oxidase. Taxonomically, it belongs to class *Gammaproteobacteria*, order *Enterobacteriales*, and family *Enterobacteriaceae* (Adeolu et al., 2016). Bacteria of this species inhabit the intestinal tract of humans and other animals as an important member of their microbiota (Leimbach et al., 2013). Moreover, the high adaptive capacity of *E. coli* permits it to survive for long periods of no growth and in a variety of niches such as soil, water, food, and sediments (Leimbach et al., 2013). Although most are innocuous, some strains of this species are pathogenic and can cause

intestinal or extraintestinal diseases, which are related to a variety of virulence genes acquired by the horizontal transfer of plasmids, pathogenicity islands, transposons, and bacteriophages (Kaper et al., 2004; Croxen and Finlay, 2010; Leimbach et al., 2013; Johnson and Russo, 2018).

The pathogenic *E. coli* strains are classified according to the infection site of isolation. Strains capable of causing diseases in the human intestinal tract are designated as diarrheagenic *E. coli* (DEC), which is subclassified into seven different pathotypes: enterotoxigenic *E. coli* (ETEC), enteroinvasive *E. coli* (EIEC), enteroaggregative *E. coli* (EAEC), and enteropathogenic *E. coli* (EPEC), both sub-grouped in typical and atypical Shiga toxin-producing *E. coli* (STEC), diffusely adherent *E. coli* (DAEC), and adherent-invasive *E. coli* (AIEC) (Kaper et al., 2004; Croxen et al., 2013; Leimbach et al., 2013; Gomes et al., 2016). Except for AIEC and DAEC, the differences among most of these pathotypes are typically due to specific virulence encoding genes that are directly related to the development of the disease and host symptomatology and are used for diagnostic purposes (**Table 1**). AIEC has been postulated as a cause of inflammatory bowel disease. However, at present, there is no consensus on this issue (Palmela et al., 2018; Perna et al., 2020), and the putative virulence factors described as involved in AIEC pathogenesis are common to strains isolated from extraintestinal infections (Martinez-Medina et al., 2009; Yang et al., 2017). Furthermore, although DAEC is a recognized enteric pathogen and the presence of genes encoding afimbrial adhesins are occasionally used for screening this pathotype, these genes are also present in other intestinal and extraintestinal pathogenic *E. coli* as well as in commensal strains, limiting their usefulness in defining the DAEC pathotype (Croxen et al., 2013).

Unlike DEC, extraintestinal pathogenic *E. coli* (ExPEC) are defined primarily by their site of isolation. The most clinically important ExPEC groups are uropathogenic *E. coli* (UPEC), neonatal meningitis-associated *E. coli* (NMEC), avian pathogenic *E. coli* (APEC), and septicemic *E. coli* (SEPEC) (Ewers et al., 2007; Santos et al., 2013; Johnson and Russo, 2018). ExPEC strains can cause infection in diverse extraintestinal sites. Furthermore, a strain that causes urinary tract infection in humans can also cause infections in other human body sites or in animals, which makes the use of the term ExPEC more appropriate than the pathotype designation (Russo and Johnson, 2000). There is no single or set of virulence factors exclusively associated with a specific host or disease, but Picard et al. (1999) and Johnson et al. (2003) have shown that the ability of ExPEC strains to cause disease in immunocompetent subjects was associated with the presence of two among five virulence markers (**Table 1**). The strains that bear these traits were referred to as "intrinsic virulent" because they are considered more pathogenic than those that do not harbor these factors. Similarly, Spurbeck et al. (2012) have proposed a set of four other genes to identify ExPEC strains with uropathogenic potential (**Table 1**). In general, ExPEC virulence factors appear partially redundant, involved in the ability of these strains to colonize, evade immune system clearance, and survive in diverse extraintestinal sites (Croxen and Finlay, 2010; Leimbach et al., 2013; Johnson and Russo, 2018).

After the increased access to genome sequencing technologies, several pathogenic *E. coli* genomes became available. These data highlighted *E. coli* genomic plasticity and showed the distribution of virulence factors among the pathotypes, including those traits related to DEC definition. A remarkable example of plasticity was the *E. coli* strain involved in 2011's outbreak that displayed the characteristics of two different pathotypes and led to severe host symptoms. Consequently, the terms "hybrid" and "hetero-pathogens" have emerged to designate potentially more virulent strains that present a combination of virulence factors, which were previously believed to be specific to each *E. coli* pathotype. In this review, we bring together the reports on hybrid- and hetero-pathogenic *E. coli* strains and discuss their potential implication in more severe diseases.

DEFINING HETERO-PATHOGENS AND HYBRID-PATHOGENS WITHOUT DECONSTRUCTING PRIMARY CONCEPTS

Here we adopt the terms "hetero-pathogenic" or "hetero-pathogen" to refer to strains that harbor virulence genes that are characteristic of two or more DEC pathotypes. Hence, the hetero-pathogens are strictly entero-pathogens, and their designation is based on the presence of specific virulence factors-associated DEC pathotypes. Their definition is straightforward because genes that delineate DEC are well-defined. A limitation is that the absence of defined virulence markers prevents the inclusion of DAEC and AIEC in these definitions.

In contrast, "hybrid-pathogenic" or "hybrid-pathogen" strains exhibit both DEC and ExPEC defining virulence factors or, alternatively, are isolated from an extraintestinal infection and encode DEC defining virulence factors. The alternate criterion for designation as a hybrid-pathogen is required due to ambiguity in the gene sets required to define ExPEC strains.

COMBINATIONS OF VIRULENCE FACTORS THAT LEAD TO MORE SEVERE DISEASES

The current challenge concerning the hybrid- or hetero-pathogenic *E. coli* strain classification is understanding whether these virulence factors are, in fact, involved in disease development and have clinical relevance that could be considered in diagnosis. We present below some examples of virulence marker combinations that were associated with more severe diseases.

EAEC/STEC

The higher virulence of the hetero-pathogenic EAEC/STEC group was highlighted when it caused the foodborne outbreak that started in Germany in 2011 and spread out to Europe and North America (Bielaszewska et al., 2011; Mellmann et al., 2011; Rasko et al., 2011), affecting more than 4,000 persons in 16 countries (Center for Disease Control Prevention, 2013). In Germany, as many as 3,816 cases were reported, 845 of which progressed to hemolytic uremic syndrome (HUS) and with 54 deaths (Frank et al., 2011).

TABLE 1 | *Escherichia coli* pathotypes and the virulence genetic markers used for their classification[a].

Pathotype	Subgroup	Virulence genetic markers (function or virulence factor)	Observations
EAEC	Typical (tEAEC)	*aggR* (transcriptional activator)	The occurrence of the aggregative adhesion pattern in HeLa/Hep-2 cells is the standard method to characterize EAEC
	Atypical (aEAEC)	*aatA* and *aaiG* (plasmid and chromosomal secretion system, respectively)	
EPEC	Typical (tEPEC)	*bfp* (bundle-forming pilus), *eae* (intimin), and absence of *stx* (Shiga toxin)	Characterized by the presence of LEE
	Atypical (aEPEC)	*eae* (intimin) and the absence of *bfp* and *stx*	
STEC	–	*stx* (Shiga toxin)	–
			The presence of LEE pathogenicity island confers to EHEC the ability to cause A/E lesion in the intestinal epithelium, as EPEC
	EHEC	*stx* (Shiga toxin) and *eae* (intimin)	
ETEC	–	*elt* (heat-label toxin—LT) and/or *est* (heat-stable toxin—ST)	–
EIEC	–	*ipaH* (multicopy family of effectors present in invasion plasmid and chromosome)	–
DAEC[b]	–	*dra* or *afa* (AFA-Dr adhesins)	No virulence factor confirmed as determinant of diarrhea was described
AIEC[b]	–	Unknown	No virulence factor confirmed as determinant of inflammatory disease
ExPEC[c]	–	Presence of at least two of five genes: *pap* (P fimbriae), *sfa* (S fimbriae), *afa/dra* (AFA-Dr adhesins), *iuc/iut* (aerobactin), and *kpsMT*II (capsular group II)	Intrinsic virulent strains are lethal in an animal model of sepsis; not all extraintestinal isolates harbor this set of virulence genes
UPEC[d]	–	Simultaneous presence of the following genes: *yfcV* (fimbriae Yfc), *vat* (vacuolating autotransporter toxin), *chuA* (heme receptor), and *fyuA* (yersiniabactin)	Strains harboring these four genes can cause urinary tract infection in animal models; not all strains isolated from UTI harbor these four genes

[a] *The table displays the virulence factors often used in surveillance studies and the diagnosis of intestinal infections. It does not represent the complete list of virulence factors that each pathotype can harbor.*

[b] *The classification of DAEC and AIEC was not based on the presence of specific virulence factors; consequently, it is not possible to identify the hybrid/hetero-pathogenic strains of these pathotypes.*

[c] *All E. coli strains isolated from any extraintestinal infection are ExPEC. This term can also be used to classify strains isolated from diverse sources that harbor specific virulence factors and are intrinsically virulent, being lethal to mice in the animal model (Picard et al., 1999; Russo and Johnson, 2000; Johnson et al., 2003).*

[d] *UPEC is the pathotype designation used to refer to ExPEC strains that were isolated from urinary tract infections or strains isolated from diverse sources that are capable of causing urinary tract infections in an animal model (Spurbeck et al., 2012; Johnson and Russo, 2018).*

Studies conducted in Germany and France showed no evidence of zoonotic origin for this outbreak and that this hetero-pathogen became well-established in the human population (Monecke et al., 2011; Wieler et al., 2011; Auvray et al., 2012). The success of this hetero-pathogen can be explained by its genetic background, which combines the EAEC O104:H4 and the STEC virulence profiles, comprising the aggregative adherence (AA) pattern and the Stx2 production (Bielaszewska et al., 2011; Mellmann et al., 2011; Rasko et al., 2011). Another factor that makes the EAEC/STEC outbreak alarming is that infections caused by this hetero-pathogen frequently progress to HUS, possibly because they present a set of proteins involved in intestinal colonization such as IrgA homologue adhesin (Iha), aggregative adherence fimbriae I (AAF/I), long polar fimbriae (Lpf), and different serine-protease autotransporters of Enterobacteriaceae (like Pic, SepA, etc.). These proteins could work synergistically to make these strains better colonizers, leading to persistent diarrhea and facilitating Shiga-toxin (Stx) absorption (Navarro-Garcia, 2014).

Besides that, a study conducted at the German National Reference Center with 2,400 STEC strains, isolated between 2008 and 2012, identified two additional hetero-pathogenic EAEC/STEC strains that were isolated from a patient with diarrhea and exhibited the AA pattern and the *stx* gene. One of these strains produced AAF/ IV, while a new type of aggregative fimbriae was described in the other (Prager et al., 2014; Lang et al., 2018). Furthermore, before the German outbreak, other EAEC/STEC hetero-pathogens were described in HUS cases associated with outbreaks that occurred in France (serotype O111: H2) and HUS and bloody diarrhea in Japan (serotype O89: HNM) (Boudailliez et al., 1997; Morabito et al., 1998; Iyoda et al., 2000).

EHEC as a Long-Standing EPEC/STEC Hetero-Pathogen

The enterohemorrhagic *E. coli* (EHEC) pathotype is involved worldwide in many outbreaks, severe symptomatology, and lethal outcomes to the human host (Levine, 1987; Kaper et al., 2004; Croxen et al., 2013; Gomes et al., 2016). This pathotype has been classified based on different concepts. Some researchers classify any STEC strain as EHEC based only on the patients' clinical manifestations, including hemorrhagic colitis or HUS due to Stx production (Doughty et al., 2002; Navarro-Garcia, 2014; Krause et al., 2018; Lang et al., 2018; Torres et al., 2018). Others, instead,

use molecular criteria based on the simultaneous presence of Stx and the locus of enterocyte effacement (LEE) pathogenicity island (PAI) to classify as EHEC (Kaper et al., 2004; Croxen et al., 2013; Sadiq et al., 2014; Silva et al., 2019).

Herein the EHEC nomenclature has been used to refer to the STEC subset that simultaneously harbors Stx and LEE. As STEC strains can cause diarrhea and HUS in human subjects independently of the presence of LEE (Luck et al., 2005; Croxen et al., 2013; Krause et al., 2018), this PAI is an accessory set of virulence genes that enhances STEC pathogenicity; thus, we can consider it as a hetero-pathogen. Nevertheless, LEE PAI is the major factor associated with the occurrence of attaching and effacing (A/E) lesion and diarrhea by EPEC strains (Croxen et al., 2013; Silva et al., 2019). LEE bears several virulence genes encoding, e.g., intimin (*eae*), a type 3 secretion system, and other effectors involved in A/E lesion formation, which are used to clinically classify pathogenic *E. coli* strains as EPEC (**Table 1**).

The EPEC pathotype is sub-grouped based on the presence of the bundle-forming pilus (BFP) in the strains classified as typical and, on its absence, in the strains classified as atypical. In general, EPEC/STEC hetero-pathogens comprise atypical EPEC carrying Stx (Croxen et al., 2013; Eichhorn et al., 2015; Gomes et al., 2016; Silva et al., 2019). The first description of a typical EPEC strain bearing Stx was reported by Gioia-Di Chiacchio et al. (2018), who identified eight *E. coli* strains isolated from birds that carried Stx2, LEE, and BFP simultaneously. The production of Stx2 was shown in all strains, and two strains induced A/E lesions in cell cultures. All these isolates belonged to the same serotype (O137:H6) and sequence type (ST2678).

EPEC/ETEC

The first reported case of these hetero-pathogenic isolates was of a 6-month-old child presenting acute watery and bloody diarrhea (Dutta et al., 2015), a more severe symptom. The virulence of this strain was assessed *in vitro*, showing that it induced A/E lesions and produced a functional heat-label toxin (LT) (Dutta et al., 2015). In 2016, a new type of EPEC/ETEC strain bearing the heat-stable toxin (ST) instead of LT-encoding genes was reported in healthy cattle (Askari Badouei et al., 2016), but the ST expression was not evaluated. Hazen et al. (2017) reported the identification of four EPEC/ETEC hetero-pathogenic strains isolated from children, two of them being with diarrhea, one asymptomatic, and another with lethal outcome. The EPEC/ETEC strain isolated from the stools of the latter child presented the autotransporter *eatA* accessory gene of ETEC, which prompted the authors to suggest its consideration as a hetero-pathogen (Hazen et al., 2017). However, from our point of view, the presence of *eatA* is not an adequate criterion since this factor is neither an ETEC pathotype defining marker nor a marker related to the ETEC infection symptomatology. Although this is the most recent report concerning these pathogens, the study comprised strains that were isolated between 2008 and 2009 in Africa and Asia (Kotloff et al., 2012). Additionally, in all cases, the EPEC strains had acquired plasmids bearing the ETEC toxin-encoding genes.

ExPEC/STEC

The ExPEC/STEC hybrid is a high-risk pathogen for humans due to the possibility of a systemic infection occurring in concomitance with HUS, which might be aggravated by the presence of a multidrug resistance phenotype, making treatment even more difficult. Reports on the occurrence of HUS just after *E. coli* urinary tract infection (UTI) are rare but have been noted in different countries since 1979 (reviewed by Lavrek et al., 2018). Many studies have reported the presence of Stx-converting phages among UTI isolates, mainly in humans but also in animals (Beutin et al., 1994; de Brito et al., 1999; Mariani-Kurkdjian et al., 2014; Toval et al., 2014b; Cointe et al., 2018; Nüesch-Inderbinen et al., 2018; Gati et al., 2019).

However, few reports have shown the occurrence of diarrhea and extraintestinal infection, in the same patient, as being caused by a single *E. coli* strain. Mariani-Kurkdjian et al. (2014) reported the occurrence of an EHEC strain that caused diarrhea, HUS, and bloodstream infection in an adult in France. This hetero-hybrid pathogen harbors two variants of Stx2, the LEE PAI and one virulence plasmid—(pAPEC-like plasmid) carrying the *ompTp*, *etsC*, *iss*, *hlyF*, *sitA*, *cvaA*, *iroN*, and *iucC* virulence genes—which is often present in APEC and NMEC strains. Moreover, the strain fulfills the intrinsic virulence criteria by Johnson et al. (2003) (**Table 1**) for consideration of ExPEC (Nüesch-Inderbinen et al., 2018), which may explain the capacity of this pathogen to reach the bloodstream and cause severe neurological symptomatology (Mariani-Kurkdjian et al., 2014; Wijnsma et al., 2017). Other studies from Switzerland and France have shown that this hetero-hybrid pathogen, which belongs to serotype O80:H2 and ST301-A, was also isolated from HUS cases followed by bacteremia (confirmed by blood culture positive) (Soysal et al., 2016; Cointe et al., 2018; Nüesch-Inderbinen et al., 2018). This hetero-hybrid pathogen was also reported in human cases of diarrhea and HUS without bacteremia and from calves with diarrhea in Belgium, Switzerland, and the Netherlands (Fierz et al., 2017; Wijnsma et al., 2017; De Rauw et al., 2019). Cointe et al. (2018) also showed the occurrence of this hetero-hybrid pathogen in human and animal subjects in other European countries, such as Germany, Switzerland, Spain, and Slovakia. It is noteworthy that the report of unusual severe neurological conditions was linked with these hybrid strains, even in the absence of bacteremia, and the HUS occurrence is higher than average (about 80%) (Soysal et al., 2016).

Toval et al. (2014b) have shown other types of ExPEC/STEC hybrid strains isolated from humans in Germany. Some of these were also hetero-hybrid pathogenic strains carrying different subtypes of intimin. In addition, the authors demonstrated the Shiga-toxin functionality in bladder cells and that some strains cause UTI and pyelonephritis in animals. These data were corroborated by another study (Gati et al., 2019) and by the occurrence of one case of diarrhea followed by urosepsis and HUS found to have been caused by another ExPEC/STEC hybrid-pathogen isolated in the Netherlands (Ang et al., 2016).

ExPEC/EPEC

Diarrhea followed by bacteremia and multiorgan dysfunction was the outcome of the patient from whom this hybrid-pathogen

was isolated (Kessler et al., 2015). This hybrid strain called attention also by the fact that a pathogen simultaneously bearing PAIs from DEC and ExPEC could reach additional niches and cause a severe disease. This ExPEC/EPEC strain harbored ExPEC defining virulence factors, LEE, and BFP and belonged to serotype O4:H1 and to ST12-B2, a recognized ST related to extraintestinal infections. The phylogenetic analyses of the strain showed that it clustered with other ExPEC lineages but not with EPEC from phylogroup B2, as the EPEC prototype strain E2348/69 (Kessler et al., 2015). Although not thoroughly characterized, another ExPEC/EPEC hybrid strain of serotype O12:K1: HNM was described, which drove a similar outcome. This strain expressed a functional LEE PAI and invaded diverse cell lineages (Bratoeva et al., 1994).

Not all ExPEC/EPEC hybrids cause a disease in intestinal and in extraintestinal niches. Although rare, these hybrid strains have been isolated from diverse extraintestinal infections from human subjects without diarrhea (Abe et al., 2008; Toval et al., 2014a; Riveros et al., 2017; Valiatti et al., 2019). These strains harbored the LEE, no ExPEC defining virulence factors, and belonged to phylogroups A or B2. However, the reason why these strains caused only extraintestinal infections is unclear.

COMBINATIONS OF VIRULENCE FACTORS WITH UNCERTAIN INVOLVEMENT IN MORE SEVERE DISEASES

The studies on the majority of the hybrid/hetero-pathogenic strains that were reported so far lacked information regarding host symptomatology or the expression of virulence factors. Therefore, there is not enough data to determine if the acquisition of new virulence factors necessarily implicates different or more severe symptoms. The combination of virulence traits might not implicate new pathogenicity features or increased virulence because some of the hybrid/hetero-pathogenic strains identified by molecular methods do not express both traits.

STEC/ETEC

Many reports on STEC/ETEC have shown its high frequency among strains isolated from post-weaning diarrhea and edema disease in piglets (Cheng et al., 2006; Barth et al., 2007, 2011; Beutin et al., 2008; Byun et al., 2013). These hetero-pathogenic strains were also isolated from other animals, food, diarrheic human subjects, and some cases of HUS (Monday et al., 2006; Müller et al., 2007; Barth et al., 2011; Prager et al., 2011; Steyert et al., 2012; Nyholm et al., 2015b; Leonard et al., 2016; Michelacci et al., 2018; Bai et al., 2019; Yang et al., 2020).

Although often reported worldwide, studies conducted in Finland and Sweden, which evaluated a large number of human isolates, demonstrated that the occurrence of STEC/ETEC hetero-pathogens was low (Nyholm et al., 2015b; Bai et al., 2019). In one of these studies, four STEC/ETEC strains were reported, corresponding to 2.05% of the total 195 clinical strains initially characterized as STEC isolated over 15 years. Severe symptomatology promoted by this hetero-pathogen was reported only in piglets, and little is known about the impact of these strains, leading to different clinical conditions in human subjects.

The occurrence of multidrug-resistant (MDR) hetero-pathogenic *E. coli* strains emphasizes their genome plasticity and points to the role of horizontal gene exchange in favoring the emergence of higher virulent MDR clones (Rasko et al., 2011), such as certain STEC/ETEC strains. García et al. (2018) showed a STEC/ETEC strain isolated from pig suffering from post-weaning diarrhea, which carried a plasmid containing multiple resistance genes and another one containing multiple virulence genes. Other authors also reported a multidrug-resistant phenotype among strains of this hetero-pathogenic pathotype (Brilhante et al., 2019).

It is interesting to note the diversity of sequence types (STs), phylogroups, and serotypes (more than 40) that was observed among the STEC/ETEC hetero-pathogenic strains (**Table 2**). Such diversity suggests that both the ETEC virulence plasmid and Shiga-toxin-converting bacteriophages could be spread to a broad range of genetic backgrounds, including those serotypes related to more pathogenic strains previously described to cause human disease such as O2:H27, O15:H16, O101:H-, O128:H8, and O141:H8 (Nyholm et al., 2015b).

ExPEC Harboring EAEC Virulence Markers

In 1991, a community-acquired UTI outbreak occurred in Copenhagen (Olesen et al., 1994). The genotypic and the phenotypic characterization of the outbreak-related strains showed that they belonged to the O78:H10 serotype, commonly associated with diarrhea. The outbreak strains harbored the complete set of EAEC defining virulence genes, expressed the aggregative pattern of adherence, and belonged to ST10, like the EAEC strains isolated from diarrhea. Interestingly, they were also lethal in an animal model and hence considered as ExPEC, clearly different from other EAEC strains isolated from diarrhea (Olesen et al., 2012). To our knowledge, these findings were the first evidence that some EAEC strains could cause an extraintestinal infection. Nevertheless, it is important to consider that, in the Copenhagen outbreak, there was no evidence that the EAEC strains could cause diarrhea, although diarrheagenic EAEC harboring ExPEC intrinsic virulence factors have already been reported (Nunes et al., 2017).

It is important to note that strains classified as EAEC by their virulence markers are not always causing diarrhea in their hosts. In fact, Nataro et al. (1995) demonstrated that only strain 042 among four EAEC strains studied induced diarrhea in human volunteers, although all the strains carried the EAEC virulence plasmid. Subsequently, many reports came out, registering the isolation of strains from various extraintestinal infections, which presented the EAEC defining genotype and expressed the aggregative adherence pattern *in vitro* (Abe et al., 2008; Nazemi et al., 2011; Toval et al., 2014a; Lara et al., 2017; Riveros et al., 2017; Freire et al., 2020). However, differently from the EAEC strains of the Copenhagen outbreak, the presence of the ExPEC markers are rare among the reported EAEC isolates from extraintestinal infections (Abe et al., 2008; Toval et al., 2014a). Moreover, it is still unclear if the same strain can cause infections in intestinal and in extraintestinal niches.

TABLE 2 | Summarized characteristics of hybrid- and hetero-pathogens.

	Isolation source	Virulence traits		Expression of the virulence traits	Disease	Outbreaks	Serogroup or serotype	MLST-phylogroup[a]	References
EAEC/STEC	Intestinal infections	Stx and aggregative fimbriae with *aggR* regulator		Yes	Diarrhea, bloody diarrhea, and HUS	Yes	O104:H4 O59:H- Orough:H- O111:H2 O89:H- O23:H28	ST678-B1 ST26-B1 ST1136-B1	Morabito et al., 1998; Iyoda et al., 2000; Frank et al., 2011; Prager et al., 2014; Lang et al., 2018
EPEC/STEC	Intestinal infections in humans, animals' gut, environment, and food	LEE PAI and Stx	Intimin (various subtypes) and Stx	Yes	Diarrhea, bloody diarrhea, and HUS	Yes	O157:H7 O145 O103 O26 O111	ST11-E ST32cplx-D ST20cplx-B1 ST29cplx-B1 ST29cplx-B1	Eichhorn et al., 2015
	Normal fecal sample	LEE PAI, Stx-2f, and BFP	Identified only in birds	Yes		No	O137:H6	ST2678-B2	Gioia-Di Chiacchio et al., 2018
EPEC/ETEC	Intestinal infections	LEE PAI and LT or ST	Regardless of the presence of BFP	Yes	Watery diarrhea	No	Unknown	ST278cplx-B1 ST1788-A	Dutta et al., 2015; Askari Badouei et al., 2016; Hazen et al., 2017
ExPEC/STEC and ExPEC/EHEC[b]	Diarrhea and extraintestinal infections simultaneously or extraintestinal infections only	Stx and ExPEC intrinsic virulence factors		Yes—both characteristics are expressed In general, harbor Stx2 variant	UTI, hemorrhagic cystitis, HUS, bacteremia	Yes[c]	O2:H6 O76:H19 Ont:H- O80:H2 O145:H-	ST141-B2 ST675-B1 ST10cplx-A ST165cplx-A ST32cplx-D	Mariani-Kurkdjian et al., 2014; Toval et al., 2014b; Gati et al., 2019
ExPEC/EPEC	Extraintestinal infections only or diarrhea followed by extraintestinal infection	LEE PAI only or LEE PAI and ExPEC intrinsic virulence factors	Regardless of the presence of BFP	LA or LAL pattern was observed in some studies	Cystitis, pyelonephritis, UTI-related bacteremia, and diarrhea with multiple organ dysfunction	No	O71 O78:H- O4:H1 O12:K1:H-	Unknown ST2018-B2 ST12-B2 Unknown	Vieira et al., 2001; Abe et al., 2008; Toval et al., 2014a; Kessler et al., 2015; Riveros et al., 2017; Lindstedt et al., 2018; Valiatti et al., 2019
STEC/ETEC	Intestinal infections in human and animals	Stx and ST toxin	Various Stx2 variants; Stx1 is frequently low	Yes, but some strains express just one toxin	Diarrhea, bloody diarrhea, and HUS	No	Various serogroups (>40 serotypes)	ST10cplx-A ST40cplx-B1 ST325-A ST329-A	Nyholm et al., 2015b; García et al., 2018; Bai et al., 2019

(Continued)

TABLE 2 | Continued

	Isolation source	Virulence traits	Expression of the virulence traits	Disease	Outbreaks	Serogroup or serotype	MLST-phylogroup[a]	References
ExPEC/EAEC	Extraintestinal infections	Aggregative fimbriae with *aggR* regulator only or with ExPEC intrinsic virulence factors	Yes[d]	Extraintestinal infections not related to diarrhea	Yes	Various serogroups (O5, O6, O11, O15, O18, O78, etc.)	Various ST10cplx-A is the most frequently reported ST69-D ST131-B2	Abe et al., 2008; Olesen et al., 2012; Toval et al., 2014a; Lara et al., 2017; Riveros et al., 2017
ExPEC/ETEC	Extraintestinal infections	ETEC virulence factors only	ST was detected in human, while LT was detected in pigs	Urinary tract infections	No	Unknown	Unknown	de Brito et al., 1999; Riveros et al., 2017

LEE PAI, locus of enterocyte effacement pathogenicity island; HUS, hemolytic uremic syndrome; BFP, bundle-forming pilus; Stx, Shiga toxin; ST, heat-stable toxin of ETEC; LT, heat-labile toxin of ETEC; UTI, urinary tract infection; LA, localized adherence; LAL, localized adherence-like.

ExPEC intrinsic virulence factors—presence of two virulence factors or genetic markers among the following: P fimbriae (pap), S fimbriae (sfa/foc), afimbrial adhesin family (afa/dra), aerobactin (iut/iuc), and capsule from capsular group II (kpsMTII).

[a]*Multilocus sequence typing (MLST) and phylogroup relationship were described as available in Escherichia/Shigella EnteroBase of Warwick Medical School (Zhou et al., 2020); STn°–sequence type number; STn°cplx–sequence type complex; ST complex referred to STs that are grouped into clonal complexes by their similarity to a central allelic profile.*

[b]*EHEC is used to refer to strains that harbor LEE and Stx simultaneously.*

[c]*Only EHEC/ExPEC strains were related to an outbreak.*

[d]*An aggregative adherence pattern was classified in HeLa or HEp-2 cell lineages. The expression of extraintestinal virulence (capacity to cause UTI or sepsis) was observed for some strains in specific animal models.*

FAVORABLE BACKGROUND FOR THE MIX-UP OF VIRULENCE FACTORS

The *E. coli* population can be divided into eight different phylogroups (A, B1, B2, C, D, E, F, and G) (Clermont et al., 2019). Although pathogenic *E. coli* are distributed among all, some pathotypes are frequently assigned to specific phylogroups; for example, ExPEC strains are often referred to as belonging to phylogroups B2 and D, while many DEC strains are of phylogroup B1. In this context, phylogroup A strains are classically related to those that make up the gut microbiota and are avirulent, such as the *E. coli* K-12 prototype strain MG1655 (Leimbach et al., 2013; Clermont et al., 2017; Johnson and Russo, 2018). However, virulent strains, including those associated with both ExPEC and DEC outbreaks, are also assigned into phylogroup A.

Interestingly, some clonal groups inside phylogroup A are frequently reported to be involved in a myriad of infections and multidrug-resistance, such as ST10 (Olesen et al., 2012; Hauser et al., 2013; Riley, 2014; Toval et al., 2014a; Nyholm et al., 2015a; Arais et al., 2018; García et al., 2018; Yamaji et al., 2018). The strains belonging to this ST seem to be very flexible and receptive, bearing many hybrid- and hetero-pathogenic strains (**Table 2**). These findings suggest that some specific genetic backgrounds could be more permissive to acquire and stably maintain a variety of mobile genetic elements, allowing the emergence of hybrid- or hetero-pathogenic strains.

Gati et al. (2019) have shown that the ST141-B2, which includes both STEC and ExPEC strains, was the origin of some STEC/ExPEC hybrid strains. Accordingly, their analysis suggested that ST141, allocated between well-defined pathogenic clusters, could be a hotspot for the emergence of hybrid strains. These authors have also concluded that the development of the STEC/ExPEC hybrid was a recent event. These events might happen in all clonal groups that harbor more than one of the *E. coli* pathotypes and could not be seen as restricted to any ST or phylogroup. The characteristics of the hybrid/hetero-pathogenic strains are detailed in **Table 2**.

WHAT MIGHT BE THE CONSEQUENCES OF *E. COLI* GENOME PLASTICITY?

Some hybrid- and hetero-pathogenic strains have been isolated from human and animal infections since the extensive study of pathogenic *E. coli* strains began. Some of these pathogens were reported long ago, like EPEC/STEC strains, while others, like ExPEC/STEC strains, emerged in recent years and are being pointed only now as the cause of diseases. Although the hybrid- and hetero-pathogenic strains might have appeared long ago, the interest in their significance as more virulent pathogens is a recent phenomenon.

Sequencing technologies have helped to understand the events involved in hybrid/hetero-pathogen evolution, the most common being the transference of virulence genes by mobile plasmids and the acquisition of converting phages. Most of the hybrid strains described until now are related to the STEC

pathotype, probably because of the broad host range of Shiga-toxin-converting bacteriophages, since their occurrence has been reported in different species including *Citrobacter freundii* and *Enterobacter cloacae*, which were associated with HUS and one outbreak (Tschäpe et al., 1995; Paton and Paton, 1996). Additionally, Fogolari et al. (2018) recently reported that the presence of the Stx-converting phage could be found in other *Shigella* species besides *Shigella dysenteriae* type 1, mainly in *Shigella flexneri*. Moreover, viable Stx-converting phages were shown to be present in water and sewage (Muniesa and Jofre, 1998; Beutin et al., 2008). Therefore, the prevalence in the environment and the broad host range explain the capacity of these phages to reach new bacteria. Interestingly, there has been no report on the occurrence of the EIEC virulence plasmid among other DEC or ExPEC pathotypes. Nevertheless, the presence in EIEC of some ExPEC virulence genetic markers, including those of UPEC pathogenicity islands, has already been reported (da Silva et al., 2017). However, the reported strains cannot be considered as hybrid pathogens since they do not fulfill the molecular criteria proposed by Johnson et al. (2003) for the classification of intrinsic virulent ExPEC (da Silva et al., 2017).

Currently, there is not enough published data to confirm if hybrid/hetero-pathogens are always more virulent than their parental pathotypes. Although some studies pointed out that the disease prognoses were worst (Bratoeva et al., 1994; Navarro-Garcia, 2014; Kessler et al., 2015; Ang et al., 2016; Soysal et al., 2016; Wijnsma et al., 2017), this question has not been adequately addressed in all hybrid/hetero-pathogenic strains, and more information about the host symptomatology are necessary to better understand their significance.

It is well-known that the *E. coli* genome is a dynamic entity; thus, hybrid- and hetero-pathogens will probably continue to emerge and expand the current set of recognized *E. coli* pathotypes. The great challenge for both human and veterinary medicine will be to promptly identify and hinder these pathogens from spreading and causing massive outbreaks, such as the German outbreak of 2011. Considering that these hybrid/hetero-pathogens can carry virulence-associated makers as well as multidrug resistance genes, there is an urgency to identify them and address appropriate measures of containment.

AUTHOR CONTRIBUTIONS

AS and FS designed and conceptualized this review, wrote the first draft, and edited the manuscript. RS and TG wrote and revised it critically. All authors contributed to manuscript revision, read, and approved the submitted version.

FUNDING

This research was supported by Fundação de Amparo à Pesquisa do Estado de São Paulo (FAPESP) (process numbers 2018/17353-7 and 2017/14821-7) that provided research grant to the authors and by Coordenação de Aperfeiçoamento de Pessoal de Nível Superior (CAPES) grant 001 to AS and FS (both PNPD fellowship). The funding agencies did not have any influence on the research work described in the manuscript.

ACKNOWLEDGMENTS

We would like to thank Editage (http://www.editage.com.br) for editing and reviewing this manuscript for the English language.

REFERENCES

Abe, C. M., Salvador, F. A., Falsetti, I. N., Vieira, M. A. M., Blanco, J., Blanco, J. E., et al. (2008). Uropathogenic *Escherichia coli* (UPEC) strains may carry virulence properties of diarrhoeagenic *E. coli*. *FEMS Immunol. Med. Microbiol.* 52, 397–406. doi: 10.1111/j.1574-695X.2008.00388.x

Adeolu, M., Alnajar, S., Naushad, S., and Gupta, R. (2016). Genome-based phylogeny and taxonomy of the 'Enterobacteriales': proposal for *Enterobacterales* ord. nov. divided into the families *Enterobacteriaceae, Erwiniaceae* fam. nov., *Pectobacteriaceae* fam. nov., *Yersiniaceae*. *Int. J. Syst. Evol. Microbiol.* 66, 5575–5599. doi: 10.1099/ijsem.0.001485

Ang, C. W., Bouts, A. H. M., Rossen, J. W. A., Van der Kuip, M., Van Heerde, M., and Bökenkamp, A. (2016). Diarrhea, urosepsis and hemolytic uremic syndrome caused by the same heteropathogenic *Escherichia coli* Strain. *Pediatr. Infect. Dis. J.* 35, 1045–1047. doi: 10.1097/INF.0000000000001226

Arais, L. R., Barbosa, A. V., Andrade, J. R. C., Gomes, T. A. T., Asensi, M. D., Aires, C. A. M., et al. (2018). Zoonotic potential of atypical enteropathogenic *Escherichia coli* (aEPEC) isolated from puppies with diarrhoea in Brazil. *Vet. Microbiol.* 227, 45–51. doi: 10.1016/j.vetmic.2018.10.023

Askari Badouei, M., Morabito, S., Najafifar, A., and Mazandarani, E. (2016). Molecular characterization of enterohemorrhagic *Escherichia coli* hemolysin gene (EHEC-hlyA)-harboring isolates from cattle reveals a diverse origin and hybrid diarrheagenic strains. *Infect. Genet. Evol.* 39, 342–348. doi: 10.1016/j.meegid.2016.02.002

Auvray, F., Dilasser, F., Bibbal, D., Kérourédan, M., Oswald, E., and Brugère, H. (2012). French cattle is not a reservoir of the highly virulent enteroaggregative Shiga toxin-producing *Escherichia coli* of serotype O104:H4. *Vet. Microbiol.* 158, 443–445. doi: 10.1016/j.vetmic.2012.02.029

Bai, X., Zhang, J., Ambikan, A., Jernberg, C., Ehricht, R., Scheutz, F., et al. (2019). Molecular characterization and comparative genomics of clinical hybrid shiga toxin-producing and enterotoxigenic *Escherichia coli* (STEC/ETEC) strains in Sweden. *Sci. Rep.* 9:5619. doi: 10.1038/s41598-019-42122-z

Barth, S., Schwanitz, A., and Bauerfeind, R. (2011). Polymerase chain reaction-based method for the typing of F18 fimbriae and distribution of F18 fimbrial subtypes among porcine Shiga toxin-encoding *Escherichia coli* in Germany. *J. Vet. Diagn. Invest.* 23, 454–464. doi: 10.1177/1040638711403417

Barth, S., Tscholshiew, A., Menge, C., Weiss, R., Baljer, G., and Bauerfeind, R. (2007). Virulence and fitness gene patterns of Shiga toxin-encoding Escherichia coli isolated from pigs with edema disease or diarrhea in Germany. *Berl. Munch. Tierarztl. Wochenschr.* 120, 307–16. doi: 10.2376/0005-9366-120-307

Beutin, L., Karch, H., Aleksic, S., Spencker, F. B., and Rosenbaum, U. (1994). Occurrence of verotoxin (Shiga-like toxin) producing *Escherichia coli* in human urinary tract infection. *Infection* 22:425. doi: 10.1007/BF01715504

Beutin, L., Kruger, U., Krause, G., Miko, A., Martin, A., and Strauch, E. (2008). Evaluation of major types of Shiga toxin 2e-producing *Escherichia coli* bacteria present in food, pigs, and the environment as potential pathogens for humans. *Appl. Environ. Microbiol.* 74, 4806–4816. doi: 10.1128/AEM.00623-08

Bielaszewska, M., Mellmann, A., Zhang, W., Köck, R., Fruth, A., Bauwens, A., et al. (2011). Characterisation of the *Escherichia coli* strain associated with an outbreak of haemolytic uraemic syndrome in Germany, 2011: a microbiological study. *Lancet Infect. Dis.* 11, 671–676. doi: 10.1016/S1473-3099(11)70165-7

Boudailliez, B., Berquin, P., Mariani-Kurkdjian, P., Ilef, D., and Cuvelier, B. (1997). Possible person-to-person transmission of *Escherichia coli* O111-associated hemolytic uremic syndrome. *Pediatr. Nephrol.* 11, 36–39. doi: 10.1007/s004670050229

Bratoeva, M. P., Wolf, M. K., Marks, J. K., and Cantey, J. R. (1994). A case of diarrhea, bacteremia, and fever caused by a novel strain of *Escherichia coli*. *J. Clin. Microbiol.* 32, 1383–1386.

Brilhante, M., Perreten, V., and Donà, V. (2019). Multidrug resistance and multivirulence plasmids in enterotoxigenic and hybrid Shiga toxin-producing/enterotoxigenic *Escherichia coli* isolated from diarrheic pigs in Switzerland. *Vet. J.* 244, 60–68. doi: 10.1016/j.tvjl.2018.12.015

Byun, J. W., Jung, B. Y., Kim, H. Y., Fairbrother, J. M., Lee, M. H., and Lee, W. K. (2013). Real-time PCR for differentiation of F18 variants among enterotoxigenic and Shiga toxin-producing *Escherichia coli* from piglets with diarrhoea and oedema disease. *Vet. J.* 198, 538–540. doi: 10.1016/j.tvjl.2013.07.021

Center for Disease Control and Prevention (2013). *Outbreak of Escherichia coli O104:H4 Infections Associated With Sprout Consumption - Europe and North America, May-July 2011.*

Cheng, D., Sun, H., Xu, J., and Gao, S. (2006). PCR detection of virulence factor genes in *Escherichia coli* isolates from weaned piglets with edema disease and/or diarrhea in China. *Vet. Microbiol.* 115, 320–328. doi: 10.1016/j.vetmic.2006.02.013

Clermont, O., Couffignal, C., Blanco, J., Mentré, F., Picard, B., and Denamur, E. (2017). Two levels of specialization in bacteraemic *Escherichia coli* strains revealed by their comparison with commensal strains. *Epidemiol. Infect.* 145, 872–882. doi: 10.1017/S0950268816003010

Clermont, O., Dixit, O. V. A., Vangchhia, B., Condamine, B., Dion, S., Bridier-Nahmias, A., et al. (2019). Characterization and rapid identification of phylogroup G in *Escherichia coli*, a lineage with high virulence and antibiotic resistance potential. *Environ. Microbiol.* 21, 3107–3117. doi: 10.1111/1462-2920.14713

Cointe, A., Birgy, A., Mariani-Kurkdjian, P., Liguori, S., Courroux, C., Blanco, J., et al. (2018). Emerging multidrug-resistant hybrid pathotype Shiga toxin-producing *Escherichia coli* O80 and related strains of clonal complex 165, Europe. *Emerg. Infect. Dis.* 24, 2262–2269. doi: 10.3201/eid2412.180272

Croxen, M. A., and Finlay, B. B. (2010). Molecular mechanisms of *Escherichia coli* pathogenicity. *Nat. Rev. Microbiol.* 8, 26–38. doi: 10.1038/nrmicro2265

Croxen, M. A., Law, R. J., Scholz, R., Keeney, K. M., Wlodarska, M., and Finlay, B. B. (2013). Recent advances in understanding enteric pathogenic *Escherichia coli*. *Clin. Microbiol. Rev.* 26, 822–880. doi: 10.1128/CMR.00022-13

da Silva, L. C., de Mello Santos, A. C., and Silva, R. M. (2017). Uropathogenic *Escherichia coli* pathogenicity islands and other ExPEC virulence genes may contribute to the genome variability of enteroinvasive *E. coli*. *BMC Microbiol.* 17:68. doi: 10.1186/s12866-017-0979-5

de Brito, B. G., Leite, D. D. S., Linhares, R. E. C., and Vidotto, M. C. (1999). Virulence-associated factors of uropathogenic *Escherichia coli* strains isolated from pigs. *Vet. Microbiol.* 65, 123–132. doi: 10.1016/S0378-1135(98)00277-6

De Rauw, K., Thiry, D., Caljon, B., Saulmont, M., Mainil, J., and Piérard, D. (2019). Characteristics of Shiga toxin producing- and enteropathogenic *Escherichia coli* of the emerging serotype O80:H2 isolated from humans and diarrhoeic calves in Belgium. *Clin. Microbiol. Infect.* 25, 111.e5–111.e8. doi: 10.1016/j.cmi.2018.07.023

Doughty, S., Sloan, J., Bennett-Wood, V., Robertson, M., Robins-Browne, R. M., and Hartland, E. L. (2002). Identification of a novel fimbrial gene cluster related to long polar fimbriae in locus of enterocyte effacement-negative strains of enterohemorrhagic *Escherichia coli*. *Infect. Immun.* 70, 6761–6769. doi: 10.1128/IAI.70.12.6761-6769.2002

Dutta, S., Pazhani, G. P., Nataro, J. P., and Ramamurthy, T. (2015). Heterogenic virulence in a diarrheagenic *Escherichia coli*: evidence for an EPEC expressing heat-labile toxin of ETEC. *Int. J. Med. Microbiol.* 305, 47–54. doi: 10.1016/j.ijmm.2014.10.006

Eichhorn, I., Heidemanns, K., Semmler, T., Kinnemann, B., Mellmann, A., Harmsen, D., et al. (2015). Highly virulent Non-O157 enterohemorrhagic *Escherichia coli* (EHEC) serotypes reflect similar phylogenetic lineages, providing new insights into the evolution of EHEC. *Appl. Environ. Microbiol.* 81, 7041–7047. doi: 10.1128/AEM.01921-15

Ewers, C., Li, G., Wilking, H., Kiebling, S., Alt, K., Antão, E., et al. (2007). Avian pathogenic, uropathogenic, and newborn meningitis-causing *Escherichia coli*: how closely related are they? *Int. J. Med. Microbiol.* 297, 163–176. doi: 10.1016/j.ijmm.2007.01.003

Fierz, L., Cernela, N., Hauser, E., Nüesch-Inderbinen, M., and Stephan, R. (2017). Characteristics of Shigatoxin-producing *Escherichia coli* strains isolated during 2010-2014 from human infections in Switzerland. *Front. Microbiol.* 8:1471. doi: 10.3389/fmicb.2017.01471

Fogolari, M., Mavian, C., Angeletti, S., Salemi, M., Lampel, K. A., and Maurelli, A. T. (2018). Distribution and characterization of Shiga toxin converting temperate phages carried by *Shigella flexneri* in Hispaniola HHS public access. *Infect. Genet. Evol.* 65, 321–328. doi: 10.1016/j.meegid.2018.07.038

Frank, C., Werber, D., Cramer, J. P., Askar, M., Faber, M., an der Heiden, M., et al. (2011). Epidemic profile of Shiga-toxin-producing *Escherichia coli* O104:H4 outbreak in Germany. *N. Engl. J. Med.* 365, 1771–1780. doi: 10.1056/NEJMoa1106483

Freire, C. A., Santos, A. C. M., Pignatari, A. C., Silva, R. M., and Elias, W. P. (2020). Serine protease autotransporters of Enterobacteriaceae (SPATEs) are largely distributed among *Escherichia coli* isolated from the bloodstream. *Brazilian J. Microbiol.* 51, 447–454. doi: 10.1007/s42770-020-00224-1

García, V., García-Meniño, I., Mora, A., Flament-Simon, S. C., Díaz-Jiménez, D., Blanco, J. E., et al. (2018). Co-occurrence of mcr-1, mcr-4 and mcr-5 genes in multidrug-resistant ST10 Enterotoxigenic and Shiga toxin-producing *Escherichia coli* in Spain (2006-2017). *Int. J. Antimicrob. Agents* 52, 104–108. doi: 10.1016/j.ijantimicag.2018.03.022

Gati, N. S., Middendorf-Bauchart, B., Bletz, S., Dobrindt, U., and Mellmann, A. (2019). Origin and evolution of hybrid Shiga toxin-producing and uropathogenic (STEC/UPEC) *Escherichia coli* of sequence type 141. *J. Clin. Microbiol.* 58:e01309-19. doi: 10.1128/JCM.01309-19

Gioia-Di Chiacchio, R. M., Cunha, M. P. V., de Sá, L. R. M., Davies, Y. M., Pereira, C. B. P., Martins, F. H., et al. (2018). Novel hybrid of typical enteropathogenic *Escherichia coli* and Shiga-toxin-producing *E. coli (tEPEC/STEC)* emerging from pet birds. *Front. Microbiol.* 9:2975. doi: 10.3389/fmicb.2018.02975

Gomes, T. A. T., Elias, W. P., Scaletsky, I. C. A., Guth, B. E. C., Rodrigues, J. F., Piazza, R. M. F., et al. (2016). Diarrheagenic *Escherichia coli*. *Brazilian J. Microbiol.* 47, 3–30. doi: 10.1016/j.bjm.2016.10.015

Hauser, E., Mellmann, A., Semmler, T., Stoeber, H., Wieler, L. H., Karch, H., et al. (2013). Phylogenetic and molecular analysis of food-borne shiga toxin-producing *Escherichia coli*. *Appl. Environ. Microbiol.* 79, 2731–2740. doi: 10.1128/AEM.03552-12

Hazen, T. H., Michalski, J., Luo, Q., Shetty, A. C., Daugherty, S. C., Fleckenstein, J. M., et al. (2017). Comparative genomics and transcriptomics of *Escherichia coli* isolates carrying virulence factors of both enteropathogenic and enterotoxigenic *E. coli*. *Sci. Rep.* 7:3513. doi: 10.1038/s41598-017-03489-z

Iyoda, S., Tamura, K., Itoh, K., Izumiya, H., Ueno, N., Nagata, K., et al. (2000). Inducible stx2 phages are lysogenized in the enteroaggregative and other phenotypic *Escherichia coli* O86:HNM isolated from patients. *FEMS Microbiol. Lett.* 191, 7–10. doi: 10.1111/j.1574-6968.2000.tb09311.x

Johnson, J. R., Murray, A. C., Gajewski, A., Sullivan, M., Snippes, P., Kuskowski, M. A., et al. (2003). Isolation and molecular characterization of nalidixic acid-resistant extraintestinal pathogenic *Escherichia coli* from retail chicken products. *Antimicrob. Agents Chemother.* 47, 2161–2168. doi: 10.1128/AAC.47.7.2161-2168.2003

Johnson, J. R., and Russo, T. A. (2018). Molecular epidemiology of extraintestinal pathogenic *Escherichia coli*. *EcoSal Plus* 8:ESP-0004-2017. doi: 10.1128/ecosalplus.ESP-0004-2017

Kaper, J. B., Nataro, J. P., and Mobley, H. L. T. (2004). Pathogenic *Escherichia coli*. *Nat. Rev. Microbiol.* 2, 123–140. doi: 10.1038/nrmicro818

Kessler, R., Nisa, S., Hazen, T. H., Horneman, A., Amoroso, A., Rasko, D. A., et al. (2015). Diarrhea, bacteremia and multiorgan dysfunction due to an extraintestinal pathogenic *Escherichia coli* strain with enteropathogenic *E. coli* genes. *Pathog. Dis.* 73:ftv076. doi: 10.1093/femspd/ftv076

Kotloff, K. L., Blackwelder, W. C., Nasrin, D., Nataro, J. P., Farag, T. H., Van Eijk, A., et al. (2012). The Global Enteric Multicenter Study (GEMS) of diarrheal disease in infants and young children in developing countries: epidemiologic and clinical methods of the case/control study. *Clin. Infect. Dis.* 55, S232–S245. doi: 10.1093/cid/cis753

Krause, M., Barth, H., and Schmidt, H. (2018). Toxins of locus of enterocyte effacement-negative Shiga toxin-producing *Escherichia coli*. *Toxins* 10:241. doi: 10.3390/toxins10060241

Lang, C., Fruth, A., Holland, G., Laue, M., Mühlen, S., Dersch, P., et al. (2018). Novel type of pilus associated with a Shiga-toxigenic *E. coli* hybrid pathovar conveys aggregative adherence and bacterial virulence. *Emerg. Microbes Infect.* 7, 1–16. doi: 10.1038/s41426-018-0209-8

Lara, F. B. M., Nery, D. R., de Oliveira, P. M., Araujo, M. L., Carvalho, F. R. Q., Messias-Silva, L. C. F., et al. (2017). Virulence markers and phylogenetic analysis of *Escherichia coli* strains with hybrid EAEC/UPEC genotypes recovered from sporadic cases of extraintestinal infections. *Front. Microbiol.* 8:146. doi: 10.3389/fmicb.2017.00146

Lavrek, D., Lava, S. A. G., Milani, G. P., Simonetti, G. D., Bianchetti, M. G., and Giannini, O. (2018). Hemolytic-uremic syndrome after *Escherichia coli* urinary tract infection in humans: systematic review of the literature. *J. Nephrol.* 31, 919–924. doi: 10.1007/s40620-018-0543-x

Leimbach, A., Hacker, J., and Dobrindt, U. (2013). *E. coli* as an all-rounder: The thin line between commensalism and pathogenicity. *Curr. Top. Microbiol. Immunol.* 358, 3–32. doi: 10.1007/82_2012_303

Leonard, S. R., Mammel, M. K., Rasko, D. A., and Lacher, D. W. (2016). Hybrid shiga toxin-producing and enterotoxigenic Escherichia sp. cryptic lineage 1 strain 7v harbors a hybrid plasmid. *Appl. Environ. Microbiol.* 82, 4309–4319. doi: 10.1128/AEM.01129-16

Levine, M. M. (1987). *Escherichia coli* that cause diarrhea: enterotoxigenic, enteropathogenic, enteroinvasive, enterohemorrhagic, and enteroadherent. *J. Infect. Dis.* 155, 377–389. doi: 10.1093/infdis/155.3.377

Lindstedt, B.-A., Finton, M. D., Porcellato, D., and Brandal, L. T. (2018). High frequency of hybrid *Escherichia coli* strains with combined Intestinal Pathogenic *Escherichia coli* (IPEC) and Extraintestinal Pathogenic *Escherichia coli* (ExPEC) virulence factors isolated from human faecal samples. *BMC Infect. Dis.* 18:544. doi: 10.1186/s12879-018-3449-2

Luck, S. N., Bennett-Wood, V., Poon, R., Robins-Browne, R. M., and Hartland, E. L. (2005). Invasion of epithelial cells by locus of enterocyte effacement-negative enterohemorrhagic *Escherichia coli*. *Infect. Immun.* 73, 3063–3071. doi: 10.1128/IAI.73.5.3063-3071.2005

Mariani-Kurkdjian, P., Lemaître, C., Bidet, P., Perez, D., Boggini, L., Kwon, T., et al. (2014). Haemolytic-uraemic syndrome with bacteraemia caused by a new hybrid *Escherichia coli* pathotype. *New Microbes New Infect.* 2, 127–131. doi: 10.1002/nmi2.49

Martinez-Medina, M., Mora, A., Blanco, M., López, C., Alonso, M. P., Bonacorsi, S., et al. (2009). Similarity and divergence among adherent-invasive *Escherichia coli* and extraintestinal pathogenic *E. coli strains. J. Clin. Microbiol.* 47, 3968–3979. doi: 10.1128/JCM.01484-09

Mellmann, A., Harmsen, D., Cummings, C. A., Zentz, E. B., Leopold, S. R., Rico, A., et al. (2011). Prospective genomic characterization of the German enterohemorrhagic *Escherichia coli* O104:H4 outbreak by rapid next generation sequencing technology. *PLoS ONE* 6:e22751. doi: 10.1371/journal.pone.0022751

Michelacci, V., Maugliani, A., Tozzoli, R., Corteselli, G., Chiani, P., Minelli, F., et al. (2018). Characterization of a novel plasmid encoding F4-like fimbriae present in a Shiga-toxin producing enterotoxigenic *Escherichia coli* isolated during the investigation on a case of hemolytic-uremic syndrome. *Int. J. Med. Microbiol.* 308, 947–955. doi: 10.1016/j.ijmm.2018.07.002

Monday, S. R., Keys, C., Hanson, P., Shen, Y., Whittam, T. S., and Feng, P. (2006). Produce isolates of the *Escherichia coli* Ont:H52 serotype that carry both Shiga toxin 1 and stable toxin genes. *Appl. Environ. Microbiol.* 72, 3062–3065. doi: 10.1128/AEM.72.4.3062-3065.2006

Monecke, S., Patricia, M. K., Bingen, E., Weill, F. X., Balière, C., Slickers, P., et al. (2011). Presence of enterohemorrhagic *Escherichia coli* ST678/O104:H4 in France prior to 2011. *Appl. Environ. Microbiol.* 77, 8784–8786. doi: 10.1128/AEM.06524-11

Morabito, S., Karch, H., Mariani-Kurkdjian, P., Schmidt, H., Minelli, F., Bingen, E., et al. (1998). Enteroaggregative, Shiga toxin-producing *Escherichia coli* O111:H2 associated with an outbreak of hemolytic-uremic syndrome. *J. Clin. Microbiol.* 36, 840–842. doi: 10.1128/JCM.36.3.840-842.1998

Müller, D., Greune, L., Heusipp, G., Karch, H., Fruth, A., Tschäpe, H., et al. (2007). Identification of unconventional intestinal pathogenic *Escherichia coli* isolates expressing intermediate virulence factor profiles by using a novel single-step multiplex PCR. *Appl. Environ. Microbiol.* 73, 3380–3390. doi: 10.1128/AEM.02855-06

Muniesa, M., and Jofre, J. (1998). Abundance in sewage of bacteriophages that infect *Escherichia coli* O157:H7 and that carry the Shiga toxin 2 gene. *Appl. Environ. Microbiol.* 64, 2443–2448. doi: 10.1128/AEM.64.7.2443-2448.1998

Nataro, J. P., Yikang, D., Cookson, S., Cravioto, A., Savarino, S. J., Guers, L. D., et al. (1995). Heterogeneity of enteroaggregative *Escherichia coli* virulence demonstrated. *J. Infect. Dis.* 171, 465–468. doi: 10.1093/infdis/171.2.465

Navarro-Garcia, F. (2014). *Escherichia coli* O104:H4 pathogenesis: an enteroaggregative *E. coli*/Shiga toxin-Producing *E. coli* explosive cocktail of high virulence. *Microbiol. Spectr.* 2:EHEC-0008-2013. doi: 10.1128/microbiolspec.EHEC-0008-2013

Nazemi, A., Mirinargasi, M., Merikhi, N., and Sharifi, S. H. (2011). Distribution of pathogenic genes aatA, aap, aggR, among Uropathogenic *Escherichia coli* (UPEC) and their linkage with StbA Gene. *Indian J. Microbiol.* 51, 355–358. doi: 10.1007/s12088-011-0175-5

Nüesch-Inderbinen, M., Cernela, N., Wüthrich, D., Egli, A., and Stephan, R. (2018). Genetic characterization of Shiga toxin producing *Escherichia coli* belonging to the emerging hybrid pathotype O80:H2 isolated from humans 2010-2017 in Switzerland. *Int. J. Med. Microbiol.* 308, 534–538. doi: 10.1016/j.ijmm.2018.05.007

Nunes, K. O., Santos, A. C. P., Bando, S. Y., Silva, R. M., Gomes, T. A. T., and Elias, W. P. (2017). Enteroaggregative *Escherichia coli* with uropathogenic characteristics are present in feces of diarrheic and healthy children. *Pathog. Dis.* 75:106. doi: 10.1093/femspd/ftx106

Nyholm, O., Halkilahti, J., Wiklund, G., Okeke, U., Paulin, L., Auvinen, P., et al. (2015a). Comparative genomics and characterization of hybrid shigatoxigenic and enterotoxigenic *Escherichia coli* (STEC/ETEC) Strains. *PLoS ONE* 10:e0135936. doi: 10.1371/journal.pone.0135936

Nyholm, O., Heinikainen, S., Pelkonen, S., Hallanvuo, S., Haukka, K., and Siitonen, A. (2015b). Hybrids of Shigatoxigenic and Enterotoxigenic *Escherichia coli* (STEC/ETEC) among human and animal isolates in Finland. *Zoonoses Public Health* 62, 518–524. doi: 10.1111/zph.12177

Olesen, B., Kolmos, H. J., Ørskov, F., and Ørskov, I. (1994). Cluster of multiresistant *Escherichia coli* O78:H10 in greater Copenhagen. *Scand. J. Infect. Dis.* 26, 406–410. doi: 10.3109/00365549409008613

Olesen, B., Scheutz, F., Andersen, R. L., Menard, M., Boisen, N., Johnston, B., et al. (2012). Enteroaggregative *Escherichia coli* O78:H10, the cause of an outbreak of urinary tract infection. *J. Clin. Microbiol.* 50, 3703–3711. doi: 10.1128/JCM.01909-12

Palmela, C., Chevarin, C., Xu, Z., Torres, J., Sevrin, G., Hirten, R., et al. (2018). Adherent-invasive *Escherichia coli* in inflammatory bowel disease. *Gut* 67, 574–587. doi: 10.1136/gutjnl-2017-314903

Paton, A. W., and Paton, J. C. (1996). Enterobacter cloacae producing a Shiga-like toxin II-related cytotoxin associated with a case of hemolytic-uremic syndrome. *J. Clin. Microbiol.* 34, 463–465. doi: 10.1128/JCM.34.2.463-465.1996

Perna, A., Hay, E., Contieri, M., De Luca, A., Guerra, G., and Lucariello, A. (2020). Adherent-invasive *Escherichia coli* (AIEC): cause or consequence of inflammation, dysbiosis, and rupture of cellular joints in patients with IBD? *J. Cell. Physiol.* 235, 5041–5049. doi: 10.1002/jcp.29430

Picard, B., Garcia, J. S., Gouriou, S., Duriez, P., Brahimi, N., Bingen, E., et al. (1999). The link between phylogeny and virulence in *Escherichia coli* extraintestinal infection. *Infect. Immun.* 67, 546–553.

Prager, R., Fruth, A., Busch, U., and Tietze, E. (2011). Comparative analysis of virulence genes, genetic diversity, and phylogeny of Shiga toxin 2g and heat-stable enterotoxin STIa encoding *Escherichia coli* isolates from humans, animals, and environmental sources. *Int. J. Med. Microbiol.* 301, 181–191. doi: 10.1016/j.ijmm.2010.06.003

Prager, R., Lang, C., Aurass, P., Fruth, A., Tietze, E., and Flieger, A. (2014). Two novel EHEC/EAEC hybrid strains isolated from human infections. *PLoS ONE* 9:e95379. doi: 10.1371/journal.pone.0095379

Rasko, D. A., Webster, D. R., Sahl, J. W., Bashir, A., Boisen, N., Scheutz, F., et al. (2011). Origins of the *E. coli* strain causing an outbreak of hemolytic-uremic syndrome in Germany. *N. Engl. J. Med.* 365, 709–717. doi: 10.1056/NEJMoa1106920

Riley, L. W. (2014). Pandemic lineages of extraintestinal pathogenic *Escherichia coli*. *Clin. Microbiol. Infect.* 20, 380–390. doi: 10.1111/1469-0691.12646

Riveros, M., García, W., García, C., Durand, D., Mercado, E., Ruiz, J., et al. (2017). Molecular and phenotypic characterization of diarrheagenic *Escherichia coli* strains isolated from bacteremic children. *Am. J. Trop. Med. Hyg.* 97, 1329–1336. doi: 10.4269/ajtmh.17-0066

Russo, T. A., and Johnson, J. R. (2000). Proposal for a new inclusive designation for extraintestinal pathogenic isolates of *Escherichia coli*: ExPEC. *J. Infect. Dis.* 181, 1753–1754. doi: 10.1086/315418

Sadiq, S. M., Hazen, T. H., Rasko, D. A., and Eppinger, M. (2014). EHEC genomics: past, present, and future. *Microbiol. Spectr.* 2:EHEC-0020-2013. doi: 10.1128/microbiolspec.EHEC-0020-2013

Santos, A. C. M., Zidko, A. C. M., Pignatari, A. C., and Silva, R. M. (2013). Assessing the diversity of the virulence potential of *Escherichia coli* isolated from bacteremia in São Paulo, Brazil. *Brazilian J. Med. Biol. Res.* 46, 968–973. doi: 10.1590/1414-431X20133184

Silva, M., Santos, A., Rocha, L., Caetano, B., Mitsunari, T., Santos, L., et al. (2019). Development and validation of Shiga toxin-producing *Escherichia coli* immunodiagnostic assay. *Microorganisms* 7:276. doi: 10.3390/microorganisms7090276

Soysal, N., Mariani-Kurkdjian, P., Smail, Y., Liguori, S., Gouali, M., Loukiadis, E., et al. (2016). Enterohemorrhagic *Escherichia coli* hybrid pathotype O80:H2 as a new therapeutic challenge. *Emerg. Infect. Dis.* 22, 1604–1612. doi: 10.3201/eid2209.160304

Spurbeck, R. R., Dinh, P. C., Walk, S. T., Stapleton, A. E., Hooton, T. M., Nolan, L. K., et al. (2012). *Escherichia coli* isolates that carry vat, fyuA, chuA, and yfcV efficiently colonize the urinary tract. *Infect. Immun.* 80, 4115–4122. doi: 10.1128/IAI.00752-12

Steyert, S. R., Sahl, J. W., Fraser, C. M., Teel, L. D., Scheutz, F., and Rasko, D. A. (2012). Comparative genomics and stx phage characterization of LEE-negative Shiga toxin-producing *Escherichia coli*. *Front. Cell. Infect. Microbiol.* 2:133. doi: 10.3389/fcimb.2012.00133

Torres, A., Amaral, M., Bentancor, L., Galli, L., Goldstein, J., Krüger, A., et al. (2018). Recent advances in Shiga toxin-producing *Escherichia coli* research in Latin America. *Microorganisms* 6:100. doi: 10.3390/microorganisms6040100

Toval, F., Köhler, C. D., Vogel, U., Wagenlehner, F., Mellmann, A., Fruth, A., et al. (2014a). Characterization of *Escherichia coli* isolates from hospital inpatients or outpatients with urinary tract infection. *J. Clin. Microbiol.* 52, 407–418. doi: 10.1128/JCM.02069-13

Toval, F., Schiller, R., Meisen, I., Putze, J., Kouzel, I. U., Zhang, W., et al. (2014b). Characterization of urinary tract infection-associated Shiga toxin-producing *Escherichia coli*. *Infect. Immun.* 82, 4631–4642. doi: 10.1128/IAI.01701-14

Tschäpe, H., Prager, R., Streckel, W., Fruth, A., Tietze, E., and Böhme, G. (1995). Verotoxinogenic *Citrobacter freundii* associated with severe gastroenteritis and cases of haemolytic uraemic syndrome in a nursery school: green butter as the infection source. *Epidemiol. Infect.* 114, 441–450. doi: 10.1017/S0950268800052158

Valiatti, T. B., Santos, F. F., de, Santos, A. C. M., Silva, R. M., Carvalho, E., and Gomes, T. A. T. (2019). Draft whole-genome sequence of a uropathogenic *Escherichia coli* strain carrying the eae gene. *Microbiol. Resour. Announc.* 8:e00980-19. doi: 10.1128/MRA.00980-19

Vieira, M. A. M., Andrade, J. R. C., Trabulsi, L. R., Rosa, A. C. P., Dias, A. M. G., Ramos, S. R. T. S., et al. (2001). Phenotypic and genotypic characteristics of *Escherichia coli* strains of non-enteropathogenic *E. coli* (EPEC) serogroups that carry eae and lack the EPEC adherence factor and Shiga toxin DNA probe sequences. *J. Infect. Dis.* 183, 762–772. doi: 10.1086/318821

Wieler, L. H., Semmler, T., Eichhorn, I., Antao, E. M., Kinnemann, B., Geue, L., et al. (2011). No evidence of the Shiga toxin-producing *E. coli* O104:H4 outbreak strain or enteroaggregative *E. coli* (EAEC) found in cattle faeces in northern Germany, the hotspot of the 2011 HUS outbreak area. *Gut Pathog.* 3:17. doi: 10.1186/1757-4749-3-17

Wijnsma, K. L., Schijvens, A. M., Rossen, J. W. A., Kooistra-Smid, A. M. D., Schreuder, M. F., and van de Kar, N. C. A. J. (2017). Unusual severe case of hemolytic uremic syndrome due to Shiga toxin 2d-producing *E. coli* O80:H2. *Pediatr. Nephrol.* 32, 1263–1268. doi: 10.1007/s00467-017-3642-3

Yamaji, R., Friedman, C. R., Rubin, J., Suh, J., Thys, E., McDermott, P., et al. (2018). A population-based surveillance study of shared genotypes of *Escherichia coli* isolates from retail meat and suspected cases of urinary tract infections. *mSphere* 3, e00179–e00118. doi: 10.1128/mSphere.00179-18

Yang, X., Bai, X., Zhang, J., Sun, H., Fu, S., Fan, R., et al. (2020). *Escherichia coli* strains producing a novel Shiga toxin 2 subtype circulate in China. *Int. J. Med. Microbiol.* 310:151377. doi: 10.1016/j.ijmm.2019.151377

Yang, Y., Liao, Y., Ma, Y., Gong, W., and Zhu, G. (2017). The role of major virulence factors of AIEC involved in inflammatory bowl disease-a mini-review. *Appl. Microbiol. Biotechnol.* 101, 7781–7787. doi: 10.1007/s00253-017-8507-y

Zhou, Z., Alikhan, N. F., Mohamed, K., Fan, Y., and Achtman, M. (2020). The EnteroBase user's guide, with case studies on *Salmonella* transmissions, *Yersinia pestis* phylogeny, and *Escherichia* core genomic diversity. *Genome Res.* 30, 138–152. doi: 10.1101/gr.251678.119

Conflict of Interest: The authors declare that the research was conducted in the absence of any commercial or financial relationships that could be construed as a potential conflict of interest.

frontiers in Cellular and Infection Microbiology

METHODS
published: 29 July 2020
doi: 10.3389/fcimb.2020.00378

Multiplex PCR Assays for the Detection of One Hundred and Thirty Seven Serogroups of Shiga Toxin-Producing *Escherichia coli* Associated With Cattle

Justin B. Ludwig[1], Xiaorong Shi[1], Pragathi B. Shridhar[1], Elisabeth L. Roberts[2], Chitrita DebRoy[2], Randy K. Phebus[3], Jianfa Bai[4] and T. G. Nagaraja[1]**

[1] Department of Diagnostic Medicine/Pathobiology, Kansas State University, Manhattan, KS, United States, [2] E. coli Reference Center, Department of Veterinary and Biomedical Sciences, The Pennsylvania State University, University Park, PA, United States, [3] Department of Animal Sciences and Industry/Food Science Institute, Kansas State University, Manhattan, KS, United States, [4] Veterinary Diagnostic Laboratory, Industry/Food Science Institute, Kansas State University, Manhattan, KS, United States

OPEN ACCESS

Edited by:
Roxane M. Piazza, Butantan Institute, Brazil

Reviewed by:
Nora Lía Padola, National University of Central Buenos Aires, Argentina
Beatriz Arellano Reynoso, National Autonomous University of Mexico, Mexico

***Correspondence:**
Jianfa Bai
jbai@vet.k-state.edu
T. G. Nagaraja
tnagaraj@vet.k-state.edu

Specialty section:
This article was submitted to Bacteria and Host, a section of the journal Frontiers in Cellular and Infection Microbiology

Received: *06 April 2020*
Accepted: *18 June 2020*
Published: *29 July 2020*

Citation:
Ludwig JB, Shi X, Shridhar PB, Roberts EL, DebRoy C, Phebus RK, Bai J and Nagaraja TG (2020) Multiplex PCR Assays for the Detection of One Hundred and Thirty Seven Serogroups of Shiga Toxin-Producing Escherichia coli Associated With Cattle. Front. Cell. Infect. Microbiol. 10:378. doi: 10.3389/fcimb.2020.00378

Escherichia coli carrying prophage with genes that encode for Shiga toxins are categorized as Shiga toxin-producing *E. coli* (STEC) pathotype. Illnesses caused by STEC in humans, which are often foodborne, range from mild to bloody diarrhea with life-threatening complications of renal failure and hemolytic uremic syndrome and even death, particularly in children. As many as 158 of the total 187 serogroups of *E. coli* are known to carry Shiga toxin genes, which makes STEC a major pathotype of *E. coli*. Seven STEC serogroups, called top-7, which include O26, O45, O103, O111, O121, O145, and O157, are responsible for the majority of the STEC-associated human illnesses. The STEC serogroups, other than the top-7, called "non-top-7" have also been associated with human illnesses, more often as sporadic infections. Ruminants, particularly cattle, are principal reservoirs of STEC and harbor the organisms in the hindgut and shed in the feces, which serves as a major source of food and water contaminations. A number of studies have reported on the fecal prevalence of top-7 STEC in cattle feces. However, there is paucity of data on the prevalence of non-top-7 STEC serogroups in cattle feces, generally because of lack of validated detection methods. The objective of our study was to develop and validate 14 sets of multiplex PCR (mPCR) assays targeting serogroup-specific genes to detect 137 non-top-7 STEC serogroups previously reported to be present in cattle feces. Each assay included 7–12 serogroups and primers were designed to amplify the target genes with distinct amplicon sizes for each serogroup that can be readily identified within each assay. The assays were validated with 460 strains of known serogroups. The multiplex PCR assays designed in our study can be readily adapted by most laboratories for rapid identification of strains belonging to the non-top-7 STEC serogroups associated with cattle.

Keywords: shiga toxin-producing *Escherichia coli* (STEC), top-7 STEC, non-top-7 STEC, Multiplex PCR assays, cattle, feces

INTRODUCTION

The polysaccharide portion, called the O-antigen, of the lipopolysaccharide layer of the outer membrane of *Escherichia coli* provides antigenic specificity and is the basis of serogrouping. As many as 187 *E. coli* serogroups have been described based on the nucleotide sequences of O-antigen gene clusters (DebRoy et al., 2016). *Escherichia coli* serogroups that cause disease in humans and animals are categorized into several pathotypes. The serogroups that carry Shiga toxin genes on a prophage are categorized as the Shiga toxin-producing *E. coli* (STEC) pathotype. As many as 158 serogroups of *E. coli* are known to carry Shiga toxin gene(s), which make STEC the most predominant *E. coli* pathotype (**Table 1**). Illnesses caused by STEC in humans, which are often foodborne, range from mild to bloody diarrhea with life-threatening complications of renal failure and hemolytic uremic syndrome (HUS), and even death, particularly in children (Karmali et al., 2010; Davis et al., 2014). Seven serogroups of STEC, O26, O45, O103, O111, O121, O145, and O157, called "top-7," are responsible for the majority of human STEC illnesses, including food borne-outbreaks (Brooks et al., 2005; Scallan et al., 2011; Gould et al., 2013; Valilis et al., 2018). However, STEC serogroups other than the top-7, called "non-top-7" have also been reported to cause human illnesses, more often as sporadic infections, although a few are also known to cause severe infections, such as hemorrhagic colitis and HUS (Hussein and Bollinger, 2005; Bettelheim, 2007; Hussein, 2007; Bettelheim and Goldwater, 2014; Valilis et al., 2018). In a recent systematic review done by Valilis et al. (2018), 129 O-serogroups of STEC were identified to be associated with clinical cases of diarrhea in humans.

Ruminants, especially cattle, are a major reservoir of STEC and harbor the organisms in the hindgut and shed them in their feces. A number of studies have reported on the fecal prevalence of the top-7 STEC in cattle because of the availability of detection methods. For these serogroups, culture method involving serogroup-specific immunomagnetic separation and media for selective isolation and PCR assays to identify serogroups of putative isolates have been developed, validated and widely used (Bielaszewska and Karch, 2000; Chapman, 2000; Bettelheim and Beutin, 2003; Noll et al., 2015a). A number of studies have reported shedding of non-top-7 STEC in cattle feces (**Table 2**). However, not much is known about the prevalence of these STEC serogroups in cattle feces, in terms of their distribution and proportion of animals in a herd positive for various serogroups, largely because of lack of isolation and detection methods. Traditionally, identification of serogroups or serotyping of *E. coli,* conducted by agglutination reaction using serogroup-specific antisera, is restricted to a few reference laboratories that possess the required antisera. However, the method is time consuming and often exhibits cross-reactions with other serogroups (DebRoy et al., 2011a). A number of PCR-based assays, end point or real time, have been developed and validated for the detection of one or more clinically relevant serogroups of *E. coli* (Perelle et al., 2004; Monday et al., 2007; Fratamico et al., 2009; Bai et al., 2010, 2012; DebRoy et al., 2011b; Madic et al., 2011; Luedtke et al., 2014; Iguchi et al., 2015b; Noll et al., 2015b; Sanchez et al., 2015; Shridhar et al., 2016a). However, only a few mPCR assays have been described to detect certain STEC serogroups that are non-top-7 (Iguchi et al., 2015b; Sanchez et al., 2015; DebRoy et al., 2018).

In recent years, DNA microarray and whole genome sequencing have been widely used to identify *E. coli* serogroups and serotypes (Liu and Fratamico, 2006; Lacher et al., 2014; Joensen et al., 2015; Norman et al., 2015). However, mPCR assays targeting serogroup-specific genes to identify STEC is a

TABLE 1 | Serogroups that belong to the Shiga toxin-producing *Escherichia coli* pathotype.

O1	O2/O50	O3	O4	O5	O6	O7	O8	O9	O10
O11/OX19	O12	O13/O129/O135	O14	O15	O16	O17/O44/O73/O77/O106	O18ab/O18ac	O19	O20/O137
O21	O22	O23	O25	O26[a]	O27	O28ac/O42	O29	O30	O32
O33	O35	O36[b]	O37	O38	O39	O40	O41	O43	O45[a]
O46/O134	O48	O49	O51	O52	O53	O54	O55	O56	O57
O58	O59	O60	O62/O68	O63	O64	O65	O66[b]	O69	O70
O71	O74	O75	O76	O78	O79	O80	O81	O82	O83
O84	O85	O86	O87	O88	O89/O101/O162	O90/O127	O91	O92	O93
O95[b]	O96	O97	O98	O100	O102	O103[a]	O104	O105	O107/O117
O108	O109	O110	O111[a]	O112	O113	O114	O115	O116	O118/O151
O119	O120	O121[a]	O123/O186	O124/O164	O125	O126	O128/OX3	O130	O131
O132	O133	O136	O138	O139	O140	O141	O142	O143	O144
O145[a]	O146	O147	O148	O149	O150	O152	O153	O154	O156
O157[a]	O158	O159	O160	O161	O163	O165	O166	O167	O168/OX6
O169	O170	O171	O172	O173	O174	O175	O176	O177	O178
O179	O180	O181	O182	O183	O184[b]	O185	O187[b]		

[a] *Serogroups (highlighted in blue color) considered as top-7 STEC.*

[b] *Serogroups (highlighted in green color) have not yet been reported in cattle feces, beef, or beef products.*

TABLE 2 | Serogroups of Shiga toxin-producing *Escherichia coli* other than the top-7 in gut contents or feces of cattle.

Cattle type	Sample type	O-serogroups reported	References
Calves with diarrhea or dysentery	Feces	O2, O5, O8, O29, O55, O149, O153	(Smith et al., 1988)
Calves	Feces	O2, O104, O128, O153	(Gonzalez and Blanco, 1989)
Bulls and dairy cows	Colonic contents of bulls at slaughter, rectal content of dairy cows	O3, O10, O22, O39, O75, O82, O91, O104, O105, O113, O116, O126, O136, O139, O156	(Montenegro et al., 1990)
Beef and dairy cattle, water buffalo	Rectal swab	O11, O25, O113, O116	(Suthienkul et al., 1990)
Dairy cattle: cows, heifers, calves; feedlot cattle	Rectal swab	O10, O15, O22, O76, O84, O116, O153, O163, O171	(Wells et al., 1991)
Dairy cows and calves	Fecal swab	O2, O3,O 4, O6, O8, O9, O11, O15, O22, O25, O32, O40, O43, O82, O87, O106, O109, O113, O117, O146, O153, O163, X3, X8	(Wilson et al., 1992)
Cattle	Rectal swab	O2, O8, O20, O22, O76, O82, O87, O88, O113, O146, O152, O156	(Beutin et al., 1993)
Cattle	Culture from cattle	O8, O9, O11, O15, O17, O20, O78, O86, O101	(Wray et al., 1993)
Dairy cows and calves	Rectal swab	O5, O18, O49, O69, O74, O76, O80, O84, O98, O118, O119, O156, O172	(Sandhu et al., 1996)
Calves, diarrheic	Feces	O4, O5, O15, O17, O53, O80, O84, O92, O118, O119, O128, O153	(Wieler et al., 1996)
Cattle	Feces	O74, O87, O90, O91, O116	(Beutin et al., 1997)
Cows and calves	Fecal swab	O2, O4, O8, O9, O20, O22, O41, O74, O77, O78, O82, O90, O91, O92, O105, O113, O116, O132, O136, O146, O150, O162, O163, O165, O171	(Blanco et al., 1997)
Calves with diarrhea	Feces	O6, O8, O25, O52, O86, O113, O167, ONT	(Beutin and Muller, 1998)
Cattle	Feces or rectal contents	O2, O16, O22, O42, O70, O74, O84, O87, O105, O109, O113, O132, O136, O146, O153, O156	(Miyao et al., 1998)
Calves, healthy and diarrheic	Feces	O118	(Wieler et al., 1998)
Dairy cows and calves	Fecal swabs	O5, O8, O22, 38, O69, O84, O98, O113, O116, O119, O132, O153, O156	(Sandhu et al., 1999)
Dairy cow with diarrhea and calves with a herd history of ill-thrift and diarrhea	Feces	O84	(Hornitzky et al., 2000)
Beef and dairy cattle: healthy and diarrheic calves; Cattle at slaughter; Grazing cows	Rectal swab	O2, O5, O20, O38, O39, O74, O79, O91, O113, O116, O117, O118, O141, O165, O168, O171	(Parma et al., 2000)
Cattle at slaughter	Feces	OX3, O1, O2, O6, O8, O15, O20, O22, O23, O39, O40, O46, O49, O74, O77, O84, O87, O88, O91, O96, O98, O102, O105, O106, O109, O112, O113, O116, O117, O120, O130, O132, O136, O140, O141, O150, O159, O163, O171, O172, OX177, OX7, OX178	(Pradel et al., 2000)
Cattle at slaughter	Rectal swab	O2, O8, O22, O43, O91, O110, O113, O116, O119, O132, O136, O153, O172	(Schurman et al., 2000)
Dairy cows and calves	Feces	O12, O35, O98, O165	(Cobbold and Desmarchelier, 2001)
Cattle	Feces	O5, O6, O7, O21, O28, O91, O113, O130, ONT	(Hornitzky et al., 2001)
Cattle at slaughter	Rectal swab	O15, O84, O91, O172	(Leung et al., 2001)
Beef and dairy cattle	Rectal swab	O20, O22, O74, O79, O84, O110, O112, O119, O125, O126, O128, O149, O156, O159, O165, O172, ONT	(Geue et al., 2002)
Beef cattle at slaughter	Fecal from cecum	O2, O8, O11, O116	(Gioffré et al., 2002)
Beef and feedlot cattle	Feces	O2, O3, O5, O6, O8, O28, O51, O68, O75, O76, O77, O81, O82, O84, O91, O93, O101, O104, O108, O110, O113, O116, O130, O149, O153, O154, O160, O163, ONT	(Hornitzky et al., 2002)
Beef or dairy cattle, calves	Feces (diagnostic samples, gastrointestinal infections)	O2, O5, O7, O8, O15, O22, O28, O41, O53, O71, O74, O75, O81, O84, O88, O98, O112, O113, O118, O119, O123, O130, O146, O159, O163, O174, O175, O177, O178, O179, O181	(Hornitzky et al., 2005)
Dairy cows, heifers, calves	Rectal swab	O29, O91, O112, O119, O125	(Moreira et al., 2003)

(Continued)

TABLE 2 | Continued

Cattle type	Sample type	O-serogroups reported	References
Cattle	Fecal swab	O22, O91, O113, O117, OX179	(Urdahl et al., 2003)
Calves	Feces	O7, O22, O113, O118, O119, O123	(Leomil et al., 2003)
Cattle, diarrheic and healthy	Feces	O2, O4, O6, O7, O8, O9, O15, O17, O20, O22, O28, O38, O39, O41, O49, O60, O64, O65, O74, O77, O79, O80, O81, O82, O84, O88, O90, O91, O96, O104, O105, O110, O113, O116, O117, O118, O123, O126, O127, O128, O132, O136, O138, O140, O141, O146, O148, O149, O150, O156, O162, O163, O165, O166, O167, O168, O171, O174, OX177, OX178, ONT	(Blanco et al., 2004a)
Cattle, grazing or feedlot	Feces	O2, O5, O8, O15, O20, O25, O38, O39, O74, O79, O91, O113, O116, O117, O118, O120, O141, O165, O168, O171, O174, O175, O177, O178, O185, ONT	(Blanco et al., 2004b)
Cattle at slaughter	Cecal content	O74, O91, O109, O110, O116, O117	(Bonardi et al., 2004)
Cattle at slaughter	Cecal content	O2, O8, O11, O25, O91, O104, O112, O113, O143, O171, O174, ONT	(Meichtri et al., 2004)
Cows and calves	Feces	O2, O8, O77, O113, O116, O136, O171, O177	(Muniesa et al., 2004)
Cattle at slaughter	Feces	O2, O5, O8, O10, O15, O35, O64, O77, O113, O119, O128, O156, O177, ONT	(Blanco et al., 2005)
Dairy cows, heifers, calves, some diarrheic	Rectal swab	O22, O44, O77, O79, O87, O88, O91, O98, O105, O112, O113, O136, O178, O181, ONT	(Irino et al., 2005)
Cattle	Feces	O2, O4, O8, O20, O22, O41, O64, O77, O82, O91, O105, O113, O116, O117, O118, O126, O128, O136, O141, O146, O150, O156, O162, O163, O168, O171, O174, O177, ONT	(Mora et al., 2005)
Cattle at slaughter	Feces	O1, O2, O5, O8, O15, O22, O86, O91, O113, O116, O117, O136, O148, O174, O182, ONT	(Zweifel et al., 2005)
Beef and dairy cattle	Feces	O2, O10, O15, O22, O74, O82, O96, O113, O116, O119, O124, O128, O137, O141, O159, O160, O63, O174, O177, O178, ONT	(Timm et al., 2007)
Steers, feedlot	Feces	O2, O8, O9, O10, O23, O37, O49, O87, O98, O132, O135, O136, O139, O153, O154, O156, O172	(Diarra et al., 2009)
Cattle	Feces	O2, O63, O148, O149, O174, ONT	(Scott et al., 2009)
Dairy cows	Feces	O2, O3, O5, O8, O11, O22, O39, O46, O64, O74, O79, O84, O88, O91, O105, O113, O130, O136, O139, O141, O163, O166, O168, O171, O1788, O179, ONT	(Fernández et al., 2010)
Beef cattle	Feces	O2, O7, O8, O15, O22, O39, O46, O73, O74, O79, O82, O91, O113, O116, O130, O136, O139, O141, O153, O163, O165, O178, O179, ONT	(Masana et al., 2011)
Cattle, beef and dairy	Pen-floor feces	O2, O13, O20, O86, O109, O113, O116, O119, O136, O168, O171, O174, ONT	(Monaghan et al., 2011)
Cattle, beef and dairy	Feces	O2, O3, O33, O69, O76, O88, O113, O118, O136, O150, O153, O171, OR, OX18	(Ennis et al., 2012)
Calves	Rectal swabs	O8, O11, O15, O91, O101, O171, ONT	(Fernández et al., 2012)
Dairy cows	Feces	O8, O21, O116, O118, O141, O153, NT	(Polifroni et al., 2012)
Beef Cattle	Rectal swabs	O2, O7, O8, O15, O22, O79, O84, O91, O107, O124, O130, O136, O141, O163, O174, O179, ONT	(Tanaro et al., 2012)
Cattle	Feces	O1, O2, O5, O8, O55, O84, O91, O109, O113, O136, O150, O156, O163, O168, O174, 177, UT	(Mekata et al., 2014)
Feedlot heifer	Colonic mucosal tissue at necropsy	O165	(Moxley et al., 2015)
Dairy Cattle	Feces	O2, O8, O10, O15, O20, O22, O39, O46, O55, O74, O77, O79, O82, O89, O91, O105, O113, O116, O141, O171, O172, O153, O165	(Gonzalez et al., 2016)
Cattle	Feces	O113, NT	(Jajarmi et al., 2017)
Cattle	Feces	O2, O3, O6, O8, O22, O28ac, O55, O71, O74, O76, O82, O87, O88, O96, O100, O104, O108, O109, O113, O115, O116, O123, O130, O132, O136, O140, O150, O153, O156, O163, O168, O171, O174, O178, O179, O183, O185	(Lee et al., 2017)
Steers	Recto anal mucosal swab	O101, O109, O177	(Stromberg et al., 2018)
Beef cattle	Feces	O178	(Paquette et al., 2018)
Dairy cattle	Feces	O3, O8, O18ac, O39, O48, O58, O77, O80, O88, O104, O112ac, O116, O146, O154, O174, O175, O176, O178, O179, O180	(Navarro et al., 2018)
Dairy cattle	Feces	O21, O22, O54, O55, O64, O69, O75, O78, O91, O92, O97, O100, O149, O173	(Peng et al., 2019)
Beef cattle	Feces	O5, O8, O15, O22, O65, O74, O76, O81, O84, O96, O116, O165, O166, O177, ONT	(Fan et al., 2019)
Beef and dairy cattle	Feces	O17, O22, O40, O76, O87, O99, O102, O108, O116, O124, O129, O136, O140, O154, O156, O163	(Bumunang et al., 2019)

ONT, Non typeable O; UT, Untypeable; NT, nontypeable.

TABLE 3 | Multiplex PCR assays running conditions for the detection of Shiga toxin-producing *Escherichia coli* (STEC) serogroups, other than top-7 serogroups.

Assays	Number of O groups	PCR cycles	Annealing temperature (°C)	O-serogroups (amplicon size in bp)
Set-1	8	25	65	O109 (204), O91 (277), O168 (336), O80 (406), O156 (452), O84 (501), O86 (562), O4 (832)
Set-2	10	30	65	O5 (176), O22 (246), O171 (281), O175 (343), O13/O129/O135 (364), O119 (421), O120 (535), O123/O186 (619), O138 (696), O128 (768)
Set-3	9	30	64	O25 (230), O79 (266), O150 (313), O116 (355), O33 (413), O75 (511), O181 (595), O98 (675), O6 (783)
Set-4	10	30	63	O147 (230), O15 (288), O118/O151 (344), O113 (419), O126 (465), O178 (495), O76 (533), O146 (640), O2/O50 (819), O78 (992)
Set-5	9	30	61	O20 (204), O55 (262), O87 (306), O92 (375), O8 (448), O136 (528), O163 (596), O7 (753), O62/O68 (906)
Set-6	12	30	66	O115 (158), O39 (201), O38 (253), O74 (303), O107/O117 (357), O88 (394), O96 (457), O108 (515), O130 (567), O132 (652), O153 (741), O141 (880)
Set-7	12	30	63	O1 (152), O18ab/O18ac (199), O28 (O28ac/O42; 255), O35 (305), O37 (353), O40 (396), O43 (445), O17/O44/O73/O77/ O106 (500), O51 (566), O69 (649), O53 (735), O70 (863)
Set-8	11	25	68	O140 (155), O148 (201), O81 (248), O82 (301), O85 (353), O105 (407), O102 (453), O90/O127 (498), O124/O164 (570), O125ab/O125ac (652), O139 (859)
Set-9	9	25	63	O21 (145), O49 (197), O149 (253), O93 (299), O110 (346), O114 (396), O154 (499), O161 (646), O169 (865)
Set-10	12	25	59	O152 (150), O159 (202), O170 (233), O172 (278), O174 (317), O176 (356), O177 (395), O46/O134 (455), O179 (505), O182 (566), O160 (655), O165 (735)
Set-11	11	30	62	O3 (145), O10 (187), O11 (225), O112ab (270), O101/O162 (309), O29 (348), O23 (403), O63 (455), O16 (505), O19 (574), O131 (655)
Set-12	9	25	63	O56 (250), O9 (309), O54 (351), O27 (382), O60 (443), O143 (500), O142 (538), O48 (793), O41 (942)
Set-13	7	25	58	O133 (294), O83 (362), O167 (403), O166 (462), O64 (727), O12 (885), O58 (1046)
Set-14	8	25	58	O100 (193), O144 (245), O66 (301), O71 (344), O65 (381), O32 (452), O173 (606), O180 (744)

simpler, low-cost alternative method, readily adaptable to most laboratories. Iguchi et al. (2015a) and DebRoy et al. (2016) have analyzed the nucleotide sequences of O-antigen gene clusters of 184 serogroups of *E. coli* and reported remarkable diversity among different serogroups and a high level of conservation of genes within a given serogroup in the O-antigen encoding gene clusters and suggested that these gene sequences can be targeted for serogroup identification. To understand the ecology and prevalence of these STEC serogroups in cattle, it is essential to detect the non-top-7 STEC serogroups shed in cattle feces in order to determine their impact on food safety and human health. Therefore, the objectives of the present study were to develop and validate mPCR assays targeting serogroup-specific genes to detect 137 non-top-7 STEC serogroups known to be associated with cattle.

MATERIALS AND METHODS

Design of the Assays

A total of 14 mPCR assays, each targeting 7–12 STEC serogroups were designed. The targeted genes to design primers for serogroup detection included: *wzx,* which encodes for the O-antigen flippase required for O-polysaccharide export (Liu et al., 1996), *wzy,* which encodes for the O-antigen polymerase required for O antigen biosynthesis (Samuel and Reeves, 2003), *gnd,* which encodes for 6-phosphogluconate dehydrogenase for O antigen biosynthesis (Nasoff et al., 1984), *wzm,* which encodes for transport permease for O antigen transport, and *orf469* and *wbdC,* which encode for mannosyltransferase for O antigen biosynthesis (Kido et al., 1995). The primers were designed based on the available nucleotide sequences of the target genes for each of the STEC serogroups from the GenBank database. The sequences for each serogroup were aligned using ClustalX version 2.0. The primers were designed to amplify the target genes with distinct amplicon sizes for each serogroup within an assay for easier visualization. The forward and reverse primer sequences for these serogroups are provided in **Supplementary Tables 1A–N.**

PCR Assay Conditions

The working concentrations of all primers in a primer mix were 4–7 pM/μl of each primer. The reaction consisted of 1 μL of primer mix, 10 μL of BioRad iQ Multiplex Powermix, 7 μL of sterile PCR grade water, and 2 μL of DNA template. The total reaction volume was 20 μL. The number of PCR cycles and annealing temperatures varied based on optimization for each set (**Table 3**). The PCR protocol for specific gene target, for sets no. 1–11, included an initial denaturation at 94°C for 5 min, followed by 25 or 30 cycles of denaturation at 94° C for 30 s, annealing for 30 s at 58–68°C, extension for 75 s at 68°C and a final step of extension at 68° C for 7 min. The assay conditions for PCR sets no. 12, 13, and 14 were initial denaturation at 94°C for 1 min, followed by 25 cycles of denaturation at 94°C for 30 s, annealing for 30 s at 58–63°C, extension for 60–80 s at 72°C and final step of extension at 72°C (**Table 3**). All the other conditions were similar for all 14 sets of assays. Amplicon size of PCR products was determined using a capillary electrophoresis system, QIAxcel Advanced System with QIAxcel DNA Screening

TABLE 4 | Validation of multiplex PCR (mPCR) assays to detect "non-top-7" Shiga toxin-producing *Escherichia coli.*.

mPCR assay	Serogroups (No. of strains positive/No. of strains tested)
1	O4 (5/5)[a,b], O80 (6/6)[b,c], O84 (4/4)[a,c], O86 (6/6)[b,c], O91 (4/4)[a,c], O109 (5/5)[a,b,d], O156 (6/6)[b,c], O168 (5/5)[b]
2	O5 (4/4)[b,c], O13/O129/O135 (2/2)[b], O22 (7/7)[a,b,c], O119 (2/2)[b,c], O120 (5/5)[b], O123/O186 (5/5)[b], O128 (6/6)[b,c], O138 (4/4)[b,c], O171 (4/4)[a,c], O175 (5/5)[b]
3	O6 (4/4)[a,c], O25 (6/6)[b], O33 (5/5)[b], O75 (6/6)[b,c], O79 (2/2)[b], O98 (3/3)[a,b], O116 (8/8)[a,c], O150 (6/6)[b,c], O181 (4/4)[b]
4	O2/O50 (4/4)[a,b,c], O15 (8/8)[a,b,c], O76 (6/6)[b,c], O78 (4/4)[a,b], O113 (5/5)[a,c], O118/O151 (4/4)[a,b,c], O126 (5/5)[a,b,c], O146 (7/7)[a,c], O147 (2/2)[a,c], O178 (5/5)[b]
5	O7 (4/4)[b,c], O8 (20/20)[a,b,c], O20 (1/1)[a], O55 (6/6)[a,c], O62/O68 (4/4)[b], O87 (3/3)[b], O92 (1/1)[b], O136 (6/6)[a,b,c], O163 (4/4)[a,c]
6	O38 (3/3)[a], O39 (3/3)[b], O74 (4/4)[a], O88 (5/5)[a], O96 (4/4)[a], O107/O117 (3/3)[a], O108 (1/1)[a], O115 (1/1)[b], O130 (4/4)[a], O132 (2/2)[a], O141 (3/3)[b], O153 (2/2)[a]
7	O1 (2/2)[b,e], O17/O44/O73/O77/O106 (6/6)[b,e], O18 (4/4)[b,e], O28 (3/3)[b,e], O35 (3/3)[b,e], O37 (3/3)[b,e], O40 (2/2)[b], O43 (4/4)[b,e], O51 (4/4)[b,e], O53 (2/2)[b,e], O69 (3/3)[b,e], O70 (3/3)[b,e]
8	O81 (3/3)[b,e], O82 (3/3)[b,e], O85 (3/3)[b,e], O90/O127 (2/2)[b,c], O102 (4/4)[b,e], O105 (3/3)[b,e], O124/O164 (2/2)[b], O125 (3/3)[b,e], O139 (3/3)[b,e], O140 (2/2)[b,e], O148 (2/2)[e]
9	O21 (3/3)[b,e], O49 (2/2)[b,e], O93 (2/2)[b,e], O110 (2/2)[b,e], O114 (3/3)[b,e], O149 (3/3)[b,e], O154 (3/3)[b,e], O161 (1/1)[e], O169 (2/2)[b,e]
10	O46/O134 (5/5)[a,b,e], O152 (2/2)[b], O159 (2/2)[a,b], O160 (2/2)[b], O165 (4/4)[a,b,e], O170 (3/3)[b,e], O172 (2/2)[a], O174 (2/2)[b,e], O176 (2/2)[b,e], O177 (5/5)[b,d], O179 (4/4)[b], O182 (4/4)[a,b,e]
11	O3 (3/3)[b,e], O10 (2/2)[b,e], O11 (3/3)[b,e], O16 (1/1)[e], O19 (3/3)[b], O23 (3/3)[b,e], O29 (3/3)[a,b,e], O63 (3/3)[b,e], O101/O162 (1/1)[d], O112 (3/3)[b,e], O131 (3/3)[b,e]
12	O9 (2)[e], O27 (1/1)[e], O41 (2/2)[e], O48 (2/2)[e], O54 (2/2)[e], O56 (1/1)[e], O60 (2/2)[e], O142 (2/2)[e], O143 (2/2)[e]
13	O12 (2/2)[e], O58 (2/2)[e], O64 (2/2)[e], O83 (2/2)[e], O133 (1/1)[e], O166 (2/2)[e], O167 (1/1)[e]
14	O32 (3/3)[e], O65 (2/2)[e], O66 (2/2)[e], O71 (2/2)[e], O100 (2/2)[e], O144 (1/1)[e], O173 (1/1)[e], O180 (2/2)[e]

[a] *Strains obtained from our culture collection.*
[b] *Strains obtained from Pennsylvania State University.*
[c] *Strains obtained from Michigan State University.*
[d] *Strains obtained from University of Nebraska.*
[e] *Strains obtained from Food and Drug administration.*

Kit (Qiagen, Germantown, MD). DNA extracted from pooled strains of known serogroups for each specific set was used as positive controls and size markers for each set of assay.

Validation of PCR assays

The specificity of each assay was determined with pooled DNA of the positive controls from the other 13 sets and top-7 STEC plus O104 PCR assays. Additionally, each assay was validated with one or more strains of the targeted serogroups. A total of 460 STEC strains belonging to 137 targeted serogroups were used for the validation of the assays (**Table 4**; **Supplementary Tables 2A–N**). The strains were obtained from our culture collection (n = 104), *E. coli* Reference Center at Pennsylvania State University (n = 223), Michigan State University (n = 42), University of Nebraska (n = 5), and Food and Drug Administration (n = 86). Strains stored in CryoCare beads (CryoCare, Key Scientific Products, Round Rock, TX) at −80°C were streaked onto blood agar plates (Remel, Lenexa, KS) and incubated overnight at 37°C. Following incubation, colonies from the blood agar plates were suspended in 1 ml of distilled water, boiled for 10 min, centrifuged at 9,300 × g for 5 min and the supernatant was used for the PCR assays.

RESULTS

Out of the 158 serogroups of STEC, only five, which include O36, O66, O95, O184, and O187, have not been reported to be present in cattle feces, beef or beef products (**Table 1**). A total of 14 mPCR assays, each targeting 7–12 O-types of 137 non-top-7 serogroups, were designed (**Table 3**). Each set of mPCR assay contained primer pairs that generated amplicons of different sizes for each target serogroup that were readily differentiated using a capillary electrophoresis system (**Table 3**; **Figures 1A–N**). The PCR product size for all the assays ranged from 145 to 1,046 bp (**Table 3**; **Figures 1A–N**). The specificity of each assay was confirmed when only the genes of the targeted serogroups were amplified and none of the serogroups targeted by the other 13 sets and top-7 plus O104 PCR assays was amplified (data not shown). The assays were validated with 460 strains of known serogroups, and the results indicated that all the assays correctly identified the target serogroups (**Table 4**). The 14 sets of mPCR assays did not include the following 14 serogroups: O14, O30, O36, O52, O57, O59, O95, O97, O104, O158, O183, O184, O185, and O187.

DISCUSSION

Of the known 187 serogroups of *E. coli*, 158 serogroups have been shown to possess genes that encode for Shiga toxin 1, 2 or both. Serogroups, O26, O45, O103, O111, O121, O145, and O157, are top-7 serogroups responsible for a majority of human STEC illness outbreaks (Scallan et al., 2011; Gould et al., 2013). Among the top-7, fecal shedding of the O157 serogroup has been studied extensively, but relatively fewer studies have examined fecal shedding of the other six non-O157 serogroups in cattle, particularly in the United States (Renter et al., 2005; Cernicchiaro et al., 2013; Dargatz et al., 2013; Baltasar et al., 2014; Ekiri

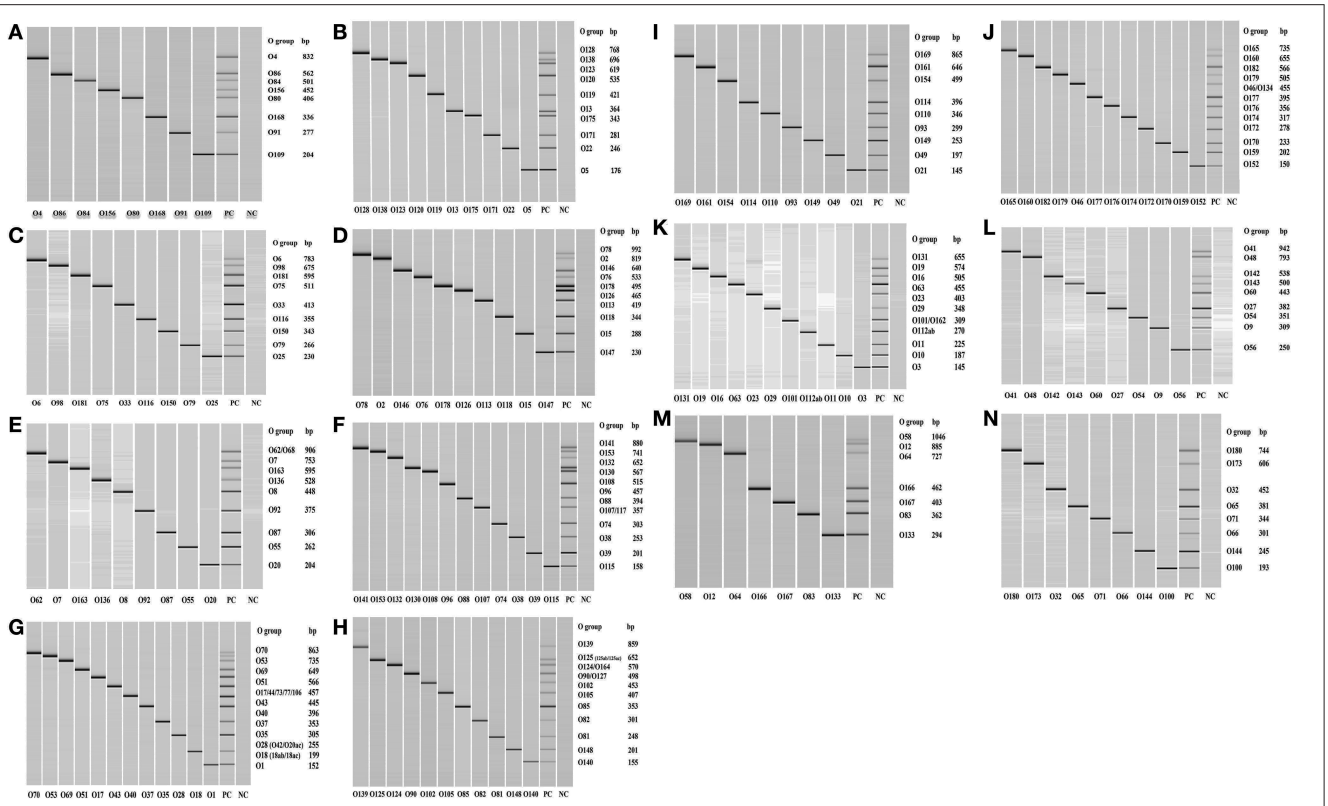

FIGURE 1 | QIAxcel images of the amplicons of serogroup-specific genes of 137 serogroups of Shiga toxin-producing *Escherichia coli* amplified by 14 sets **(A–N)** of multiplex PCR assays. Positive control (PC) included pooled cultures of the known serogroups within each assay. Negative control (NC) included all reagents except the DNA template.

et al., 2014; Paddock et al., 2014; Dewsbury et al., 2015; Noll et al., 2015a; Cull et al., 2017). Among the six top-7 non-O157 serogroups, O26, O45, and O103 are the dominant serogroups in cattle feces with prevalence ranging from 40 to 50%. However, only a small proportion of these serogroups (2–6%) carry Shiga toxin genes (Noll et al., 2015a). Because Shiga toxin genes are located on a prophage, it is suggested that the serogroups lacking these genes either have lost the prophage or have the potential to acquire the prophage (Bielaszewska et al., 2007). A majority of the non-O157 top-six STEC have been show to carry Shiga toxin 1 gene (Shridhar et al., 2017). There is evidence that the type of *stx* gene carried by STEC in cattle is dependent on the age of the animal and season. Shiga toxin gene of STEC strains in adult cattle are predominantly of the *stx*2 type, whereas the strains from calves primarily possess *stx*1 type (Cho et al., 2006; Fernández et al., 2012). In a study on *E. coli* O157 in Argentina, strains of O157 detected in all seasons were predominantly of the *stx*2 type, the proportion of strains containing *stx*1 decreased and proportion of strains possessing both types increased in warm seasons (Fernández et al., 2009).

Many PCR assays have been developed and validated, generally targeting top-7 STEC serogroups, and often in combination with major virulence genes (Shiga toxins 1 and 2, intimin, and enterohemolysin: Bai et al., 2010, 2012; DebRoy et al., 2011b; Fratamico et al., 2011; Lin et al., 2011; Anklam et al., 2012; Paddock et al., 2012; Noll et al., 2015b; Shridhar et al., 2016a). There is limited development of PCR assays targeting the non-top-7 STEC in cattle feces. Individual primer pairs have been described and PCR assays have been developed for each of the 187 serogroups of *E. coli* (DebRoy et al., 2018). However, there are only a few multiplex PCR assays targeting non-top-7 STEC serogroups (Iguchi et al., 2015b; Sanchez et al., 2015). Sanchez et al. (2015) reported the development of three mPCR assays targeting 21 of the most clinically relevant STEC serogroups associated with infections in humans. The assays included, top-7 serogroups and O5, O15, O55, O76, O91, O104, O118, O113, O123, O128, O146, O165, O172, and O177. Iguchi et al. (2015b) designed primer pairs to develop 20 mPCR assays, with each set containing six to nine serogroups, to detect 147 serogroups that included STEC and non-STEC.

Because cattle are a major reservoir of STEC, we designed a series of multiplex PCR assays targeting serogroups, other than the top-7, that have been shown to be associated with feces, beef, or beef products. The nucleotide sequences of some of the targeted serogroups included in our assays have been previously shown to be 98–99.9% identical to other *E. coli* serogroups (O2/O50, O13/O129/O135, O17/O44/O73/O77/O106, O42/O28ac, O46/O134, O62/O68, O90/O127, O107/O117, O118/O151, O123/O186, O124/O164, O118/O51; DebRoy et al., 2016). Of the 158 known STEC serogroups, only five serogroups,

O36, O66, O95, O184, and O187, have not been detected in cattle. The 14 sets of PCR assays did not include O104 because we have published a mPCR assay for the top-7 STEC and O104 (Paddock et al., 2013). The reason for including O104 with the top-7 STEC was because O104:H4, a hybrid pathotype of STEC and enteroaggregative *E. coli,* was involved in a major foodborne outbreak in Germany in 2011 (Bielaszewska et al., 2011). Cattle have been shown to harbor serogroup O104 in the gut and shed in the feces, however, none of the isolates was the H4 serotype and none possessed traits characteristic of the enteroaggregative *E. coli* (Paddock et al., 2013; Shridhar et al., 2016b). The 14 sets of mPCR assays did not include the following 13 serogroups: O14, O30, O36, O52, O57, O59, O95, O97, O158, O183, O184, O185, and O187. Of the 13 serogroups, O14 and O57 have been shown to contain no O-antigen biosynthesis gene clusters (Iguchi et al., 2015a; DebRoy et al., 2016). The reason for not including the remaining 11 serogroups (O30, O36, O52, O59, O95, O97, O158, O183, O184, O185, and O187) was because we were unable to procure known strains of the serogroups required for validation.

STEC serogroups other than the top-7 have been reported to be involved in sporadic cases and a few outbreaks of human illness (McLean et al., 2005; Espie et al., 2006; Buchholz et al., 2011; Mingle et al., 2012). Among the non-top-7 STEC, certain serogroups, such as O1, O2, O8, O15, O25, O43, O75, O76, O86, O91, O101, O102, O113, O116, O156, O160, and O165, specifically certain serotypes within these serogroups, have been involved in outbreaks associated with consumption of contaminated beef in the US and European countries (Eklund et al., 2001; Hussein, 2007). Many of the outbreaks included cases of hemorrhagic colitis and HUS. Serogroups O91 (mostly H21 and H14 serotypes) and O113 (mostly H21 serotype) have been associated with severe cases of hemorrhagic colitis and HUS in the US and other countries (Feng et al., 2014, 2017). Obviously, the difference in virulence between serogroups and serotypes is attributable to specific virulence factors encoded by genes in the chromosome, particularly on large horizontally acquired pathogenicity islands, or on plasmids (Levine, 1987; Bolton, 2011).

In contrast to humans, cattle are generally considered to be not susceptible to STEC infections. Only new born calves, particularly those that are immunocompromised because of deprived colostrum, have been shown to exhibit *E. coli* O157:H7 infections characterized by bloody diarrhea and attaching and effacing lesions (Dean-Nystrom et al., 1998; Moxley and Smith, 2010). Other serogroups that have been associated with diarrheal diseases of calves include O5, O8, O20, O26, O111, and O113 (Mainil and Daube, 2005). The majority of the serotypes causing infections in calves carried only Shiga toxin 1 gene (Mainil and Daube, 2005). Moxley et al. (2015) have reported isolation of STEC O165:H25 from the colonic mucosal tissue of an adult heifer that died of hemorrhagic colitis.

Some of the serogroups detected in cattle feces such as O5, O8, O9, O11, O15, O20, O49, O59, O62, O65, O69, O71, O76, O78, O86, O87, O89, O91, O100, O114, O115, O116, O119, O120, O128, O138, O139, O141, O143, O147, O159, O163, O167, O172, O174, and O180 have also been detected in swine feces (Cha et al., 2018; Peng et al., 2019). A few of the swine STEC serogroups, particularly O8, O138, O139, O141, and O147, are more often implicated in edema disease in weaned piglets and young finishing pigs (Kaper et al., 2004; Melton-Celsa et al., 2012).

Of the 158 STEC serogroups, 130 serogroups have been associated with clinical cases of diarrhea in humans (Mainil and Daube, 2005; Hussein, 2007; Valilis et al., 2018). Therefore, there are 28 STEC serogoups that have not been reported to cause human infections, which is interesting because Shiga toxins are potent virulence factors. Either these STEC have not yet been linked to an illness or they lack other virulence factors, such as those needed for attachment and colonization, necessary to cause infections. A further understanding and assessment of the virulence potential of these serogroups will require sequencing of the whole genome to obtain a comprehensive gene profile.

In conclusion, the multiplex PCR assays designed in our study, which can be readily performed in most microbiology laboratories, will allow for rapid identification of isolates belonging to the non-top-7 *E. coli* STEC serogroups that are prevalent in cattle feces, beef or beef products.

DATA AVAILABILITY STATEMENT

The raw data supporting the conclusions of this article will be made available by the authors, without undue reservation.

AUTHOR CONTRIBUTIONS

JB, TN, and CD conceived and designed the experiments. JL and XS performed the experiments. XS, JB, CD, ER, RP, and TN contributed reagents, materials, and analysis tools. PS, CD, XS, JB, and TN wrote the paper. All authors contributed to the article and approved the submitted version.

FUNDING

This material is based upon work that is supported by the National Institute of Food and Agriculture, U. S. Department of Agriculture, under award number 2012-68003-30155. The funders had no role in the study design, data collection and analyses, preparation of the manuscript or decision to publish.

ACKNOWLEDGMENTS

The authors thank Dr. Shannon Manning (Michigan State University), Dr. Rod Moxley (University of Nebraska) and Ms. Isha Patel (U. S. Food and Drug Administration) for providing us with known serogroups of *E. coli* and Neil Wallace and Leigh Ann George for assistance in the laboratory. This publication is contribution no. 20-251-J of the Kansas Agricultural Experiment Station.

SUPPLEMENTARY MATERIAL

The Supplementary Material for this article can be found online at: https://www.frontiersin.org/articles/10.3389/fcimb.2020.00378/full#supplementary-material

REFERENCES

Anklam, K. S., Kanankege, K. S. T., Gonzales, T. K., Kaspar, C. W., and Döpfer, D. (2012). Rapid and reliable detection of Shiga toxin-producing *Escherichia coli* by real-time multiplex PCR. *J. Food Prot.* 75, 643–650. doi: 10.4315/0362-028X.JFP-11-392

Bai, J., Paddock, Z. D., Shi, X., Li, S., An, B., and Nagaraja, T. G. (2012). Applicability of a multiplex PCR to detect the seven major Shiga toxin-producing *Escherichia coli* based on genes that code for serogroup-specific O-antigens and major virulence factors in cattle feces. *Foodborne Pathog. Dis.* 9, 541–548. doi: 10.1089/fpd.2011.1082

Bai, J., Shi, X., and Nagaraja, T. G. (2010). A multiplex PCR procedure for the detection of six major virulence genes in *Escherichia coli* O157:H7. *J. Microbiol. Meth.* 82, 85–89. doi: 10.1016/j.mimet.2010.05.003

Baltasar, P., Milton, S., Swecker, W., Elvinger, F., and Ponder, M. (2014). Shiga toxin-producing *Escherichia coli* distribution and characterization in a pasture-based cow-calf production system. *J. Food. Prot.* 77, 722–731. doi: 10.4315/0362-028X.JFP-13-420

Bettelheim, K. A. (2007). The non-O157 shiga-toxigenic (verocytotoxigenic) *Escherichia coli*; under-rated pathogens. *Crit. Rev. Microbiol.* 33, 67–87. doi: 10.1080/10408410601172172

Bettelheim, K. A., and Beutin, L. (2003). Rapid laboratory identification and characterization of verocytotoxigenic (Shiga toxin producing) *Escherichia coli* (VTEC/STEC). *J. Appl. Microbiol.* 95, 205–217. doi: 10.1046/j.1365-2672.2003.02031.x

Bettelheim, K. A., and Goldwater, P. N. (2014). Serotypes of non-O157 shigatoxigenic *Escherichia coli* (STEC). *Adv. Microbiol.* 04:13. doi: 10.4236/aim.2014.47045

Beutin, L., Geier, D., Steinruck, H., Zimmermann, S., and Scheutz, F. (1993). Prevalence and some properties of verotoxin (Shiga-like toxin)-producing *Escherichia coli* in seven different species of healthy domestic animals. *J. Clin. Microbiol.* 31, 2483–2488. doi: 10.1128/JCM.31.9.2483-2488.1993

Beutin, L., Geier, D., Zimmermann, S., Aleksic, S., Gillespie, H. A., and Whittam, T. S. (1997). Epidemiological relatedness and clonal types of natural populations of *Escherichia coli* strains producing Shiga toxins in separate populations of cattle and sheep. *Appl. Environ. Microbiol.* 63, 2175–2180. doi: 10.1128/AEM.63.6.2175-2180.1997

Beutin, L., and Muller, W. (1998). Cattle and verotoxigenic *Escherichia coli* (VTEC), an old relationship? *Vet. Rec.* 142, 283–284. doi: 10.1136/vr.142.11.283

Bielaszewska, M., Dobrindt, U., Gärtner, J., Gallitz, I., Hacker, J., Karch, H., et al. (2007). Aspects of genome plasticity in pathogenic *Escherichia coli*. *Int. J. Med. Microbiol.* 297, 625–639. doi: 10.1016/j.ijmm.2007.03.001

Bielaszewska, M., and Karch, H. (2000). Non-O157:H7 Shiga toxin (verocytotoxin)-producing *Escherichia coli* strains: epidemiological significance and microbiological diagnosis. *World J. Microbiol. Biotechnol.* 16, 711–718. doi: 10.1023/A:1008972605514

Bielaszewska, M., Mellmann, A., Zhang, W., Köck, R., Fruth, A., Bauwens, A., et al. (2011). Characterisation of the *Escherichia coli* strain associated with an outbreak of haemolytic uraemic syndrome in Germany, 2011: a microbiological study. *Lancet Infect. Dis.* 11, 671–676. doi: 10.1016/S1473-3099(11)70165-7

Blanco, M., Blanco, J. E., Blanco, J., Mora, A., Prado, C., Alonso, M. P., et al. (1997). Distribution and characterization of faecal verotoxin-producing *Escherichia coli* (VTEC) isolated from healthy cattle. *Vet. Microbiol.* 54, 309–319. doi: 10.1016/S0378-1135(96)01292-8

Blanco, M., Blanco, J. E., Mora, A., Dahbi, G., Alonso, M. P., Gonzalez, E. A., et al. (2004a). Serotypes, virulence genes, and intimin types of Shiga toxin (Verotoxin)-producing *Escherichia coli* isolates from cattle in Spain and identification of a new intimin variant gene (*eae-*). *J. Clin. Microbiol.* 42, 645–651. doi: 10.1128/JCM.42.2.645-651.2004

Blanco, M., Padola, N. L., Kruger, A., Sanz, M. E., Blanco, J. E., Gonzalez, E. A., et al. (2004b). Virulence genes and intimin types of Shiga-toxin-producing *Escherichia coli* isolated from cattle and beef products in Argentina. *Int. Microbiol.* 7, 269–276.

Blanco, M., Schumacher, S., Tasara, T., Zweifel, C., Blanco, J. E., Dahbi, G., et al. (2005). Serotypes, intimin variants and other virulence factors of eae positive *Escherichia coli* strains isolated from healthy cattle in Switzerland. Identification of a new intimin variant gene (eae-eta2). *BMC Microbiol.* 5:23. doi: 10.1186/1471-2180-5-23

Bolton, D. J. (2011). Verocytotoxigenic (Shiga toxin-producing) *Escherichia coli*: virulence factors and pathogenicity in the farm to fork paradigm. *Foodborne Pathog Dis.* 8, 357–365. doi: 10.1089/fpd.2010.0699

Bonardi, S., Foni, E., Brindani, F., Bacci, C., Chiapponi, C., and Cavallini, P. (2004). Detection and characterization of verocytotoxin-producing *Escherichia coli* (VTEC) O157 and non-O157 in cattle at slaughter. *New Microbiol.* 27, 255–261.

Brooks, J. T., Sowers, E. G., Wells, J. G., Greene, K. D., Griffin, P. M., Hoekstra, R. M., et al. (2005). Non-O157 Shiga toxin-producing *Escherichia coli* infections in the United States, 1983-2002. *J. Infect. Dis.* 192, 1422–1429. doi: 10.1086/466536

Buchholz, U., Bernard, H., Werber, D., Böhmer, M. M., Remschmidt, C., Wilking, H., et al. (2011). German outbreak of *Escherichia coli* O104:H4 associated with sprouts. *N. Engl. J. Med.* 365, 1763–1770. doi: 10.1056/NEJMoa1106482

Bumunang, E. W., McAllister, T. A., Zaheer, R., Ortega Polo, R., Stanford, K., King, R., et al. (2019). Characterization of non-O157 *Escherichia coli* from cattle faecal samples in the North-West province of South Africa. *Microorganisms* 7:8. doi: 10.3390/microorganisms7080272

Cernicchiaro, N., Cull, C. A., Paddock, Z. D., Shi, X., Bai, J., Nagaraja, T. G., et al. (2013). Prevalence of Shiga toxin-producing *Escherichia coli* and associated virulence genes in feces of commercial feedlot cattle. *Foodborne Pathog Dis.* 10, 835–841. doi: 10.1089/fpd.2013.1526

Cha, W., Fratamico, P. M., Ruth, L. E., Bowman, A. S., Nolting, J. M., Manning, S. D., et al. (2018). Prevalence and characteristics of Shiga toxin-producing *Escherichia coli* in finishing pigs: Implications on public health. *Int. J. Food Microbiol.* 264, 8–15. doi: 10.1016/j.ijfoodmicro.2017.10.017

Chapman, P. A. (2000). Methods available for the detection of *Escherichia coli* O157 in clinical, food and environmental samples. *World J. Microbiol. Biotechnol.* 16, 733–740. doi: 10.1023/A:1008985008240

Cho, S., Diez-Gonzales, F., Fossler, C. P., Wells, S. J., Hedberg, C. W., Kaneene, J. B., et al. (2006). Prevalence of Shiga toxin-encoding bacteria and Shiga toxin-producing *Escherichia coli* isolates from dairy farms and county fairs. *Vet. Microbiol.* 118, 289–298. doi: 10.1016/j.vetmic.2006.07.021

Cobbold, R., and Desmarchelier, P. (2001). Characterisation and clonal relationships of Shiga-toxigenic *Escherichia coli* (STEC) isolated from Australian dairy cattle. *Vet. Microbiol.* 79, 323–335. doi: 10.1016/S0378-1135(00)00366-7

Cull, C. A., Renter, D. G., Dewsbury, D. M., Noll, L. W., Shridhar, P. B., Ives, S. E., et al. (2017). Feedlot- and pen-level prevalence of enterohemorrhagic *Escherichia coli* in feces of commercial feedlot cattle in two major U.S. cattle feeding areas. *Foodborne Pathog. Dis.* 14, 309–317. doi: 10.1089/fpd.2016.2227

Dargatz, D. A., Bai, J., Lubbers, B. V., Kopral, C. A., An, B., and Anderson, G. A. (2013). Prevalence of *Escherichia coli* O-types and Shiga toxin genes in fecal samples from feedlot cattle. *Foodborne Pathog. Dis.* 10, 392–396. doi: 10.1089/fpd.2012.1289

Davis, T. K., Van De Kar, N. C. A. J., and Tarr, P. I. (2014). Shiga toxin/Verocytotoxin-producing *Escherichia coli* infections: Practical clinical perspectives. *Microbiol. Spect.* 2:4. doi: 10.1128/microbiolspec.EHEC-0025-2014

Dean-Nystrom, E. A., Bosworth, B. T., Moon, H. W., and O'Brien, A. D. (1998). "Bovine infection with Shiga toxin-producing *Escherichia coli*," in *Escherichia coli O157:H7 and Other Shiga Toxin-producing E. coli Strains*, eds J. B. Kaper and A. D. O'Brien (Washington, DC: ASM Press), 261–267.

DebRoy, C., Fratamico, P. M., and Roberts, E. (2018). Molecular serogrouping of *Escherichia coli*. *Anim. Hlth. Res. Rev.* 19, 1–16. doi: 10.1017/S1466252317000093

DebRoy, C., Fratamico, P. M., Yan, X., Baranzoni, G., Liu, Y., Needleman, D. S., et al. (2016). Comparison of O-antigen gene clusters of all O-serogroups of *Escherichia coli* and proposal for adopting a new nomenclature for O-typing. *PLoS ONE* 11:e0147434. doi: 10.1371/journal.pone.0147434

DebRoy, C., Roberts, E., and Fratamico, P. M. (2011a). Detection of O antigens in *Escherichia coli*. *Anim. Health Res. Rev.* 12, 169–185. doi: 10.1017/S1466252311000193

DebRoy, C., Roberts, E., Valadez, A. M., Dudley, E. G., and Cutter, C. N. (2011b). Detection of Shiga toxin-producing Escherichia coli O26, O45, O103, O111, O113, O121, O145, and O157 serogroups by multiplex polymerase chain reaction of the wzx gene of the O-antigen gene cluster. *Foodborne Pathog. Dis.* 8, 651–652. doi: 10.1089/fpd.2010.0769

Dewsbury, D. M. A., Renter, D. G., Shridhar, P. B., Noll, L. W., Shi, X., Nagaraja, T. G., et al. (2015). Summer and winter prevalence of Shiga toxin-producing *Escherichia coli* (STEC) O26, O45, O103, O111, O121, O145, and O157 in feces of feedlot cattle. *Foodborne Pathog. Dis.* 12, 726–732. doi: 10.1089/fpd.2015.1987

Diarra, M. S., Giguère, K., Malouin, F., Lefebvre, B., Bach, S., Delaquis, P., et al. (2009). Genotype, serotype, and antibiotic resistance of sorbitol-negative *Escherichia coli* isolates from feedlot cattle. *J. Food Prot.* 72, 28–36. doi: 10.4315/0362-028X-72.1.28

Ekiri, A. B., Landblom, D., Doetkott, D., Olet, S., Shelver, W. L., and Khaitsa, M. L. (2014). Isolation and characterization of Shiga toxin-producing *Escherichia coli* serogroups O26, O45, O103, O111, O113, O121, O145, and O157 shed from range and feedlot cattle from postweaning to slaughter. *J. Food Prot.* 77, 1052–1061. doi: 10.4315/0362-028X.JFP-13-373

Eklund, M., Scheutz, F., and Siitonen, A. (2001). Clinical isolates of non-O157 Shiga toxin-producing *Escherichia coli:* serotypes, virulence characteristics, and molecular profiles of strains of the same serotype. *J. Clin. Microbiol.* 39, 2829–2834. doi: 10.1128/JCM.39.8.2829-2834.2001

Ennis, C., McDowell, D., and Bolton, D. J. (2012). The prevalence, distribution and characterization of Shiga toxin-producing *Escherichia coli* (STEC) serotypes and virulotypes from a cluster of bovine farms. *J. Appl. Microbiol.* 113, 1238–1248. doi: 10.1111/j.1365-2672.2012.05421.x

Espie, E., Grimont, F., Vaillant, V., Montet, M. P., Carle, I., Bavai, C., et al. (2006). O148 Shiga toxin-producing *Escherichia coli* outbreak: microbiological investigation as a useful complement to epidemiological investigation. *Clin. Microbiol. Infect.* 12, 992–998. doi: 10.1111/j.1469-0691.2006.01468.x

Fan, R., Shao, K., Yang, X., Bai, X., Fu, S., Sun, H., et al. (2019). High prevalence of non-O157 Shiga toxin-producing *Escherichia coli* in beef cattle detected by combining four selective agars. *BMC Microbiology* 19:213. doi: 10.1186/s12866-019-1582-8

Feng, P. C. H., Delannoy, S., Lacher, D. W., Bosilavac, J. M., Fach, P., and Beutin, L. (2017). Shiga toxin-producing serogroup O91 *Escherichia coli* strains isolated from food and environmental samples. *Appl. Environ. Microbiol.* 83:e01231–e012317. doi: 10.1128/AEM.01231-17

Feng, P. C. H., Delannoy, S., Lacher, D. W., Fernando dos Santos, L., Beutin, L., Fach, P., et al. (2014). Genetic diversity and virulence potential of Shiga toxin-producing *Escherichia coli* O113:H21 strains isolated from clinical, environmental, and food sources. *Appl. Environ. Microbiol.* 80, 4757–4763. doi: 10.1128/AEM.01182-14

Fernández, D., Irino, K., Sanz, M. E., Padola, N. L., and Parma, A. E. (2010). Characterization of Shiga toxin-producing *Escherichia coli* isolated from dairy cows in Argentina. *Lett. Appl. Micribiol.* 51, 377–382. doi: 10.1111/j.1472-765X.2010.02904.x

Fernández, D., Rodriguez, E. M., Arroyo, G. H., Padola, N. L., and Parma, A. E. (2009). Seasonal variation of Shiga toxin-encoding genes (*stx*) and detection of *E. coli* O157 in dairy cattle from Argentina. *J. Appl. Micribiol.* 106, 1250–1267. doi: 10.1111/j.1365-2672.2008.04088.x

Fernández, D., Sanz, M. E., Parma, A. E., and Padola, N. L. (2012). Short communiaction: Characterization of Shiga toxin-producing *Escherichia coli* isolated from newborn, milk-fed, and growing calves in Argentina. *J. Dairy Sci*, 95, 5340–5343. doi: 10.3168/jds.2011-5140

Fratamico, P. M., Bagi, L. K., Cray, W. C., Narang, N., Yan, X., Medina, M., et al. (2011). Detection by multiplex real-time polymerase chain reaction assays and isolation of Shiga toxin-producing *Escherichia coli* serogroups O26, O45, O103, O111, O121, and O145 in ground beef. *Foodborne Pathog. Dis.* 8, 601–607. doi: 10.1089/fpd.2010.0773

Fratamico, P. M., DebRoy, C., Miyamoto, T., and Liu, Y. (2009). PCR detection of enterohemorrhagic *Escherichia coli* O145 in food by targeting genes in the E. coli O145 O-antigen gene cluster and the Shiga toxin 1 and Shiga toxin 2 genes. *Foodborne Pathog. Dis.* 6, 605–611. doi: 10.1089/fpd.2008.0254

Geue, L., Segura-Alvarez, M., Conraths, F., Kuczius, T., Bockemühl, J., Karch, H., et al. (2002). A long-term study on the prevalence of shiga toxin-producing *Escherichia coli* (STEC) on four German cattle farms. *Epidemiol. Infect.* 129, 173–185. doi: 10.1017/S0950268802007288

Gioffré, A., Meichtri, L., Miliwebsky, E., Baschkier, A., Chillemi, G., Romano, M. I., et al. (2002). Detection of Shiga toxin-producing *Escherichia coli* by PCR in cattle in Argentina: Evaluation of two procedures. *Vet. Microbiol.* 87, 301–313. doi: 10.1016/S0378-1135(02)00079-2

Gonzalez, A. G., Cerqueira, A. M., Guth, B. E., Coutinho, C. A., Liberal, M. H., Souza, R. M., et al. (2016). Serotypes, virulence markers and cell invasion ability of Shiga toxin-producing *Escherichia coli* strains isolated from healthy dairy cattle. *J. Appl. Microbiol.* 121, 1130–1143. doi: 10.1111/jam.13230

Gonzalez, E. A., and Blanco, J. (1989). Serotypes and antibiotic resistance of verotoxigenic (VTEC) and necrotizing (NTEC) *Escherichia coli* strains isolated from calves with diarrhoea. *FEMS Microbiol. Lett.* 51, 31–36. doi: 10.1111/j.1574-6968.1989.tb03414.x

Gould, L. H., Mody, R. K., Ong, K. L., Clogher, P., Cronquist, A. B., Garman, K. N., et al. (2013). Increased recognition of non-O157 Shiga toxin-producing *Escherichia coli* infections in the United States during 2000-2010: epidemiologic features and comparison with *E. coli* O157 Infections. *Foodborne Pathog. Dis.* 10, 453–460. doi: 10.1089/fpd.2012.1401

Hornitzky, M. A., Bettelheim, K. A., and Djordjevic, S. P. (2000). The isolation of enterohaemorrhagic *Escherichia coli* O111:H- from Australian cattle. *Aust. Vet. J.* 78, 636–637. doi: 10.1111/j.1751-0813.2000.tb11941.x

Hornitzky, M. A., Bettelheim, K. A., and Djordjevic, S. P. (2001). The detection of Shiga toxin-producing *Escherichia coli* in diagnostic bovine faecal samples using vancomycin-cefixime-cefsulodin blood agar and PCR. *FEMS Microbiol. Lett.* 198, 17–22. doi: 10.1111/j.1574-6968.2001.tb10613.x

Hornitzky, M. A., Mercieca, K., Bettelheim, K. A., and Djordjevic, S. P. (2005). Bovine feces from animals with gastrointestinal infections are a source of serologically diverse atypical enteropathogenic *Escherichia coli* and Shiga toxin-producing *E. coli* strains that commonly possess intimin. *Appl. Environ. Microbiol.* 71, 3405–3412. doi: 10.1128/AEM.71.7.3405-3412.2005

Hornitzky, M. A., Vanselow, B. A., Walker, K., Bettelheim, K. A., Corney, B., Gill, P., et al. (2002). Virulence properties and serotypes of Shiga toxin-producing *Escherichia coli* from healthy Australian cattle. *Appl. Eenviron. Microbiol.* 68, 6439–6445. doi: 10.1128/AEM.68.12.6439-6445.2002

Hussein, H. S. (2007). Prevalence and pathogenicity of Shiga toxin-producing *Escherichia coli* in beef cattle and their products. *J. Anim. Sci.* 85, E63–E72. doi: 10.2527/jas.2006-421

Hussein, H. S., and Bollinger, L. M. (2005). Prevalence of Shiga toxin–producing *Escherichia coli* in beef cattle. *J. Food Protect.* 68, 2224–2241. doi: 10.4315/0362-028X-68.10.2224

Iguchi, A., Iyoda, S., Kikuchi, T., Ogura, Y., Katsura, K., Ohnishi, M., et al. (2015a). A complete view of the genetic diversity of the *Escherichia coli* O-antigen biosynthesis gene cluster. *DNA Res.* 22, 101–107. doi: 10.1093/dnares/dsu043

Iguchi, A., Iyoda, S., Seto, K., Morita-Ishihara, T., Scheutz, F., and Ohnishi, M. (2015b). *Escherichia coli* O-Genotyping PCR: a comprehensive and practical platform for molecular O serogrouping. *J. Clin. Microbiol.* 53, 2427–2432. doi: 10.1128/JCM.00321-15

Irino, K., Kato, M. A. M. F., Vaz, T. M. I., Ramos, I. I., Souza, M. A. C., Cruz, A. S., et al. (2005). Serotypes and virulence markers of Shiga toxin-producing *Escherichia coli* (STEC) isolated from dairy cattle in São Paulo State, Brazil. *Vet. Microbiol.* 105, 29–36. doi: 10.1016/j.vetmic.2004.08.007

Jajarmi, M., Imani Fooladi, A. A., Badouei, M. A., and Ahmadi, A. (2017). Virulence genes, Shiga toxin subtypes, major O-serogroups, and phylogenetic background of Shiga toxin-producing *Escherichia coli* strains isolated from cattle in Iran. *Microb. Pathog.* 109, 274–279. doi: 10.1016/j.micpath.2017.05.041

Joensen, K. G., Tetzschner, A. M., Iguchi, A., Aarestrup, F. M., and Scheutz, F. (2015). Rapid and easy *In Silico* serotyping of *Escherichia coli* isolates by use of whole-genome sequencing data. *J. Clin. Microbiol.* 53, 2410–2426. doi: 10.1128/JCM.00008-15

Kaper, J. B., Nataro, J. P., and Mobley, H. L. (2004). Pathogenic *Escherichia coli. Nat. Rev. Microbiol.* 2, 123–140. doi: 10.1038/nrmicro818

Karmali, M. A., Gannon, V., and Sargeant, J. M. (2010). Verocytotoxin-producing *Escherichia coli* (VTEC). *Vet. Microbiol.* 140, 360–370. doi: 10.1016/j.vetmic.2009.04.011

Kido, N., Torgov, V. I., Sugiyama, T., Uchiya, K., Sugihara, H., Komatsu, T., et al. (1995). Expression of the O9 polysaccharide of *Escherichia coli:* sequencing of the *E. coli* O9 rfb gene cluster, characterization of mannosyl transferases, and evidence for an ATP-binding cassette transport system. *J. Bacteriol.* 177, 2178–2187. doi: 10.1128/JB.177.8.2178-2187.1995

Lacher, D. W., Gangiredla, J., Jackson, S. A., Elkins, C. A., and Feng, P. C. H. (2014). Novel Microarray design for molecular serotyping of shiga toxin-producing *Escherichia coli* strains isolated from fresh produce. *Appl. Environ. Microbiol.* 80, 4677–4682. doi: 10.1128/AEM.01049-14

Lee, K., Kusumoto, M., Iwata, T., Iyoda, S., and Akiba, M. (2017). Nationwide investigation of Shiga toxin-producing *Escherichia coli* among cattle in Japan revealed the risk factors and potentially virulent subgroups. *Epidemiol. Infect.* 145, 1557–1566. doi: 10.1017/S0950268817000474

Leomil, L., Aidar-Ugrinovich, L., Guth, B. E. C., Irino, K., Vettorato, M. P., Onuma, D. L., et al. (2003). Frequency of Shiga toxin-producing *Escherichia coli* (STEC) isolates among diarrheic and non-diarrheic calves in Brazil. *Vet. Microbiol.* 97, 103–109. doi: 10.1016/j.vetmic.2003.08.002

Leung, P. H., Yam, W. C., Ng, W. W., and Peiris, J. S. (2001). The prevalence and characterization of verotoxin-producing *Escherichia coli* isolated from cattle and pigs in an abattoir in Hong Kong. *Epidemiol. Infect.* 126, 173–179. doi: 10.1017/S0950268801005210

Levine, M. (1987). *Escherichia coli* that cause diarrhea - enterotoxigenic, enteropathogenic, enteroinvasive, enterohemorrhagic, and enteroadherent. *Am. J. Infect. Dis.* 155, 377–389. doi: 10.1093/infdis/155.3.377

Lin, A., Sultan, O., Lau, H. K., Wong, E., Hartman, G., and Lauzon, C. R. (2011). O serogroup specific real time PCR assays for the detection and identification of nine clinically relevant non-O157 STECs. *Food Microbiol.* 28, 478–483. doi: 10.1016/j.fm.2010.10.007

Liu, D., Cole, R. A., and Reeves, P. R. (1996). An O-antigen processing function for Wzx (RfbX): a promising candidate for O-unit flippase. *J. Bacteriol.* 178, 2102–2107. doi: 10.1128/JB.178.7.2102-2107.1996

Liu, Y., and Fratamico, P. (2006). *Escherichia coli* O antigen typing using DNA microarrays. *Mol. Cell Probes* 20, 239–244. doi: 10.1016/j.mcp.2006.01.001

Luedtke, B. E., Bono, J. L., and Bosilevac, J. M. (2014). Evaluation of real time PCR assays for the detection and enumeration of enterohemorrhagic *Escherichia coli* directly from cattle feces. *J. Microbiol. Methods* 105, 72–79. doi: 10.1016/j.mimet.2014.07.015

Madic, J., Vingadassalon, N., de Garam, C. P., Marault, M., Scheutz, F., Brugere, H., et al. (2011). Detection of Shiga toxin-producing *Escherichia coli* serotypes O26:H11, O103:H2, O111:H8, O145:H28, and O157:H7 in raw-milk cheeses by using multiplex real-time PCR. *Appl. Environ. Microbiol.* 77, 2035–2041. doi: 10.1128/AEM.02089-10

Mainil, J. G., and G., Daube (2005). Verotoxigenic *Escherichia coli* from animals, humans and foods: who's who? *J. Appl. Microbiol.* 98, 1332–1344. doi: 10.1111/j.1365-2672.2005.02653.x

Masana, M. O., D'Astek, B. A., Palladino, P. M., Galli, L., and Del Castillo, L. L., Carbonari, etal. (2011). Genotypic chatcterization of non-O157 Shiga toxin-producing *Escherichia coli* in beef abattoirs of Argentina. *J. Food Prot.* 74, 2008–2017. doi: 10.4315/0362-028X.JFP-11-189

McLean, C., Bettelheim, K. A., Kuzevski, A., Falconer, L., and Djordjevic, S. P. (2005). Isolation of *Escherichia coli* O5:H-, possessing genes for Shiga toxin 1, intimin-beta and enterohaemolysin, from an intestinal biopsy from an adult case of bloody diarrhoea: evidence for two distinct O5:H- pathotypes. *J. Med. Microbiol.* 54(Pt 6), 605–607. doi: 10.1099/jmm.0.45938-0

Meichtri, L., Miliwebsky, E., Gioffre, A., Chinen, I., Baschkier, A., Chillemi, G., et al. (2004). Shiga toxin-producing *Escherichia coli* in healthy young beef steers from Argentina: prevalence and virulence properties. *Int. J. Food Microbiol.* 96, 189–198. doi: 10.1016/j.ijfoodmicro.2004.03.018

Mekata, H., Iguchi, A., Kawano, K., Kirino, Y., Kobayashi, I., and Misawa, N. (2014). Identification of O serotypes, genotypes, and virulotypes of Shiga toxin-producing *Escherichia coli* isolates, including non-O157 from beef cattle in Japan. *J. Food Prot.* 77, 1269–1274. doi: 10.4315/0362-028X.JFP-13-506

Melton-Celsa, A., Mohawk, K., Teel, L., and O'Brien, A. (2012). Pathogenesis of Shiga-toxin producing *Escherichia coli*. *Curr Top Microbiol Immunol.* 357, 67–103. doi: 10.1007/82_2011_176

Mingle, L. A., Garcia, D. L., Root, T. P., Halse, T. A., Quinlan, T. M., Armstrong, L. R., et al. (2012). Enhanced identification and characterization of non-O157 Shiga toxin-producing *Escherichia coli:* a six-year study. *Foodborne Pathog. Dis.* 9, 1028–1036. doi: 10.1089/fpd.2012.1202

Miyao, Y., Kataoka, T., Nomoto, T., Kai, A., Itoh, T., and Itoh, K. (1998). Prevalence of verotoxin-producing *Escherichia coli* harbored in the intestine of cattle in Japan. *Vet. Microbiol.* 61, 137–143. doi: 10.1016/S0378-1135(98)00165-5

Monaghan, A., Byrne, B., Fanning, S., Sweeney, T., McDowell, D., and Bolton, D. J. (2011). Serotypes and virulence profiles of non-O157 Shiga toxin-producing *Escherichia coli* isolates from bovine farms. *Appl. Environ. Microbiol.* 77, 8662–8668. doi: 10.1128/AEM.06190-11

Monday, S. R., Beisaw, A., and Feng, P. C. H. (2007). Identification of Shiga toxigenic *Escherichia coli* seropathotypes A and B by multiplex PCR. *Mol. Cell Probes.* 21, 308–311. doi: 10.1016/j.mcp.2007.02.002

Montenegro, M. A., Bulte, M., Trumpf, T., Aleksic, S., Reuter, G., Bulling, E., et al. (1990). Detection and characterization of fecal verotoxin-producing *Escherichia coli* from healthy cattle. *J. Clin. Microbiol.* 28, 1417–1421. doi: 10.1128/JCM.28.6.1417-1421.1990

Mora, A., Blanco, J., s,.E., Blanco, M., Alonso, M. P., Dhabi, G., et al. (2005). Antimicrobial resistance of Shiga toxin (verotoxin)-producing *Escherichia coli* O157: H7 and non-O157 strains isolated from humans, cattle, sheep and food in Spain. *Res. Microbiol.* 156, 793–806. doi: 10.1016/j.resmic.2005.03.006

Moreira, C. N., Pereira, M. A., Brod, C. S., Rodrigues, D. P., Carvalhal, J. B., and Aleixo, J. A. (2003). Shiga toxin-producing *Escherichia coli* (STEC) isolated from healthy dairy cattle in southern Brazil. *Vet. Microbiol.* 93, 179–183. doi: 10.1016/S0378-1135(03)00041-5

Moxley, R. A., and Smith, D. R. (2010). Attaching and effacing *Escherichia coli* infections in cattle. *Vet. Clin. North Amer. Food Anim.* 26, 29–56. doi: 10.1016/j.cvfa.2009.10.011

Moxley, R. A., Stromberg, Z. R., Lewis, G. L., Loy, J. D., Brodersen, B. W., Patel, I. R., et al. (2015). Haemorrhagic colitis associated with enterohaemorrhagic *Escherichia coli* O165:H25 infection in a yearling feedlot heifer. *J. Microbiol. Mtds Case Rep.* 2, 1–6. doi: 10.1099/jmmcr.0.005004

Muniesa, M., Blanco, J. E., de Simon, M., Serra-Moreno, R., Blanch, A. R., and Jofre, J. (2004). Diversity of *stx*2 converting bacteriophages induced from Shiga-toxin-producing *Escherichia coli* strains isolated from cattle. *Microbiology* 150(Pt 9), 2959–2971. doi: 10.1099/mic.0.27188-0

Nasoff, M. S., Baker, H. V. II., and Wolf, R. E. Jr. (1984). DNA sequence of the *Escherichia coli* gene, gnd, for 6-phosphogluconate dehydrogenase. *Gene* 27, 253–264. doi: 10.1016/0378-1119(84)90070-2

Navarro, A., Cauich-Sanchez, P. I., Trejo, A., Gutierrez, A., Diaz, S. P., Diaz, C. M., et al. (2018). Characterization of diarrheagenic strains of *Escherichia coli* isolated from cattle raised in three regions of Mexico. *Front. Microbiol.* 9:2373. doi: 10.3389/fmicb.2018.02373

Noll, L. W., Shridhar, P. B., Dewsbury, D. M., Shi, X., Cernicchiaro, N., Renter, D. G., et al. (2015a). A comparison of culture- and PCR-based methods to detect six major non-O157 serogroups of Shiga toxin-producing *Escherichia coli* in cattle feces. *PLoS ONE* 10:e0135446. doi: 10.1371/journal.pone.0135446

Noll, L. W., Shridhar, P. B., Shi, X., An, B., Cernicchiaro, N., Renter, D. G., et al. (2015b). A four-plex real-time PCR assay, based on *rfb*E, *stx*1, *stx*2, and *eae* genes, for the detection and quantification of Shiga toxin-producing *Escherichia coli* O157 in cattle feces. *Foodborne Pathog Dis.* 12, 787–794. doi: 10.1089/fpd.2015.1951

Norman, K. N., Clawson, M. L., Strockbine, N. A., Mandrell, R. E., Johnson, R., Ziebell, K., et al. (2015). Comparison of whole genome sequences from human and non-human *Escherichia coli* O26 strains. *Front. Cell Infect. Microbiol.* 5:21. doi: 10.3389/fcimb.2015.00021

Paddock, Z., Shi, X., Bai, J., and Nagaraja, T. G. (2012). Applicability of a multiplex PCR to detect O26, O45, O103, O111, O121, O145, and O157 serogroups of *Escherichia coli* in cattle feces. *Vet. Microbiol.* 156, 381–388. doi: 10.1016/j.vetmic.2011.11.017

Paddock, Z. D., Bai, J., Shi, X., Renter, D. G., and Nagaraja, T. G. (2013). Detection of *Escherichia coli* O104 in the feces of feedlot cattle by a multiplex PCR assay designed to target major genetic traits of the virulent hybrid strain responsible for the 2011 German outbreak. *Appl. Environ. Microbiol.* 79, 3522–3525. doi: 10.1128/AEM.00246-13

Paddock, Z. D., Renter, D. G., Cull, C. A., Shi, X., Bai, J., and Nagaraja, T. G. (2014). *Escherichia coli* O26 in feedlot cattle: fecal prevalence, isolation, characterization, and effects of an *E. coli* O157 vaccine and a direct-fed microbial. *Foodborne Pathog. Dis.* 11, 186–193. doi: 10.1089/fpd.2013.1659

Paquette, S.-J., Stanford, K., Thomas, J., and Reuter, T. (2018). Quantitative surveillance of shiga toxins 1 and 2, *Escherichia coli* O178 and O157 in feces of western-Canadian slaughter cattle enumerated by droplet digital PCR with a focus on seasonality and slaughterhouse location. *PLoS ONE* 13:e0195880. doi: 10.1371/journal.pone.0195880

Parma, A. E., Sanz, M. E., Blanco, J. E., Blanco, J., Vinas, M. R., Blanco, M., et al. (2000). Virulence genotypes and serotypes of verotoxigenic *Escherichia coli* isolated from cattle and foods in Argentina. Importance in public health. *Eur. J. Epidemiol.* 16, 757–762. doi: 10.1023/A:1026746016896

Peng, Z., Liang, W., Hu, Z., Li, X., Guo, R., Hua, L., et al. (2019). O-serogroups, virulence genes, antimicrobial susceptibility, and MLST genotypes of Shiga toxin-producing *Escherichia coli* from swine and cattle in Central China. *BMC Veterinary Res.* 15, 427–427. doi: 10.1186/s12917-019-2177-1

Perelle, S., Dilasser, F., Grout, J., and Fach, P. (2004). Detection by 5'-nuclease PCR of Shiga-toxin producing Escherichia coli O26, O55, O91, O103, O111, O113, O145 and O157:H7, associated with the world's most frequent clinical cases. *Mol. Cell. Probes* 18, 185–192. doi: 10.1016/j.mcp.2003.12.004

Polifroni, R., Etcheverría, A. I., Sanz, M. E., Cepeda, R. E., Krüger, A., Lucchesi, P. M., et al. (2012). Molecular characterization of Shiga toxin-producing *Escherichia coli* isolated from the environment of a dairy farm. *Curr. Microbiol.* 3, 337–343. doi: 10.1007/s00284-012-0161-0

Pradel, N., Livrelli, V., De Champs, C., Palcoux, J. B., Reynaud, A., Scheutz, F., et al. (2000). Prevalence and characterization of Shiga toxin-producing *Escherichia coli* isolated from cattle, food, and children during a one-year prospective study in France. *J. Clin. Microbiol.* 38, 1023–1031. doi: 10.1128/JCM.38.3.1023-1031.2000

Renter, D. G., Morris, J. G., Sargeant, J. M., Hungerford, L. L., Berezowski, J., Ngo, T., et al. (2005). Prevalence, risk factors, O serogroups, and virulence profiles of Shiga toxin-producing bacteria from cattle production environments. *J. Food Prot.* 68, 1556–1565. doi: 10.4315/0362-028X-68.8.1556

Samuel, G., and Reeves, P. (2003). Biosynthesis of O-antigens: genes and pathways involved in nucleotide sugar precursor synthesis and O-antigen assembly. *Carbohydr. Res.* 338, 2503–2519. doi: 10.1016/j.carres.2003.07.009

Sanchez, S., Llorente, M. T., Echeita, M. A., and Herrera-Leon, S. (2015). Development of three multiplex PCR assays targeting the 21 most clinically relevant serogroups associated with Shiga toxin-producing *E. coli* infection in humans. *PLoS ONE* 10:e0117660. doi: 10.1371/journal.pone.0117660

Sandhu, K. S., Clarke, R. C., and Gyles, C. L. (1999). Virulence markers in Shiga toxin-producing *Escherichia coli* isolated from cattle. *Can. J. Vet. Res.* 63, 177–184.

Sandhu, K. S., Clarke, R. C., McFadden, K., Brouwer, A., Louie, M., Wilson, J., et al. (1996). Prevalence of the *eaeA* gene in verotoxigenic *Escherichia coli* strains from dairy cattle in Southwest Ontario. *Epidemiol. Infect.* 116, 1–7. doi: 10.1017/S095026880005888X

Scallan, E., Hoekstra, R. M., Angulo, F. J., Tauxe, R. V., Widdowson, M.-A., and Roy, S. L. (2011). Foodborne illness acquired in the United States—major pathogens. *Emerg. Infect. Dis.* 17, 7–15. doi: 10.3201/eid1701.P11101

Schurman, R. D., Hariharan, H., Heaney, S. B., and Rahn, K. (2000). Prevalence and characteristics of Shiga toxin-producing *Escherichia coli* in beef cattle slaughtered on Prince Edward Island. *J. Food Prot.* 63, 1583–1586. doi: 10.4315/0362-028X-63.11.1583

Scott, L., McGee, P., Walsh, C., Fanning, S., Sweeney, T., Blanco, J., et al. (2009). Detection of numerous verotoxigenic *E. coli* serotypes, with multiple antibiotic resistance from cattle faeces and soil. *Vet. Microbiol.* 134, 288–293. doi: 10.1016/j.vetmic.2008.08.008

Shridhar, P. B., Noll, L. W., Shi, X., An, B., Cernicchiaro, N., Renter, D. G., et al. (2016a). Multiplex quantitative PCR assays for the detection and quantification of the six major non-O157 *Escherichia coli* serogroups in cattle feces. *J. Food Prot.* 79, 66–74. doi: 10.4315/0362-028X.JFP-15-319

Shridhar, P. B., Noll, L. W., Shi, X., Cernicchiaro, N., Renter, D. G., Bai, J., et al. (2016b). *Escherichia coli* O104 in feedlot cattle feces: prevalence, isolation and characterization. *PLoS ONE* 11:e0152101. doi: 10.1371/journal.pone.0152101

Shridhar, P. B., Siepker, C., Noll, L. W., Shi, X., Nagaraja, T. G., and Bai, J. (2017). Shiha toxin subtypes of non-O157 *Escherichia coli* serogroups isolated from cattle feces. *Front. Cell. Infect. Microbiol.* 7:121. doi: 10.3389/fcimb.2017.00121

Smith, H. R., Scotland, S. M., Willshaw, G. A., Wray, C., McLaren, I. M., Cheasty, T., et al. (1988). Vero cytotoxin production and presence of VT genes in *Escherichia coli* strains of animal origin. *Microbiology* 134, 829–834. doi: 10.1099/00221287-134-3-829

Stromberg, Z. R., Lewis, G. L., Schneider, L. G., Erickson, G. E., Patel, I. R., Smith, D. R., et al. (2018). Culture-based quantification with molecular characterization of non-O157 and O157 enterohemorrhagic *Escherichia coli* isolates from rectoanal mucosal swabs of feedlot cattle. *Foodborne Pathog. Dis.* 15, 26–32. doi: 10.1089/fpd.2017.2326

Suthienkul, O., Brown, J. E., Seriwatana, J., Tienthongdee, S., Sastravaha, S., and Echeverria, P. (1990). Shiga-like-toxin-producing *Escherichia coli* in retail meats and cattle in Thailand. *Appl. Environ. Microbiol.* 56, 1135–1139. doi: 10.1128/AEM.56.4.1135-1139.1990

Tanaro, J. D., Galli, L., Lound, L. H., Leotta, G. A., Piaggio, M. C., Carbonari, C. C., et al. (2012). Non-O157:H7 Shiga toxin-producing Escherichia coli in bovine rectums and surface water streams on a beef cattle farm in Argentina. *Foodborne Pathog Dis.* 9, 878–884. doi: 10.1089/fpd.2012.1182

Timm, C. D., Irino, K., Gomes, T. A. T., Viera, M. M., Guth, B. E. C., Vaz, T. M. I., et al. (2007). Virulence markers and serotypes of Shiga toxin-producing *Escherichia coli* isolated from cattle in Rio Grande do Sul, Brazil. *Lett. Appl. Microbiol.* 44, 419–425. doi: 10.1111/j.1472-765X.2006.02085.x

Urdahl, A. M., Beutin, L., Skjerve, E., Zimmermann, S., and Wasteson, Y. (2003). Animal host associated differences in Shiga toxin-producing *Escherichia coli* isolated from sheep and cattle on the same farm. *J. Appl. Microbiol.* 95, 92–101. doi: 10.1046/j.1365-2672.2003.01964.x

Valilis, E., Ramsey, A., Sidiq, S., and DuPont, H. L. (2018). Non-O157 Shiga toxin-producing *Escherichia coli*-A poorly appreciated enteric pathogen: systematic review. *Int. J. Infect. Dis.* 76, 82–87. doi: 10.1016/j.ijid.2018.09.002

Wells, J. G., Shipman, L. D., Greene, K. D., Sowers, E. G., Green, J. H., Cameron, D. N., et al. (1991). Isolation of *Escherichia coli* serotype O157:H7 and other Shiga-like-toxin-producing *E. coli* from dairy cattle. *J. Clin. Microbiol.* 29, 985–989. doi: 10.1128/JCM.29.5.985-989.1991

Wieler, L., Vieler, E., Erpenstein, C., Schlapp, T., Steinruck, H., Bauerfeind, R., et al. (1996). Shiga toxin-producing *Escherichia coli* strains from bovines: association of adhesion with carriage of *eae* and other genes. *J. Clin. Microbiol.* 34, 2980–2984. doi: 10.1128/JCM.34.12.2980-2984.1996

Wieler, L. H., Schwanitz, A., Vieler, E., Busse, B., Steinrück, H., Kaper, J. B., et al. (1998). Virulence properties of Shiga toxin-producing *Escherichia coli* (STEC) strains of serogroup O118, a major group of STEC pathogens in calves. *J. Clin. Microbiol.* 36, 1604–1607. doi: 10.1128/JCM.36.6.1604-1607.1998

Wilson, J. B., McEwen, S. A., Clarke, R. C., Leslie, K. E., Wilson, R. A., Waltner-Toews, D., et al. (1992). Distribution and characteristics of verocytotoxigenic *Escherichia coli* isolated from Ontario dairy cattle. *Epidemiol. Infect.* 108, 423–439. doi: 10.1017/S0950268800049931

Wray, C., McLaren, I. M., and Carroll, P. J. (1993). *Escherichia coli* isolated from farm animals in England and Wales between 1986 and 1991. *Vet. Rec.* 133, 439–442. doi: 10.1136/vr.133.18.439

Zweifel, C., Schumacher, S., Blanco, M., Blanco, J. E., Tasara, T., Blanco, J., et al. (2005). Phenotypic and genotypic characteristics of non-O157 Shiga toxin-producing *Escherichia coli* (STEC) from Swiss cattle. *Vet. Microbiol.* 105, 37–45. doi: 10.1016/j.vetmic.2004.10.007

Conflict of Interest: The authors declare that the research was conducted in the absence of any commercial or financial relationships that could be construed as a potential conflict of interest.

frontiers in Cellular and Infection Microbiology

MINI REVIEW
published: 21 August 2020
doi: 10.3389/fcimb.2020.00381

Siderophore-Microcins in *Escherichia coli*: Determinants of Digestive Colonization, the First Step Toward Virulence

Clémence Massip [1,2]* *and Eric Oswald* [1,2]*

[1] IRSD, Université de Toulouse, INSERM, INRA, ENVT, UPS, Toulouse, France, [2] Service de Bactériologie-Hygiène, Hôpital Purpan, CHU de Toulouse, Toulouse, France

Siderophore-microcins are antimicrobial peptides produced by enterobacteria, especially *Escherichia coli* and *Klebsiella pneumoniae* strains. The antibiotic peptide is post-translationally modified by the linkage of a siderophore moiety. Therefore, it can enter and kill phylogenetically related bacteria by a "Trojan Horse" stratagem, by mimicking the iron–siderophore complexes. Consequently, these antimicrobial peptides are key determinants of bacterial competition within the intestinal niche, which is the reservoir for pathogenic *E. coli.* The most frequent extraintestinal infections caused by *E. coli* are urinary tract infections. Uropathogenic *E. coli* (UPEC) can produce many virulence factors, including siderophore-microcins. Siderophore-microcins are chromosomally encoded by small genomic islands that exhibit conserved organization. In UPEC, the siderophore-microcin gene clusters and biosynthetic pathways differ from the "archetypal" models described in fecal strains. The gene cluster is shorter. Thus, active siderophore-microcin production requires proteins from two other genomic islands that also code for virulence factors. This functional and modular synergy confers a strong selective advantage for the domination of the colonic niche, which is the first step toward infection. This optimization of genetic resources might favor the selection of additional virulence factors, which are essential in the subsequent steps of pathogenesis in *E. coli* infection.

Keywords: microcins, *Escherichia coli*, ExPEC, UPEC, genomic island (GI), intestinal colonization, pathogenesis, B2 phylogroup

OPEN ACCESS

Edited by:
Mauricio J. Farfan, University of Chile, Chile

Reviewed by:
Arun K. Bhunia, Purdue University, United States
Xingmin Sun, University of South Florida, United States

***Correspondence:**
Clémence Massip
massip.c@chu-toulouse.fr
Eric Oswald
eric.oswald@inserm.fr

Specialty section:
This article was submitted to Bacteria and Host, a section of the journal Frontiers in Cellular and Infection Microbiology

Received: *01 April 2020*
Accepted: *22 June 2020*
Published: *21 August 2020*

Citation:
Massip C and Oswald E (2020) Siderophore-Microcins in Escherichia coli: Determinants of Digestive Colonization, the First Step Toward Virulence. Front. Cell. Infect. Microbiol. 10:381. doi: 10.3389/fcimb.2020.00381

INTRODUCTION

Escherichia coli lives as a commensal in the gut of warm-blooded animals (Tenaillon et al., 2010). It is also a major pathogen that causes intestinal and extraintestinal diseases, such as neonatal meningitis, nosocomial pneumonia, and bacteremia (Johnson and Russo, 2002; Kaper et al., 2004). The most common extraintestinal *E. coli* infections are urinary tract infections (UTIs) caused by uropathogenic *E. coli* (UPEC; Kaper et al., 2004; Flores-Mireles et al., 2015). UTIs are a serious public health issue in terms of morbidity, mortality, selection of antibiotic-resistant bacteria, and health care costs (Flores-Mireles et al., 2015).

E. coli strains are divided into eight phylogroups: A, B1, B2, C, D, E, F, and G (Tenaillon et al., 2010; Chaudhuri and Henderson, 2012; Clermont et al., 2019). Most extraintestinal pathogenic *E. coli*, including UPEC, belong to the *E. coli* phylogenetic group B2 (Picard et al., 1999; Johnson and Russo, 2002; Jaureguy et al., 2008; Tourret and Denamur, 2016). The reservoir of UPEC is gut microbiota, and *E. coli* from the B2 phylogroup are now the most frequently recovered in human fecal samples in industrialized countries (Touchon et al., 2009; Tenaillon et al., 2010). They produce more virulence factors than strains from other phylogroups (Picard et al., 1999), especially siderophore-microcins (Mcc; Budič et al., 2011; Micenková et al., 2016; Massip et al., 2020).

Mcc are antimicrobial peptides with a molecular mass below 10 kDa, produced by enterobacteria (Asensio et al., 1976; Pons et al., 2002). Siderophore-Mcc constitute a subclass of Mcc characterized by their molecular masses (between 5 and 10 kDa) and their post-translational modifications. They are post-translationally linked with a siderophore moiety derived from enterobactin (Azpiroz and Laviña, 2004; Thomas et al., 2004). Enterobactin is an iron uptake system produced by a non-ribosomal peptide synthetase (NRPS) pathway (for reviews, see Fischbach et al., 2006; Miethke and Marahiel, 2007).

Four siderophore-Mcc have been described so far: MccE492, MccH47, MccI47, and MccM. MccE492 is produced by *Klebsiella pneumoniae* and was first described in human fecal strain RYC492 (de Lorenzo and Pugsley, 1985). MccH47 was initially studied in human fecal strain *E. coli* H47 (Laviña et al., 1990). Like MccM, it is synthesized by *E. coli* fecal strains Nissle 1917, CA46, and CA58 (Davies and Reeves, 1975; Patzer, 2003; Vassiliadis et al., 2010) but also by many UPEC strains (Azpiroz et al., 2009; Šmajs et al., 2010; Abraham et al., 2012; Massip et al., 2020). MccI47 has only been mentioned in one study that focuses on the genetic systems that encode Mcc in *E. coli* strains H47 and CA46 (Poey et al., 2006).

In this review, we provide an overview of the current knowledge concerning siderophore-Mcc genetic systems and biosynthesis, their mechanisms of action, and their biological relevance in *E. coli*.

SIDEROPHORE-Mcc GENE CLUSTERS, SMALL GENOMIC ISLANDS

The overall organization of siderophore-Mcc gene clusters is conserved. The G+C contents of siderophore-Mcc gene clusters are significantly lower (from 33 to 43%) than those of their host *E. coli* (51%) or *K. pneumoniae* (57.5%), which indicates that they might have been acquired from different bacteria by horizontal transfer (Duquesne et al., 2007). Moreover, siderophore-Mcc gene clusters are generally flanked by direct repeats described as acting as attachment sites in genomic islands (Azpiroz et al., 2011). Genomic islands are mobile genetic elements that help in the adaptation to a given environment. They contribute to the evolution of bacteria and undergo repeated rearrangements, deletions, and insertions (Dobrindt et al., 2010). Azpiroz et al. (2011) demonstrated that the MccH47 genetic system can be mobilized by site-specific recombination. Therefore, it was suggested that the siderophore-Mcc gene cluster is a small genomic island (Azpiroz et al., 2011).

Genes responsible for siderophore-Mcc biosynthesis and export are gathered in large clusters (up to 13 kb) on the bacterial chromosome (**Figure 1**). The minimal structure comprises the gene that encodes the Mcc precursor peptide and the self-immunity gene, which are grouped in an operon, and genes responsible for the export of the siderophore-Mcc. Genes *mceA*, *mchB*, *mchS2*, and *mcmA* encode precursor peptides of 103, 75, 77, and 92 amino acids for MccE492, MccH47, MccI47, and MccM, respectively (Gaggero et al., 1993; Lagos et al., 2001; Poey et al., 2006; Duquesne et al., 2007). The mechanism of self-immunity to siderophore-Mcc remains largely elusive. MccE492, MccH47, MccI47, and MccM have specific self-immunity proteins. Studies of their sequence indicate that they are probably membrane-bound, with two or three transmembrane helices (Rodríguez et al., 1999; Lagos et al., 2001; Duquesne et al., 2007).

In general, the siderophore-Mcc gene cluster also bears genes that encode post-translational modifications enzymes (Poey et al., 2006; Duquesne et al., 2007). When several siderophore-Mcc are encoded by a single gene cluster (e.g., MccH47 and MccM in *E. coli* Nissle), genes responsible for post-translational modifications and export can be shared (Poey et al., 2006). Genes involved in post-translational modifications *mceC*, *mchA*, and *mcmL* are homologous to *iroB* encoding a glycosyltransferase from the salmochelin genetic system *iroA* (Lagos et al., 2001; Patzer, 2003). Salmochelins are siderophores derived from enterobactin through glycosylation (Fischbach et al., 2006). Similarly, *mceD*, *mchS1*, and *mcmK* are homologous to *iroD* encoding an enterobactin esterase (Lagos et al., 2001; Patzer, 2003). Proteins MceI, MceJ, and their homologs MchC, MchD link the Mcc precursor peptides with the siderophore moiety derived from enterobactin, but the precise function of these proteins remains unknown (Nolan and Walsh, 2008).

Siderophore-Mcc are transported outside the producing bacteria by a three-component ATP-binding cassette (ABC) exporter. Two components are encoded as an operon on the Mcc gene cluster: the ABC transporter protein (MchF for MccH47 and MccM, MceG for MccE492) and the accessory protein of the membrane fusion protein (MFP) family (MchE for MccH47 and MccM, MceH for MccE492). These proteins are highly similar with 92 and 94% identical amino acids between the two types of ABC and MFP proteins, respectively. The third component of this export system is the outer membrane protein TolC (Azpiroz et al., 2001; Lagos et al., 2001; Patzer, 2003).

Although the general organization of the siderophore-Mcc island is conserved, substantial differences can be found between strains. Traces of recombination events can be detected at the center of siderophore-Mcc gene clusters. In *E. coli* strain CA58, genes encoding transposases are inserted between genes *mchS2* and *mchS3* encoding MccI47 precursor and immunity peptides. Since these two genes are normally organized in an operon, the translation process is compromised, at least for *mchS2*, which is downstream of the insertion sequence. Consequently, unlike strain CA46, *E. coli* CA58 does not produce MccI47 (Patzer, 2003; Poey et al., 2006; Vassiliadis et al., 2010).

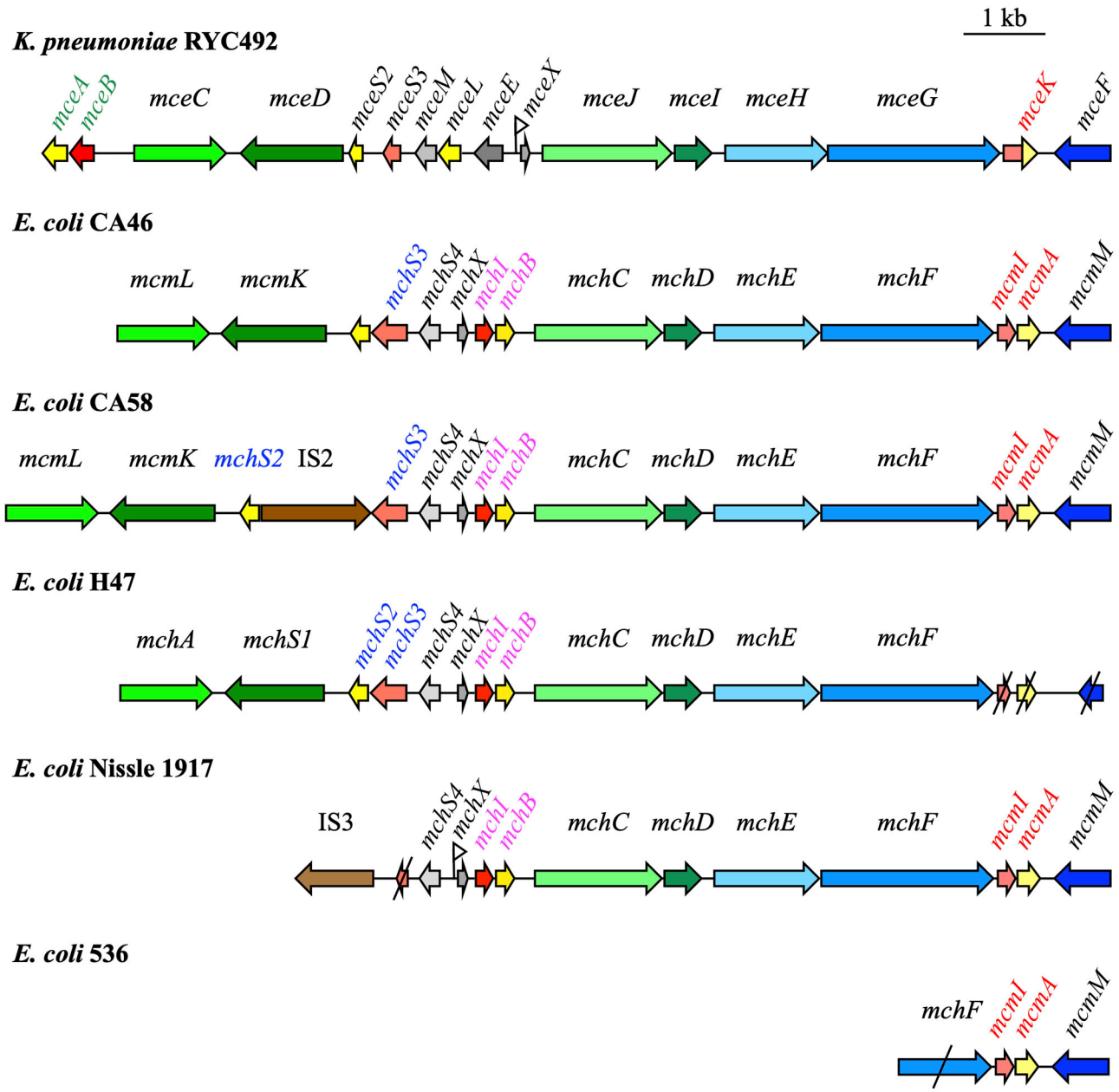

FIGURE 1 | Microcin (Mcc) gene clusters in *Klebsiella pneumoniae* RYC492, *Escherichia coli* CA46, CA58, H47, Nissle 1917, and 536 [modified from Massip et al. (2019)]. Mcc precursor genes, immunity genes, and genes involved in Mcc export and post-translational modifications are indicated in yellow, red, blue, and green, respectively. Truncated genes are shown with slashes. The names of the genes specifically involved in MccE492, MccM, MccH47, and MccI47 are in green, red, pink, and blue, respectively. Fur boxes proved important in the regulation of Mcc production are marked by a small flag.

In UPEC strain 536, the siderophore-Mcc island has undergone considerable changes if strain CA46 is considered as a reference. Only four genes remain: genes encoding MccM precursor and immunity peptides, and two genes involved in Mcc export, *mcmM* and *mchF*, which are truncated. In the absence of a functional export system (association between ABC and MFP proteins), strain 536 might not be able to secrete siderophore-Mcc.

Finally, in *E. coli* Nissle and in the UPEC strains CFT073 and ABU83972, the island is truncated in the 5′ region. Compared to the strain CA46 island, it is deprived of the MccI47 precursor peptide and self-immunity genes, as well as post-translational modification genes *mcmL* and *mcmK* (Patzer, 2003; Poey et al., 2006). In strains bearing such a truncated island, genes encoding transposases flank the 5′ region as remnants of recombination events (Patzer, 2003). In the three *E. coli* strains Nissle, CFT073,

and ABU83972, the truncated Mcc gene cluster is located on the genomic island I that covers the *serX* tRNA locus [for reviews, see Dobrindt et al. (2004, 2010)]. This genomic island also carries the *iroA* locus with the *mcmL* and *mcmK* homologs *iroB* and *iroD*. It is highly conserved in the three strains and in the Mcc gene cluster in particular, with 100% similarity (Grozdanov et al., 2004; Vejborg et al., 2010; Reister et al., 2014). Therefore, Poey et al. (2006) suggested considering the siderophore-Mcc gene cluster as "an islet inside an island." It provides a selective advantage, is acquired by horizontal transfer, and can undergo significant rearrangements.

BIOSYNTHESIS OF SIDEROPHORE-Mcc AND MODE OF ACTION

Siderophore-Mcc biosynthesis begins with the production of two separate moieties: (1) a precursor peptide encoded by the Mcc island and (2) enterobactin by an NRPS pathway (**Figure 2A**). Glycosyltransferases MceC, MchA, or McmL catalyze the transfer of one glucose to the 2,3-dihydroxybenzoic acid moieties of enterobactin (Nolan et al., 2007; Vassiliadis et al., 2007). In fact, unlike its homolog IroB, the catalytic efficiency of MceC decreases with enterobactin glycosylation (Nolan et al., 2007). MceIJ or their homolog MchCD then links the C-glycosylated enterobactin to the serine and glycine-rich C-terminal region of the precursor peptide (Nolan and Walsh, 2008; Vassiliadis et al., 2010). The enterobactin esterase MceD, MchS1, or McmK hydrolyzes the C-glycosylated enterobactin into a glycosylated linear trimer of 2,3-dihydroxybenzoyl-serine (Nolan et al., 2007; Vassiliadis et al., 2007). Alternatively, the glycosylated enterobactin could be linearized prior to its linkage to the precursor peptide. None of these pathways could be excluded in *in vitro* MccE492 synthesis experiments. MceIJ complex catalyzes the attachment of glycosylated enterobactin, whether or not it is linearized, and MceD can hydrolyze glycosylated enterobactin whether or not it is linked to the precursor peptide (Nolan et al., 2007; Nolan and Walsh, 2008). Enterobactin glycosylation is catalyzed before linearization, because the catalytic efficiency of MceC decreases with the linearization of the enterobactin scaffold (Nolan et al., 2007).

The last step of the siderophore-Mcc maturation process is concomitant with export. Siderophore-Mcc precursors carry an N-terminal leader peptide of 15–19 amino acids, which probably acts as a recognition signal for the ABC transporter (MceG or MchF; Pons et al., 2002; Vassiliadis et al., 2010). The ABC transporter N-terminal domain with a protease activity cleaves the leader peptide during export (Azpiroz et al., 2001; Vassiliadis et al., 2010). The precise role of the accessory protein (MceH or MchE) has not been examined. However, it may act as a connector between the ABC transporter and the outer membrane protein TolC (Pons et al., 2002; Duquesne et al., 2007).

In strains such as *E. coli* Nissle, deprived of *mcmL* and *mcmK*, the siderophore-Mcc synthesis pathway is slightly different (**Figure 2B**). The enterobactin moiety is glycosylated by IroB from the salmochelin pathway instead of the missing McmL. Moreover, the periplasmic protein ClbP involved in colibactin synthesis (Nougayrède et al., 2006) is essential for MccH47 and MccM production (Massip et al., 2019). Even if the exact production pathway in such strains has not been elucidated, the C-terminal domain of ClbP has been suggested to facilitate the export of MccH47 and MccM, in which enterobactin moiety would not be linearized in the absence of the esterase McmK (Massip et al., 2019).

Siderophore-Mcc were labeled "Trojan Horse" toxins because they enter target bacteria by the catecholate siderophore receptors FepA, Fiu, or Cir (**Figure 3**), thanks to their post-translational modification with an enterobactin moiety (Patzer, 2003; Thomas et al., 2004; Vassiliadis et al., 2010). Consequently, they target enterobacteria that are phylogenetically similar and can be competitors for space and resources in a given niche. Once recognized by siderophore receptors, siderophore-Mcc are translocated through the outer membrane using the energy produced by the TonB machinery (Destoumieux-Garzón et al., 2003). Once in the periplasm, MccE492 interacts with the ManY/ManZ inner-membrane components of the mannose permease. It triggers channel or pore formation and TonB-dependent inner-membrane depolarization, followed by cell death (Bieler et al., 2006). MccH47 has a different cellular target: the ATP synthase (Trujillo et al., 2001). To be more precise, the F_0 proton channel is required for MccH47 activity. MccH47 provokes an unregulated entry of protons, which dissipates the membrane potential (Rodriguez and Lavina, 2003). The mechanism of action of MccM has never been established, but it is suspected to be the same as that of MccH47.

Siderophore-Mcc production is highly regulated by iron concentration through the ferric uptake regulator (Fur) protein (Patzer, 2003; Vassiliadis et al., 2007). This protein acts as a transcriptional repressor and senses intracellular iron availability (Bagg and Neilands, 1987). Fur boxes are located upstream of *mceX* and *mchX* genes (Patzer, 2003; Vassiliadis et al., 2007). At high iron availability, Fur–Fe^{2+} complexes repress *mceX*, in which transcription is coupled with *mceIJ* genes. Therefore, MceIJ cannot catalyze the attachment of the enterobactin moiety with the MccE492 precursor. Moreover, MceX acts as a negative regulator of *mceA* and *mceB* genes. Therefore, a high iron concentration allows a high expression of the MccE492 precursor, leading to a predominant synthesis of unmodified Mcc (Marcoleta et al., 2018). This form has a low antibacterial activity because it is not recognized by siderophore receptors (Thomas et al., 2004).

IMPACTS OF SIDEROPHORE-Mcc PRODUCED BY *E. coli*

E. coli causes various extraintestinal infections, of which UTIs are the most frequent. *E. coli* is also a frequent cause of neonatal meningitis, bacteremia, and nosocomial infections such as nosocomial pneumonia (Johnson and Russo, 2002; Kaper et al., 2004). The patient's own intestinal flora is the reservoir for these so-called extraintestinal pathogenic *E. coli* (Russo and Johnson, 2000; Starčič Erjavec and Žgur-Bertok, 2015), especially for UPEC (Yamamoto et al., 1997; Moreno et al., 2008). A

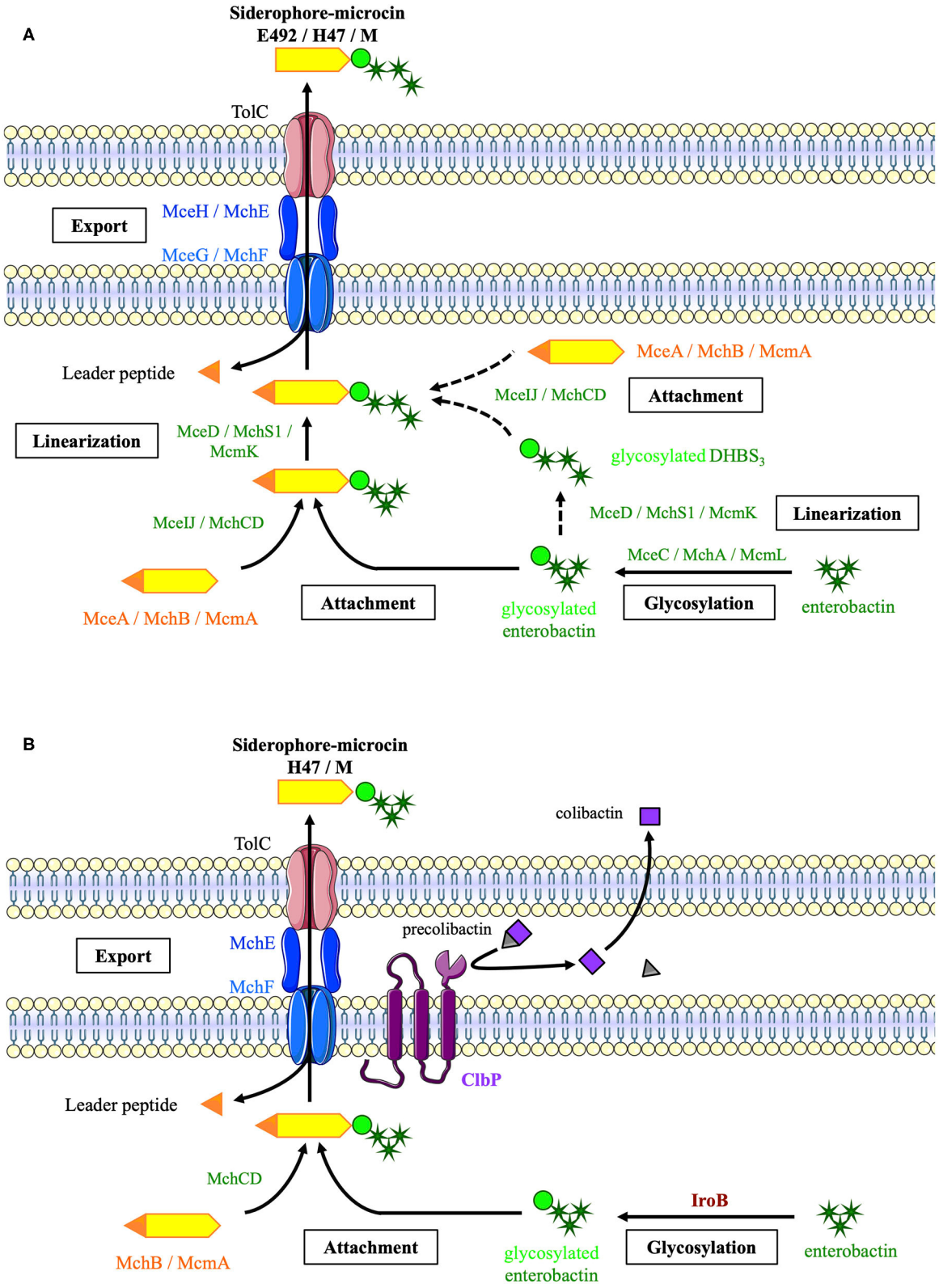

FIGURE 2 | Biosynthetic pathways of siderophore-microcins (Mcc) **(A)** in strains carrying an "archetypal Mcc gene cluster" with genes encoding the enterobactin esterase and glycosyltransferase **(B)** in *E. coli* strains from the B2 phylogroup carrying a "truncated Mcc gene cluster." This biosynthesis requires the glycosyltransferase IroB encoded by the salmochelin gene cluster and the ClbP protein encoded by the *pks* island, which are indicated in brown and purple, respectively [adapted from Massip et al. (2019)]. Mcc precursor peptides and proteins involved in Mcc export and post-translational modifications are indicated in orange, blue, and green, respectively.

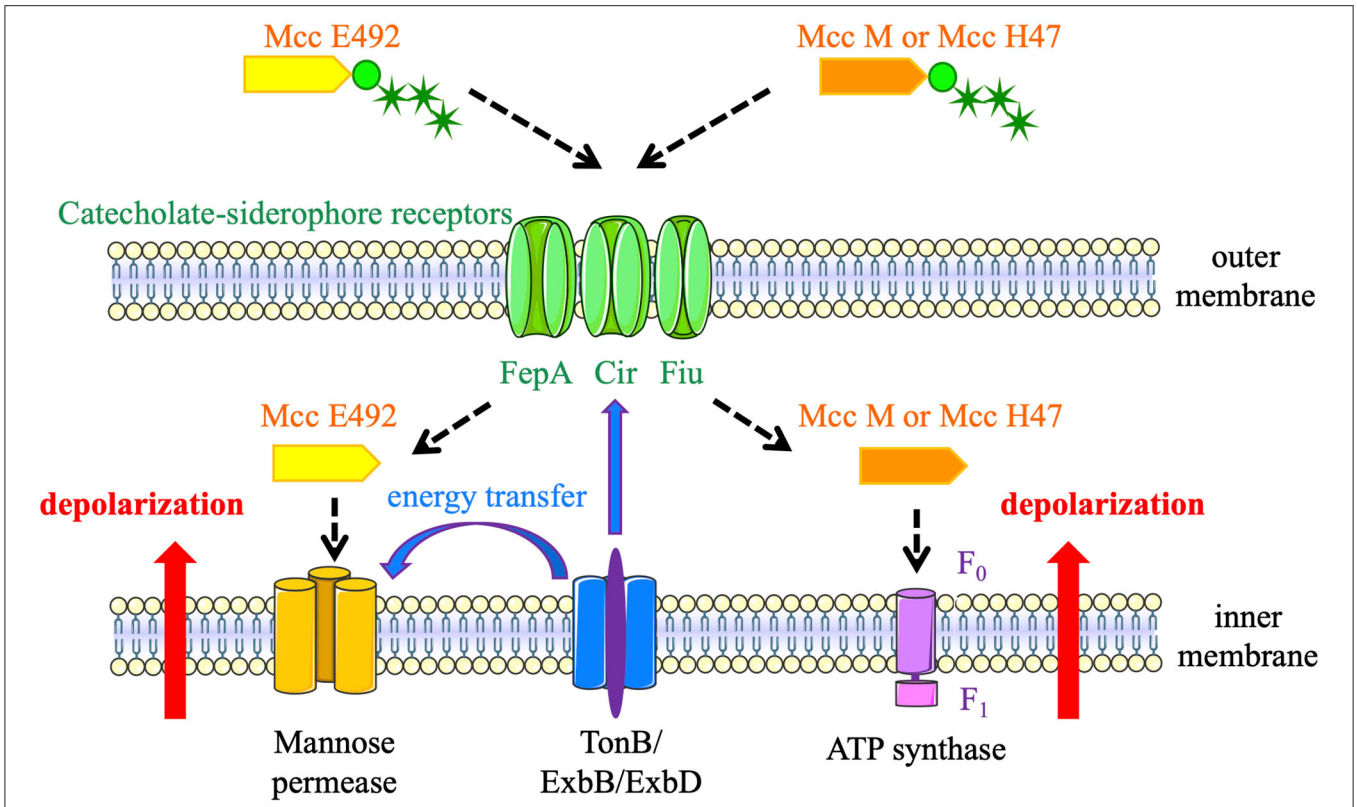

FIGURE 3 | Siderophore-microcins (Mcc) mechanisms of action. MccE492, MccH47, and MccM enter target bacteria by catecholate siderophore receptors (FepA, Fiu, or Cir). MccE492 interacts with the mannose permease, whereas MccH47 and MccM target the F_0 proton channel of the ATP synthase. These interactions trigger inner-membrane depolarization and cell death. The energy produced by the TonB machinery is required for translocation of the three siderophore-Mcc and the formation of channels or pores by MccE492 linkage with the mannose permease.

UPEC strain residing in the gut emerges from the rectal flora, colonizes the perineal region and the urethra, and then migrates to the bladder (Flores-Mireles et al., 2015). Therefore, effective intestinal colonization is a prerequisite for UTI development.

In industrialized countries, most human fecal strains belong to the B2 phylogroup, whereas most strains from Africa, Asia, or South America belong to the A phylogroup (Gordon and O'Brien, 2006; Tenaillon et al., 2010). The differences in phylogroup distribution are probably linked to socioeconomic factors, such as dietary and hygiene habits, which condition the gut microbiota (Tenaillon et al., 2010). A 1-year study in which the fecal strains of Swedish infants were monitored revealed that *E. coli* from the B2 phylogroup had a capacity for enhanced persistence in their intestinal microflora (Nowrouzian et al., 2005). Studies of fecal *E. coli* in Australia and the Czech Republic revealed that MccH47- and MccM-producing strains are overrepresented in the B2 phylogroup (Gordon and O'Brien, 2006; Micenková et al., 2016). Since *E. coli* siderophore-Mcc target phylogenetically related *Enterobacteriaceae*, they probably confer a selective advantage in the intestinal niche.

The proportion of B2 phylogroup strains seems to be higher in UPEC than in fecal strains: 72 and 69% in UPEC (Abraham et al., 2012; Massip et al., 2020), and 45 and 30% in fecal strains (Tenaillon et al., 2010) in Australia and France, respectively. Similarly, siderophore-Mcc-producing strains represent ∼30% of UPEC (Šmajs et al., 2010; Abraham et al., 2012; Massip et al., 2020), compared to ∼15% of fecal strains (Gordon and O'Brien, 2006; Micenková et al., 2016). Like in fecal *E. coli*, there are significantly more UPEC strains carrying siderophore-Mcc genes among B2 phylogroup strains than among non-B2 strains (Azpiroz et al., 2009; Abraham et al., 2012; Massip et al., 2020).

Most UPEC strains that produce siderophore-Mcc carry a "truncated" Mcc gene cluster deprived of genes *mcmL* and *mcmK*. Besides very rare exceptions, they also bear the *pks* and salmochelin islands (Azpiroz et al., 2009; Massip et al., 2020), which correspond with the functional synergy recently demonstrated between these three gene clusters used to synthetize MccH47 and MccM (Massip et al., 2019). The triple combination of "truncated" Mcc gene cluster, *pks*, and salmochelin islands enables the production of at least five virulence factors in addition to Mcc: the siderophores enterobactin, salmochelins, and yersiniabactin (Martin et al., 2013), colibactin (Nougayrède et al., 2006), and analgesic lipopeptides (Pérez-Berezo et al., 2017). The versatility of these three genomic islands leads to "genomic economy." At least three pleiotropic proteins are encoded by this triad: IroB, which intervenes in Mcc and salmochelins syntheses (Fischbach et al., 2005; Massip et al., 2019); ClbA, which triggers colibactin,

analgesic lipopeptide, and enterobactin production (Nougayrède et al., 2006; Martin et al., 2013; Pérez-Berezo et al., 2017); and ClbP, which is involved in Mcc and colibactin pathways (Dubois et al., 2011; Massip et al., 2019). Therefore, this type of *E. coli* strain can adapt to various environments with a limited impact on genome size. They persist and emerge from the polymicrobial intestinal niche, adapt to a nutrient-poor environment, and evade the host defense system.

Although this triple combination is frequent among UPEC, it is not correlated with the clinical severity of the infection (Abraham et al., 2012; Massip et al., 2020). Thus, it might not be a virulence factor *per se* within the urinary tract. However, a transcriptional analysis of the pyelonephritis strain CFT073 grown in urine revealed that *mchB* and *iroB* are among the 50 most upregulated genes (Snyder et al., 2004). A similar study performed with the asymptomatic bacteriuria strain ABU83972 and the probiotic strain Nissle, in addition to CFT073, showed that microcin, colibactin, and salmochelin genes are induced when the strains are grown in urine (Hancock et al., 2010). Considering that MccH47 and MccM are the most frequent Mcc in UPEC (Šmajs et al., 2010; Abraham et al., 2012), it suggests that the synergistic triad between microcin, colibactin, and salmochelin islands could promote urinary tract colonization (Massip et al., 2020). This hypothesis is supported by a study that compared the whole genome sequences of UTI and fecal isolates from the same patients. The microcin M activity protein (McmM) was significantly overrepresented in UTI isolates compared to strictly fecal isolates, unlike the classical UPEC virulence factors (e.g., fimbriae; Nielsen et al., 2017).

Moreover, UPEC strains that carry MccM and MccH47 determinants possess a greater number of other virulence factors (e.g., *hlyA* and *cnf1*) than isolates deprived of these siderophore-Mcc genes (Abraham et al., 2012; Massip et al., 2020). It suggests that the triad of the truncated Mcc gene cluster, the *pks* island, and the *iroA* locus enables the domination of the rectal niche with minimal genetic cost, which might favor the selection of additional virulence factors. The accumulation of these virulence factors eventually determines the strain pathogenicity level in a given host urinary tract.

In conclusion, MccH47 and MccM seem to be key determinants for effective intestinal colonization by B2 phylogroup *E. coli*. They might be particularly important in UPEC strains, for which domination and emergence from the rectal reservoir is a prerequisite for urinary tract colonization. Their production in B2 phylogroup strains seems to be optimized to minimize genetic cost and allow further selection of virulence factors. Hence, siderophore-Mcc could be a cornerstone of extraintestinal pathogenic *E. coli* versatility.

AUTHOR CONTRIBUTIONS

CM wrote the first draft of the manuscript. Both authors contributed to manuscript revision, read, and approved the submitted version.

FUNDING

This work was supported by research grant ANR-17-CE35-0010 from the Agence Nationale de la Recherche.

REFERENCES

Abraham, S., Chapman, T. A., Zhang, R., Chin, J., Mabbett, A. N., Totsika, M., et al. (2012). Molecular characterization of *Escherichia coli* strains that cause symptomatic and asymptomatic urinary tract infections. *J. Clin. Microbiol.* 50:1027. doi: 10.1128/JCM.06671-11

Asensio, C., Pérez-Díaz, J. C., Martínez, M. C., and Baquero, F. (1976). A new family of low molecular weight antibiotics from enterobacteria. *Biochem. Biophys. Res. Commun.* 69, 7–14. doi: 10.1016/S0006-291X(76)80264-1

Azpiroz, M. F., Bascuas, T., and Laviña, M. (2011). Microcin H47 system: an *Escherichia coli* small genomic island with novel features. *PLoS ONE* 6:e26179. doi: 10.1371/journal.pone.0026179

Azpiroz, M. F., and Laviña, M. (2004). Involvement of enterobactin synthesis pathway in production of microcin H47. *Antimicrob. Agents Chemother.* 48, 1235–1241. doi: 10.1128/AAC.48.4.1235-1241.2004

Azpiroz, M. F., Poey, M. E., and Laviña, M. (2009). Microcins and urovirulence in *Escherichia coli*. *Microb. Pathog.* 47, 274–280. doi: 10.1016/j.micpath.2009.09.003

Azpiroz, M. F., Rodríguez, E., and Laviña, M. (2001). The structure, function, and origin of the microcin H47 ATP-binding cassette exporter indicate its relatedness to that of colicin V. *Antimicrob. Agents Chemother.* 45, 969–972. doi: 10.1128/AAC.45.3.969-972.2001

Bagg, A., and Neilands, J. B. (1987). Ferric uptake regulation protein acts as a repressor, employing iron(II) as a cofactor to bind the operator of an iron transport operon in *Escherichia coli*. *Biochemistry* 26, 5471–5477. doi: 10.1021/bi00391a039

Bieler, S., Silva, F., Soto, C., and Belin, D. (2006). Bactericidal activity of both secreted and nonsecreted microcin E492 requires the mannose permease. *J. Bacteriol.* 188:7049. doi: 10.1128/JB.00688-06

Budič, M., Rijavec, M., Petkovšek, Z., and Zgur-Bertok, D. (2011). *Escherichia coli* bacteriocins: antimicrobial efficacy and prevalence among isolates from patients with bacteraemia. *PLoS ONE* 6:e28769. doi: 10.1371/journal.pone.0028769

Chaudhuri, R. R., and Henderson, I. R. (2012). The evolution of the *Escherichia coli* phylogeny. *Infect. Genet. Evol.* 12, 214–226. doi: 10.1016/j.meegid.2012.01.005

Clermont, O., Dixit, O. V. A., Vangchhia, B., Condamine, B., Dion, S., Bridier-Nahmias, A., et al. (2019). Characterization and rapid identification of phylogroup G in *Escherichia coli*, a lineage with high virulence and antibiotic resistance potential. *Environ. Microbiol.* 21, 3107–3117. doi: 10.1111/1462-2920.14713

Davies, J. K., and Reeves, P. (1975). Genetics of resistance to colicins in *Escherichia coli* K-12: cross-resistance among colicins of group A. *J. Bacteriol.* 123, 102–117. doi: 10.1128/JB.123.1.102-117.1975

de Lorenzo, V., and Pugsley, A. P. (1985). Microcin E492, a low-molecular-weight peptide antibiotic which causes depolarization of the *Escherichia coli* cytoplasmic membrane. *Antimicrob. Agents Chemother.* 27:666. doi: 10.1128/AAC.27.4.666

Destoumieux-Garzón, D., Thomas, X., Santamaria, M., Goulard, C., Barthélémy, M., Boscher, B., et al. (2003). Microcin E492 antibacterial activity: evidence for a TonB-dependent inner membrane permeabilization on *Escherichia coli*. *Mol. Microbiol.* 49, 1031–1041. doi: 10.1046/j.1365-2958.2003.03610.x

Dobrindt, U., Chowdary, M. G., Krumbholz, G., and Hacker, J. (2010). Genome dynamics and its impact on evolution of Escherichia coli. *Med. Microbiol. Immunol.* 199, 145–154. doi: 10.1007/s00430-010-0161-2

Dobrindt, U., Hochhut, B., Hentschel, U., and Hacker, J. (2004). Genomic islands in pathogenic and environmental microorganisms. *Nat. Rev. Microbiol.* 2:414. doi: 10.1038/nrmicro884

Dubois, D., Baron, O., Cougnoux, A., Delmas, J., Pradel, N., Boury, M., et al. (2011). ClbP is a prototype of a peptidase subgroup involved in biosynthesis of nonribosomal peptides. *J. Biol. Chem.* 286, 35562–35570. doi: 10.1074/jbc.M111.221960

Duquesne, S., Destoumieux-Garzón, D., Peduzzi, J., and Rebuffat, S. (2007). Microcins, gene-encoded antibacterial peptides from enterobacteria. *Nat. Prod. Rep.* 24, 708–734. doi: 10.1039/b516237h

Fischbach, M. A., Lin, H., Liu, D. R., and Walsh, C. T. (2005). *In vitro* characterization of IroB, a pathogen-associated C-glycosyltransferase. *Proc. Natl. Acad. Sci. U.S.A.* 102:571. doi: 10.1073/pnas.0408463102

Fischbach, M. A., Lin, H., Liu, D. R., and Walsh, C. T. (2006). How pathogenic bacteria evade mammalian sabotage in the battle for iron. *Nat. Chem. Biol.* 2, 132–138. doi: 10.1038/nchembio771

Flores-Mireles, A. L., Walker, J. N., Caparon, M., and Hultgren, S. J. (2015). Urinary tract infections: epidemiology, mechanisms of infection and treatment options. *Nat. Rev. Microbiol.* 13, 269–284. doi: 10.1038/nrmicro3432

Gaggero, C., Moreno, F., and Laviña, M. (1993). Genetic analysis of microcin H47 antibiotic system. *J. Bacteriol.* 175, 5420–5427. doi: 10.1128/JB.175.17.5420-5427.1993

Gordon, D. M., and O'Brien, C. L. (2006). Bacteriocin diversity and the frequency of multiple bacteriocin production in *Escherichia coli*. *Microbiology* 152, 3239–3244. doi: 10.1099/mic.0.28690-0

Grozdanov, L., Raasch, C., Schulze, J., Sonnenborn, U., Gottschalk, G., Hacker, J., et al. (2004). Analysis of the genome structure of the nonpathogenic probiotic *Escherichia coli* strain Nissle 1917. *J. Bacteriol.* 186, 5432–5441. doi: 10.1128/JB.186.16.5432-5441.2004

Hancock, V., Vejborg, R. M., and Klemm, P. (2010). Functional genomics of probiotic *Escherichia coli* Nissle 1917 and 83972, and UPEC strain CFT073: comparison of transcriptomes, growth and biofilm formation. *Mol. Genet. Genomics* 284, 437–454. doi: 10.1007/s00438-010-0578-8

Jaureguy, F., Landraud, L., Passet, V., Diancourt, L., Frapy, E., Guigon, G., et al. (2008). Phylogenetic and genomic diversity of human bacteremic *Escherichia coli* strains. *BMC Genomics* 9:560. doi: 10.1186/1471-2164-9-560

Johnson, J. R., and Russo, T. A. (2002). Extraintestinal pathogenic *Escherichia coli*: "The other bad *E. coli*." *J. Lab. Clin. Med.* 139, 155–162. doi: 10.1067/mlc.2002.121550

Kaper, J. B., Nataro, J. P., and Mobley, H. L. T. (2004). Pathogenic *Escherichia coli*. *Nat. Rev. Microbiol.* 2, 123–140. doi: 10.1038/nrmicro818

Lagos, R., Baeza, M., Corsini, G., Hetz, C., Strahsburger, E., Castillo, J. A., et al. (2001). Structure, organization and characterization of the gene cluster involved in the production of microcin E492, a channel-forming bacteriocin. *Mol. Microbiol.* 42, 229–243. doi: 10.1046/j.1365-2958.2001.02630.x

Laviña, M., Gaggero, C., and Moreno, F. (1990). Microcin H47, a chromosome-encoded microcin antibiotic of *Escherichia coli*. *J. Bacteriol.* 172, 6585–6588. doi: 10.1128/JB.172.11.6585-6588.1990

Marcoleta, A. E., Gutiérrez-Cortez, S., Hurtado, F., Argandoña, Y., Corsini, G., Monasterio, O., et al. (2018). The Ferric uptake regulator (Fur) and iron availability control the production and maturation of the antibacterial peptide microcin E492. *PLoS ONE* 13:e0200835. doi: 10.1371/journal.pone.0200835

Martin, P., Marcq, I., Magistro, G., Penary, M., Garcie, C., Payros, D., et al. (2013). Interplay between siderophores and colibactin genotoxin biosynthetic pathways in *Escherichia coli*. *PLoS Pathog.* 9:e1003437. doi: 10.1371/journal.ppat.1003437

Massip, C., Branchu, P., Bossuet-Greif, N., Chagneau, C. V., Gaillard, D., Martin, P., et al. (2019). Deciphering the interplay between the genotoxic and probiotic activities of *Escherichia coli* Nissle 1917. *PLoS Pathog.* 15:e1008029. doi: 10.1371/journal.ppat.1008029

Massip, C., Chagneau, C. V., Boury, M., and Oswald, E. (2020). The synergistic triad between microcin, colibactin, and salmochelin gene clusters in uropathogenic *Escherichia coli*. *Microbes Infect.* 22, 144–147. doi: 10.1016/j.micinf.2020.01.001

Micenková, L., Bosák, J., Štaudová, B., Kohoutová, D., Cejková, D., Woznicová, V., et al. (2016). Microcin determinants are associated with B2 phylogroup of human fecal *Escherichia coli* isolates. *MicrobiologyOpen* 5, 490–498. doi: 10.1002/mbo3.345

Miethke, M., and Marahiel, M. A. (2007). Siderophore-based iron acquisition and pathogen control. *Microbiol. Mol. Biol. Rev.* 71, 413–451. doi: 10.1128/MMBR.00012-07

Moreno, E., Andreu, A., Pigrau, C., Kuskowski, M. A., Johnson, J. R., and Prats, G. (2008). Relationship between *Escherichia coli* strains causing acute cystitis in women and the fecal *E. coli* population of the host. *J. Clin. Microbiol.* 46, 2529–2534. doi: 10.1128/JCM.00813-08

Nielsen, K. L., Stegger, M., Kiil, K., Godfrey, P. A., Feldgarden, M., Lilje, B., et al. (2017). Whole-genome comparison of urinary pathogenic *Escherichia coli* and faecal isolates of UTI patients and healthy controls. *Int. J. Med. Microbiol.* 307, 497–507. doi: 10.1016/j.ijmm.2017.09.007

Nolan, E. M., Fischbach, M. A., Koglin, A., and Walsh, C. T. (2007). Biosynthetic tailoring of microcin E492m: post-translational modification affords an antibacterial siderophore-peptide conjugate. *J. Am. Chem. Soc.* 129, 14336–14347. doi: 10.1021/ja074650f

Nolan, E. M., and Walsh, C. T. (2008). Investigations of the MceIJ-catalyzed posttranslational modification of the microcin E492 C-terminus: linkage of ribosomal and nonribosomal peptides to form "Trojan Horse" antibiotics. *Biochemistry* 47, 9289–9299. doi: 10.1021/bi800826j

Nougayrède, J.-P., Homburg, S., Taieb, F., Boury, M., Brzuszkiewicz, E., Gottschalk, G., et al. (2006). *Escherichia coli* induces DNA double-strand breaks in eukaryotic cells. *Science* 313, 848–851. doi: 10.1126/science.1127059

Nowrouzian, F. L., Wold, A. E., and Adlerberth, I. (2005). *Escherichia coli* strains belonging to phylogenetic group B2 have superior capacity to persist in the intestinal microflora of infants. *J. Infect. Dis.* 191, 1078–1083. doi: 10.1086/427996

Patzer, S. I. (2003). The colicin G, H and X determinants encode microcins M and H47, which might utilize the catecholate siderophore receptors FepA, Cir, Fiu and IroN. *Microbiology* 149, 2557–2570. doi: 10.1099/mic.0.26396-0

Pérez-Berezo, T., Pujo, J., Martin, P., Faouder, P., Galano, J.-M., Guy, A., et al. (2017). Identification of an analgesic lipopeptide produced by the probiotic *Escherichia coli* strain Nissle 1917. *Nat. Commun.* 8:1314. doi: 10.1038/s41467-017-01403-9

Picard, B., Garcia, J. S., Gouriou, S., Duriez, P., Brahimi, N., Bingen, E., et al. (1999). The link between phylogeny and virulence in *Escherichia coli* extraintestinal infection. *Infect. Immun.* 67, 546–553. doi: 10.1128/IAI.67.2.546-553.1999

Poey, M. E., Azpiroz, M. F., and Laviña, M. (2006). Comparative analysis of chromosome-encoded microcins. *Antimicrob. Agents Chemother.* 50, 1411–1418. doi: 10.1128/AAC.50.4.1411-1418.2006

Pons, A.-M., Lanneluc, I., Cottenceau, G., and Sable, S. (2002). New developments in non-post translationally modified microcins. *Biochimie* 84, 531–537. doi: 10.1016/S0300-9084(02)01416-5

Reister, M., Hoffmeier, K., Krezdorn, N., Rotter, B., Liang, C., Rund, S., et al. (2014). Complete genome sequence of the gram-negative probiotic *Escherichia coli* strain Nissle 1917. *J. Biotechnol.* 187, 106–107. doi: 10.1016/j.jbiotec.2014.07.442

Rodríguez, E., Gaggero, C., and Laviña, M. (1999). The structural gene for microcin H47 encodes a peptide precursor with antibiotic activity. *Antimicrob. Agents Chemother.* 43, 2176–2182. doi: 10.1128/AAC.43.9.2176

Rodriguez, E., and Lavina, M. (2003). The proton channel is the minimal structure of ATP synthase necessary and sufficient for microcin H47 antibiotic action. *Antimicrob. Agents Chemother.* 47, 181–187. doi: 10.1128/AAC.47.1.181-187.2003

Russo, T. A., and Johnson, J. R. (2000). Proposal for a new inclusive designation for extraintestinal pathogenic isolates of *Escherichia coli*: ExPEC. *J. Infect. Dis.* 181, 1753–1754. doi: 10.1086/315418

Šmajs, D., Micenková, L., Šmarda, J., Vrba, M., Ševčíková, A., Vališová, Z., et al. (2010). Bacteriocin synthesis in uropathogenic and commensal *Escherichia coli*: colicin E1 is a potential virulence factor. *BMC Microbiol.* 10:288. doi: 10.1186/1471-2180-10-288

Snyder, J. A., Haugen, B. J., Buckles, E. L., Lockatell, C. V., Johnson, D. E., Donnenberg, M. S., et al. (2004). Transcriptome of uropathogenic *Escherichia coli* during urinary tract infection. *Infect. Immun.* 72, 6373–6381. doi: 10.1128/IAI.72.11.6373-6381.2004

Starčič Erjavec, M., and Žgur-Bertok, D. (2015). Virulence potential for extraintestinal infections among commensal *Escherichia coli* isolated from healthy humans—the Trojan horse within our gut. *FEMS Microbiol. Lett.* 362:fnu061. doi: 10.1093/femsle/fnu061

Tenaillon, O., Skurnik, D., Picard, B., and Denamur, E. (2010). The population genetics of commensal *Escherichia coli*. *Nat. Rev. Microbiol.* 8, 207–217. doi: 10.1038/nrmicro2298

Thomas, X., Destoumieux-Garzón, D., Peduzzi, J., Afonso, C., Blond, A., Birlirakis, N., et al. (2004). Siderophore peptide, a new type of post-translationally modified antibacterial peptide with potent activity. *J. Biol. Chem.* 279, 28233–28242. doi: 10.1074/jbc.M400228200

Touchon, M., Hoede, C., Tenaillon, O., Barbe, V., Baeriswyl, S., Bidet, P., et al. (2009). Organised genome dynamics in the *Escherichia coli* species results in highly diverse adaptive paths. *PLoS Genet.* 5:e1000344. doi: 10.1371/journal.pgen.1000344

Tourret, J., and Denamur, E. (2016). Population phylogenomics of extraintestinal pathogenic *Escherichia coli*. *Microbiol. Spectr.* 4:UTI-0010-2012. doi: 10.1128/microbiolspec.UTI-0010-2012

Trujillo, M., Rodríguez, E., and Laviña, M. (2001). ATP synthase is necessary for microcin H47 antibiotic action. *Antimicrob. Agents Chemother.* 45, 3128–3131. doi: 10.1128/AAC.45.11.3128-3131.2001

Vassiliadis, G., Destoumieux-Garzón, D., Lombard, C., Rebuffat, S., and Peduzzi, J. (2010). Isolation and characterization of two members of the siderophore-microcin family, microcins M and H47. *Antimicrob. Agents Chemother.* 54, 288–297. doi: 10.1128/AAC.00744-09

Vassiliadis, G., Peduzzi, J., Zirah, S., Thomas, X., Rebuffat, S., and Destoumieux-Garzón, D. (2007). Insight into siderophore-carrying peptide biosynthesis: enterobactin is a precursor for microcin E492 posttranslational modification. *Antimicrob. Agents Chemother.* 51, 3546–3553. doi: 10.1128/AAC.00261-07

Vejborg, R. M., Friis, C., Hancock, V., Schembri, M. A., and Klemm, P. (2010). A virulent parent with probiotic progeny: comparative genomics of *Escherichia coli* strains CFT073, Nissle 1917 and ABU 83972. *Mol. Genet. Genomics* 283, 469–484. doi: 10.1007/s00438-010-0532-9

Yamamoto, S., Tsukamoto, T., Terai, A., Kurazono, H., Takeda, Y., and Yoshida, O. (1997). Genetic evidence supporting the fecal-perineal-urethral hypothesis in cystitis caused by *Escherichia coli*. *J. Urol.* 157, 1127–1129. doi: 10.1016/S0022-5347(01)65154-1

Conflict of Interest: The authors declare that the research was conducted in the absence of any commercial or financial relationships that could be construed as a potential conflict of interest.

frontiers in Cellular and Infection Microbiology

ORIGINAL RESEARCH
published: 18 September 2020
doi: 10.3389/fcimb.2020.00485

Gut Microbiota-Metabolome Changes in Children With Diarrhea by Diarrheagenic *E. coli*

Pablo Gallardo[1], *Mariana Izquierdo*[1], *Roberto M. Vidal*[2], *Francisco Soto*[1], *Juan C. Ossa*[1] *and Mauricio J. Farfan*[1]*

[1] *Departamento de Pediatría y Cirugía Infantil, Facultad de Medicina, Hospital Dr. Luis Calvo Mackenna, Universidad de Chile, Santiago, Chile,* [2] *Programa de Microbiología y Micología, Facultad de Medicina, Instituto de Ciencias Biomédicas, Universidad de Chile, Santiago, Chile*

Background: Diarrheagenic *Escherichia coli* (DEC) strains are a main cause of diarrhea worldwide in children under 5 years old. DEC virulence is strongly regulated by environmental conditions and metabolites produced by the gut microbiota in the intestinal tract. In this study, we evaluated changes in gut microbiota-metabolome in children with or without diarrhea produced by DEC pathotypes.

Goal: To determine gut microbiota composition and metabolome in stool samples obtained from healthy children and children with diarrhea positive for DEC pathotypes.

Methods: We analyzed a total of 16 age-paired stool samples: 8 diarrheal samples positive for one DEC pathotype and 8 stool samples from healthy children. To identify the microbiota composition, we sequenced the V3-V4 region of the 16S rRNA and determined operational phylogenetic units (OPU). OPU were then used to predict metabolic pathways using the PICRUSt2 software. The presence of metabolites in stool samples was determined by LC-MS. A correlation analysis was performed with the main genera from each group and main metabolites. Bacteria associated with variance of main metabolites were identified using the MIMOSA2 software.

Results: DEC and healthy groups showed a statistically different microbiota composition. A decrease in *Firmicutes* together with an increase in *Bacteroidetes* and *Proteobacteria* was found in the DEC group compared to the healthy group. Metabolic pathway predictions based on microbiota diversity showed that pathways involved in histidine and L-ornithine metabolism were significantly different between groups. A total of 88 metabolites detected by LC-MS were included in the metabolome analysis. We found higher levels of histamine and lower levels of ornithine in DEC samples than in the healthy group. Histamine and L-ornithine were associated with a specific microbiota species and the corresponding metabolic pathways.

Conclusion: Stool samples from healthy children and children positive for DEC displayed a differential metabolome and microbiota composition. A strong correlation between a gut microbiota species and certain metabolites, such as histamine and L-ornithine, was found in the DEC group. This information might be useful to identify mechanisms and signaling molecules involved in the crosstalk between microbiota and DEC pathotypes.

Keywords: Diarrheagenic *Escherichia coli*, microbiota, metabolome, diarrhea, children

OPEN ACCESS

Edited by:
Natarajaseenivasan Kalimuthusamy, Bharathidasan University, India

Reviewed by:
Luis Fernando Dos Santos, Adolfo Lutz Institute, Brazil
Philip R. Hardwidge, Kansas State University, United States

***Correspondence:**
Mauricio J. Farfan
mfarfan@uchile.cl

Specialty section:
This article was submitted to Bacteria and Host, a section of the journal Frontiers in Cellular and Infection Microbiology

Received: *08 April 2020*
Accepted: *05 August 2020*
Published: *18 September 2020*

Citation:
Gallardo P, Izquierdo M, Vidal RM, Soto F, Ossa JC and Farfan MJ (2020) Gut Microbiota-Metabolome Changes in Children With Diarrhea by Diarrheagenic E. coli. Front. Cell. Infect. Microbiol. 10:485. doi: 10.3389/fcimb.2020.00485

INTRODUCTION

Diarrheagenic *Escherichia coli* (DEC) is the most common bacterial etiological agent of diarrhea in diverse subpopulations, both in developing and industrialized regions, and it primarily affects children under 5 years of age (Press, 2014). Generally, DEC infection involves adherence and colonization of the intestinal surface, production and secretion of virulence factors, and diarrhea, along with intestinal inflammation (Croxen et al., 2013). Even though there are data available about the regulation of DEC virulence associated with induction of an inflammatory response, information is limited to the environmental conditions in the intestine that may modulate infection. Under well-defined environmental conditions, expression of virulence genes occurs at specific sites, allowing the bacteria to initiate the infection process (Carlson-Banning and Sperandio, 2018; Alvestegui et al., 2019). Most studies have focused on unraveling the molecular mechanisms occurring inside the bacteria and little is known about the environmental factors that regulate pathogenesis at a specific time or place (Carlson-Banning and Sperandio, 2018). Therefore, an understanding of the molecular basis of DEC pathogenesis is necessary to design new strategies aimed at controlling these infections worldwide.

In recent years, gut microbiota has played a significant role in the regulation of pathogenic mechanisms. Published evidence has supported the role of specific strains from the normal gut microbiota in DEC virulence (Pacheco et al., 2012; Curtis et al., 2014; Rolhion and Chassaing, 2016). Additionally, several metabolites produced by the gut microbiota in the intestinal tract could be mediating interactions between the intestinal microbiota and enteric pathogens, such as DEC (Vogt et al., 2015). Given their abundance in the intestinal milieu, short-chain fatty acids (SCFA) have been extensively studied as signaling molecules for enteropathogens (Sun and O'riordan, 2013), including DEC, but the role of other metabolites must be explored in order to get a broader picture of virulence regulation by metabolites present in the intestinal lumen.

In this study, we determined gut microbiota and metabolome composition in stool samples obtained from healthy children and children with diarrhea positive for DEC pathotypes. Our data shows that stool samples from healthy children and children positive for DEC displayed a differential pattern of metabolites and bacterial microbiota.

METHODS

Patients and Samples

Diarrheal and non-diarrheal stool samples were collected from September 2018 to February 2019 from patients under 5 years old treated at the Hospital Dr. Luis Calvo Mackenna (HLCM) and the HLCM daycare center, respectively, located in Santiago, Chile. All stool samples were stored at −80°C. Frozen stool samples were screened for 22 enteric pathogens using FilmArray® GI testing and selected samples were grouped as healthy (non-diarrheal, no pathogens detected) and DEC (diarrheal, with only one DEC pathotype detected). We excluded from the study children who received antibiotics, probiotics, steroidal and non-steroidal anti-inflammatory drugs 2 months prior to enrollment. Eight age-paired samples for each group were chosen for this study (**Table 1**).

Ethics

This study was conducted in accordance with Declaration of Helsinki guidelines. The study protocol was approved by the Ethics Committee of the Universidad de Chile. Written informed consent was obtained from all parents on behalf of their children.

DNA Extraction and Sequencing

Total DNA was extracted from each stool using the QIAamp Fast DNA Stool Mini kit (Qiagen), quantified using a Synergy HT® spectrophotometer (Biotek™) and stored at −20°C. DNA samples were shipped to Molecular Research LP (TX, USA) for DNA amplification and sequencing of the V3-V4 regions of the 16S rRNA, using the Illumina miSeq 2x300 PE.

Microbiota Identification

Illumina raw amplicons were processed as previously described (Gallardo et al., 2017). Briefly, raw sequences were trimmed and processed using MacQiime V1.9.1-20150604, according to the default parameters for trimming (Caporaso et al., 2010). Sequences were aligned using the SINA (Pruesse et al., 2012) built-in resource on the ARB software (Ludwig et al., 2004) and OPU were assigned using the Silva132 database as the reference (Quast et al., 2013). OPU abundance was coded as an entry matrix. Data were transformed applying double square root to reduce variance between detected OPU. A redundancy analysis (RDA) and ANOVA was performed using the *Vegan* (Oksanen et al., 2019) and *ggplot2* (Wickham, 2016) packages from the RStudio 1.0.136 software. The most statistically representative genera for each group were determined using the *Indicspecies* package (De Caceres and Legendre, 2009) for R. Abundance of taxa at different levels was determined, expressing OPU abundance as percentages.

Metabolomic Analysis

The presence of metabolites in stool samples was determined by liquid chromatography mass spectrometry (LC-MS) at MS-Omics (Denmark). Briefly, PCR grade water was added to

TABLE 1 | Overall microbiota findings in stool samples for DEC and healthy groups.

Characteristics	DEC group	Healthy group
Number of samples	8	8
Age in months (Interquartile range)	37 (27.8–48.3)	36.5 (34.3–48.5)
Pathogen detected (number of samples)	*Shigella*/EIEC (1) STEC (1) EAEC (3) EPEC (3)	
Exclusive OPUs	228	185

DEC, Diarrheagenic E. coli.
EAEC, Enteroaggregative E. coli.
EPEC, Enteropathogenic E. coli.
EIEC, Enteroinvasive E. coli.
STEC, Shiga toxin-producing E. coli.

500 mg of stool sample, vortexed and centrifuged. Supernatants were filtered with a 0.2 μm filter and filtered supernatants were shipped to MS-Omics. A total of 156 metabolites were detected. We used the KEGG database (Kanehisa and Goto, 2000) for filtering only those with a bacterial or human origin and that were present in at least 5 of 8 samples within groups; thus, a total of 88 metabolites were selected for analysis. Metabolomic analysis was done using the *MetaboAnalystR* package (Chong and Xia, 2018) for R considering peak intensities as the input format. Data were normalized by sample median and log transformation without other data scaling. A redundancy analysis for determining metabolic structures was performed using the *vegan* package (Oksanen et al., 2019). Exploratory research on metabolites was performed using fold change analysis and a *t*-test; important features were selected by volcano plot, selecting those with a fold change of 2 or more and setting the *t*-test threshold at 0.05. Sample clustering of exploratory selected metabolites was based on their levels in samples, using hierarchical clustering, Euclidean distance and Ward algorithms of the *MetaboAnalystR* package (Chong and Xia, 2018) for R.

Combined Analysis and Statistics

Correlation between the main genera of each group and the main metabolites detected was done using the *corrplot* package (Wei and Simko, 2017) for R. Later, a metabolic prediction was done based on the sequences of the representative OPU, using the PICRUSt2 (Douglas et al., 2020) algorithm and the PICRUSt (Langille et al., 2013) default Greengenes database as the reference (Desantis et al., 2006). Graphs were obtained with STAMP 2.9 (Parks et al., 2014), and Welch's *t*-test was used to determine significance of sequence contribution to predicted pathways. Finally, using the Web version of the MIMOSA2 (www.borensteinlab.com/software_MIMOSA2.html) package (Noecker et al., 2016) and the AGORA model, sequences from the representative OPU and metabolites selected from the prior volcano plot were used to determine a microbiota explanation for the presence of metabolite levels within the DEC groups. Representative OPUs were used to construct a metabolic model containing the metabolic reactions that each taxon is potentially capable of performing, assigning a score to each taxon-metabolite relation. Total scores were compared to metabolite measurements across all samples, and a regression analysis to assess whether scores were positively or negatively predictive of the observed metabolite levels in the samples was done. Finally, decomposing the model allowed us to identify the individual taxon contributions. The sum of the contributions of all listed taxa is equal to the unadjusted R-squared of the regression model used to predict each metabolite.

RESULTS

Metabolic Pathway Predictions Using Microbiota Composition in Diarrheal and Non-diarrheal Stool Samples

We identified a total of 755 OPU within 16 stool samples. The redundancy analysis showed that microbiota composition was statistically different among DEC and healthy groups, with a distinctive community structure clustering (**Figure 1**; $p = 0.002$). At *phylum* level, the DEC group presented a decreasing number of Firmicutes (81.8 ± 3.6% vs. 68.3 ± 7.5%, $p < 0.001$), as well as an increasing number of Proteobacteria (4.1 ± 1.5% vs. 11.6 ± 6%, $p = 0.009$) compared to the healthy group. We also found differences in the proportion of Bacteroidetes (7.1 ± 3.9% vs. 12.7 ± 6.7%, $p = 0.06$). All the taxa comparisons are shown in **Supplementary Figure 1**.

Representative sequences of each OPU were used to predict metabolic pathways that could be related to the gut microbiota composition. Pathways involved in L-histidine degradation presented a higher representation of sequences associated with DEC groups compared to healthy groups. By contrast, L-ornithine and L-histidine biosynthesis pathways were less represented in DEC groups compared to healthy groups (**Figure 2**). All metabolic predictions are shown in **Supplementary Figure 2**.

DEC Group Displayed a Distinctive Metabolome Composition Compared to Healthy Group

A total of 156 metabolites were identified in the 16 stool samples included in this work. We discarded molecules that are not metabolized by bacteria, such as sweeteners or food additives. Therefore, a total of 88 metabolites were included in the analysis. The redundancy analysis of normalized data showed a distinctive metabolic composition for each group (**Figure 3**; $p = 0.001$). Using a univariate analysis of samples by volcano plot, we found 13 metabolites with

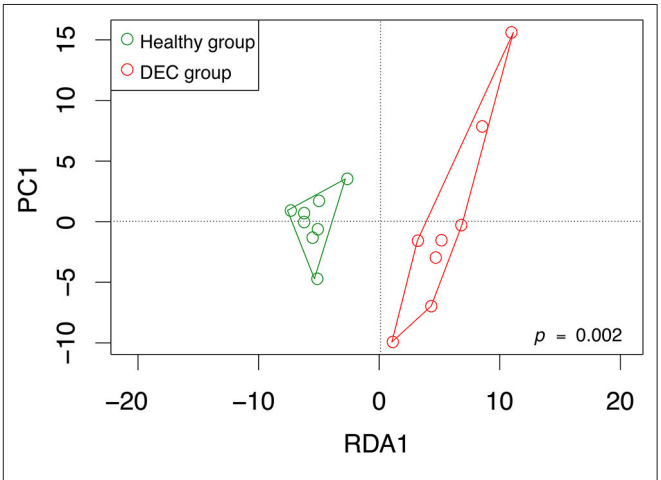

FIGURE 1 | OPU community structure of healthy and DEC-positive stool samples. Microbiota community distribution of each sample and its clustering according to the sample group were analyzed by redundancy analysis. Green and red circles represent microbiota compositions found in healthy and DEC-positive stool samples, respectively. The analysis was conducted using a sample classification as the explanatory matrix and relative OPU abundance as the response matrix. Data were normalized with a double square root transformation. Clustering significance was analyzed by ANOVA, using the *vegan* package for R.

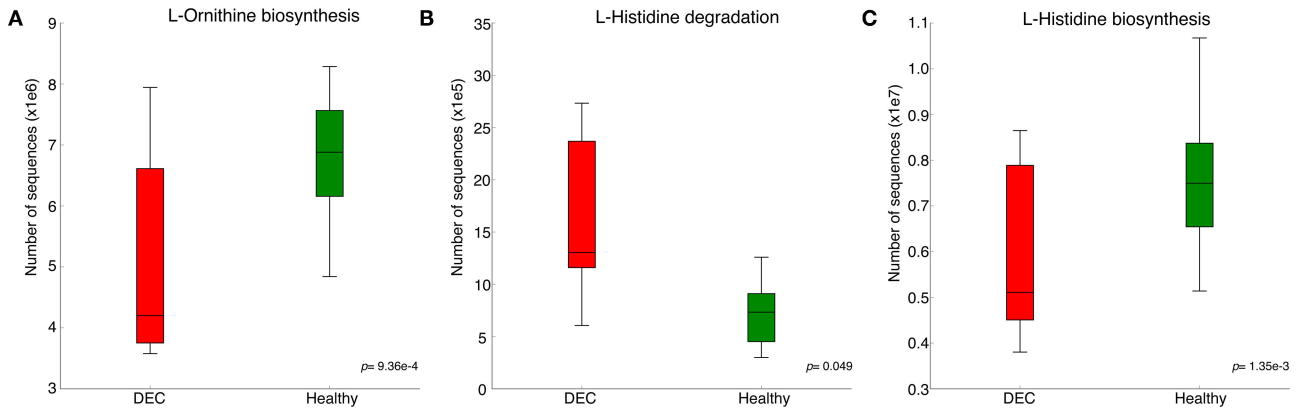

FIGURE 2 | Predicted metabolic pathways related to the gut microbiota composition. Principal pathway prediction by PICRUSt2 algorithm using representative sequences of main OPUs from each group and the Greengenes database as the reference. Graphs of predictions and significance values were obtained using STAMP v. 2.1.3. Graphs represent the number of sequences in microbiota that have known genes involved in L-ornithine biosynthesis **(A)**, L-histidine degradation **(B)**, and L-histidine biosynthesis **(C)**. Box plots denote the top quartile, median, and bottom quartile, analyzed using Welch's *t*-test.

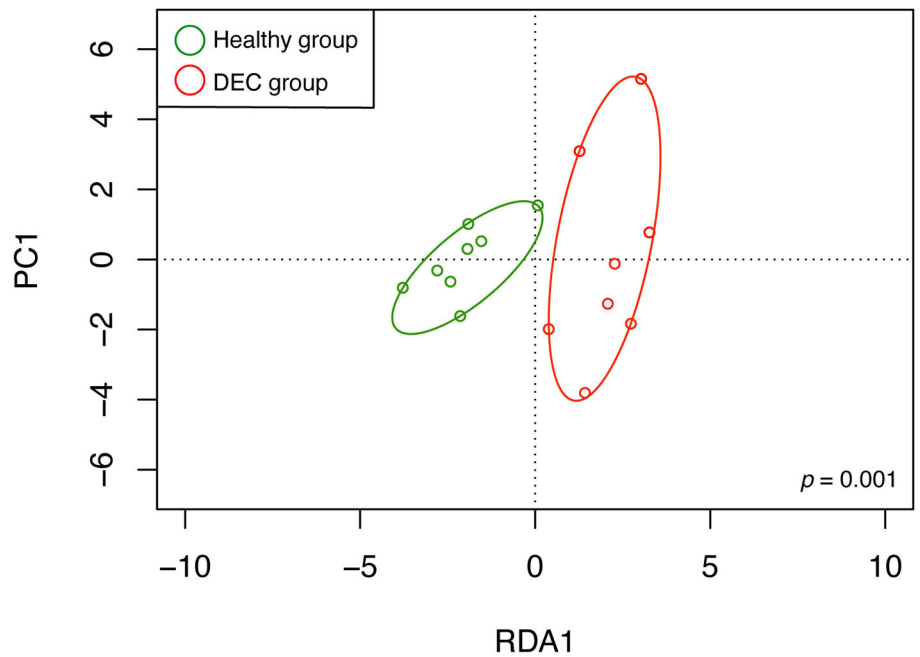

FIGURE 3 | Metabolomic structure of healthy and DEC-positive stool samples. Metabolomic structure of each sample and its organization according to the sample group were analyzed by redundancy analysis. Green and red circles represent metabolome compositions found in healthy and DEC-positive stool samples, respectively. The analysis was conducted using peak intensities of 88 LC-MS-detected metabolites from stool samples. Clustering significance was analyzed by ANOVA, using the *vegan* package for R.

a fold change >2 and *p*-value of *t*-test < 0.05 (**Table 2**; **Figure 4**). Alanine, N-butylformamide, piperidine, cadaverine and histamine were significantly associated with the DEC group compared to the healthy group. On the other hand, aspartic acid, ornithine, citrulline, dimethylformamide, dehydroalanine, ethyl acetoacetate, glucosamine and benzoic acid were significantly associated with the healthy group compared to the DEC group. We included guaiacol and diethyl malonate in the DEC and healthy groups in the following analysis since these metabolites where close to significance (fold change >2 and $p = 0.05$). Dendrograms and heatmaps of the significantly associated metabolites described above displayed a hierarchical organization of samples similar to the *a priori* grouping of samples based on health status (**Figure 5**).

TABLE 2 | Changes of peak intensities of the 15 main LC-MS-detected metabolites in DEC-positive stool samples compared to the healthy stool samples.

	Compounds	Fold Change (FC)	*p*
Metabolites associated to DEC group	Alanine	12.66*	0.0005
	N-Butylformamide	6.34*	0.0085
	Piperidine	11.09*	0.0183
	Cadaverine	11.55*	0.0185
	Histamine	9.32*	0.0204
	Guaiacol	15.67	0.0517
Metabolites associated to healthy group	Aspartic acid	−2.17*	0.0003
	Ornithine	−2.19*	0.0014
	Citrulline	−2.21*	0.0013
	Dimethylformamide	−2.59*	0.0029
	Dehydroalanine	−2.37*	0.0031
	Benzoic acid	−12.25*	0.0055
	Glucosamine	−4.61*	0.0073
	Ethyl acetoacetate	−2.56*	0.0154
	Diethyl malonate	−2.31	0.0582

*Metabolites with statistically significant differential levels according to the t-test p-value and fold-change value are indicated as main metabolites for each group. *p < 0.05.*

Microbiota-Metabolome Correlation in Samples From DEC and Healthy Groups

Among the identified taxa on samples, we found that *Gemella* ($p = 0.005$), *Escherichia* ($p = 0.003$), *Prevotella* ($p = 0.027$), *Erwinia* ($p = 0.010$), and *Buttiauxella* ($p = 0.016$) were the genera significantly associated with the DEC groups. Instead, *Faecalitalea* ($p = 0.001$), *Lactococcus* ($p = 0.032$), and *Clostridium* ($p = 0.010$) were the genera significantly associated with the healthy groups. Correlation between the abundance of these main genera and the 15 metabolites with a fold change >2 showed a clear pattern of link between the group's associated genera and metabolites in each group (**Figure 6**).

Using the MIMOSA2 software, a tool for the metabolic model-based estimation of paired microbiome and metabolomic datasets, we evaluated the representative microbiota sequences and the abundance of the 15 metabolites described above. We found specific genera and species that could explain the variance of histamine and ornithine, metabolites distinctively found in the DEC and healthy groups. In the case of metabolomic screening for these metabolites, we found higher levels of histamine in the DEC groups compared to healthy groups, which according

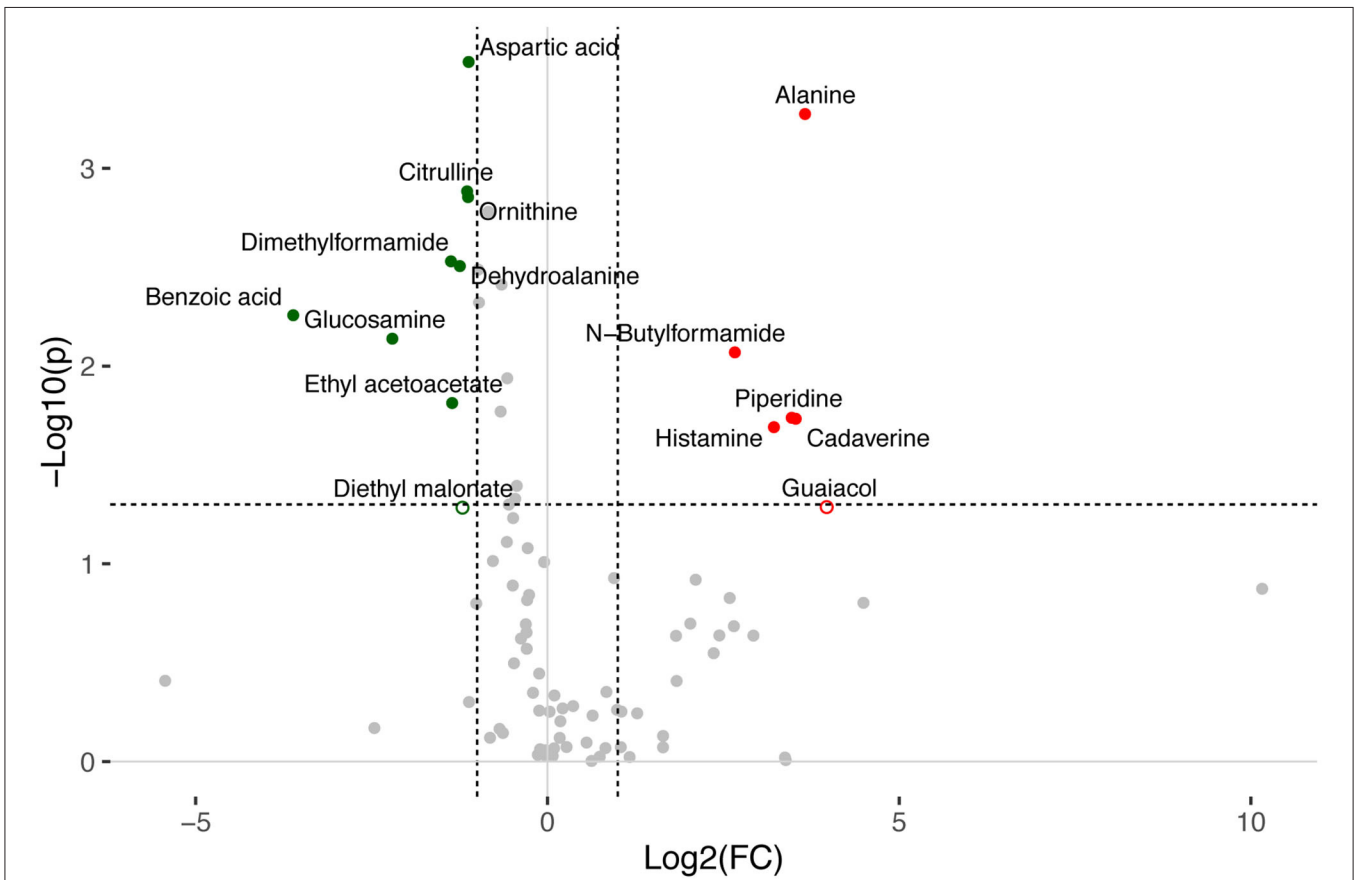

FIGURE 4 | Volcano plot of LC-MS-detected metabolites in healthy and DEC-positive stool samples. Changes in normalized peak intensities of metabolites detected in samples from the DEC group compared to healthy samples. The volcano plot summarizes both fold-change and *t*-test criteria for all metabolites. Metabolites with significant differential levels according to the *t*-test *p*-value ($p < 0.05$) and fold-change value (FC > 2) were colored. Red and green dots represent metabolites found significantly higher and lower, respectively, in the DEC group compared to the healthy group. Borderline metabolites (diethyl malonate and guaiacol) are represented as empty circles.

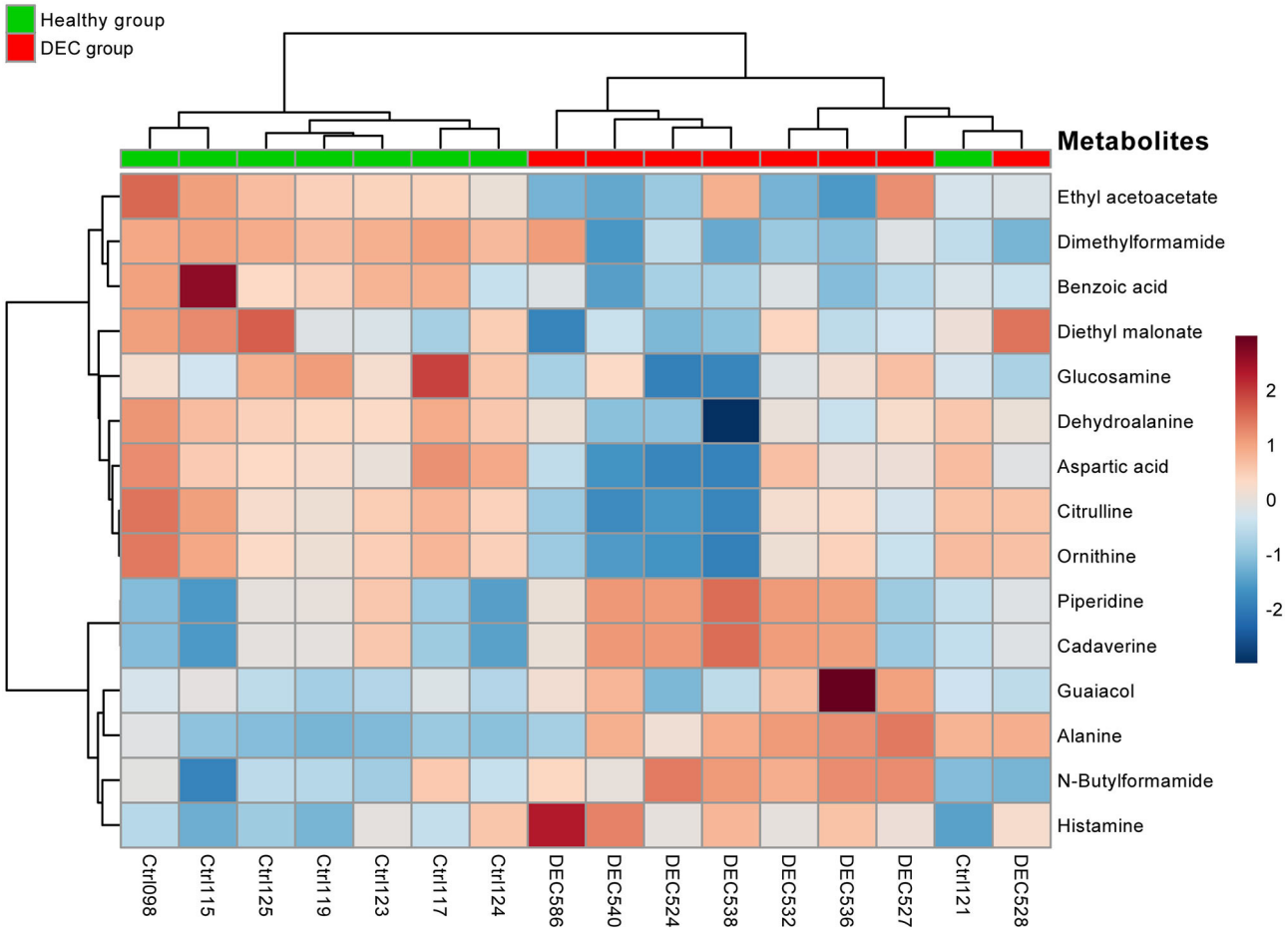

FIGURE 5 | Heatmap of main metabolites found in healthy and DEC-positive stool samples. Heatmap showing the clustering of the 15 main metabolites present in stool samples found in the DEC and healthy groups. Each colored cell on the map corresponds to a metabolite peak intensity. The row displays the metabolites and the column represents the samples (red = elevated; blue = reduced). A distinct pattern of group-associated metabolite ordination was observed. Metabolites and samples were hierarchically clustered by Ward's method and Pearson's distance using the *MetaboAnalyst* package for R.

to the MIMOSA2 model could be explained mainly by the presence of *Enterobacter hormaechei*, *Bifidobacterium stercoris*, *Shigella* spp., and *Citrobacter werkmanii/freundii*. We also found lower levels of ornithine in the DEC samples compared to healthy groups (**Table 2**), which could be due mainly to the presence of *Streptococcus anginosus, Enterococcus faecalis* and *Escherichia* sp. (**Figure 7**).

DISCUSSION

Current knowledge of gut microbiota in diarrheal infections reveals a distinctive composition and abundance of commensal bacteria (Jeffery et al., 2019), but these differences are insufficient to explain the mechanisms involved in infections by enteric pathogens. Several reports strongly suggest that DEC pathogenicity along the transit of the pathogen across the gastrointestinal tract is finely regulated by gut microbiota, the immune system and metabolites of the intestinal milieu (Thaiss and Elinav, 2014). Therefore, gut metabolome could provide relevant information to reveal the environmental signals produced by gut microbiota that regulate DEC pathogenesis at a specific time or place (Kumar and Sperandio, 2019).

Our previous evidence has indicated that children with diarrhea by DEC display a distinctive microbiota composition (Gallardo et al., 2017). In this current study we have confirmed our previous observations by analyzing microbiota composition in stool samples from 8 age-paired children, either healthy or with diarrhea by DEC (**Figure 1**). Considering that dysbiosis could be related to a distinct metabolomic composition (Noorbakhsh et al., 2019), we sought to identify the metabolome composition of the samples included in this study. Interestingly, our data showed a clear metabolomic structure statistically different for each group (**Figure 3**), suggesting that metabolic environment associated with DEC infection may contain specific metabolites related to DEC pathogenicity. We identified 15 metabolites in stool samples significantly different between the DEC and healthy groups (**Figure 4**), the levels of which were associated with the main genera from DEC and healthy groups

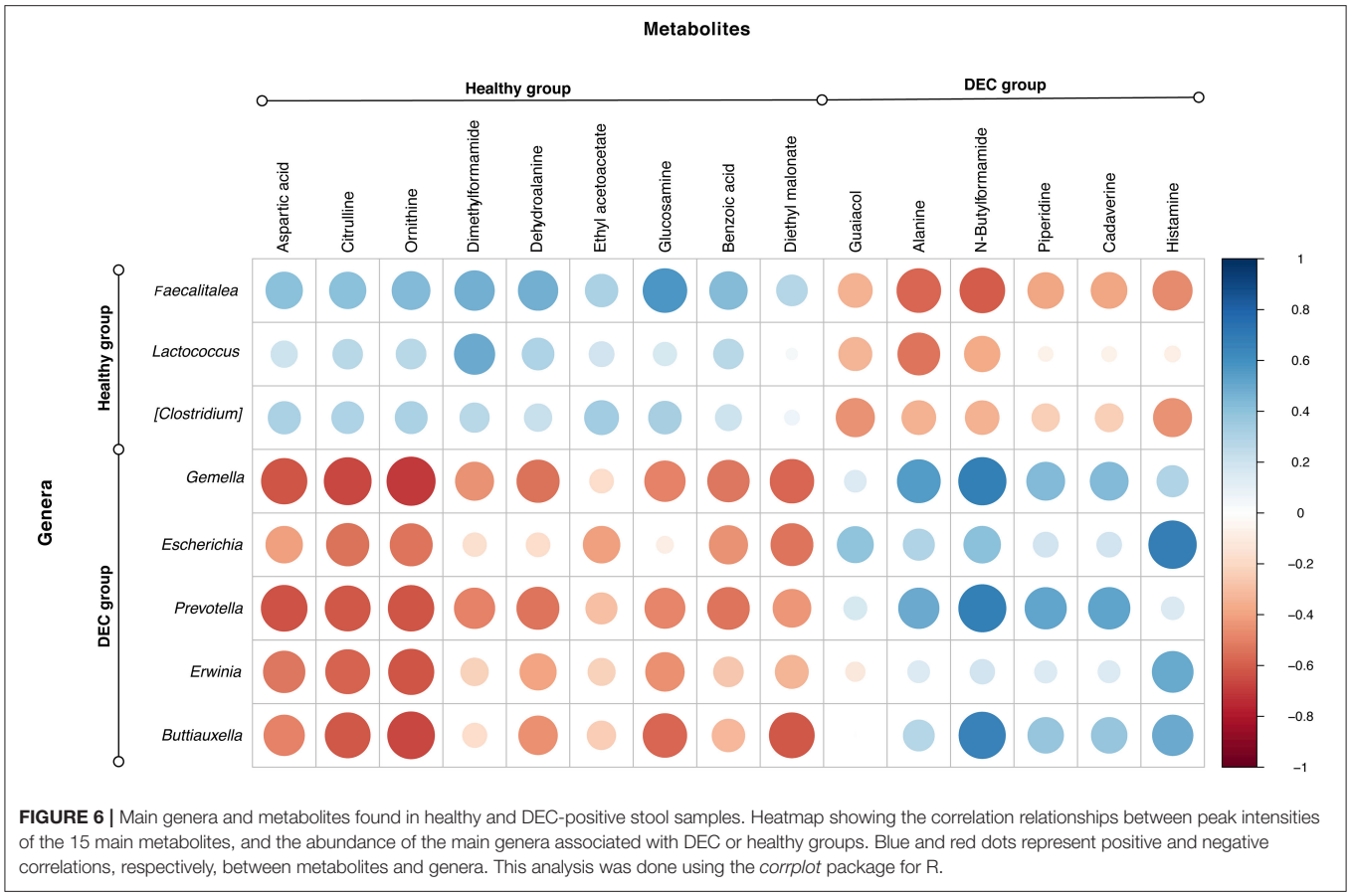

FIGURE 6 | Main genera and metabolites found in healthy and DEC-positive stool samples. Heatmap showing the correlation relationships between peak intensities of the 15 main metabolites, and the abundance of the main genera associated with DEC or healthy groups. Blue and red dots represent positive and negative correlations, respectively, between metabolites and genera. This analysis was done using the *corrplot* package for R.

(**Figure 5**). Considering this well-conserved metabolomic and commensal community structure among the groups, we then sought to identify which metabolic pathways could be involved in what was observed. We found by functional predictions from amplicon sequences that L-histidine biosynthesis and degradation pathways, as well as the L-ornithine biosynthesis route, were significantly different between the DEC and healthy groups (**Figure 6**). These predictions are in agreement with the low levels of ornithine and histidine detected in the DEC group compared to healthy groups (**Table 2**; **Supplementary Table 1**). Interestingly, we found that histamine, a product of L-histidine decarboxylation, was significantly higher in the DEC group compared to the healthy groups (**Figure 4**). In the gut, histamine is produced by immune cells such as mast cells, and its secretion could be influenced by cytokines such as IL-18, TNF-α, IL-12, and IL-1, among others (O'mahony et al., 2011). In commensal bacteria, such as *E. coli*, histamine has been linked to endogenous biosynthetic pathways (Kyriakidis et al., 2008) in Ca^{2+}-mediated signals (Theodorou et al., 2009) and its chemotaxis (Theodorou et al., 2012). The role of histamine could be directly linked to *E. coli* adherence, as evidence has shown that histamine inhibits the clearance of *E. coli* from the host peritoneal cavity in a peritonitis mouse model (Hori et al., 2002). Related to ornithine, we found lower levels of this metabolite in the DEC samples than in the healthy ones. L-ornithine can be produced in the urea cycle by the enzyme arginase, using arginine as the substrate. Once produced, L-ornithine is transformed to citrulline by the enzyme ornithine carbamoyltransferase (Wu, 1998). Arginine levels were similar in both groups, but citrulline and ornithine levels were higher in healthy samples (**Table 2**). L-ornithine production has been associated with a healthy gut mucosa. A recent study showed that L-ornithine administered to mice resulted in goblet cell production, mucin secretion and cell proliferation, which are associated with a healthier gut environment (Qi et al., 2019). Together with these results, L-ornithine also induces accumulation of IL-22 in intestinal tissues (Qi et al., 2019), a cytokine involved in the reconstitution of gut epithelial cells, improving mucus production by goblet cells, increasing the production of antimicrobial peptides and modulating genes involved in wound healing (Sun et al., 2012). Overall, these observations suggest that histamine and L-ornithine might be important signaling molecules in DEC pathogenesis and merit further investigation.

MIMOSA2 modeling of the 15 metabolites statistically associated with the study groups suggested that only 2 metabolite (ornithine and histamine) variations depend on the presence of specific taxa. Among the taxa associated with the positive contribution of histamine and ornithine levels, *Escherichia* sp., *Streptococcus anginosus*, *Citrobacter werkmanii/Citrobacter freundii,* and other species were found to increase the variability

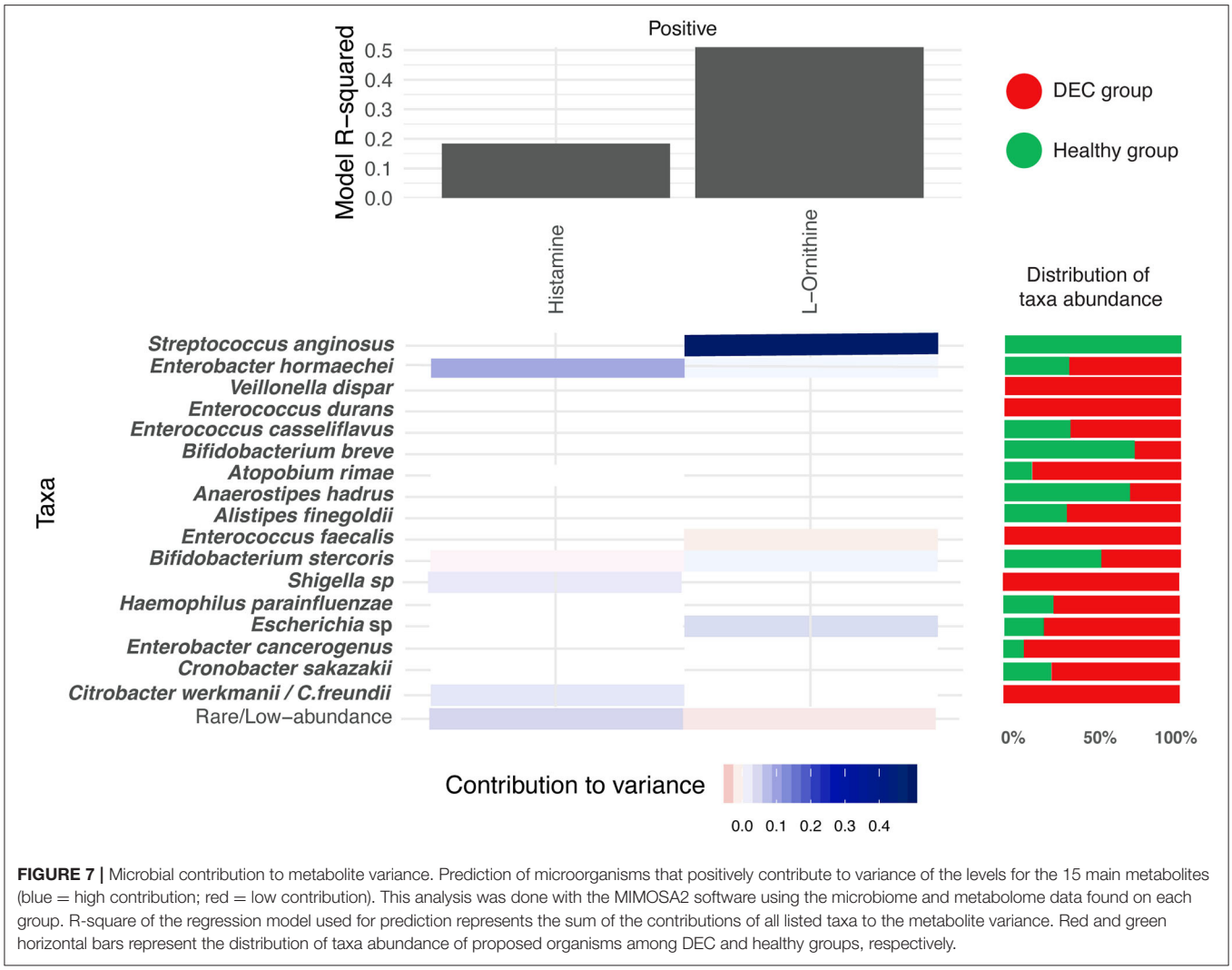

FIGURE 7 | Microbial contribution to metabolite variance. Prediction of microorganisms that positively contribute to variance of the levels for the 15 main metabolites (blue = high contribution; red = low contribution). This analysis was done with the MIMOSA2 software using the microbiome and metabolome data found on each group. R-square of the regression model used for prediction represents the sum of the contributions of all listed taxa to the metabolite variance. Red and green horizontal bars represent the distribution of taxa abundance of proposed organisms among DEC and healthy groups, respectively.

of these metabolites (**Figure 7**). Within these genera, *Escherichia coli* has been identified as being responsible for histamine production (Barcik et al., 2016, 2017), suggesting that during DEC infection, histamine levels could be modulated by pathogen metabolism. For the other 13 metabolites, the metabolic potential scores of identified taxa were not predictive according to the MIMOSA2, meaning that metabolite levels could not be attributed to specific taxa of the DEC or the healthy group. However, piperidine and cadaverine have been associated with virulence in enteropathogens. A decrease in *S. flexneri* invasion to cells was found in the presence of ornithine; this effect was found to be counteracted by the presence of cadaverine, a polyamine produced by lysine decarboxylation (Durand and Bjork, 2009). In the intestine, cadaverine is cyclated to piperidine, a molecule that reduces the invasion of *S. typhimurium* and the recruitment of polymorphonuclear neutrophils (Kohler et al., 2002). It would be interesting to evaluate the role that piperidine and cadaverine might play in the virulence of DEC, as well as the other metabolites significantly associated with the DEC group.

Our study has limitations. We analyzed a small number of samples and therefore our results should be considered as an exploratory approach. However, our data provided valuable information about the importance of gut microbiota and metabolome analysis in understanding the regulatory mechanism of DEC virulence. It is important to note that our metabolome analysis did not include metabolites that have been previously proven to have an impact on DEC virulence, such as SCFAs, because the primary goal of this study was to identify new pathways or metabolites that might be important to DEC pathogenicity. From this study we obtained an effect size value of 0.4377, which will be used to obtain the required sample size for further studies to confirm our observations, as well as *in vitro* infection experiments to evaluate the role of metabolites significantly associated with the DEC group as signaling molecules involved in DEC virulence regulation.

In conclusion, our study showed that stool samples from healthy children and children positive for DEC displayed a differential metabolome and microbiota composition. We found a correlation between gut microbiota species and certain

metabolites, information that might be useful in identifying mechanisms and signaling molecules implicated in the crosstalk between microbiota and DEC pathotypes that might participate in the virulence of these pathogens.

DATA AVAILABILITY STATEMENT

The datasets presented in this study can be found in online repositories. The names of the repository/repositories and accession number(s) can be found below: https://www.ncbi.nlm.nih.gov/, PRJNA623942.

ETHICS STATEMENT

The studies involving human participants were reviewed and approved by Ethical Committee of Universidad de Chile. Written informed consent to participate in this study was provided by the participants' legal guardian/next of kin.

AUTHOR CONTRIBUTIONS

PG participated in sample processing, performed sequences and metabolites analyses, interpreted the data, and participated in manuscript writing. MI participated in data analysis and manuscript writing. RV participated in study design and data analysis. FS participated in data analysis and manuscript writing. JO participated in data analysis. MF participated in study design, data acquisition and interpretation, manuscript writing, and final approval of the manuscript. All authors contributed to the article and approved the submitted version.

FUNDING

This work was supported by FONDECYT grants 1160426 and 1200994 awarded to MF and 1161161 to RV. PG and MI were supported by a doctoral fellowship from ANID.

ACKNOWLEDGMENTS

We are very thankful to Dr. Cecilia Noecker for her help and guidance with MIMOSA2 settings.

SUPPLEMENTARY MATERIAL

The Supplementary Material for this article can be found online at: https://www.frontiersin.org/articles/10.3389/fcimb.2020.00485/full#supplementary-material

REFERENCES

Alvestegui, A., Olivares-Morales, M., Munoz, E., Smith, R., Nataro, J. P., Ruiz-Perez, F., et al. (2019). TLR4 participates in the inflammatory response induced by the AAF/II fimbriae from enteroaggregative *Escherichia coli* on intestinal epithelial cells. *Front. Cell Infect. Microbiol.* 9:143. doi: 10.3389/fcimb.2019.00143

Barcik, W., Pugin, B., Westermann, P., Perez, N. R., Ferstl, R., Wawrzyniak, M., et al. (2016). Histamine-secreting microbes are increased in the gut of adult asthma patients. *J. Allergy Clin. Immunol.* 138, 1491–1494 e1497. doi: 10.1016/j.jaci.2016.05.049

Barcik, W., Wawrzyniak, M., Akdis, C. A., and O'mahony, L. (2017). Immune regulation by histamine and histamine-secreting bacteria. *Curr. Opin. Immunol.* 48, 108–113. doi: 10.1016/j.coi.2017.08.011

Caporaso, J. G., Kuczynski, J., Stombaugh, J., Bittinger, K., Bushman, F. D., Costello, E. K., et al. (2010). QIIME allows analysis of high-throughput community sequencing data. *Nat. Methods* 7, 335–336. doi: 10.1038/nmeth.f.303

Carlson-Banning, K. M., and Sperandio, V. (2018). Enterohemorrhagic *Escherichia coli* outwits hosts through sensing small molecules. *Curr. Opin. Microbiol.* 41, 83–88. doi: 10.1016/j.mib.2017.12.002

Chong, J., and Xia, J. (2018). MetaboAnalystR: an R package for flexible and reproducible analysis of metabolomics data. *Bioinformatics* 34, 4313–4314. doi: 10.1093/bioinformatics/bty528

Croxen, M. A., Law, R. J., Scholz, R., Keeney, K. M., Wlodarska, M., and Finlay, B. B. (2013). Recent advances in understanding enteric pathogenic *Escherichia coli*. *Clin. Microbiol. Rev.* 26, 822–880. doi: 10.1128/CMR.00022-13

Curtis, M. M., Hu, Z., Klimko, C., Narayanan, S., Deberardinis, R., and Sperandio, V. (2014). The gut commensal *Bacteroides thetaiotaomicron* exacerbates enteric infection through modification of the metabolic landscape. *Cell Host Microbe* 16, 759–769. doi: 10.1016/j.chom.2014.11.005

De Caceres, M., and Legendre, P. (2009). Associations between species and groups of sites: indices and statistical inference. *Ecology* 90, 3566–3574. doi: 10.1890/08-1823.1

Desantis, T. Z., Hugenholtz, P., Larsen, N., Rojas, M., Brodie, E. L., Keller, K., et al. (2006). Greengenes, a chimera-checked 16S rRNA gene database and workbench compatible with ARB. *Appl. Environ. Microbiol.* 72, 5069–5072. doi: 10.1128/AEM.03006-05

Douglas, G. M., Maffei, V. J., Zaneveld, J., Yurgel, S. N., Brown, J. R., Taylor, C. M., et al. (2020). PICRUSt2 for prediction of metagenome functions. *Nat. Biotechnol.* 38, 685–688. doi: 10.1038/s41587-020-0548-6

Durand, J. M. B., and Bjork, G. R. (2009). Metabolic control through ornithine and uracil of epithelial cell invasion by *Shigella flexneri*. *Microbiology* 155, 2498–2508. doi: 10.1099/mic.0.028191-0

Gallardo, P., Izquierdo, M., Vidal, R. M., Chamorro-Veloso, N., Rossello-Mora, R., O'ryan, M., et al. (2017). Distinctive gut microbiota is associated with Diarrheagenic *Escherichia coli* infections in Chilean children. *Front. Cell. Infect. Microbiol.* 7:424. doi: 10.3389/fcimb.2017.00424

Hori, Y., Nihei, Y., Kurokawa, Y., Kuramasu, A., Makabe-Kobayashi, Y., Terui, T., et al. (2002). Accelerated clearance of *Escherichia coli* in experimental peritonitis of histamine-deficient mice. *J. Immunol.* 169, 1978–1983. doi: 10.4049/jimmunol.169.4.1978

Jeffery, I. B., Das, A., O'herlihy, E., Coughlan, S., Cisek, K., Moore, M., et al. (2019). Differences in fecal microbiomes and metabolomes of people with vs without irritable Bowel syndrome and bile acid malabsorption. *Gastroenterology* 158, 1016–1028.e8. doi: 10.1053/j.gastro.2019.11.301

Kanehisa, M., and Goto, S. (2000). KEGG: kyoto encyclopedia of genes and genomes. *Nucleic Acids Res.* 28, 27–30. doi: 10.1093/nar/28.1.27

Kohler, H., Rodrigues, S. P., Maurelli, A. T., and Mccormick, B. A. (2002). Inhibition of *Salmonella typhimurium* enteropathogenicity by piperidine, a metabolite of the polyamine cadaverine. *J. Infect. Dis.* 186, 1122–1130. doi: 10.1086/344236

Kumar, A., and Sperandio, V. (2019). Indole signaling at the host-microbiota-pathogen interface. *mBio* 10:e01031-19. doi: 10.1128/mBio.01031-19

Kyriakidis, D. A., Theodorou, M. C., Filippou, P. S., Kyriakidis, K. D., and Tiligada, E. (2008). Effect of histamine on the signal transduction of the AtoS-AtoC two component system and involvement in poly-(R)-3-hydroxybutyrate biosynthesis in *Escherichia coli*. *Amino Acids* 35, 45–52. doi: 10.1007/s00726-007-0635-8

Langille, M. G., Zaneveld, J., Caporaso, J. G., Mcdonald, D., Knights, D., Reyes, J. A., et al. (2013). Predictive functional profiling of microbial communities

using 16S rRNA marker gene sequences. *Nat. Biotechnol.* 31, 814–821. doi: 10.1038/nbt.2676

Ludwig, W., Strunk, O., Westram, R., Richter, L., Meier, H., Buchner, A., et al. (2004). ARB: a software environment for sequence data. *Nucleic Acids Res.* 32, 1363–1371. doi: 10.1093/nar/gkh293

Noecker, C., Eng, A., Srinivasan, S., Theriot, C. M., Young, V. B., Jansson, J. K., et al. (2016). Metabolic model-based integration of microbiome taxonomic and metabolomic profiles elucidates mechanistic links between ecological and metabolic variation. *mSystems* 1:e00013-15. doi: 10.1128/mSystems.00013-15

Noorbakhsh, H., Yavarmanesh, M., Mortazavi, S. A., Adibi, P., and Moazzami, A. A. (2019). Metabolomics analysis revealed metabolic changes in patients with diarrhea-predominant irritable bowel syndrome and metabolic responses to a synbiotic yogurt intervention. *Eur. J. Nutr.* 58, 3109–3119. doi: 10.1007/s00394-018-1855-2

Oksanen, J., Blanchet, F. G., Friendly, M., Kindt, R., Legendre, P., Mcglinn, D., et al. (2019). *vegan: Community Ecology Package.* Retrieved from https://CRAN.R-project.org/package=vegan

O'mahony, L., Akdis, M., and Akdis, C. A. (2011). Regulation of the immune response and inflammation by histamine and histamine receptors. *J. Allergy Clin. Immunol.* 128, 1153–1162. doi: 10.1016/j.jaci.2011.06.051

Pacheco, A. R., Curtis, M. M., Ritchie, J. M., Munera, D., Waldor, M. K., Moreira, C. G., et al. (2012). Fucose sensing regulates bacterial intestinal colonization. *Nature* 492, 113–117. doi: 10.1038/nature11623

Parks, D. H., Tyson, G. W., Hugenholtz, P., and Beiko, R. G. (2014). STAMP: statistical analysis of taxonomic and functional profiles. *Bioinformatics* 30, 3123–3124. doi: 10.1093/bioinformatics/btu494

Press, W. (2014). *World Health Statistics*. Geneva.

Pruesse, E., Peplies, J., and Glockner, F. O. (2012). SINA: accurate high-throughput multiple sequence alignment of ribosomal RNA genes. *Bioinformatics* 28, 1823–1829. doi: 10.1093/bioinformatics/bts252

Qi, H., Li, Y., Yun, H., Zhang, T., Huang, Y., Zhou, J., et al. (2019). *Lactobacillus* maintains healthy gut mucosa by producing L-Ornithine. *Commun. Biol.* 2:171. doi: 10.1038/s42003-019-0424-4

Quast, C., Pruesse, E., Yilmaz, P., Gerken, J., Schweer, T., Yarza, P., et al. (2013). The SILVA ribosomal RNA gene database project: improved data processing and web-based tools. *Nucleic Acids Res.* 41, D590–D596. doi: 10.1093/nar/gks1219

Rolhion, N., and Chassaing, B. (2016). When pathogenic bacteria meet the intestinal microbiota. *Philos. Trans. R. Soc. Lond. B. Biol. Sci.* 371:20150504. doi: 10.1098/rstb.2015.0504

Sun, X., Chalmers, L., Fu, X., and Zhao, M. (2012). A molecular link between interleukin 22 and intestinal mucosal wound healing. *Adv. Wound Care* 1, 231–237. doi: 10.1089/wound.2011.0334

Sun, Y., and O'riordan, M. X. (2013). Regulation of bacterial pathogenesis by intestinal short-chain fatty acids. *Adv. Appl. Microbiol.* 85, 93–118. doi: 10.1016/B978-0-12-407672-3.00003-4

Thaiss, C. A., and Elinav, E. (2014). Exploring new horizons in microbiome research. *Cell Host Microbe* 15, 662–667. doi: 10.1016/j.chom.2014.05.016

Theodorou, M. C., Theodorou, E. C., and Kyriakidis, D. A. (2012). Involvement of AtoSC two-component system in *Escherichia coli* flagellar regulon. *Amino Acids* 43, 833–844. doi: 10.1007/s00726-011-1140-7

Theodorou, M. C., Tiligada, E., and Kyriakidis, D. A. (2009). Extracellular Ca2+ transients affect poly-(R)-3-hydroxybutyrate regulation by the AtoS-AtoC system in *Escherichia coli*. *Biochem. J.* 417, 667–672. doi: 10.1042/BJ20081169

Vogt, S. L., Pena-Diaz, J., and Finlay, B. B. (2015). Chemical communication in the gut: effects of microbiota-generated metabolites on gastrointestinal bacterial pathogens. *Anaerobe* 34, 106–115. doi: 10.1016/j.anaerobe.2015.05.002

Wei, T., and Simko, V. (2017). *R Package "corrplot": Visualization of a Correlation Matrix*. Available online at: https://github.com/taiyun/corrplot.

Wickham, H. (2016). *ggplot2: Elegant Graphics for Data Analysis*. New York, NY: Springer-Verlag.

Wu, G. (1998). Intestinal mucosal amino acid catabolism. *J. Nutr.* 128, 1249–1252. doi: 10.1093/jn/128.8.1249

Conflict of Interest: The authors declare that the research was conducted in the absence of any commercial or financial relationships that could be construed as a potential conflict of interest.

frontiers in Cellular and Infection Microbiology

ORIGINAL RESEARCH
published: 25 September 2020
doi: 10.3389/fcimb.2020.549919

Prevalence of Enteropathogens and Virulence Traits in Brazilian Children With and Without Diarrhea

Victor R. Merino[1†], Viviane Nakano[1†‡], Sabine Delannoy[2], Patrick Fach[2], Gabriela G. F. Alberca[1], Mauricio J. Farfan[3], Roxane M. F. Piazza[4]* and Mario J. Avila-Campos[1]*

[1] Laboratório de Anaeróbios, Departamento de Microbiologia, Instituto de Ciências Biomédicas, Universidade of São Paulo, São Paulo, Brazil, [2] Agence Nationale de Sécurité Sanitaire de l'Alimentation, de l'Environnement et du Travail, Food Safety Laboratory, Université Paris-Est, Champs-sur-Marne, France, [3] Departamento de Pediatría y Cirugía Infantil, Facultad de Medicina, Campus Oriente-Hospital Dr. Luis Calvo Mackenna, Universidad de Chile, Santiago, Chile, [4] Laboratório de Bacteriologia, Instituto Butantan, São Paulo, Brazil

The use of molecular diagnostics for pathogen detection in epidemiological studies have allowed us to get a wider view of the pathogens associated with diarrhea, but the presence of enteropathogens in asymptomatic individuals has raised several challenges in understanding the etiology of diarrhea, and the use of these platforms in clinical diagnosis as well. To characterize the presence of the most relevant bacterial enteropathogens in diarrheal episodes, we evaluated here the prevalence of diarrheagenic *E. coli* pathotypes, *Salmonella* spp., and *Yersinia enterocolitica* in stool samples of children with and without diarrhea using real-time quantitative PCR (qPCR). We found that the presence of genetic markers associated with bacterial pathogens was significantly higher in stool samples from the diarrhea group compared to the control ($P < 0.001$). Bacterial loads in samples positive for *eae* and *aggR* markers were also determined. Compared to samples from asymptomatic children, a significantly higher number of copies of the *eae* gene were found in diarrhea samples. Also, the presence of genetic markers associated with STEC strains with clinical significance was evaluated in *eae*-positive samples by high-throughput real-time PCR. The data presented herein demonstrated that asymptomatic children of an urban area in Brazil might be enteropathogen reservoirs, especially for STEC.

Keywords: enteric pathogens, *Escherichia coli* pathotypes, diarrheal children, healthy children, molecular diagnostics

OPEN ACCESS

Edited by:
Jorge Eugenio Vidal, University of Mississippi Medical Center, United States

Reviewed by:
Javier Sanchez-Villamil, The University of Texas Medical Branch at Galveston, United States
Miguel Angel Garcia Bereguiain, University of the Americas, Ecuador

***Correspondence:**
Roxane M. F. Piazza
roxane.piazza@butantan.gov.br
Mauricio J. Farfan
mfarfan@med.uchile.cl

In Memoriam:
This work is dedicated to Prof. Dr. Mario J. Avila-Campos who conceived and supervised this project

†These authors have contributed equally to this work

‡Present address:
Viviane Nakano, GeneOne, DASA, São Paulo, Brazil

Specialty section:
This article was submitted to Clinical Microbiology, a section of the journal Frontiers in Cellular and Infection Microbiology

Received: *07 April 2020*
Accepted: *25 August 2020*
Published: *25 September 2020*

Citation:
Merino VR, Nakano V, Delannoy S, Fach P, Alberca GGF, Farfan MJ, Piazza RMF and Avila-Campos MJ (2020) Prevalence of Enteropathogens and Virulence Traits in Brazilian Children With and Without Diarrhea. Front. Cell. Infect. Microbiol. 10:549919. doi: 10.3389/fcimb.2020.549919

INTRODUCTION

Diarrheal disease is the second most important cause of child morbidity and mortality in the world, and is frequently due to contaminated food and water. Worldwide, 780 million individuals lack access to safe drinking water and 2.5 billion lack adequate sanitation. Diarrhea is widespread throughout developing countries. In low-income countries, children under 3 years old experience on average three episodes of diarrhea every year (World Health Organization, 2017).

Rotavirus and diarrheagenic *Escherichia coli* (DEC) are the two most common etiological agents of moderate-to-severe diarrhea in low-income countries (World Health Organization, 2017). Other pathogens such as Cryptosporidium, Shigella, *Campylobacter*, *Salmonella*, and *Yersinia* species also cause human bacterial gastroenteritis, but location-specific etiological patterns also need to be considered (Bottone, 1999; Freitas Neto et al., 2010; Marinou et al., 2012; Nunes et al., 2012; World Health Organization, 2017; Lima F. M. et al., 2019; Leli et al., 2020).

Enterotoxigenic *E. coli* (ETEC), enteroinvasive *E. coli* (EIEC), typical and atypical enteropathogenic *E. coli* (tEPEC and aEPEC), typical and atypical enteroaggregative *E. coli* (tEAEC and aEAEC), and Shiga toxin-producing *E. coli* (STEC) and its subgroup enterohemorrhagic *E. coli* (EHEC), enteroinvasive *E. coli* (EIEC), and diffusely adherent *E. coli* (DAEC) comprise DEC pathotypes (Kaper et al., 2004; Gomes et al., 2016). These pathogens use many common features to colonize the intestinal mucosa and trigger disease, but its initiation, progression, and complications vary considerably (Croxen et al., 2013). Thus, ETEC isolates carry the enterotoxins LT and/or ST on plasmids, as well as colonization factors (CFs). tEPEC, aEPEC, and LEE-positive STEC strains (EHEC) carry the locus of enterocyte effacement (LEE) which contains *eae*, the gene that encodes intimin, but only tEPEC has the bundle-forming pilus gene (bfp). STEC strains, LEE-positive and -negative, carry the Shiga toxin genes (stx1 and/or stx2). Some virulence factors for EAEC for a certain group of isolates are found on the pAA plasmid, and the presence of the *aggR* gene differentiates tEAEC from aEAEC. EIEC and also *Shigella spp*. have the ability to invade cells mainly through the pINV plasmid and acquired additional virulence attributes mainly from chromosomal pathogenicity islands (PAIs) (Croxen et al., 2013).

Nevertheless, the designation of certain isolates into a pathotype is complicated due to the plasticity of the *E. coli* genome resulting in the emergence of hybrid strains; besides, DEC epidemiology varies in different regions of the world and may depend on the host and environmental factors (Croxen et al., 2013). It is important to note that DEC pathotypes have been largely disregarded because of the lack of laboratory capabilities (Piazza et al., 2010; Miliwebsky et al., 2016). Moreover, in several case-control studies, it shows almost equal distribution, especially in EPEC and EAEC pathotypes (Bueris et al., 2007; Hernandes et al., 2009; Gomes et al., 2016; Imdad et al., 2018; Dias et al., 2020).

Besides LEE-positive pathogens and *Shigella*, *Salmonella* also uses the type III secretion system (T3SS) apparatus to deliver effector proteins into the host cell, and *invA*, an inner-membrane component, is critical to the functioning of *Salmonella* T3SS (Galán et al., 1992; Ginocchio and Galán, 1995). In addition, the most common virulence-associated gene in pathogenic Yersinia enterocolitica proved to be *ystA*, which can therefore be considered the best target gene to be amplified to evaluate the presence of pathogenic biotypes (Peruzy et al., 2017).

The use of multiple pathogen detection platforms in epidemiological studies have allowed us to get a broader view of the pathogens associated with diarrhea, but the presence of enteropathogens in asymptomatic individuals has raised several challenges in understanding the etiology of diarrhea, as well as the use of these platforms in clinical diagnosis (Liu et al., 2012; Lima A. A. M et al., 2019). The use of real-time quantitative PCR (qPCR) to determine bacterial loads in stool samples appears as an alternative to associate a pathogen with diarrheal cases.

To determine the most prevalent bacterial pathogens of diarrhea in children, we used qPCR to detect and quantify the presence of EPEC, ETEC, EAEC, STEC, EIEC, *Shigella*, *Salmonella*, and *Y. enterocolitica*. Furthermore, in a subset of *eae*-positive samples, we analyzed by high-throughput real-time PCR the presence of genetic markers related to EHEC strains with clinical significance.

MATERIALS AND METHODS

Sample Collection, Ethical, and Biosafety Procedures

Stool samples were obtained from 110 children with diarrhea (54 boys and 56 girls) and 150 children without diarrhea (71 boys and 79 girls), aged from 1 month to 7 years old. Stool samples were collected from March 2008 through November 2010 at Hospital Municipal do Tatuapé, Hospital Infantil Cândido Fontoura, Hospital Infantil Menino Jesus and Centro Educacional Unificado (CEU-Butantã) in Sao Paulo city, SP, Brazil. Children did not display illnesses or comorbidities other than diarrhea, and they were not under antibiotic treatment for at least 3 months prior to sample collection. Diarrhea was defined as three or more unformed stools in the 24 h prior to enrollment. The Ethics Committee of the Biomedical Science Institute at the University of Sao Paulo approved this study (2006/743). All procedures followed the management of biosafety and biosecurity, since Biomedical Science Institute at São Paulo University guarantees excellent conditions for workers and population, and environmental protection from biohazards exposure.

DNA Extraction

Total DNA from 200 mg of stool was obtained by using a QIAamp DNA Stool Mini Kit (QIAGEN) according to the manufacturer's instructions, resuspended in 100 μL of ultrapure water and stored at −80°C until use. DNA concentrations were determined by spectrophotometer (NanoDrop 2000, Thermo Scientific, USA), and 5 μL of each DNA sample were checked for integrity on 1% agarose gel.

Identification of the Main Enteric Pathogens by qPCR

qPCR assays for genes *eae* (attaching and effacing lesions), *ipaH* (enteroinvasive mechanism), *lt* (heat-labile toxin), *st* (heat-stable toxin), *aggR* (aggregative fimbriae regulator), *invA* [inner membrane component of the *Salmonella* T3SS apparatus], and *ystA* (enterotoxin YstA *Yersinia* virulence plasmid) were carried out in duplicate and performed in a total volume of 25 μL, containing 2X TaqMan universal master mix (Applied Biosystems, USA), 10 μM of each primer, 10 μM of TaqMan probe, and 2 ng of DNA. Amplifications were performed in a

thermal cycler programmed as follows: denaturation at 95°C for 10 min, followed by 45 cycles of two steps: denaturation at 95°C for 15 s and an annealing temperature at 60°C for 1 min. The primer/probe sets used are shown in **Supplementary Table 1**. A standard curve was also derived using 10-fold DNA dilutions from the reference strains with their respective primer pairs. Amplifications were adjusted to $R^2 > 0.900$. A $P < 0.05$ was considered statistically significant. A sample was considered positive for a target gene when the detected fluorescence generated a curve above the background fluorescence, which was established by the Rotor-Gene Q6000 analytical software (Qiagen, Brazil).

Differentiation of Enteric Pathogens by PCR

Samples positive for *eae* ($n = 57$) and *ipaH* ($n = 15$) by real-time PCR were further screened for the *eae*, *bfpA* (bundle-forming pilus for typical EPEC), *ipaH*, *lacY* (lactose permease), and *stx1* and *stx2* (Shiga toxins) genes by multiplex PCR according to the protocol of Aranda et al. (2004) and Pavlovic et al. (2011) for differentiation between EPEC/STEC and EIEC/*Shigella* samples.

Characterization of the *eae*-positive Samples by High-Throughput Real-Time PCR

A LightCycler® 1536 (Roche, Meylan, France) was used to perform high-throughput real-time PCR amplifications as described previously (Delannoy et al., 2012b), except that 1 μL of sample DNA was used in each reaction for a final reaction volume of 2 μL. The thermal profile was modified as follows: 95°C for 1 min, followed by 45 cycles of 95°C for 0 s, and 58°C for 30 s. All ramp rates were set to 2°C/s. The primers and probes used targeted genes encoding intimin (*eae*, *eae*-alpha, *eae*-beta, *eae*-gamma, *eae*-epsilon, and *eae*-theta), O group-associated genes for the top 7 serogroups (wzx_{O26}, $rfbE_{\_O157}$, $wzy_{\_O145}$, $wzx_{\_O103}$, $wbdl_{\_O111}$, $wzx_{\_O121}$, $wzx_{\_O45}$,), flagellar antigens H11, H19, H2, H28, H7, and H8 (*fliC*H11, *fliC*H19, *fliC*H2, *fliC*H28, *fliC*H7, and *fliC*H8), urease (*ureD*), effector proteins translocated by T3SS (EspL2 [*ent* {or *espL2*}], NleB [*nleB*], NleE [*nleE*], NleA [*nleA*], NleF [*nleF*], EfA1 [*efa1*], EspN [*espN*], EspK [*espK*], and EspM1 [*espM1*]), and other genetic markers including Z6065, *Z2098, Z2099, terE, hlyA, ehxA, and pagC* and markers related to the CRISPR loci *SP_O157_A, SP_O157_B, SP_O157_C, SP_O26_C, SP_O26_D, SP_O26_E* (Perelle et al., 2004; Fratamico et al., 2009, 2010; Bugarel et al., 2010; Delannoy et al., 2012a, 2013, 2015, 2016; Piazza et al., 2013). The *wecA* gene was used as a reference genetic marker for *E. coli* (Bugarel et al., 2011). An inhibition control (IC) was introduced in each sample to check for potential inhibition of the PCR reaction due to intrinsic characteristics of the sample. IC is a recombinant pBluescriptIISK+ plasmid containing the *dsb* gene from *Ehrlichia canis* (Michelet et al., 2014). The plasmid was added to each sample at a concentration of ∼0.3 pg/μL. Primers and probe specific for the *Ehrlichia canis dsb* gene were used to detect IC (Michelet et al., 2014).

Statistical Analyses

We compared the presence of pathogen between groups using the Fisher exact test. A comparison of bacterial loads in *eae*- and *aggR*-positive samples between samples from children with and without diarrhea was performed with a Mann-Whitney *U*-test. A $P < 0.05$ was considered statistically significant. All statistical analyses were performed in Stata v.12.1.

RESULTS

Prevalence of Enteropathogens in Stool Samples Obtained From Children With and Without Diarrhea

A total of 260 stool samples (110 from children with diarrhea and 150 children without diarrhea) were collected from public hospitals and schools, respectively, in Sao Paulo city (the largest city in South America) from March 2008 through November 2010. The groups studied consisted of children between 1 month and 7 years old, representing much of childhood. Each group was further divided into 3 age groups: 0–11 months, 12–23 months, and older than 24 months. The pathogens detected through their representative genetic markers in the stool samples from children with and without diarrhea of different age are reported in **Table 1**.

No genetic markers were detected in 39 of 110 (35%) children with diarrhea and 92 out of 150 (61%) without diarrhea. The presence of genetic markers associated with bacterial pathogens was significantly higher in stool samples from the diarrhea group (71/110) compared to the control (58/150) ($P < 0.001$). A significant increase in the number of samples positive for one pathogen was found in the diarrhea samples (46/110) compared to asymptomatic group (39/150) ($P = 0.0036$). Although we observed statistical differences between groups in samples with 3 or 4 pathogens, in both groups, the number of samples is low, not allowing further conclusions (**Table 2**).

Bacterial Loads in *eae*- and *aggR*-Positive Samples

Quantification of bacterial loads was shown to be a promising tool to identify the etiological agent of diarrheal diseases. Of all the genes evaluated, *aggR* and *eae* were the markers most found in diarrheal and asymptomatic children (71 and 56 samples, respectively). We compared the copy number of *eae* and *aggR* genes in all the samples positive for these markers in both diarrhea and asymptomatic groups (**Figure 1**). A significantly higher copy number of *eae* was found in diarrhea samples ($P < 0.039$); no differences in *aggR* copy number were found between groups ($P = 0.43$).

Prevalence of EHEC-Associated Virulence Markers in *eae*-positive Stool Samples From Children With and Without Diarrhea

In the control group, we detected 13% *eae*-positive samples and 11% *stx*-positive samples, while in the diarrhea group, 34% *eae*-positive samples, and 27%-*stx* positive samples were present,

TABLE 1 | Distribution of virulence genes from enteric pathogens in fecal samples from children with and without diarrhea.

Pathogens detected	Genetic markers	Asymptomatic group ($n = 150$)				Diarrhea group ($n = 110$)				*P*-value
		0–11 months ($n = 54$)	12–23 months ($n = 59$)	> 24 months ($n = 37$)	Total	0–11 months ($n = 55$)	12–23 months ($n = 50$)	> 24 months ($n = 5$)	Total	
STEC	eae, stx1/stx2	2	4	0	6	2	9	0	11	0.19
EAEC	aagR	15	9	1	25	10	8	0	18	0.016
EPEC Typ	eae, bfp	0	1	0	1	1	0	0	1	0.44
EPEC atyp	eae	0	0	0	0	3	1	0	4	0.033
ETEC	lt/st	3	1	0	4	1	3	0	4	0.38
EIEC	ipaH, LacY	0	1	2	3	4	3	1	8	0.088
STEC EAEC	eae, aggR, stx1/stx2	3	1	0	4	1	2	0	3	0.25
STEC EPECtyp	eae, bfp, stx1/stx2	1	1	0	2	3	5	0	8	0.049
STEC ETEC	eae, stx1/stx2, lt/st	1	0	0	1	0	0	0	0	0.13
EAEC ETEC	aggR, lt/st	3	3	0	6	1	0	0	1	0.013
EAEC EPECtyp	aggR, eae, bfp	2	1	0	3	0	0	0	0	0.02
EAEC EIEC	aggR, ipaH, LacY	0	0	0	0	1	0	0	1	0.182
EAEC EPECatyp	aggR, eae	0	0	0	0	1	1	0	2	0.098
EAEC Salmonella	aagR, invA	0	0	0	0	0	1	0	1	0.18
STEC EAEC ETEC	eae, stx1/stx2, aggR, lt/st	1	1	0	2	0	0	0	0	0.057
STEC EAEC EPECtyp	eae, aggR, stx1/stx2, bfp	0	1	0	1	2	0	1	3	0.2
STEC EPECtyp EIEC	eae, stx1/stx2, bfp, ipaH, LacY	0	0	0	0	1	0	0	1	0.18
STEC EPECtyp ETEC	eae, stx1/stx2, bfp, lt/st	0	0	0	0	1	0	0	1	0.18
STEC EPECtyp Yersinia	eae, stx1/stx2, bfp, invA	0	0	0	0	1	0	0	1	0.18
STEC ETEC EIEC	eae, stx1/stx2, lt/st, ipaH, LacY	0	0	0	0	1	0	0	1	0.18
STEC EPECtyp ETEC EIEC	eae, stx1/stx2, bfp, lt/st, ipaH, Lacy	0	0	0	0	0	2	0	2	0.098

$P < 0.05$ was considered statistically significant.

TABLE 2 | Association of enteric pathogens in fecal samples from children with and without diarrhea determined by virulence genes presence.

Number of pathogens detected	Asymptomatic group ($n = 150$) Total	Diarrhea group ($n = 110$) Total	*P*-value
None	92	39	>0.001
Positive for 1 or more pathogens	58	71	>0.001
1 pathogen	39	46	0.0036
2 pathogens	16	16	0.1734
3 pathogens	3	7	0.0354
4 pathogens	0	2	0.0486

and thus, the presence of these genes were significantly higher in the diarrhea group. Surprisingly, our results indicated higher percentages of the majority of the additional genetic markers that are reported to be mostly predominant in EHEC in asymptomatic children (**Table 3**). Comparing all genetic markers, no differences were observed between the groups ($P = 0.312$), but the presence of the genes *stx2*, *ehxA*, *nleB*, *nleE*, *nleF*, *espM1*, *pagC*, *ent*, *efa1*, espV, Z2098, Z2099, Z6065, *terE*, *ureD*, and SP_O157 A, B, and C were statistically significant in the asymptomatic children compared to the diarrhea groups (*P*-values varying from 0.0001 to 0.0035) (**Table 3**).

DISCUSSION

A better knowledge of the distribution of pathogens linked to stool contamination is important for evaluating the pathogen loads in the environment as well as the associated health risks (Zhang et al., 2016). Over the last few decades, new molecular methods have become essential in allowing the rapid detection and characterization of pathogens (Miliwebsky et al., 2016).

The present study was performed to determine the molecular epidemiology of enteropathogens among children under seven years old with and without acute gastroenteritis in Sao Paulo, SP, Brazil. Virulence markers for DEC pathotypes were largely detected confirming some other surveys in Latin America and China (Ochoa et al., 2009; Moreno et al., 2010; Zhang et al., 2016; Lima A. A. M et al., 2019; Lima F. M. et al., 2019). Different results were reported in Western Kenya among bacterial pathogens, where two species of *Shigella* were the most prevalent (Swierczewski et al., 2013).

Our results showed that the genes encoding virulence factors for *Salmonella* and *Yersinia* were detected in very low frequencies, in agreement with another survey in counties near Sao Paulo city (Lima F. M. et al., 2019).

Herein, DEC-associated genetic markers were detected in 71 out of 110 (65%) children with diarrhea and 58 out of 150 (39%) without diarrhea and significant differences were observed between the two groups. These results are in agreement with other studies in South American countries. In Northeast Brazil, the presence of EPEC and EAEC were consistently associated

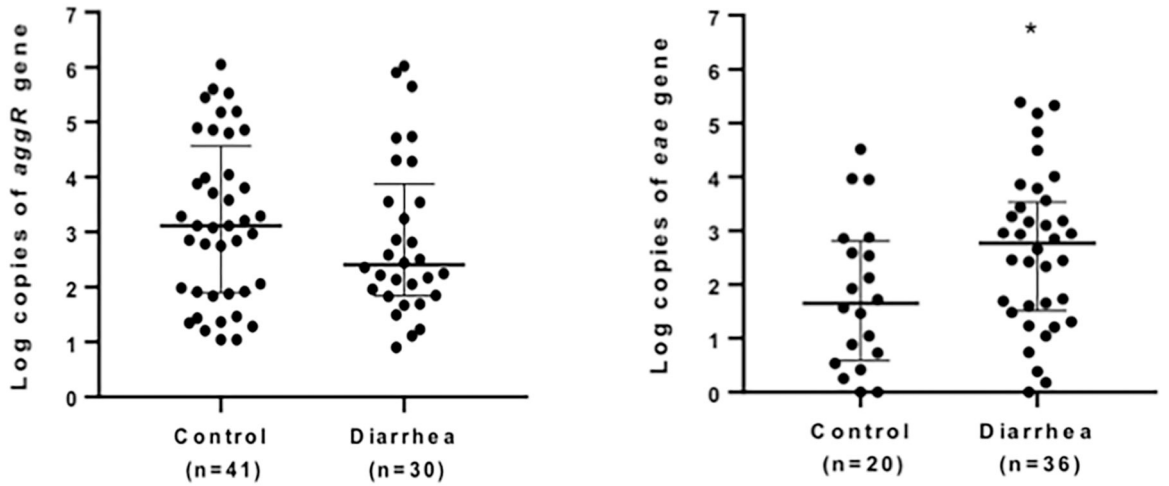

FIGURE 1 | Quantification of *eae*- and *aggR*- markers in stool. Positive stool samples for *aggR* (left) or *eae* (right) markers from children with (diarrhea group) or without (control) diarrhea were analyzed by quantitative qPCR. Data are presented as median log copy number/mg of stool sample ± IQR. *$P < 0.05$ (Mann-Whitney *U*-test).

with diarrhea (Maranhão et al., 2008; Moreno et al., 2010). Furthermore, EAEC and STEC showed by multivariate logistic regression analysis significant odds of being associated with a risk for diarrheal diseases as well as norovirus, adenovirus, rotavirus, and *Giardia* infection. Furthermore, EAEC enteric infections are associated with a high clinical severity score plus moderate-to-severe dehydration (Lima A. A. M et al., 2019).

The shifting in DEC epidemiology has been described in different studies and geographical regions (Pérez et al., 2010; Torres, 2017; Imdad et al., 2018; Pérez-Corrales and Leandro-Sandí, 2019) including Brazil, where until the 1990s, EPEC, mainly the typical EPEC serotypes producing EPEC adherence factor (EAF), was the main cause of infantile diarrhea (Gomes et al., 1991; Rosa et al., 1998; Regua-Mangia et al., 2004), and also *Salmonella* species (8%), ETEC (7%), and *Shigella* species (5%) were associated with diarrhea (Gomes et al., 1991), but it seems that they are becoming more and more rare, as presented herein and described elsewhere (Franzolin et al., 2005; Bueris et al., 2007; Moreno et al., 2010; Lima A. A. M et al., 2019; Lima F. M. et al., 2019; Ori et al., 2018).

The distribution of genes encoding either for one single pathogen in the diarrhea group (66%) and in control (67%) or in multiple coinfections, 34 and 33%, respectively, was similar in the present study. However, except for *Salmonella* plus *E. coli* and *Yersinia* plus *E. coli*, we cannot assure that we detected different strains, since they were not isolated from stools. Nevertheless, coinfections have been described, suggesting associations among potential enteropathogens in the etiology of diarrhea (Orlandi et al., 2006; Lima F. M. et al., 2019). Indeed, some hybrid strains possessing typical genes from different pathotypes (heteropathogens) have recently emerged (Santos et al., 2020). For example, the O104:H4 strain associated with the severe German outbreak in 2011 was a hybrid of both EAEC and EHEC (Brzuszkiewicz et al., 2011). More recently, enterohemorrhagic *E. coli* hybrid pathotype O80:H2 has emerged in Europe as an important serotype responsible for hemolytic uremic syndrome (HUS) associated with extraintestinal infections in children (Cointe et al., 2018). Also, coinfections have been reported, detecting in stool samples the presence of EPEC and EAEC and *S. enterica houtenae* and EAEC (Lima F. M. et al., 2019).

The incidence of intestinal infection caused by STEC is low in the Brazilian population (de Souza et al., 2011; Ori et al., 2018; Lima F. M. et al., 2019). Thus, it was surprising to find more EHEC-associated genetic markers in the asymptomatic group than in the diarrhea group, since these genetic markers are usually more associated with *E. coli* strains of greater clinical significance (Delannoy et al., 2012a,b, 2016; Piazza et al., 2013). This suggests that these potential EHEC strains are not the etiological agent of diarrhea in this sampled group, which remains to be investigated.

Current methods for either screening or detecting of enteropathogens by PCR, multiplex PCR, and qPCR have been used worldwide, given the high sensitivity and specificity, which are satisfactory parameters to ensure an adequate diagnosis (Panchalingam et al., 2012). However, the presence of several pathogens in diarrhea samples, as we observed, and the high frequency of enteropathogens in asymptomatic children has made it difficult to use these methods as a tool to identify the etiological agent of diarrhea.

Here, we found a significantly higher copy number of *eae* in diarrhea samples compared to samples from asymptomatic children, suggesting that LEE-containing pathogens could be the etiological agents responsible for diarrhea in children. Even though we did not find differences between groups in the number of copies for *aggR*, our data must be complemented with a larger number of samples and/or selection of other EAEC markers to support the use of qPCR for molecular diagnosis for this pathogen.

Our study had the following limitations. The number of samples was limited and we did not search for other

TABLE 3 | Virulence profile determination of *eae*+ *Escherichia coli* from fecal samples of children with and without diarrhea*.

Genetic markers	32 fecal samples with diarrhea (%)	19 fecal samples without diarrhea (%)	*P*-value
bfp	1 (3.1)	0 (0)	0.2192
stx1	1 (3.1)	3 (15.8)	0.0513
stx2	8 (25.0)	12 (63.2)	0.0035
ehxA	6 (18.8)	13 (68.4)	0.0002
hlyA	12 (37.5)	7 (37.0)	0.4858
nleA	5 (15.6)	2 (10.5)	0.3043
nleB	12 (37.5)	14 (73.7)	0.0062
nleE	12 (37.5)	15 (79.0)	0.0020
nleF	13 (40.6)	15 (79.0)	0,0039
espM1	12 (37.5)	14 (73.7)	0.0062
pagC	6 (18.8)	15 (79.0)	0.0001
ent	7 (22.0)	15 (79.0)	0.0001
efa1	3 (9.4)	9 (47.4)	0.0010
espK	6 (18.8)	4 (21.0)	0.4242
espN	1 (3.1)	1 (5.3)	0.3477
espV	8 (25.0)	13 (68.4)	0.0012
Z2098	7 (22.0)	12 (63.2)	0.0016
Z2099	12 (37.5)	16 (84.2)	0,0006
Z6065	12 (37.5)	13 (68.4)	0.0164
terE	29 (91.0)	18 (94.7)	0.3151
ureD	14 (44.0)	15 (79.0)	0.0073
SP_O157-A	6 (18.8)	11 (58.0)	0.0021
SP_O157-B	1 (3.1)	7 (37.0)	0.0007
SP_O157-C	6 (18.8)	11 (58.0)	0.0021
O26_C	4 (12.5)	1 (5.3)	0.2017
O26_D	2 (6.2)	1 (5.3)	0.4474

*$P < 0.05$ was considered statistically significant. *General P value between groups 0.312.*

relevant pathogens, such as rotavirus, norovirus, protozoa, and helminthes. For bacterial loads, we only evaluated two markers, which might be insufficient, considering that DEC harbors several virulence determinants that can be used as a target for diagnosis. Another limitation of the study was that we did not isolate the pathogenic strains. This would be helpful to identify if asymptomatic children might shed the bacteria and possibly be contagious.

In conclusion, we found that the presence of genetic markers associated with bacterial pathogens was significantly higher in stool samples from the diarrhea group compared to the control. Also, compared to samples from asymptomatic children, there was a significantly higher copy number of the *eae* gene in diarrhea samples. The data presented herein demonstrated that asymptomatic children of an urban area in Brazil might be enteropathogen reservoirs, especially for STEC, thus favoring their widespread.

DATA AVAILABILITY STATEMENT

All datasets generated for this study are included in the article/**Supplementary Material**.

ETHICS STATEMENT

The studies involving human participants were reviewed and approved by Ethics Committee of the Biomedical Science Institute at the University of Sao Paulo. Written informed consent to participate in this study was provided by the participants' legal guardian/next of kin.

AUTHOR CONTRIBUTIONS

VM, VN, SD, PF, RP, and MA-C participated in the design of the study. VM, VN, SD, PF, MF, RP, and MA-C participated in data analysis. MF, RP, SD, and PF participated in writing the manuscript. VM and VN carried out the qPCR experiments. GA carried out the multiplex PCR experiments. SD and PF carried out the high-throughput real-time PCR experiments. All authors read and approved the final manuscript.

FUNDING

This study was supported by grants from CNPq 158799/2012-7, FAPESP 2013/17739-9, 2017/14821-7, and FONDECYT 1200994.

ACKNOWLEDGMENTS

The authors thank Mrs. Marcia H. Fukugaiti for her technical support. Standard strains were kindly donated by Dr. Juliana Pfrimer Falcão, Faculdade de Ciências Farmacêuticas de Ribeirão Preto (FCFRP-USP), SP, Brazil and Dr. Marcia Regina Franzolin from Instituto Butantan, SP, Brazil. Dr. A. Leyva (USA) helped with English editing of the manuscript.

SUPPLEMENTARY MATERIAL

The Supplementary Material for this article can be found online at: https://www.frontiersin.org/articles/10.3389/fcimb.2020.549919/full#supplementary-material

REFERENCES

Aranda, K. R. S., Fagundes-Neto, U., and Scaletsky, I. C. A. (2004). Evaluation of multiplex PCRs for diagnosis of infection with diarrheagenic *Escherichia coli* and *Shigella* spp. *J. Clin. Microbiol.* 42, 5849–5853. doi: 10.1128/JCM.42.12.5849-5853.2004

Bottone, E. J. (1999). *Yersinia enterocolitica*: overview and epidemiologic correlates. *Microbes Infect.* 1, 323–333. doi: 10.1016/S1286-4579(99)80028-8

Brzuszkiewicz, E., Thürmer, A., Schuldes, J., Leimbach, A., Liesegang, H., Meyer, F. D., et al. (2011). Genome sequence analyses of two isolates from the recent *Escherichia coli* outbreak in Germany reveal the emergence of a new pathotype:

entero-aggregative-haemorrhagic *Escherichia coli* (EAHEC). *Arch. Microbiol.* 193, 883–891. doi: 10.1007/s00203-011-0725-6

Bueris, V., Sircili, M. P., Taddei, C. R., dos Santos, M. F., Franzolin, M. R., Martinez, M. B., et al. (2007). Detection of diarrheagenic *Escherichia coli* from children with and without diarrhea in Salvador, Bahia, Brazil. *Mem. Inst. Oswaldo Cruz.* 102, 839–844. doi: 10.1590/S0074-02762007005000116

Bugarel, M., Beutin, L., and Fach, P. (2010). Low-density macroarray targeting non-locus of enterocyte effacement effectors (*nle* genes) and major virulence factors of Shiga toxin-producing *Escherichia coli* (STEC): a new approach for molecular risk assessment of STEC isolates. *Appl. Environ. Microbiol.* 76, 203–211. doi: 10.1128/AEM.01921-09

Bugarel, M., Beutin, L., Scheutz, F., Loukiadis, E., and Fach, P. (2011). Identification of genetic markers for differentiation of Shiga toxin-producing, enteropathogenic, and avirulent strains of *Escherichia coli* O26. *Appl. Environ. Microbiol.* 77, 2275–2281. doi: 10.1128/AEM.02832-10

Cointe, A., Birgy, A., Mariani-Kurkdjian, P., Liguori, S., Courroux, C., Blanco, J., et al. (2018). Emerging multidrug-resistant hybrid pathotype Shiga toxin-producing *Escherichia coli* O80 and related strains of clonal complex 165, Europe. *Emerg. Infect Dis.* 24, 2262–2269. doi: 10.3201/eid2412.180272

Croxen, M. A., Law, R. J., Scholz, R., Keeney, K. M., Wlodarska, M., and Finlay, B. B. (2013). Recent advances in understanding enteric pathogenic *Escherichia coli*. *Clin. Microbiol. Rev.* 26, 822–880. doi: 10.1128/CMR.00022-13

de Souza, R. L., Carvalhaes, J. T. A., Nishimura, L. S., de Andrade, M. C., and Guth, B. E. C. (2011). Hemolytic uremic syndrome in pediatric intensive care units in São Paulo, Brazil. *Open Microbiol J.* 5, 76–82. doi: 10.2174/1874285801105010076

Delannoy, S., Beutin, L., Burgos, Y., and Fach, P. (2012a). Specific detection of enteroaggregative hemorrhagic *Escherichia coli* O104:H4 strains by use of the CRISPR locus as a target for a diagnostic real-time PCR. *J. Clin. Microbiol.* 50, 3485–3492. doi: 10.1128/JCM.01656-12

Delannoy, S., Beutin, L., and Fach, P. (2012b). Use of clustered regularly interspaced short palindromic repeat sequence polymorphisms for specific detection of enterohemorrhagic *Escherichia coli* strains of serotypes O26:H11, O45:H2, O103:H2, O111:H8, O121:H19, O145:H8, and O157:H7 by real time PCR. *J. Clin. Microbiol.* 50, 4035–4040. doi: 10.1128/JCM.02097-12

Delannoy, S., Beutin, L., and Fach, P. (2013). Towards a molecular definition of enterohemorrhagic *Escherichia coli* (EHEC): detection of genes located on O island 57 as markers to distinguish EHEC from closely related enteropathogenic *Escherichia coli* strains. *J. Clin. Microbiol.* 51, 1083–1088. doi: 10.1128/JCM.02864-12

Delannoy, S., Chaves, B. D., Ison, S. A., Webb, H. E., Beutin, L., Delaval, J., et al. (2016). Revisiting the STEC testing approach: using *espK* and *espV* to make enterohemorrhagic *Escherichia coli* (EHEC) detection more reliable in beef. *Front. Microbiol.* 7:1. doi: 10.3389/fmicb.2016.00001

Delannoy, S., Mariani-Kurkdjian, P., Bonacorsi, S., Liguori, S., Ison, S. A., and Fach, P. (2015). Draft genome sequences of human-pathogenic *Escherichia coli* O26:H11 strains carrying the *stx2* gene only and circulating in France. *Genome Announc.* 3:e00852–e00815. doi: 10.1128/genomeA.00852-15

Dias, R. C. B., Tanabe, R. H. S., Vieira, M. A., Cergole-Novella, M. C., Dos Santos, L. F., Gomes, T. A. T., et al. (2020). Analysis of the virulence profile and phenotypic features of typical and atypical enteroaggregative *Escherichia coli* (EAEC) isolated from diarrheal patients in Brazil. *Front. Cell. Infect. Microbiol.* 10:144. doi: 10.3389/fcimb.2020.00144

Franzolin, M. R., Alves, R. C., Keller, R., Gomes, T. A., Beutin, L., Barreto, M. L., et al. (2005). Prevalence of diarrheagenic *Escherichia coli* in children with diarrhea in Salvador, Bahia, Brazil. *Mem. Inst. Oswaldo Cruz.* 100, 359–363. doi: 10.1590/S0074-02762005000400004

Fratamico, P. M., DebRoy, C., Miyamoto, T., and Liu, Y. (2009). PCR detection of enterohemorrhagic *Escherichia coli* O145 in food by targeting genes in the *E. coli* O145 O-antigen gene cluster and the Shiga toxin 1 and Shiga toxin 2 genes. *Foodborne Pathog. Dis.* 6, 605–611. doi: 10.1089/fpd.2008.0254

Fratamico, P. M., Yan, X. H., Liu, Y. H., DebRoy, C., Byrne, B., Monaghan, A., et al. (2010). *Escherichia coli* serogroup O2 and O28ac O-antigen gene cluster sequences and detection of pathogenic *E. coli* O2 and O28ac by PCR. *Can. J. Microbiol.* 56, 308–316. doi: 10.1139/W10-010

Freitas Neto, O. C., Penha Filho, R. A. C., Barrow, P., and Berchieri Junior, A. (2010). Sources of human non-typhoid Salmonellosis: a review. *Rev. Bras. Cienc. Avic.* 12, 1–11. doi: 10.1590/S1516-635X2010000100001

Galán, J. E., Ginocchio, C., and Costeas, P. (1992). Molecular and functional characterization of the *Salmonella* invasion gene InvA homology of InvA to members of a new protein family. *J. Bacteriol.* 174, 4338–4349. doi: 10.1128/JB.174.13.4338-4349.1992

Ginocchio, C. C., and Galán, J. E. (1995). Functional conservation among members of the *Salmonella typhimurium* InvA family of proteins. *Infect. Immun.* 63, 729–732. doi: 10.1128/IAI.63.2.729-732.1995

Gomes, T. A., Elias, W. P., Scaletsky, I. C., Guth, B. E., Rodrigues, J. F., Piazza, R. M. F., et al. (2016). Diarrheagenic *Escherichia coli*. *Braz. J. Microbiol.* 47(Suppl. 1), 3–30. doi: 10.1016/j.bjm.2016.10.015

Gomes, T. A., Rassi, V., MacDonald, K. L., Ramos, S. R., Trabulsi, L. R., Vieira, M. A., et al. (1991). Enteropathogens associated with acute diarrheal disease in urban infants in São Paulo, Brazil. *J. Infect. Dis.* 164, 331–337. doi: 10.1093/infdis/164.2.331

Hernandes, R. T., Elias, W. P., Vieira, M. A., and Gomes, T. A. (2009). An overview of atypical enteropathogenic *Escherichia coli*. *FEMS. Microbiol. Lett.* 297, 137–149. doi: 10.1111/j.1574-6968.2009.01664.x

Imdad, A., Foster, M. A., Iqbal, J., Fonnesbeck, C., Payne, D. C., Zhang, C., et al. (2018). Diarrheagenic *Escherichia coli* and acute gastroenteritis in children in Davidson County, Tennessee, United States: a case-control study. *Pediatr. Infect. Dis. J.* 37, 543–548. doi: 10.1097/INF.0000000000001908

Kaper, J. B., Nataro, J. P., and Mobley, H. L. (2004). Pathogenic *Escherichia coli*. *Nat. Rev. Microbiol.* 2, 123–140. doi: 10.1038/nrmicro818

Leli, C., Di Matteo, L., Gotta, F., Vay, D., Cavallo, V., Mazzeo, R., et al. (2020). Evaluation of a multiplex gastrointestinal PCR panel for the aetiological diagnosis of infectious diarrhoea. *Infect. Dis.* 52, 114–120. doi: 10.1080/23744235.2019.1688861

Lima, A. A. M., Oliveira, D. B., Quetz, J. S., Havt, A., Prata, M. M. G., Lima, I. F. N., et al. (2019). Etiology and severity of diarrheal diseases in infants at the semiarid region of Brazil: a case-control study. *PLoS Negl. Trop. Dis.* 13:e0007154. doi: 10.1371/journal.pntd.0007154

Lima, F. M., de Paulo Daurelio, F., Mucci, E. R., Ahagon, C. M., Dos Santos Carmo, A. M., Eterovic, A., et al. (2019). Epidemiology and genetic screening of diarrheagenic *Escherichia coli* among symptomatic and asymptomatic children. *J. Med. Microbiol.* 68, 1033–1041. doi: 10.1099/jmm.0.001020

Liu, L., Johnson, H. L., Cousens, S., Perin, J., Scott, S., Lawn, J. E., et al. (2012). Global, regional, and national causes of child mortality: an updated systematic analysis for 2010 with time trends since 2000. *Lancet* 379, 2151–2161. doi: 10.1016/S0140-6736(12)60560-1

Maranhão, H. S., Medeiros, M. C., Scaletsky, I. C., Fagundes-Neto, U., and Morais, M. B. (2008). The epidemiological and clinical characteristics and nutritional development of infants with acute diarrhoea, in north-eastern Brazil. *Ann. Trop. Med. Parasitol.* 102, 357–365. doi: 10.1179/136485908X278865

Marinou, I., Bersimis, S., Ioannidis, A., Nicolaou, C., Mitroussia-Ziouva, A., Legakis, N. J., et al. (2012). Identification and antimicrobial resistance of Campylobacter species isolated from animal sources. *Front. Microbiol.* 3:58. doi: 10.3389/fmicb.2012.00058

Michelet, L., Delannoy, S., Devillers, E., Umhang, G., Aspan, A., Juremalm, M., et al. (2014). High-throughput screening of tick-borne pathogens in Europe. *Front. Cell. Infect. Microbiol.* 4:103. doi: 10.3389/fcimb.2014.00103

Miliwebsky, E., Schelotto, F., Varela, G., Luz, D., Chinen, I., and Piazza, R. M. F. (2016). "Human diarrheal infections: diagnosis of diarrheagenic *Escherichia coli* pathotypes," in *Escherichia coli in the Americas,* ed A. G. Torres (Cham: Springer), 343–369. doi: 10.1007/978-3-319-45092-6_15

Moreno, A. C., Fernandes-Filho, A., Gomes, T. A., Ramos, S. T. S., Montemor, L. P., Tavares, V. C., et al. (2010). Etiology of childhood diarrhea in the northeast of Brazil: significant emergent diarrheal pathogens. *Diagn. Microbiol. Infect. Dis.* 66, 50–57. doi: 10.1016/j.diagmicrobio.2008.03.017

Nunes, M. R., Magalhães, P. P., Penna, F. J., Nunes, J. M., and Mendes, E. N. (2012). Diarrhea associated with *Shigella* in children and susceptibility to antimicrobials. *J. Pediatr.* 88, 125–128. doi: 10.2223/JPED.2131

Ochoa, T. J., Ecker, L., Barletta, F., Mispireta, M. L., Gil, A. I., Contreras, C., et al. (2009). Age-related susceptibility to infection with diarrheagenic *Escherichia coli* among infants from periurban areas in Lima, Peru. *Clin. Infect. Dis.* 49, 1694–1702. doi: 10.1086/648069

Ori, E. L., Takagi, E. H., Andrade, T. S., Miguel, B. T., Cergole-Novella, M. C., Guth, B. E. C., et al. (2018). Diarrhoeagenic *Escherichia coli* and *Escherichia albertii* in

Brazil: pathotypes and serotypes over a 6-year period of surveillance. *Epidemiol. Infect*. 147:e10. doi: 10.1017/S0950268818002595

Orlandi, P. P., Magalhães, G. F., Matos, N. B., Silva, T., Penatti, M., Nogueira, P. A., et al. (2006). Etiology of diarrheal infections in children of Porto Velho (Rondonia, Western Amazon region, Brazil). *Braz. J. Med. Biol. Res*. 39, 507–517. doi: 10.1590/S0100-879X2006000400011

Panchalingam, S., Antonio, M., Hossain, A., Mandomando, I., Ochieng, B., Oundo, J., et al. (2012). Diagnostic microbiologic methods in the GEMS-1 case/control study. *Clin. Infect. Dis*. 55(Suppl. 4), S294–302. doi: 10.1093/cid/cis754

Pavlovic, M., Luze, A., Konrad, R., Buger, A., Sing, A., Busch, U., et al. (2011). Development of a duplex real time PCR for differentiation between *Escherichia coli* and *Shigella* spp. *J. Appl. Microbiol*. 110, 1245–1251. doi: 10.1111/j.1365-2672.2011.04973.x

Perelle, S., Dilasser, F., Grout, J., and Fach, P. (2004). Detection by 5′- nuclease PCR of Shiga-toxin producing *Escherichia coli* O26, O55, O91, O103, O111, O113, O145 and O157:H7, associated with the world's most frequent clinical cases. *Mol. Cell Probes*. 18, 185–192. doi: 10.1016/j.mcp.2003.12.004

Pérez, C., Gómez-Duarte, O. G., and Arias, M. L. (2010). Diarrheagenic *Escherichia coli* in children from Costa Rica. *Am. J. Trop. Med. Hyg*. 83, 292–297. doi: 10.4269/ajtmh.2010.09-0412

Pérez-Corrales, C., and Leandro-Sandí, K. (2019). Diarrheagenic *Escherichia coli* in Costa Rican children: a 9-year retrospective study. *BMC Res. Notes*. 12:297. doi: 10.1186/s13104-019-4313-1

Peruzy, M. F., Murru, N., Perugini, A. G., Capuano, F., Delibato, E., Mercogliano, R., et al. (2017). Evaluation of virulence genes in *Yersinia enterocolitica* strains using SYBR Green real-time PCR. *Food Microbiol*. 65, 231–235. doi: 10.1016/j.fm.2017.03.004

Piazza, R. M. F., Abe, C. M., Horton, D. S. P. Q., Miliwebsky, E., Chinen, I., Vaz, T. M. I., et al. (2010). "Detection and subtyping methods of diarrheagenic *Escherichia coli* strains," in *Pathogenic Escherichia coli in Latin America,* ed A. G. Torres (Sharjah: Bentham Science Publishers), 95–115.

Piazza, R. M. F., Delannoy, S., Fach, P., Saridakis, H. O., Pedroso, M. Z., Rocha, L. B., et al. (2013). Molecular and phenotypic characterization of *Escherichia coli* O26:H8 among diarrheagenic *Escherichia coli* O26 strains isolated in Brazil. *Appl. Environ. Microbiol*. 79, 6847–6854. doi: 10.1128/AEM.01693-13

Regua-Mangia, A. H., Gomes, T. A. T., Vieira, M. A. M., Andrade, J. R., Irino, K., and Teixeira, L. M. (2004). Frequency and characteristics of diarrhoeagenic *Escherichia coli* strains isolated from children with and without diarrhoea in Rio de Janeiro, Brazil. *J. Infect*. 48, 161–167. doi: 10.1016/S0163-4453(03)00138-5

Rosa, A. C., Mariano, A. T., Pereira, A. M., Tibana, A., Gomes, T. A. T., and Andrade, J. R. (1998). Enteropathogenicity markers in *Escherichia coli* isolated from infants with acute diarrhoea and healthy controls in Rio de Janeiro, Brazil. *J. Med. Microbiol*. 47, 781–790. doi: 10.1099/00222615-47-9-781

Santos, A. C. M., Santos, F. F., Silva, R. M., and Gomes, T. A. T. (2020). Diversity of hybrid- and hetero-pathogenic *Escherichia coli* and their potential implication in more severe diseases. *Front. Cell. Infect. Microbiol*. 10:339. doi: 10.3389/fcimb.2020.00339

Swierczewski, B. E., Odundo, E. A., Koech, M. C., Ndonye, J. N., Kirera, R. K., Odhiambo, C. P., et al. (2013). Enteric pathogen surveillance in a case-control study of acute diarrhoea in the town of Kisii, Kenya. *J. Med. Microbiol*. 62, 1774–1776. doi: 10.1099/jmm.0.059139-0

Torres, A. G. (2017). *Escherichia coli* diseases in Latin America-a "One Health" multidisciplinary approach. *Pathog. Dis*. 1:75. doi: 10.1093/femspd/ftx012

World Health Organization (2017). *Diarrhoeal Disease*. Available online at: https://www.who.int/news-room/fact-sheets/detail/diarrhoeal-disease (accessed July 21, 2020).

Zhang, S.-X., Yang, C.-L., Gu, W.-P., Ai, L., Serrano, E., Yang, P., et al. (2016). Case-control study of diarrheal disease etiology in individuals over 5 years in Southwest China. *Gut Pathog*. 8:58. doi: 10.1186/s13099-016-0141-1

Conflict of Interest: The authors declare that the research was conducted in the absence of any commercial or financial relationships that could be construed as a potential conflict of interest.

frontiers in Cellular and Infection Microbiology

ORIGINAL RESEARCH
published: 29 September 2020
doi: 10.3389/fcimb.2020.00492

Genetic and Virulence Characteristics of a Hybrid Atypical Enteropathogenic and Uropathogenic *Escherichia coli* (aEPEC/UPEC) Strain

Tiago B. Valiatti[1†], *Fernanda F. Santos*[1†], *Ana C. M. Santos*[1], *Júllia A. S. Nascimento*[1], *Rosa M. Silva*[1], *Eneas Carvalho*[2], *Rita Sinigaglia*[3] *and Tânia A. T. Gomes*[1*]

[1] Departamento de Microbiologia, Imunologia e Parasitologia, Escola Paulista de Medicina, Universidade Federal de São Paulo, São Paulo, Brazil, [2] Laboratório de Bacteriologia, Instituto Butantan, São Paulo, Brazil, [3] Centro de Microscopia Eletrônica, Escola Paulista de Medicina, Universidade Federal de São Paulo, São Paulo, Brazil

Hybrid strains of *Escherichia coli* combine virulence traits of diarrheagenic (DEC) and extraintestinal pathogenic *E. coli* (ExPEC), but it is poorly understood whether these combined features improve the virulence potential of such strains. We have previously identified a uropathogenic *E. coli* (UPEC) strain (UPEC 252) harboring the *eae* gene that encodes the adhesin intimin and is located in the locus of enterocyte effacement (LEE) pathogenicity island. The LEE-encoded proteins allow enteropathogenic *E. coli* (EPEC) and enterohemorrhagic *E. coli* (EHEC) to form attaching and effacing (A/E) lesions in enterocytes. We sought to characterize UPEC 252 through whole-genome sequencing and phenotypic virulence assays. Genome analysis unveiled that this strain harbors a complete LEE region, with more than 97% of identity comparing to E2348/69 (EPEC) and O157:H7 Sakai (EHEC) prototype strains, which was functional, since UPEC 252 expressed the LEE-encoded proteins EspB and intimin and induced actin accumulation foci in HeLa cells. Phylogenetic analysis performed comparing 1,000 single-copy shared genes clustered UPEC 252 with atypical EPEC strains that belong to the sequence type 10, phylogroup A. Additionally, UPEC 252 was resistant to the bactericidal power of human serum and colonized cells of the urinary (T24 and HEK293-T) and intestinal (Caco-2 and LS174T) tracts. Our findings suggest that UPEC 252 is an atypical EPEC strain that emerges as a hybrid strain (aEPEC/UPEC), which could colonize new niches and potentially cause intestinal and extraintestinal infections.

Keywords: ***Escherichia coli*, UPEC, hybrid pathogenic strain, virulence factor, ExPEC, urinary tract infection, atypical EPEC**

OPEN ACCESS

Edited by:
Nora Lía Padola, National University of Central Buenos Aires, Argentina

Reviewed by:
Jorge Blanco, University of Santiago de Compostela, Spain
Roberto Mauricio Vidal, University of Chile, Chile
Laura A. Mike, University of Michigan, United States

****Correspondence:***
Tânia A. T. Gomes
tatg.amaral@unifesp.br

†Present address:
Tiago B. Valiatti and Fernanda F. Santos, Laboratório Alerta, Disciplina de Infectologia, Departamento de Medicina, Escola Paulista de Medicina, Universidade Federal de São Paulo, São Paulo, Brazil

Specialty section:
This article was submitted to Molecular Bacterial Pathogenesis, a section of the journal Frontiers in Cellular and Infection Microbiology

Received: *08 April 2020*
Accepted: *08 August 2020*
Published: *29 September 2020*

Citation:
Valiatti TB, Santos FF, Santos ACM, Nascimento JAS, Silva RM, Carvalho E, Sinigaglia R and Gomes TAT (2020) Genetic and Virulence Characteristics of a Hybrid Atypical Enteropathogenic and Uropathogenic Escherichia coli (aEPEC/UPEC) Strain. Front. Cell. Infect. Microbiol. 10:492. doi: 10.3389/fcimb.2020.00492

INTRODUCTION

Urinary tract infection (UTI) is one of the most prevalent diseases worldwide, affecting both community and hospitalized subjects, resulting in impairment of the patients' life quality (Terpstra and Geerlings, 2016; Wurpel et al., 2016). Several factors, such as surgical manipulation, diabetes, previous hospitalizations, and catheterization, are related to a

higher risk for developing this disease (Saltoglu et al., 2015; Redder et al., 2016). UTI most often results from bacteria transitorily present in the gut microbiota that colonize the perineum and ascend through the urethra. Alternatively, UTI may occur after the introduction of bacteria directly into the urinary tract, during the use of a bladder catheter or certain sexual practices (Donnenberg and Welch, 1996; Finer and Landau, 2004). Characteristics of the host, especially those associated with immunity, also contribute to the occurrence and severity of infections in the urinary tract.

The main agents of UTI are Gram-negative bacilli of the family *Enterobacteriaceae*. Among them, uropathogenic *Escherichia coli* (UPEC) are the most frequent (Donnenberg and Welch, 1996; Heilberg and Schor, 2003), responding for about 80% of all cases worldwide (Ronald, 2003; Hooton, 2012; Korbel et al., 2017). UPEC strains belong to a group of *E. coli* clones that are collectively referred to as extraintestinal pathogenic *E. coli* (ExPEC), which are adapted to colonize and cause disease in different extraintestinal host sites (Russo and Johnson, 2000). The ability of ExPEC strains to colonize and develop extraintestinal diseases is due to the presence of a variety of virulence factors, including adhesins, toxins, capsules, invasins, and iron uptake systems that are encoded in Pathogenicity islands (PAI) present in chromosomes or plasmids (Dale and Woodford, 2015). Currently, more than 50 virulence factors have their role in ExPEC pathogenicity established (Johnson and Russo, 2018), but the ability of ExPEC to colonize a variety of host sites varies among strains reflecting their genetic diversity.

Despite the number of virulence factors related to ExPEC pathogenicity, its classification is primarily performed by the isolation site, and their pathotypes defined by the infection source, with uropathogenic *E. coli* (UPEC) being the most prevalent ExPEC pathotype. Many studies focus on UPEC virulence and epidemiology, mainly because of the disease's burden. Johnson et al. (2003) described a set of virulence factors that could identify ExPEC strains by their intrinsic virulence, and are thus considered more virulent strains (presence of at least two among five markers: *pap, sfa/foc, afa/dra, iuc/iut, kpsMTII*). Later, Spurbeck et al. (2012) described another set of virulence markers that are epidemiologically linked with the uropathogenic potential (simultaneous presence of *chuA*, *fyuA*, *vat*, and *yfcV*). Together these methodologies enable the screening of the ExPEC strains that either harbor intrinsic virulence or uropathogenic potential, in diverse sources, like water, food, and gut, favoring the identification of their reservoirs. However, these criteria fail to classify all strains isolated from extraintestinal infections (Spurbeck et al., 2012; Santos et al., 2013, 2020b; Freire et al., 2020) and some clinical lineages with epidemiological importance also do not meet these criteria (Bert et al., 2010; Olesen et al., 2012; Manges and Johnson, 2015; Manges et al., 2017, 2019; Campos et al., 2018; Yamaji et al., 2018; Santos et al., 2020a,b).

Other clones of *E. coli* can cause intestinal infections by different mechanisms and are collectively referred to as diarrheagenic *E. coli* (DEC). DEC strains are classified into six pathotypes named enterotoxigenic *E. coli* (ETEC), enteroinvasive *E. coli* (EIEC), enteroaggregative *E. coli* (EAEC), Shiga toxin-producing *E. coli* (STEC), diffusely adherent *E. coli* (DAEC), and enteropathogenic *E. coli* (EPEC) (Kaper and Nataro, 1998; Croxen et al., 2013; Gomes et al., 2016). EPEC strains are divided into typical (tEPEC) and atypical (aEPEC) based on the presence of the EAF (EPEC adherence factor) plasmid (pEAF) in tEPEC and its absence in aEPEC (Trabulsi et al., 2002). pEAF encodes a bundle forming pilus (BFP) that promotes bacterial aggregation and, consequently, the formation of compact microcolonies that characterize a localized adhesion (LA) pattern on the surface of HeLa and HEp-2 epithelial cells (Scaletsky et al., 1984; Girón et al., 1991).

Reports of *E. coli* strains that caused intestinal and extraintestinal infections in the same host are uncommon. However, recent studies have identified ExPEC strains promoting intestinal infections followed by bloodstream infections (Mariani-Kurkdjian et al., 2014; Kessler et al., 2015). These strains that contain virulence factors of intestinal and extraintestinal pathotypes are considered hybrid and potentially more virulent pathogens. In these studies, the horizontal gene transfer (HGT) of virulence factors occurred from ExPEC to DEC and DEC to ExPEC.

Despite the recognized potential of HGT between pathogenic *E. coli* strains, only a few studies have described this phenomenon among DEC and UPEC in strains isolated from UTI and in these studies the genetic background of strains involved was not evaluated (Olesen et al., 1994; Garcia et al., 2000; Keller et al., 2002; Matar et al., 2005; Ogura et al., 2007; Wallace-Gadsden et al., 2007; Abe et al., 2008; Lara et al., 2017; Santos et al., 2020a). A study evaluating fecal EAEC isolates identified that some strains produced alpha-hemolysin (*hlyA*) and P fimbria (*pap*) (Suzart et al., 1999), characteristics often found in UPEC strains, suggesting that certain EAEC strains with specific virulence genes would be potentially uropathogenic. Assessing the virulence factors of strains isolated from UTI, we have previously (Falsetti, 1998; Abe et al., 2008) demonstrated in some UPEC isolates the presence of the *aggR* and *aat* genes, as well as the aggregative adhesion (AA) pattern on HeLa cells, which are properties that define the EAEC pathotype. In addition to the UPEC isolates bearing EAEC virulence genes, in the referred study, we identified a UPEC strain (UPEC 252) carrying the *eae* gene (Abe et al., 2008), which encodes intimin, an outer membrane adhesive protein that is fundamental for the intimate adhesion of EPEC and EHEC strains to intestinal cells and subsequent formation of attaching/effacing (A/E) lesions (Kaper et al., 2004). A/E lesions are characterized by intimate bacterial adhesion to the host cells, which undergoes the eradication of microvilli and accumulation of actin filaments underneath the adhered bacteria, thus promoting the formation of pedestal-like structures on the cell surface (Moon et al., 1983). This type of lesion can be identified in non-intestinal (HeLa and HEp-2 cells) and intestinal epithelial (Caco-2) cell lineages *in vitro*, as well as in animal and human enterocytes *in vivo* (Kaper et al., 2004). The genes involved in A/E lesion formation are contained in a chromosomal PAI called the locus of enterocyte effacement (LEE). Besides *eae*, LEE encodes a type III secretion system (T3SS) and several effectors and regulatory proteins, whose activities culminate in

the production of the lesion (Mcdaniel et al., 1995). Regardless of the detection of the *eae* gene in UPEC 252, the genetic background of the strain has not been properly evaluated, and its relationship with other pathogenic *E. coli* is unknown. Furthermore, it is not known whether the DEC virulence genes found in this strain are complete, nor if they are expressed and play a role in the bacterial interaction with intestinal and urinary tract cells. Therefore, this study aimed to provide information about the genetic and virulence properties of UPEC 252, an *E. coli* that was isolated from UTI and carries the *eae* gene characteristic of EPEC and EHEC.

MATERIALS AND METHODS

Bacterial Strain

UPEC 252 was isolated, in 1998, from a 1-month-old female patient hospitalized at Hospital São Paulo, São Paulo, Brazil, with urinary tract infection (Falsetti, 1998; Abe et al., 2008). The strain was stored in Lysogeny broth (LB) supplemented with 15% glycerol and kept at −80°C. For routine use, it was grown in LB at 37°C for ∼18 h.

Genome Sequencing, Assembly, Annotation, and Data Analysis

The genome of UPEC 252 was sequenced as previously published (Valiatti et al., 2019). Briefly, DNA was extracted using the Wizard® Genomic DNA Purification Kit and sequenced on an Illumina Hiseq1500 platform. The paired-end reads were assembled *de novo* using SPAdes (version 3.12.0) (Bankevich et al., 2012) and the annotation was performed using Prokka version 1.13.3 (Seemann, 2014). The reads used for UPEC 252 genome assembly were deposited in the Sequence Read Archive (SRA) at NCBI under the accession number SRR9317828, and the whole-genome sequences (WGS) were deposited in the GenBank database under the accession number VFST00000000 (Valiatti et al., 2019).

The WGS of UPEC 252 was submitted to the Center for Genomic Epidemiology (CGE) to determine the strain sequencing type (Multi-Locus Sequence Typing - MLST version 2.0) (Larsen et al., 2012), virulence profile (VirulenceFinder 2.0) (Joensen et al., 2014), resistance profile (ResFinder 3.1) (Zankari et al., 2012), and serotype (SerotypeFinder version 1.1) (Joensen et al., 2015). To analyze the presence of virulence and resistance genes, we also used ecoli_VF collection v0.1 (Leimbach, 2016) and the ABRicate program[1], which employes multiple databases: VFDB (Chen et al., 2016), ARG-ANNOT (Gupta et al., 2014), CARD (Jia et al., 2017), PlasmidFinder (Carattoli et al., 2014), EcOH (Ingle et al., 2016), MEGARes 2.0 (Doster et al., 2020), and NCBI AMRFinderPlus (Feldgarden et al., 2019). The phylogenetic typing of the strain was determined using the ClermonTyping tool (Beghain et al., 2018). Confirmation of the identified genes of the LEE region and the non-LEE encoded genes was carried out by aligning the DNA sequences of UPEC 252 with the DNA sequences deposited at the National Center for Biotechnological Information (NCBI) using the BLAST program.

[1]Seemann, T. *ABRicate*. Available online at: https://github.com/tseemann/abricate

Comparative Genome Analyses of UPEC 252

To identify the UPEC 252 genome rearrangement, gain and loss, different strategies were used. First, the annotated genome of UPEC 252 was aligned using progressiveMAUVE (Darling et al., 2010). In another approach, pangenome analysis was performed using the Roary pipeline (Page et al., 2015). In both methods, the genome of UPEC 252 was compared with the genome of the following strains: prototype EPEC E2348/69 (GCF_000026545.1), aEPEC 4581-2 (QYYF00000000.1), prototype EHEC O157:H7 Sakai (GCF_000008865.2), EHEC O111:H- 11128 (GCF_000010765.1), prototype UPEC CFT073 (GCF_000007445.1), prototype UPEC 536 (GCF_000013305.1), prototype UPEC UMN026 (GCF_000026325.1), an isolate from asymptomatic bacteriuria VR50 (GCF_000968515.1), and K12 derived MG1655 (GCF_000005845.2).

UPEC 252 Phylogenetic Analysis

The phylogenetic tree that includes UPEC 252 was built using the Phylogenetic tree tool of the Pathosystems Resource Integration Center (PATRIC) (Wattam et al., 2017). A total of 140 *E. coli* public genomes were used to build the tree, 95 genomes of which were randomly chosen among strains belonging to ST10 (**Supplementary Table 1**), while 45 others were selected by similarity using the Mash algorithm in the PATRIC similarity genome service (**Supplementary Table 1**). The tree was built applying the codon tree methodology employing the alignment of 1,000 single-copy coding-genes in the RAxML matrix. The *E. coli* strains UMN026 (ST597-D), CFT073 (ST73-B2), 536 (ST127-B2), S88 (ST95-B2), E2348/69 (ST15-B2), O157:H7 Sakai (ST11-E), and O111:H- 11128 (ST16-B1) were added to the phylogenetic tree as outgroups as well as the *Escherichia fergusonni* strain ATCC35469. The final layout and annotation were accomplished using iTOL v.4. (Letunic and Bork, 2019).

Analysis of Intimin Production and EspB Secretion by Immunoblotting

For the immunoblotting assays, the bacterial inoculum was standardized sub-culturing the strains at a dilution of 1/50 into DMEM until they reached an OD600 ≅1.

Intimin production was analyzed using total protein extract, followed by immunoblotting, as previously described by Towbin et al. (1979) using a monospecific polyclonal antibody against the conserved region of this protein (Int388-667) (Menezes et al., 2010).

Secreted proteins were extracted as described by Zarivach et al. (2007), and an immunoblotting assay using an anti-EspB primary antibody (Guirro et al., 2013) and anti-rabbit secondary IgG antibody (whole molecule)-Peroxidase (Sigma, Saint Louis, EUA) was employed to evaluate the ability of UPEC 252 to produce T3SS. A protein extract from the typical EPEC prototype strain E2348/69 was used as a positive control (Santos et al., 2019).

Cell Culture and Maintenance

HeLa (ATCC® CCL-2), HEK293T (ATCC® CRL-1573), Caco-2 (ATCC® HTB-37TM), and LS174T (ATCC® CL-188) cell lineages were cultivated using Dulbecco's Modified

Eagle Medium (DMEM), high glucose, GlutaMax™ (Gibco-ThermoFisher Scientific, USA) (2 g/L sodium bicarbonate, 4.5 g/L glucose) containing 15 mM HEPES (Sigma, Saint Louis, USA), 1x Penicillin-Streptomycin-Neomycin (PSN) antibiotic mixture (GiBCO, USA), and 10% bovine fetal serum (BFS) (GIBCO, USA). T24 cells (ATCC® HTB-4) were grown using McCoy 5A (modified) medium (Gibco, USA) supplemented with 10% BFS and 1x PSN. All cell lineages were kept in 5% CO_2 atmosphere at 37°C.

Suspensions of each cell type were seeded into 24-well plates (1×10^5 cells/ mL per well) and kept in culture according to the assay type. For qualitative assays, all cell lineages were cultivated for 2–5 days until they reached 80% confluency, except for Caco-2 cells, which were cultivated for 10 days to reach confluency, polarization, and differentiation. For quantitative assays, all cells were cultivated until they reached full confluency.

Determination of the Bacterial Adherence Pattern

The adherence pattern was determined as described (Santos et al., 2019) using HeLa cells in 6 h of interaction in the presence of 2% D-mannose (Sigma - USA) to prevent Type 1 fimbria-mediated adhesion. Bacteria previously grown in LB for 18 h at 37°C were inoculated in 1 mL of cell media, at a 1:50 dilution, and incubated at 37°C for 3 h. The preparation was then washed with phosphate-buffered saline (PBS), fresh medium was added, and incubation proceeded for an additional 3 h. After the 6 h period, the cells were washed, fixed with methanol, stained with May Grünwald and Giemsa (Merck, New Jersey, USA) and evaluated by light microscopy (Hernandes et al., 2013). As controls, the *E. coli* prototype strains producing the LA (tEPEC E2348/69), AA (EAEC 042), and diffuse adhesion (DA) (DAEC C1845) patterns were used, as well as a non-adherent laboratory strain (*E. coli* HB101) (Hernandes et al., 2013).

Fluorescence Actin Staining (FAS) Assay

The FAS test was used as an indirect approach to verify the ability of UPEC 252 to cause A/E lesions (Knutton et al., 1989). The test was performed in HeLa cells precisely as described for the determination of adhesion patterns. At the end of the assay, cells were fixed in 3% formaldehyde in PBS, permeabilized with 1% Triton X-100, and incubated with phalloidin for 20 min. Subsequently, coverslips were washed in PBS, mounted on glycerol, and observed under fluorescence microscopy (OLYMPUS BX60) (Olympus, Tokyo, Japan) with immersion lenses. As positive and negative controls, the *E. coli* E2348/69 (Jerse et al., 1990) and C1845 strains, respectively, were used.

The percentage of cells with pedestal produced by the UPEC 252 and EPEC E2348/69 strains was quantified in three different fields of view in a triplicated FAS assay. The results were shown by the means of the number of infected cells with F-actin accumulation foci (pedestals) ± SD. The unpaired bi-directional Student's *t*-test was used to compare means of the two strains, in which $P \leq 0.05$ was considered statistically significant.

Transmission Electron Microscopy

For Transmission Electron Microscopy (TEM), HeLa cells were grown onto ACLAR® film inserted into 24-wells plates, and subsequently subjected to an adhesion assay for 3 h as described above. In the end, the preparation was washed twice with 2% formaldehyde and 2.5% glutaraldehyde in 0.1 M sodium cacodylate buffer pH 7.2 and kept overnight in the same buffer. The material used was gradually infiltrated and embedded in gelatin capsules and allowed to polymerize for 48 h in an oven at 60°C; semi-thin sections (300–500 μm) were obtained and hot-stained with 1% toluidine blue. Finally, ultrathin sections (70 nm) were contrasted with uranium and lead citrate and visualized on a Jeol JEM 1200EX II transmission electron microscope. The typical EPEC E2348/69 and DAEC C1845 prototype strains were used as a positive and negative controls, respectively.

Bacterial Interaction With Intestinal and Urinary Tract Cell Lineages

The ability of UPEC 252 to interact with intestinal (Caco-2 and LS174T) and urinary tract (T24 and HEK293) cell lineages was evaluated.

Adherence assays were performed as described above but in 3 h and the absence of D-mannose. For the quantitative adhesion assays, after the 3 h incubation period, cells were incubated for ∼30 min with 1 mL sterile distilled water for cell lysis (Santos et al., 2019). Then, the suspension containing lysed cells and bacteria was subjected to serial dilutions and seeding onto MacConkey Agar to determine the number of colony-forming units (CFU) associated with the cells. The UPEC CFT073, aEPEC 4581-2 and non-adherent *E. coli* HB101 were included as controls. The One-way ANOVA followed by *post hoc* Tukey HSD test was used to compare the results obtained in this experiment.

The quantitative invasion assay was performed in duplicates, however, at the end of 3 h of incubation, one of the duplicates was washed with PBS, lysed by incubation with sterile distilled water for about 30 min, serially diluted, and plated onto MacConkey Agar to obtain the total number of bacteria interacting with the cells. The second duplicate was washed with PBS, incubated for an additional hour with DMEM containing 100 μg/mL gentamicin to kill the extracellular bacteria; after the incubation period, cells were washed, lysed, and the resulting preparations, diluted and seeded onto MacConkey agar to obtain the number of internalized bacteria (Luck et al., 2005). The invasion index was defined by the ratio of the total number of internalized CFUs by the total number of CFUs associated with the cells (externally and internally), expressed as a percentage. The invasive *Shigella flexneri* strain M90T was used as positive control while the non-invasive strain *Escherichia albertii* 1551-2::*eae*, mutated in the *eae* gene (Hernandes et al., 2008), was employed as a non-invasive control in all cellular lineages tested, except for the HEK293T cell lineage, where the DAEC C1845 strain was used as a negative control. All quantitative assays were performed in biological and experimental triplicates. The One-way ANOVA followed by *post*

hoc Tukey HSD test was used to compare the results obtained in this experiment.

Bacterial Resistance to the Human Serum Complement

To determine the resistance of UPEC 252 to the human serum complement, lyophilized human complement (Sigma, USA) reconstituted in PBS was used. Bacterial cells grown overnight in LB were washed twice and resuspended in PBS. The bacterial suspension was seeded onto MacConkey agar for CFU determination. The bacterial culture concentration was then adjusted to $\sim 1 \times 10^7$ CFU / mL in PBS. Then, 200 μl of the adjusted inoculum and 200 μl of human serum pool were mixed and incubated at 37°C for 4 h. Aliquots of the preparation were collected at three different times (30, 60, and 240 min), serially diluted, and plated onto MacConkey agar to obtain the survived bacterial counts. Simultaneously, another assay using serum inactivated by heating for 30 min at 56°C was performed. The experiments were carried out in biological triplicates, and the *E. coli* strain C600 and the *Enterobacter* spp. strain EB046 were used as serum sensitive and resistant controls, respectively (Keller et al., 1998). Additionally, the UPEC CFT073 and aEPEC 4581-2 strains were used as controls.

Biofilm Formation

Analysis of biofilm formation was carried out as described previously (Lima et al., 2019). UPEC 252 was grown in LB at 37°C for 18 h. Then, 20 μl of the culture were added to 24-well polystyrene plates containing 1 mL of DMEM GlutaMax™ and incubated at 37°C for 24 or 48 h. After incubation, bacteria were washed with PBS, fixed overnight with 1 mL of formaldehyde (3%), and stained with 1% violet crystal. After successive washes, the dye impregnated in the cells was solubilized with 95% ethanol (Merck), supernatants were transferred to 96-well plates, and the optical density of the solution was measured in a spectrophotometer at 620 nm (Hernandes et al., 2013). The experiments were carried out in biological and experimental triplicates. The EAEC 042, UPEC CFT073, aEPEC 4581-2, and *E. coli* HB101 strains were used as controls. The One-way ANOVA followed by *post hoc* Tukey HSD test was used to compare the results obtained in this experiment.

Antimicrobial Sensitivity Test

The diffusion disc technique was used as proposed by Bauer et al. (1966) to evaluate the antimicrobial susceptibility profile. The diameters of growth inhibition halos were measured and interpreted following the standards of the Brazilian Committee on Antimicrobial Susceptibility Testing - BrCAST breakpoints (EUCAST, 2020).

The antibiotics employed in this test were: amoxicillin-clavulanic acid (20 + 10 μg), aztreonam (30 μg), cefepime (30 μg), ceftazidime (10 μg), ceftriaxone (30 μg), meropenem (10 μg), imipenem (10 μg), ertapenem (10 μg), gentamicin (10 μg), amikacin (30 μg), tigecycline (15 μg), cefoxetin (30 μg), and ciprofloxacin (5 μg).

RESULTS

Genetic Characterization of the LEE Region and Non-LEE Effectors in UPEC 252

UPEC 252 was originally reported to harbor the *eae* gene, which is a property characteristic of the EPEC and EHEC pathotypes (Abe et al., 2008). This fact raised the question of whether this strain would carry an intact LEE region, where the *eae* gene is located, and, therefore, could be potentially more virulent. Based on manual verification of the recently published genome sequence of UPEC 252 (Valiatti et al., 2019), we observed that the strain carried a complete LEE region (**Table 1**). Moreover, of all the 55 non-LEE effectors screened, only the *cif, nleB, nleB1, nleB2, nleC, nleE, nleF, nleG, nleH1*, *nleH2, espL,* and *espJ* genes were found.

By examining the sequence of the LEE region using the BLAST program, UPEC 252 showed identities ranging from 93 to 99% with EPEC, EHEC, and *E. albertii* strains isolated from different sources and countries (**Table 2**). The highest identity was found between UPEC 252 and aEPEC strain 13E0767 isolated from cattle in Germany, and eight EHEC strains, five of them belonging to the O111 serogroup, including the EHEC O111:H-strain 11128 (**Table 2**).

Assessment of the LEE Region Functionality

The functionality of the LEE was verified phenotypically. Initially, Intimin and EspB expression was confirmed by immunoblotting, in which both proteins exhibited their predicted molecular sizes (**Figure 1**).

The ability of UPEC 252 to promote A/E lesion was then assessed in HeLa cells, where it presented a mixed adherence pattern either in the presence or absence of D-mannose, with occasional loose clusters resembling the Localized Adherence-Like (LAL) pattern (**Figure 2**), as well as bacteria diffusely attached to the cell surface, after 6 h of interaction. The ability of UPEC 252 to produce A/E lesion was then assessed by the FAS test, which revealed the capacity of the strain to mobilize actin. However, as observed by optical microscopy, actin mobilization occurred only occasionally, ∼30% of the infected cells, 3-fold less of the mobilization caused by E2348/69 (**Supplementary Figures 1**, **2**). Pedestal formation due to actin mobilization was found on the cells surface by TEM (**Figure 3**), showing that UPEC 252 bears a functional LEE capable of producing A/E lesion *in vitro*.

UPEC 252 Genetic Background and Other Virulence-Associated Genes

To understand the general genomic relationship of UPEC 252 with other *E. coli* isolates, phylogenetic analyses were performed, showing that it belongs to serotype O71:H40 and to phylogroup A. Multilocus sequence analysis conducted according to the Warwick scheme identified the strain as belonging to ST10. The phylogenetic tree built with strains of the ST10 showed that this ST is composed of strains from various DEC pathotypes, including strains presenting virulence encoding-genes of different DEC pathotypes and ExPEC strains isolated

TABLE 1 | Genes that comprise the LEE region of UPEC252[a].

Gene	Coverage	%Coverage	%Identity	Accession
espG	1–1,197/1,197	100.00	100.00	gi:260869665
escE	1–219/219	100.00	99.54	NP_290287
escK	1–199/199	100.00	99.50	AF022236.1
escR	1–654/654	100.00	100.00	gi:215488994
escT	1–777/777	100.00	99.87	gi:260869699
etgA	1–459/459	100.00	99.35	NP_290279
grlA	1–414/414	100.00	99.76	gi:260869695
escC	1–1,539/1,539	100.00	99.94	gi:215488986
escJ	1–573/573	100.00	99.83	gi:260869691
espZ	1–297/297	100.00	99.66	gi:260869689
escV	1–2,028/2,028	100.00	100.00	gi:260869687
escO	1–378/378	100.00	98.41	NP_290267
sepQ/escQ	1–918/918	100.00	93.14	NP_290265
cesF	1–363/363	100.00	99.45	gi:260869681
tir	1–1,656/1,656	100.00	99.94	gi:260869679
eae	1-2808/2808	100.00	100.00	gi:260869677
sepL	1–1,056/1,056	100.00	100.00	gi:260869675
espD	1–1,143/1,143	100.00	100.00	gi:260869673
cesD2	135–408/408	67.16	99.27	gi:260869671
escG	1–279/279	100.00	96.77	NP_290251
espF	1–504/789	63.88	90.71	gi:260869668
escF	1–222/222	100.00	100.00	gi:260869670
espB	1–963/963	100.00	100.00	gi:260869672
espA	1–579/579	100.00	100.00	gi:260869674
escD	1–1,221/1,221	100.00	99.84	gi:260869676
cesT	1–471/471	100.00	100.00	gi:260869678
map	1–612/612	100.00	99.84	gi:260869680
espH	1–510/510	100.00	100.00	gi:260869682
escP	1–276/276	100.00	98.19	NP_290266
escN	1–1,341/1,341	100.00	99.92	gi:260869686
cesL	1–354/354	100.00	99.44	NP_290270
escI	1–429/429	100.00	93.24	NP_290272
sepD	1–456/456	100.00	100.00	gi:260869692
cesD	1–456/456	100.00	100.00	gi:260869694
grlR	1–372/372	100.00	100.00	gi:260869696
escU	1–1,038/1,038	100.00	100.00	gi:260869698
escS	1–273/273	100.00	99.63	gi:291285070
escL	1–615/615	100.00	99.67	NP_290284
cesAB	1–324/324	100.00	99.69	gi:15804247
ler	1–390/390	100.00	99.74	gi:215488999
rorf1	1–272/272	100.00	90.81	AF022236.1

[a]*Summary of LEE genes identified by the ABRicate program. The percentage of coverage and identity displayed were the highest identified, comparing UPEC 252 with O157: H7 Sakai (EHEC), O127: H6 E2348/69 (EPEC), and O111: H- 11128 (EHEC). Most proteins presented belong to the E. coli O111:H- str 11128.*

from different sites of infection (**Figure 4**). UPEC 252 was allocated in a cluster composed of aEPEC strains and two *E. coli* strains isolated from extraintestinal infections (**Figure 4**). Among the aEPEC strains with higher similarity, most were isolated from humans without intestinal infection (**Figure 4** and **Supplementary Table 1**).

Regarding the virulence-encoding genes investigated, *in silico* analysis revealed the presence of 17 virulence genes/operons, as shown in **Table 3**, which are related to several pathogenicity mechanisms. Genes related to iron acquisition, serum resistance, and some adhesins were identified; although none of them are recognized as classically related to extraintestinal infections, except for *malX* (**Table 3**), they might contribute to the occurrence of extraintestinal infections. Several genes of different efflux pumps related to resistance to antimicrobials and other organic compounds were found in the UPEC 252 genome (**Supplementary Table 2**). However, no gene directly related to antimicrobial resistance was identified. Additionally, a phenotypic assay demonstrated that our strain was sensitive to all tested antimicrobials (**Supplementary Table 3**). The pangenome analyzes performed reinforced the phylogenetic relationship of UPEC 252 and aEPEC (**Supplementary Figure 3**), but did not evidence any gene that could be related to the establishment of UTI. Moreover, the genome alignment performed using progressiveMAUVE highlighted some insertion regions (composed of genes with unknown function or bacteriophages) in the UPEC 252 genome (**Supplementary Figure 4**) in comparison with EPEC/EHEC strains.

UPEC 252 Is Resistant to Serum Complement Activity

As the analyses of the genome revealed the presence of the *traT* and *iss* genes, UPEC 252 was tested regarding its ability to resist the bactericidal power of human serum. Data demonstrated that UPEC 252 was serum resistant in the assayed condition, in which bacteria were incubated with serum complement in the physiologic concentration (50%) for at least 4 h, like the serum-resistant control *Enterobacter* sp. strain EB046 (**Figure 5**).

UPEC 252 Does Not Produce Biofilm on Abiotic Surfaces

The ability to form biofilm on an abiotic surface (polystyrene) was tested at two different periods (24 and 48 h), however, under the conditions tested (cultivation in DMEM at 37°C) and regardless of the incubation period, the UPEC 252 was not able to form biofilm *in vitro* (**Supplementary Figure 5**).

Evaluation of the Ability of UPEC 252 to Colonize and Invade Urinary and Intestinal Tract Cells *in vitro*

The ability of UPEC 252 to adhere to urinary (T24 and HEK 293T) and intestinal (Caco-2 and LS174T) epithelial cells was assessed using qualitative (**Supplementary Figures 6**, **7**) and quantitative (**Figure 6**) adherence assays, with incubation periods of 3 h. UPEC 252 was able to adhere efficiently to all cell lines tested, and, when compared to UPEC (CFT073) and aEPEC (4581-2) controls, it showed higher adherence capacity in HEK293T, T24, and Caco-2 cells ($p < 0.0001$) than in the LS174T cell lineage ($p < 0.001$).

Comparing UPEC 252 adherence capacity among the diverse cell lineages used, the number of bacteria that adhered to the cells

TABLE 2 | Comparison of the LEE region of UPEC 252 with strains available at the NCBI.

Strain	Isolation year	Place	Pathotype	Serogroup	Source	Identity	Access number
Escherichia coli 13E0767	1998	Germany	EPEC	O156	Cattle	99.97%	CP020107.1
Escherichia coli FORC_042	2013	South Korea	EPEC	NA[a]	Pork meat	99.93%	CP025318.1
Escherichia coli 2013C-3304	2013	USA	EHEC	O71	Stool human	99.92%	CP027593.1
Escherichia coli O111 RM9322	2009	USA	EHEC	O111	Stream	99.92%	CP028117.1
Escherichia coli 2015C-3101	2014	USA	EHEC	O111	Stool human	99.92%	CP027221.1
Escherichia coli O111:H- 11128	2001	Japan	EHEC	O111	Stool human	99.92%	AP010960.1
Escherichia coli RM9975	2009	USA	EHEC	O111	Stool human	99.91%	CP028432.1
Escherichia coli 95JB1	1995	Australia	EHEC	O111	Stool human	99.91%	CP021335.1
Escherichia coli O157:H7 Sakai	1996	Japan	EHEC	O157	Stool human	97.46%	BA000007.3
Escherichia coli O127:H6 E2348/69	1969	United kingdom	EPEC	O127	Stool human	97.19%	FM180568.1
Escherichia coli O121 RM8352	2009	USA	EHEC	O121	Sediment[b]	93.17%	CP028110.1
Escherichia coli O121:H19 16-9255	2016	Canada	EHEC	O121	Flour	93.17%	CP022407.1
Escherichia albertii _EC06_170	2006	Japan	NA	NA	Human	93.20%	AP014857.1

[a] *NA – Information not available or not applicable.*
[b] *the strain was isolated from sediments from a stream.*

of the urinary tract was higher when compared to the cells of the intestinal tract (*** $p < 0.01$) (**Supplementary Figure 8**).

Invasion assays were performed to verify the ability of UPEC 252 to invade epithelial cells. To this end, HeLa, HEK293T, and Caco-2 cells were infected for 3 h in the absence of mannose. Despite recovering internalized bacterial counts in the order of 10^4 CFU/mL, the invasion indexes observed were 0.028% (HeLa cells), 0.024% (HEK293T cells), and 0.05% (Caco-2 cells) (**Supplementary Figures 9–11**). These indexes were considerably low in comparison with the index of the classical invasive strain, *Shigella flexneri* M90T, used as a positive control.

DISCUSSION

In this study, we sought to perform a genotypic and phenotypic characterization of UPEC 252, which carried the *eae* gene (Falsetti, 1998; Abe et al., 2008) that is characteristic of the EPEC and EHEC pathotypes, what suggested that this strain could be capable of producing intestinal and extraintestinal infections in the same patient.

The alignment of the sequence of the LEE of UPEC 252 with the LEE of other strains revealed high similarities (more than 99.9% of identity) with aEPEC and EHEC strains isolated in Europe, Asia, Oceania, and North America. Interestingly, the strain whose genome showed the highest similarity was an aEPEC strain isolated in Germany in the same year as UPEC 252 (1998). In addition, we investigated if UPEC 252 harbored non-LEE genes that encode effector proteins that are secreted by A/E lesion-producing pathogens by a T3SS (Deng et al., 2012). Twelve among 55 known non-LEE genes (*cif, nleB, nleB*1, *nleB*2, *nleC, nleE, nleF, nleG, nleH*1, *nleH*2, *espL,* and *espJ*) were identified. It should be noted that the non-LEE proteins are not directly related to A/E lesion formation, but their activities may contribute to increased bacterial virulence by other pathways (reviewed by Gomes et al., 2016). The non-LEE genes found in UPEC 252 are related to several pathogenic mechanisms, such as inhibition of cell detachment and modulation of cell death (*cif* and *nleF*); inhibition of phagocytosis (*nleG*, *espJ, nleH*1, and *nleH*2), modulation of pro-inflammatory signaling (*nleB, nleB*1, *nleB*2, *nleC, nleE*, *nleG, nleH*1, and *nleH*2), and cytoskeleton modulation (*espL*) (Dean and Kenny, 2009; Vieira et al., 2010; Vossenkämper et al., 2011; Wong et al., 2011; Salvador et al., 2014).

Immunoblotting assays revealed that UPEC 252 produced intimin and secreted the EspB protein, thus suggesting that the LEE region was functional in this strain. Given the similarity of UPEC 252 with aEPEC strains (presence of the LEE region, and absence of pEAF and the *stx* genes), its adhesion pattern was investigated on HeLa cells, using prolonged assays (6-h assay) in the presence of D-mannose. Although UPEC 252 presented a non-characteristic adhesion pattern, it adhered randomly, forming loose microcolonies, which is the same pattern observed in some aEPEC strains. Thus, the presence of the LEE region in the UPEC 252 genome is probably contributing to the formation of the observed loose clusters, but further studies should be performed to confirm this hypothesis.

To corroborate the hypothesis of the ability of the UPEC 252 to produce A/E lesion, we employed the FAS test, which is commonly used as an indirect measure to determine the capacity of EPEC, EHEC, *E. albertii,* and *Citrobacter rodentium* strains to remodel the host cell cytoskeleton (Knutton et al., 1991; Lima et al., 2019; Tanabe et al., 2019). Although we have verified that UPEC 252 can promote actin accumulation in HeLa cells at the site of bacterial adhesion at only some fields and 3-fold less than a typical EPEC strain, TEM images revealed the occurrence of pedestal-like structures on the cell surface. Additional experiments are necessary to confirm further the ability of this strain to promote A/E lesions *in vivo* since it has been shown that not all LEE-positive strains that produce these lesions are FAS positive *in vitro* (Bai et al., 2008).

Genomic analyses have improved our understanding of how *E. coli* strains have evolved, revealing their genetic backgrounds,

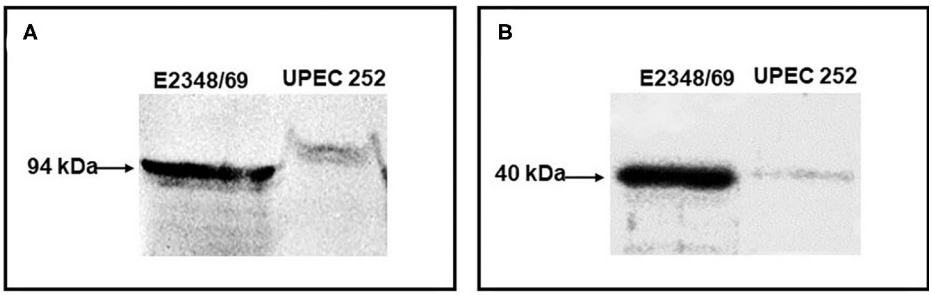

FIGURE 1 | Immunodetection of Intimin and EspB. The production of the adhesin intimin and the secreted protein EspB were detected by immunoblotting. **(A)** Immunoblotting assay of UPEC 252 using an anti-intimin antibody (1:100) against the conserved region of the protein (Int388-667); **(B)** Immunoblotting assay of UPEC 252 using an anti-EspB antibody (1:3000). tEPEC strain E2348/69, positive control of production of intimin (94 kDa) and EspB (∼ 40 kDa).

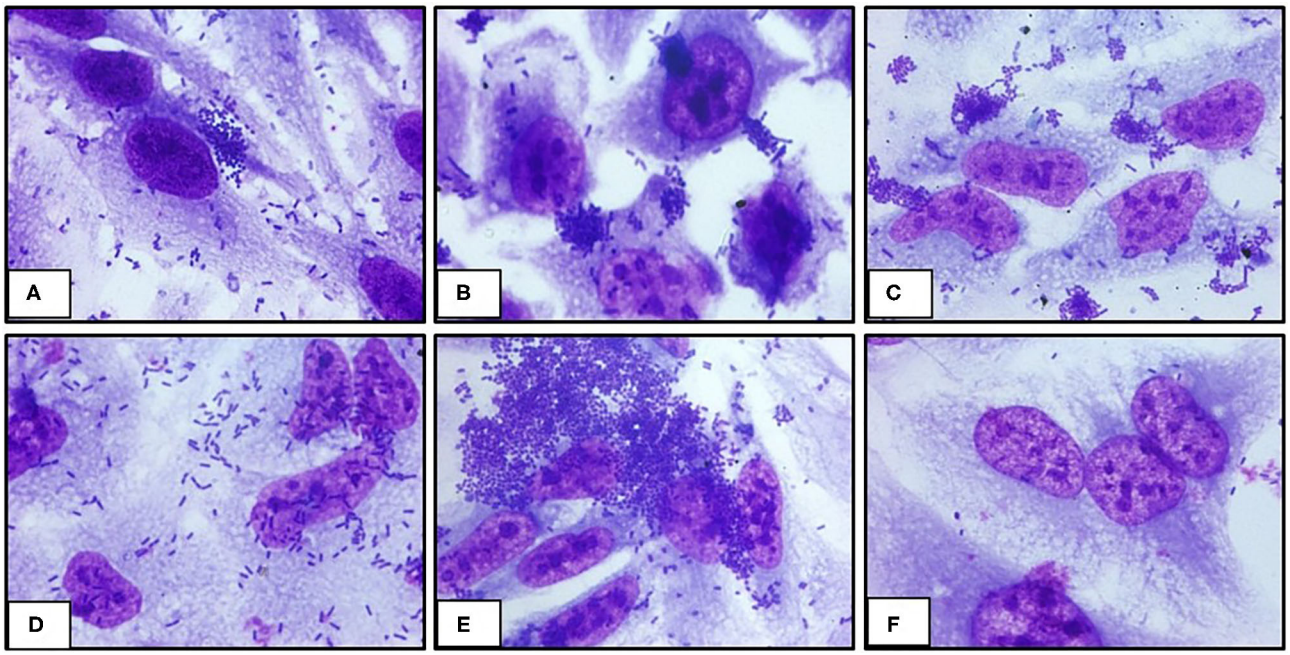

FIGURE 2 | Adherence pattern of UPEC 252 to HeLa cells. The adherence pattern of the UPEC 252 **(A)** was obtained in a 6-h interaction assay in the presence of 2% D-mannose. Light microscopy images (microscopic magnification 1,000 ×) shows the production of loose bacterial microcolonies similar to the LAL (localized adherence-like) pattern of atypical EPEC. Controls: Localized adhesion: typical EPEC E2348/69 **(B)**; LAL: aEPEC 3991-1 **(C)**; Diffuse adhesion: DAEC C1845 **(D)**, Aggregative adhesion: EAEC 042 **(E)**; Non-adherent: *E. coli* HB101 **(F)**.

and highlighting the occurrence of horizontal gene transfer. Our phylogenetic analysis evidenced that UPEC 252 belonged to phylogroup A, ST10, and serotype O71:H40. *E. coli* strains of the ST10 have been frequently associated with UTI in several countries, including Brazil (Gonçalves et al., 2016; Hertz et al., 2016; Campos et al., 2018). Other studies have also reported the isolation of *E. coli* strains of the ST10 from the environment and food, as well as from bloodstream infections and diarrhea, evidencing the versatility of colonization of this ST (Arais et al., 2018; Liu et al., 2018; Mohsin et al., 2018; Yamaji et al., 2018).

In addition, our analysis showed that ST10 is composed of *E. coli* strains from various DEC pathotypes (ETEC, STEC, EPEC), as well as commensals and strains isolated from a variety of extraintestinal infections. Moreover, strains harboring combined virulence-encoding-genes used as diagnostic markers of the different DEC pathotypes (*e.g.,* ETEC/STEC) were identified among the ST10 strains. Furthermore, two strains isolated in Europe (Sweden and England) from extraintestinal infections and harboring the LEE region were detected. One of them was isolated in 1995 from the urine of an inpatient that developed urosepsis, while the other was isolated in a surveillance program from a bloodstream infection in 2008 (Kallonen et al., 2017). Altogether, these data corroborate with the hypotheses that some *E. coli* STs could be considered a "melting pot" that

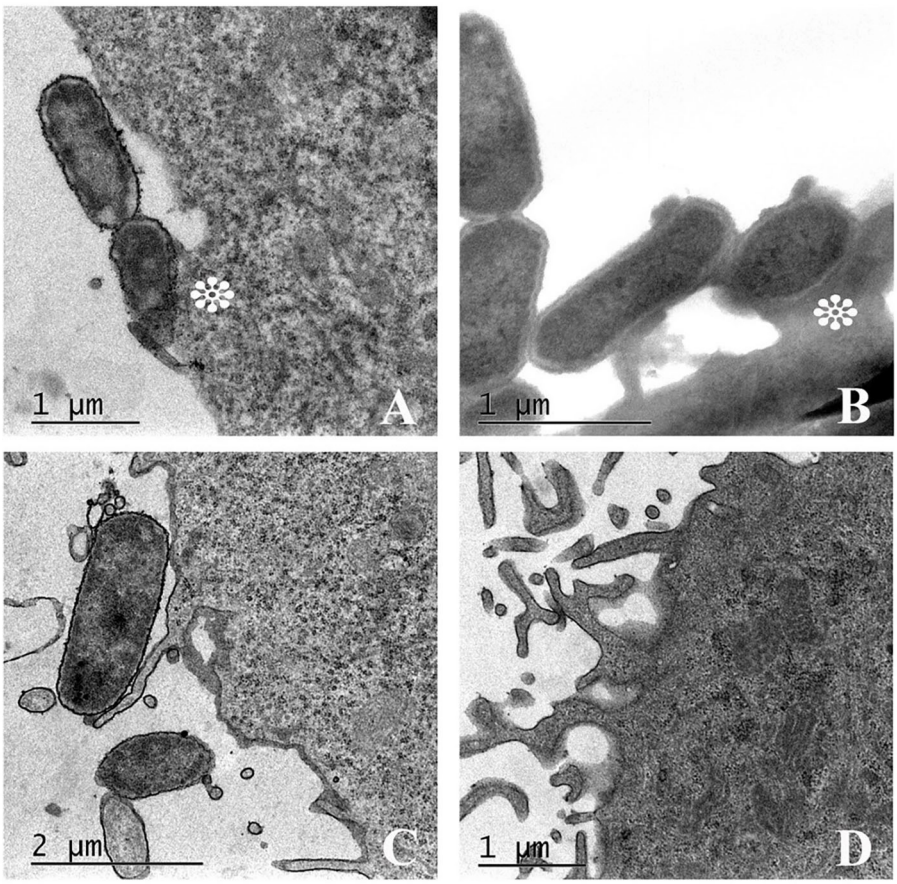

FIGURE 3 | Attaching-effacing lesion promoted by UPEC 252. Transmission electron microscopy (TEM) of UPEC 252 evidencing cytoskeleton rearrangement and pedestal formation under the intimate bacterial adherence to HeLa cell. **(A)** A/E lesion produced by UPEC 252; **(B)** A/E lesion produced by positive control typical EPEC E2348/69; **(C)** Absence of A/E lesion in cells infected with the DAEC strain C1845, used as a negative control; **(D)** Non-infected cells. Asterisks indicate the pedestal-like structure formed under the adhered bacterium.

favors the emergence of hybrid strains, i.e., strains presenting concomitantly virulence markers that define different *E. coli* pathotypes (Gati et al., 2019). The ST10 complex could be a candidate for this emergence because it encompasses all *E. coli* pathotypes, and a variety of hybrid strains have been identified in this ST (STEC/ETEC, EAEC/UPEC, and EPEC/ExPEC).

In this context, two hypotheses were raised: UPEC 252 could be an ExPEC strain that acquired the LEE island, or an aEPEC strain that, over time, received ExPEC genes that allowed it to establish UTI. Our phylogenetic analyses supported the latter hypothesis because UPEC 252 is inserted into a cluster composed of aEPEC strains, suggesting that it has an EPEC genomic background. The diversity of aEPEC strains and their ability to acquire virulence genes by horizontal transfer were demonstrated by Hazen et al. (2017) through genome analyses. These authors showed that EPEC/ETEC hybrid strains were genetically closer to EPEC, and later acquired ETEC virulence genes. It is worth to mention that most aEPEC strains in the UPEC 252 cluster were isolated from the gut of asymptomatic human carriers, besides the two ExPEC strains that also harbored the LEE and were isolated from extraintestinal infection of non-diarrheic inpatients. These data suggested that this specific cluster could harbor strains with an attenuated diarrheagenic phenotype, which is reinforced by the few FAS positive signals produced by UPEC 252 in HeLa cells mentioned above. However, more studies are necessary to confirm this hypothesis because ST10 bears other EPEC clusters in which several pathogenic EPEC strains that had been isolated from diarrhea were detected (Ferdous et al., 2016; Arais et al., 2018; Santos et al., 2019). Besides the EPEC related genes, other virulence factors were identified in the genome of UPEC 252, among which genes that are involved in bacterial adherence to host cells, like *E. coli* laminin-binding fimbriae (ELF), *E. coli* common pilus (ECP), and Type 1 fimbriae. In UPEC strains, Type I fimbriae were demonstrated to be essential for adherence to the bladder epithelium (Paneth cells) at the early stage of UTI establishment (Connell et al., 1996; Sokurenko et al., 1998). Analysis of the genome of UPEC 252 also revealed the presence of the *iss* and *traT* genes, which confer to *E. coli* strains resistance to the bactericidal power of human serum (Binns et al., 1979) that is the first line of

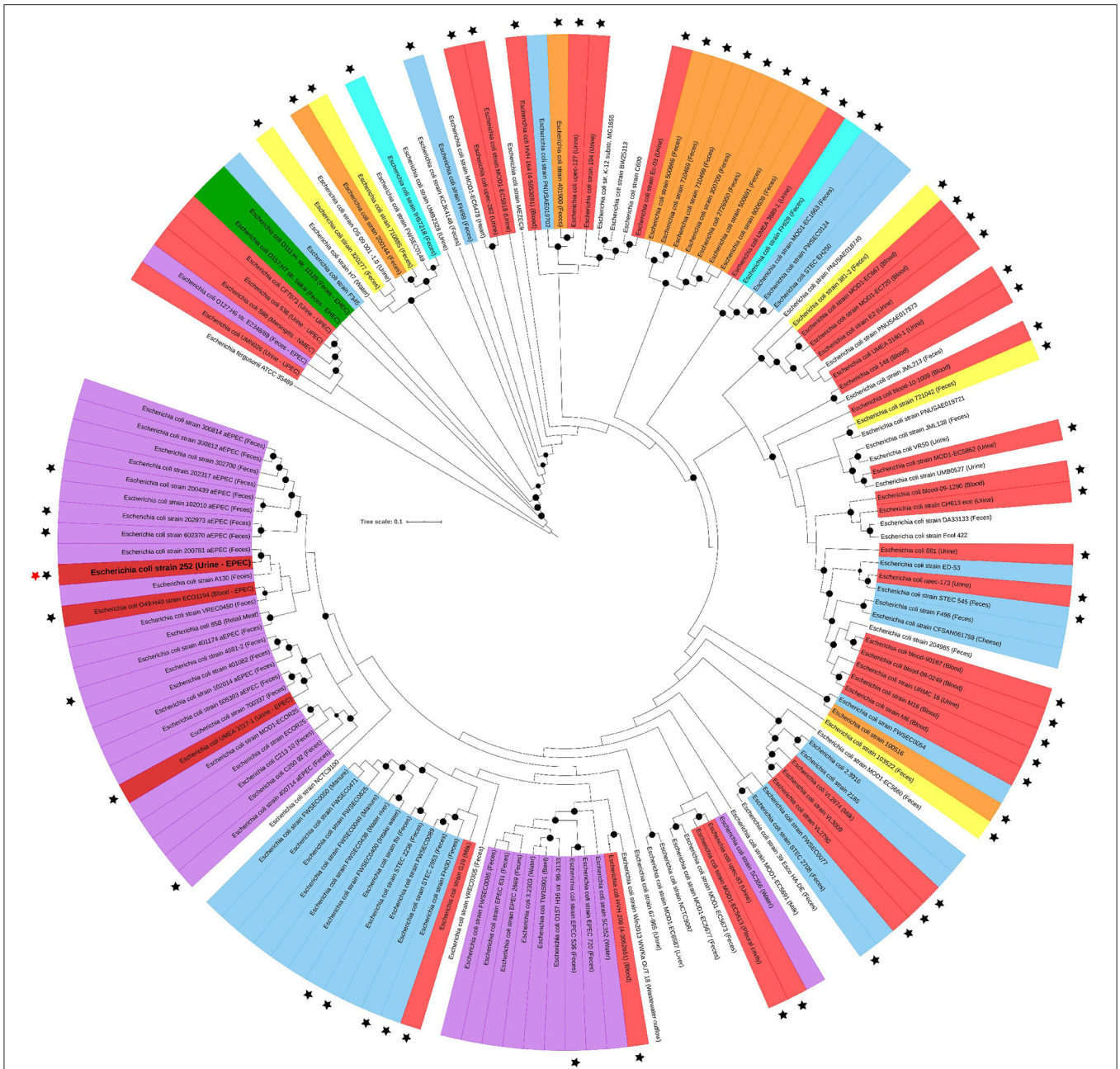

FIGURE 4 | UPEC 252 phylogenetic tree. The phylogenetic tree was built with 140 public *E. coli* genomes belonging to ST10 using the codon-tree methodology of 1,000 single-copy proteins in the Maximum Likelihood-based matrix (RAxML). Labels are colored according to the *E. coli* pathotypes, which were determined by the presence of specific virulence factors or type of infection: red, extraintestinal pathogenic *E. coli* (strains isolated from extraintestinal infections); orange, enterotoxigenic *E. coli* (*elt* or *est* positive); light blue, Shiga toxin-producing *E. coli* (*stx* positive and *eae* and *escV* negative); green, enterohemorrhagic *E. coli* (*stx, eae* and *escV* positive) cyan, strains harboring *elt* and *stx* (ETEC/STEC); yellow, strains isolated from diarrhea but of unknown DEC pathotype; lilac, enteropathogenic *E. coli* (*eae* and *escV* positive, *stx* negative); dark red, extraintestinal pathogenic *E. coli* strains that, like UPEC 252, were isolated from extraintestinal infections but harbored EPEC virulence genes; uncolored, strains with no pathotype assignment or not confirmed as causing disease. Strains from known origins are indicated in parenthesis. Black stars indicate strains isolated from confirmed infections. UPEC 252 is labeled with a bold letter and indicated by a red star aside from the label. Bootstrap values higher than 90 are indicated by a black circle in the branch.

host defense (Walport, 2001). The serum resistance ability of UPEC 252 was confirmed in experiments conducted *in vitro*. This mechanism is essential for the pathogenicity of strains that reach the bloodstream since it allows bacteria to move across the whole human body, evading such a system and, consequently, aggravating the patient's clinical condition.

We also identified the presence of *mal*X in the genome of UPEC 252, which encodes enzyme II of the phosphotransferase

system, and is used as the pathogenicity island marker of the UPEC prototype strain CFT073, whose relationship with UTI persistence and recurrence was previously demonstrated (Ejrnæs, 2011; Ejrnæs et al., 2011). It is noteworthy that *mal*X is essential for the persistence of *E. coli* strains in the intestinal tract of healthy babies (Östblom et al., 2011).

TABLE 3 | Virulence-encoding genes detected in UPEC 252.

Traits	Virulence factor	Gene/operon
Adhesins/Invasins	*E. coli* laminin-binding fimbriae (ELF)	*elfACDG*
	Hemorrhagic *E. coli* pilus (HCP)	*hcpABC*
	Type I fimbriae	*fimABCDEFGHI*
	E. coli common pilus (ECP)	*ecpRABCDE*
	Curli adhesin	*csgABC-csgEFG*
	Intimin-like adhesin FdeC	*eaeH*
	IbeB (CusC) invasive protein	*cusC*
	EhaB autotransporter Protein	*ehaB*
Protectins	Surface exclusion protein	*traT*
	Increased serum survival	*iss*
	Colicin V production protein	*cvpA*
Iron acquisition system	Ferric hydroxamate system	*fhuACDB*
	Fe^{3+} uptake coprogen receptor	*fhuE*
	Ferric enterobactin receptor	*fepA*
Toxins	Hemolysin/cytolysin A	*hlyE*
	Cytoskeleton-binding toxin CbtA	*cbtA*
Pathogenicity island marker	PTS system maltose-specific	*malX*

Virulence genes detected by VFBD and manually confirmed by BLAST.

Biofilm production allows bacteria to persist in the host and can be associated with the gravity of the infection (Høiby et al., 2011). UPEC strains have been shown to present varying levels of biofilm production (Watts et al., 2010; Novais et al., 2012; Ponnusamy et al., 2012; Agarwal et al., 2013; Tapiainen et al., 2014; Flament-Simon et al., 2019). Herein, we showed that UPEC 252 is not capable of producing biofilm on abiotic surfaces under the conditions tested.

The ability of bacterial strains to adhere to and invade host cells are important mechanisms of virulence, which directly implicates increased pathogenicity since these processes are associated with persistent infections. We showed that UPEC 252 could adhere to different cell lines of the urinary and intestinal tracts *in vitro*. A higher affinity with the urinary tract epithelial cells was observed, which was expected, considering that it was isolated from a urinary tract infection. However, whether UPEC 252 can interact with the intestinal epithelium and cause disease in the intestinal tract remains to be investigated. Furthermore, the ability to invade the host cells allows bacteria to overcome the actions of the immune system and certain antibiotics (Lewis et al., 2016). Especially in female patients, UTIs often recur even after antibiotic therapy (Dielubanza and Schaeffer, 2011; Barber et al., 2013). Studies estimate that ∼1-3rd of women up to 24 years old will be affected by UTI, and about 25% of these women will have at least one recurrent UTI in the following 6 months (Foxman, 2014). According to Lewis et al. (2016), recurrent UTIs are probably related to the invasiveness, persistence, and multiplication of bacteria within the urinary

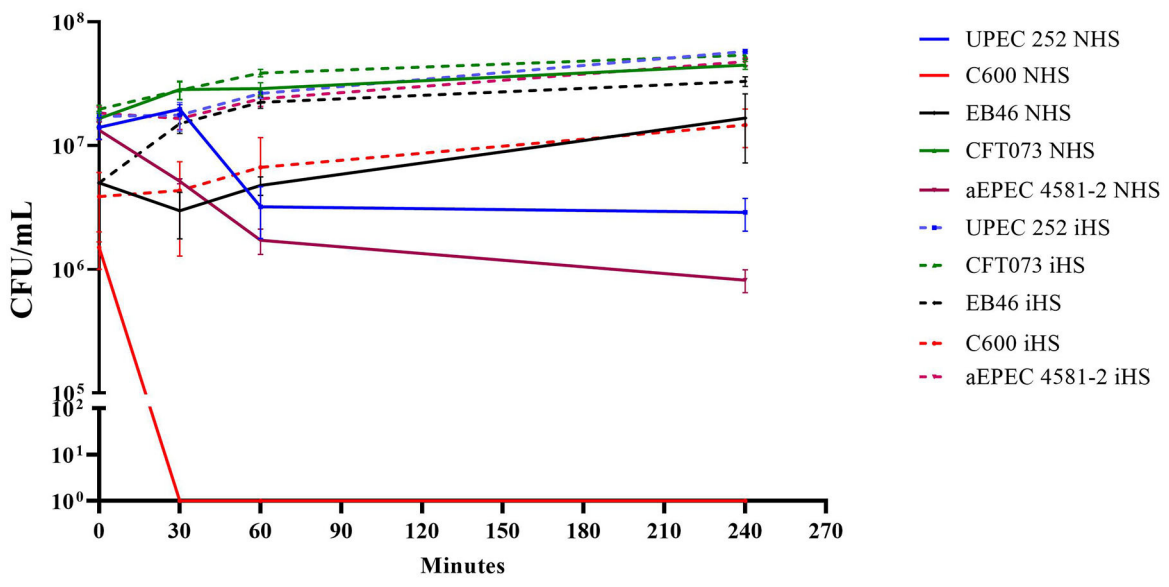

FIGURE 5 | UPEC 252 serum resistance assay. Resistance to the bactericidal effect of the human serum was evaluated using a pool of human serum in PBS (50% of final serum concentration) in a 4-h assay. NHS, normal human serum; iHS, heat-inactivated human serum. The prototypical K-12 derived laboratory strain, *E. coli* C600, was used as a negative control, and the *Enterobacter* sp. strain EB046 was used as a positive control. Strains CFT073 and aEPEC4581 were also included in the experiment. The experiments were performed in biological triplicates.

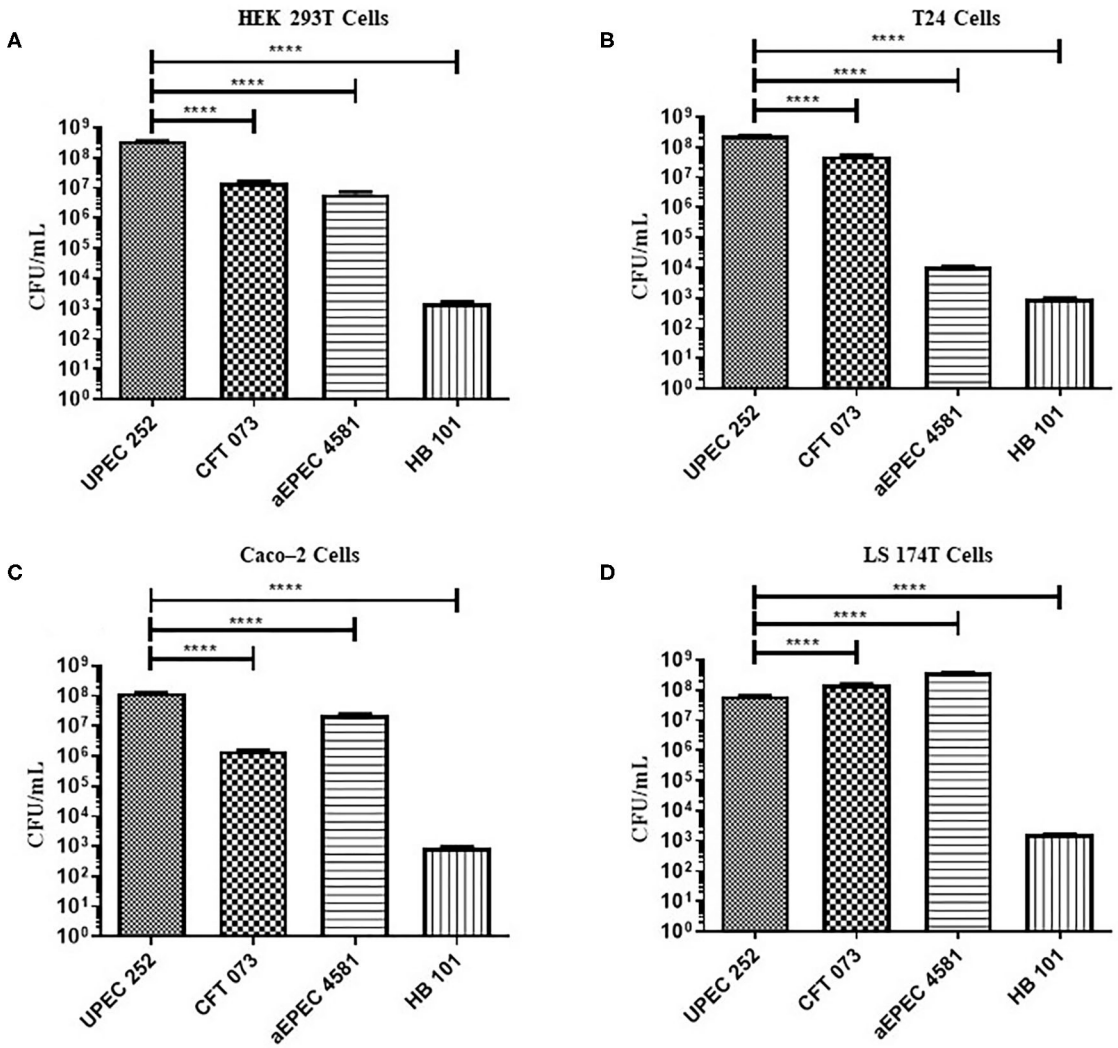

FIGURE 6 | Quantitative adherence of UPEC 252 in different eukaryotic cell lineages. Quantitative assays were performed in a 3-h incubation period, in urinary (T24 and HEK 293T), and intestinal (Caco-2 and LS174T) tract cell lineages, in the absence of D-mannose. **(A)** HEK-293T cells; **(B)** T24 cells; **(C)** Caco-2 cells; **(D)** LS174T cells. The bacterial strains CFT073, aEPEC 4581-2, and *E. coli* HB101 were used as UPEC, aEPEC and poorly adherent controls, respectively. ****$P \leq 0.0001$.

epithelium. Although the internalization rates of UPEC 252 were considerably lower than those of a classical invasive strain (*S. flexneri*), our findings evidenced the ability of this strain to invade the three different cell lines tested (HeLa, HEK293T, and Caco-2), suggesting that it may cause recurrent UTI, or even persistent diarrhea, since it was also able to invade differentiated intestinal Caco-2 cells. As in the present study, Owrangi et al. (2018) verified the ability of UPEC strains to adhere to and invade Caco-2 cells, with 10^4 CFU being recovered from the intracellular compartment.

The occurrence in UPEC 252 of genes characteristic of DEC, the isolation of an symptomatic urinary tract infection, and the presence of ExPEC traits simultaneously suggests that it may cause infections in both the intestinal and extraintestinal tracts, and can be classified as a hybrid aEPEC/UPEC strain (Santos et al., 2020a). Likewise, Lara et al. (2017) identified two UPEC strains carrying EAEC and UPEC genes simultaneously. In the same study, an *E. coli* strain isolated from bacteremia with the same hybrid characteristics as the UPEC strains was also found. By analyzing the presence of specific genes of the DEC pathotypes, Salmani et al. (2016) identified UPEC strains that carried the *st*, *lt*, *agg*R, *inv*E, and *daa*D genes; however, none of them was positive for the *eae* gene. In contrast, Kim et al. (2018) found six UPEC strains of serogroups O2, O15, O18, and O25 that carried *eae*; however, these authors did not demonstrate whether these strains had complete and functional LEE regions.

In addition to our previous study (Abe et al., 2008), four other studies have reported the occurrence of EPEC/ExPEC hybrid strains (Toval et al., 2014; Kessler et al., 2015; Riveros et al., 2017; Lindstedt et al., 2018). In two of them, the strains were isolated from urinary tract infections and carried EPEC virulence genes but were devoid of the most common ExPEC virulence factors, like P fimbriae (Toval et al., 2014; Riveros et al., 2017). Interestingly, these strains also lacked the virulence

genes used to classify the intrinsic virulence of pathogenic ExPEC strains, which is determined by the presence of at least two among the following virulence genes: *iuc/iut, pap, sfa, afa*, and *kpsMTII* (Johnson et al., 2003). In this context, these strains were similar to UPEC 252, whose genome carried a few ExPEC virulence-encoding genes. The other two studies reported on the occurrence of *E. coli* strains from diarrheal patients that harbored the ExPEC intrinsic virulence encoding-genes; in one of these patients, bacteremia and multiorgan dysfunction development were reported (Kessler et al., 2015; Lindstedt et al., 2018). Notably, these reports included strains from three different STs (ST12, ST28, and ST2018) of phylogroups B2 (Toval et al., 2014; Kessler et al., 2015; Lindstedt et al., 2018) and one strain from phylogroup A, whose ST was not determined (Riveros et al., 2017).

Although some *E. coli* clones of ST10 are recognized as ExPEC strains involved in various human extraintestinal infections (Bert et al., 2010; Manges et al., 2017; Yamaji et al., 2018), they do not fulfill the molecular criteria to be recognized as intrinsic virulent (Johnson et al., 2003, 2015) or uropathogenic (Spurbeck et al., 2012) strains. The absence of the most common traits related to ExPEC virulence does not limit their capacity to cause more than 10% of infections in some countries (Manges and Johnson, 2015; Campos et al., 2018; Manges et al., 2019) nor their importance as a recognized foodborne cause of extraintestinal infections that has been continuously reported worldwide (Campos et al., 2018; Yamaji et al., 2018; Manges et al., 2019). Additionally, we identified two other strains that harbored the LEE and were isolated from extraintestinal infections in the same phylogenetic cluster of UPEC 252.

Despite the frequent reports about *E. coli* from ST10 harboring multidrug resistance genes, including *mcr-1*, bla_{NDM}, and bla_{CTX} (Zhang et al., 2017; García et al., 2018; Mohsin et al., 2018; dos Anjos et al., 2019), UPEC 252 was shown to be sensitive to the tested antimicrobials. The detection of some resistance-related genes in UPEC 252 suggests that there is a potential phenotype of resistance for this strain, which perhaps was not detected due to the lack of other essential genes and /or gene expression.

Finally, the data presented here contribute to the discussion about hybrid *E. coli* strains, more specifically, hybrid strains of UPEC, which have additional virulence mechanisms that are characteristic of other *E. coli* pathotypes. Therefore, hybrid UPEC strains may emerge as important pathogens in the world scenario, and further studies are necessary to better understand their virulence mechanisms, so that prevention, diagnosis, and treatment can be more appropriately addressed.

CONCLUSION

UPEC 252 strain exhibits characteristics of ExPEC, EPEC and EHEC strains, along with the ability to adhere to and invade cells of the urinary and intestinal tracts *in vitro*. Our findings suggest that UPEC 252 is an atypical EPEC strain that emerges as a hybrid strain (aEPEC/UPEC), which could colonize new niches and potentially cause intestinal and extraintestinal infections.

DATA AVAILABILITY STATEMENT

The reads used for UPEC 252 genome assembly were deposited in the Sequence Read Archive (SRA) at NCBI under the accession number SRR9317828, and the whole-genome sequences (WGS) were deposited in the GenBank database under the accession number VFST00000000.

ETHICS STATEMENT

This work was evaluated and approved by the local Research Ethics Committee of the Federal University of São Paulo-UNIFESP/São Paulo Hospital, under CEP N 8580081117. Written and informed consent was not required in accordance with local guidelines.

AUTHOR CONTRIBUTIONS

TG, TV, RMS, AS, and FS conceptualized the study. TV, AS, FS, EC, and TG contributed to the formal analysis. TG and TV were responsible for funding acquisition. TV, FS, AS, JN, and EC carried out the investigation. TV, FS, AS, JN, EC, and RS worked on the methodology and validated the study. TG helped with the project administration. TG and RMS supervised the study. TV, FS, and AS wrote the original draft. TV, FS, AS, JN, EC, and TG reviewed and edited the manuscript. All authors read and approved the final manuscript.

FUNDING

This study was conducted with a scholarship funded by grant 2017/21947-7 to TV and grant 2018/17353-7 to TG from the São Paulo Research Foundation (FAPESP).

ACKNOWLEDGMENTS

We thank The Electronic Microscopy Center (CEME) of the Federal University of São Paulo for support with electron microscopy experiments.

SUPPLEMENTARY MATERIAL

The Supplementary Material for this article can be found online at: https://www.frontiersin.org/articles/10.3389/fcimb.2020.00492/full#supplementary-material

REFERENCES

Abe, C. M., Salvador, F. A., Falsetti, I. N., Vieira, M. A. M., Blanco, J., Blanco, J. E., et al. (2008). Uropathogenic *Escherichia coli* (UPEC) strains may carry virulence properties of diarrhoeagenic *E. coli*. *FEMS Immunol. Med. Microbiol.* 52, 397–406. doi: 10.1111/j.1574-695X.2008.00388.x

Agarwal, J., Mishra, B., Srivastava, S., and Srivastava, R. (2013). Genotypic characteristics and biofilm formation among *Escherichia coli* isolates from Indian women with acute cystitis. *Trans. R. Soc. Trop. Med. Hyg.* 107, 183–187. doi: 10.1093/trstmh/trs090

Arais, L. R., Barbosa, A. V., Andrade, J. R. C., Gomes, T. A. T., Asensi, M. D., Aires, C. A. M., et al. (2018). Zoonotic potential of atypical enteropathogenic *Escherichia coli* (aEPEC) isolated from puppies with diarrhoea in Brazil. *Vet. Microbiol.* 227, 45–51. doi: 10.1016/j.vetmic.2018.10.023

Bai, L., Schüller, S., Whale, A., Mousnier, A., Marches, O., Wang, L., et al. (2008). Enteropathogenic *Escherichia coli* O125:H6 triggers attaching and effacing lesions on human intestinal biopsy specimens independently of Nck and TccP/TccP2. *Infect. Immun.* 76, 361–368. doi: 10.1128/IAI.01199-07

Bankevich, A., Nurk, S., Antipov, D., Gurevich, A. A., Dvorkin, M., Kulikov, A. S., et al. (2012). SPAdes: a new genome assembly algorithm and its applications to single-cell sequencing. *J. Comput. Biol.* 19, 455–477. doi: 10.1089/cmb.2012.0021

Barber, A. E., Norton, J. P., Spivak, A. M., and Mulvey, M. A. (2013). Urinary tract infections: current and emerging management strategies. *Clin. Infect. Dis.* 57, 719–724. doi: 10.1093/cid/cit284

Bauer, A. W., Kirby, W. M., Sherris, J. C., and Turck, M. (1966). Antibiotic susceptibility testing by a standardized single disk method. *Am. J. Clin. Pathol.* 45, 493–496. doi: 10.1093/ajcp/45.4_ts.493

Beghain, J., Bridier-Nahmias, A., Le Nagard, H., Denamur, E., and Clermont, O. (2018). ClermonTyping: an easy-to-use and accurate *in silico* method for Escherichia genus strain phylotyping. *Microb. Genomics* 4:e000192. doi: 10.1099/mgen.0.000192

Bert, F., Johnson, J. R., Ouattara, B., Leflon-Guibout, V., Johnston, B., Marcon, E., et al. (2010). Genetic diversity and virulence profiles of *Escherichia coli* isolates causing spontaneous bacterial peritonitis and bacteremia in patients with cirrhosis. *J. Clin. Microbiol.* 48, 2709–2714. doi: 10.1128/JCM.00516-10

Binns, M. M., Davies, D. L., and Hardy, K. G. (1979). Cloned fragments of the plasmid ColV,I-K94 specifying virulence and serum resistance. *Nature* 279, 778–781. doi: 10.1038/279778a0

Campos, A. C. C., Andrade, N. L., Ferdous, M., Chlebowicz, M. A., Santos, C. C., Correal, J. C. D., et al. (2018). Comprehensive molecular characterization of *Escherichia coli* isolates from urine samples of hospitalized patients in Rio de Janeiro, Brazil. *Front. Microbiol.* 9:243. doi: 10.3389/fmicb.2018.00243

Carattoli, A., Zankari, E., García-Fernández, A., Voldby Larsen, M., Lund, O., Villa, L., et al. (2014). *In silico* detection and typing of plasmids using plasmidfinder and plasmid multilocus sequence typing. *Antimicrob. Agents Chemother.* 58, 3895–3903. doi: 10.1128/AAC.02412-14

Chen, L., Zheng, D., Liu, B., Yang, J., and Jin, Q. (2016). VFDB 2016: hierarchical and refined dataset for big data analysis-10 years on. *Nucleic Acids Res.* 44, D694–D697. doi: 10.1093/nar/gkv1239

Connell, H., Agace, W., Klemm, P., Schembri, M., Mårild, S., and Svanborg, C. (1996). Type 1 fimbrial expression enhances *Escherichia coli* virulence for the urinary tract. *Proc. Natl. Acad. Sci. U.S.A.* 93, 9827–9832. doi: 10.1073/pnas.93.18.9827

Croxen, M. A., Law, R. J., Scholz, R., Keeney, K. M., Wlodarska, M., and Finlay, B. B. (2013). Recent advances in understanding enteric pathogenic *Escherichia coli*. *Clin. Microbiol. Rev.* 26, 822–880. doi: 10.1128/CMR.00022-13

Dale, A. P., and Woodford, N. (2015). Extra-intestinal pathogenic *Escherichia coli* (ExPEC): disease, carriage and clones. *J. Infect.* 71, 615–626. doi: 10.1016/j.jinf.2015.09.009

Darling, A. E., Mau, B., and Perna, N. T. (2010). Progressivemauve: multiple genome alignment with gene gain, loss and rearrangement. *PLoS ONE* 5:e11147. doi: 10.1371/journal.pone.0011147

Dean, P., and Kenny, B. (2009). The effector repertoire of enteropathogenic *E. coli:* ganging up on the host cell. *Curr. Opin. Microbiol.* 12, 101–109. doi: 10.1016/j.mib.2008.11.006

Deng, W., Yu, H. B., De Hoog, C. L., Stoynov, N., Li, Y., Foster, L. J., et al. (2012). Quantitative proteomic analysis of type III secretome of enteropathogenic *Escherichia coli* reveals an expanded effector repertoire for attaching/effacing bacterial pathogens. *Mol. Cell. Proteomics* 11, 692–709. doi: 10.1074/mcp.M111.013672

Dielubanza, E. J., and Schaeffer, A. J. (2011). Urinary tract infections in women. *Med. Clin. North Am.* 95, 27–41. doi: 10.1016/j.mcna.2010.08.023

Donnenberg, M. S., and Welch, R. A. (1996). "Virulence determinants of uropathogenic *Escherichia coli*," in *Urinary Tract Infections: Molecular Pathogenesis and Clinical Management*, eds H. L. T. Mobley, and J. W. Warren (Washington, DC: ASM Press), 135–174.

dos Anjos, C., Sabino, C. P., Bueris, V., Fernandes, M. R., Pogliani, F. C., Lincopan, N., et al. (2019). Antimicrobial blue light inactivation of international clones of multidrug-resistant *Escherichia coli* ST10, ST131 and ST648. *Photodiagnosis Photodyn. Ther.* 27, 51–53. doi: 10.1016/j.pdpdt.2019.05.014

Doster, E., Lakin, S. M., Dean, C. J., Wolfe, C., Young, J. G., Boucher, C., et al. (2020). MEGARes 2.0: a database for classification of antimicrobial drug, biocide and metal resistance determinants in metagenomic sequence data. *Nucleic Acids Res.* 48, 561–569. doi: 10.1093/nar/gkz1010

Ejrnæs, K. (2011). Bacterial characteristics of importance for recurrent urinary tract infections caused by *Escherichia coli*. *Dan. Med. Bull.* 58:B4187. Available online at: https://ugeskriftet.dk/files/scientific_article_files/2018-11/b4187.pdf

Ejrnæs, K., Stegger, M., Reisner, A., Ferry, S., Monsen, T., Holm, S. E., et al. (2011). Characteristics of *Escherichia coli* causing persistence or relapse of urinary tract infections: phylogenetic groups, virulence factors and biofilm formation. *Virulence* 2, 528–537. doi: 10.4161/viru.2.6.18189

EUCAST (2020). *The European Committee on Antimicrobial Susceptibility Testing. Breakpoint tables for interpretation of MICs and zone diameters*. Available online at: http://www.eucast.org (accessed March 16, 2020).

Falsetti, I. N. (1998). *Identificação de Caracteristicas Fenotipicas e Genotipicas de Escherichia coli Enteroagregativa (EAEC) em Amostras de Escherichia coli Uropatogenica (UPEC)*. Available online at: http://repositorio.unifesp.br/handle/11600/16065 (acessed January 19, 2020).

Feldgarden, M., Brover, V., Haft, D. H., Prasad, A. B., Slotta, D. J., Tolstoy, I., et al. (2019). Validating the AMRFINder tool and resistance gene database by using antimicrobial resistance genotype-phenotype correlations in a collection of isolates. *Antimicrob. Agents Chemother.* 63:e00483-19. doi: 10.1128/AAC.00483-19

Ferdous, M., Friedrich, A. W., Grundmann, H., de Boer, R. F., Croughs, P. D., Islam, M. A., et al. (2016). Molecular characterization and phylogeny of Shiga toxin–producing *Escherichia coli* isolates obtained from two Dutch regions using whole genome sequencing. *Clin. Microbiol. Infect.* 22, 642.e1–642.e9. doi: 10.1016/j.cmi.2016.03.028

Finer, G., and Landau, D. (2004). Pathogenesis of urinary tract infections with normal female anatomy. *Lancet Infect. Dis.* 4, 631–635. doi: 10.1016/S1473-3099(04)01147-8

Flament-Simon, S. C., Duprilot, M., Mayer, N., García, V., Alonso, M. P., Blanco, J., et al. (2019). Association between kinetics of early biofilm formation and clonal lineage in *Escherichia coli*. *Front. Microbiol.* 10:1183. doi: 10.3389/fmicb.2019.01183

Foxman, B. (2014). Urinary tract infection syndromes. Occurrence, recurrence, bacteriology, risk factors, and disease burden. *Infect. Dis. Clin. North Am.* 28, 1–13. doi: 10.1016/j.idc.2013.09.003

Freire, C. A., Santos, A. C. M., Pignatari, A. C., Silva, R. M., and Elias, W. P. (2020). Serine protease autotransporters of enterobacteriaceae (SPATEs) are largely distributed among *Escherichia coli* isolated from the bloodstream. *Brazilian J. Microbiol.* 51, 447–454. doi: 10.1007/s42770-020-00224-1

Garcia, M. I., Jouve, M., Nataro, J. P., Gounon, P., and Le Bouguénec, C. (2000). Characterization of the AfaD-like family of invasins encoded by pathogenic *Escherichia coli* associated with intestinal and extra-intestinal infections. *FEBS Lett.* 479, 111–117. doi: 10.1016/S0014-5793(00)01898-6

García, V., García-Meniño, I., Mora, A., Flament-Simon, S. C., Díaz-Jiménez, D., Blanco, J. E., et al. (2018). Co-occurrence of mcr-1, mcr-4 and mcr-5 genes in multidrug-resistant ST10 Enterotoxigenic and Shiga toxin-producing *Escherichia coli* in Spain (2006-2017). *Int. J. Antimicrob. Agents* 52, 104–108. doi: 10.1016/j.ijantimicag.2018.03.022

Gati, N. S., Middendorf-Bauchart, B., Bletz, S., Dobrindt, U., and Mellmann, A. (2019). Origin and evolution of hybrid Shiga toxin-producing and

uropathogenic (STEC/UPEC) *Escherichia coli* of sequence type 141. *J. Clin. Microbiol.* 58:01309–19. doi: 10.1128/JCM.01309-19

Girón, J. A., Ho, A. S. Y., and Schoolnik, G. K. (1991). An inducible bundle-forming pilus of enteropathogenic *Escherichia coli*. *Science* 254, 710–713. doi: 10.1126/science.1683004

Gomes, T. A. T., Elias, W. P., Scaletsky, I. C. A., Guth, B. E. C., Rodrigues, J. F., Piazza, R. M. F., et al. (2016). Diarrheagenic *Escherichia coli*. *Br. J. Microbiol.* 47, 3–30. doi: 10.1016/j.bjm.2016.10.015

Gonçalves, L. F., de Oliveira Martins, P., De Melo, A. B. F., Da Silva, R. C. R. M., de Paulo Martins, V., Pitondo-Silva, A., et al. (2016). Multidrug resistance dissemination by extended-spectrum β-lactamase-producing *Escherichia coli* causing community-acquired urinary tract infection in the Central-Western Region, Brazil. *J. Glob. Antimicrob. Resist.* 6, 1–4. doi: 10.1016/j.jgar.2016.02.003

Guirro, M., de Souza, R. L., Piazza, R. M. F., and Guth, B. E. C. (2013). Antibodies to intimin and *Escherichia coli*-secreted proteins EspA and EspB in sera of Brazilian children with hemolytic uremic syndrome and healthy controls. *Vet. Immunol. Immunopathol.* 152, 121–125. doi: 10.1016/j.vetimm.2012.09.016

Gupta, S. K., Padmanabhan, B. R., Diene, S. M., Lopez-Rojas, R., Kempf, M., Landraud, L., et al. (2014). ARG-annot, a new bioinformatic tool to discover antibiotic resistance genes in bacterial genomes. *Antimicrob. Agents Chemother.* 58, 212–220. doi: 10.1128/AAC.01310-13

Hazen, T. H., Michalski, J., Luo, Q., Shetty, A. C., Daugherty, S. C., Fleckenstein, J. M., et al. (2017). Comparative genomics and transcriptomics of *Escherichia coli* isolates carrying virulence factors of both enteropathogenic and enterotoxigenic *E. coli*. *Sci. Rep.* 7:3513. doi: 10.1038/s41598-017-03489-z

Heilberg, I. P., and Schor, N. (2003). Diagnosis and clinical management of urinary tract infection. *Rev. Assoc. Med. Bras.* 49, 109–116. doi: 10.1590/S0104-42302003000100043

Hernandes, R. T., De la Cruz, M. A., Yamamoto, D., Girón, J. A., and Gomes, T. A. T. (2013). Dissection of the role of pili and type 2 and 3 secretion systems in adherence and biofilm formation of an atypical enteropathogenic *Escherichia coli* strain. *Infect. Immun.* 81, 3793–3802. doi: 10.1128/IAI.00620-13

Hernandes, R. T., Silva, R. M., Carneiro, S. M., Salvador, F. A., Fernandes, M. C. D. C., Padovan, A. C. B., et al. (2008). The localized adherence pattern of an atypical enteropathogenic *Escherichia coli* is mediated by intimin omicron and unexpectedly promotes HeLa cell invasion. *Cell. Microbiol.* 10, 415–425. doi: 10.1111/j.1462-5822.2007.01054.x

Hertz, F. B., Nielsen, J. B., Schønning, K., Littauer, P., Knudsen, J. D., Løbner-Olesen, A., et al. (2016). Population structure of drug-susceptible, -resistant and ESBL-producing *Escherichia coli* from community-acquired urinary tract infections. *BMC Microbiol.* 16:63. doi: 10.1186/s12866-016-0725-4

Høiby, N., Ciofu, O., Johansen, H. K., Song, Z. J., Moser, C., Jensen, P. Ø., et al. (2011). The clinical impact of bacterial biofilms. *Int. J. Oral Sci.* 3, 55–65. doi: 10.4248/IJOS11026

Hooton, T. M. (2012). Uncomplicated urinary tract infection. *N. Engl. J. Med.* 366, 1028–1037. doi: 10.1056/NEJMcp1104429

Ingle, D. J., Valcanis, M., Kuzevski, A., Tauschek, M., Inouye, M., Stinear, T., et al. (2016). *In silico* serotyping of *E. coli* from short read data identifies limited novel O-loci but extensive diversity of O:H serotype combinations within and between pathogenic lineages. *Microb. Genomics* 2:e000064. doi: 10.1099/mgen.0.000064

Jerse, A. E., Yu, J., Tall, B. D., and Kaper, J. B. (1990). A genetic locus of enteropathogenic *Escherichia coli* necessary for the production of attaching and effacing lesions on tissue culture cells. *Proc. Natl. Acad. Sci. U.S.A.* 87, 7839–7843. doi: 10.1073/pnas.87.20.7839

Jia, B., Raphenya, A. R., Alcock, B., Waglechner, N., Guo, P., Tsang, K. K., et al. (2017). CARD 2017: expansion and model-centric curation of the comprehensive antibiotic resistance database. *Nucleic Acid Res.* 45, D566–D573. doi: 10.1093/nar/gkw1004

Joensen, K. G., Scheutz, F., Lund, O., Hasman, H., Kaas, R. S., Nielsen, E. M., et al. (2014). Real-time whole-genome sequencing for routine typing, surveillance, and outbreak detection of verotoxigenic *Escherichia coli*. *J. Clin. Microbiol.* 52, 1501–1510. doi: 10.1128/JCM.03617-13

Joensen, K. G., Tetzschner, A. M. M., Iguchi, A., Aarestrup, F. M., and Scheutz, F. (2015). Rapid and easy *in silico* serotyping of *Escherichia coli* isolates by use of whole-genome sequencing data. *J. Clin. Microbiol.* 53, 2410–2426. doi: 10.1128/JCM.00008-15

Johnson, J. R., Murray, A. C., Gajewski, A., Sullivan, M., Snippes, P., Kuskowski, M. A., et al. (2003). Isolation and molecular characterization of nalidixic acid-resistant extraintestinal pathogenic *Escherichia coli* from retail chicken products. *Antimicrob. Agents Chemother.* 47, 2161–2168. doi: 10.1128/AAC.47.7.2161-2168.2003

Johnson, J. R., Porter, S., Johnston, B., Kuskowski, M. A., Spurbeck, R. R., Mobley, H. L. T., et al. (2015). Host characteristics and bacterial traits predict experimental virulence for *Escherichia coli* bloodstream isolates from patients with urosepsis. *Open Forum Infect. Dis.* 2:eofv083. doi: 10.1093/ofid/ofv083

Johnson, J. R., and Russo, T. A. (2018). Molecular epidemiology of extraintestinal pathogenic *Escherichia coli*. *EcoSal. Plus* 8:ESP-0004-2017. doi: 10.1128/ecosalplus.ESP-0004-2017

Kallonen, T., Brodrick, H. J., Harris, S. R., Corander, J., Brown, N. M., Martin, V., et al. (2017). Systematic longitudinal survey of invasive *Escherichia coli* in England demonstrates a stable population structure only transiently disturbed by the emergence of ST131. *Genome Res.* 27, 1437–1449. doi: 10.1101/gr.216606.116

Kaper, J. B., and Nataro, J. P. (1998). Diarrheagenic *Escherichia coli* strains. *Clin. Microbiol. Rev.* 11, 142–201. doi: 10.1128/CMR.11.1.142

Kaper, J. B., Nataro, J. P., and Mobley, H. L. T. (2004). Pathogenic *Escherichia coli*. *Nat. Rev. Microbiol.* 2, 123–140. doi: 10.1038/nrmicro818

Keller, R., Ordoñez, J. G., De Oliveira, R. R., Trabulsi, L. R., Baldwin, T. J., and Knutton, S. (2002). Afa, a diffuse adherence fibrillar adhesin associated with enteropathogenic *Escherichia coli*. *Infect. Immun.* 70, 2681–2689. doi: 10.1128/IAI.70.5.2681-2689.2002

Keller, R., Pedroso, M. Z., Ritchmann, R., and Silva, R. M. (1998). Occurrence of virulence-associated properties in enterobacter cloacae. *Infect. Immun.* 66, 645–649. doi: 10.1128/IAI.66.2.645-649.1998

Kessler, R., Nisa, S., Hazen, T. H., Horneman, A., Amoroso, A., Rasko, D. A., et al. (2015). Diarrhea, bacteremia and multiorgan dysfunction due to an extraintestinal pathogenic *Escherichia coli* strain with enteropathogenic *E. coli* genes. *Pathog. Dis.* 73:ftv076. doi: 10.1093/femspd/ftv076

Kim, D. H., Subhadra, B., Kang, H. Y., Woo, K., Kim, J., Son, Y. J., et al. (2018). Virulence properties of uropathogenic *Escherichia coli* isolated from children with urinary tract infection in Korea. *Genes Genomics* 40, 625–634. doi: 10.1007/s13258-018-0664-6

Knutton, S., Baldwin, T., Williams, P. H., and McNeish, A. S. (1989). Actin accumulation at sites of bacterial adhesion to tissue culture cells: basis of a new diagnostic test for enteropathogenic and enterohemorrhagic *Escherichia coli*. *Infect. Immun.* 57, 1290–1298. doi: 10.1128/IAI.57.4.1290-1298.1989

Knutton, S., Phillips, A. D., Smith, H. R., Gross, R. J., Shaw, R., Watson, P., et al. (1991). Screening for enteropathogenic *Escherichia coli* in infants with diarrhea by the fluorescent-actin staining test. *Infect. Immun.* 59, 365–371. doi: 10.1128/IAI.59.1.365-371.1991

Korbel, L., Howell, M., and Spencer, J. D. (2017). The clinical diagnosis and management of urinary tract infections in children and adolescents. *Paediatr. Int. Child Health* 37, 273–279. doi: 10.1080/20469047.2017.1382046

Lara, F. B. M., Nery, D. R., de Oliveira, P. M., Araujo, M. L., Carvalho, F. R. Q., Messias-Silva, L. C. F., et al. (2017). Virulence markers and phylogenetic analysis of *Escherichia coli* strains with hybrid EAEC/UPEC genotypes recovered from sporadic cases of extraintestinal infections. *Front. Microbiol.* 8:146. doi: 10.3389/fmicb.2017.00146

Larsen, M. V., Cosentino, S., Rasmussen, S., Friis, C., Hasman, H., Marvig, R. L., et al. (2012). Multilocus sequence typing of total-genome-sequenced bacteria. *J. Clin. Microbiol.* 50, 1355–1361. doi: 10.1128/JCM.06094-11

Leimbach, A. (2016). *Database: ecoli_VF_collection: v0.1.* Zenodo. doi: 10.5281/zenodo.56686

Letunic, I., and Bork, P. (2019). Interactive Tree Of Life (iTOL) v4: recent updates and new developments. *Nucleic Acids Res.* 47, W256–W259. doi: 10.1093/nar/gkz239

Lewis, A. J., Richards, A. C., and Mulvey, M. A. (2016). Invasion of host cells and tissues by uropathogenic bacteria. *Microbiol. Spectr.* 4:UTI-0026-2016. doi: 10.1128/microbiolspec.UTI-0026-2016

Lima, M. P., Yamamoto, D., Santos, A. C., de, M., Ooka, T., Hernandes, R. T., et al. (2019). Phenotypic characterization and virulence-related properties of *Escherichia albertii* strains isolated from children with diarrhea in Brazil. *Pathog. Dis.* 77:ftz014. doi: 10.1093/femspd/ftz014

Lindstedt, B.-A., Finton, M. D., Porcellato, D., and Brandal, L. T. (2018). High frequency of hybrid *Escherichia coli* strains with combined intestinal pathogenic *Escherichia coli* (IPEC) and extraintestinal pathogenic *Escherichia coli* (ExPEC) virulence factors isolated from human faecal samples. *BMC Infect. Dis*. 18:544. doi: 10.1186/s12879-018-3449-2

Liu, X., Liu, H., Wang, L., Peng, Q., Li, Y., Zhou, H., et al. (2018). Molecular characterization of extended-spectrum β-lactamase-producing multidrug resistant *Escherichia coli* from Swine in Northwest China. *Front. Microbiol*. 9:1756. doi: 10.3389/fmicb.2018.01756

Luck, S. N., Bennett-Wood, V., Poon, R., Robins-Browne, R. M., and Hartland, E. L. (2005). Invasion of epithelial cells by locus of enterocyte effacement-negative enterohemorrhagic *Escherichia coli*. *Infect. Immun*. 73, 3063–3071. doi: 10.1128/IAI.73.5.3063-3071.2005

Manges, A. R., Geum, H. M., Guo, A., Edens, T. J., Fibke, C. D., and Pitout, J. D. D. (2019). Global extraintestinal pathogenic *Escherichia coli* (Expec) lineages. *Clin. Microbiol. Rev*. 32:e00135-18. doi: 10.1128/CMR.00135-18

Manges, A. R., and Johnson, J. R. (2015). Reservoirs of extraintestinal pathogenic *Escherichia coli*. *Microbiol. Spectr*. 3:UTI-0006-2012. doi: 10.1128/microbiolspec.UTI-0006-2012

Manges, A. R., Mende, K., Murray, C. K., Johnston, B. D., Sokurenko, E. V., Tchesnokova, V., et al. (2017). Clonal distribution and associated characteristics of *Escherichia coli* clinical and surveillance isolates from a military medical center. *Diagn. Microbiol. Infect. Dis*. 87, 382–385. doi: 10.1016/j.diagmicrobio.2017.01.007

Mariani-Kurkdjian, P., Lemaître, C., Bidet, P., Perez, D., Boggini, L., Kwon, T., et al. (2014). Haemolytic-uraemic syndrome with bacteraemia caused by a new hybrid *Escherichia coli* pathotype. *New Microbes New Infect*. 2, 127–131. doi: 10.1002/nmi2.49

Matar, G. M., Daou, R., Araj, G. F., and Uwaydah, M. (2005). Expression of DR-II adhesins encoded by the draE2 genes in *Escherichia coli* strains from urinary tract infections-related bacteremia. *J. Appl. Res.* 5, 275–281.

Mcdaniel, T. K., Jarvis, K. G., Donnenberg, M. S., and Kaper, J. B. (1995). A genetic locus of enterocyte effacement conserved among diverse enterobacterial pathogens. *Proc. Natl. Acad. Sci. U.S.A*. 92, 1664–1668. doi: 10.1073/pnas.92.5.1664

Menezes, M. A., Rocha, L. B., Koga, P. C. M., Fernandes, I., Nara, J. M., Magalhães, C. A., et al. (2010). Identification of enteropathogenic and enterohaemorrhagic *Escherichia coli* strains by immunoserological detection of intimin. *J. Appl. Microbiol*. 108, 878–887. doi: 10.1111/j.1365-2672.2009.04484.x

Mohsin, J., Pál, T., Petersen, J. E., Darwish, D., Ghazawi, A., Ashraf, T., et al. (2018). Plasmid-mediated colistin resistance gene mcr-1 in an *Escherichia coli* ST10 bloodstream isolate in the sultanate of Oman. *Microb. Drug Resist*. 24, 278–282. doi: 10.1089/mdr.2017.0131

Moon, H. W., Whipp, S. C., Argenzio, R. A., Levine, M. M., and Giannella, R. A. (1983). Attaching and effacing activities of rabbit and human enteropathogenic *Escherichia coli* in pig and rabbit intestines. *Infect. Immun*. 41, 1340–1351. doi: 10.1128/IAI.41.3.1340-1351.1983

Novais, Â., Pires, J., Ferreira, H., Costa, L., Montenegro, C., Vuotto, C., et al. (2012). Characterization of globally spread *Escherichia coli* ST131 isolates (1991 to 2010). *Antimicrob. Agents Chemother*. 56, 3973–3976. doi: 10.1128/AAC.00475-12

Ogura, Y., Ooka, T., Asadulghani, Terajima, J., Nougayrède, J. P., Kurokawa, K., et al. (2007). Extensive genomic diversity and selective conservation of virulence-determinants in enterohemorrhagic *Escherichia coli* strains of O157 and non-O157 serotypes. *Genome Biol.* 8:R138. doi: 10.1186/gb-2007-8-7-r138

Olesen, B., Kolmos, H. J., Ørskov, F., and Ørskov, I. (1994). Cluster of multiresistant *Escherichia coli* O78:H10 in greater copenhagen. *Scand. J. Infect. Dis*. 26, 406–410. doi: 10.3109/00365549409008613

Olesen, B., Scheutz, F., Andersen, R. L., Menard, M., Boisen, N., Johnston, B., et al. (2012). Enteroaggregative *Escherichia coli* O78:H10, the cause of an outbreak of urinary tract infection. *J. Clin. Microbiol*. 50, 3703–3711. doi: 10.1128/JCM.01909-12

Östblom, A., Adlerberth, I., Wold, A. E., and Nowrouzian, F. L. (2011). Pathogenicity island markers, virulence determinants malX and usp, and the capacity of *Escherichia coli* to persist in infants' commensal microbiotas. *Appl. Environ. Microbiol*. 77, 2303–2308. doi: 10.1128/AEM.02405-10

Owrangi, B., Masters, N., Kuballa, A., O'Dea, C., Vollmerhausen, T. L., and Katouli, M. (2018). Invasion and translocation of uropathogenic *Escherichia coli* isolated from urosepsis and patients with community-acquired urinary tract infection. *Eur. J. Clin. Microbiol. Infect. Dis*. 37, 833–839. doi: 10.1007/s10096-017-3176-4

Page, A. J., Cummins, C. A., Hunt, M., Wong, V. K., Reuter, S., Holden, M. T. G., et al. (2015). Roary: Rapid large-scale prokaryote pan genome analysis. *Bioinformatics* 31, 3691–3693. doi: 10.1093/bioinformatics/btv421

Ponnusamy, P., Natarajan, V., and Sevanan, M. (2012). *In vitro* biofilm formation by uropathogenic *Escherichia coli* and their antimicrobial susceptibility pattern. *Asian Pac. J. Trop. Med*. 5, 210–213. doi: 10.1016/S1995-7645(12)60026-1

Redder, J. D., Leth, R. A., and Møller, J. K. (2016). Analysing risk factors for urinary tract infection based on automated monitoring of hospital-acquired infection. *J. Hosp. Infect*. 92, 397–400. doi: 10.1016/j.jhin.2015.12.009

Riveros, M., García, W., García, C., Durand, D., Mercado, E., Ruiz, J., et al. (2017). Molecular and phenotypic characterization of diarrheagenic *Escherichia coli* strains isolated from bacteremic children. *Am. J. Trop. Med. Hyg*. 97, 1329–1336. doi: 10.4269/ajtmh.17-0066

Ronald, A. (2003). The etiology of urinary tract infection: traditional and emerging pathogens. *Dis. Mon.* 49, 71–82. doi: 10.1067/mda.2003.8

Russo, T. A., and Johnson, J. R. (2000). Proposal for a new inclusive designation for extraintestinal pathogenic isolates of *Escherichia coli*: ExPEC. *J. Infect. Dis*. 181, 1753–1754. doi: 10.1086/315418

Salmani, H., Azarnezhad, A., Fayazi, M. R., and Hosseini, A. (2016). Pathotypic and phylogenetic study of diarrheagenic *Escherichia coli* and uropathogenic *E. coli* using multiplex polymerase chain reaction. *Jundishapur J. Microbiol.* 9:e28331. doi: 10.5812/jjm.28331

Saltoglu, N., Karali, R., Yemisen, M., Ozaras, R., Balkan, I. I., Mete, B., et al. (2015). Comparison of community-onset healthcare-associated and hospital-acquired urinary infections caused by extended-spectrum beta-lactamase-producing *Escherichia coli* and antimicrobial activities. *Int. J. Clin. Pract*. 69, 766–770. doi: 10.1111/ijcp.12608

Salvador, F. A., Hernandes, R. T., Vieira, M. A. M., Rockstroh, A. C., and Gomes, T. A. T. (2014). Distribution of non-LEE-encoded type 3 secretion system dependent effectors in enteropathogenic *Escherichia coli*. *Brazilian J. Microbiol.* 45, 851–855. doi: 10.1590/S1517-83822014000300014

Santos, A. C. M., Santos, F. F., Silva, R. M., and Gomes, T. A. T. (2020a). Diversity of Hybrid- and Hetero-Pathogenic *Escherichia coli* and their potential implication in more severe diseases. *Front. Cell. Infect. Microbiol*. 10:339. doi: 10.3389/fcimb.2020.00339

Santos, A. C. M., Silva, R. M., Valiatti, T. B., Santos, F. F., Santos-Neto, J. F., Cayô, R., et al. (2020b). Virulence potential of a multidrug-resistant *Escherichia coli* strain belonging to the emerging clonal group ST101-B1 isolated from bloodstream infection. *Microorganisms* 8:827. doi: 10.3390/microorganisms8060827

Santos, A. C. M., Zidko, A. C. M., Pignatari, A. C., and Silva, R. M. (2013). Assessing the diversity of the virulence potential of *Escherichia coli* isolated from bacteremia in São Paulo, Brazil. *Br. J. Med. Biol. Res*. 46, 968–973. doi: 10.1590/1414-431X20133184

Santos, F. F., Yamamoto, D., Abe, C. M., Bryant, J. A., Hernandes, R. T., Kitamura, F. C., et al. (2019). The Type III Secretion System (T3SS)-translocon of atypical enteropathogenic *Escherichia coli* (aEPEC) can mediate adherence. *Front. Microbiol*. 10:1527. doi: 10.3389/fmicb.2019.01527

Scaletsky, I. C. A., Silva, M. L. M., and Trabulsi, L. R. (1984). Distinctive patterns of adherence of enteropathogenic *Escherichia coli* to HeLa cells. *Infect. Immun*. 45, 534–536. doi: 10.1128/IAI.45.2.534-536.1984

Seemann, T. (2014). Genome analysis prokka: rapid prokaryotic genome annotation. *Bioinformatics* 30, 2068–2069. doi: 10.1093/bioinformatics/btu153

Sokurenko, E. V., Chesnokova, V., Dykhuizen, D. E., Ofek, I., Wu, X. R., Krogfelt, K. A., et al. (1998). Pathogenic adaptation of *Escherichia coli* by natural variation of the FimH adhesin. *Proc. Natl. Acad. Sci. U.S.A*. 95, 8922–8926. doi: 10.1073/pnas.95.15.8922

Spurbeck, R. R., Dinh, P. C., Walk, S. T., Stapleton, A. E., Hooton, T. M., Nolan, L. K., et al. (2012). *Escherichia coli* isolates that carry *vat, fyuA, chuA,* and *yfcV* efficiently colonize the urinary tract. *Infect. Immun*. 80, 4115–4122. doi: 10.1128/IAI.00752-12

Suzart, S., Gomes, T. A. T., and Guth, B. E. C. (1999). Characterization of serotypes and outer membrane protein profiles in enteroaggregative *Escherichia coli* strains. *Microbiol. Immunol*. 43, 201–205. doi: 10.1111/j.1348-0421.1999.tb02394.x

Tanabe, R. H. S., Vieira, M. A., Mariano, N. A. B., Dias, R. C. B., da Silva, R. V., Castro, C. M., et al. (2019). Identification and characterization of atypical enteropathogenic and Shiga toxin-producing *Escherichia coli* isolated from ground beef and poultry breast purchased in Botucatu, Brazil. *Brazilian J. Microbiol.* 50, 1099–1103. doi: 10.1007/s42770-019-00101-6

Tapiainen, T., Hanni, A. M., Salo, J., Ikäheimo, I., and Uhari, M. (2014). *Escherichia coli* biofilm formation and recurrences of urinary tract infections in children. *Eur. J. Clin. Microbiol. Infect. Dis.* 33, 111–115. doi: 10.1007/s10096-013-1935-4

Terpstra, M. L., and Geerlings, S. E. (2016). Urinary tract infections: how new findings create new research questions. *Curr. Opin. Infect. Dis.* 29, 70–72. doi: 10.1097/QCO.0000000000000232

Toval, F., Köhler, C. D., Vogel, U., Wagenlehner, F., Mellmann, A., Fruth, A., et al. (2014). Characterization of *Escherichia coli* isolates from hospital inpatients or outpatients with urinary tract infection. *J. Clin. Microbiol.* 52, 407–418. doi: 10.1128/JCM.02069-13

Towbin, H., Staehelin, T., and Gordon, J. (1979). Electrophoretic transfer of proteins from polyacrylamide gels to nitrocellulose sheets: Procedure and some applications. *Proc. Natl. Acad. Sci. U.S.A.* 76, 4350–4354. doi: 10.1073/pnas.76.9.4350

Trabulsi, L. R., Keller, R., and Tardelli Gomes, T. A. (2002). Typical and atypical enteropathogenic *Escherichia coli*. *Emerg. Infect. Dis.* 8, 508–513. doi: 10.3201/eid0805.010385

Valiatti, T. B., Santos, F. F., Santos, A. C., de, M., Silva, R. M., Carvalho, E., et al. (2019). Draft whole-genome sequence of a uropathogenic *Escherichia coli* strain carrying the *eae* gene. *Microbiol. Resour. Announc.* 8:e00980-19. doi: 10.1128/MRA.00980-19

Vieira, M. A. M., Salvador, F. A., Silva, R. M., Irino, K., Vaz, T. M. I., Rockstroh, A. C., et al. (2010). Prevalence and characteristics of the O122 pathogenicity Island in typical and atypical enteropathogenic Escherichia coli strains. *J. Clin. Microbiol.* 48, 1452–1455. doi: 10.1128/JCM.01944-09

Vossenkämper, A., MacDonald, T. T., and Marchès, O. (2011). Always one step ahead: how pathogenic bacteria use the type III secretion system to manipulate the intestinal mucosal immune system. *J. Inflamm.* 8:11. doi: 10.1186/1476-9255-8-11

Wallace-Gadsden, F., Johnson, J. R., Wain, J., and Okeke, I. N. (2007). Enteroaggregative *Escherichia coli* related to uropathogenic clonal group A. *Emerg. Infect. Dis.* 13, 757–760. doi: 10.3201/eid1305.061057

Walport, M. J. (2001). Advances in immunology: complement (first of two parts). *N. Engl. J. Med.* 344, 1058–1066. doi: 10.1056/NEJM200104053441406

Wattam, A. R., Davis, J. J., Assaf, R., Boisvert, S., Brettin, T., Bun, C., et al. (2017). Improvements to PATRIC, the all-bacterial bioinformatics database and analysis resource center. *Nucleic Acids Res.* 45, D535–D542. doi: 10.1093/nar/gkw1017

Watts, R. E., Hancock, V., Ong, C. L. Y., Vejborg, R. M., Mabbett, A. N., Totsika, M., et al. (2010). *Escherichia coli* isolates causing asymptomatic bacteriuria in catheterized and noncatheterized individuals possess similar virulence properties. *J. Clin. Microbiol.* 48, 2449–2458. doi: 10.1128/JCM.01611-09

Wong, A. R. C., Pearson, J. S., Bright, M. D., Munera, D., Robinson, K. S., Lee, S. F., et al. (2011). Enteropathogenic and enterohaemorrhagic *Escherichia coli*: even more subversive elements. *Mol. Microbiol.* 80, 1420–1438. doi: 10.1111/j.1365-2958.2011.07661.x

Wurpel, D. J., Totsika, M., Allsopp, L. P., Webb, R. I., Moriel, D. G., and Schembri, M. A. (2016). Comparative proteomics of uropathogenic *Escherichia coli* during growth in human urine identify UCA-like (UCL) fimbriae as an adherence factor involved in biofilm formation and binding to uroepithelial cells. *J. Proteomics* 131, 177–189. doi: 10.1016/j.jprot.2015.11.001

Yamaji, R., Friedman, C. R., Rubin, J., Suh, J., Thys, E., McDermott, P., et al. (2018). A Population-based surveillance study of shared genotypes of *Escherichia coli* isolates from retail meat and suspected cases of urinary tract infections. *mSphere* 3, e00179–e00118. doi: 10.1128/mSphere.00179-18

Zankari, E., Hasman, H., Cosentino, S., Vestergaard, M., Rasmussen, S., Lund, O., et al. (2012). Identification of acquired antimicrobial resistance genes. *J. Antimicrob. Chemother.* 67, 2640–2644. doi: 10.1093/jac/dks261

Zarivach, R., Vuckovic, M., Deng, W., Finlay, B. B., and Strynadka, N. C. J. (2007). Structural analysis of a prototypical ATPase from the type III secretion system. *Nat. Struct. Mol. Biol.* 14, 131–137. doi: 10.1038/nsmb1196

Zhang, Y., Liao, K., Gao, H., Wang, Q., Wang, X., Li, H., et al. (2017). Decreased fitness and virulence in ST10 *Escherichia coli* harboring *blaNDM-5* and mcr-1 against a ST4981 strain with *blaNDM-5*. *Front. Cell. Infect. Microbiol.* 7:242. doi: 10.3389/fcimb.2017.00242

Conflict of Interest: The authors declare that the research was conducted in the absence of any commercial or financial relationships that could be construed as a potential conflict of interest.

frontiers in Cellular and Infection Microbiology

ORIGINAL RESEARCH
published: 15 October 2020
doi: 10.3389/fcimb.2020.572951

New Insights Into DAEC and EAEC Pathogenesis and Phylogeny

*Mario Meza-Segura[1], Mussaret B. Zaidi[2,3], Arturo Vera-Ponce de León[4], Nadia Moran-Garcia[1], Esperanza Martinez-Romero[4], James P. Nataro[5] and Teresa Estrada-Garcia[1]**

[1] Molecular Biomedicine Department, Centro de Investigación y de Estudios Avanzados del Instituto Politécnico Nacional, Mexico City, Mexico, [2] Infectious Diseases Research Unit, Hospital General O'Horan, Mérida, Mexico, [3] Department of Epidemiology and Biostatistics, Michigan State University, Lansing, MI, United States, [4] Centro de Ciencias Genómicas, Universidad Nacional Autónoma de México, Cuernavaca, Mexico, [5] Department of Pediatrics, University of Virginia, Charlottesville, VI, United States

Diarrheagenic *E. coli* can be separated into six distinct pathotypes, with enteroaggregative (EAEC) and diffusely-adherent *E. coli* (DAEC) among the least characterized. To gain additional insights into these two pathotypes we performed whole genome sequencing of ten DAEC, nine EAEC strains, isolated from Mexican children with diarrhea, and one EAEC plus one commensal *E. coli* strains isolated from an adult with diarrhea and a healthy child, respectively. These genome sequences were compared to 85 *E. coli* genomes available in public databases. The EAEC and DAEC strains segregated into multiple different clades; however, six clades were heavily or exclusively comprised of EAEC and DAEC strains, suggesting a phylogenetic relationship between these two pathotypes. EAEC strains harbored the typical virulence factors under control of the activator AggR, but also several toxins, bacteriocins, and other virulence factors. DAEC strains harbored several iron-scavenging systems, toxins, adhesins, and complement resistance or Immune system evasion factors that suggest a pathogenic paradigm for this poorly understood pathotype. Several virulence factors for both EAEC and DAEC were associated with clinical presentations, not only suggesting the importance of these factors, but also potentially indicating opportunities for intervention. Our studies provide new insights into two distinct but related diarrheagenic organisms.

Keywords: DAEC, EAEC, genomes, phylogeny, virulence factors, DAEC pathogenesis

OPEN ACCESS

Edited by:
Roxane M. Piazza, Butantan Institute, Brazil

Reviewed by:
David A. Montero, University of Chile, Chile
Brandon Luedtke, University of Nebraska at Kearney, United States
Claire Jenkins, Public Health England, United Kingdom

***Correspondence:**
Teresa Estrada-Garcia
testrada@cinvestav.mx

Specialty section:
This article was submitted to Molecular Bacterial Pathogenesis, a section of the journal Frontiers in Cellular and Infection Microbiology

Received: *15 June 2020*
Accepted: *09 September 2020*
Published: *15 October 2020*

Citation:
Meza-Segura M, Zaidi MB, Vera-Ponce de León A, Moran-Garcia N, Martinez-Romero E, Nataro JP and Estrada-Garcia T (2020) New Insights Into DAEC and EAEC Pathogenesis and Phylogeny. Front. Cell. Infect. Microbiol. 10:572951. doi: 10.3389/fcimb.2020.572951

INTRODUCTION

Worldwide, diarrheal disease remains a major cause of morbidity and is the eighth leading cause of mortality, among children under 5 years of age from less developed regions of the world (GBD 2016 Diarrhoeal Disease Collaborators, 2018). Diarrheagenic *Escherichia coli* pathotypes (DEP) are important etiological agents of acute and persistent diarrhea in children (Ochoa et al., 2009; Patzi-Vargas et al., 2015; Zhou et al., 2018), that can lead to death (Lanata et al., 2013; GBD 2016 Diarrhoeal Disease Collaborators, 2018), and cause traveler's diarrhea in adults (Paredes-Paredes et al., 2011; Jennings et al., 2017). Recent studies by our group have shown that DEP have become the main etiologic agents of diarrheal disease among children requiring hospitalization; DAEC and EAEC are the most prevalent pathotypes, surpassing *Salmonella* and *Shigella* (Patzi-Vargas et al., 2015).

DEP are classified into six well-described categories: shiga toxin producing *E. coli* (STEC), which encompasses the enterohemorrhagic *E. coli* group (EHEC); enterotoxigenic *E. coli* (ETEC); enteroaggregative *E. coli* (EAEC); enteroinvasive *E. coli* (EIEC); diffusely adherent *E. coli* (DAEC); and enteropathogenic *E. coli* (EPEC). The latter is subdivided into typical EPEC (tEPEC) and atypical EPEC (aEPEC) (Kaper et al., 2004). Overall, pathogenic *E. coli* use adhesins, sugars (capsular polysaccharides and lipopolysaccharides), toxins, invasion-promoting proteins, iron acquisition systems, complement resistance factors or immune evasion factors, to colonize, survive in, and injure their hosts (Kaper et al., 2004; Nataro, 2005; Meza-Segura and Estrada-Garcia, 2016). EAEC strains are characterized by their ability to form a stacked-brick or aggregative adherence (AA) pattern on HEp-2 cells, which is mediated by the aggregative adherence fimbriae (AAF) (Kaper et al., 2004). AAF transcription and that of at least other 44 EAEC chromosomal (aaiC) and plasmid-borne genes (the anti-aggregative secreted protein dispersin), are regulated by the Aggregative Adherence Regulator (AggR) (Nataro et al., 1994; Estrada-Garcia and Navarro-Garcia, 2012).

Due to the importance of AggR, EAEC isolates were subdivided into typical (tEAEC), i.e., *aag*R-positive, and atypical (aEAEC), i.e., *aag*R-negative, groups (Nataro, 2005). The recognition of tEAEC as strains carrying the *agg*R regulon was a major step in EAEC molecular identification, since it was shown that most EAEC strains previously characterized by the HEp-2 adherence assay harbored the *agg*R gene (Cerna et al., 2003). It is noteworthy that tEAEC, as well as other DEP, may also acquire other virulence factors (VF) by horizontal transfer and increase their virulence. In 2011, for example, a hybrid pathogenic EAEC-STEC O104:H4 that was responsible for a massive outbreak of bloody diarrhea in 16 countries, mostly harbored tEAEC (*agg*A, *agg*R, *set*1, *pic,* and *aap*) virulence genes and produced shiga toxin 2 (*stx*2) (World Health Organization, 2018).

Like EAEC, DAEC was classified based on its diffusely adherent (DA) pattern on HEp-2 cells, promoted by Afa, F1845, and Dr adhesins encoded by the *afa*, *daa,* and *dra* operons, respectively. Most of these adhesins have affinity for the human decay accelerating factor (hDAF; also known as CD55) or for carcinoembryonic antigen cell adhesion molecules (hCEACAMs), and both molecules are localized on the surface of intestinal epithelial cells (Servin, 2014; Meza-Segura and Estrada-Garcia, 2016). In contrast with EAEC, DAEC strains, aside from the adhesins, have only been associated with one other VF, the secreted autotransporter toxin (Sat) (Servin, 2014; Meza-Segura and Estrada-Garcia, 2016).

With the exception of tEPEC, aEPEC, STEC, and ETEC strains, the phylogenetic relationship among different DEP remains unclear (Lacher et al., 2007; Hazen et al., 2016; Montero et al., 2019; Rasko et al., 2019).

To date, not a single DAEC genome, and only a few different tEAEC genomes have been sequenced. Whole genome sequencing (WGS) of these pathotypes, in conjunction with previously reported *E. coli* genomes, will contribute to a greater understanding of the *E. coli* pan- and core-genomes. The pan-genome comprises the whole repertoire of genes identified in a bacterial species or group, while the core-genome includes the genes shared by all strains that encode for the proteins necessary for basic biological functions. *E. coli* species are considered to have an infinitely open pan-genome (Rouli et al., 2015), as it includes commensals and several pathogenic groups of strains capable of causing a wide variety of diseases, such as diarrhea, urinary tract infection, sepsis, and neonatal meningitis (Kaper et al., 2004). Therefore, *E. coli* phylogenetic analysis needs recognize *E. coli* pathogenic groups (Rasko et al., 2011; Rouli et al., 2015). WGS of DAEC and tEAEC may also help to identify new VF and potential novel pathogenetic mechanisms.

In this study, we sequenced the whole genome of ten DAEC and ten tEAEC strains identified as the sole pathogens isolated from the stools of patients with diarrhea, as well as one commensal *E. coli* strain isolated from a healthy child. These genomes were analyzed for their phylogenetic association with other *E. coli* strains and for the presence of genes encoding for VF. The results revealed that DAEC and tEAEC are phylogenetically related. However, strains of the different pathotypes harbor genes encoding for different sets of VF. DAEC carry more genes encoding for iron acquisition factors, while tEAEC harbor genes encoding toxins and bacteriocins. These findings will help to understand the molecular mechanisms that underlie the ability of DAEC and tEAEC to cause disease and will facilitate the identification of virulence gene profiles associated with more virulent strains. Moreover, this study will give insight into the origin and diversification of DAEC and tEAEC in reference to other DEP and ExPEC genomes.

MATERIALS AND METHODS

Study Population

A 4-year study was conducted from March 2010 to July 2014 on 1,043 children < 10 years of age who sought medical care for acute community-acquired diarrhea at the Hospital O'Horan in Merida, Yucatan. The clinical severity of each diarrheal episode was determined by the Ruuska-Vesikari scoring system (RVSS) (Ruuska and Vesikari, 1990). In addition, children who presented bloody diarrhea but no shock, were classified as moderate diarrhea, and those who presented hypovolemic shock, severe electrolyte imbalance and/or seizures were classified as severe. On admission, a trained nurse obtained demographic and clinical information for each child on a standardized questionnaire. Stools from each child were collected and screened for *Escherichia coli*, *Campylobacter* spp., *Salmonella* sp., *Shigella* spp., *Vibrio* spp., and rotavirus, as previously described (Patzi-Vargas et al., 2015).

Ethics Statement

This study was approved by both the Hospital General O'Horan Ethics Committee and the CINVESTAV Committee of Bioethics for Human Research. Legal guardians were required to sign an informed consent form. All children received medical treatment according to the hospital protocols.

Identification of Diarrheagenic *E. coli*

From each patient, five *E. coli* like strains were selected. All isolates were both biochemically confirmed as *E. coli* and screened by two multiplex PCR for DEP genes. The first multiplex

TABLE 1 | Patient's clinical profile and strains genome characteristics.

Group	Patient	Gender	Age (years)	DWD	DWV	Complications	Clinical outcome	Strain
DAEC	CA0022	M	2.3	3	1	None	Moderate	MEX-1
	CA0030	M	4.8	5	3	None	Severe	MEX-2
	CA0063	F	2.4	4	3	None	Moderate	MEX-3
	CA0170	M	0.1	4	1	S	Severe	MEX-4
	CA0209	F	1.5	7	2	HS, S	Severe	MEX-5
	CA0273	F	1.1	8	1	None	Moderate	MEX-6
	CA0437	M	1.8	6	2	BIS, HN	Severe	MEX-7
	CA0472	M	1.0	8	1	None	Severe	MEX-8
	CA0582	M	2.7	5	2	HN, HK	Severe	MEX-9
	CA1035	M	0.9	5	1	None	Moderate	MEX-10
tEAEC	CA0008	F	0.9	3	2	None	Moderate	MEX-11
	CA0036	F	2.8	2	1	BIS	Severe	MEX-12
	CA0041	M	1.3	5	3	BIS	Severe	MEX-13
	CA0155	M	1.5	4	1	None	Mild	MEX-14
	CA0345	F	0.6	6	1	None	Moderate	MEX-15
	CA0577	F	1.4	6	2	HN, HK	Severe	MEX-16
	CA0603	M	1.3	8	4	HN, HK	Severe	MEX-17
	CA0714	M	1.1	7	1	None	Moderate	MEX-18
	CA1036	F	1.2	9	1	HN, S	Severe	MEX-19
	TE-001	F	54.0	3	1	None	Moderate	MEX-20
Commensal	SE-001	F	2.0	–	–	–	–	MEX-21

DWD, Days with diarrhea; DWV, Days with vomit; HS, Hypovolemic shock; S, seizures; BIS, Blood in stool; HN, Hyponatremia; HK, hypokalemia.

PCR identifies the presence of distinctive loci defining ETEC, EPEC, STEC and EIEC (Lopez-Saucedo et al., 2003), while the second multiplex PCR specific genes for DAEC and tEAEC (modified from Patzi-Vargas et al., 2013), including two plasmid-borne (*aap* and *aat*A) and one chromosomal (*aai*C) EAEC genes (**Supplementary Table 1**).

DAEC and EAEC Strains Included for the VF -Clinical Severity Study

Thirty-eight DAEC and 30 EAEC strains isolated as the sole pathogen from children with diarrhea were selected for the characterization of 29 VF-encoding genes by four different multiplex PCR; one previously described (Guzman-Hernandez et al., 2016) and three newly developed in this study. The full description of the VF identified by each PCR assay, primers and PCR conditions, are described in **Supplementary Table 1**.

DAEC and tEAEC Strains Included for WGS

For WGS, ten DAEC and nine tEAEC isolates were selected from those children with the most severe diarrhea who were not malnourished (**Table 1**). A tEAEC strain isolated as the only enteric pathogen from a 56-year-old woman with acute diarrhea, and a commensal *E. coli* strain from a healthy 2-year-old girl, both from Mexico City, were included for comparison.

Genomic DNA was extracted by a phenol/chloroform method (Neumann et al., 1992). DNA libraries were prepared using the illumine TrueSeq DNA nano sample preparation kit and sequenced on the Illumina MiSeq platform at CINVESTAV-Langebio to generate tagged paired-end reads of 250 bases in length. Quality control, trimming and filtering of raw sequencing data was performed using Trim Galore v0.4.1[1]. Genomes were assembled with SPAdes v3.9.0 (Nurk et al., 2013; Prjibelski et al., 2014; Vasilinetc et al., 2015), and the accuracy of the assemblies was evaluated with REAPR 1.0.16 (Hunt et al., 2013). Pre-assembled contigs were scaffolded using SSPACE_Standard_v3.0.pl (Boetzer et al., 2011) and GapFiller_v1-10 (Boetzer and Pirovano, 2012).

Phylogenomic Analysis

Phylogenetic trees were constructed using a total of 107 genomes, including the 21 genomes sequenced in this study and 79 publicly available genomes for pathogenic *E. coli*, six commensal *E. coli* and one *Escherichia fergusonii* (**Supplementary Table 2**). Open reading frames (ORFs) of all genomes were predicted by GeneMark (Besemer and Borodovsky, 2005) and a Maximum Parsimony pan-genome phylogenetic tree was constructed with GetHomologues (Contreras-Moreira and Vinuesa, 2013), based on the translated protein sequences of each genome, using a combination of the orthoMCL and COGS as clustering

[1]Krueger F. *Trim Galore 0.4.1*. Available online at: https://www.bioinformatics.babraham.ac.uk/projects/trim_galore/ (accessed on November 12th, 2015).

algorithms. Single-copy genes of the *E. coli* core-genome were retrieved with a custom Bash/Perl script deposited in Github[2] MAFFT 7.3.10 was used to align all sequences (Katoh and Standley, 2013). After alignment all sequences were concatenated using the multigenomes2blocks pipeline (Vera-Ponce de Leon et al., 2020) and the GTR+F+R10 nucleotide substitution model was obtained by ModelFinder (Kalyaanamoorthy et al., 2017). The maximum-likelihood (ML) phylogenetic tree was then calculated by IQtree v1.6.12 (Minh et al., 2020) with 1,000 Bootstrap replicates for internal branch support. Population structure was calculated using a Bayesian analysis approach (BAPS) by RhierBAPS package (Tonkin-Hill et al., 2018) in R 3.6.3. For this, two depth levels and a maximum clustering size of 20 (default = number of isolates/5; 107/5 = 21.4) were specified. Seven different sequence clusters (SC) were identified, which were further divided into 24 lineages (**Supplementary Figure 1**). All scripts to replicate this experiment are deposited in Github[2]. Pan- and core-genome phylogenetic trees were visualized and edited using iTOL (Letunic and Bork, 2016).

Identification of ORFs Encoding for Virulence Factors

For this study, we defined VF as molecules that enable a microorganism to establish itself on or within a host of a particular species and enhance its potential to cause disease. A commensal *E. coli* strain was defined as an isolate from the stool of subjects exhibiting no signs of diarrheal illness and that did not display any known molecular markers that are associated with DEP. The presence of genes encoding for bacterial VF was analyzed by a Protein-Protein BLAST (BLAST 2.2.28+), using the translated protein sequences of all predicted ORFs and the virulence factor database (VFDB) (Liu et al., 2019). VF were annotated when their coverage and identities were $\geq$ 80%, after BLAST searches. VF were included for the analysis only when all genes or operons involved in their production or secretion were identified (i.e., the Sit iron/manganese transport system was only included when the genes encoding for *sit*A, *sit*B, sitC, and *sit*D were present). Individual VF were grouped together based on their function, including adhesins, bacteriocins, toxins, iron acquisition systems (IAS), and complement resistance or immune system evasion factors (CR/ISEF). The relative frequency (RF) of these groups was calculated by adding together the individual frequency of each VF in that group and dividing the result by the total number of genomes.

Statistical Analysis

All statistical analyses were performed using GraphPad PRISM® version 5.0 software. The incidence of individual VF was evaluated by Fisher's exact test (FET) and the RF of VF groups by Mann-Whitney *U*-Test (MWUT). $P < 0.05$ were considered statistically significant.

Data Availability

The genome sequence assemblies generated in this study have been deposited in GenBank as part of the Bioproject PRJNA588567 under the accession numbers listed in **Supplementary Table 2**. The remaining data that support the findings of this study are available from the corresponding author upon request.

[2]Available online at: https://github.com/avera1988/E.coli_PopulationStructure.

RESULTS AND DISCUSION

Pan-Genome and Core-Genome of *E. coli*, DAEC, and EAEC

The clinical characteristics of each subject and the general genomic features of their sequenced strains are summarized in **Table 1** and **Supplementary Table 3**, respectively. Almost all children presented with moderate to severe diarrhea (95%) and were < 5 years of age (95%). *E. coli* genome sizes obtained ranged from 4.9 to 5.5 Mbp, similar to those reported for other DEP genomes (Lukjancenko et al., 2010). To our knowledge, these are the first DAEC genomes to be reported.

In order to establish the phylogenetic relationships among the 21 genomes described in this work, 85 previously sequenced *E. coli* genomes were used for comparison, including six tEAEC, one aEAEC and ten tEAEC-STEC O104:H4, forty-nine DEP, ten uropathogenic *E. coli* (UPEC), three neonatal meningitis-causing *E. coli* (NMEC), six commensal and MG1655 K12 genomes (**Supplementary Table 2**). *E. fergusonni* (ATCC® 35469™) (Farmer et al., 1985) was used as an outgroup to root the phylogenetic trees. The comparative genomic analysis revealed a pan-genome containing 25,726 genes, including 1,452 core-genes, of which only 1,144 were single copy. This pan-genome contained more genes than those previously described with a similar number of genomes analyzed, reported with 13,000–16,373 genes (Rasko et al., 2008; Lukjancenko et al., 2010; Kaas et al., 2012). The number of genes included in the core-genome, however, were comparable to previously published studies, in which an average number of 1,631 genes was reported (Rasko et al., 2008; Lukjancenko et al., 2010; Kaas et al., 2012).

Pan- and Core-Genome Phylogenetic Clades Revealed DAEC and EAEC Relatedness

For the pan-genome tree we selected those clades harboring more than one DAEC or tEAEC genomes (I–VII), each of which included some of the sequenced strains (**Figure 1**). Clade VI contained only one tEAEC strain sequenced in this study, as well as one hybrid EAEC-STEC and one aEAEC reference strain, revealing that these three EAEC groups share a common set of genes.

To analyze the evolutionary relationships among DEP we built a core-genome phylogenetic tree, and the population structure was analyzed using a Bayesian approach. All 107 genomes were grouped into seven sequence clusters (SC), which were further divided into 24 lineages (**Supplementary Figure 1**). Nineteen of these lineages were selected and illustrated in the core-genome tree as clades I-VI and a-m (**Figure 2**). The tree revealed six different phylogenetic origins for each DAEC and tEAEC pathotypes. Even though these two DEP were outnumbered by other *E. coli* genomes, clades I–VI mostly comprised DAEC or

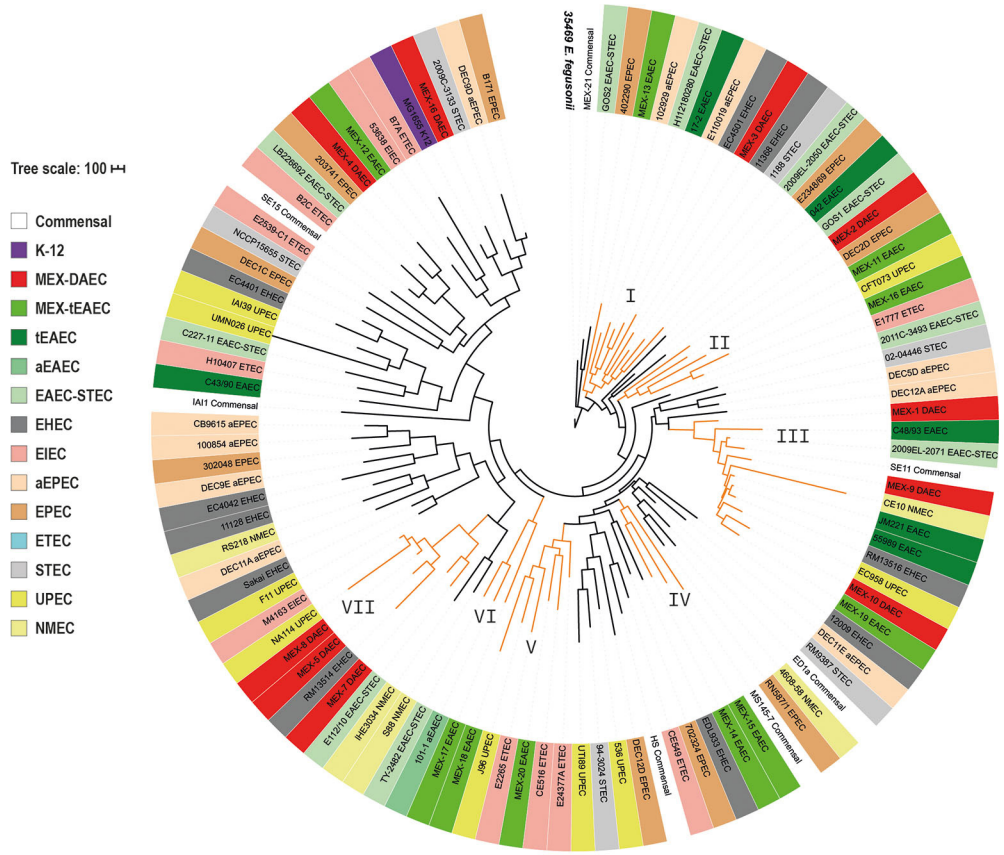

Clade	Groups (# genomes)
I	MEX-DAEC (1), MEX-tEAEC (1), tEAEC (1), EAEC-STEC (2), aEPEC (2), EHEC (2), STEC (1)
II	MEX-DAEC (1), MEX-tEAEC (2), EPEC (1), UPEC (1)
III	MEX-DAEC (3), MEX-tEAEC (1), tEAEC (3) EAEC-STEC (1), EHEC (1), UPEC (1), NMEC (1), Commensal (1)
IV	MEX- tEAEC (2), Commensal (1)
V	MEX-tEAEC (2), ETEC (3), UPEC (1)
VI	MEX-tEAEC (1), EAEC-STEC (1), aEAEC (1)
VII	MEX-DAEC (3), EAEC-STEC (1), EHEC (1), EIEC (1), UPEC (1)

FIGURE 1 | Pan-genome phylogenetic tree. The tree was built up based on the presence or absence of 25,726 genes comprised in the *E. coli* pan-genome. *E. fergusonii* 35,469 (in bold) was included to root the tree. Each *E. coli* group is indicated by a different color listed in the left box. Clades including more than one DAEC or tEAEC genomes are highlighted in orange and the roman numeral indicates the clade number. The scale bar represents the number of differences in the presence or absence of genes among all genomes.

tEAEC strains. Clades I and IV exclusively contained DAEC and tEAEC genomes. Additionally, clade V, which mostly harbored these two pathotypes (two DAEC and nine tEAEC), also contained one aEPEC, one commensal and K12 strains. Altogether, this results strongly suggest that DAEC and tEAEC are phylogenetically related. Of note, nine of the 14 genomes (64.3%) included in clade V were isolated from Mexican children, suggesting a geographical cluster: two MEX-DAEC, five MEX-tEAEC, the commensal MEX-21 and the JM221 tEAEC reference strain, which was isolated from a Mexican child with diarrhea in the 1980s (Mathewson et al., 1987). Clade VI solely contained tEAEC and EAEC-STEC O104:H4 genomes, confirming that EAEC-STEC O104:H4 is more closely related to tEAEC than to EHEC 0157:H7 (Rasko et al., 2011).

The core-genome tree also revealed that DAEC clustered together with UPEC strains (clades III, c, and d). Clade III and c harbored exclusively DAEC and UPEC genomes, whereas clade d also included an aEPEC and a commensal strain. This was not unexpected, given that UPEC strains carrying *afa*/*daa*/*dra* operons have been identified among UTI patients (Servin, 2014).

Additionally, the core-genome tree revealed associations between other *E. coli* groups (clades a, b, e–m). Clades a and b encompassed typical EPEC strains that resemble previously described EPEC9 and EPEC1 phylogenomic lineages, respectively, whereas clade m belongs to the B1 phylogroup and comprises two aEPEC strains, including the prototype E110019 strain (Lacher et al., 2007; Hazen et al., 2016). Moreover, clade h supports the notion that EHEC O157:H7 evolved from O55:H7 aEPEC (Zhou et al., 2010). Clade k harbors EPEC, aEPEC and EHEC genomes, similar to EPEC2 phylogenomic lineage (Lacher et al., 2007; Hazen et al., 2016). Phylogenetic relatedness was also observed between aEPEC and EHEC strains belonging to the O26:H11 serotype (clade L); these strains undergo transient interconversions via loss and gain of Stx-encoding phages (Bielaszewska et al., 2007).

Of interest, four ETEC (40%) and two EIEC (66.6%) genomes formed clades i and j, respectively, suggesting a specific phylogenetic origin for each pathotype (Rasko et al., 2019). In addition, clades e and f, containing NMEC and UPEC strains, revealed that these ExPEC groups are phylogenetically related. The fact that commensal *E. coli* genomes were widely distributed

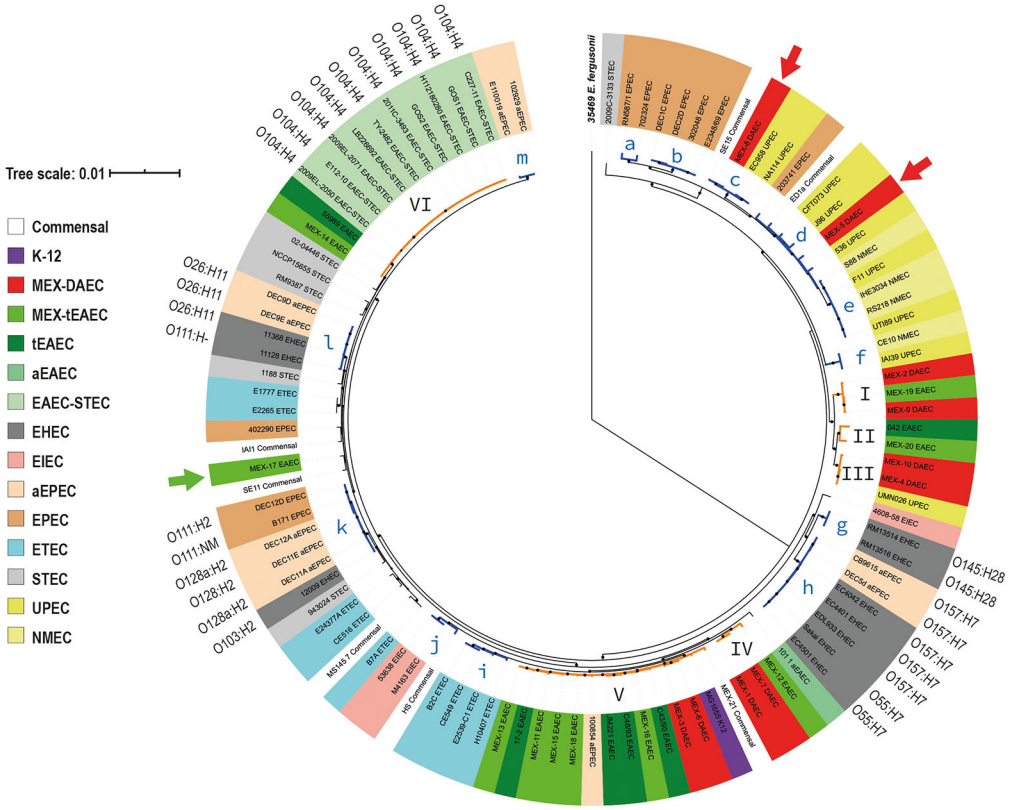

Clade	Groups (# genomes)
I	MEX-DAEC (2), MEX-tEAEC(1)
II	MEX-tEAEC (1), tEAEC (1)
III	MEX-DAEC (2), UPEC (1)
IV	MEX-DAEC (2), MEX-tEAEC (1)
V	MEX-DAEC (2), MEX-tEAEC (5), tEAEC (4), aEPEC (1), Commensal (1), K12
VI	MEX-tEAEC (1), tEAEC (1), EAEC-STEC (10)
a	EPEC (2)
b	EPEC (4)
c	MEX-DAEC (1), UPEC (2), Commensal (1)
d	MEX-DAEC (1), EPEC (1), UPEC (3), Commensal (1)
e	NMEC (3), UPEC (2)
f	NMEC (1), UPEC (1)
g	EHEC (2)
h	aEPEC (2), EHEC (5)
i	ETEC (4)
j	EIEC (2), Commensal (1)
k	aEPEC (3), EPEC (2), EHEC (1)
l	aEPEC (2), EHEC (2)
m	aEPEC (2)

FIGURE 2 | Core-genome (GTR + F + R10) phylogenetic tree. A maximum likelihood tree was constructed based on 1,144 single copy genes from the *E. coli* core-genome. *E. fergusonii* 35,469 (in bold) was used as an out-group. The tree was then calculated by IQtree v1.6.12 (Minh et al., 2020) with 1,000 Bootstrap replicates for internal branch support and values over 70% are indicated at each node with a black circle. Population structure was calculated using a Bayesian approach by RhierBAPS package (Tonkin-Hill et al., 2018) in R 3.6.3. *E. coli* groups are indicated by different color labels listed in the left chart. Clades including more than one DAEC or tEAEC genomes are highlighted in orange and the roman numerals in front of them indicate the clade number. Two DAEC (red arrows) and one tEAEC (green arrow) genomes were located outside these clades. Clades highlighted in blue (a–m) contain other pathogenic *E. coli* genomes that had important associations. The scale bar represents the number of nucleotide substitutions per site.

and clustered with strains from different pathogenic groups, confirms the great diversity of *E. coli* genomes (**Figure 2**).

Analysis of DAEC and tEAEC VF by Function Reveals Different and Novel Pathogenic Mechanisms

In order to identify new DAEC and tEAEC pathogenic mechanisms, virulence factors were grouped by function: adhesins, bacteriocins, toxins, iron acquisition factors (IAF), complement resistance or Immune system evasion factors (CR/ISEF), and bacterial secretion systems. With the exception of adhesins, all genes identified among these groups are mentioned in **Table 2**. In addition, the genes encoding for the following 14 adhesins were identified: antigen 43 (Agn43), calcium-binding antigen 43 homolog (Cah), curli, EaeH surface protein, *E. coli* common pilus (ECP), EHEC autotransporter encoding genes A (EhaA) and B (EhaB), *E. coli* YcbQ laminin-binding fimbriae (Elf/Ycb), pyelonephritis-associated pilus (Pap), Stg fimbria, toxigenic invasion loci A/haemagglutinin from *E. coli* K1 (Tia/Hek), type 1 fimbria (TIF), trimeric autotransporter adhesin UpaG, and autotransporter adhesin UpaH. Most of these adhesins have been implicated in adhesion to epithelial cells, autoaggregation and biofilm formation. The relative frequency (RF) of adhesins was similar among DAEC (RF 7.4), tEAEC (RF 7.5), and commensal (RF 7.0) *E. coli* strains, revealing that adherence is a key event for initiating *E. coli* commensal and pathogen colonization, and that its success relies on multiple adhesins that recognize receptors on the intestinal and bladder epithelium (Kaper et al., 2004; Flores-Mireles et al., 2015).

Since the information on DAEC VF is scarce, it was interesting to find that DAEC harbored significantly more IAF than both tEAEC (4.30 vs. 3.06 $p = 0.0023$) and commensal *E. coli* (4.30 vs. 2.29 $p = 0.0256$), suggesting that IAF may play an important role in DAEC virulence (**Table 2**). Iron is essential for *E. coli* survival, facilitating numerous essential cellular activities, such as peroxide

TABLE 2 | Distribution of groups of virulence factors among DAEC, EAEC, and commensal *E. coli* genomes.

Genome	Bacteriocins		CR/ISEF		IAF		Toxins		Secretion systems		Total
	#	VF	#	VF	#	VF	#	VF	#	VF	#
MEX-1-DAEC	1	CcdAB	2	OmpA, TraT	4	Aer, Ent, Sit, Ybt	0	–	0	–	7
MEX-2-DAEC	0	–	4	Iss, KPS, OmpA, TraT	5	Aer, Ent, Chu, Sit, Ybt	3	HlyE, Sat, TieB	1	ETT2	13
MEX-3-DAEC	1	CcdAB	4	Iss, KPS, OmpA, TraT	4	Aer, Ent, Sit, Ybt	3	HlyE, Sat, TieB	0	–	12
MEX-4-DAEC	1	CcdAB	4	Iss, KPS, OmpA, TraT	5	Aer, Chu, Ent, Sit, Ybt	2	HlyE, Sat	1	ETT2	13
MEX-5-DAEC	1	CcdAB	5	Iss, KPS, OmpA, TcpC, TraT	4	Aer, Chu, Ent, Ybt	1	Vat	0	–	11
MEX-6-DAEC	1	CcdAB	4	Iss, KPS, OmpA, TraT	4	Aer, Ent, Sit, Ybt	3	HlyE, Sat, TieB	0	–	12
MEX-7-DAEC	1	CcdAB	3	Iss, OmpA, TraT	4	Aer, Ent, Sit, Ybt	0	0	0	–	8
MEX-8-DAEC	1	CcdAB	3	KPS, OmpA, TraT	6	Aer, Chu, Ent, Hbp, Sit, Ybt	3	EspC, Sat, TieB	0	–	13
MEX-9-DAEC	0	–	3	Iss, KPS, OmpA	3	Chu, Ent, Ybt	3	EAST1, EatA, HlyE	1	ETT2	10
MEX-10-DAEC	1	CcdAB	4	Iss, KPS, OmpA, TraT	4	Chu, Ent, Sit, Ybt	2	HlyE, Sat	1	ETT2	12
RF	0.80		3.60		4.30		2.00		0.40		11.10
MEX-11-tEAEC	1	CcdAB	4	Iss, KPS, OmpA, Pic	3	3: Aer, Ent, Ybt	2	2: HlyE, ShET1	1	Aai	11
MEX-12-tEAEC	1	MccH47	3	OmpA, Pic, TraT	2	EntA, Ybt	3	3: EAST1, HlyE, ShET1	1	Aai	10
MEX-13- tEAEC	2	CcdAB, MccH47	4	Iss, KPS, OmpA, Pic	3	Aer, Ent, Ybt	5	EAST1, HlyA, HlyE, Sat, ShET1	1	Aai	15
MEX-14-EAEC	2	CcdAB, MccH47	2	OmpA, Pic	3	Aer, Ent, Ybt	5	HlyA, Pet, SepA, ShET1, SigA	1	Aai	13
MEX-15-EAEC	2	CcdAB, MccH47	2	OmpA, Pic	2	Ent, Ybt	4	EAST1, HlyE, Sat, ShET1	1	Aai	11
MEX-16-EAEC	1	CcdAB	3	OmpA, Pic, TraT	1	Ent	2	2: HlyE, ShET1	1	Aai	8
MEX-17-EAEC	1	CcdAB	2	OmpA, Pic	3	Aer, Ent, Ybt	4	EAST1, Sat, SepA, ShET1	1	Aai	11
MEX-18-EAEC	1	CcdAB	2	Iss, OmpA	3	Ent, Sit, Ybt	1	HlyE	0	–	7
MEX-19-EAEC	1	CcdAB	3	KPS, OmpA, TraT	5	Aer, Chu, Ent, Sit, Ybt	3	HlyA, HlyE, Sat	1	ETT2	13
MEX-20-EAEC	0	–	5	Iss, KPS, OmpA, Pic, TraT	4	Chu, Ent, Sit, Ybt	4	EAST1, HlyE, SepA, ShET1	1	Aai	14
042-EAEC	2	CcdAB, MccH47	4	KPS, OmpA, Pic, TraT	4	Chu, Ent, Sit, Ybt	4	EAST1, HlyE, Pet, ShET1	2	Aai, ETT2	16
55989-EAEC	1	CcdAB	2	OmpA, Pic	3	Aer, Ent, Ybt	4	EAST1, Pet, ShET1, SigA	1	Aai	11
C43/90-EAEC	2	CcdAB, MccH47	3	OmpA, Pic, TraT	3	Aer, Ent, Ybt	4	EAST1, HlyE, Sat, ShET1	1	Aai	13
48/93-EAEC	2	CcdAB, MccH47	3	Iss, OmpA, Pic	3	Aer, Ent, Ybt	3	HlyE, Sat, ShET1	1	Aai	12
JM221-EAEC	1	CcdAB	3	Iss, OmpA, Pic	3	Aer, Ent, Ybt	3	HlyE, Sat, ShET1	1	Aai	11
17-2-EAEC	1	CcdAB	3	Iss, KPS, OmpA	4	Aer, Ent, Sit, Ybt	5	EAST1, HlyA, HlyE, Sat, ShET1	1	Aai	14
RI	1.31		3.00		3.06		3.50		1.00		11.88
MEX-21-Com	0	–	3	Iss, OmpA, TraT	3	Aer, Ent, Sit	1	HlyE	0	–	7
HS-Com	0	–	1	OmpA	1	Ent	0	–	0	–	2
SE11-Com	1	CcdAB	2	Iss, OmpA	1	Ent	0	–	0	–	4
SE15-Com	1	CcdAB	3	KPS, OmpA, TraT	4	Chu, Ent, Sit, Ybt	2	EspC, TieB	0	–	10
IAI1-Com	0	–	2	Iss, OmpA	1	Ent	0	–	0	–	3
ED1A-Com	1	CcdAB	2	KPS, OmpA	5	Aer, Chu, Ent, Sit, Ybt	2	Sig, TieB	0	–	10
MS145-7-Com	1	CcdAB	2	OmpA, TraT	1	Ent	0	–	0	–	4
RI	0.57		2.14		2.29		0.71		0.00		5.71

CR/ISEF, Complement resistance/Immune system evasion factors; IAF, Iron acquisition factors; RI, Relative incidence; VF, Virulence factors; CcdAB, CcdA/CcdB type-II toxin-antitoxin system; MccH47, Microcin H47; Iss, Increased serum survival protein; KPS, group II Capsule; OmpA, Outer membrane protein A; Pic, Protein involved in colonization; TcpC, Tir domain containing protein; ChuA, E. coli hemin uptake system; Ybt, Yersiniabactin; Aer, Aerobactin; SitA, Sit iron/manganese transport system; EAST1, EAEC heat stable toxin 1; HlyA, α-Hemolysin; HlyE, Hemolysin E; Pet, Plasmid encoded toxin; Sat, Secreted autotransporter toxin; SepA, Secreted serine srotease A; ShET-1, Shigella enterotoxin 1; SigA, Shigella IgA-like protease homolog; Vat, Vacuolating autotransporter toxin; Aai, Aai-type VI secretion system; ETT2, E. coli Type III secretion system 2.

reduction, electron transport, and nucleotide biosynthesis (Gao et al., 2012). In other pathogenic *E. coli* groups, such as UPEC, IAS play an important role in virulence *in vivo* (Torres et al., 2001; Flores-Mireles et al., 2015). *Shigella* has also evolved multiple strategies for sequestering iron and other elements from the host (Wei and Murphy, 2016).

As shown in **Table 2**, tEAEC carried significantly more bacteriocins than DAEC ($p = 0.0005$) and commensal *E. coli* ($p = 0.0167$). tEAEC genomes were the only ones to harbor the Microcin H47 (43%) system. Microcin H47 was first found in the non-pathogenic, probiotic Nissle 1917 *E. coli* strain and is highly prevalent among ExPEC strains (Micenkova et al., 2014). It exhibits antibacterial activity against enteric pathogens such as Adherent Invasive *E. coli* (AIEC) and *S. enterica* serovar Typhimurium (Sassone-Corsi et al., 2016; Palmer et al., 2018). It is plausible that DAEC, and particularly tEAEC, use bacteriocins to eliminate competing bacteria in the gut, including other pathogenic species. Likewise, tEAEC had significantly more toxins (**Figure 2**) than DAEC (3.50 vs. 2.0, $p = 0.007$) and commensal *E. coli* (3.50 vs. 0.71, $p = 0.0321$), providing evidence that toxins play an important role in tEAEC virulence (Estrada-Garcia and Navarro-Garcia, 2012). DAEC had significantly more toxins than commensal strains (2.00 vs. 071, $P = 0.0418$), thus maybe toxins play a role in DAEC pathogenesis as well.

Two secretion systems were identified among the sequenced genomes: (1) the *E. coli* Type III secretion system 2 (ETT2), which was first discovered through the genome analysis of enterohemorrhagic *E. coli* O157:H7 (Ren et al., 2004), and (2) the tEAEC Aai type six secretion system (T6SS), which is regulated by AggR and its function is as yet unknown (Dudley et al., 2006).

ETT2 was more prevalent in DAEC (40%) than in tEAEC (12.5%) and was absent in all commensal strains (**Table 2**). With exception of MEX-20 tEAEC genome, the whole ETT2 gene cluster was identified in all strains of clades I, II, III, g and h. It has been reported that ETT2 participates in the invasion of endothelial cells by NMEC strain EC10 (Yao et al., 2009) and may have functional importance in infection among human pathogenic *E. coli* strains isolated from blood samples (Fox et al., 2020). Aai-T6SS was only identified among tEAEC genomes ($P < 0.0001$). T6SS was initially associated with bacterial virulence in eukaryotic host cells, but currently the main role of T6SS is thought to involve bacterial competition via killing of neighboring bacteria by the injection of antibacterial proteins directly into their periplasm after cell-cell contact (Navarro-Garcia et al., 2019).

CR/ISEF were significantly more prevalent in DAEC (RF 3.60 vs. 2.14, $P = 0.0043$) and tEAEC (RF 3.00 vs. 2.14, $P = 0.0008$) than among commensal strains, but there was no difference between these two pathotypes. CR/ISEF may play an essential role in DAEC pathogenesis, since the initial binding of Afa/F1845/Dr adhesins to hDAF could potentially result in a decreased inactivation of the complement cascade, thus production of CR/ISEF could protect DAEC from the action of complement (Duan and Mukherjee, 2016; Meza-Segura and Estrada-Garcia, 2016).

Novel and Common VF Genes Found Among DAEC and tEAEC Strains

Because very little is known about DAEC VF this section highlights the new VF genes identified for this pathotype. We also describe common tEAEC and commensal VF genes (**Table 3**). When compared to tEAEC, Cah was highly prevalent among DAEC genomes (90% vs. 37.5%, $p = 0.0143$), and was absent from commensal bacteria (**Table 3**). *cah* has been described to be widespread among STEC and has only been identified in one commensal *E. coli* strain (Torres et al., 2002; Montero et al., 2014; Carter et al., 2018). Cah shares high sequence similarity with AIDA-1, an adhesin that mediates DAEC diffuse adherence pattern to HeLa cells, and with Antigen 43. In *E. coli* O157:H7, Cah is known to be involved in autoaggregation and biofilm formation (Carter et al., 2018). The gene encoding for the enterotoxin TieB (*sen*B) was also significantly more prevalent in DAEC, since it was absent in tEAEC genomes ($p = 0.0140$, **Table 3**); there was no significant difference between DAEC and commensal *E. coli* genomes in the frequency of *sen*B. TieB is an enterotoxin that was initially described in EIEC (Nataro et al., 1995). Additionally, UPEC strains carrying *sen*B have been associated with both pyelonephritis and urosepsis, suggesting that TieB may play a role in UPEC virulence in humans (Mao et al., 2012).

Similarly, the gene encoding for the plasmid-encoded outer membrane protein TraT was more prevalent in DAEC than in tEAEC (90 vs. 37.5%, $P = 0.0143$). TraT is a complement-resistance molecule that is believed to enhance *E. coli* serum resistance by inhibiting later stages of the membrane attack complex activity or by altering C3 deposition on the bacterial surface and affecting outer membrane permeability (Miajlovic and Smith, 2014). *tra*T was detected in a significantly higher proportion of *E. coli* strains isolated from patients with bacteraemia/septicaemia and enteric infections when compared to *E. coli* strains isolated from healthy subjects (Montenegro et al., 1985).

IAS is the most prevalent functional group associated with DAEC and we identified two genes that were significantly more prevalent in DAEC than in tEAEC genomes: Chu, which binds host hemoproteins (60 vs. 18.8%, $p = 0.0461$), and Sit iron/manganese transport system, for the utilization of ferric iron (80 vs. 31.25%, $p = 0.0414$) (**Table 3**). Mice infected with *chu*A-inactivated UPEC strains resulted in attenuation of UPEC virulence *in vivo*, indicating that this heme receptor is a VF in UPEC (Torres et al., 2001). Sit has been described as the sole iron-uptake system in *S. flexneri* that allows this strain to survive and form plaques in a monolayer of eukaryotic cells, suggesting a direct role in *S. flexneri* pathogenesis (Runyen-Janecky et al., 2003). Furthermore, in *S. enterica* serovar Typhimurium the Sit system transports manganese (Kehres et al., 2002).

In contrast with DAEC, toxins play an important role in tEAEC virulence (Estrada-Garcia and Navarro-Garcia, 2012). As shown in **Table 3**, ShET1 (81%) and HlyA (25%) were only identified among tEAEC genomes, as both toxins play a role in tEAEC pathogenesis. ShET1 is an oligomeric toxin that induces intestinal secretion via intracellular increase of cAMP

TABLE 3 | Virulence factors encoded in DAEC, tEAEC, and commensal *E. coli* genomes.

Virulence factor	DAEC *n* = 10 (%)	EAEC *n* = 16 (%)	Commensal *n* = 7 (%)
Adhesins			
Antigen 43	10 (100.00)[I]	16 (100.00)[§]	3 (42.86)
Calcium-binding antigen 43 homolog (Cah)	9 (90.00)*[I]	6 (37.5)	0 (0)
Curli	10 (100)	15 (93.75)	7 (100)
EaeH surface protein	8 (80.00)	10 (62.5)	6 (85.71)
E. coli common pilus (ECP)	7 (70.00)	11 (68.75)	5 (71.43)
EHEC autotransporter encoding gene A (EhaA)	0 (0)	4 (25.00)	3 (42.86)
EHEC autotransporter encoding gene B (EhaB)	9 (90.00)	16 (100)	5 (71.43)
E. coli YcbQ laminin-binding fimbriae (Elf/Ycb)	3 (30.00)	14 (87.50)*	5 (71.43)
Pyelonephritis-associated pilus (Pap)	0 (0)	3 (18.75)	0 (0)
Stg fimbriae	2 (20.00)	5 (31.25)	3 (42.86)
Toxigenic invasion loci A/ haemagglutinin from *E. coli* K1 (Tia/Hek)	3 (30.00)	4 (25.00)	0 (0)
Type 1 fimbriae	8 (80.00)	11 (68.75)	6 (85.71)
Trimeric autotransporter adhesin UpaG	4 (40.00)	5 (31.25)	6 (85.71)[§]
Autotransporter adhesin UpaH	1 (10.00)	0 (0)	0 (0)
Bacteriocins			
CcdA/CcdB type-II toxin-antitoxin system	8 (80.00)	14 (87.50)	4 (57.14)
Microcin H47 (MccH47)	0 (0)	7 (43.75)*	0 (0)
Complement resistance/Immune system evasion factors			
Increased serum survival protein (Iss)	8 (80.00)	7 (43.75)	3 (42.86)
Group II Capsule (KPSMII)	8 (80.00)	6 (37.5)	2 (28.57)
Outer membrane protein A (OmpA)	10 (100)	16 (100)	7 (100)
Protein involved in colonization (Pic)	0 (0)	13 (81.25)*[§]	0 (0)
TIR domain-containing protein C (TcpC)	1 (10.00)	0 (0)	0 (0)
Plasmid-encoded outer membrane protein TraT	9 (90.00)*	6 (37.5)	3 (42.86)
Iron acquisition factors			
Aerobactin	8 (80.00)	10 (62.5)	2 (28.57)
E. coli hemin uptake system (Chu)	6 (60.00)*	3 (18.75)	2 (28.57)
Enterobactin	10 (100)	16 (100)	7 (100)
Hemoglobin-binding protease (Hbp)	1 (10.00)	0 (0)	0 (0)
Sit iron/manganese transport system	8 (80.00)*	5 (31.25)	3 (42.86)
Yersiniabactin	10 (100)[I]	15 (93.75)[§]	2 (28.57)
Secretion systems			
Aai Type VI secretion system	0 (0)	14 (87.50)*[§]	0 (0)
E. coli Type III secretion system 2 (ETT2)	4 (40.00)	2 (12.50)	0 (0)
Toxins			
EAEC heat-stable enterotoxin 1 (EAST1)	1 (10.00)	9 (56.25)*[§]	0 (0)
α-Hemolysin (HlyA)	0 (0)	4 (25.00)	0 (0)
Hemolysin E (HlyE)	6 (60.00)	13 (81.25)[§]	1 (14.29)
Plasmid-encoded toxin (Pet)	0 (0)	3 (18.75)	0 (0)
Secreted autotransporter toxin (Sat)	6 (60.00)[I]	8 (50.00)	0 (0)
Secreted serine protease A (SepA)	0 (0)	3 (18.75)	0 (0)
Shigella enterotoxin 1 (ShET1)	0 (0)	13 (81.25)*[§]	0 (0)
Shigella IgA-like protease homolog (SigA)	0 (0)	2 (12.50)	1 (14.29)
Enterotoxin TieB	4 (40.00)*	0 (0)	2 (28.57)
Vacuolating autotransporter toxin (Vat)	1 (10.00)	0 (0)	0 (0)
Other			
Escherichia coli putative arylsulfatase (AslA)	1 (10.00)	13 (81.25)	3 (42.86)[I]
Dispersin	0 (0)	15 (93.75)*[§]	0 (0)
Dispesin translocator (Aat)	0 (0)	15 (93.75)*[§]	0 (0)
ETEC autotransporter A (EatA)	1 (10.00)	0 (0)	0 (0)
Shigella flexneri Homolog Shf	1 (10.00)	7 (43.75)	2 (28.57)

*$P < 0.05$ between DAEC and EAEC, Fisher exact test.
[I]$P < 0.05$ between DAEC and commensal, Fisher exact test.
[§]$P < 0.05$ between EAEC and commensal, Fisher exact test.

and cGMP (Fasano et al., 1997). Sat toxin, previously reported to be significantly associated with DAEC strains (Meza-Segura and Estrada-Garcia, 2016), was similarly distributed among the genomes of both pathotypes (**Table 3**).

The Protein involved in colonization (Pic) was exclusively found and highly prevalent (81%) in tEAEC. Pic and ShET1 are encoded on the same chromosomal locus, encoded on opposite strands. Pic was first described in tEAEC (Henderson et al., 1999), since then it has been identified in EHEC, EPEC, and UPEC, as well as in other pathogens of the Enterobacteriaceae family (Abreu and Barbosa, 2017). Pic is a secreted autotransporter able to cleave C2, C3/C3b, and C4/C4b, and works synergistically with human Factor I and Factor H (FH), thereby promoting inactivation of C3b. It is thereby considered a CR/ISEF (Abreu and Barbosa, 2017). Also, *E. coli* Ycb laminin-binding fimbriae (Elf/Ycb) was significantly more frequent among tEAEC than DAEC genomes (87.5 vs. 30%, $P = 0085$). Elf contributes to the adherence of STEC to human intestinal epithelial cells, and to cow and pig gut tissue *in vitro* (Samadder et al., 2009). To the best of our knowledge, this is the first time Elf/Ycb has been described among DAEC and tEAEC strains. As expected, the genes encoding for dispersin (*aap*) and its translocator (*aat*A) were significantly associated with tEAEC (Patzi-Vargas et al., 2015). Obviously, the presence of these virulence genes should be corroborated among tEAEC and DAEC strains from other regions of the world, to confirm its importance in the pathogenesis of these strains.

Association of DAEC and tEAEC Virulence Genes With Clinical Severity of Diarrheal Disease

The presence of 29 *E. coli* virulence genes, identified by PCR, among the 38 DAEC and 30 tEAEC strains is shown in **Table 4**. In agreement with the comparative genome analysis, genes encoding for ChuA and SitA were more prevalent among DAEC isolates, while AaiC (T6SS), AatA, dispersin (*aap*), EAST1 (*ast*A), MccH47 (*mch*B) and Pic, among tEAEC isolates. In addition, PCR results revealed for the first time the presence of five genes significantly associated with DAEC strains: *iss*, *kps* MII, *fyu*A, and *iut*A. On the other hand, *hly*A, *pap*C, *pet* and *sep*A were significantly associated with tEAEC isolates.

DAEC strains harbored significantly more IAS encoding genes, while tEAEC strains harbored more toxin and bacteriocin genes (**Figure 3**), as previously shown in the ORF genome analysis (**Table 2**).

Of the 38 DAEC strains, 20 (52.6%) had the *afa*C-*ang*43-*fyu*A-*iut*A-*kps*MII-*sat*-*fim*A virulence gene profile (VGP), which harbors two genes encoding for IAS yersianiabactin (*fyu*A) and aerobactin (*iut*A) siderophore receptors. Both yersiniabactin and aerobactin genes are found more frequently among pathogenic *E. coli* strains and have been involved in UPEC virulence (Garcia et al., 2011; Flores-Mireles et al., 2015). Yersiniabactin binds copper to protect pathogens during infection; direct mass spectrometroscopy showed that it also binds nickel, cobalt, and chromium, and transports these metals by its receptor FyuA (Koh et al., 2017). Detection of urinary Ybt and serological detection of the outer membrane Ybt importer (*fyu*A) have been implicated in clinical UTI (Koh et al., 2017). It also appears that the aerobactin system is important in UPEC virulence (Gao et al., 2012). Therefore, the presence of several IAF in DAEC

TABLE 4 | Prevalence of 29 selected virulence genes among DAEC and tEAEC strains identified as the only pathogens isolated from children with diarrhea.

Group	Gene	DAEC, $n = 38$ (%)	tEAEC, $n = 30$ (%)
Adhesins	*agn*43	36 (94.74)	30 (100)
	*fim*A	27 (71.05)	23 (76.67)
	*pap*C	1 (2.63)	6 (20.00)*
Bacteriocins	*ccd*B	26 (68.42)	26 (86.67)
	*mch*B	0 (0)	9 (30.00)*
Complement resistance/Immune system evasion	*iss*	25 (65.79)*	12 (40.00)
	*kps*MII	28 (73.68)*	13 (43.33)
	pic	0 (0)	21 (70.00)§
	*tra*T	23 (60.53)	17 (56.67)
Dispersin	*aap*	2 (5.26)	29 (96.67)§
Dispesin translocator	*aat*A	0 (0)	28 (93.33)§
Iron acquisition systems	*iro*N	0 (0)	0 (0)
	*chu*A	22 (57.89)*	8 (26.67)
	*fyu*A	38 (100)*	24 (80.00)
	*iut*A	33 (86.84)*	13 (43.33)
	*sit*A	24 (66.16)§	3 (10.00)
Secretion systems	*aai*C	0 (0)	21 (70.00)§
	*eiv*A	12 (31.58)	6 (20.00)
Toxins	*ast*A	4 (10.53)	13 (43.33)*
	*cdt*B	0 (0)	0 (0)
	*cnf*1	0 (0)	1 (3.33)
	*hly*A	0 (0)	8 (26.67)*
	*hly*E	18 (47.37)	18 (60.00)
	pet	0 (0)	5 (16.67)*
	sat	23 (60.53)	11 (36.67)
	*sep*A	0 (0)	4 (13.33)*
	*sig*A	0 (0)	2 (6.67)
	*sub*AB	0 (0)	0 (0)
	vat	2 (5.26)	0 (0)

*$P < 0.05$, Fisher exact test.

§$P < 0.0001$, Fisher exact test.

agn43, Antigen 43; fimA, Type I fimbriae; papC, P fimbriae; ccdB, CcdA/CcdB type-II toxin-antitoxin system; mchB, Microcin H47; iss, Increased serum survival protein; kpsMII, group II Capsule; pic, Protein involved in colonization; iroN, Salmochelin; chuA, E. coli hemin uptake system; fyuA, Yersiniabactin; iutA, Aerobactin; sitA, Sit iron/manganese transport system; aaiC, Aai-type VI secretion system subunit C; eivA, E. coli Type III secretion system 2 subunit eivA; astA, EAEC heat stable toxin 1; cnf-1, Cytotoxic Necrotizing Factor-1; cdtB, Cytolethal Distending Toxin; hlyA, α-Hemolysin; hlyE, Hemolysin E; pet, Plasmid encoded toxin; sat, Secreted autotransporter toxin; sepA, Secreted serine srotease A; sigA, Shigella IgA-like protease homolog; subAB, Subtilase cytotoxin; vat, Vacuolating autotransporter tox.

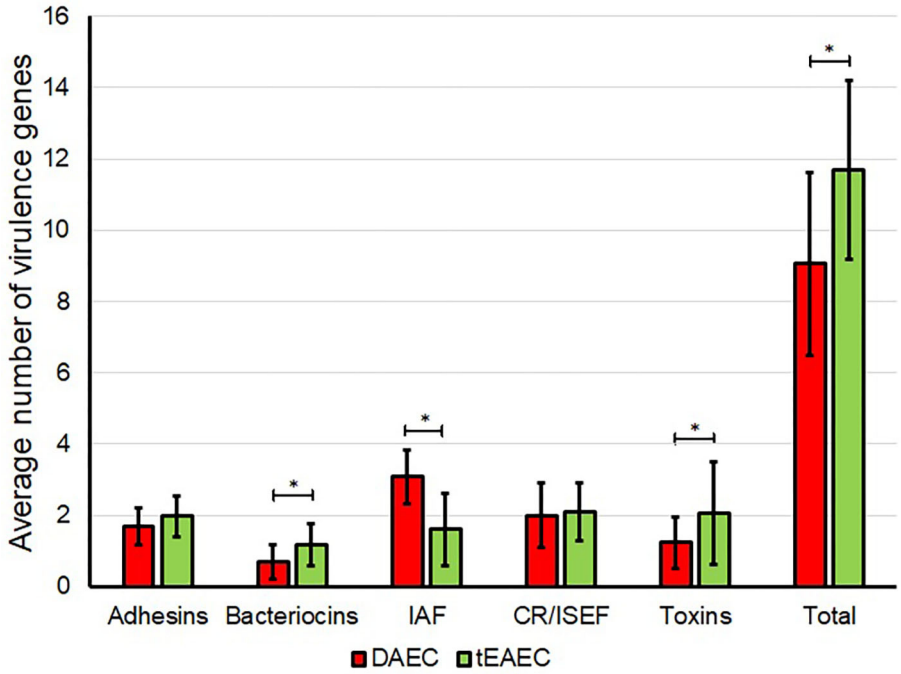

FIGURE 3 | Distribution of virulence genes in DAEC and tEAEC strains. The average number of different groups of virulence genes detected by PCR in DAEC (red) and tEAEC (green) strains are shown. Asterisks indicate a significant difference in the number of virulence genes between both pathotypes ($P < 0.05$, MWUT). CR/ISEF, Complement resistance/Immune system evasion factors; IAF, Iron acquisition factors.

genomes should be advantageous not only for its virulence, but to overcome the host "nutritional immunity" which limits bacterial growth by sequestering metals in the intestine (Lopez and Skaar, 2018). *sat*, *kps*MII, and *fim*A, also included in this common VGP, belong to the functional groups of toxins, CR/ISEF and adhesins, respectively. In animal models, SAT-producing UPEC and DAEC strains may cause damage to the renal and intestinal epithelium, respectively (Guyer et al., 2002; Taddei et al., 2005). Seventy percent of NMEC strains harbored the *kps*MII gene that encodes for the K2 capsule (Wijetunge et al., 2015). K2 provides protection against complement-mediated killing of UPEC CFT073 strain and has been shown to be important for UTI pathogenesis (Buckles et al., 2009). Among UPEC strains it has been shown that type 1 pilus (*fim*A) participates in the colonization of both the uroepithelium and the intestinal epithelium (Flores-Mireles et al., 2015; Spaulding et al., 2017). Furthermore, the type 1 pilus plays an essential role in ETEC virulence, acting in concert with specific ETEC colonization factors (CF) promoting optimal bacterial adhesion to cultured intestinal epithelium and to epithelial monolayers differentiated from human small intestinal stem cells (Sheikh et al., 2017).

Of the 30 tEAEC strains, *agg*R-*ang*43-*aap*-*aat*A-*aai*C-*pic*-*ccd*B was the predominant VGP (56.67%). *pic* also comprised part of the most prevalent gene profile (*set1*A-*set1*B-*pic*) identified in tEAEC strains isolated from Peruvian children with diarrhea, but not in strains isolated from asymptomatic children, and was also significantly associated with both acute diarrhea and prolonged diarrhea (Duan and Mukherjee, 2016). Pic's role in EAEC pathogenesis is multi-factorial: it is a mucinase, induces intestinal mucus hypersecretion, and is involved in gut colonization and complement inactivation; thus it appears that *pic* is a potential marker for virulent tEAEC strains (Estrada-Garcia and Navarro-Garcia, 2012; Abreu and Barbosa, 2017). CcdA/CcdB toxin-antitoxin system may increase the probability of tEAEC colonization by inhibiting the growth of competing organisms in the gut. To the best of our knowledge, this is the first study to identify this bacteriocin among tEAEC strains.

Specific DAEC or tEAEC VGP and Adhesins Were Associated With Fever, Age, Hyponatremia, and Disease Severity

We explored associations between the clinical characteristics of the diarrheal episode and specific VGP in DAEC and tEAEC. The *agn*43-*ccd*B-*fyu*A-*iut*A-*kps*MII-*sat*-*sit*A-*tra*T DAEC VGP was significantly associated with fever $\geq$ 38°C (7/12, 58.3% vs. 3/26, 11.5% $p = 0.0047$). It is unknown whether any of the molecules encoded by these genes directly induces secretion of IL-1, the cytokine that induces fever (Endres et al., 1987). However, we have previously shown that both DAEC reference strain C1845 and a clinical DAEC isolate induce the production of IL-1ß from Caco-2 confluent cells *in vitro* (Patzi-Vargas et al., 2013). Furthermore, DAEC and tEAEC strains isolated from patients with fever had a higher number of toxin-encoding genes (RF 2.0 vs. 1.3, $P = 0.0231$) and overall more virulence genes

(RF 11.5 vs. 9.43, $P = 0.0037$) than strains isolated from children without fever.

The *aap-aat*A-*agn*43-*fim*A-*fyu*A VGP was only found among tEAEC isolates from children aged < 2-years (18/24, 75%, $P = 0.0157$), while the *mch*B-*hly*E-*iut*A-*kps*MII VGP was exclusive to older children (3/5, 60%, $P = 0.0027$). It has been suggested that DAEC strains from children and adults constitute two different populations (Mansan-Almeida et al., 2013); this may be the case for tEAEC strains as well. *Sat* was found to be associated with hyponatremia in tEAEC diarrhea (4/5, 80% vs. 7/25, 28%, $p = 0.0472$). In a ligated rabbit ileal loop assay, SAT produced a copious amount of fluid similar to that observed with ETEC LT toxin, as well as villous edema, vacuolization and loss of internal villous structure (Taddei et al., 2005), that may result in loss of electrolytes and hyponatremia. In both DAEC and tEAEC strains, *fim*A (type 1 pilus) was more common in isolates from children ≤ 24 months than in older children (22/27, 81.5% vs. 5/11, 45.45%, $P = 0.0471$; and 22/24, 91.67% vs. 1/6,16.67%, $P = 0.0008$; respectively). As observed for ETEC, type 1 pilus may enable more effective bacterial adhesion of DAEC and tEAEC strains to the intestinal epithelium of younger children (Sheikh et al., 2017). tEAEC strains isolated from cases with dehydration signs had a higher number of genes encoding for adhesins (RF 3.43 vs. RF 2.74, $P = 0.0126$).

Hypothetical DAEC Model of Pathogenesis

Based on the variety of novel genes identified among DAEC genomes, we propose the following model for DAEC pathogenesis (**Figure 4**). Afa/F1845/Dr adhesins bind to hDAF/CD55 and hCEACAMs, localized on the apical pole of human intestinal epithelial cells, which results in DAEC characteristic diffuse adherence pattern. A novel adhesin, Cah, was found among most DAEC strains, suggesting that it could also participate in the initial adherence of DAEC, in the aggregation of bacteria and in the formation of biofilm, as it has been described before for STEC (Torres et al., 2002; Carter et al., 2018). Also, Cah shares high sequence similarity with AIDA-1, an adhesin that also mediates DAEC diffuse adherence pattern to HeLa cells (Torres

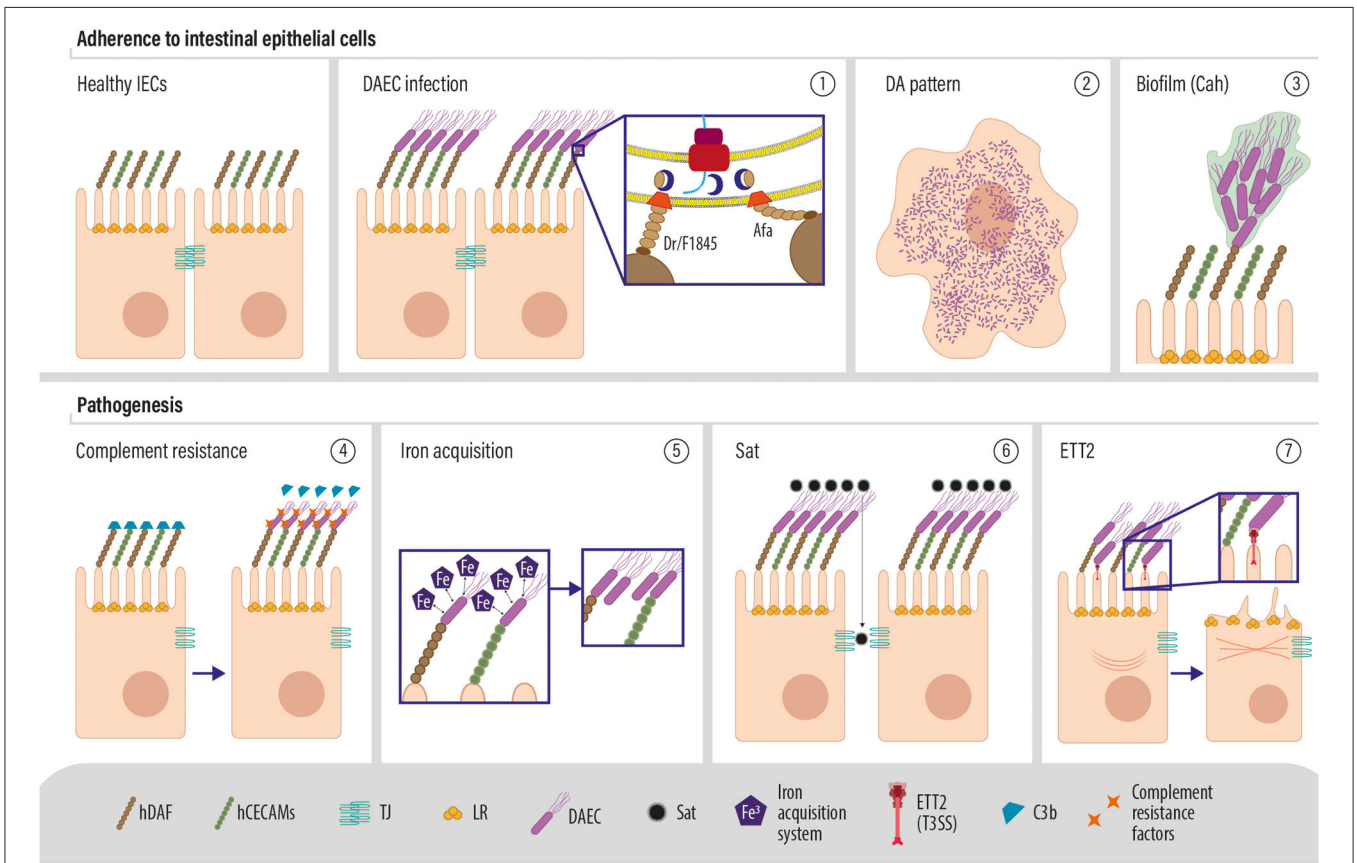

FIGURE 4 | Molecular pathogenesis of DAEC (1). DAEC expresses Afa/F1845/Dr adhesins that interact with the decay accelerating factor (also known as Dr or CD55) and (2) are responsible for the characteristic diffuse adherence (DA) pattern exhibited by this pathotype (3). The production of Cah may assist in the initial adherence to enterocytes or with production of biofilm (3). Adherence of the bacteria may dampen the inhibitory activity of hDAF, which could result in a decreased inactivation of the complement. However, DAEC strains carry a wide variety of complement resistance factors, which might protect the bacteria (4). Iron acquisition systems are common among DAEC, suggesting an important role for iron scavenging in DAEC infection, which may facilitate bacterial replication and colonization (5). The serine protease Sat is also common among DAEC strains and it is associated with the loss of cell shape and potentially detachment from epithelial layers. Finally, the ETT2 type 3 secretion system may deliver intracellular effectors to the enterocytes, which may induce cytoskeletal modifications.

et al., 2002). DAEC intrinsically has an effect on the host complement system since it binds hDAF/C55, hampering the capacity of this molecule to inhibit the complement-cascade amplification. The expression of CR/ISEF by DAEC could protect the bacteria from the action of the complement. For example, *tra*T, which inhibits later stages of the membrane attack complex activity, was highly prevalent among DAEC strains. Moreover, these strains also express a wide variety of iron acquisition systems, such as Chu, which binds host hemoproteins, and Sit iron/manganese transport system for the utilization of ferric iron, allowing DAEC to capture these elements that are indispensable for bacterial growth and to replicate faster than resident microbiota. Also, the most common DAEC VGP *afaC-ang43-fyuA-iutA-kpsMII-sat-fimA*, contained two IAS, the yersianiabactin and aerobactin siderophore receptors.

Among DAEC strains, we found the whole gene cluster encoding ETT2, which could be potentially involved in the polymerization of actin observed during DAEC infection (Riveros et al., 2011), as it has been shown for the type three secretion system of EPEC and EHEC (Kaper et al., 2004). Sat, the only previously described DAEC VF, was also identified in the most common DAEC VGP. Sat may be responsible for tight junction alteration and increased secretion of fluids into the lumen during the course of DAEC infection. We identified a gene encoding for a second toxin, TieB, for which a mechanism of action has not yet been described.

CONCLUSIONS

Comprehensive WGS and identification of VF for DAEC and tEAEC strains reveal for the first time that these two pathotypes are phylogenetically related. Given this relationship, we hypothesized that the two pathotypes would harbor a shared set of VF (as do EPEC and STEC, for example), supplemented by different factors that mediate their divergent pathogenic lifestyles. This was in fact the case, as most VF were shared between the two pathogens with few exceptions. Moreover, our work is the first comprehensive genomic analysis of DAEC, and as such identified several novel VF groups and genes among DAEC strains, including the ones encoding for Cah, Iss, Kps MII, Sit, TieB, and TraT; the analysis has allowed us to suggest for the first time a pathogenetic paradigm for this pathotype. Lastly, our work suggests clinical application by identifying common and conserved VF that may offer promise as immunogens to control DAEC and tEAEC infections.

DATA AVAILABILITY STATEMENT

The genome sequence assemblies generated in this study have been deposited in GenBank under the accession numbers listed in **Supplementary Table 2**. The remaining data that support the findings of this study are available from the corresponding author upon request.

ETHICS STATEMENT

The studies involving human participants were reviewed and approved by both the Hospital General O'Horan Ethics Committee and the CINVESTAV Committee of Bioethics for Human Research. Legal guardians were required to sign an informed consent form. All children received medical treatment according to the hospital protocols. Written informed consent to participate in this study was provided by the participants' legal guardian/next of kin.

AUTHOR CONTRIBUTIONS

MM-S and TE-G conceived the experiments. TE-G was Co-PI of the epidemiological study. MM-S and NM-G performed the experiments. MM-S, AV-P, and EM-R performed all bioinformatic analysis. MBZ was Co-PI of the epidemiological study, collected clinical samples data, and strains data. MM-S, MBZ, JPN, and TE-G wrote the manuscript, which was reviewed and approved by all authors. All authors contributed to the article and approved the submitted version.

ACKNOWLEDGMENTS

CONACYT scholarship 368026 to MM-S, 261884 to AV-P, and 368716 to NM-G. TE-G was recipient of CONACYT Grant 254990. We thank Diego Meza-Segura for realization of drawings.

SUPPLEMENTARY MATERIAL

The Supplementary Material for this article can be found online at: https://www.frontiersin.org/articles/10.3389/fcimb.2020.572951/full#supplementary-material

REFERENCES

Abreu, A. G., and Barbosa, A. S. (2017). How *Escherichia coli* circumvent complement-mediated killing. *Front. Immunol.* 8:452. doi: 10.3389/fimmu.2017.00452

Besemer, J., and Borodovsky, M. (2005). GeneMark: web software for gene finding in prokaryotes, eukaryotes and viruses. *Nucleic Acids Res.* 33, W451–454. doi: 10.1093/nar/gki487

Bielaszewska, M., Prager, R., Kock, R., Mellmann, A., Zhang, W., Tschape, H., et al. (2007). Shiga toxin gene loss and transfer *in vitro* and *in vivo* during enterohemorrhagic *Escherichia coli* O26 infection in humans. *Appl. Environ. Microbiol.* 73, 3144–3150. doi: 10.1128/AEM.02937-06

Boetzer, M., Henkel, C. V., Jansen, H. J., Butler, D., and Pirovano, W. (2011). Scaffolding pre-assembled contigs using SSPACE. *Bioinformatics* 27, 578–579. doi: 10.1093/bioinformatics/btq683

Boetzer, M., and Pirovano, W. (2012). Toward almost closed genomes with GapFiller. *Genome Biol.* 13:R56. doi: 10.1186/gb-2012-13-6-r56

Buckles, E. L., Wang, X., Lane, M. C., Lockatell, C. V., Johnson, D. E., Rasko, D. A., et al. (2009). Role of the K2 capsule in *Escherichia coli* urinary tract infection and serum resistance. *J. Infect. Dis.* 199, 1689–1697. doi: 10.1086/598524

Carter, M. Q., Brandl, M. T., Kudva, I. T., Katani, R., Moreau, M. R., and Kapur, V. (2018). Conditional function of autoaggregative protein cah and common cah mutations in shiga toxin-producing *Escherichia coli*. *Appl. Environ. Microbiol.* 84, e01739–17. doi: 10.1128/AEM.01739-17

Cerna, J. F., Nataro, J. P., and Estrada-Garcia, T. (2003). Multiplex PCR for detection of three plasmid-borne genes of enteroaggregative *Escherichia coli* strains. *J. Clin. Microbiol.* 41, 2138–2140. doi: 10.1128/JCM.41.5.2138-2140.2003

Contreras-Moreira, B., and Vinuesa, P. (2013). GET_HOMOLOGUES, a versatile software package for scalable and robust microbial pangenome analysis. *Appl. Environ. Microbiol.* 79, 7696–7701. doi: 10.1128/AEM.02411-13

Duan, L., and Mukherjee, E. (2016). Janeway's immunobiology, ninth edition. *Yale J. Biol. Med.* 89, 424–425.

Dudley, E. G., Thomson, N. R., Parkhill, J., Morin, N. P., and Nataro, J. P. (2006). Proteomic and microarray characterization of the AggR regulon identifies a pheU pathogenicity island in enteroaggregative *Escherichia coli*. *Mol. Microbiol.* 61, 1267–1282. doi: 10.1111/j.1365-2958.2006.05281.x

Endres, S., van der Meer, J. W., and Dinarello, C. A. (1987). Interleukin-1 in the pathogenesis of fever. *Eur. J. Clin. Invest.* 17, 469–474. doi: 10.1111/j.1365-2362.1987.tb01144.x

Estrada-Garcia, T., and Navarro-Garcia, F. (2012). Enteroaggregative *Escherichia coli* pathotype: a genetically heterogeneous emerging foodborne enteropathogen. *FEMS Immunol. Med. Microbiol.* 66, 281–298. doi: 10.1111/j.1574-695X.2012.01008.x

Farmer, J. J. III., Fanning, G. R., Davis, B. R., O'Hara, C. M., Riddle, C., Hickman-Brenner, F. W., et al. (1985). *Escherichia fergusonii* and enterobacter taylorae, two new species of enterobacteriaceae isolated from clinical specimens. *J. Clin. Microbiol.* 21, 77–81. doi: 10.1128/JCM.21.1.77-81.1985

Fasano, A., Noriega, F. R., Liao, F. M., Wang, W., and Levine, M. M. (1997). Effect of *Shigella Enterotoxin* 1 (ShET1) on rabbit intestine *in vitro* and *in vivo*. *Gut* 40, 505–511. doi: 10.1136/gut.40.4.505

Flores-Mireles, A. L., Walker, J. N., Caparon, M., and Hultgren, S. J. (2015). Urinary tract infections: epidemiology, mechanisms of infection and treatment options. *Nat. Rev. Microbiol.* 13, 269–284. doi: 10.1038/nrmicro3432

Fox, S., Goswami, C., Holden, M., Connolly, J. P. R., Mordue, J., O'Boyle, N., et al. (2020). A highly conserved complete accessory *Escherichia coli* type III secretion system 2 is widespread in bloodstream isolates of the ST69 lineage. *Sci. Rep.* 10:4135. doi: 10.1038/s41598-020-61026-x

Gao, Q., Wang, X., Xu, H., Xu, Y., Ling, J., Zhang, D., et al. (2012). Roles of iron acquisition systems in virulence of extraintestinal pathogenic *Escherichia coli*: salmochelin and aerobactin contribute more to virulence than heme in a chicken infection model. *BMC Microbiol.* 12:143. doi: 10.1186/1471-2180-12-143

Garcia, E. C., Brumbaugh, A. R., and Mobley, H. L. (2011). Redundancy and specificity of *Escherichia coli* iron acquisition systems during urinary tract infection. *Infect. Immun.* 79, 1225–1235. doi: 10.1128/IAI.01222-10

GBD 2016 Diarrhoeal Disease Collaborators (2018). Estimates of the global, regional, and national morbidity, mortality, and aetiologies of diarrhoea in 195 countries: a systematic analysis for the Global Burden of Disease Study 2016. *Lancet. Infect. Dis.* 18, 1211–1228. doi: 10.1016/S1473-3099(18)30362-1

Guyer, D. M., Radulovic, S., Jones, F. E., and Mobley, H. L. (2002). Sat, the secreted autotransporter toxin of uropathogenic *Escherichia coli*, is a vacuolating cytotoxin for bladder and kidney epithelial cells. *Infect. Immun.* 70, 4539–4546. doi: 10.1128/IAI.70.8.4539-4546.2002

Guzman-Hernandez, R., Contreras-Rodriguez, A., Hernandez-Velez, R., Perez-Martinez, I., Lopez-Merino, A., Zaidi, M. B., et al. (2016). Mexican unpasteurised fresh cheeses are contaminated with salmonella spp., non-O157 shiga toxin producing *Escherichia coli* and potential uropathogenic *E. coli* strains: a public health risk. *Int. J. Food Microbiol.* 237, 10–16. doi: 10.1016/j.ijfoodmicro.2016.08.018

Hazen, T. H., Donnenberg, M. S., Panchalingam, S., Antonio, M., Hossain, A., Mandomando, I., et al. (2016). Genomic diversity of EPEC associated with clinical presentations of differing severity. *Nat. Microbiol.* 1:15014. doi: 10.1038/nmicrobiol.2015.14

Henderson, I. R., Czeczulin, J., Eslava, C., Noriega, F., and Nataro, J. P. (1999). Characterization of pic, a secreted protease of shigella flexneri and enteroaggregative *Escherichia coli*. *Infect. Immun.* 67, 5587–5596. doi: 10.1128/IAI.67.11.5587-5596.1999

Hunt, M., Kikuchi, T., Sanders, M., Newbold, C., Berriman, M., and Otto, T. D. (2013). REAPR: a universal tool for genome assembly evaluation. *Genome Biol.* 14:R47. doi: 10.1186/gb-2013-14-5-r47

Jennings, M. C., Tilley, D. H., Ballard, S. B., Villanueva, M., Costa, F. M., Lopez, M., et al. (2017). Case-case analysis using 7 years of travelers' diarrhea surveillance data: preventive and travel medicine applications in cusco, Peru. *Am. J. Trop. Med. Hyg.* 96, 1097–1106. doi: 10.4269/ajtmh.16-0633

Kaas, R. S., Friis, C., Ussery, D. W., and Aarestrup, F. M. (2012). Estimating variation within the genes and inferring the phylogeny of 186 sequenced diverse *Escherichia coli* genomes. *BMC Genomics* 13:577. doi: 10.1186/1471-2164-13-577

Kalyaanamoorthy, S., Minh, B. Q., Wong, T. K. F., von Haeseler, A., and Jermiin, L. S. (2017). ModelFinder: fast model selection for accurate phylogenetic estimates. *Nat. Methods* 14, 587–589. doi: 10.1038/nmeth.4285

Kaper, J. B., Nataro, J. P., and Mobley, H. L. (2004). Pathogenic *Escherichia coli*. *Nat. Rev. Microbiol.* 2, 123–140. doi: 10.1038/nrmicro818

Katoh, K., and Standley, D. M. (2013). MAFFT multiple sequence alignment software version 7: improvements in performance and usability. *Mol. Biol. Evol.* 30, 772–780. doi: 10.1093/molbev/mst010

Kehres, D. G., Janakiraman, A., Slauch, J. M., and Maguire, M. E. (2002). SitABCD is the alkaline Mn^{2+} transporter of Salmonella enterica serovar typhimurium. *J. Bacteriol.* 184, 3159–3166. doi: 10.1128/JB.184.12.3159-3166.2002

Koh, E. I., Robinson, A. E., Bandara, N., Rogers, B. E., and Henderson, J. P. (2017). Copper import in *Escherichia coli* by the yersiniabactin metallophore system. *Nat. Chem. Biol.* 13, 1016–1021. doi: 10.1038/nchembio.2441

Lacher, D. W., Steinsland, H., Blank, T. E., Donnenberg, M. S., and Whittam, T. S. (2007). Molecular evolution of typical enteropathogenic *Escherichia coli*: clonal analysis by multilocus sequence typing and virulence gene allelic profiling. *J. Bacteriol.* 189, 342–350. doi: 10.1128/JB.01472-06

Lanata, C. F., Fischer-Walker, C. L., Olascoaga, A. C., Torres, C. X., Aryee, M. J., Black, R. E., et al. (2013). Global causes of diarrheal disease mortality in children <5 years of age: a systematic review. *PLoS ONE.* 8, e72788. doi: 10.1371/journal.pone.0072788

Letunic, I., and Bork, P. (2016). Interactive tree of life (iTOL) v3: an online tool for the display and annotation of phylogenetic and other trees. *Nucleic Acids Res.* 44, W242–245. doi: 10.1093/nar/gkw290

Liu, B., Zheng, D., Jin, Q., Chen, L., and Yang, J. (2019). VFDB 2019: a comparative pathogenomic platform with an interactive web interface. *Nucleic Acids Res.* 47, D687–D692. doi: 10.1093/nar/gky1080

Lopez, C. A., and Skaar, E. P. (2018). The impact of dietary transition metals on host-bacterial interactions. *Cell Host Microbe* 23, 737–748. doi: 10.1016/j.chom.2018.05.008

Lopez-Saucedo, C., Cerna, J. F., Villegas-Sepulveda, N., Thompson, R., Velazquez, F. R., Torres, J., et al. (2003). Single multiplex polymerase chain reaction to detect diverse loci associated with diarrheagenic *Escherichia coli*. *Emerg. Infect. Dis.* 9, 127–131. doi: 10.3201/eid0901.010507

Lukjancenko, O., Wassenaar, T. M., and Ussery, D. W. (2010). Comparison of 61 sequenced *Escherichia coli* genomes. *Microb. Ecol.* 60, 708–720. doi: 10.1007/s00248-010-9717-3

Mansan-Almeida, R., Pereira, A. L., and Giugliano, L. G. (2013). Diffusely adherent *Escherichia coli* strains isolated from children and adults constitute two different populations. *BMC Microbiol.* 13:22. doi: 10.1186/1471-2180-13-22

Mao, B. H., Chang, Y. F., Scaria, J., Chang, C. C., Chou, L. W., Tien, N., et al. (2012). Identification of *Escherichia coli* genes associated with urinary tract infections. *J. Clin. Microbiol.* 50, 449–456. doi: 10.1128/JCM.00640-11

Mathewson, J. J., Oberhelman, R. A., Dupont, H. L., Javier de la Cabada, F., and Garibay, E. V. (1987). Enteroadherent *Escherichia coli* as a cause of diarrhea among children in Mexico. *J. Clin. Microbiol.* 25, 1917–1919. doi: 10.1128/JCM.25.10.1917-1919.1987

Meza-Segura, M., and Estrada-Garcia, T. (2016). "Diffusely adherent *Escherichia coli*," in *Escherichia coli in the Americas,* ed A. G. Torres (Cham: Springer International Publishing), 125–147. doi: 10.1007/978-3-319-45092-6_6

Miajlovic, H., and Smith, S. G. (2014). Bacterial self-defence: how *Escherichia coli* evades serum killing. *FEMS Microbiol. Lett.* 354, 1–9. doi: 10.1111/1574-6968.12419

Micenkova, L., Staudova, B., Bosak, J., Mikalova, L., Littnerova, S., Vrba, M., et al. (2014). Bacteriocin-encoding genes and ExPEC virulence determinants are associated in human fecal *Escherichia coli* strains. *BMC Microbiol.* 14:109. doi: 10.1186/1471-2180-14-109

Minh, B. Q., Schmidt, H. A., Chernomor, O., Schrempf, D., Woodhams, M. D., von Haeseler, A., et al. (2020). IQ-TREE 2: new models and efficient methods for phylogenetic inference in the genomic era. *Mol. Biol. Evol.* 37, 1530–1534. doi: 10.1093/molbev/msaa015

Montenegro, M. A., Bitter-Suermann, D., Timmis, J. K., Aguero, M. E., Cabello, F. C., Sanyal, S. C., et al. (1985). traT gene sequences, serum resistance and pathogenicity-related factors in clinical isolates of *Escherichia coli* and other gram-negative bacteria. *J. Gen. Microbiol.* 131, 1511–1521. doi: 10.1099/00221287-131-6-1511

Montero, D., Orellana, P., Gutierrez, D., Araya, D., Salazar, J. C., Prado, V., et al. (2014). Immunoproteomic analysis to identify Shiga toxin-producing *Escherichia coli* outer membrane proteins expressed during human infection. *Infect. Immun.* 82, 4767–4777. doi: 10.1128/IAI.02030-14

Montero, D. A., Canto, F. D., Velasco, J., Colello, R., Padola, N. L., Salazar, J. C., et al. (2019). Cumulative acquisition of pathogenicity islands has shaped virulence potential and contributed to the emergence of LEE-negative Shiga toxin-producing *Escherichia coli* strains. *Emerg. Microbes Infect.* 8, 486–502. doi: 10.1080/22221751.2019.1595985

Nataro, J. P. (2005). Enteroaggregative *Escherichia coli* pathogenesis. *Curr. Opin. Gastroenterol.* 21, 4–8.

Nataro, J. P., Seriwatana, J., Fasano, A., Maneval, D. R., Guers, L. D., Noriega, F., et al. (1995). Identification and cloning of a novel plasmid-encoded enterotoxin of enteroinvasive *Escherichia coli* and shigella strains. *Infect. Immun.* 63, 4721–4728. doi: 10.1128/IAI.63.12.4721-4728.1995

Nataro, J. P., Yikang, D., Yingkang, D., and Walker, K. (1994). AggR, a transcriptional activator of aggregative adherence fimbria I expression in enteroaggregative *Escherichia coli*. *J. Bacteriol.* 176, 4691–4699. doi: 10.1128/JB.176.15.4691-4699.1994

Navarro-Garcia, F., Ruiz-Perez, F., Cataldi, A., and Larzabal, M. (2019). Type VI secretion system in pathogenic *Escherichia coli*: structure, role in virulence, and acquisition. *Front. Microbiol.* 10:1965. doi: 10.3389/fmicb.2019.01965

Neumann, B., Pospiech, A., and Schairer, H. U. (1992). Rapid isolation of genomic DNA from gram-negative bacteria. *Trends Genet.* 8, 332–333. doi: 10.1016/0168-9525(92)90269-A

Nurk, S., Bankevich, A., Antipov, D., Gurevich, A. A., Korobeynikov, A., Lapidus, A., et al. (2013). Assembling single-cell genomes and mini-metagenomes from chimeric MDA products. *J. Comput. Biol.* 20, 714–737. doi: 10.1089/cmb.2013.0084

Ochoa, T. J., Ecker, L., Barletta, F., Mispireta, M. L., Gil, A. I., Contreras, C., et al. (2009). Age-related susceptibility to infection with diarrheagenic *Escherichia coli* among infants from periurban areas in Lima, Peru. *Clin. Infect. Dis.* 49, 1694–1702. doi: 10.1086/648069

Palmer, J. D., Piattelli, E., McCormick, B. A., Silby, M. W., Brigham, C. J., and Bucci, V. (2018). Engineered probiotic for the inhibition of salmonella via tetrathionate-induced production of microcin H47. *ACS Infect. Dis.* 4, 39–45. doi: 10.1021/acsinfecdis.7b00114

Paredes-Paredes, M., Okhuysen, P. C., Flores, J., Mohamed, J. A., Padda, R. S., Gonzalez-Estrada, A., et al. (2011). Seasonality of diarrheagenic *Escherichia coli* pathotypes in the US students acquiring diarrhea in Mexico. *J. Travel Med.* 18, 121–125. doi: 10.1111/j.1708-8305.2010.00488.x

Patzi-Vargas, S., Zaidi, M., Bernal-Reynaga, R., Leon-Cen, M., Michel, A., and Estrada-Garcia, T. (2013). Persistent bloody diarrhoea without fever associated with diffusely adherent *Escherichia coli* in a young child. *J. Med. Microbiol.* 62(Pt 12), 1907–1910. doi: 10.1099/jmm.0.062349-0

Patzi-Vargas, S., Zaidi, M. B., Perez-Martinez, I., Leon-Cen, M., Michel-Ayala, A., Chaussabel, D., et al. (2015). Diarrheagenic *Escherichia coli* carrying supplementary virulence genes are an important cause of moderate to severe diarrhoeal disease in Mexico. *PLoS Negl. Trop. Dis.* 9:e0003510. doi: 10.1371/journal.pntd.0003510

Prjibelski, A. D., Vasilinetc, I., Bankevich, A., Gurevich, A., Krivosheeva, T., Nurk, S., et al. (2014). ExSPAnder: a universal repeat resolver for DNA fragment assembly. *Bioinformatics* 30, i293–301. doi: 10.1093/bioinformatics/btu266

Rasko, D. A., Del Canto, F., Luo, Q., Fleckenstein, J. M., Vidal, R., and Hazen, T. H. (2019). Comparative genomic analysis and molecular examination of the diversity of enterotoxigenic *Escherichia coli* isolates from Chile. *PLoS Negl. Trop. Dis.* 13:e0007828. doi: 10.1371/journal.pntd.0007828

Rasko, D. A., Rosovitz, M. J., Myers, G. S., Mongodin, E. F., Fricke, W. F., Gajer, P., et al. (2008). The pangenome structure of *Escherichia coli*: comparative genomic analysis of *E. coli* commensal and pathogenic isolates. *J. Bacteriol.* 190, 6881–6893. doi: 10.1128/JB.00619-08

Rasko, D. A., Webster, D. R., Sahl, J. W., Bashir, A., Boisen, N., Scheutz, F., et al. (2011). Origins of the *E. coli* strain causing an outbreak of hemolytic-uremic syndrome in Germany. *N Engl. J. Med.* 365, 709–717. doi: 10.1056/NEJMoa1106920

Ren, C. P., Chaudhuri, R. R., Fivian, A., Bailey, C. M., Antonio, M., Barnes, W. M., et al. (2004). The ETT2 gene cluster, encoding a second type III secretion system from *Escherichia coli*, is present in the majority of strains but has undergone widespread mutational attrition. *J. Bacteriol.* 186, 3547–3560. doi: 10.1128/JB.186.11.3547-3560.2004

Riveros, M., Barletta, F., Cabello, M., Durand, D., Mercado, E. H., Contreras, C., et al. (2011). Adhesion patterns in diffusely adherent *Escherichia coli* (DAEC) strains isolated from children with and without diarrhea. *Rev. Peru Med. Exp. Salud. Publica* 28, 21–28. doi: 10.1590/S1726-46342011000100004

Rouli, L., Merhej, V., Fournier, P. E., and Raoult, D. (2015). The bacterial pangenome as a new tool for analysing pathogenic bacteria. *N Microbes N Infect.* 7, 72–85. doi: 10.1016/j.nmni.2015.06.005

Runyen-Janecky, L. J., Reeves, S. A., Gonzales, E. G., and Payne, S. M. (2003). Contribution of the shigella flexneri sit, Iuc, and Feo iron acquisition systems to iron acquisition *in vitro* and in cultured cells. *Infect. Immun.* 71, 1919–1928. doi: 10.1128/IAI.71.4.1919-1928.2003

Ruuska, T., and Vesikari, T. (1990). Rotavirus disease in finnish children: use of numerical scores for clinical severity of diarrhoeal episodes. *Scand. J. Infect. Dis.* 22, 259–267. doi: 10.3109/00365549009027046

Samadder, P., Xicohtencatl-Cortes, J., Saldana, Z., Jordan, D., Tarr, P. I., Kaper, J. B., et al. (2009). The *Escherichia coli* ycbQRST operon encodes fimbriae with laminin-binding and epithelial cell adherence properties in Shiga-toxigenic *E. coli* O157:H7. *Environ. Microbiol.* 11, 1815–1826. doi: 10.1111/j.1462-2920.2009.01906.x

Sassone-Corsi, M., Nuccio, S. P., Liu, H., Hernandez, D., Vu, C. T., Takahashi, A. A., et al. (2016). Microcins mediate competition among enterobacteriaceae in the inflamed gut. *Nature* 540, 280–283. doi: 10.1038/nature20557

Servin, A. L. (2014). Pathogenesis of human diffusely adhering *Escherichia coli* expressing Afa/Dr adhesins (Afa/Dr DAEC): current insights and future challenges. *Clin. Microbiol. Rev.* 27, 823–869. doi: 10.1128/CMR.00036-14

Sheikh, A., Rashu, R., Begum, Y. A., Kuhlman, F. M., Ciorba, M. A., Hultgren, S. J., et al. (2017). Highly conserved type 1 pili promote enterotoxigenic E. *coli* pathogen-host interactions. *PLoS Negl. Trop. Dis.* 11:e0005586. doi: 10.1371/journal.pntd.0005586

Spaulding, C. N., Klein, R. D., Ruer, S., Kau, A. L., Schreiber, H. L., Cusumano, Z. T., et al. (2017). Selective depletion of uropathogenic E. *coli* from the gut by a FimH antagonist. *Nature* 546, 528–532. doi: 10.1038/nature22972

Taddei, C. R., Fasano, A., Ferreira, A. J., Trabulsi, L. R., and Martinez, M. B. (2005). Secreted autotransporter toxin produced by a diffusely adhering *Escherichia coli* strain causes intestinal damage in animal model assays. *FEMS Microbiol. Lett.* 250, 263–269. doi: 10.1016/j.femsle.2005.07.013

Tonkin-Hill, G., Lees, J. A., Bentley, S. D., Frost, S. D. W., and Corander, J. (2018). RhierBAPS: an R implementation of the population clustering algorithm hierBAPS. *Wellcome Open Res.* 3:93. doi: 10.12688/wellcomeopenres.14694.1

Torres, A. G., Perna, N. T., Burland, V., Ruknudin, A., Blattner, F. R., and Kaper, J. B. (2002). Characterization of Cah, a calcium-binding and heat-extractable autotransporter protein of enterohaemorrhagic *Escherichia coli*. *Mol. Microbiol.* 45, 951–966. doi: 10.1046/j.1365-2958.2002.03094.x

Torres, A. G., Redford, P., Welch, R. A., and Payne, S. M. (2001). TonB-dependent systems of uropathogenic *Escherichia coli*: aerobactin and heme transport and TonB are required for virulence in the mouse. *Infect. Immun.* 69, 6179–6185. doi: 10.1128/IAI.69.10.6179-6185.2001

Vasilinetc, I., Prjibelski, A. D., Gurevich, A., Korobeynikov, A., and Pevzner, P. A. (2015). Assembling short reads from jumping libraries with large insert sizes. *Bioinformatics* 31, 3262–3268. doi: 10.1093/bioinformatics/btv337

Vera-Ponce de Leon, A., Jahnes, B. C., Duan, J., Camuy-Velez, L. A., and Sabree, Z. L. (2020). Cultivable, host-specific bacteroidetes symbionts exhibit diverse polysaccharolytic strategies. *Appl. Environ. Microbiol.* 86, e00091–20. doi: 10.1128/AEM.00091-20

Wei, Y., and Murphy, E. R. (2016). Shigella iron acquisition systems and their regulation. *Front. Cell. Infect. Microbiol.* 6:18. doi: 10.3389/fcimb.2016.00018

Wijetunge, D. S., Gongati, S., DebRoy, C., Kim, K. S., Couraud, P. O., Romero, I. A., et al. (2015). Characterizing the pathotype of neonatal meningitis causing *Escherichia coli* (NMEC). *BMC Microbiol.* 15:211. doi: 10.1186/s12866-015-0547-9

World Health Organization. (2018). *Outbreaks of E. coli O104: H4 infection: update 30*. Available online at: https://www.euro.who.int/en/countries/germany/news/news/2011/07/outbreaks-of-e.-coli-o104h4-infection-update-30 (accessed June 12, 2020).

Yao, Y., Xie, Y., Perace, D., Zhong, Y., Lu, J., Tao, J., et al. (2009). The type III secretion system is involved in the invasion and intracellular survival of *Escherichia coli* K1 in human brain microvascular endothelial cells. *FEMS Microbiol. Lett.* 300, 18–24. doi: 10.1111/j.1574-6968.2009.01763.x

Zhou, Y., Zhu, X., Hou, H., Lu, Y., Yu, J., Mao, L., et al. (2018). Characteristics of diarrheagenic *Escherichia coli* among children under 5 years of age with acute diarrhea: a hospital based study. *BMC Infect. Dis.* 18:63. doi: 10.1186/s12879-017-2936-1

Zhou, Z., Li, X., Liu, B., Beutin, L., Xu, J., Ren, Y., et al. (2010). Derivation of *Escherichia coli* O157:H7 from its O55:H7 precursor. *PLoS ONE* 5:e8700. doi: 10.1371/journal.pone.0008700

Conflict of Interest: The authors declare that the research was conducted in the absence of any commercial or financial relationships that could be construed as a potential conflict of interest.

frontiers in Cellular and Infection Microbiology

MINI REVIEW
published: 21 December 2020
doi: 10.3389/fcimb.2020.548492

Escherichia coli as a Multifaceted Pathogenic and Versatile Bacterium

Vânia Santos Braz[†], *Karine Melchior and Cristiano Gallina Moreira*[*†]

Department of Biological Sciences, School of Pharmaceutical Sciences, São Paulo State University (UNESP), Araraquara, Brazil

Genetic plasticity promotes evolution and a vast diversity in *Escherichia coli* varying from avirulent to highly pathogenic strains, including the emergence of virulent hybrid microorganism. This ability also contributes to the emergence of antimicrobial resistance. These hybrid pathogenic *E. coli* (HyPEC) are emergent threats, such as O104:H4 from the European outbreak in 2011, aggregative adherent bacteria with the potent Shiga-toxin. Here, we briefly revisited the details of these *E. coli* classic and hybrid pathogens, the increase in antimicrobial resistance in the context of a genetically empowered multifaceted and versatile bug and the growing need to advance alternative therapies to fight these infections.

Keywords: treatment, genetic mobility, pathogenesis, *Escherichia*, multiresistant

OPEN ACCESS

Edited by:
Mauricio J. Farfan, University of Chile, Chile

Reviewed by:
Sanjana Mukherjee, United States Food and Drug Administration, United States
Cecilia Shirley Toro, University of Chile, Chile

***Correspondence:**
Cristiano Gallina Moreira
cg.moreira@unesp.br

[†]***ORCID:***
Vânia Santos Braz
orcid.org/0000-0002-1389-1055
Cristiano Gallina Moreira
orcid.org/0000-0002-0689-4119

Specialty section:
This article was submitted to Bacteria and Host, a section of the journal Frontiers in Cellular and Infection Microbiology

Received: *02 April 2020*
Accepted: *17 November 2020*
Published: *21 December 2020*

Citation:
Braz VS, Melchior K and Moreira CG (2020) Escherichia coli as a Multifaceted Pathogenic and Versatile Bacterium. Front. Cell. Infect. Microbiol. 10:548492. doi: 10.3389/fcimb.2020.548492

INTRODUCTION

Escherichia coli (or *E. coli*) is a Gram-negative versatile bacterium, easily found and amenable to natural and random genetic alteration. There is a vast collection of sequenced *E. coli* genomes which exhibit different sizes and genomic diversity among commensal and pathogens, indicating a great assortment within the same bacterial species. They comprise of non-pathogenic bacteria that may act as commensals and belong to the normal intestinal microbiota of humans and many animals. There are also pathogenic variants, divided as diarrheagenic and extraintestinal pathogens, with different pathotypes and various natural hybrid strains (**Tables 1** and **2**). These variants can be facultative or obligate pathogens. The facultative bacteria are part of the intestinal tract and may act as opportunistic pathogens when outside of their natural habitat, causing various types of extraintestinal infections. On the other hand, intestinal obligate pathogenic variants cause infections in distinct conditions, from moderate diarrhea to more threatening cases, as lethal outcome (Kaper et al., 2004; Köhler and Dobrindt, 2011).

E. coli pangenome studies indicate enormous capacity to evolve by gene acquisition and genetic modification. Besides, these genomes have a mosaic-like structure consisting of a core genome, encoding essential cellular functions, and an accessory genome with flexible strain-specific sequences. Thus, *E. coli* is a model well established for studying the interdependence of genome architecture and the lifestyle of bacteria (Touchon et al., 2009; Dobrindt et al., 2010).

Based on virulence factors in *E. coli* genomes and phenotypic traits, the human pathotypes of diarrheagenic *E. coli* (DEC) are differentiated from non-pathogenic *E. coli* and extraintestinal pathogenic *E. coli* (ExPEC). The ExPEC are classified as uropathogenic *E. coli* (UPEC), sepsis-causing *E. coli* (SEPEC) and neonatal meningitis-associated *E. coli* (NMEC) (Kaper et al., 2004). Recent pathogenomics and phenotypic classification have revisited the DEC group as nine distinct

TABLE 1 | Classic *E. coli* pathotypes main features: extraintestinal (ExPEC) and diarrheagenic (DEC).

E. coli Pathotype (DEC and ExPEC)	Main virulence traits	Clinical manifestation	Antimicrobial resistance (AMR) commonly found	Mobile genetic resistance determinants	References
Shiga toxin-producing (STEC)	Shiga-toxin	Not associated with human diseases	Streptomycin, Ampicillin, Tetracyclin and sulphonamides	ND	Jerse et al., 1990; Kaper et al., 2004; Day et al., 2017
Enterohemorrhagic (EHEC)	EscF, EscC, EspA, EspB, EspD, Intimin, Tir, and Shiga-toxin	Foodborne Bloody diarrhea and HUS	Streptomycin, Ampicillin, Tetracyclin and sulphonamides	Resistance plasmid-mediated (as pO157, pO111-CRL115, pO26-CRL125, pO145-13514)	Knutton et al., 1989; Mellies et al., 1999; Kaper et al., 2004; Garmendia et al., 2005; Day et al., 2017
Enteropathogenic (EPEC)	EscF, EscC, EspA, EspB, EspD, Intimin, Tir, EAF plasmid (tEPEC) and Bfp (tEPEC)	Watery diarrhea	Streptomycin, Ampicillin, Tetracyclin, Trimethoprim and Sulfamethoxazole	Resistance plasmid-mediated (as pEAF, MB80, pB171_90, pED208)	Tobe et al., 1999; Trabulsi et al., 2002; Kaper et al., 2004; Ingle et al., 2018
Enteroaggregative (EAEC)	pAA plasmid, aggregated fimbriae adhesion (AAF), AggR regulator and dispersin	Acute and chronic diarrhea	Ampicillin, Trimethoprim, Sulfamethoxazole, Nalidixic acid, and ciprofloxacin	Resistance plasmid-mediated (as pAA), chromosomal *gyrB* and *parC* mutations	Regua-Mangia et al., 2009; Aslani et al., 2011; Gomes et al., 2016; Pawłowska and Sobieszczańska, 2017; Chattaway et al., 2017
Enteroinvasive (EIEC)	Plasmid pINV and invasins	Bacillary Dysentery	Carbapenem, fosfomycin-trometanol, nitrofurantoin, chloramphenicol, β-lactams, nalidixic acid, ampicillin and fluoroquinolones	Resistance plasmid-mediated, chromosomal *gyrB* and *parC* mutations	Kaper et al., 2004; Baylis et al., 2006; Gomes et al., 2016; Pawłowska and Sobieszczańska, 2017
Enterotoxigenic (ETEC)	Thermostable (ST) and thermolabile (LT) enterotoxins	Watery diarrhea, known as traveler's diarrhea	Ampicillin, sulfamethoxazole, tetracycline and azithromycin	Resistance plasmid-mediated (distinct Inc type conjugative plasmids)	Kaper et al., 2004; Medina et al., 2015; Gomes et al., 2016; Pawłowska and Sobieszczańska, 2017
Diffusely-adhering (DAEC)	Afa/Dr adhesins	Acute diarrhea to assypmtomatic cases	Ampicillin, Trimethoprim, Sulfamethoxazole, Fosfomycin, piperacillin, tetracycline, ciprofloxacin, co-trimoxazole, nitrofurantoin, oxacillin, bactericin, cloxacillin, chloramphenicol, and nalidixic acid	Resistance plasmid-mediated, chromosomal *gyrB* and *parC* mutations	Kaper et al., 2004; Nash et al., 2010; Servin, 2014; Gomes et al., 2016
Adherent-invasive (AIEC)	type VI secretion system, type I pili, long polar fimbriae	Chronic gut inflammation and Crohn´s disease	Ampicillin and ciprofloxacin	Resistance plasmid-mediated, chromosomal *gyrB* and *parC* mutations	Kaper et al., 2004; Nash et al., 2010; Barrios-Villa et al., 2018
Cell-detaching (CDEC)	K-hemolysin, pyelonephritis-associated pili and cytotoxic necrotizing factor 1 (CNF1)	Diarrhea in infants, cell detaching, and inked to Crohn´s disease cases	Amoxicillin-clavulanic acid, ampicillin, mezlocillin, piperacillin, tetracycline, trimethoprim, trimethoprim-sulfamethoxazole, spectinomycin, streptomycin and sulfonamide	Resistance plasmid-mediated, integrons	Elliott et al., 1998; Fábrega et al., 2002; Okeke et al., 2002; Kaper et al., 2004; Rakitina et al., 2017
Uropathogenic (UPEC)	P fimbriae, certain other mannose-resistant adhesins, and type 1 fimbriae, K capsule, Hemolysin, Aerobactin	Urinary and Bloodstream infections	Fluoroquinolone, aminoglycosides, trimethoprim-sulfamethoxazole and carbapenems	Resistance plasmid-mediated, transposons, integrons, chromosomal	Kaper et al., 2004; Mobley et al., 2009; Petty et al., 2014

(Continued)

TABLE 1 | Continued

E. coli Pathotype (DEC and ExPEC)	Main virulence traits	Clinical manifestation	Antimicrobial resistance (AMR) commonly found	Mobile genetic resistance determinants	References
				gyrA, gyrB, parE, parC and *marA* mutations	
Sepsis-causing (SEPEC)	Type 1, P, and S fimbriae, K capsule K1/K5, hemolysin, aerobactin, yersiniabactin, salmochelin, CNF1, secreted autotransporter toxin, serum resistance, and colicin V	Bacteremia and sepsis	Carbapenems	Resistance plasmid-mediated, integrons	Kaper et al., 2004; Mokady et al., 2005; Nagarjuna et al., 2018
Neonatal meningitis-associated (NMEC)	*ompTp*, *hlyF*, *cvaC*, *etsA*, *cvaA*, *etsB*, *cvaB*, *iss*, *iutA*, and *tsh*	Meningitis, and bacteremia in neonates	Streptomycin sulfisoxazole, ampicillin, tetracycline, chloramphenicol, kanamycin and trimethoprim-sulfamethoxazole	Resistance plasmid-mediated	Korhonen et al., 1985; Kaper et al., 2004; Logue et al., 2012

ND, non-described.

pathotypes, proposed by their differential features and the essential virulence genes defining each subgroup, such as Shiga toxin-producing *E. coli* (STEC), enterohemorrhagic *E. coli* (EHEC), enteropathogenic *E. coli* (EPEC), enterotoxigenic *E. coli* (ETEC), enteroinvasive *E. coli* (EIEC), enteroaggregative *E. coli* (EAEC), diffusely-adhering *E. coli* (DAEC), adherent-invasive *E. coli* (AIEC), and cell-detaching *E. coli* (CDEC) (Kaper et al., 2004; Pawłowska and Sobieszczańska, 2017) (**Table 1**).

Herein, we briefly describe the diversity of these classic and novel emerging *E. coli* pathotypes and their genetic plasticity in a multifaceted organism. The mobile genetic elements are responsible for the appearance of novel hybrid strains with distinct assortment of virulence and antimicrobial resistance traits, bringing up the urgent need to reconsider the forms of treatment for these infections.

TYPES OF *E. COLI*: MANY FLAVORS WITHIN A SINGLE BACTERIAL SPECIES

E. coli is one of the most genetically versatile microorganisms and is able to colonize and persist in several niches, both in the environment or in hosts. Commensal *E. coli* strains colonize the gastrointestinal tract of humans a few hours after birth, resulting in a symbiotic relationship between the microbiota and its host (Ducarmon et al., 2019). However, the mechanisms by which *E. coli* ensures this efficient symbiosis is not well known. It could be related to its high ability to use nutrients in the colon (Fabich et al., 2008; Ducarmon et al., 2019). Several studies have shown that competition for nutrients between microbiota and pathogens limits the colonization of the pathogens, leading to fierce competition among these microorganisms (Lustri et al., 2017).

Occasionally, pathogenic *E. coli* cannot be distinguished from commensal *E. coli*, only based on specific virulence factors, as some previously described in ExPEC strains (Köhler and Dobrindt, 2011). However, this scenario is changing due to sophistication and availability of molecular typing methodologies. New computational approaches bring countless important information about host-pathogen relationships, reservoir, clinical diagnoses, and novel ExPEC transmission pathways (Johnson and Russo, 2018). Often, virulence genes are located in transmissible genetic elements such as genomic islands, bacteriophages, insertion sequences (ISs), integrons, plasmids, and transposons; hence, they can be easily exchanged among different bacteria (Hacker et al., 2003; Dobrindt et al., 2010). They also carry multiple antibiotic resistance genes that have been under strong selective pressure as consequence of the extensive use of antibiotics (Brzuszkiewicz et al., 2009).

Common genetic changes in *E. coli* genomes ensure high diversity due to the gain and loss of genes through genetic modification events. There are many strains of ExPEC that normally colonize the gut asymptomatically, as members of the intestinal microbiota. Nonetheless, only a subset of ExPEC as UPEC, SEPEC and NMEC are responsible for the vast majority of infections such as urinary tract infections, sepsis, and meningitis (Kaper et al., 2004). There is a great variety of virulence factors in ExPEC strains, such as adhesins (fimbrial and non-fimbrial), siderophores, toxins, invasins, the ability to survive in serum, among others. Moreover, many of these virulence factors may occur combined within the same strain and act synergistically. Despite extra factors, the septic strains always possess at least an adherence system, an iron uptake system and genes for serum survival (Biran and Ron, 2018; Johnson and Russo, 2018) (**Table 1**).

The genetic evolution in *E. coli* pathogenesis employs horizontal transfer mechanisms within same and across similar species. Therefore, the IS, transposons and integrons may facilitate novel rearrangements within the genome, such as duplication and suppression of genes and also capture of new genes. This genetic material transit can result in greater flexibility concerning various features, such as the transition of pathogenic bacteria between humans and animals, resistance to antimicrobials, appearance of emerging pathogens due to the gain of virulence genes, increased pathogenicity, among other features (Frost et al., 2005; Brigulla and Wackernagel, 2010; Dobrindt et al., 2010; Jackson et al., 2011; Sheppard et al., 2018). All these conditions may contribute to the virulence of these bacteria, like the bacteriophage importance in the pathogenesis. The horizontal transfer between different strains favors the emergence of new pathogenic strains with discrepancies in the bacteriophage repertoire affecting directly their virulence (Manning et al., 2008; Ogura et al., 2009; Dobrindt et al., 2010; Jackson et al., 2011).

TABLE 2 | Hybrid pathogenic (HyPEC) main features described.

HyPEC	Main features	Hybrid virulence traits identified	Clinical manifestation	Antimicrobial resistance (AMR) described	References
O1O4:H4 EAEC/STEC	Hybrid EAEC with STEC	Aggregative typical fimbriae, Shiga toxin	Diarrhea, HUS	Quinolones and β-lactams	Bielaszewska et al., 2011; Rasko et al., 2011; Muniesa et al., 2012; Navarro-Garcia, 2014; Ribeiro et al., 2019
O80:H2 STEC/ExPEC	Hybrid STEC with ExPEC	Intimin, Shiga toxin and pS88-like plasmid	HUS, Bacteremia	β-lactams	Peigne et al., 2009; Mariani-Kurkdjian et al., 2014
O2:H6 STEC/UPEC	Hybrid STEC with UPEC	*α-hlyA*, *cnf1* and *clb* genes	Diarrhea, Urinary tract infections, HUS	ND	Bielaszewska et al., 2014
ST131 UPEC/EAEC	Hybrid ExPEC with EAEC	pAA plasmid	Urinary infections, Bloodstream infections and Diarrhea	β-lactams	Boll et al., 2018
EPEC/ETEC	Hybrid EPEC and ETEC	Intimin, LEE island, ST and LT toxin	Diarrhea, Mild fever and cough	β-lactams, SUT, and quinolones	Dutta et al., 2015
STEC/ETEC	Hybrid STEC and ETEC	Intimin, Shiga toxin (Stx2) and LT toxin	Acute diarrhea and HUS	ND	Lindstedt et al., 2018
O137:H6 (ST2678) EPEC/STEC	Hybrid EPEC and STEC	Intimin, BFP, Shiga toxin (Stx2) and AIDA-I autotransporter	Diarrhea and HUS	ND	Gioia-Di Chiacchio et al., 2018
STEC/ETEC	Hybrid STEC and ETEC	Intimin, Shiga toxin, ST and LT toxins	Acute diarrhea and HUS	ND	Nyholm et al., 2015
EPEC/ETEC	Hybrid EPEC and ETEC	Intimin, BFP, ST and LT toxins	Diarrhea, Mild fever and cough	ND	Hazen et al., 2017

HyPEC, Hybrid Pathogenic E. coli; HUS, Hemolytic Uremic Syndrome; ND, non-described; SUT, Trimethoprim-sulfamethoxazole.

The co-evolution of bacterial genomes with plasmids, besides potential genetic and phenotypic gain may impact cellular metabolism to ensure the maintenance and stability of the plasmid (Jackson et al., 2011). Many ExPEC virulence genes are encoded within plasmids, often belonging to the ColV family, which encodes colicin, serum survival factors and iron uptake systems (Biran and Ron, 2018). Similarly, intestinal pathogens carry a variety of types of plasmids, associated with virulence, majorly belonging to the incompatibility group IncF, which has transfer functions (Carattoli, 2009). There are virulence plasmids essential for some pathotypes of *E. coli*, such as pINV and pAA, respectively, in EIEC and EAEC, according to each own group features (Kaper et al., 2004).

Although, all ExPEC and DEC pathotypes are not enough to fully classify all pathogenic *E. coli* strains, since these bacteria are so variable, allowing constant appearance of distinct hybrid-formed strains within this dynamic bacterial species. The carriage of virulence genes essential to the pathogenesis of each pathotype and the ability to adapt to different conditions allow the emergence of hybrid pathogenic *E. coli* (HyPEC).

GENETIC PLASTICITY AND EMERGENT *E. COLI* PATHOGEN: HYPEC

E. coli has an astonishing facility to amend very well, replicate and disseminate. These features allowed the advent of novel HyPEC. Acquired virulence genes and novel functions appear from mutation, recombination and other genetic changes. All these genetic differences have increased the occurrence of novel hybrid and antimicrobial resistance among DEC and ExPEC (Dobrindt et al., 2003; Bielaszewska et al., 2007; Khan et al., 2018).

Recently, a HyPEC strain received widespread attention after an outbreak of foodborne bloody diarrhea and hemorrhagic uremic syndrome (HUS) in Germany. This outbreak of *E. coli* O1O4:H4 was associated with consumption of raw fenugreek sprouts, as a hybrid EAEC strain with STEC features, like Shiga toxin presence. This HyPEC was quickly sequenced and unraveled its intricate nature, but even with a quick response and identification it was not enough to avoid 3,842 hospitalizations with many fatalities in Europe and North Africa (Bielaszewska et al., 2011; Rasko et al., 2011). Emerging processes are responsible for the HyPEC occurrences. Herein, the combined enteroaggregative features in a rare serotype was responsible to high attachment to cells and a biofilm formation (Navarro-Garcia, 2014; Ribeiro et al., 2019). Moreover, this strain has gained *stx2* gene lambdoid phage integrated in the genome, thus it may release the Shiga-toxin. These features have increased HUS occurrence during the outbreak on this HyPEC when compared to STEC (Muniesa et al., 2012).

Many distinct genetic hybrid examples are reported in *E. coli*, such as STEC/ExPEC O80:H2 serotype, which caused HUS and bacteremia due the presence of *stx2* and *eae* genes from STECs and pS88-like plasmid, described in meningitis, urosepsis and avian pathogenic strains of ExPEC (Peigne et al., 2009; Mariani-

Kurkdjian et al., 2014). The STEC/UPEC strain O2:H6 serotype, a STEC with virulence genes as *α-hlyA*, *cnf1*, and *clb* from UPEC that have ability to cause diarrhea and urinary tract infections (Bielaszewska et al., 2014). The EPEC/ETEC strain has acquired the LEE island and encodes the LT toxin (Dutta et al., 2015). The broadly reported multidrug resistant *E. coli* ST131 is example of highly virulent ExPEC associated with urinary and bloodstream infections. It has also acquired enteroaggregative diarrheagenic phenotype due to pAA plasmid presence (Boll et al., 2018). Many others HyPEC are described as case report, but not fully characterized. Here, we have briefly sampled some of the acquired genes by these strains, their direct impact in virulence and their hybrid nature (**Table 2**). Comparable to these HyPEC, the coined terms hybrid- and hetero-pathogenic *E. coli* have been recently described as new combination of virulence factors among classic *E. coli* groups. Together, they show differences between typical and atypical subgroups within the EAEC and EPEC pathotypes and hybrids, such as EPEC/STEC, ExPEC/EPEC and ExPEC/EAEC hybrids (Santos et al., 2020). Similar to our approach here, this study shows how this topic is critical in the field.

The high prevalence of classic pathogenic *E. coli* and appearance of HyPEC occur *via* similar genetic mechanisms, which also enable bacteria to resist the presence of distinct antimicrobials. Bacteria resistant to various classes of antibiotics are related to the complex combination of intrinsic and acquired resistance genes, which may act synergistically (Cag et al., 2016; Khan et al., 2018). Together that brings multiresistant bacteria, as an alarming factor reported worldwide in several bacterial species. WHO has prioritized studies on AMR bacteria, including Enterobacteriaceae, based on recent surveillance reports (WHO, 2018).

EMERGING HYBRIDS AND ALTERNATIVE THERAPIES

The complex combination of multidrug-resistant bacteria and emerging hybrid bacteria with intrinsic or acquired bacterial virulence factors disseminated by genetic mobility elements, the intense and inappropriate use of antibiotics have simultaneously favored the emergence of resistance to various antibiotics (Khan et al., 2018). That is a special challenge to these hybrid strains, since these HyPEC gathered virulence traits and acquired antibiotic resistance, together these points raise the importance to alternative treatments. These options are crucial to reduce the use of antibiotics and the consequent increase of antimicrobial resistance. Novel therapies are urgent to replace prophylactic and treatment with antibiotics by probiotics, prebiotics, enzymatic compounds, vaccines, monoclonal antibodies, phage therapy, antivirulence compounds, among other possibilities (Gadde et al., 2017).

Recently, different vaccine strategies have been used for pathogenic *E. coli* infection as an alternative to antibiotic therapy (Rojas-Lopez et al., 2018), including vaccines with attenuated toxins (McKenzie et al., 2007; Bitzan et al., 2009), attenuated bacterial cell (Calderon Toledo et al., 2011), individual components of virulence factors such as Shiga toxin (Liu et al., 2009), EspA or Intimin (Oliveira et al., 2012), small peptides (Zhang et al., 2011), DNA (García-Angulo et al., 2014) or polysaccharides (Ahmed et al., 2006; van den Dobbelsteen, 2016), as well detailed in the literature. Commercial vaccines have aimed the use to protect livestock, such as poultry, swine and bovine herds, against respectively to APEC, like Poulvac® *E. coli*, ETEC and EHEC infections (Sadeyen et al., 2015; Nesta and Pizza, 2018). Vaccines with a modern approach and technology still are a promising strategy to protect against emergent HyPECs infections in humans and livestock.

Recent studies have revisited the phage therapy as a biological alternative, which employs strictly lytic phages uncapable of lysogenization (Carter et al., 2012). Studies have demonstrated ability of phages to decrease biofilm formation in UPEC (Chibeu et al., 2012), increased mice rate survival in *E. coli*-induced pneumonia (Dufour et al., 2015). Moreover, lytic bacteriophages were used to infect and kill bacteria harboring phage-dependent conjugative plasmid to avoid emergence of multiresistant bacteria (Ojala et al., 2013; Tagliaferri et al., 2019). The phages cocktail EcoShield™ is already commercialized (Intralytix) and it has been reported to significantly reduce the *E. coli* O157:H7 contamination on surfaces and food (Abuladze et al., 2008; Carter et al., 2012). Additionally, mutual use of phages with antibiotics have emerged, with SPR02 and DAF6 phages combined with enrofloxacin have shown promising data, rescuing chickens challenged with avian pathogenic *E. coli* infection (Tagliaferri et al., 2019).

The novel approach *via* antivirulence-directed compounds works disarming the pathogens' ability to cause disease by inhibiting their virulence factors, favoring the host's immune defenses during the bacterial clearance. These compounds do not induce bacterial resistance as antibiotics, because they disarm the pathogen, instead of directly targeting its growth. Therefore, as they are directed to specific factors for pathogenesis, they potentially reduce the selection of resistance and limit collateral damage to the microbiota. Some virulence inhibitors are effective against many pathogens, molecules such as LED209, HC102A, HC103A, Artemisinin, and Ethoxzolamide, by inhibit different two-component systems as QseBC in *E. coli* and other enteropathogens (Sperandio et al., 2003; Rasko et al., 2008; Yang et al., 2014; Xue et al., 2015; Kim et al., 2020), Bicyclic 2-pyridones, Biaryl mannoside, Nitazoxanide and FN075, avoiding the initial bacterial adhesion; and compounds like Toxtazins A and B, Ebselen, 7086, 7812, 7832, BPT15, and BBH7, blocking toxins and secretion systems (Payne, 2008; Johnson and Abramovitch, 2017).

CONCLUSION

The forces that shape the evolution in *E. coli* comprise vast repertoire, affecting genetic flexibility and excessive permissiveness to acquire and donate DNA *via* horizontal gene

transfer. These features guarantee the spread of antibiotic resistance as well as virulence factors inherited among the various pathotypes of *E. coli*. The exact identification and assessment assist researchers to better understand this bacterium modification, diagnosis, public health and treatment. *E. coli* strains with multiple and distinct factors are probably very common but unreported, since these *E. coli* strains have developed many strategies to persist in different settings and successfully infect the host. These strategies result in an immense variety of microorganisms, ranging from avirulent to extremely virulent strains that can cause intestinal or extraintestinal diseases. *E. coli* strains have great potential for dissemination and capacity to pass along hereditary elements. Currently, these HyPEC strains are a very concerning threat that demands more studies and the development of novel treatment methods.

AUTHOR CONTRIBUTIONS

VB: writing and organization. KM: writing. CM: writing and mentoring. All authors contributed to the article and approved the submitted version.

FUNDING

Financially supported by FAPESP (grants 2014/06779-2, 2018/22412-2, 2018/22042-0, and 2019/03049-7), CNPq (307418/2017-0), and "Programa de Apoio ao Desenvolvimento Científico da Faculdade de Ciências Farmacêuticas da UNESP-PADC. This study was financed in part by the Coordenação de Aperfeiçoamento de Pessoal de Nível Superior - Brasil (CAPES) - Finance Code 001.

REFERENCES

Abuladze, T., Li, M., Menetrez, M. Y., Dean, T., Senecal, A., and Sulakvelidze, A. (2008). Bacteriophages reduce experimental contamination of hard surfaces, tomato, spinach, broccoli, and ground beef by *Escherichia coli* O157:H7. *Appl. Environ. Microbiol.* 74, 6230–62 8. doi: 10.1128/AEM.01465-08.21

Ahmed, A., Li, J., Shiloach, Y., Robbins, J. B., and Szu, S. C. (2006). Safety and immunogenicity of *Escherichia coli* O157 O-specific polysaccharide conjugate vaccine in 2-5-year-old children. *J. Infect. Dis.* 193, 515–521. doi: 10.1086/499821

Aslani, M. M., Alikhani, M. Y., Zavari, A., Yousefi, R., and Zamani, A. R. (2011). Characterization of enteroaggregative *Escherichia coli* (EAEC) clinical isolates and their antibiotic resistance pattern. *Int. J. Infect. Dis. IJID Off. Publ. Intern. Soc Infec. Dis.* 15 (2), e136–e139. doi: 10.1016/j.ijid.2010.10.002

Barrios-Villa, E., Cortés-Cortés, G., Lozano-Zaraín, P., Arenas-Hernández, M., Martínez de la Peña, C. F., Martínez-Laguna, Y., et al. (2018). Adherent/invasive Escherichia coli (AIEC) isolates from asymptomatic people: new *E. coli* ST131 O25:H4/H30-Rx virotypes. *Ann. Clin. Mic. Antim.* 17 (1), 42. doi: 10.1186/s12941-018-0295-4

Baylis, C. L., Penn, C. W., Thielman, N. M., Guerrant, R. L., Jenkins, C., and Gillespie, S. H. (2006). "Escherichia coli and Shigella spp," in *Principles and Practice of Clinical Bacteriology*, *2nd ed.* Eds. S. H. Gillespie and P. M. Hawkey (England, UK: John Wiley and Sons Ltd), 347–365. doi: 10.1002/9780470017968.ch28

Bielaszewska, M., Dobrindt, U., Gärtner, J., Gallitz, I., Hacker, J., Karch, J., et al. (2007). Aspects of genome plasticity in pathogenic *Escherichia coli*. *Int. J. Med. Microbiol.* 297 (7-8), 625–639. doi: 10.1016/j.ijmm.2007.03.001

Bielaszewska, M., Mellmann, A., Zhang, W., Köck, R., Fruth, A., Bauwens, A., et al. (2011). Characterisation of the *Escherichia coli* strain associated with an outbreak of haemolytic uraemic syndrome in German: a microbiological study. *Lancet Infect. Dis.* 11 (9), 671–676. doi: 10.1016/S1473-3099(11)70165-7

Bielaszewska, M., Schiller, R., Lammers, L., Bauwens, A., Fruth, A., Middendorf, B., et al. (2014). Heteropathogenic virulence and phylogeny reveal phased pathogenic metamorphosis in *Escherichia coli* O2:H6. *EMBO Mol. Med.* 6, 347–357. doi: 10.1002/emmm.201303133

Biran, D., and Ron, E. Z. (2018). Extraintestinal Pathogenic *Escherichia coli*. *Curr. Top. Microbiol. Immunol.* 416, 149–161. doi: 10.1007/82_2018_108

Bitzan, M., Poole, R., Mehran, M., Sicard, E., Brockus, C., Thuning-Roberson, C., et al. (2009). Safety and pharmacokinetics of chimeric anti-Shiga toxin 1 and anti-Shiga toxin 2 monoclonal antibodies in healthy volunteers. *Antimicrob. Agents Chemother.* 53, 3081–3087. doi: 10.1128/AAC.01661-08

Boll, E. J., Overballe-Petersen, S., Hasman, H., Roer, L., Ng, K., Scheutz, F., et al. (2018). Emergence of enteroaggregative*Escherichia coli* within the ST131 lineage as a cause of extraintestinal infections. *mBio* 11 (3), e00353–e00420. doi: 10.1128/mBio.00353-20

Brigulla, M., and Wackernagel, W. (2010). Molecular aspects of gene transfer and foreign DNA acquisition in prokaryotes with regard to safety issues. *Appl. Microbiol. Biotechnol.* 86 (4), 1027–1041. doi: 10.1007/s00253-010-2489-3

Brzuszkiewicz, E., Gottschalk, G., Ron, E., Hacker, J., and Dobrindt, U. (2009). Adaptation of Pathogenic *E. coli* to Various Niches: Genome Flexibility is the Key. *Genome Dyn.* 6, 110–125. doi: 10.1159/000235766

Cag, Y., Caskurlu, H., Fan, Y., Cao, B., and Vahaboglu, H. (2016). Resistance mechanisms. *Ann. Transl. Med.* 4 (17), 326. doi: 10.21037/atm.2016.09.14

Calderon Toledo, C., Arvidsson, I., and Karpman, D. (2011). Cross-reactive protection against enterohemorrhagic *Escherichia coli* infection by enteropathogenic *E. coli* in a mouse model. *Infect. Immun.* 79, 2224–2233. doi: 10.1128/IAI.01024-10

Carattoli, A. (2009). Resistance plasmid families in Enterobacteriaceae. *Ant. Agents Chemother.* 53 (6), 2227–2238. doi: 10.1128/AAC.01707-08

Carattoli, A. (2013). Plasmids and the spread of resistance. *Int. J. Med. Microbiol.* 303, 298–304. doi: 10.1016/j.ijmm.2013.02.001

Carter, C. D., Parks, A., Abuladze, T., Li, M., Woolston, J., Magnone, J., et al. (2012). Bacteriophage cocktail significantly reduces *Escherichia coli* O157: H7 contamination of lettuce and beef, but does not protect against recontamination. *Bacteriophage* 2 (3), 178–185. doi: 10.4161/bact.22825

Chahales, P., Hoffman, P. S., and Thanassi, D. G. (2016). Nitazoxanide Inhibits Pilus Biogenesis by Interfering with Folding of the Usher Protein in the Outer Membrane. *Antimicrob. Agents Chemother.* 60, 2028–2038. doi: 10.1128/AAC.02221-15

Chattaway, M. A., Day, M., Mtwale, J., White, E., Rogers, J., Day, M., et al. (2017). Clonality, virulence and antimicrobial resistance of enteroaggregative *Escherichia coli* from Mirzapur, Bangladesh. *J. Med. Microbiol.* 66 (10), 1429–1435. doi: 10.1099/jmm.0.000594

Chibeu, A., Lingohr, E. J., Masson, L., Manges, A., Harel, J., Ackermann, H.-W., et al. (2012). Bacteriophages with the ability to degrade uropathogenic *Escherichia coli* biofilms. *Viruses* 4, 471–487. doi: 10.3390/v4040471

Curtis, M. M., Russell, R., Moreira, C. G., Adebesin, A. M., Wang, C., Williams, N. S., et al. (2014). QseC inhibitors as an antivirulence approach for Gram-negative pathogens. *MBio* 5 (6), e02165. doi: 10.1128/mBio.02165-14

Day, M., Doumith, M., Jenkins, C., Dallman, T. J., Hopkins, K. L., Elson, R., et al. (2017). Antimicrobial resistance in Shiga toxin-producing *Escherichia coli* serogroups O157 and O26 isolated from human cases of diarrhoeal disease in Englan. *J. Antimicrob. Chemother.* 72 (1), 145–152. doi: 10.1093/jac/dkw371

Dobrindt, U., Agerer, F., Michaelis, K., Janka, A., Buchrieser, C., Samuelson, M., et al. (2003). Analysis of genome plasticity in pathogenic and commensal *Escherichia coli* isolates by use of DNA arrays. *J. Bacteriol.* 185 (6), 1831–1840. doi: 10.1128/jb.185.6.1831-1840.2003

Dobrindt, U., Chowdary, M. G., Krumbholz, G., and Hacker, J. (2010). Genome dynamics and its impact on evolution of *Escherichia coli*. *Med. Microbiol. Immunol.* 199 (3), 145–154. doi: 10.1007/s00430-010-0161-2

Ducarmon, Q. R., Zwittink, R. D., Hornung, B. V. H., van Schaik, W., Young, V. B., and Kuijper, E. J. (2019). Gut Microbiota and Colonization Resistance against Bacterial Enteric Infection. *Microbiol. Mol. Biol. Rev.* 83 (3), e00007–e00019. doi: 10.1128/MMBR.00007-19

Dufour, N., Debarbieux, L., Fromentin, M., and Ricard, J. D. (2015). Treatment of highly virulent extraintestinal pathogenic *Escherichia coli* pneumonia with bacteriophages. *Crit. Care Med.* 43 (6), e190–e198. doi: 10.1097/CCM.0000000000000968

Dutta, S., Pazhani, G. P., Nataro, J. P., and Ramamurthy, T. (2015). Heterogenic virulence in a diarrheagenic *Escherichia coli*: evidence for an EPEC expressing heat-labile toxin of ETEC. *Int. J. Med. Microbiol.* 305, 47–54. doi: 10.1016/j.ijmm.2014.10.006

Elbediwi, M., Li, Y., Paudyal, N., Pan, H., Li, X., Xie, S., et al. (2019). Global Burden of Colistin-Resistant Bacteria: Mobilized Colistin Resistance Genes Study, (1980-2018). *Microorganisms* 7 (10), E461. doi: 10.3390/microorganisms7100461

Elliott, S. J., Srinivas, S., Albert, M. J., Alam, K., Robins-Browne, R. M., Gunzburg, S. T., et al. (1998). Characterization of the roles of hemolysin and other toxins in enteropathy caused by alpha-hemolytic *Escherichia coli* linked to human diarrhea. *Infect. Immun.* 66, 2040–2051. doi: 10.1128/IAI.66.5.2040-2051.1998

Fabich, A. J., Jones, S. A., Chowdhury, F. Z., Cernosek, A., Anderson, A., Smalley, D., et al. (2008). Comparison of carbon nutrition for pathogenic and commensal *Escherichia coli* strains in the mouse intestine. *Infect. Immun.* 76, 1143–1152. doi: 10.1128/IAI.01386-07

Fábrega, V. L. A., Ferreira, A. J. P., Patrício, F. R. S., Brinkley, C., and Scaletsky, I. C. A. (2002). Cell-detaching *Escherichia coli*(CDEC) strains from children with diarrhea: Identification of a protein with toxigenic activity. *FEMS Microbiol. Lett.* 217 (2), 191–197. doi: 10.1111/j.1574-6968.2002.tb11474.x

Fernandes, M. R., McCulloch, J. A., Vianello, M. A., Moura, Q., Perez-Chaparro, P. J., Esposito, F., et al. (2016). First Report of the Globally Disseminated IncX4 Plasmid Carrying the mcr-1 Gene in a Colistin-Resistant *Escherichia coli* Sequence Type 101 Isolate from a Human Infection in Brazil. *Antimic. Agents Chemother.* 60 (10), 6415–6417. doi: 10.1128/AAC.01325-16

Frost, L. S., Leplae, R., Summers, A. O., and Toussaint, A. (2005). Mobile genetic elements: the agents of open source evolution. *Nat. Rev. Microbiol.* 3 (9), 722–732. doi: 10.1038/nrmicro1235

Gadde, U., Kim, W. H., Oh, S. T., and Lillehoj, H. S. (2017). Alternatives to antibiotics for maximizing growth performance and feed efficiency in poultry: a review. *Anim. Health Res. Rev.* 18 (1), 26–45. doi: 10.1017/S1466252316000207

García-Angulo, V. A., Kalita, A., Kalita, M., Lozano, L., and Torres, A. G. (2014). Comparative genomics and immunoinformatics approach for the identification of vaccine candidates for enterohemorrhagic *Escherichia coli* O157:H7. *Infect. Immun.* 82, 2016–2026. doi: 10.1128/IAI.01437-13

Garmendia, J., Frankel, G., and Crepin, V. F. (2005). Enteropathogenic and enterohemorrhagic *Escherichia coli* infections: translocation, translocation, translocation. *Infect. Immun.* 73 (5), 2573–2585. doi: 10.1128/IAI.73.5.2573-2585.2005

Gioia-Di Chiacchio, R. M., Cunha, M. P. V., de Sá, L. R. M., Davies, Y. M., Pereira, C. B. P., Martins, F. H., et al. (2018). Novel Hybrid of Typical Enteropathogenic *Escherichia coli* and Shiga-Toxin-Producing *E. coli* (tEPEC/STEC) Emerging From Pet Birds. *Front. Microbiol.* 9:2975:2975. doi: 10.3389/fmicb.2018.02975

Gomes, T. A., Elias, W. P., Scaletsky, I. C., Guth, B. E., Rodrigues, J. F., and Piazza, R. M. (2016). Diarrheagenic *Escherichia coli*. *Braz. J. Microbiol.* 47 Suppl 1, 3–30. doi: 10.1016/j.bjm.2016.10.015

Gunzburg, S. T., Chang, B. J., Elliott, S. J., Burke, V., and Gracey, M. (1993). Diffuse and enteroaggregative patterns of adherence of enteric *Escherichia coli* isolated from aboriginal children from the Kimberley region of Western Australia. *J. Infect. Dis.* 167, 755–758. doi: 10.1093/infdis/167.3.755

Hacker, J., Hentschel, U., and Dobrindt, U. (2003). Prokaryotic chromosomes and disease. *Science* 301 (5634), 790–793. doi: 10.1126/science.1086802

Hadjifrangiskou, M., Kostakioti, M., Chen, S. L., Henderson, J. P., Greene, S. E., and Hultgren, S. J. (2011). A central metabolic circuit controlled by QseC in pathogenic *Escherichia coli*. *Mol. Microbiol.* 80 (6), 1516–1529. doi: 10.1111/j.1365-2958.2011.07660.x

Han, Z., Pinkner, J. S., Ford, B., Chorell, E., Crowley, J. M., Cusumano, C. K., et al. (2012). Lead optimization studies on FimH antagonists: discovery of potent and orally bioavailable ortho-substituted biphenyl mannosides. *J. Med. Chem.* 55, 3945–3959. doi: 10.1021/jm300165m

Hazen, T. H., Michalski, J., Luo, Q., Shetty, A. C., Daugherty, S. C., Fleckenstein, J. M., et al. (2017). Comparative genomics and transcriptomics of *Escherichia coli* isolates carrying virulence factors of both enteropathogenic and enterotoxigenic *E. coli*. *Sci. Rep.* 7, 3513. doi: 10.1038/s41598-017-03489-z

Ingle, D. J., Levine, M. M., Kotloff, K. L., Holt, K. E., and Robins-Browne, R. M. (2018). Dynamics of antimicrobial resistance in intestinal Escherichia coli from children in community settings in South Asia and sub-Saharan Africa. *Nat. Microbiol.* 3 (9), 1063–1073. doi: 10.1038/s41564-018-0217-4

Jackson, R. W., Vinatzer, B., Arnold, D. L., Dorus, S., and Murillo, J. (2011). The influence of the accessory genome on bacterial pathogen evolution. *Mob. Genet. Elements* 1 (1), 55–65. doi: 10.4161/mge.1.1.16432

Jarvis, C., Han, Z., Kalas, V., Klein, R., Pinkner, J. S., Ford, B., et al. (2016). Antivirulence Isoquinolone Mannosides: Optimization of the Biaryl Aglycone for FimH Lectin Binding Affinity and Efficacy in the Treatment of Chronic UTI. *ChemMedChem* 11 (4), 367–373. doi: 10.1002/cmdc.201600006

Jerse, A. E., Yu, J., Tall, B. D., and Kaper, J. B. (1990). A genetic locus of enteropathogenic *Escherichia coli* necessary for the production of attaching and effacing lesions on tissue culture cells. *Proc. Natl. Acad. Sci. U.S.A.* 87 (20), 7839–7843. doi: 10.1073/pnas.87.20.7839

Johnson, B. K., and Abramovitch, R. B. (2017). Small Molecules That Sabotage Bacterial Virulence. *Trends Pharmacol. Sci.* 38 (4), 339–362. doi: 10.1016/j.tips.2017.01.004

Johnson, J. R., and Russo, T. A. (2018). Molecular Epidemiology of Extraintestinal Pathogenic *Escherichia coli*. *EcoSal. Plus* 8 (1), 4–22. doi: 10.1128/ecosalplus.ESP-0004-2017

Kaper, J. B., Nataro, J. P., and Mobley, H. L. (2004). Pathogenic *Escherichia coli*. *Nat. Rev. Microbiol.* 2 (2), 123–140. doi: 10.1038/nrmicro818

Khan, A., Miller, W. R., and Arias, C. A. (2018). Mechanisms of antimicrobial resistance among hospital-associated pathogens. *Expert Rev. Anti. Infect. Ther.* 16 (4), 269–287. doi: 10.1080/14787210.2018.1456919

Kim, C. S., Gatsios, A., Cuesta, S., Lam, Y. C., Wei, Z., Chen, H., et al. (2020). Characterization of Autoinducer-3 Structure and Biosynthesis in *E. coli*. *ACS Cent. Sci.* 6 (2), 197–206. doi: 10.1021/acscentsci.9b01076

Knutton, S., Baldwin, T., Williams, P. H., and McNeish, A. S. (1989). Actin accumulation at sites of bacterial adhesion to tissue culture cells: basis of a new diagnostic test for enteropathogenic and enterohemorrhagic *Escherichia coli*. *Infect. Immun.* 57 (4), 1290–1298. doi: 10.1128/IAI.57.4.1290-1298.1989

Köhler, C. D., and Dobrindt, U. (2011). What defines extraintestinal pathogenic *Escherichia coli*? *Int. J. Med. Microbiol.* 301 (8), 642–647. doi: 10.1016/j.ijmm.2011.09.006

Korhonen, T. K., Valtonen, M. V., Parkkinen, J., Väisänen-Rhen, V., Finne, J., Orskov, F., et al. (1985). Serotypes, hemolysin production, and receptor recognition of *Escherichia coli* strains associated with neonatal sepsis and meningitis. *Infect. Immun.* 48 (2), 486–491. doi: 10.1128/IAI.48.2.486-491.1985

Lindstedt, B. A., Finton, M. D., Porcellato, D., and Brandal, L. T. (2018). High frequency of hybrid *Escherichia coli* strains with combined Intestinal Pathogenic *Escherichia coli*(IPEC) and Extraintestinal Pathogenic *Escherichia coli* (ExPEC) virulence factors isolated from human faecal samples. *BMC Infect. Dis.* 18, 544. doi: 10.1186/s12879-018-3449-2

Liu, J., Sun, Y., Feng, S., Zhu, L., Guo, X., and Qi, C. (2009). Towards an attenuated enterohemorrhagic *Escherichia coli* O157:H7 vaccine characterized by a deleted ler gene and containing apathogenic Shiga toxins. *Vaccine* 27, 5929–5935. doi: 10.1016/j.vaccine.2009.07.097

Logue, C. M., Doetkott, C., Mangiamele, P., Wannemuehler, Y. M., Johnson, T. J., Tivendale, K. A., et al. (2012). Genotypic and phenotypic traits that distinguish neonatal meningitis-associated *Escherichia coli* from fecal E. coli isolates of healthy human hosts. *Appl. Environ. Microbiol.* 78 (16), 5824–5830. doi: 10.1128/AEM.07869-11

Lustri, B. C., Sperandio, V., and Moreira, C. G. (2017). Bacterial chat: intestinal metabolites and signals in host-microbiota-pathogen interactions. *Infec. Immun.* 85 (12), e00476. doi: 10.1128/IAI.00476-17

Maltby, R., Leatham-Jensen, M. P., Gibson, T., Cohen, P. S., and Conway, T. (2013). Nutritional basis for colonization resistance by human commensal

Escherichia coli strains HS and Nissle 1917 against *E. coli* O157:H7 in the mouse intestine. *PloS One* 8, e53957. doi: 10.1371/journal.pone.0053957

Manning, S. D., Motiwala, A. S., Springman, A. C., Qi, W., Lacher, D. W., Ouellette, L. M., et al. (2008). Variation in virulence among clades of *Escherichia col*i O157:H7 associated with disease outbreaks. *Proc. Natl. Acad. Sci. U.S.A.* 105 (12), 4868–4873. doi: 10.1073/pnas.0710834105

Mariani-Kurkdjian, P., Lemaitre, C., Bidet, P., Perez, D., Boggini, L., Kwon, T., et al. (2014). Haemolytic-uraemic syndrome with bacteraemia caused by a new hybrid *Escherichia coli* pathotype. *New Microbes New Infect.* 2, 127–131. doi: 10.1002/nmi2.49

Marques, L. R., Abe, C. M., Grin, P. M., and Gomes, T. A. T. (1995). Association between alpha-hemolysin production and HeLa cell-detaching activity in fecal isolates of *Escherichia coli*. *J. Clin. Microbiol.* 33, 2707–2709. doi: 10.1128/JCM.33.10.2707-2709.1995

McKenzie, R., Bourgeois, A. L., Frech, S. A., Flyer, D. C., Bloom, A., Kazempour, K., et al. (2007). Transcutaneous immunization with the heat-labile toxin (LT) of enterotoxigenic *Escherichia coli* (ETEC): protective efficacy in a double-blind, placebo-controlled challenge study. *Vaccine* 25, 3684–3691. doi: 10.1016/j.vaccine.2007.01.043

Medina, A. M., Rivera, F. P., Pons, M. J., Riveros, M., Gomes, C., Bernal, M., et al. (2015). Comparative analysis of antimicrobial resistance in enterotoxigenic *Escherichia coli* isolates from two paediatric cohort studies in Lima, Peru. *Trans. R. Soc Trop. Med. Hyg.* 109 (8), 493–502. doi: 10.1093/trstmh/trv054

Mellies, J. L., Elliott, S. J., Sperandio, V., Donnenberg, M. S., and Kaper, J. B. (1999). The Per regulon of enteropathogenic *Escherichia coli*: identification of a regulatory cascade and a novel transcriptional activator, the locus of enterocyte effacement (LEE)-encoded regulator (Ler). *Mol. Microbiol.* 33 (2), 296–306. doi: 10.1046/j.1365-2958.1999.01473.x

Mobley, H., Donnenberg, M., and Hagan, E. (2009). Uropathogenic *Escherichia coli*, EcoSal Plus 2009. *EcoSal Plus* 3 (2), 1–27. doi: 10.1128/ecosalplus.8.6.1.3

Mokady, D., Gophna, U., and Ron, E. Z. (2005). Virulence factors of septicemic *Escherichia coli* strains. *Int. J. Med. Microbiol.* 295 (6-7), 455–462. doi: 10.1016/j.ijmm.2005.07.007

Muniesa, M., Hammerl, J. A., Hertwig, S., Appel, B., and Brüssow, H. (2012). Shiga toxin-producing *Escherichia coli* O104: H4: a new challenge for microbiology. *Appl. Environ. Microbiol.* 78 (12), 4065–4073. doi: 10.1128/AEM.00217-12

Nagarjuna, D., Mittal, G., Dhanda, R. S., Gaind, R., and Yadav, M. (2018). Alarming levels of antimicrobial resistance among sepsis patients admitted to ICU in a tertiary care hospital in India - a case control retrospective study. *Antimicrob. Resist. Infect. Control* 7, 150. doi: 10.1186/s13756-018-0444-8

Nash, J. H., Villegas, A., Kropinski, A. M., Aguilar-Valenzuela, R., Konczy, P., Mascarenhas, M., et al. (2010). Genome sequence of adherent-invasive *Escherichia coli* and comparative genomic analysis with other *E. coli* pathotypes. *BMC Genomics* 11, 667. doi: 10.1186/1471-2164-11-667

Navarro-Garcia, F. (2014). *Escherichia coli* O104:H4 Pathogenesis: an Enteroaggregative*E.coli*/Shiga Toxin-Producing *E. coli* Explosive Cocktail of HighVirulence. *Microbiol. Spectr.* 2 (6), 2–15. doi: 10.1128/microbiolspec.EHEC-0008-2013

Nesta, B., and Pizza, M. (2018). *"Vaccines against Escherichia coli." In Escherichia coli, a Versatile Pathogen* (Cham: Springer), 213–242. doi: 10.1007/82_2018_111

Nyholm, O., Halkilahti, J., Wiklund, G., Okeke, U., Paulin, L., Auvinen, P., et al. (2015). Comparative genomics and characterization of hybrid Shigatoxigenic and Enterotoxigenic *Escherichia coli* (STEC/ETEC) strains. *PloS One* 10, e0135936. doi: 10.1371/journal.pone.0135936

Ogura, Y., Ooka, T., Iguchi, A., Toh, H., Asadulghani, M., Oshima, K., et al. (2009). Comparative genomics reveal the mechanism of the parallel evolution of O157 and non-O157 enterohemorrhagic *Escherichia coli*. *Proc. Natl. Acad. Sci. U.S.A.* 106 (42), 17939–17944. doi: 10.1073/pnas.0903585106

Ojala, V., Laitalainen, J., and Jalasvuori, M. (2013). Fight evolution with evolution: plasmid-dependent phages with a wide host range prevent the spread of antibiotic resistance. *Evol. Appl.* 6, 925–932. doi: 10.1111/eva.12076

Okeke, I. N., Steinrück, H., Kanack, K. J., Elliott, S. J., Sundström, L., Kaper, J. B., et al. (2002). Antibiotic-resistant cell-detaching *Escherichia coli* strains from Nigerian children. *J. Clin. Microb.* 40 (1), 301–305. doi: 10.1128/jcm.40.1.301-305.2002

Oliveira, A. F., Cardoso, S. A., Almeida, F. B., de Oliveira, L. L., Pitondo-Silva, A., Soares, S. G., et al. (2012). Oral immunization with attenuated *Salmonella* vaccine expressing *Escherichia coli* O157:H7 intimin gamma triggers both systemic and mucosal humoral immunity in mice. *Microbiol. Immunol.* 56, 513–522. doi: 10.1111/j.1348-0421.2012.00477.x

Pawłowska, B., and Sobieszczańska, B. M. (2017). Intestinal epithelial barrier: The target for pathogenic *Escherichia coli*. *Adv. Clin. Exp. Med.* 26 (9), 1437–1445. doi: 10.17219/acem/64883

Payne, D. J. (2008). *Microbiology.* Desperately seeking new antibiotics. *Science* 321 (5896), 1644–1645. doi: 10.1126/science.1164586

Peigne, C., Bidet, P., Mahjoub-Messai, F., Plainvert, C., Barbe, V., Médigue, C., et al. (2009). The plasmid of *Escherichia coli* strain S88 (O45:K1:H7) that causes neonatal meningitis is closely related to avian pathogenic *E. coli* plasmids and is associated with high-level bacteremia in a neonatal rat meningitis model. *Infect. Immune* 77 (6), 2272–2284. doi: 10.1128/IAI.01333-08

Petty, N. K., Ben Zakour, N. L., Stanton-Cook, M., Skippington, E., Totsika, M., Forde, B. M., et al. (2014). Global dissemination of a multidrug resistant Escherichia coli clone. *Proc. Nat. Acad. Sci. U.S.A.* 111 (15), 5694–5699. doi: 10.1073/pnas.1322678111

Pinkner, J. S., Remaut, H., Buelens, F., Miller, E., Aberg, V., Pemberton, N., et al. (2006). Rationally designed small compounds inhibit pilus biogenesis in uropathogenic bacteria. *Proc. Natl. Acad. Sci. U.S.A.* 103, 17897–17902. doi: 10.1073/pnas.0606795103

Rakitina, D. V., Manolov, A. I., Kanygina, A. V., Garushyants, S. K., Baikova, J. P., Alexeev, D. G., et al. (2017). Genome analysis of *E. coli* isolated from Crohn's disease patients. *BMC Genomics* 18 (1), 544. doi: 10.1186/s12864-017-3917-x

Rasko, D. A., Moreira, C. G., de Li, R., Reading, N. C., Ritchie, J. M., Waldor, M. K., et al. (2008). Targeting QseC signaling and virulence for antibiotic development. *Science* 321 (5892), 1078–1080. doi: 10.1126/science.1160354

Rasko, D. A., Webster, D. R., Sahl, J. W., Bashir, A., Boisen, N., Scheutz, F., et al. (2011). Origins of the *E. coli* strain causing an outbreak of hemolytic-uremic syndrome in Germany. *N Engl. J. Med.* 365 (8), 709–717. doi: 10.1056/NEJMoa1106920

Regua-Mangia, A. H., Gomes, T. A., Vieira, M. A., Irino, K., and Teixeira, L. M. (2009). Molecular typing and virulence of enteroaggregative *Escherichia coli* strains isolated from children with and without diarrhoea in Rio de Janeiro city, Brazil. *J. Med. Microbiol.* 58, 414–422. doi: 10.1099/jmm.0.006502-0

Ribeiro, T. R. M., Lustri, B. C., Elias, W. P., and Moreira, C. G. (2019). QseC Signaling in the Outbreak O104:H4 *Escherichia coli* Strain Combines Multiple Factors during Infection. *J. Bacteriol. Aug.* 8, e00203–e00219, 201(17). doi: 10.1128/JB.00203-19

Rodríguez-Martínez, J. M., Machuca, J., Cano, M. E., Calvo, J., Martínez-Martínez, L., and Pascual, A. (2016). Plasmid-mediated quinolone resistance: two decades on. *Drug Resist. Update* 29, 13–29. doi: 10.1016/j.drup.2016.09.001

Rojas-Lopez, M., Monterio, R., Pizza, M., Desvaux, M., and Rosini, R. (2018). Intestinal pathogenic *Escherichia coli*: insights for vaccine development. *Front. Microbiol.* 9, 440. doi: 10.3389/fmicb.2018.00440

Rooks, M. G., Veiga, P., Reeves, A. Z., Lavoie, S., Yasuda, K., Asano, Y., et al. (2017). QseC inhibition as an antivirulence approach for colitis-associated bacteria. *Proc. Natl. Acad. Sci. U.S.A.* 114 (1), 142–147. doi: 10.1073/pnas.1612836114

Sadeyen, J.-R., Wu, Z., Davies, H., van Diemen, P. M., Milicic, A., La Ragione, R. M., et al. (2015). Immune responses associated with homologous protection conferred by commercial vaccines for control of avian pathogenic *Escherichia coli* in turkeys. *Vet. Res.* 461), 5. doi: 10.1186/s13567-014-0132-5

Santos, A. C. M., Santos, F. F., Silva, R. M., and Gomes, T. A. T. (2020). Diversity of Hybrid- and Hetero-Pathogenic *Escherichia coli* and Their Potential Implication in More Severe Diseases. *Front. Cell. Infect. Microbiol.* 10, 339. doi: 10.3389/fcimb.2020.00339

Servin, A. L. (2014). Pathogenesis of human diffusely adhering *Escherichia coli* expressing Afa/Dr adhesins (Afa/Dr DAEC): current insights and future challenges. *Clin. Mic. Rev.* 27 (4), 823–869. doi: 10.1128/CMR.00036-14

Shamir, E. R., Warthan, M., Brown, S. P., Nataro, J. P., Guerrant, R. L., and Hoffman, P. S. (2010). Nitazoxanide inhibits biofilm production and hemagglutination by enteroaggregative *Escherichia coli* strains by blocking assembly of AafA fimbriae. *Antimicrob. Agents Chemother.* 54, 1526–1533. doi: 10.1128/AAC.01279-09

Sheppard, S. K., Guttman, D. S., and Fitzgerald, J. R. (2018). Population genomics of bacterial host adaptation. *Nat. Rev. Genet.* 19 (9), 549–565. doi: 10.1038/s41576-018-0032-z

Sperandio, V., Torres, A. G., Jarvis, B., Nataro, J. P., and Kaper, J. B. (2003). Bacteria-host communication: the language of hormones. *PNAS* 22100 (15), 8951–8956. doi: 10.1073/pnas.1537100100

Tagliaferri, T. L., Mathias, J., and Hans-Peter, H. (2019). Fighting pathogenic bacteria on two fronts: phages and antibiotics as combined strategy. *Front. Cel. Infect. Microb.* 9, 22. doi: 10.3389/fcimb.2019.00022

Tobe, T., Hayashi, T., Han, C. G., Schoolnik, G. K., Ohtsubo, E., and Sasakawa, C. (1999). Complete DNA sequence and structural analysis of the enteropathogenic *Escherichia coli* adherence factor plasmid. *Infect. Immun.* 67 (10), 5455–5462. doi: 10.1128/IAI.67.10.5455-5462.1999

Touchon, M., Hoede, C., Tenaillon, O., Barbe, V., Baeriswyl, S., Bidet, P., et al. (2009). Organised genome dynamics in the *Escherichia coli* species results in highly diverse adaptive paths. *PloS Genet.* 5 (1), e1000344. doi: 10.1371/journal.pgen.1000344

Trabulsi, L. R., Keller, R., and Tardelli Gomes, T. A. (2002). Typical and atypical enteropathogenic *Escherichia coli*. *Emerg. Infect. Dis.* 8 (5), 508–513. doi: 10.3201/eid0805.010385

van den Dobbelsteen, G., Fae, K. C., Serroyen, J., van den Nieuwenhof, I. M., Braun, M., Haeuptle, M. A., et al. (2016). Immunogenicity and safety of a tetravalent *E. coli* O-antigen bioconjugate vaccine in animal models. *Vaccine* 34, 4152e60. doi: 10.1016/j.vaccine.2016.06.067

World Health Organization. (2018). *Global antimicrobial resistance surveillance system (GLASS) report. Early implemetantion 2016-2017*, ISBN: .

Xue, X. Y., Mao, X. G., Li, Z., Chen, Z., Zhou, Y., Hou, Z., et al. (2015). A potent and selective antimicrobial poly(amidoamine) dendrimer conjugate with LED209 targeting QseC receptor to inhibit the virulence genes of gram-negative bacteria. *Nanomedicine* 11 (2), 329–339. doi: 10.1016/j.nano.2014.09.016

Yang, Q., Anh, N. D., Bossier, P., and Defoirdt, T. (2014). Norepinephrine and dopamine increase motility, biofilm formation, and virulence of *Vibrio harveyi*. *Front. Microbiol.* 5:584:584. doi: 10.3389/fmicb.2014.00584

Zhang, X. H., He, K. W., Zhang, S. X., Lu, W. C., Zhao, P. D., Luan, X. T., et al. (2011). Subcutaneous and intranasal immunization with Stx2B-Tir-Stx1B-Zot reduces colonization and shedding of *Escherichia coli* O157:H7 in mice. *Vaccine* 29, 3923–3929. doi: 10.1016/j.vaccine.2011.02.007

Zheng, B., Dong, H., Xu, H., Lv, J., Zhang, J., Jiang, X., et al. (2016). Coexistence of MCR-1 and NDM-1 in Clinical *Escherichia coli* Isolates. *Clin. Infect. Dis.* 63 (10), 1393–1395. doi: 10.1093/cid/ciw553

Zhong, L. L., Zhang, Y. F., Doi, Y., Huang, X., Zhang, X. F., Zeng, K. J., et al. (2017). Coproduction of MCR-1 and NDM-1 by Colistin-Resistant *Escherichia coli* Isolated from a Healthy Individual. *Antimicrob. Agents Chemother.* 61 (1), e01962–e01916. doi: 10.1128/AAC.01962-16

Conflict of Interest: The authors declare that the research was conducted in the absence of any commercial or financial relationships that could be construed as a potential conflict of interest.

Advantages of publishing in Frontiers

OPEN ACCESS
Articles are free to read for greatest visibility and readership

FAST PUBLICATION
Around 90 days from submission to decision

HIGH QUALITY PEER-REVIEW
Rigorous, collaborative, and constructive peer-review

TRANSPARENT PEER-REVIEW
Editors and reviewers acknowledged by name on published articles

Frontiers
Avenue du Tribunal-Fédéral 34
1005 Lausanne | Switzerland

Visit us: www.frontiersin.org
Contact us: frontiersin.org/about/contact

REPRODUCIBILITY OF RESEARCH
Support open data and methods to enhance research reproducibility

DIGITAL PUBLISHING
Articles designed for optimal readership across devices

FOLLOW US
@frontiersin

IMPACT METRICS
Advanced article metrics track visibility across digital media

EXTENSIVE PROMOTION
Marketing and promotion of impactful research

LOOP RESEARCH NETWORK
Our network increases your article's readership